Getting Up To Speed

Society of Petroleum Engineers

Artificial Intelligence & Data Mining Applications in the E&P Industry

Shahab D. Mohaghegh
Intelligent Solutions, Inc. & West Virginia University

Saud M. Al-Fattah
Saudi Aramco & King Abdullah Petroleum Studies & Research

Andrei S. Popa
Chevron Corporation

Society of Petroleum Engineers

© Copyright 2011 Society of Petroleum Engineers

All rights reserved. No portion of this publication may be reproduced in any form or by any means, including electronic storage retrieval systems, except by explicit, prior written permission of the publisher, except for brief passages excerpted for review and critical purposes.

Manufactured in the United States of America.

ISBN 978-1-61399-064-3

11 12 13 14 15 16 / 10 9 8 7 6 5 4 3 2 1

Society of Petroleum Engineers
222 Palisades Creek Drive
Richardson, TX 75080-2040 USA

http://store.spe.org/
books@spe.org
1.972.952.9393

The purpose of this collection of papers is to introduce the subject of artificial intelligence and data mining to engineers interested in gaining a basic overview of the technology and its applications. It is intended not to offer a comprehensive look at the topic but, rather, to provide the reader with enough knowledge to allow for more advanced study or work in the field.

Foreword

The application of artificial intelligence and data mining (AI&DM) in the petroleum industry dates back to the late 1980s; at the time, artificial intelligence was a new technology and was called by other names (this is true even today) such as soft computing, virtual intelligence, and computational intelligence, among others. Artificial intelligence may be defined as a collection of complementary technologies that imitate life to solve complex nonlinear and dynamic problems. AI&DM presents a new set of solutions outside of the toolbox traditionally available to and used by engineers and scientists in the exploration and production industry. Successful usage of these tools requires a new way of looking at problems because first principle physics is not used as the key to unlock the problem; rather, fundamental principles play the role of the gatekeeper to ensure that any new solutions developed make physical sense. This is because when AI&DM is used to solve problems, the main source of information is data.

Unfortunately, this characteristic of AI&DM has created some confusion such that AI&DM is sometimes thought of as a type of statistical analysis; because statistics (and geostatistics, in some cases) has been around for a long time, this confusion has obstructed the realization of the novelty and the potential offered by AI&DM. Today, with the aid of AI&DM and without directly using the principles of physics, we can build reliable, data-driven predictive models that honor physics. In contrast to statistics, where predefined patterns (parametric models) are used to build models, AI&DM tools and techniques are not constrained to any predefined functional definitions.

AI&DM provides an *inductive* approach to problem solving that encourages learning by following intuitive pathways from general to specific. In contrast, the common *deductive* approach guides learning from specifics to general. In other words, instead of paying exclusive attention to the details as an Aristotelian approach to the truth, AI&DM provides the alternative of "the big picture," or the Platonic approach to the truth. Therefore, instead of using preconceived/predefined models to characterize patterns in data (i.e., decline-curve analysis in the petroleum industry), AI&DM explores and discovers existing patterns in data, regardless of how complex or invisible they may seem at first glance. AI&DM's objective is to mimic the most powerful pattern recognition engine in the universe – the human brain.

AI&DM has been used as a problem-solving tool in two different fashions, both of which are represented in the collection of SPE papers presented here. The most common use of AI&DM has been as a function approximator whereby the problem is defined as an input/output system. In this instance, the AI&DM tools are used to build models that predict the output based on a given set of input parameters. In the opinion of the authors, the least common approach, which is also more challenging and potentially game-changing, is the use of AI&DM's pattern-recognition capabilities for developing novel workflows. These workflows can only be conceived because of the potential of this powerful technology. In the following paragraphs, two workflows based on the pattern-recognition power of AI&DM are provided as specific examples.

Smart Fields and the Surrogate Reservoir Model (SRM). Given the state of the oil and gas industry, one of the most appropriate applications of this technology is in smart fields. Without using AI&DM, there are major limitations to make important use of the high-frequency data streams available in many of today's fields and wells. The questions commonly addressed by engineers and scientists are as follows:

- What kind of information about the state of the well and the reservoir can be extracted from high-frequency data coming from individual wells?
- How can this large amount of data be used in order to:
  - Proactively manage the wells?
  - Identify if a well will need intervention?
  - Learn about the compartmentalization in the reservoir?
  - Learn about reservoir heterogeneity away from the well?
  - History match the reservoir simulation models in real time?
  - Manage the reservoir in real time?

Addressing these issues makes real-time reservoir management (RTRM) a possibility. One of the solutions that has the potential of making RTRM a reality is a new utilization of AI&DM in reservoir simulation and modeling, namely surrogate reservoir models (SRMs).

SRM is developed using state-of-the-art capabilities in AI&DM. An SRM is an accurate replica of a complex reservoir-simulation model that may include tens or hundreds of wells and millions of gridblocks. SRM output includes pressure and production profiles and/or pressure and saturation distribution throughout the reservoir. Generally, SRMs are developed using a unique series of data-generation, processing, compilation, and management techniques that are designed to take maximum advantage of integration of artificial neural network characteristics and fuzzy set theory. Upon completion of the modeling and validation process, an SRM can accurately replicate the results generated by highly sophisticated reservoir-simulation models in response to changes made to the model input.

The fact that thousands of SRM runs can be performed in seconds makes uncertainty analysis a practical task. This allows the uncertainty band associated with any decisions to be identified quickly. SRMs have been successfully field-tested in the industry in the last several years. In a recent study performed on a giant oil field in the Middle East, an SRM was developed to replicate the existing simulation model; at first, the company used a commercial simulator to develop the field model, which consisted of approximately 1 million gridblocks. On a field of this size, the computing time required for a single run of the existing simulation model is 10 hours on a cluster of 12 parallel CPUs. Upon development, training, calibration, and validation of the SRM that successfully and accurately replicated the results of the simulation model, tens of millions of SRM runs were performed in a relatively short period of time. This exercise was done to comprehensively explore the reservoir model's solution space so that a successful field-development strategy could be established.

The objective was to increase oil production from the field by relaxing the rate restriction imposed on wells. The key goal was aimed at identifying well candidates that would not suffer from high water cuts once a rate-relaxation program was initiated. The SRM had to account for and quantify the uncertainties associated with the geological model while accomplishing the target objectives. Using the SRM system output, compiled from tens of millions of runs, the 165 wells in the field were divided into five clusters on the basis of rising water-cut risk. Recommendations for rate relaxation were made for wells in Clusters 1 and 2. Furthermore, for these two clusters, it was predicted that wells would produce small amounts of water and large amounts of incremental oil over the next 25 years. On the other hand, more than 100 wells in Clusters 4 and 5 were predicted to produce large amounts of water if rate restrictions were lifted. With the completion of the study, the rate restriction was lifted from 20 wells; these wells were selected from among all the clusters to provide a representative spatial distribution of the reservoir and examine the accuracy of the SRM predictions. A look-back was conducted after approximately 2.5 years of production; wells in Clusters 1 and 2 produced large amounts of incremental oil, while water production declined. The opposite effect was observed in wells that were classified in Clusters 4 and 5, which aligns entirely with SRM predictions. Results from this study (Mohaghegh 2006; Mohaghegh et al. 2006a, 2006b), as well as other similar studies, demonstrate the robustness and accuracy of SRM technology.

Top-Down Model. A workflow that is specifically designed for brown fields using AI&DM is called top-down modeling. Top-down modeling is a new approach to reservoir simulation and modeling that is not intended to be a substitution for numerical reservoir simulation, but a complement. This new modeling workflow tends to approach the modeling of fluid flow in the porous media from a completely different perspective. Instead of using Darcy's law and finite-difference calculus to model a petroleum reservoir, the top-down model workflow integrates conventional reservoir engineering techniques such as decline-curve analysis, type-curve matching, single-well numerical history matching, volumetric reserve calculation, and recovery factor estimation with statistical measures of production to simulate fluid-flow behavior in the reservoir as a function of time and space. The exploratory power of AI&DM's pattern recognition is used to discover patterns and to build a predictive model based on spatio-temporal snapshots of the reservoir's behavior. The model is history matched similar to conventional reservoir simulation models, after which it is used in predictive mode for forecasting and decision making.

The objective of top-down modeling is to provide an independent model of the fluid flow in the reservoir that should be used in concert with the existing numerical models and other engineering tools to aid in making informed decisions. To put the concept of top-down modeling into the context of reservoir

engineering and reservoir modeling, let us define production as a function of reservoir and fluid characteristics, operational constraints, and other variables in the following formulation:

$$q = f(x_1, x_2, \dots, x_n,\ y_1, y_2, \dots, y_n,\ w_1, w_2, \dots, w_n)$$

where

$q =$ production from the reservoir
$x_1, x_2, \dots, x_n =$ reservoir and fluid characteristics
$y_1, y_2, \dots, y_n =$ operational constraints
$w_1, w_2, \dots, w_n =$ other variables
$f(x) =$ constant and predetermined functional relationship

The above equation simply states that production from a field is modeled using a functional relationship between reservoir-fluid characteristics, operational constraints (e.g., drilling new wells, injecting water, shutting some wells, changing the surface facility capacity), and other variables such as well configurations and completion techniques. This formulation is applicable for both numerical reservoir simulation and top-down modeling. In both of these modeling techniques, the intent is to model production as a function of reservoir-fluid characteristics, well characteristics, and operational constraints; the major difference between the two techniques appears in the philosophy of the state of our knowledge of the phenomenon (fluid flow in porous media) and the assumptions made during the modeling process.

Numerical reservoir simulation and modeling is a bottom-up approach. It starts with building a geological model of the reservoir that is populated with the best available petrophysical and geophysical information. Engineering fluid-flow principles are then added and solved numerically to arrive at a dynamic reservoir model. The dynamic reservoir model is calibrated using the production history of multiple wells and the history-matched model is used to strategize field development in order to improve recovery.

In numerical simulation and modeling, the functional relationships used in the above equation include the law of mass conservation, Darcy's law (Fick's law of diffusion in the cases that such formulation is required), and thermodynamics and energy conservation (if we are modeling thermal recovery). These functional relationships are believed to be true, deterministic, and unchangeable. Therefore, if the production that results from numerical simulation and modeling does not match our observation from the field, we conclude that the reservoir characteristics may not be ideally measured and interpreted and therefore must be modified to achieve the match. This is the conventional wisdom and has been the common practice during the past several decades. The validity and application of this technology is not disputed; however, it should be pointed out that this functional formulation has evolved from simple relationships in the early days of reservoir simulation (single-phase, Darcy's law) to a much more complex set of relationships. These relationships enable the modeling of more complexities in the reservoir (e.g., multiphase flow, dual-porosity formulation, compositional formulation, coupling with geomechanics and surface facilities) and are bound to evolve even further as our knowledge of these physical phenomena deepens.

Therefore, during the history matching of a numerical reservoir simulation model, because the functional relationships are constant and unchangeable (i.e., our current understanding of the physical phenomena is good enough that we do not need modification, no matter which reservoir we are modeling), the engineer concentrates on modification of reservoir characterization (such as permeability) to reach a reasonable match. Because the reservoir characterization is represented by a geocellular model developed by geoscientists and is full of interpretations and "fuzzy" values, we as engineers feel comfortable changing these numbers in order to get the match we are seeking. Please note that this approach is not being criticized but merely explained in order to emphasize its differences with top-down modeling.

Top-down modeling approaches reservoir simulation and modeling from the opposite angle by attempting to build a realization of the reservoir starting with well production behavior (history). The production history is augmented by core, log, well-test, and seismic data to increase the accuracy of the top-down model. Although not intended as a substitute for the conventional reservoir simulation, this approach to reservoir modeling can be used as an alternative to conventional reservoir simulation and modeling. In cases in which a conventional model of a reservoir already exists, top-down modeling should be considered as a complement to, rather than a competitor for, the conventional technique to provide an

independent look at the data coming from the reservoir/wells for optimum development strategy and recovery enhancement.

In top-down modeling, some of the assumptions that are made in conventional numerical modeling are modified. Instead of holding the functional relationship constant, these relationships are allowed to change, in addition to the possibility of modifying the reservoir characteristics. In other words, constant, deterministic, and nonflexible functional relationships between production and reservoir characteristics are avoided. In top-down modeling, the functional relationship that generates the observed production (actual field production) from the reservoir using the set of measured reservoir characteristics is sought through pattern-recognition technology. Of course, reservoir characteristics can also be modified if one set of reservoir characteristics (measurements) is believed to be better than the one being used. Once a set of reservoir characteristics that geoscientists are reasonably comfortable with (typically using only measured and not interpreted data, unless we have a high degree of confidence on a particular interpretation) is identified, they are not modified during the history-matching process. Instead, the functional relationships are modified until a match is attained.

References

Mohaghegh, S.D. 2006. Quantifying Uncertainties Associated With Reservoir Simulation Studies Using a Surrogate Reservoir Model. Paper SPE 102492 presented at the SPE Annual Technical Conference and Exhibition, San Antonio, Texas, USA, 24–27 September. DOI: 10.2118/102492-MS.

Mohaghegh, S.D., Modavi, A., Hafez, H.H., Haajizadeh, M., Kenawy, M., and Guruswamy, S. 2006a. Development of Surrogate Reservoir Models (SRM) for Fast-Track Analysis of Complex Reservoirs. Paper SPE 99667 presented at the SPE Intelligent Energy Conference and Exhibition, Amsterdam, 11–13 April. DOI: 10.2118/99667-MS.

Mohaghegh, S.D., Hafez, H., Gaskari, R., Haajizadeh, M., and Kenawy, M. 2006b. Uncertainty Analysis of a Giant Oil Field in the Middle East Using Surrogate Reservoir Model. Paper SPE 101474 presented at the SPE Abu Dhabi International Petroleum Exhibition and Conference, Abu Dhabi, UAE, 5–8 November. DOI: 10.2118/101474-MS.

About the Editors

Shahab D. Mohaghegh is a professor of petroleum and natural gas engineering at West Virginia University and founder and president of Intelligent Solutions, Inc. With more than 18 years of experience, Mohaghegh has pioneered the application of artificial intelligence and data mining in the exploration and production industry, applying hybrid forms of neural networks, genetic algorithms and fuzzy logic to smart wells, smart completions, and smart fields as well as to drilling, completion, well stimulation, formation evaluation, reservoir characterization, reservoir simulation and reservoir management. He has published more than 100 technical papers and has been a technical reviewer for various SPE journals and other petroleum-related publications. He co-chaired the first SPE Forum Series on Artificial Intelligence in 2009 and served as an SPE Distinguished Lecturer for 2007–2008. Mohaghegh was appointed by the U.S. Secretary of Energy (in two different administrations) to serve on the Department of Energy's Unconventional Resources Advisory Committee as a subject matter expert. He holds BS and MS degrees in natural gas engineering from Texas A&I University and a PhD degree in petroleum and natural gas engineering from Pennsylvania State University.

Saud M. Al-Fattah is currently Director of Energy Markets, Policy and Strategic Research at the King Abdullah Petroleum Studies and Research Center (KAPSARC). Al-Fattah is a Saudi Aramco loanee to KAPSARC and has more than 25 years of experience working in various departments in Saudi Aramco, including Southern Area reservoir management, production and facilities development, petroleum engineering applications services, and corporate planning. His areas of specialty include reservoir engineering, energy economics, artificial intelligence, and operations research. Al-Fattah has published several technical papers in peer-reviewed journals; he is a technical editor for *SPE Reservoir Evaluation & Engineering* and several other industry publications. He holds BS and MS degrees (with honors) in

petroleum engineering from King Fahd University of Petroleum and Minerals and a PhD degree (with distinction) in petroleum engineering from Texas A&M University. Al-Fattah is currently enrolled in the Executive MBA degree program at Prince Mohammed University (PMU), Al-Khobar, Saudi Arabia.

Andrei S. Popa is the *i-field* Reservoir Management Supervisor for Chevron's San Joaquin Valley Business Unit. Prior to joining Chevron in 2002, he completed a reservoir engineer assignment with Petrom Romanian National Oil Company and a research associate assignment at West Virginia University. Since joining Chevron, Popa has completed multiple assignments including production and reservoir engineer, special projects lead engineer, artificial intelligence engineer, and subsurface team lead. He has more than 13 years of experience applying artificial intelligence technologies to complex optimization problems in the energy industry and has written or co-written more than two dozen papers on the subject. Popa holds a BS degree from the University of Ploiesti, Romania and MS and PhD degrees from West Virginia University, all in petroleum and natural gas engineering. He is a Technical Editor for *SPE Reservoir Evaluation & Engineering* and *SPE Economics & Management* and served as Chair of SPE's San Joaquin Valley Section in 2007–2008.

Contents

Mohaghegh, S.D. 2000. Virtual-Intelligence Applications in Petroleum Engineering: Part 1—Artificial Neural Networks. *J Pet Technol* **52** (9): 64–73. SPE-58046-MS. DOI: 10.2118/58046-MS.

Mohaghegh, S.D. 2000. Virtual-Intelligence Applications in Petroleum Engineering: Part 2—Evolutionary Computing. *J Pet Technol* **52** (10): 40–46. SPE-61925-MS. DOI: 10.2118/61925-MS.

Mohaghegh, S.D. 2000. Virtual-Intelligence Applications in Petroleum Engineering: Part 3—Fuzzy Logic. *J Pet Technol* **52** (11): 40–46. SPE-62415-MS. DOI: 10.2118/62415-MS.

Al-Kaabi, A.U. and Lee, W.J. 1993. Using Artificial Neural Networks To Identify the Well Test Interpretation Model (includes associated papers 28151 and 28165). *SPE Form Eval* **8** (3): 233–240. SPE-20332-PA. DOI: 10.2118/20332-PA.

Nitters, G., Davies, D.R., and Epping, W.J.M. 1995. Discriminant Analysis and Neural Nets: Valuable Tools To Optimize Completion Practices. *SPE Drill & Compl* **10** (2): 127–133. SPE-21699-PA. DOI: 10.2118/21699-PA.

Xiong, H. and Holditch, S.A. 1995. An Investigation Into the Application of Fuzzy Logic to Well Stimulation Treatment Design. *SPE Comp App* **1** (4): 18–24. SPE-27672-PA. DOI: 10.2118/27672-PA.

Boomer, R.J. 1995. Predicting Production Using a Neural Network (Artificial Intelligence Beats Human Intelligence). Paper SPE 30202 presented at the SPE Petroleum Computer Conference, Houston, 11–14 June. DOI: 10.2118/30202-MS.

Panda, M.N., Zaucha, D.E., Perez, G., and Chopra, A.K. 1996. Application of Neural Networks to Modeling Fluid Contacts in Prudhoe Bay. *SPE J.* **1** (3): 303–312. SPE-30600-PA. DOI: 10.2118/30600-PA.

Mohaghegh, S.D., McVey, D., Aminian, K., and Ameri, S. 1996. Predicting Well-Stimulation Results in a Gas-Storage Field in the Absence of Reservoir Data With Neural Networks. *SPE Res Eng* **11** (4): 268–272. SPE-31159-PA. DOI: 10.2118/31159-PA.

Mohaghegh, S.D., Platon, V., and Ameri, S. 1996. Candidate Selection for Stimulation of Gas Storage Wells Using Available Data With Neural Networks and Genetic Algorithms. Paper SPE 51080 presented at the SPE Eastern Regional Meeting, Pittsburgh, Pennsylvania, USA, 9–11 November. DOI: 10.2118/51080-MS.

Gharbi, R.B.C. and Elsharkawy, M. 1999. Neural Network Model for Estimating the PVT Properties of Middle East Crude Oils. *SPE Res Eval & Eng* **2** (3): 255–265. SPE-56850-PA. DOI: 10.2118/56850-PA.

Mohaghegh, S.D., Popa, A., and Ameri, S. 1999. Intelligent Systems Can Design Optimum Fracturing Jobs. Paper SPE 57433 presented at the SPE Eastern Regional Conference and Exhibition, Charleston, West Virginia, USA, 21–22 October. DOI: 10.2118/57433-MS.

He, Z., Yang, L., Yen, J., and Wu, C. 2001. Neural-Network Approach To Predict Well Performance Using Available Field Data. Paper SPE 68801 presented at the SPE Western Regional Meeting, Bakersfield, California, USA, 26–30 March. DOI: 10.2118/68801-MS.

Al-Fattah, S.M. and Startzman, R.A. 2003. Neural Network Approach Predicts U.S. Natural Gas Production. *SPE Prod & Fac* **18** (2): 84–91. SPE-82411-PA. DOI: 10.2118/82411-PA.

Alimonti, C. and Falcone, G. 2004. Integration of Multiphase Flowmetering, Neural Networks, and Fuzzy Logic in Field Performance Monitoring. *SPE Prod & Fac* **19** (1): 25–32. SPE-87629-PA. DOI: 10.2118/87629-PA.

Mohaghegh, S.D. 2005. Recent Developments in Application of Artificial Intelligence in Petroleum Engineering. *J Pet Technol* **57** (4): 86–91. SPE-89033-MS. DOI: 10.2118/89033-MS.

Popa, C., Popa, A., and Cover, A. 2004. Zonal Allocation and Increased Production Opportunities Using Data Mining in Kern River. Paper SPE 90266 presented at the SPE Annual Technical Conference and Exhibition, Houston, 26–29 September. DOI: 10.2118/90266-MS.

Stundner, M. and Oberwinkler, C. 2004. Self-Organizing Maps for Lithofacies Identification and Permeability Prediction. Paper 90720 presented at the SPE Annual Technical Conference and Exhibition, Houston, 26–29 September. DOI: 10.2118/90720-MS.

Patel, A., Davis, D., Guthrie, C., and Tuk, D. 2005. Optimizing Cyclic Steam Oil Production With Genetic Algorithms. Paper SPE 93906 presented at the SPE Western Regional Meeting, Irvine, California, USA, 30 March–01 April. DOI: 10.2118/93906-MS.

Mohaghegh, S.D., Gaskari, R., Popa, A., Salehi, I., and Ameri, S. 2005. Analysis of Best Hydraulic Fracturing Practices in the Golden Trend Fields of Oklahoma. Paper SPE 95942 presented at the SPE Annual Technical Conference and Exhibition, Dallas, 9–12 October. DOI: 10.2118/95942-MS.

Zangl, G., Giovannoli, M., and Stundner, M. 2006. Application of Artificial Intelligence in Gas Storage Management. Paper SPE 100133 presented at the SPE Europec/EAGE Annual Conference and Exhibition, Vienna, Austria, 12–15 June. DOI: 10.2118/100133-MS.

Saeedi, A., Camarda, K.V., and Liang, J.T. 2007. Using Neural Networks for Candidate Selection and Well-Performance Prediction in Water-Shutoff Treatments Using Polymer Gels—A Field-Case Study. *SPE Prod & Oper* **22** (4): 417–424. SPE-101028-PA. DOI: 10.2118/101028-PA.

Alajmi, M. and Ertekin, T. 2007. The Development of an Artificial Neural Network as a Pressure Transient Analysis Tool for Applications in Double-Porosity Reservoirs. Paper SPE 108604 presented at the SPE Asia Pacific Oil and Gas Conference and Exhibition, Jakarta, 30 October–1 November. DOI: 10.2118/108604-MS.

Ozbayoglu, E.M. and Ozbayoglu, M.A. 2007. Flow Pattern and Frictional-Pressure-Loss Estimation Using Neural Networks for UBD Operations. Paper SPE 108340 presented at the IADC/SPE Managed Pressure Drilling and Underbalanced Operations Conference and Exhibition, Galveston, Texas, USA, 28–29 March. DOI: 10.2118/108340-MS.

Mohaghegh, S.D., Hafez, H., Gaskari, R., Haajizadeh, M., and Kenawy, M. 2006. Uncertainty Analysis of a Giant Oil Field in the Middle East Using Surrogate Reservoir Model. Paper SPE 101474 presented at the SPE Abu Dhabi International Petroleum Exhibition and Conference, Abu Dhabi, 5–8 November. DOI: 10.2118/101474-MS.

Al-Fattah, S.M. and Al-Naim, H.A. 2009. Artificial-Intelligence Technology Predicts Relative Permeability of Giant Carbonate Reservoirs. *SPE Res Eval & Eng* **12** (1): 96–103. SPE-109018-PA. DOI: 10.2118/109018-PA.

Popa, A., Popa, C., Malamma, M., and Hicks, J. 2008. Case-Based Reasoning Approach for Well Failure Diagnostics and Planning. Paper SPE 114229 presented at the SPE Western Regional and Pacific Section AAPG Joint Meeting, Bakersfield, California, USA, 29 March–2 April. DOI: 10.2118/114229-MS.

Gomez, Y., Khazaeni, Y., Mohaghegh, S.D., and Gaskari, R. 2009. Top Down Intelligent Reservoir Modeling. Paper SPE 124204 presented at the SPE Annual Technical Conference and Exhibition, New Orleans, 4–7 October. DOI: 10.2118/124204-MS.

Kalantari-Dahaghi, A., Mohaghegh, S.D., and Khazaeni, Y. 2010. New Insight into Integrated Reservoir Management using Top-Down, Intelligent Reservoir Modeling Technique; Application to a Giant and Complex Oil Field in the Middle East. Paper SPE 132621 presented at the SPE Western Regional Meeting, Anaheim, California, USA, 27–29 May. DOI: 10.2118/132621-MS.

Virtual-Intelligence Applications in Petroleum Engineering: Part 1—Artificial Neural Networks

Shahab Mohaghegh, SPE, West Virginia U.

This is the first article of a three-article series on virtual intelligence and its applications in petroleum and natural gas engineering. In addition to discussing artificial neural networks, the series covers evolutionary programming and fuzzy logic. Intelligent hybrid systems that incorporate an integration of two or more of these paradigms and their application in the oil and gas industry are also discussed in these articles. The intended audience is the petroleum professional who is not quite familiar with virtual intelligence but would like to know more about the technology and its potential. Those with a prior understanding of and experience with the technology should also find the articles useful and informative.

Background and Definitions

This section covers some historical background of the technology, provides definitions of virtual intelligence and artificial neural networks, and offers more general information on the nature and mechanism of the artificial neural network and its relation to biological neural networks.

Virtual intelligence has been referred to by different names. Among these are artificial intelligence, computational intelligence, and soft computing. There seems to be no uniformly acceptable name for this collection of analytic tools among the researchers and practitioners of the technology. Of these, artificial intelligence is used the least as an umbrella term because artificial intelligence has historically referred to rule-based expert systems and today is used synonymously with expert systems. Expert systems made many promises of delivering intelligent computers and programs but did not fulfill these promises. Many believe that soft computing is the most appropriate term to use and that virtual intelligence is a subset of soft computing. While this argument has merit, we use the term virtual intelligence throughout these articles.

Virtual intelligence may be defined as a collection of new analytic tools that attempts to imitate life. [1] Virtual-intelligence techniques exhibit an ability to learn and deal with new situations. Artificial neural networks, evolutionary programming, and fuzzy logic are among the paradigms that are classified as virtual intelligence. These techniques possess one or more attributes of "reason," such as generalization, discovery, association, and abstraction. [2] In the last decade, virtual intelligence has matured to a set of analytic tools that facilitates solving problems that were previously difficult or impossible to solve. The trend now seems to be integration of these tools with each other as well as with conventional tools, such as statistical analysis, to

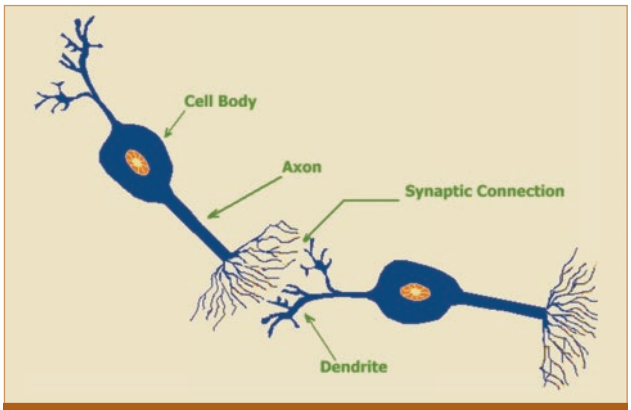

Fig. 1—Two bipolar neurons.

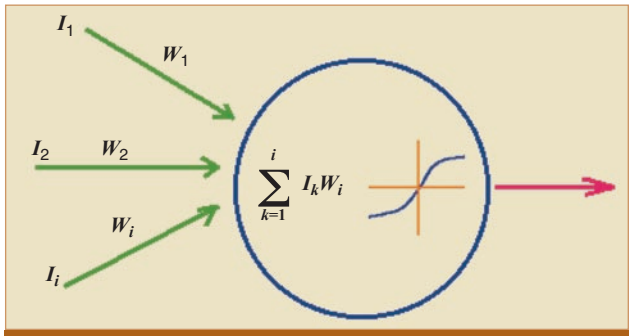

Fig. 2—Artificial neuron or a processing element.

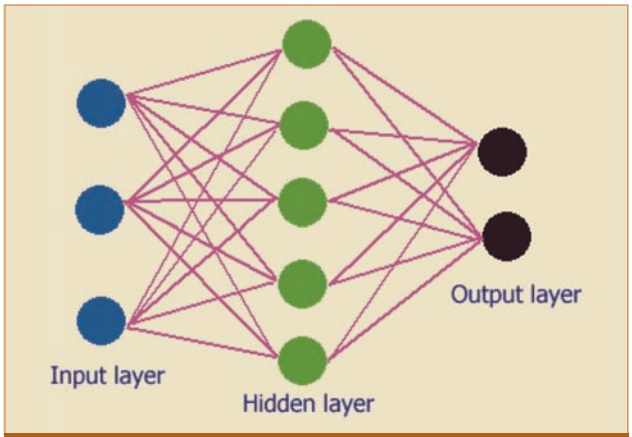

Fig. 3—Three-layer neuron network.

Copyright 2000 Society of Petroleum Engineers

This is paper SPE 58046. **Distinguished Author Series** articles are general, descriptive representations that summarize the state of the art in an area of technology by describing recent developments for readers who are not specialists in the topics discussed. Written by individuals recognized as experts in the area, these articles provide key references to more definitive work and present specific details only to illustrate the technology. **Purpose:** to inform the general readership of recent advances in various areas of petroleum engineering.

build sophisticated systems that can solve challenging problems. These tools are now used in many different disciplines and have found their way into commer cial products. Virtual intelligence is used in such ar eas as medical diagnosis, credit-card-fraud detection, bank-loan approval, smart household appliances, subway systems, automatic transmissions, financial-portfolio management, and robot-navigation systems among many others. In the oil and gas industry, these tools have been used to solve pr oblems related to pressure-transient analysis, well-log interpr etation, reservoir characterization, candidate-well selection for stimulation, and other such areas.

Short History of Neural Networks

Neural-network research can be traced back to a 1943 paper by McCulloch and Pitts.[3] In 1957, Rosenblatt[4] invented the perceptron. He proved that, given linearly separable classes, a per ceptron would, in a finite number of training trials, develop a weight vector that separates the classes (a pattern-classification task). He also showed that the starting value of the weights does not affect his proof. At approximately the same time, Widrow[5] developed a similar network called adeline. Minskey and Paper t[6] pointed out that the perceptron theorem obviously applies to those problems that the structure is capable of computing. They showed that elementary calculation, such as simple "exclusive or" problems, cannot be solved by single-layer perceptrons.

Rosenblatt[4] also studied structures with more layers and believed that they could overcome the limitations of simple perceptrons. However, no learning algorithm was known that could determine the weights necessary to implement a given calculation. Minskey and Papert[6] doubted that one could be found and recommended that other appr oaches to artificial intelligence should be pursued. Following this discussion, most of the computer science community left the neural-network paradigm for 20 years.[7] In the early 1980's, Hopfield[8] revived neural-network research. His efforts coincided with development of new learning algorithms, such as backpropagation. The growth of neural-network research and applications has been phenomenal since this revival.

Structure of a Neural Network

An artificial neural network is an information-processing system that has certain performance characteristics in common with biological neural networks. Therefore, we briefly describe a biological neural network before offering a detailed definition of artificial neural networks. All living organisms are made up of cells. The basic building blocks of the nervous system are nerve cells called neurons. **Fig. 1** is a schematic diagram of two bipolar neurons.

A typical neuron contains a cell body (where the nucleus is located), dendrites, and an axon. Information in the form of a train of electrochemical pulses (signals) enters the cell body from the dendrites. Depending on the nature of this input, the neuron activates in an excitatory or inhibitory fashion and provides an output that travels through the axon and connects to other neurons, where it becomes the input to the receiving neuron. The point between two neurons in a neural pathway, where the ter-

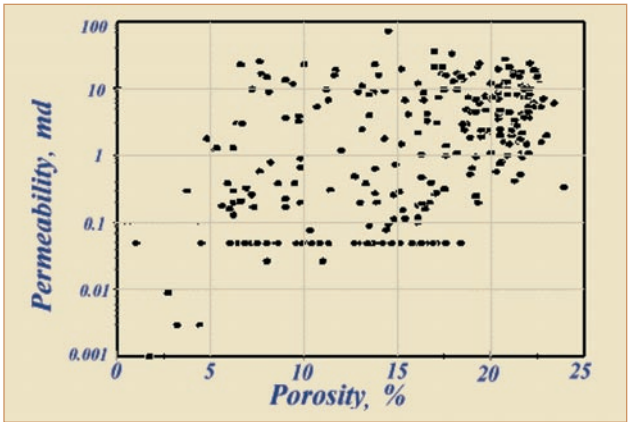

Fig. 4—Porosity and permeability crossplot for Big Injun formation.

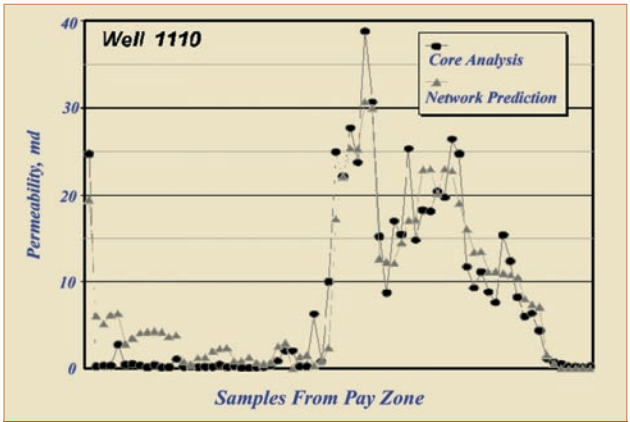

Fig. 5—Core and network permeability for Well 1110 in Big Injun formation.

mination of the axon of one neuron comes into close proximity with the cell body or dendrites of another, is called a synapse. The signals traveling from the first neuron initiate a train of electrochemical pulse (signals) in the second neuron.

It is estimated that the human brain contains on the order of 10 to 500 billion neurons.[9] These neurons are divided into modules, and each module contains approximately 500 neural networks.[10] Each network may contain approximately 100,000 neurons, where each neuron is connected to hundreds to thousands of other neurons. This architecture is the main driving force behind the complex behavior that comes to us so naturally. Simple tasks, such as catching a ball, drinking a glass of water, or walking in a crowded market, require so many complex and coordinated calculations that sophisticated computers are unable to perform them, but humans can do them routinely without a moment of thought. This becomes even more interesting when one realizes that neurons in the human brain have a cycle time of approximately 10 to 100 milliseconds, while the cycle time of a typical desktop computer chip is measured in nanoseconds. The human brain, although a million times slower than common desktop PCs, can perform many tasks at speeds that are orders of magnitude faster than computers because of its massively parallel architecture.

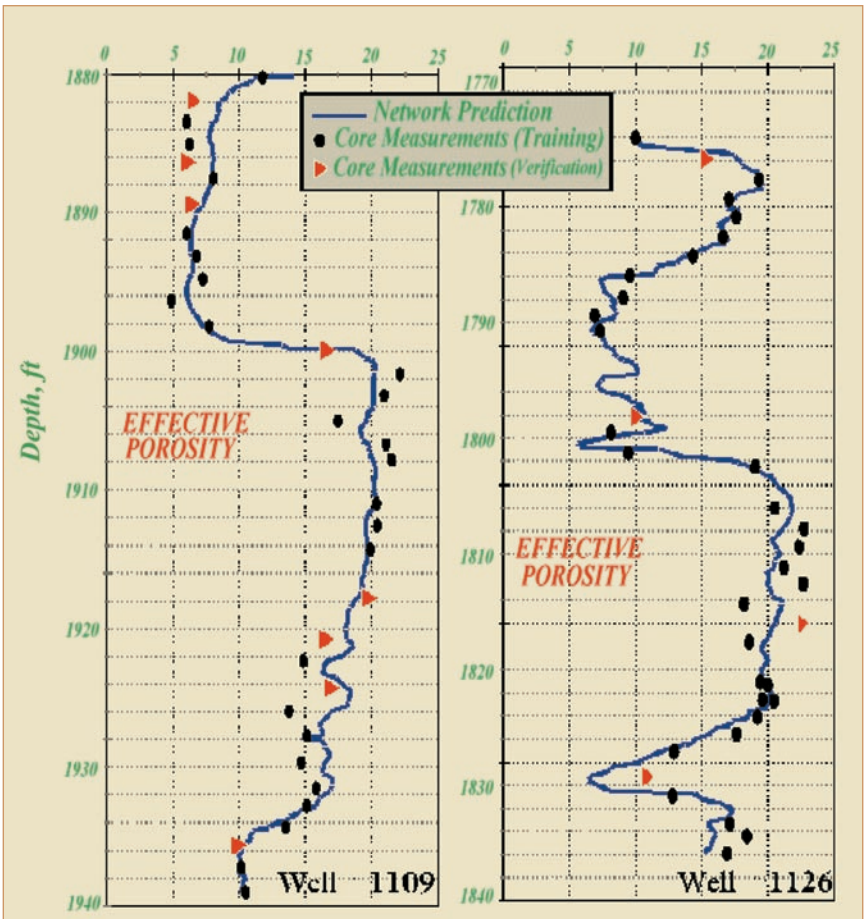

Fig. 6—Core and network effective porosity for Wells 1109 and 1126 in Big Injun formation.

Artificial neural networks are information-processing systems that are a rough approximation and simplified simulation of this biological process and have performance characteristics similar to those of biological neural networks. They have been developed as generalizations of mathematical models of human cognition or neural biology on the basis of the following assumptions.

1. Information processing occurs in many simple elements that are called neurons (processing elements).
2. Signals are passed between neurons over connecting links.
3. Each connecting link has an associated weight, which, in a typical neural network, multiplies the signal being transmitted.
4. Each neuron applies an activation function (usually nonlinear) to its net input to determine its output signal.[11]

Fig. 2 is a schematic diagram of a typical neuron (processing element)

in an artificial neural network. Output from other neurons is multiplied by the weight of the connection and enters the neuron as input; therefore, an artificial neuron has many inputs and only one output. The inputs are summed and subsequently applied to the activation function, and the result is the output of the neuron.

Mechanics of Neural-Network Operation

An artificial neural network is a collection of neurons that are arranged in specific formations. Neurons are grouped into layers. A multilayer network usually consists of an input layer, one or more hidden layers, and an output layer. The number of neurons in the input layer corresponds to the number of parameters that are being presented to the network as input. The same is true for the output layer. Note that neural-network analysis is not limited to a single output and that neural nets can be trained to build neuromodels with multiple outputs. The neurons in the hidden layer or layers are responsible primarily for feature extraction. They provide increased dimensionality and accommodate such tasks as classification and pattern recognition. **Fig. 3** is a schematic diagram of a fully connected, three-layer neural network.

Neural-network scientists and practitioners have classified the many kinds of neural networks that exist. One of the most popular classifications is based on training methods. Neural networks can be divided into two major categories on the basis of training methods: supervised and unsupervised. Unsupervised neural networks, also known as self-organizing maps, are mainly clustering and classification algorithms. They have been used in the oil and gas industry to interpret well logs and to identify lithology. They are called unsupervised because no feedback is provided to the network. The network is asked to classify the input vectors into groups and clusters. This requires a certain degree of redundancy in the input data; hence, the notion that redundancy is knowledge.[12]

Most neural-network applications in the oil and gas industry are based on supervised training algorithms. During a supervised training process, both input and output are presented to the network to permit learning on a feedback basis.

In a typical neural data-processing procedure, the database is divided into three separate portions called training, calibration, and verification sets. The training set is used to develop the desired network. In this process (depending on the paradigm used), the desired output in the training set is used to help the network adjust the weights between its neurons or processing elements. During the training process, the question of when to stop the training arises. How many times should the network go through the data in the training set to learn the system behavior? When should the training stop? These are legitimate questions because a network can be overtrained. In the neural-network-related literature, overtraining is also referred to as memorization. Once the network memorizes a data set, it is incapable of generalization even though it fits the training data set very accurately. Overtraining does not apply to neural-network paradigms simply because they are are trained with an iterative process. Memorization and overtraining are applicable to those networks that are historically among the most popular for engineering problem solving. These include

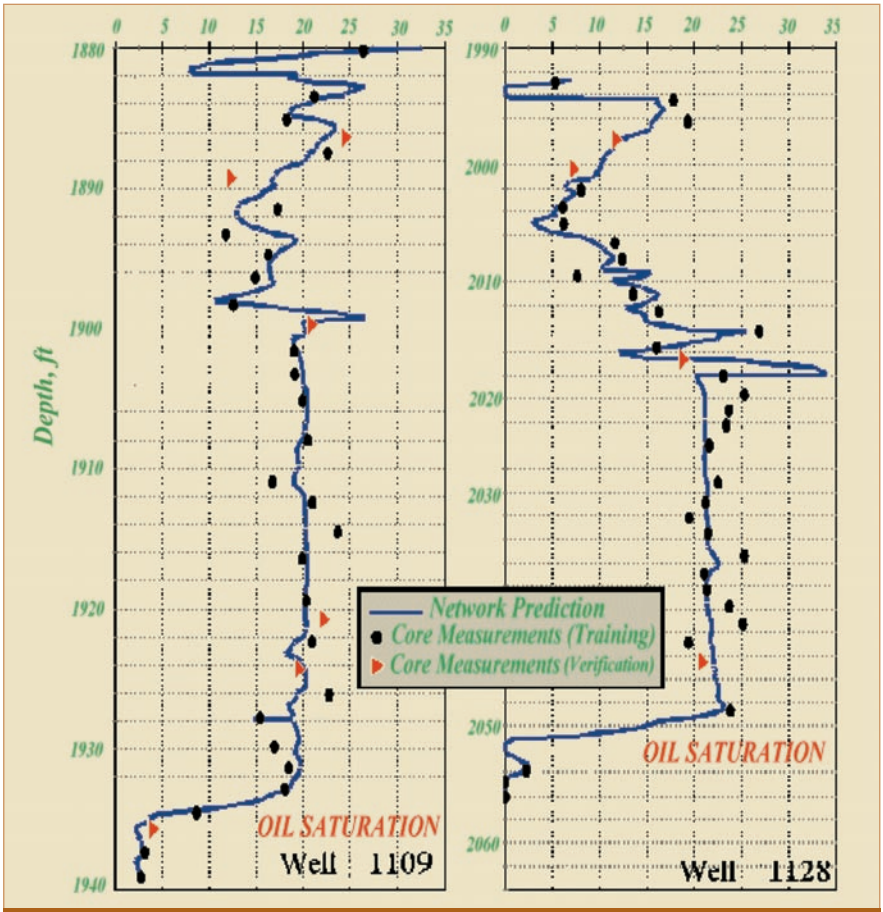

Fig. 7—Core and network oil saturation for W ells 1109 and 1128 in Big Injun formation.

backpropagation networks that use an iterative process during training.

Mathematically, we could look at the inputs and the weights on the inputs as vectors, such as $I_1, I_2 \ldots I_n$ for inputs and $W_1, W_2 \ldots W_n$ for weights. The total input signal is the dot, or inner , product of the two vectors. Geometrically, the inner product of two vectors can be considered a measure of their similarity. The inner pr oduct is at its maximum if the vectors point in the same dir ection. If the vectors point in opposite directions (180°), their inner pr oduct is at its minimum. Signals coming into a neuron can be positive (excitatory) or negative (inhibitory). T raining is accomplished by modification of the weights until conver gence is reached. The ability to change the weights allows the network to modify its behavior in r esponse to its inputs (or in other words, learn). In the backpr opagation algorithm (one of the most commonly used supervised training algorithms), network output is compared with the desir ed output—which is part of the training data set—and the difference (error) is propagated backward through the network. During this backpropagation of error, the weights of the connections between neur ons are adjusted. This pr ocess is continued in an iterative manner . The network converges when its output is within acceptable pr oximity of the desired output.

TABLE 1—RESULTS OF VIRTUAL MR LOGS FOR FOUR U.S. WELLS

Well Location	MR Log	Data Set	Correlation Coefficient
East Texas	Porosity	Verification	0.941
		Entire well	0.967
	Irreducible water	Verification	0.853
		Entire well	0.894
	Permeability	Verification	0.966
		Entire well	0.967
Utah	Porosity	Verification	0.800
		Entire well	0.831
	Irreducible water	Verification	0.887
		Entire well	0.914
	Permeability	Verification	0.952
		Entire well	0.963
Gulf of Mexico	Porosity	Verification	0.853
		Entire well	0.893
	Irreducible water	Verification	0.930
		Entire well	0.940
	Permeability	Verification	0.945
		Entire well	0.947
New Mexico	Porosity	Verification	0.957
		Entire well	0.960
	Irreducible water	Verification	0.884
		Entire well	0.926

Applications in the Oil and Gas Industry

Common sense indicates that, if a pr oblem can be solved with conventional methods, neural networks (or any other virtual-intelligence technique) should not be used to solve it. For example, balancing your checkbook with a neural network is not recommended. Although there is academic value to solving simple problems, such as polynomials and differential equations, with neural networks to show their capabilities, they should be used mainly to solve problems that otherwise are very time-consuming or simply impossible to solve by conventional methods.

Neural networks have shown gr eat potential for generating accurate analysis and r esults from large historical databases, the kind of data that engineers may not consider valuable or r elevant in conventional modeling and

TABLE 2—RECOVERABLE-RESERVE CALCULATIONS WITH ACTUAL AND VIRTUAL MR LOGS

Well Location	MR Type	Reserve (MMscf/Acre)	Difference (%)
Texas	Actual	414.58	−1.57
	Virtual	407.95	
New Mexico	Actual	192.73	−1.91
	Virtual	189.05	
Gulf of Mexico	Actual	1,904.93	+0.30
	Virtual	1,910.70	
Utah	Actual	1,364.07	−1.81
	Virtual	1,339.56	

analysis processes. Neural networks should be used in cases where mathematical modeling is not a practical option. This may be because all the parameters involved in a particular process are not known and/or the interrelation of the parameters is too complicated for mathematical modeling of the system. In such cases, a neural network can be constructed to observe the system behavior (what type of output is produced as a result of certain set of inputs) and try to mimic its functionality and behavior. In the next section, we present some examples of applying artificial neural networks to petroleum-engineering-related problems.

Reservoir Characterization

Neural networks have been used to predict or virtually measure formation characteristics, such as porosity, permeability and fluid saturation, from conventional well logs.[13,14] With well logs as input data coupled with core analysis of the corresponding depth, these reservoir characteristics were successfully predicted for a heterogeneous formation in West Virginia. Since the early 1960's, many attempts have been made to correlate permeability with core porosity and/or well logs by use of mathematical or statistical functions.[15] It has been shown that a carefully orchestrated neural-network analysis is capable of providing more accurate and repeatable results compared with previously used methods.[16]

Fig. 4 is a crossplot of porosity vs. permeability for the Big Injun formation in West Virginia. It is obvious that no apparent correlation exists between porosity and permeability in this formation. The scatter of this plot arises mainly from the complex and heterogeneous nature of this reservoir.

Well logs provide a wealth of information about the rock but fall short in measurement and calculation of its permeability. Dependencies of rock permeability on parameters that can be measured by well logs have remained one of the fundamental research areas in petroleum engineering. Using the conventional computing tools available, scientists have not been able to prove that a certain functional relationship exists that can explain the relationships in a rigorous and universal manner. Our opinion is that, if such dependency or functional relation exists, an artificial neural network is the tool to find it.

With geophysical well log data as input (bulk density, gamma ray, and induction logs), a neural network was trained to predict formation permeability measured from laboratory core analyses. Log and core permeability data were available from four wells. The network was trained with the data from three wells and attempted to predict the measurements from the fourth well. This practice was repeated twice, each time with a different well as the verification well. **Fig. 5** shows the result of neural-network prediction compared with the actual laboratory measurements. Note that the well logs and core measurements from the test well were not used during the training process.

In a similar process, well logs were used to predict (virtually measure) effective porosity and oil saturation in this formation. **Figs. 6 and 7** show the results of this study. In these figures, solid lines show the neural-network predictions and the core measurements are shown by circles for core measurements used during the training process and by triangles for those never seen by the network.

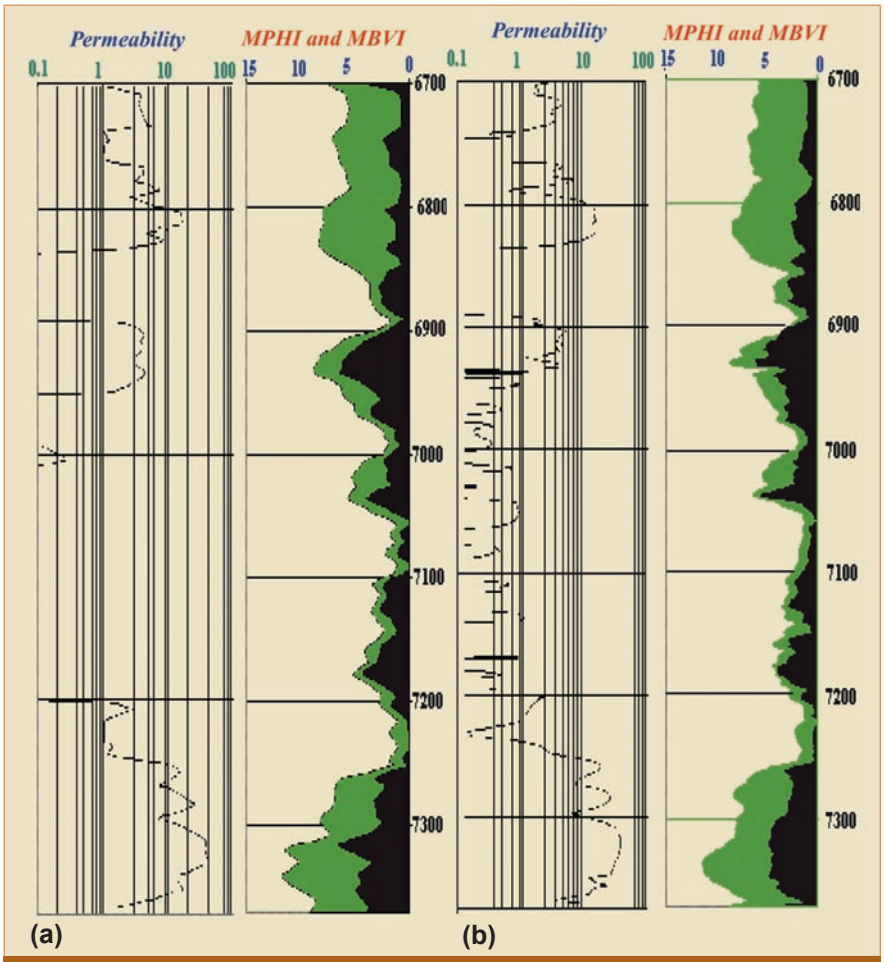

Fig. 8—(a) Actual and (b) virtual MR log results for the east Texas well; MPHI=magnetic porosity and MVBVI=magnetic bulk volume index= irreducible water.

Virtual MR Logs

Magnetic resonance (MR) logs are well logs that use nuclear magnetic resonance to measure free fluid, irreducible water, and effective porosity accurately. Permeability is then calculated with a mathematical function that incorporates these measured properties. MR logs can provide information that results in an increase in the recoverable reserve simply by including portions of the pay zone in the recoverable-reserve calculations that were excluded during analysis with conventional well logs. MR logs accomplish this by estimating the economically recoverable hydrocarbon (identification of a combination of water and hydrocarbon saturation as well as the reservoir permeability) that has been overlooked. A recent paper showed that neural networks have the potential to be used as an analytical tool for generation of synthetic MR logs from conventional geophysical well logs.[17] In Ref. 17, four wells from different locations in the U.S. (Utah, the Gulf of Mexico, east Texas, and New Mexico) were used to show the potential of this proposed approach. In each case, part of the well data are used to train a neural network and the remaining well data are used as verification. As Ref. 17 mentions, this method is most useful for fields with many wells where only a handful need to be logged with MR tools. These wells can be strategically placed to capture as much reservoir variation as possible. Then, a virtual MR application can be developed on the basis of these wells and applied to the rest of the wells in the field.

Table 1 shows the accuracy of this method when applied to the four wells being studied. For each well the methodology was applied to three different MR logs: namely, effective porosity, irreducible water saturation, and permeability. For each log, the table shows the correlation coefficient both for the entire well data set (training data and verification data) and for only the verification data set. The verification data set includes data that had not been seen previously by the network. The correlation coefficient of this method ranges from 0.80 to 0.97. As expected, the correlation coefficient for the entire well data set is better than that of the verification data set. This is because the training data set is included in the entire well data set and the correlation coefficient for the training data is usually higher than that for the verification data set.

MR logs are also used to provide a more realistic estimate of recoverable reserve compared with that from conventional well logs. **Table 2** shows the recoverable reserve calculated with actual and virtual MR logs. Recoverable-reserve calculations based on virtual MR logs are quite close to those of actual MR logs because a certain degree of averaging takes place during the reserve calculation that compensates for some of the inaccuracies associated with virtual MR logs. As Table 2 shows, in all four cases, recoverable reserves calculated with virtual MR logs are within 2% of those calculated with actual MR logs. In the case of the Gulf of Mexico well, the difference is approximately 0.3%. Although there is not enough evidence to make definitive conclusions at this point, it seems that recoverable reserves calculated with virtual MR logs are mostly on the conservative side. **Fig. 8** compares the actual and virtual MR logs for the east Texas well.

Many more areas exist for application of neural networks in the oil and gas industry. These include field development,[18] two-phase flow in pipes,[19] identification of well-test-interpretation models,[20] completion analysis,[21] formation-damage prediction,[22] permeability prediction,[23] and fractured reservoirs.[24]

Closing Remarks

Toeffler[25] said, "The responsibility for change … lies within us. We must begin with ourselves, teaching ourselves not to close our minds prematurely to the novel, the surprising, and the seemingly radical." Virtual intelligence, in general, and artificial neural networks, specifically, have advanced substantially in the past decade. There are many everyday applications and products that use these tools to make life

easier for humankind. Historically, petroleum engineers have been among the most open-minded scientists and practitioners to embrace new technology and turn it to the task of problem solving. Neural networks seem to be one of the newest tools finding their way into the oil and gas industry as an alternative analytical method.

This technology is in its infancy and has great potential. Most neural-network application of today is conducted in the software domain. Hardware implementations have already started becoming more and more popular. The integration of neural networks with fuzzy logic and genetic programming techniques, which are covered in the next two articles, is providing ever more powerful tools. JPT

Nomenclature

i,k = indices
$I_{1,2,k,n}$ = neural-network inputs
$W_{1,2,k,n}$ = neural-net connection weights

References

1. Zaruda, J.M., Marks, R.J., and Robinson, C.J.: *Computational Intelligence, Imitating Life,* IEEE Press, Piscataway, New Jersey (1994).
2. Eberhart, R., Simpson, P., and Dobbins, R.: *Computational Intelligence PC Tools,* Academic Press, Orlando, Florida (1996).
3. McCulloch, W.S. and Pitts, W.: "A Logical Calculus of Ideas Immanent in Nervous Activity," *Bull. Mathematical Biophysics* (1943) **5,** 115.
4. Rosenblatt, F: "The Perceptron: Probabilistic Model for Information Storage and Organization in the Brain," *Psychol. Rev.* (1958) **65,** 386.
5. Widrow, B.: "Generalization and Information Storage in Networks of Adeline Neurons," *Self-Organizing Systems,* M.C. Yovitz, G.T. Jacobi, and G.D. Goldstein (eds.), Spartan Books, Washington, DC (1962) 435–61.
6. Minsky, M.L. and Papert, S.A.: *Perceptrons*, MIT Press, Cambridge, Massachusetts (1969).
7. Hertz, J., Krogh, A., and Palmer, R.G.: *Introduction to the Theory of Neural Computation,* Addison-Wesley Publishing Co., Redwood City, California (1991).
8. Hopfield, J.J.: "Neural Networks and Physical Systems With Emergent Collective Computational Abilities," *Proc.*, Natl. Academy of Science (1982) **79,** 2554.
9. Rumelhart, D.E. and McClelland, J.L.: *Parallel Distributed Processing, Exploration in the Microstructure of Cognition, Foundations,* MIT Press, Cambridge, Massachusetts (1986) **1.**
10. Stubbs, D.: "Neurocomputers," *M.D. Computing* (1988) **5,** No. 3, 14.
11. Fausett, L.: *Fundamentals of Neural Networks, Architectures, Algorithms, and Applications,* Prentice-Hall Inc., Englewood Cliffs, New Jersey (1994).
12. Barlow, H.B.: "Unsupervised learning," *Neural Computation* (1988) **1,** 295.
13. Mohaghegh, S., Arefi, R., and Ameri, S.: "Petroleum Reservoir Characterization with the Aid of Artificial Neural Networks," *J. Pet. Sci. & Eng.* (1996) **16,** 263.
14. Mohaghegh, S., Ameri, S., and Arefi, R.: "Virtual Measurement of Heterogeneous Formation Permeability Using Geophysical Well Log Responses," *Log Analyst* (March/April 1996) 32.
15. Balan, B., Mohaghegh, S., and Ameri, S.: "State-of-the-Art in Permeability Determination From Well Log Data: Part 1: A Comparative Study, Model Development," paper SPE 30978 presented at the 1995 SPE Eastern Regional Meeting, Morgantown, West Virginia, 17–21 September.
16. Mohaghegh, S., Balan, B., and Ameri, S.: "State-of-the-Art in Permeability Determination From Well Log Data: Part 2: Verifiable, Accurate Permeability Prediction, the Touchstone of All Models," paper SPE 30979 presented at the 1995 SPE Eastern Regional Meeting, Morgantown, West Virginia, 17–21 September.
17. Mohaghegh, S., Richardson, M., and Ameri, M.: "Virtual Magnetic Resonance Imaging Logs: Generation of Synthetic MRI Logs From Conventional Well Logs," paper SPE 51075 presented at the 1998 SPE Eastern Regional Meeting, Pittsburgh, Pennsylvania, 9–11 November.
18. Doraisamy, H., Ertekin, T., and Grader, A.: "Key Parameters Controlling the Performance of Neuro-Simulation Applications in Field Development," paper SPE 51079 presented at the 1998 SPE Eastern Regional Meeting, Pittsburgh, Pennsylvania, 9–11 November.
19. Ternyik, J. *et al.*: "Virtual Measurement in Pipes, Part 1: Flowing Bottomhole Pressure Under Multiphase Flow and Inclined Wellbore Conditions," paper SPE 30975 presented at the 1995 SPE Eastern Regional Meeting, Morgantown, West Virginia, 17–21 September.
20. Al-Kaabi, A-A.U. and Lee, W. J.: "Using Artificial Neural Nets To Identify the Well-Test Interpretation Model," *SPEFE* (September 1993) 233; *Trans.*, AIME, **295.**
21. Shelley, R. *et al.*: "Granite Wash Completion Optimization With the Aid of Artificial Neural Networks," paper SPE 39814 presented at the 1998 SPE Gas Technology Symposium, Calgary, 15–18 March.
22. Nikravesh, M., Kovscek, A.R., and Patzek, T.W.: "Prediction of Formation Damage During Fluid Injection Into Fractured Low-Permeability Reservoirs via Neural Networks," paper SPE 31103 presented at the 1996 SPE Formation Damage Symposium, Lafayette, Louisiana, 16–18 February.
23. Wong, P.M., Taggart, I.J., and Jian, F.X.: "A Critical Comparison of Neural Networks and Discriminant Analysis in Lithofacies, Porosity and Permeability Predictions," *J. Pet. Geol.* (1995) **18,** No. 2, 191.
24. Ouenes, A. *et al.*: "Practical Use of Neural Networks in Tight Gas Fractured Reservoirs: Application to the San Juan Basin," paper SPE 39965 presented at the 1998 SPE Rocky Mountain Regional/Low Permeability Reservoirs Symposium, Denver, Colorado, 5–8 April.
25. Toeffler, A.: *The Third Wave*, Bantam Books, New York City (December 1991).

SI Metric Conversion Factors

acre	×4.046 856	E−01 =	ha
ft	×3.048*	E−01 =	m
ft^3	×2.831 685	E−01 =	m^3
md	×9.869 233	E−04 =	μm^2

*Conversion factor is exact.

Shahab Mohaghegh *is an associate professor of petroleum and natural gas engineering at West Virginia U. in Morgantown, West Virginia. e-mail: shahab@wvu.edu. Involved in R&D of virtual intelligence techniques since 1991, he has applied the techniques successfully to petroleum engineering problems in many different areas, including drilling, completion, stimulation, formation evaluation, and reservoir evaluation. Mohaghegh holds BS and MS degrees in natural gas engineering from Texas A&I U. and a PhD degree in petroleum and natural gas engineering from Pennsylvania State U. A member of the Editorial Review Committee, he served as a Review Chairman for* **SPE Reservoir Engineering and Evaluation** *during 1997–99.*

Virtual-Intelligence Applications in Petroleum Engineering: Part 2—Evolutionary Computing

Shahab Mohaghegh, SPE, West Virginia U.

Part 1 of this series discussed artificial neural networks and provided a general definition of virtual intelligence.[1] The goal of this second article is to provide an overview of evolutionary computing, its potential combination with neural networks to produce powerful intelligent applications, and its applications in the oil and gas industry. The most successful intelligent applications incorporate several virtual-intelligence tools in a hybrid manner. Virtual-intelligence tools complement each other and are able to amplify each other's effectiveness. This article also presents the background of evolutionary computation as related to Darwinian evolution theory. This is followed by a more detailed look at genetic algorithms, the primary evolutionary-computing paradigm currently used. The article concludes by exploring application of a hybrid neural network/genetic algorithm system to a petroleum-engineering-related problem.

Background

Evolutionary computing, like other virtual-intelligence tools, has its roots in nature. It is an attempt to mimic the evolutionary process by use of computer algorithms and instructions. The question, however, is why mimic the evolutionary process. The answer becomes obvious once we realize what types of problems the evolutionary process solves and consider whether we would like to solve similar problems. Evolution is an optimization process.[2] One of the major principles of evolution is heredity. Each generation inherits the evolutionary characteristics of the previous generation and passes those same characteristics to the next generation. These characteristics include progress, growth, and development. The passing of the characteristics from generation to generation is facilitated through genes.

Since the mid-1960's, new analytical tools for intelligent optimization inspired by the Darwinian evolution theory have surfaced. The term "evolutionary computing" has been used as an umbrella for many of these tools. Evolutionary computing comprises evolutionary programming, genetic algorithms, evolution strategies, and evolution programs, among others. To many people, these tools (and names) look similar and their names appear to have the same meaning. However, the names carry quite distinct meanings to scientists who are deeply involved in this area of research.

Copyright 2000 Society of Petroleum Engineers

This is paper SPE 61925. **Distinguished Author Series** articles are general, descriptive representations that summarize the state of the art in an area of technology by describing recent developments for readers who are not specialists in the topics discussed. Written by individuals recognized as experts in the area, these articles provide key references to more definitive work and present specific details only to illustrate the technology. **Purpose:** to inform the general readership of recent advances in various areas of petroleum engineering.

Evolutionary programming, introduced by Koza,[3] is concerned primarily with solving complex problems by evolving sophisticated computer programs from simple, task-specific computer programs. Genetic algorithms, the subject of this article, are discussed in detail in the next section. In evolution strategies,[4] the components of a trial solution are viewed as behavioral traits of an individual (not as genes along a chromosome) as implemented in genetic algorithms. Evolution programs[5] combine genetic algorithms with specific data structures to achieve their goals.

Genetic Algorithms

Darwin's theory of survival of the fittest (presented in his 1859 paper titled "On the Origin of Species by Means of Natural Selection"), coupled with the selectionism of Weismann and the genetics of Mendel, have formed the universally accepted set of arguments known as the evolution theory.[4]

In nature, the evolutionary process occurs when the following four conditions are satisfied.[3]

1. An entity has the ability to reproduce.
2. There is a population of such self-reproducing entities.
3. There is some variety among the self-reproducing entities.
4. This variety is associated with some difference in ability to survive in the environment.

In nature, organisms evolve as they adapt to dynamic environments. The "fitness" of an organism is defined by the degree of its adaptation to its environment. The organism's fitness determines how long it will live and how much of a chance it has to pass its genes on to the next generation. In biological evolution, only the winners survive to continue the evolutionary process. It is assumed that, if the organism lives by adapting to its environment, it must be doing something right. The characteristics of the organisms are coded in their genes, and their genes pass these characteristics to their offspring through the process of heredity. The fitter an individual, the higher is its chance to survive and, hence, reproduce.

Intelligence and evolution are intimately connected. Intelligence has been defined as the capability of a system to adapt its behavior to meet goals in a range of environments.[4] By imitating the evolutionary process with computer instructions and algorithms, researchers try to mimic the intelligence associated with the problem-solving capabilities of the evolutionary process. As in real life, this type of continuous adaptation creates very robust organisms. The whole process continues through many "generations," with the best genes being handed down to future generations. The result typically is a very good solution to the problem. In computer simulation of the

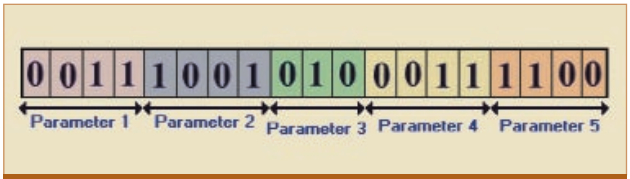

Fig. 1—Chromosome with five genes.

evolutionary process, genetic operators pass genes from generation to generation. These operators (crossover, inversion, and mutation) are the primary tools for spawning a new generation of individuals from the fit individuals of the current population. Continual cycling of these operators creates a surprisingly powerful search engine. This inherently preserves the critical balance needed with an intelligent search: the balance between exploitation (taking advantage of information already obtained) and exploration (searching new areas). Although simplistic from a biologist's viewpoint, these algorithms are sufficiently complex to provide robust and powerful search mechanisms.

Mechanism of a Genetic Algorithm

The process of genetic optimization can be divided into the following steps.

1. Generating the initial population.
2. Evaluating the fitness of each individual in the population.
3. Ranking individuals on the basis of their fitness.
4. Selecting those individuals to produce the next generation on the basis of their fitness.
5. Using genetic operations, such as crossover, inversion, and mutation, to generate a new population.
6. Continuing the process by going back to Step 2 until the problem's objectives are satisfied.

The initial population usually is generated with a random process covering the entire problem space. This ensures a wide variety in the gene pool. Each problem is encoded in the form of a chromosome. Each chromosome is a collection of a set of genes. Each set of genes represents a parameter in the problem. In classic genetic algorithms, a string of 0's and 1's or a bit string represents each set of genes (parameter). Therefore, a chromosome is a long bit string that includes all the genes (parameters) for an individual. **Fig. 1** shows a typical chromosome as an individual in a population that has five genes. Obviously, this chromosome is for a problem that has been coded to find the optimum solution with five parameters.

The fitness of each individual is determined with a fitness function. The goal of optimization usually is to find a minimum or a maximum. Examples of this include minimization of error for a problem that must converge to a target value or maximization of profit in a financial portfolio. Once the fitness of each individual in the population is evaluated, all the individuals are ranked. After ranking, parents are selected to produce the next generation of individuals. The selection process assigns a higher probability of reproduction to the highest-ranking individual, and reproduction probability is reduced with a reduction in ranking.

After the selection process is complete, genetic operators (such as crossover, inversion, and mutation) are incorpo-

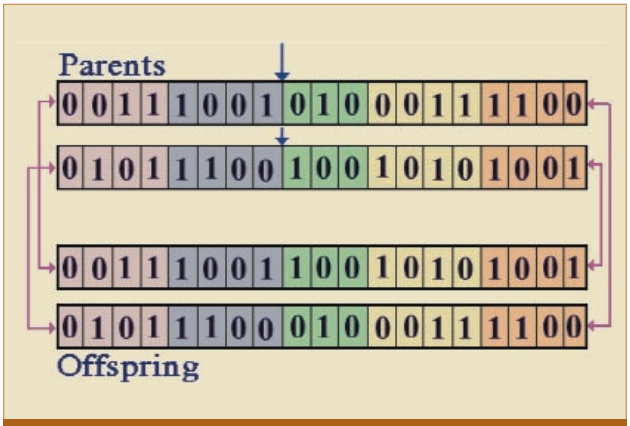

Fig. 2—Simple crossover operator.

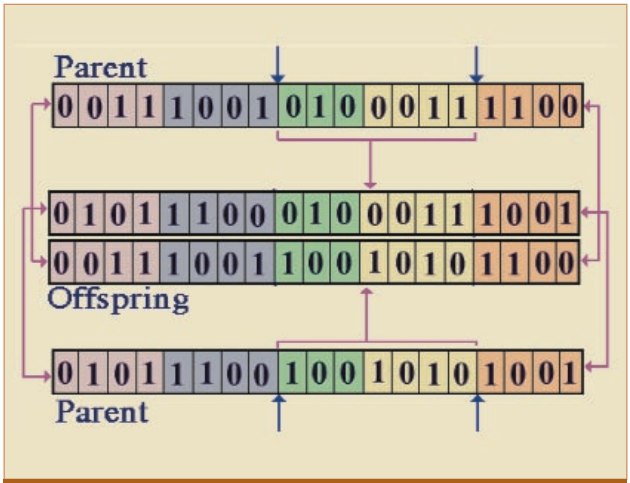

Fig. 3—Double-crossover operator.

rated to generate a new population. The evolutionary process of survival of the fittest takes place in the selection and reproduction stages. The higher the ranking of an individual, the higher the chance it has to r eproduce and pass on its gene to the next generation.

In crossover, the two parent individuals are first selected and then a break location in the chromosome is randomly identified. Both parents break at that location, and the halves switch places. This process produces two new individuals from the parents. One pair of parents may break in more than one location at different times to produce more than one pair of offspring. **Fig. 2** demonstrates the simple crossover.

Other crossover schemes exist beside simple cr ossover, such as double and random cr ossover. In double crossover, each parent breaks in two locations, and the sections are swapped. During random cr ossover, parents may break in several locations. **Fig. 3** demonstrates a double-crossover process.

As mentioned earlier, there are two other genetic operators in addition to cr ossover: inversion and mutation. In both these operators, the of fspring is reproduced from one parent rather than a pair of par ents. The inversion operator changes all the 0's to 1's and all the 1's to 0's from the parent to make the of fspring. The mutation operator chooses a random location in the bit string and changes that particular bit. The pr obability for inversion and mutation is usually lower than the pr obability for crossover. **Figs. 4 and 5** demonstrate inversion and mutation, respectively.

Once the new generation has been completed, the evaluation process with the fitness function is repeated and the steps given previously are followed. During each generation, the top-ranking individual is saved as the optimum solution to the problem. Each time a new and better individual evolves, it becomes the optimum solution. The convergence of the process can be evaluated by several criteria. If the objective is to minimize an error, then the convergence criterion can be the amount of error that the problem can tolerate. Another criterion is that convergence takes place when a new and better individual does not evolve within four to five generations. Total fitness of each generation has also been used as a convergence criterion. Total fitness of each generation can be calculated (as a sum), and the operation can stop if that value does not improve in several generations. Many applications simply use a certain number of generations as the convergence criterion.

This procedure is the classic genetic algorithm, which has many variations. For example, many classes of pr oblems would respond better to genetic optimization if a data structure other than bit strings were used. Once the data structure that best fits the pr oblem is identified, it is important to modify the genetic operators so that they accommodate the data structur e. Genetic operators ser ve specific purposes (e.g., making sure that the offspring is a combination of the par ents to satisfy the principles of heredity) that should not be undermined when the data structure is altered.

Another important issue is introduction of constraints to the algorithm. In most cases, cer tain constraints must be encoded in the process so that the generated individuals are "legal." Legality of an individual is defined as its compliance with the problem constraints. For example, in a genet-

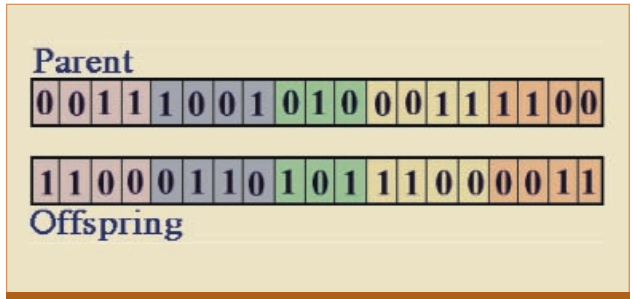

Fig. 4—Inversion operator.

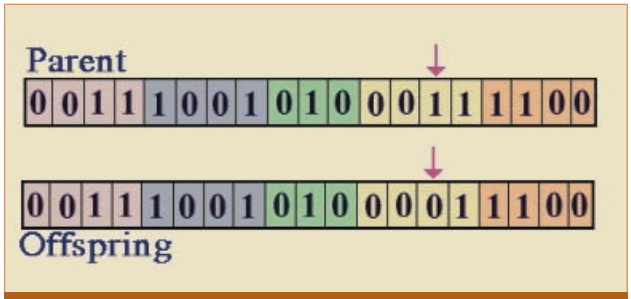

Fig. 5—Mutation operator.

ic algorithm developed for the design of new cars, basic criteria, including the fact that all four tires must be on the ground, had to be met for the design to be considered legal. Although this may seem to be quite trivial, it is the kind of knowledge that needs to be coded into an algorithm as constraints for the process to function as expected.

Application in the Petroleum Industry

There have been several applications of genetic algorithms in the petroleum and natural gas industry. Goldberg's[6] work is the first application to appear in the literature. He applied a genetic algorithm to find the optimum design for gas-transmission lines. Since then, genetic algorithms have been used in several other petroleum applications, including reservoir characterization[7] and modeling,[8] distribution of gas-lift injection,[9] petrophysics,[10] petroleum geology,[11] well-test analysis,[12] and hydraulic-fracture design.[13-15]

As mentioned earlier, virtual-intelligence techniques perform best when used to complement each other. The first hybrid neural-network/genetic-algorithm application in the oil and gas industry was used to design optimum hydraulic fractures in a gas-storage field.[13,14] The following is a brief review of the hybrid neural network/genetic algorithm.

Virtual-intelligence techniques were used to design optimum hydraulic fractures for the Clinton sand in northeast Ohio. To maintain and/or enhance deliverability of gas-storage wells in the Clinton sand, an annual restimulation program has been in place since the late 1960's. The program calls for as many as 20 hydraulic fractures and refractures per year. Several wells have been refractured three to four times, while other wells have been fractured only once in the past 30 years. Detailed reservoir engineering data were lacking for the formation. This lack of engineering data for hydraulic-fracture design and evaluation, therefore, made use of 2D or 3D hydraulic-fracture simulators impractical. As a result, prior hydraulic-fracture designs had been reduced to guesswork. In some cases, the designs depended on engineers' intuition about the formation and its potential response to different treatments; this intuitive knowledge is gained only through many years of experience with this particular field.

A wealth of relevant information, however, was found in the well files.The data set used in the study was collected from well files that included information on the design of the hydraulic fractures. The following parameters were extracted from these files for each hydraulic-fracture treatment: year the well was drilled, total number of fractures performed on the well, number of years since the last fracture, fracture fluid, amount of fluid, amount of sand used as proppant, sand concentration, acid volume, nitrogen volume, average pumping rate, and service company that performed the job. The match between hydraulic-fracture design parameters and available post-fracture deliverability data produced a data set with approximately 560 records.

The first step in the study was to develop a set of neural-network models of the hydraulic-fracturing process in the Clinton sand. These models were capable of predicting post-fracture deliverability with the input data extracted from the well files. **Fig. 6** shows the neural-network-model predictions compared with actual field results for 3 years. Data from these years were not used in the training process.

Once the neural-network-model accuracy was established, it was used as the fitness function for the genetic-

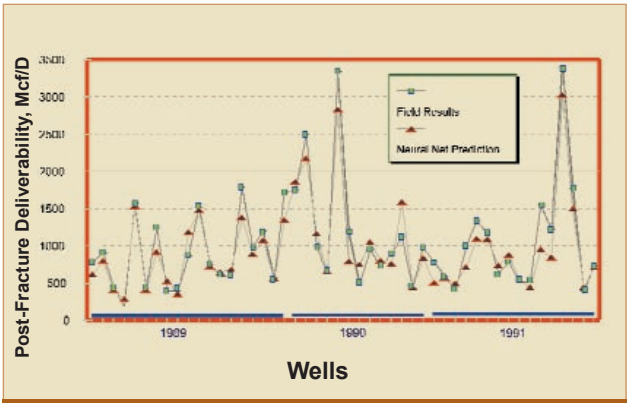

Fig. 6—Neural-network-model predictive capability in the Clinton sand.

algorithm process to form the hybrid intelligent system. The input data to the neural network can be divided into three categories: (1) basic well information; (2) well pr oduction history; and (3) hydraulic-fractur e-design parameters, such as sand concentration, rate of injection, sand mesh size, and fluid type, among others.

From these categories, only the thir d (hydraulic-fracture-design parameters) is among the contr ollable parameters. In other words, these are the parameters that can be modified for each well to achieve a better hydraulic-fracture design. A two-stage pr ocess was developed to produce the optimum hydraulic-fracture design (defined as the design that r esults in the highest possible post-fracture deliverability) for each well in the Clinton sand. **Fig. 7** is a schematic diagram of the hybrid neur o-genetic procedure.

The neural network for the first stage (Neural Module 1) is designed and trained to perform a rapid screening of the wells. This network is designed to identify so-called "dog wells," where deliverability would not be enhanced significantly even after a fracture job. This way, the genetic optimization can be concentrated on those wells that have a realistic chance of deliverability enhancement.

The second stage of the process is the genetic-optimization routine. This stage is performed on one well at a time, and its objective is to search among all possible combinations of design parameters and identify the combination of the hydraulic-fracture parameters for a specific well that results in the highest incremental post-fracture deliverability. The routine starts with the generation of 100 random solutions. Each solution is defined as a combination of hydraulic-fracture-design parameters. These solutions are then combined with other information available from the well and presented to the fitness function (neural network). The result of this process is the post-fracture deliverability for each solution. The solutions are then ranked on the basis of the highest incremental enhancement of the post-fracture deliverability. The highest-rank-

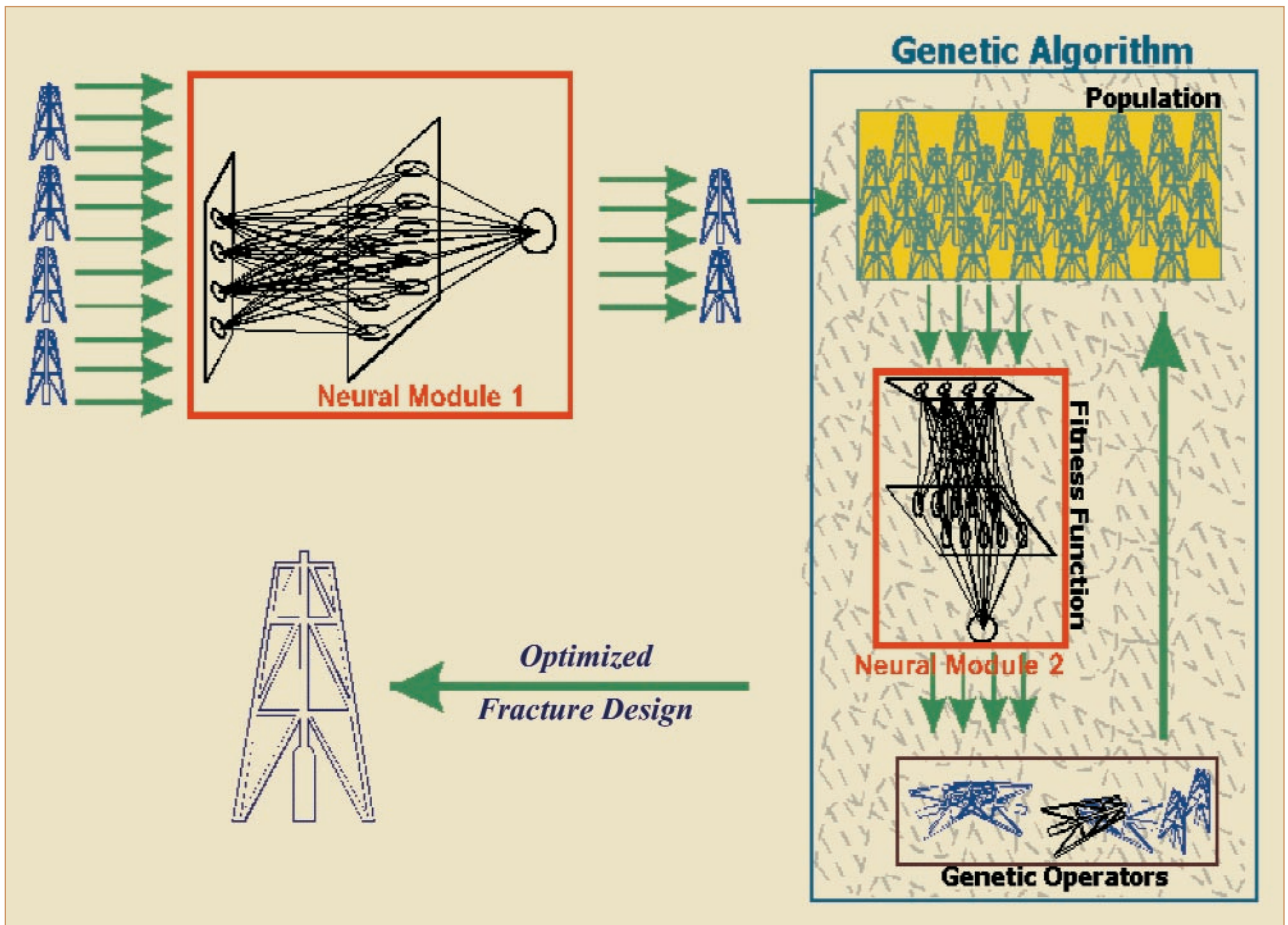

Fig. 7—Hybrid neurogenetic procedure for optimum hydraulic-fracture design in the Clinton sand.

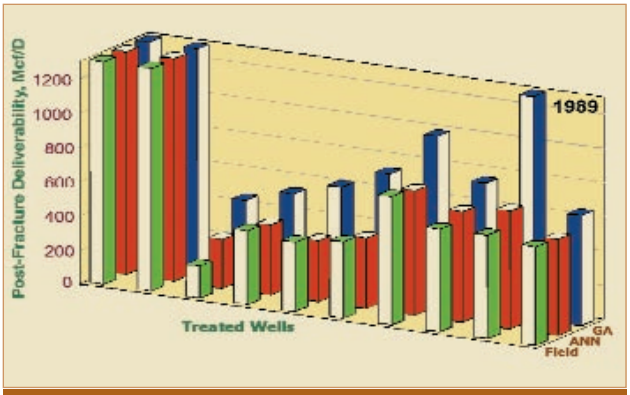

Fig. 8—Enhancement in post-fracture deliverability if method had been used in 1989.

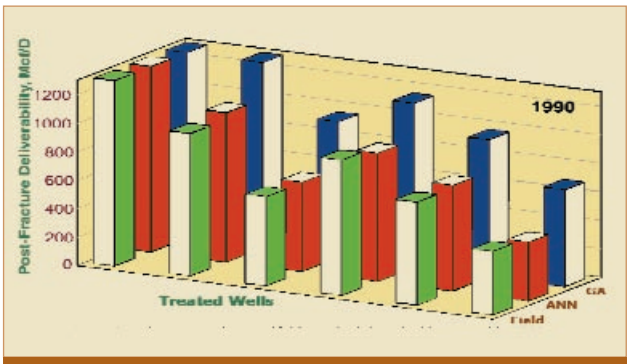

Fig. 9—Enhancement in post-fracture deliverabilities if method had been used in 1990.

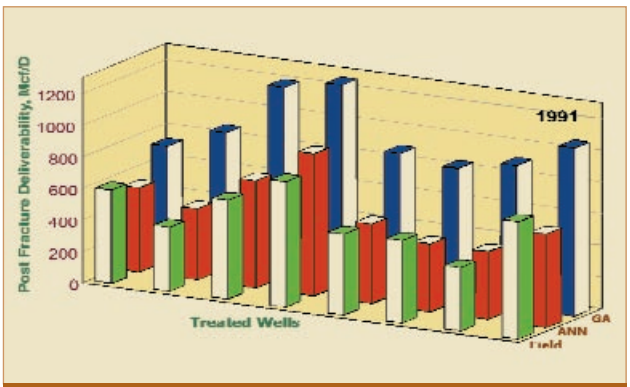

Fig. 10—Enhancement in post-fracture deliverabilities if method had been used in 1991.

ing individuals are identified, and the selection for reproduction of the next generation is made. Genetic operations, such as crossover, inversion, and mutations, are performed, and a new generation of solutions is generated. This process is continued until a convergence criterion is reached.

This process is repeated for all the wells. The wells with the highest potential for post-fracture deliverability enhancement are selected as candidate wells. The combination of the design parameters identified for each well is also provided to the operator as the guideline for achieving the well's potential. This process was performed for the wells in Fig. 6. **Figs. 8 through 10** present the results

of the genetic optimization. Because the same neural networks have generated all the post-fracture deliverabilities, post-fracture deliverabilities achieved after genetic optimization are expected to have the same degree of accuracy as those that were predicted for each well's field result. In these figures, the green bars show actual post-fracture deliverabilities of the wells achieved in the field. The red bars show the accuracy of the neural network used as the fitness function in the genetic-optimization routine when it is predicting post-fracture deliverabilities, given the design parameters used in the field. The blue bars show post-fracture deliverabilities resulting from the same neural network that produced the red bars, but with the input design parameters proposed by the genetic algorithms.

Please note that the process indicates that some wells cannot be enhanced, regardless of the modification in the fracture design, while other wells can be enhanced significantly. This finding can have important financial impact on the operation and can help management make better decisions in allocation of investment.

In another application, genetic algorithms were used in combination with neural networks to develop an expert hydraulic-fracture designer.[15] The intelligent system developed for this purpose is capable of designing hydraulic fractures in detail; providing the pumping schedule in several stages (or in a ramp scheme); and identifying fluid type and amount, proppant type and concentration, and pumping rate. Ref. 15 shows that fracture designs proposed by this intelligent system are comparable with those designed by expert engineers with several years of experience.

Conclusions

Evolutionary-computing paradigms provide a rich and capable environment for solving many search, optimization, and design problems. The larger the space of possible solutions, the more effective is the use of these paradigms. Evolutionary computing, in general, and genetic algorithms, specifically, are able to combine the exploration characteristics of an effective search algorithm with a remarkable ability to preserve and exploit the knowledge acquired during every step of the search as a guide to the next step. This provides an intelligent approach to solving search, optimization, and design problems more efficiently.

Domain expertise is a necessity in generating useful tools with evolutionary computing. It must be combined with a fundamental understanding of intelligent systems and experience in applying them in real-life problems. This produces intelligent tools that industry can use to help its bottom line. JPT

References

1. Mohaghegh, S.: "Virtual-Intelligence Applications in Petroleum Engineering: Part 1—Artificial Neural Networks," *JPT* (September 2000) 64.
2. Kayr, E.: *Toward a New Philosophy of Biology: Observations of an Evolutionist*, Belknap Press, Cambridge, Massachusetts. (1988).
3. Koza, J.R.: *Genetic Programming, On the Programming of Computers by Means of Natural Selection*, MIT Press, Cambridge, Massachusetts (1992).
4. Fogel, D.B.: *Evolutionary Computation, Toward a New Philosophy of Machine Intelligence*, IEEE Press, Piscataway, New Jersey (1995).
5. Michalewicz, Z.: *Genetic Algorithms+Data Structure=Evolution Programs*, Springer-Verlag, New York City (1992).
6. Goldberg, D.E.: "Computer Aided Gas Pipeline Operation Using Genetic Algorithms and Rule Learning," PhD dissertation, U. of Michigan, Ann Arbor, Michigan (1983).
7. Guerreiro, J.N.C. *et. al.*: "Identification of Reservoir Heterogeneities Using Tracer Breakthrough Profiles and Genetic Algorithms," paper SPE 39066 presented at the 1997 SPE Latin American and Caribbean Petroleum Engineering Conference, Rio de Janeiro, 30 August–3 September.
8. Sen, M.K. *et. al.*: "Stochastic Reservoir Modeling Using Simulated Annealing and Genetic Algorithm," paper SPE 24754 presented at the 1992 SPE Annual Technical Conference and Exhibition, Washington, DC, 4–7 October.
9. Martinez, E.R. *et. al.*: "Application of Genetic Algorithm on the Distribution of Gas-Lift Injection," paper SPE 26993 presented at the 1994 SPE Annual Technical Conference and Exhibition, New Orleans, 25–28 September.
10. Fang, J.H., Karr, C.L., and Stanley, D.A.: "Genetic Algorithm and Its Application to Petrophysics," paper SPE 26208 available from SPE, Richardson, Texas (1992).
11. Hu, L.Y., Joseph, P., and Dubrule, O.: "Random Genetic Simulation of the Internal Geometry of Deltaic Sandstone Bodies," paper SPE 24714 presented at the 1992 SPE Annual Technical Conference and Exhibition, Washington, DC, 4–7 October.
12. Yin, H. and Zhai, Y.: "An Optimum Method of Early-Time Well Test Analysis—Genetic Algorithm," paper SPE 50905 presented at the 1998 SPE International Oil and Gas Conference and Exhibition, Beijing, 2–6 November.
13. Mohaghegh, S. *et. al.*: "A Hybrid, Neurogenetic Approach to Hydraulic Fracture Treatment Design and Optimization," paper SPE 36602 presented at the 1996 SPE Annual Technical Conference and Exhibition, Denver, Colorado, 6–9 October.
14. Mohaghegh, S., Platon, V., and Ameri, S.: "Candidate Selection for Stimulation of Gas-Storage Wells Using Available Data With Neural Networks and Genetic Algorithms," paper SPE 51080 presented at the 1998 SPE Eastern Regional Meeting, Pittsburgh, Pennsylvania, 9–11 November.
15. Mohaghegh, S., Popa, A.S., and Ameri, S.: "Intelligent Systems Can Design Optimum Fracturing Jobs," paper SPE 57433 presented at the 1999 SPE Eastern Regional Meeting, Charleston, West Virginia, 21–22 October.

SI Metric Conversion Factor

$ft^3 \times 2.831\ 685\ E{-}01 = m^3$

Shahab Mohaghegh *is an associate professor of petroleum and natural gas engineering at West Virginia U. in Morgantown, West Virginia. e-mail: shahab@wvu.edu. Involved in R&D of virtual-intelligence techniques since 1991, he has applied the techniques successfully to petroleum engineering problems in many different areas, including drilling, completion, stimulation, formation evaluation, and reservoir evaluation. Mohaghegh holds BS and MS degrees in natural gas engineering from Texas A&I U. and a PhD degree in petroleum and natural gas engineering from Pennsylvania State U. A member of the Editorial Review Committee, he served as a Review Chairman for* **SPE Reservoir Engineering and Evaluation** *during 1997–99.*

Virtual-Intelligence Applications in Petroleum Engineering: Part 3—Fuzzy Logic

Shahab Mohaghegh, SPE, West Virginia U.

Parts 1 and 2 of this series of articles presented a general overview of artificial neural networks and evolutionary computing, respectively, and their applications in the oil and gas industry.[1,2] The focus of this article is fuzzy logic. The article provides overview of the subject and its potential application in solving petroleum-engineering-related problems. As the previous articles mentioned, the most successful applications of intelligent systems, especially when solving engineering problems, have been achieved by use of different intelligent tools in concert and as a hybrid system. This article reviews the application of fuzzy logic for restimulation-candidate selection in a tight-gas formation in the Rocky Mountains. We chose this particular application because it uses fuzzy logic in a hybrid manner integrated with neural networks and genetic algorithms.

Background

The science of today is based on Aristotle's crisp logic formed more than 2,000 years ago. Aristotelian logic looks at the world in a bivalent manner, such as black and white, yes and no, and 0 and 1. The set theory developed in the late 19th Century by German mathematician Cantor was based on Aristotle's bivalent logic and made this logic accessible to modern science. Subsequent superimposition of probability theory made the bivalent logic reasonable and workable. Cantor's theory defines sets as a collection of definite, distinguishable objects. **Fig. 1** is a simple example of Cantor's set theory and its most common operations, such as complement, intersection, and union.

The first work on vagueness dates back to the first decade 20th Century, when American philosopher Pierce noted that "vagueness is no more to be done away with in the world of logic than friction in mechanics."[3] In the early 1920's, Polish mathematician and logician Lukasiewicz[4] developed three-valued logic and talked about many-valued, or multivalued, logic. In 1937, quantum philosopher Black[5] published a paper on vague sets. These scientists built the foundation on which fuzzy logic was later developed.

Zadeh,[6] known as the father of fuzzy logic, published his landmark paper "Fuzzy Sets" in 1965. He developed many key concepts, including membership values, and provided a comprehensive framework to apply the theory to engineering and scientific problems. This framework included the classical operations for fuzzy sets, which comprise all the mathematical tools necessary to apply the fuzzy-set theory to real-world problems. Zadeh was the first to use the term "fuzzy," which provoked much opposition. A tireless spokesperson for the field, he was often harshly criticized. At a 1972 conference, Kalman stated that "Fuzzification is a kind of scientific permissiveness; it tends to result in socially appealing slogans unaccompanied by the discipline of hard scientific work."[7] (Note that Kalman is a former student of Zadeh's and inventor of the famous Kalman filter, a major statistical tool in electrical engineering. The Kalman filter is the technology behind the Patriot missiles used in the Gulf War. Claims have been made that it has been proved that use of fuzzy logic can significantly increase the accuracy of these missiles.[8,9]) Despite all its adversaries, fuzzy logic continued to flourish and has become a major force behind many advances in intelligent systems.

The word "fuzzy" carries a negative connotation in Western culture, and "fuzzy logic" seems to misdirect the attention and to celebrate mental fog.[10] On the other hand, Eastern culture embraces the concept of coexistence of contradictions as it appears in the yin/yang symbol (**Fig. 2**). While Aristotelian logic preaches A *or* Not-A, Buddhism is all about A *and* Not-A.

Many believe that the tolerance of Eastern culture for such ideas is the main reason behind the success of fuzzy logic in Japan. While fuzzy logic was being attacked in the U.S., Japanese industries were busy building a multibillion-dollar industry around it. Today, the Japanese hold more than 2,000 fuzzy-related patents. They have used fuzzy technology to build intelligent household appliances, such as washing machines and vacuum cleaners (Matsushita and Hitachi), rice cookers (Matsushita and Sanyo), air conditioners (Mitsubishi), and microwave ovens (Sharp, Sanyo, and Toshiba), to name a few. Matsushita used fuzzy technology to develop its digital image stabilizer for camcorders. Adaptive fuzzy systems (a hybrid with neural networks) can be found in many Japanese cars. Nissan patented a fuzzy automatic transmission that is now very popular with many other manufacturers, such as Mitsubishi and Honda.[10]

Fuzzy-Set Theory

The human thinking/reasoning/decision-making process is not crisp. We use vague, imprecise words to explain our thoughts or communicate with one another. There is a contradiction between the imprecise, vague process of human reasoning, thinking, and decision-making and the crisp, scientific reasoning of black-and-white computer algorithms and approaches. This contradiction gave rise to the impractical approach of using computers to assist humans in the decision-making process and is the main reason that tradi-

Copyright 2000 Society of Petroleum Engineers

This is paper SPE 62415. **Distinguished Author Series** articles are general, descriptive representations that summarize the state of the art in an area of technology by describing recent developments for readers who are not specialists in the topics discussed. Written by individuals recognized as experts in the area, these articles provide key references to more definitive work and present specific details only to illustrate the technology. **Purpose:** to inform the general readership of recent advances in various areas of petroleum engineering.

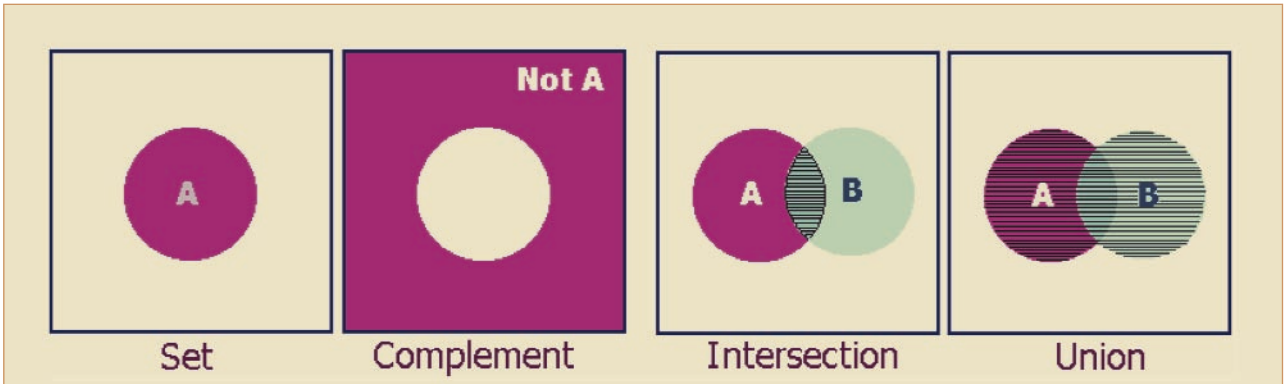

Fig. 1—Operations of conventional crisp sets.

Fig. 2—Yin/yang symbol.

tional artificial intelligence or conventional rule-based systems (also known as expert systems) have been unsuccessful. Expert systems, which started as a technology in the early 1950's, remained in research laboratories and never broke through to the consumer market.

In essence, fuzzy logic provides the means to compute with words. Using fuzzy logic, experts are no longer forced to summarize their knowledge to a language that machines or computers can understand. What traditional expert systems failed to achieve finally became reality with the use of fuzzy-expert systems. Fuzzy logic is made up of fuzzy sets, which are a way of representing nonstatistical uncertainty and approximate reasoning, which includes operations used to make inferences.[9]

Fuzzy-set theory provides a means of representing uncertainty. Uncertainty usually is the result of either the random nature of events or the imprecision and ambiguity of the information we have about the problem we are trying to solve. In a random process, the outcome of an event from among several possibilities is strictly the result of chance. When the uncertainty is a product of randomness of events, probability theory is the proper tool to use. Observations and measurements can be used to resolve statistical or random uncertainty. For example, once a coin is tossed, no further random or statistical uncertainty remains.

Most uncertainties, especially when dealing with complex systems, are the result of a lack of information. The type of uncertainty that is the outcome of the complexity of a system arises from imprecision, from our inability to perform adequate measurements, from a lack of knowledge, or from vagueness (like the fuzziness inherent in natural language). Fuzzy-set theory is a marvelous tool for modeling the kind of uncertainty associated with vagueness, imprecision, and/or a lack of information regarding a particular element of the problem at hand.[11] Fuzzy logic achieves this important task through fuzzy sets. In crisp sets, an object either belongs to a set or it does not. In fuzzy sets, everything is a matter of degrees. Therefore, an object belongs to a set to a certain degree. For example, the price of oil today is U.S.$24.30/bbl. Given the price of oil in the past few years, this price seems to be high. But what is a high price for oil? A few months ago, the price of oil was approximately U.S. $10/bbl, which everyone agrees is low. Given how much it costs to produce a barrel of oil in the U.S., one can say that the cutoff between low and high for oil price is U.S. $15/bbl. If we use crisp sets, U.S. $14.99/bbl is low and U.S. $15.01/bbl is high. Imagine if this was the criterion used by oil company executives to make decisions. The fact is, while U.S. $15.01 is a price that many people (in the oil industry) would be happy with, U.S. $16/bbl is better and U.S. $20/bbl is even better. Categorizing these three prices as high can be quite misleading. **Fig. 3** shows the fuzzy sets that fuzzy logic proposes for the price of oil.

The most popular (although not yet standard) form of representing fuzzy set and membership information is

$$\mu_A(X)=m, \quad \ldots\ldots\ldots\ldots\ldots\ldots\ldots\ldots\ldots\ldots (1)$$

where the membership μ of X in Fuzzy Set A is m. According to Fig. 3, when the price of oil is U.S. $20/bbl, it has a membership of 0.15 in the fuzzy set "Good" and a membership of 0.85 in the fuzzy set "High." With these values to represent the oil-price-membership values,

$$\mu_{\text{good}}(\$20)=0.15 \quad \ldots\ldots\ldots\ldots\ldots\ldots\ldots\ldots (2a)$$

and

$$\mu_{\text{high}}(\$20)=0.85. \quad \ldots\ldots\ldots\ldots\ldots\ldots\ldots\ldots (2b)$$

Approximate Reasoning. When decisions are made on the basis of fuzzy linguistic variables (low, good, high) with fuzzy-set operators (and, or), the process is called approximate reasoning. This process mimics the human expert's reasoning process much more realistically than do conventional expert systems. For example, if the objective is to build a fuzzy expert system to help us make a recommendation on enhanced recovery operations, we can use the oil price and the company's proven reserves to make such a recommendation. Using the fuzzy sets in Fig. 3 for the oil price and the fuzzy sets in **Fig. 4** for the company's total proven reserves, we try to build a fuzzy system that can help us in making a recommendation on engaging in enhanced-recovery operations (**Fig. 5**).

Fig. 3—Fuzzy sets representing oil price.

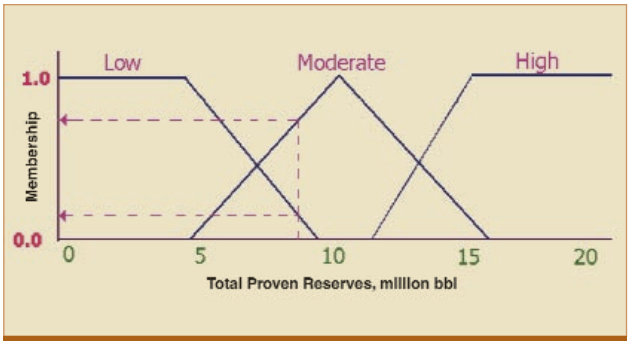

Fig. 4—Fuzzy sets representing total proven reserves.

Approximate reasoning is implemented through fuzzy rules. A fuzzy rule for the system being explained here can have the following form.

Rule 1. If the price of oil is high *and* the total proven reserves of the company is low, engaging in enhanced-recovery practices is highly recommended.

Because this fuzzy system comprises two variables and each variable consists of three fuzzy sets, the system includes nine fuzzy rules, which can be set up in a matrix (**Fig. 6**). The abbreviations in the Fig. 6 matrix correspond to the fuzzy sets defined in Fig. 5. One can conclude from this example that the number of rules in a fuzzy system increases dramatically with the addition of new variables. Adding one more variable consisting of three fuzzy sets to the example increases the number of rules from 9 to 27. This is known as the "curse of dimensionality."

Fuzzy Inference. A complete fuzzy system includes a fuzzy-inference engine. Fuzzy inference helps us build fuzzy relations based on the fuzzy rules that have been defined. During a fuzzy-inference process, several fuzzy rules are fired in parallel. Parallel-rule firing, unlike sequential evaluation of the rules in the conventional expert system, is much closer to the human reasoning process. Unlike the sequential process, where some information contained in the variables may be overlooked because of the stepwise approach, parallel firing of the rules allows simultaneous consideration of all the information. Many different fuzzy-inference methods exist. We examine a popular method called Mamdani's inference method.[12] **Fig. 7** illustrates this inference method graphically. In this figure, a case is considered when the price of oil is U.S. $20/bbl and the company has approximately 9 million bbl of proven reserves. Oil price is represented by its membership in the Good and High fuzzy sets, while total proven reserves is represented in the Low and Moderate fuzzy sets. As Fig. 7 shows, this causes the firing of four rules simultaneously. According to Fig. 6 these are Rules 1, 2, 4, and 5. In each rule, the fuzzy-set operation "and" [the intersection between the two input (antecedents) variables] is evaluated as the minimum and consequently is mapped on the corresponding output (consequent). The result of the inference is the collection of the different fuzzy sets of the output variable on the bottom of the figure.

A crisp value may be extracted from the result as mapped on the output fuzzy sets by defuzzifying the output. One of the most popular defuzzification procedures is to find the center of the mass of the shaded area in the output fuzzy sets.

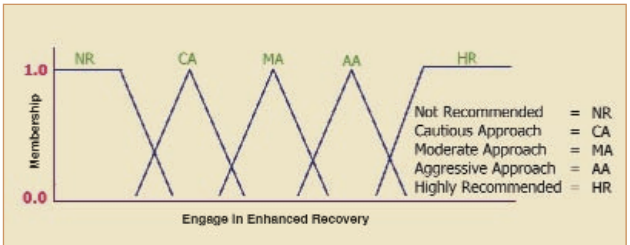

Fig. 5—Fuzzy sets representing the decision to engage in enhanced recovery.

Application in the Petroleum Industry

Fuzzy logic has been used in several petroleum-engineering-related applications. These include petrophysics,[13,14] reservoir characterization,[15] enhanced recovery,[16,17] infill drilling,[18] decision-making analysis,[19] and well stimulation.[20-22] In this section, we review an application that incorporates fuzzy logic in a hybrid manner in concert with neural networks and genetic algorithms.

In this example of use of intelligent systems in petroleum engineering, neural networks, genetic algorithms, and fuzzy logic are used to select candidates for restimulation in the Frontier formation in the Green River basin.[22] As the first step of the method, neural networks are used to build a representative model of the well performance in the Frontier formation. **Table 1** lists the input parameters

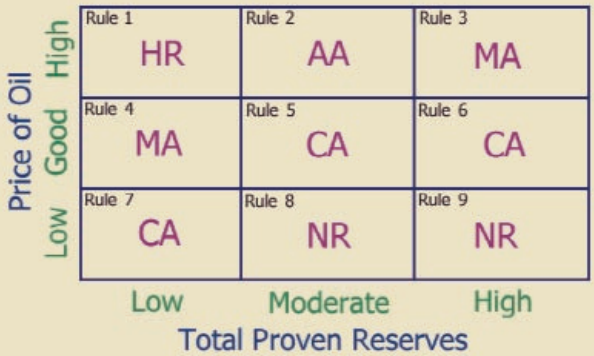

Fig. 6—Fuzzy rules for approximate reasoning.

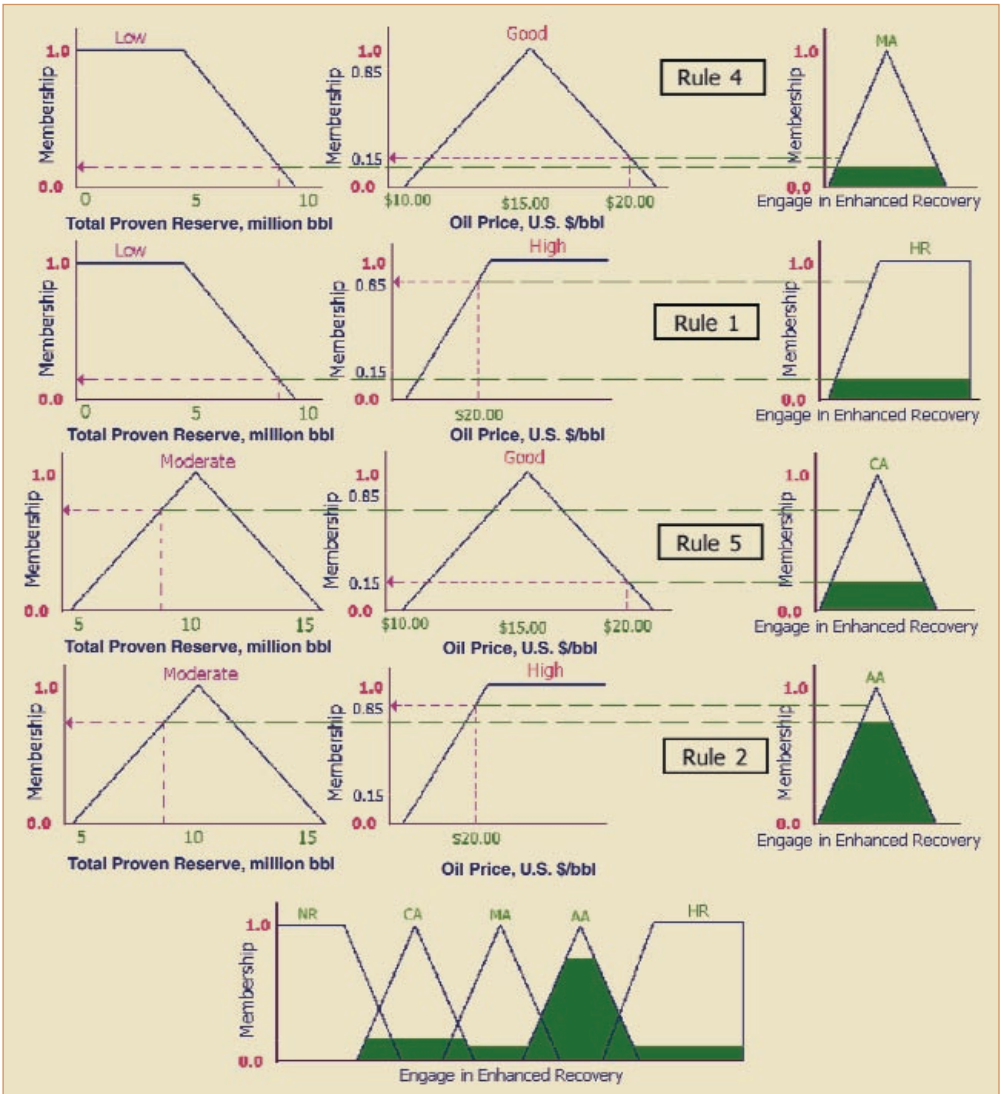

Fig. 7—Mamdani's fuzzy inference.

TABLE 1—INPUT PARAMETERS FOR NEURAL-NETWORK ANALYSIS

Category	Input Parameter	Comments
Location	*x*	x coordinates of the well (east-west)
	y	y coordinates of the well (north-south)
	KB elevation	Kelly bushing elevation
Reservoir	Permeability	From type-curve-matching analysis
	Drainage area	From type-curve-matching analysis
	Total gas-feet	Sum (porosity+gas saturation +net pay) (all zones)
Completion	Total *h* completed	Total completed thickness (all zones)
	Total number of holes	Total number of perforation holes
	Completion date	Date of well completion
	Number of zones	Total number of zones completed
Fracture	Fracture number	A well may have up to seven fracture jobs
	Fluid type	Gelled oil, ungelled oil, linear gel, crosslinked gel
	Fluid volume	Total amount of fluid pumped in all fractures
	Proppant amount	Total amount of proppant pumped in all fractures

used in the neural-network model-building process.

After training, testing, and validation of the neural networks, the training data set had a correlation coefficient of 0.96 and the verification data set had a correlation coefficient of 0.72. As a byproduct of the neural-network analysis and with a method called "backward elimination," an attempt was made to identify the most influential parameters in this data set. **Fig. 8** shows the results of neural-network backward-elimination analysis.

This figure shows all four categories of input data. The most influential category has the lowest R^2. The figure also shows that reservoir quality is the most important category, followed by the completion and stimulation categories, which seem to be equally important. The location-related input parameters seem to be the least important compared with the others. Note that, among all the parameters involved in the analysis, only the last three stimulation-related parameters in Table 1 are considered to be controllable.

The second step of the analysis involves genetic optimization of the stimulation parameters. The last three input parameters in Table 1 (fluid type, total fluid volume, and total proppant amount) are used in the optimization process. With the neural-network model developed in the first step of the analysis as the "fitness" function of the evolution process, the algorithm searches through all possible combinations of the three stimulation parameters and tries to find the combination that results in the highest 5-year cumulative production. This process is repeated for each well. The difference between the optimized and the actual 5-year cumulative production is considered to be the potentially missed production that might be recovered by restimulation. The outcome of this process is called the potential 5-year cumulative production and is used as one of the three inputs

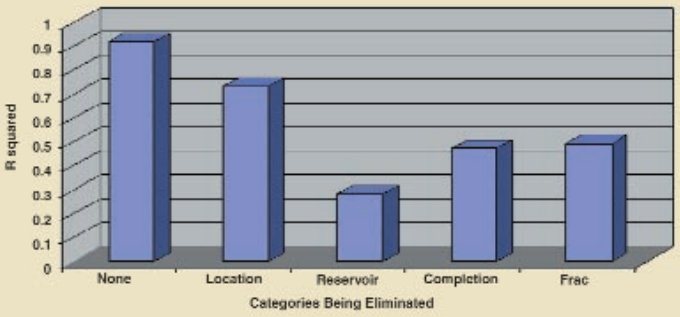

Fig. 8—Influence of parameters in the stimulation process in Frontier formation.

in Step three, which is the fuzzy-decision suppor t system that uses approximate reasoning.

Step three is a three-input/one-output fuzzy system. The inputs include the potential 5-year cumulative production, a calculated parameter called fractures per zone (FPZ), and pressure. Engineers in the field brought the FPZ parameter to our attention. They mentioned that some wells had been completed in all zones (as many as seven zones can be present) but only one hydraulic fracture had been performed. In other words, the ratio of number of treatments performed to total number of zones completed is an important factor. We also found that long-term pressure surveys had been performed on many wells in 1995. The issue with pressure surveys is that shut-in time and depth where the pressure readings were taken were not consistent throughout the field. This introduces serious imprecision in the pressure values as a comparative value from well to well. Therefore, we subjected all three input parameters to fuzzy sets using low, moderate, and high fuzzy sets. Output of the fuzzy system is the degree to which a well is a candidate for restimulation. The output fuzzy sets include (1) the well is a candidate, (2) the well may be a candidate, and (3) the well is not a candidate. The system includes 27 fuzzy rules that are qualified with a set of three truth functions. **Fig. 9** shows the 27 rules with truth qualifications for the fuzzy systems. **Fig. 10** shows the truth-qualification functions used for the approximate-reasoning implementation in the fuzzy system. As the figure shows, each rule can be true, fairly true, or very true.

With this thr ee-step process, all the wells belonging to a particular operator in the Frontier formation were processed and a list of r estimulation candidates identified.

Results. The intelligent-systems approach for this application was modified as a result of its application to thr ee different formations, two in the Rocky Mountains and one in east T exas. The fuzzy-decision support system was the most recent addition to the pr ocess. The new and improved intelligent-systems appr oach that included the fuzzy logic component picked W ell GRB 45-12 as Candidate 20, while this well was missed as a candidate before the addition of fuzzy logic to the procedure. An engineer with several years of experience in this field also had suggested this well as a candidate. The fuzzy-decision suppor t system was able to capture the engineer's knowledge and use it in an automatic process for all the wells in the study. **Fig. 11** shows the result of restimulation on Well GRB 45-12.

Conclusions

This series of articles presented a general background and some introductory information about vir tual intelligence and thr ee of its most popular tools (neural networks, genetic algorithms, and fuzzy logic). Some uses of these technologies in the oil and gas industry wer e also presented along with application examples for each of the techniques. We hope that this ef fort invokes some interest in this ar ea by demonstrating the potential that these methods have in solving challenging and complex problems. JPT

Nomenclature

h = thickness, L, ft
m = membership value
R^2 = correlation coefficient
x,y = coordinates
X = input-parameter value
μ = membership of a fuzzy set

Frac/Zone	Pressure: Low	Pressure: Medium	Pressure: High
High	NO VT; NO VT; NO T	Maybe FT; NO FT; Maybe T	Yes T; Maybe VT; Maybe VT
Med.	Maybe T; NO T; NO VT	Yes FT; Maybe T; NO FT	Yes VT; Yes T; Maybe VT
Low	Maybe FT; Maybe FT; Maybe T	Yes FT; Yes FT; Maybe T	Yes VT; Yes VT; Yes T
	Low; Medium; High	Low; Medium; High	Low; Medium; High
	Potential 5-Year Cumulative	Potential 5-Year Cumulative	Potential 5-Year Cumulative

Fig. 9—Rules used in fuzzy-decision support system.

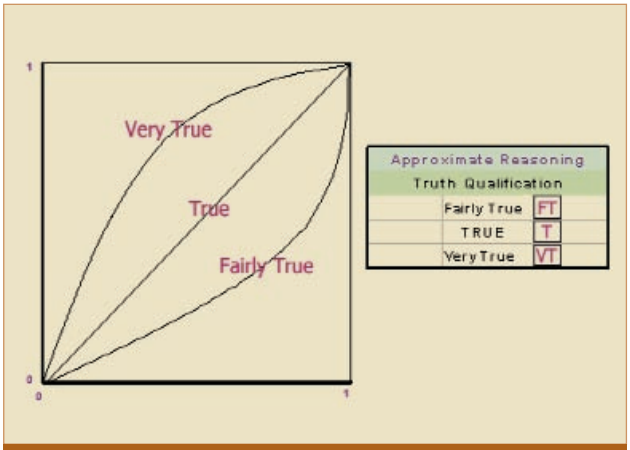

Fig. 10—Truth qualification for fuzzy rules.

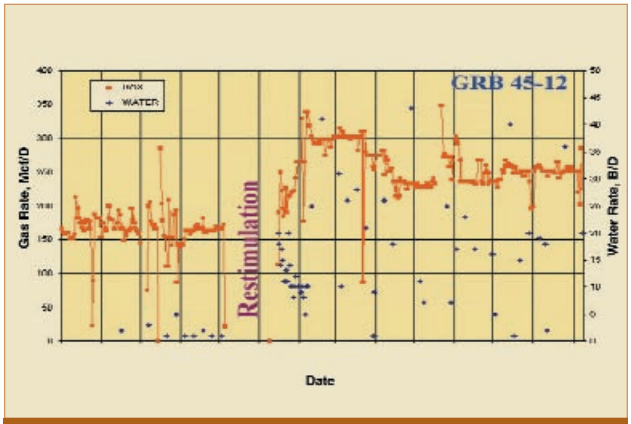

Fig. 11—Gas and water production for W ell GRB 45-12 before and after restimulation.

References

1. Mohaghegh, S.: "Virtual-Intelligence Applications in Petroleum Engineering: Par t 1—Artificial Neural Networks," *JPT* (September 2000) 64.
2. Mohaghegh, S.: "Virtual-Intelligence Applications in Petroleum Engineering: Par t 2—Evolutionary Computing," *JPT* (October 2000) 40.
3. *The Relevance of Charles Pierce*, E. Fr eeman (ed.), Monist Library of Philosophy, La Salle, Illinois (1983) 157–58.
4. Lukasiewicz, J.: *Elements of Mathematical Logic*, MacMillan Co., New York City (1963).
5. Black, M.: "Vagueness: An Exercise in Logical Analysis," *Philosophy of Science* (1937) **4,** 427.
6. Zadeh, L.A.: "Fuzzy Sets," *Information and Control* (1965) **8,** 338.
7. Eberhart, R., Simpson, P ., and Dobbins, R.: *Computational Intelligence PC Tools*, Academic Press, Orlando, Florida (1996).
8. Kosko, B.: *Fuzzy Thinking*, Hyperion, New York City (1991).
9. Kosko, B.: *Neural Networks and Fuzzy Systems*, Prentice-Hall Inc., Englewood Cliffs, New Jersey (1992).
10. McNeill, D. and Freiberger, P.: *Fuzzy Logic*, Simon & Schuster, New York City (1993).
11. Ross, T.: *Fuzzy Logic With Engineering Applications,* McGraw-Hill Inc., New York City (1995).
12. *Fuzzy Logic and Control: Software and Hardware Applications*, M. Jamshidi *et al.* (eds.) Prentice-Hall Inc., Englewood Cliffs, New Jersey (1993).
13. Zhanggui, L. *et al.*: "Integration of Fuzzy Methods Into Geostatistics for Petrophysical Property Distribution," paper SPE 49964 presented at the 1998 SPE Asia Pacific Oil and Gas Conference and Exhibition, Perth, Australia, 12–14 October.
14. Chen, H.C. *et al.*: "Novel Approaches to the Determination of Archie Parameters II: Fuzzy Regression Analysis," paper SPE 26288 available from SPE, Richardson, Texas (1993).
15. Zhou, C.-D., W u, X.-L., and Cheng, J.-A.: "Determining Reservoir Properties in Reser voir Studies Using a Fuzzy Neural Network," paper SPE 26430 pr esented at the 1993 SPE Annual Technical Conference and Exhibition, Houston, 3–6 October.
16. Chung, T.-H., Carroll, H.B. Jr., and Lindsey, R.: "Application of Fuzzy Expert Systems for EOR Project Risk Analysis," paper SPE 30741 presented at the 1995 SPE Annual T echnical Conference and Exhibition, Dallas, 22–25 October.
17. Nikravesh, M., Dobie, C.A., and Patzek, T .W.: "Field-Wise Waterflood Management in Low-Permeability , Fractured Oil Reservoirs: Neuro-Fuzzy Approach," paper SPE 37523 presented at the 1997 SPE International Thermal Operations and Heavy Oil Symposium, Bakersfield, California, 10–12 February.
18. Wu, C.H., Lu, G.F., and Yen, J.: "Statistical and Fuzzy Infill Drilling Recovery Models for Carbonate Reser voirs," paper SPE 37728 pr esented at the 1997 Middle East Oil Conference, Manama, Bahrain, 17–20 March.
19. Yong, Q., Hu, Y ., and Xiao, F .: "Fuzzy-Grey-Element Relational Decision-Making Analysis and Its Application," paper SPE 39579 presented at the 1998 SPE India Oil and Gas Conference, New Delhi, India, 17–19 Februar y.
20. Xiong, H.: "An Investigation Into the Application of Fuzzy Logic to W ell Stimulation T reatment Design," paper SPE 27672 presented at the 1994 SPE Permian Basin Oil and Gas Recovery Conference, Midland, Texas, 16–18 March.
21. Rivera, V.P.: "Fuzzy Logic Contr ols Pressure in Fracturing Fluid Characterization Facility," paper SPE 28239 pr esented at the 1994 SPE Petroleum Computer Conference, Dallas, 31 July–3 August.
22. Mohaghegh, S., Reeves, S., and Hill, D.: "Development of an Intelligent Systems Appr oach to Restimulation Candidate Selection," paper SPE 59767 pr esented at the 2000 SPE Gas Technology Symposium, Calgary, 3–5 April.

SI Metric Conversion Factor

bbl × 1.589 873 E−01 = m^3

Shahab Mohaghegh *is an associate professor of petroleum and natural gas engineering at W est Virginia U. in Morgantown, West Virginia. e-mail: shahab@wvu.edu. Involved in R&D of virtual-intelligence techniques since 1991, he has applied the techniques successfully to petroleum engineering problems in many different areas, including drilling, completion, stimulation, formation evaluation, and reservoir evaluation. Mohaghegh holds BS and MS degrees in natural gas engineering from T exas A&I U. and a PhD degree in petroleum and natural gas engineering from Pennsylvania State U. A member of the Editorial Review Committee, he served as a Review Chairman for* **SPE Reservoir Engineering and Evaluation** *during 1997–99.*

Using Artificial Neural Nets To Identify the Well-Test Interpretation Model

Abdul-Aziz U. Al-Kaabi, SPE, and **W. John Lee,** SPE, Texas A&M U.

Summary. This paper presents a new approach, based on artificial neural net technology, to identify a preliminary well-test interpretation model from derivative plot data. Artificial neural nets can identify patterns from incomplete and distorted data and also eliminate the need for elaborate data preparation, such as smoothing.

Introduction

In a pressure-transient test, a signal of pressure vs. time is recorded. When this signal is plotted with specialized plotting functions, diagnostic plots, such as derivative[1] or Horner plots, are produced that often are used in the interpretation process. The signal on these plots is deformed and shaped by underlying mechanisms in the formation and wellbore. These mechanisms are the well-test interpretation model. The objective of this work is to identify these mechanisms from the signatures on the derivative plot.

Identifying the well-test interpretation model is described in the literature as an inverse problem.[2] The traditional way of solving an inverse problem is with inverse theory[3] techniques (e.g., regression analysis). A serious disadvantage of such techniques is that we have to assume an interpretation model. The inverse theory provides estimates of the model parameters but not of the model itself. Because more than one interpretation model can produce the same signal, this approach can lead to misleading results. We seek the model itself instead of its parameters in this study.

In this study, we trained a neural net simulator to identify the well-test interpretation model from the derivative plot. The neural net simulator can be part of a well-test expert system or a computer-enhanced well-test interpretation.

Literature Review

In 1988, Allain and Horne[4] used syntactic pattern recognition[5] and a rule-based approach to identify the well-test interpretation model automatically from the derivative plot. Their approach is based on transforming the derivative plot into a symbolic form. The symbols generated (UP, DOWN, etc.) are used by a rule-based system to identify the well-test interpretation model.

In 1989, Stewart and Du[6] presented a technique to transform the derivative plot into a symbolic form for use in a knowledge-based system to identify the well-test interpretation model. This approach relies on preprocessing test data to obtain a smooth derivative plot. The data are filtered with a preselected smooth parameter incorporated in approximating spline functions. Then, the smoothed derivative plot is transformed into symbols by first approximating the curve with linear and nonlinear segments based on preselected error thresholds and measurements of inflection points. The resulting segments then are used to obtain a detailed symbolic description of the derivative plot.

In this paper, we present a new method to identify a preliminary interpretation model. Our approach eliminates the need for preprocessing and writing complex rules. The approach is based on artificial neural net technology and is fully automatic because it does not depend on threshold choice and difficult-to-measure parameters, such as inflection points. The disadvantage of this procedure is that it is useful for model selection only; the analyst must estimate the model parameters using methods totally independent of the neural net. An advantage of the symbolic approach is that it can be used to estimate model parameters. Thus, each approach has strengths and limitations.

Artificial Neural Net Approach

The dominant artificial intelligence paradigms (e.g., rule-based systems) assume a symbolic approach to describe intelligence. Such paradigms assume that such means as rules or algorithms are available that can be encoded into a computer to solve a problem. The symbolic approach is applied successfully when the problem domain model (i.e., the solution) can be mapped into a procedure. The fundamental limitation of this approach is that it cannot be used to solve problems for which a solution procedure does not exist or cannot be found. The visual recognition problem is one that cannot be solved by an exact procedure. We normally solve a vision problem without thinking of a formal procedure to carry out the recognition task. This limitation in the symbolic approach is minimized with artificial neural nets.[7-11] The neural net approach does not assume a predefined algorithm to solve a problem; instead, it learns the solution model automatically by training on examples and their expected outputs.

Artificial neural nets are computing systems based on the belief that intelligence is achieved through interaction of large numbers of simple processing units (nodes),[8] a belief based on the current understanding of brain anatomy. The brain consists of billions of small processing units called neurons. A group of highly connected neurons specializes in solving certain cognitive tasks. Experts think that learning occurs through constructing internal representations of concepts by strengthening or weakening connections between neurons. Similarly, artificial neural nets learn tasks by changing the strength of links between nodes.

Artificial Neural Net System Architecture. Fig. 1 is a schematic of a multilayer artificial neural net. It consists of nodes arranged in layers. The first layer is an input layer, the second is a middle or intermediate layer, and the last layer is an output layer. The input in each node, except for the nodes in the output layer, is propagated throughout the entire net by connections called links. Each link has a weight with either a positive (strengthening) or a negative (weakening) value. The activation level in the intermediate and output layer nodes is measured by a threshold function usually called a squashing or activation function. The threshold function approaches the limiting value 1 (i.e., the node is very active) at a very large positive argument and approaches the limiting value 0 (i.e., the node is inactive) at a very small negative argument. This function is continuous and differentiable everywhere. Any function that has such characteristics can be used as a threshold function. The sigmoidal function **(Fig. 2)** frequently is used as a threshold function and has the form

$$O_j = 1/[1+\exp(-I_j)], \quad \ldots\ldots\ldots\ldots\ldots\ldots\ldots\ldots\ldots\ldots (1)$$

where O_j = the output from a node in the j layer (Fig. 1) and I_j = the sum of the input signals to this node:

$$I_j = \sum_i w_{ji} O_i. \quad \ldots\ldots\ldots\ldots\ldots\ldots\ldots\ldots\ldots\ldots\ldots\ldots (2)$$

This summarizes the calculation that occurs in a single node.

Learning is the most important computationally and memory-intensive task in a neural net operation. In a mathematical sense, learning is the process by which we can find a set of weights that produces the expected output when a net is presented within an input. In the learning phase, the net is given a set of examples (usually called a training set) where each training set consists of an input vector and a desired output vector. In this study, we used back-

Copyright 1993 Society of Petroleum Engineers

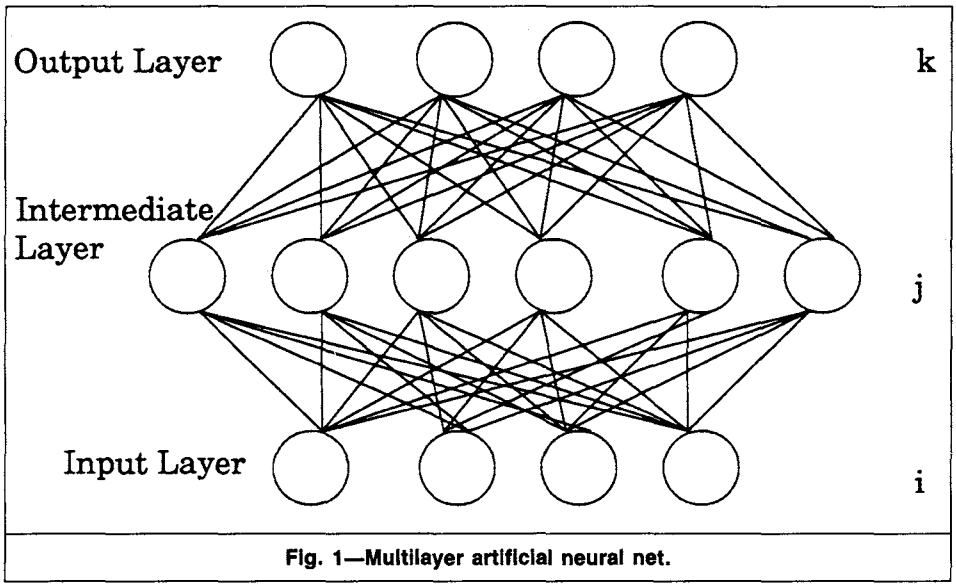

Fig. 1—Multilayer artificial neural net.

propagation as the learning algorithm. The key idea in this algorithm is that the error (difference between computed and actual output) at the output layer is propagated backward through the net with credit-assignment strategy. This means that the weight in each link is changed by an amount proportional to the error it brings to the output layer. As the error is propagated backward through the links between layers, weight changes are added or subtracted on the basis of the sign of the sigmoidal function derivative as in a gradient-descent method:

$$\Delta w_{kj} = \eta(t_k - O_k) f_k(I_k) O_j. \quad \ldots\ldots\ldots\ldots\ldots\ldots\ldots\ldots\ldots\ldots (3)$$

The left side of Eq. 3 is the weight change within a link between Layers k and j. Note that,on the right side of Eq. 3, the weight change is based on the output from a node in a previous layer (the node that caused the error). Eq. 3 is used to calculate weights in links pointing to the output layer only. Another form of Eq. 3 is used to calculate internal link weights.

Appendices A and B show the mathematical derivation of and programming steps for the backpropagation learning algorithm, respectively. In Appendix C, we discuss some practical considerations used during training. **Fig. 3** is a schematic of the learning cycle in an artificial neural net.

Well-Test Interpretation Model Identification by Artificial Neural Net. Because of the nature of neural nets, segmentation and symbolic transformation are eliminated. The net examines the whole curve simultaneously and identifies models that could have caused the signal presented by the curve.

System Description. The neural net recognition system in **Fig. 4** is used to identify the well-test interpretation model. The recognition system consists of a data input module and two trained artificial nets. Two nets are used in the recognition process because it was difficult to arrive at one set of weights that would ensure correct classification of all models considered. The second net is used whenever the output in the third node of the first net is >0.5 or when the activation level in the second node is the highest.

Data Input. The input layer in each net consists of 60 nodes that accept 30 data points (x,y) from a derivative curve. This implies that the derivative curve should be sampled for 30 points **(Fig. 5).** The output layer of the first net has 16 nodes. Each node corresponds to a specific model class (Fig. 4). In this study, the first net is trained to identify seven different model classes, which implies that only seven nodes in the output layer are active. The rest of the nodes in the output layer can be used to incorporate new models. The output layer of the second net has two nodes, which

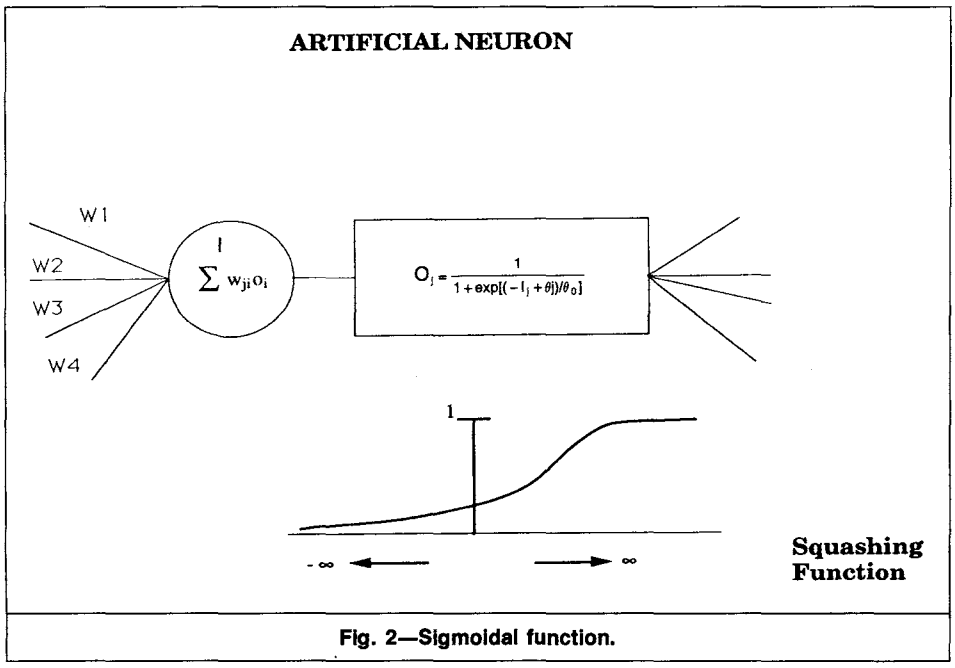

Fig. 2—Sigmoidal function.

correspond to two model classes (Fig. 4). The intermediate layer in each net has 120 nodes. The input curve is normalized between 0 and 1 by

$$x_i' = x_i / \sqrt{\Sigma (x_i)^2} \quad \ldots\ldots (4)$$

and $$y_i' = y_i / \sqrt{\Sigma (y_i)^2}. \quad \ldots\ldots (5)$$

Any normalization scheme can be used. The derivative curve must be normalized to avoid saturating the net. Saturation is the stage when the net stops learning because of very small sigmoidal function derivatives. Very small or zero derivatives occur when the argument of the sigmoidal function is large **(Fig. 6).** Note that the derivative curve on the logarithmic scale is shifted to the right or up by a value equal to the absolute value of the largest negative number on the axis on which the shift is done. This is necessary to scale all data points from 0 to 1. The output layer nodes are assigned the values 1 (firing) or 0 (silent), depending on whether the node represents the model. However, for computational accuracy, we used 0.9 and 0.1 instead of 1 and 0 because the sigmoidal function is 1 at positive infinity and 0 at negative infinity.

Training. Training is the stage when the net learns the recognition task by adjusting the weights in the links between nodes created by processing representative examples (input and output pairs). In the training set, we used models that included various combinations of inner boundary conditions (wellbore storage and skin or stimulation), reservoir types (homogeneous or dual porosity), and outer boundary conditions (infinite acting, closed outer boundary, and constant-pressure outer boundary). This phase is repeated until the net performance reaches a satisfactory level (i.e., recognition of all examples in the training set and at least 90% of test examples). Test examples are examples that are not included in the training set but that belong to the model classes that the net is trained to classify. Testing the net performance on new examples is important to ensure generalization. Generalization is the ability of the net to recognize patterns for which the net was not specifically trained. If generalization performance is poor, the net will act as a lookup table, which will limit its practical value. If the net identifies a test example with a high activation level (larger than 0.8), it is not added to the training set. If the identification was not successful or was poor, then the test example is added to the training set and the net is trained on this new set. The training set had 34 examples when training sessions were stopped.

The derivative computation took flow history effects into account by use of the derivative as a function of superposition time.

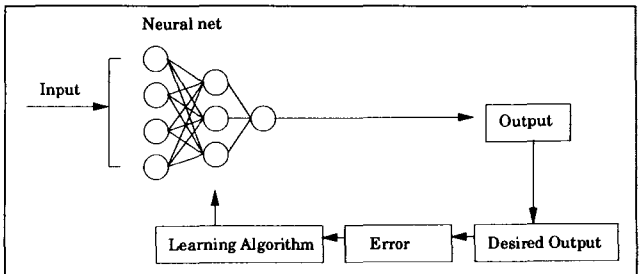

Fig. 3—Schematic of the learning cycle in an artificial net.

Each net is trained incrementally by increasing the training set size gradually until the net learns all model classes. The weights at which the net converges in each stage are used as the beginning weights for the next stage. A learning rate of 0.2 and a momentum value (explained in Appendix A) of 0.9 are used in the training sessions. The learning session is considered successful when the maximum error (Appendix A) in the output layer is <0.01.

To reduce the scaling effect (sensitivity to pattern size) during training, each derivative curve in the training set is presented to the net in different sizes (large, small, and medium). This was achieved by dividing the data points on the x and y axes after normalization by constant factors (2 and 3, respectively). An alternative method is to present the net with many examples of the same model class.

Examples

In this section, we present two examples to illustrate the application of our method.

Example 1. The first example is a buildup test in a severely damaged gas well. **Tables 1 and 2** show test data, and **Figs. 7 and 8** show diagnostic plots.

The derivative curve is sampled first for 30 data points and normalized between 0 and 1. The normalization procedure should be consistent with that used to normalize the training set examples. The normalized derivative curve is used as input to the neural nets. **Fig. 9** shows the input curve and the activation levels in the output layer. The highest activation level (0.982) indicates that the interpretation model is one in which the well response is from a well in

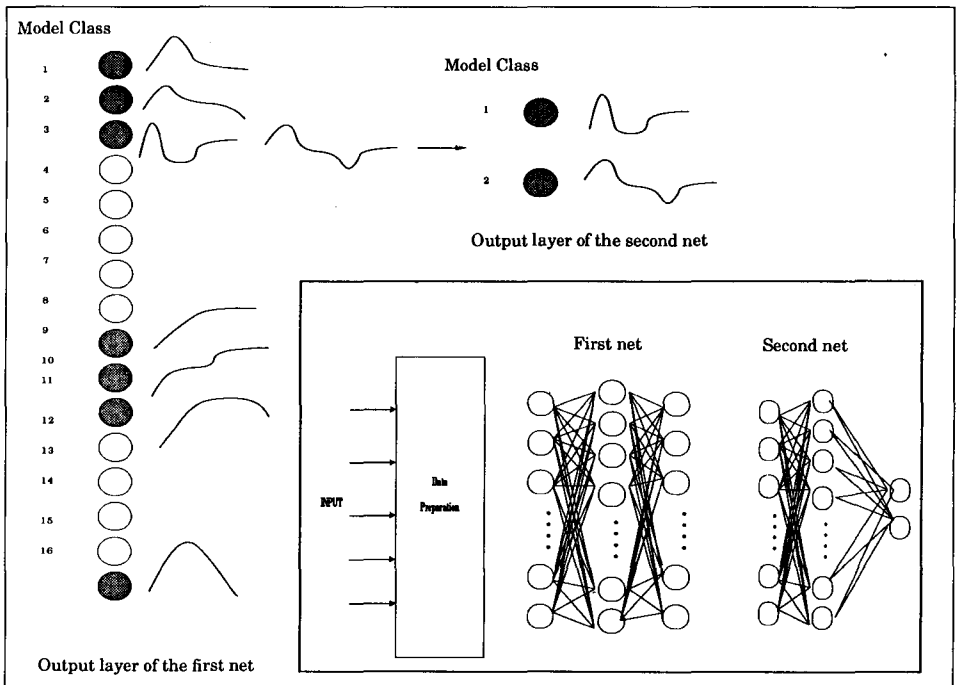

Fig. 4—Schematic of the recognition system showing output layer arrangements.

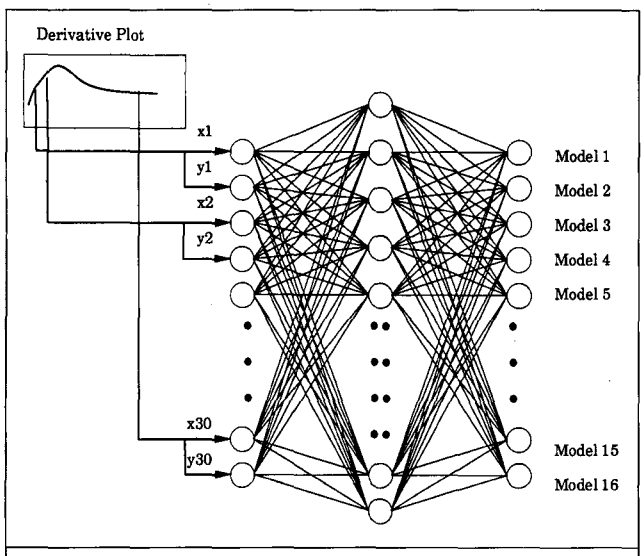

Fig. 5—Input of a derivative plot into the artificial neural net.

a homogeneous infinite-acting reservoir with wellbore storage and skin.

The second node in the ouput layer shows some activity (0.698), which indicates a response from a well affected by wellbore storage and skin in a homogeneous reservoir with a closed or constant-pressure outer boundary. This second possibility could be caused by the shallow downward trend of the last few points on the derivative plot, which suggests that the neural net approach is capable of ranking the models that could have caused the observed response on the basis of the distinctness of the features (signatures) that characterize each model.

The interpretation model suggested by the system is a preliminary model and should be verified with other information sources, such as other diagnostic plots, geologic information, well log data, and history matching, as Ref. 12 discusses.

The history-matching results indicate that the parameters obtained from analyzing the infinite-acting model accurately describe the actual pressure history of the well **(Fig. 10). Table 3** shows the interpretation model parameters.

An interesting feature of this approach is its very high tolerance to *random* noise (i.e., noise that is not correlated with the observed response). **Fig. 11** is the same input derivative curve distorted by random noise. The net was able to identify the interpretation model successfully despite the noise, as the activation levels indicated. Such performance is not guaranteed when dealing with very noisy field data. This result can be explained by the systematic (nonrandom) nature of noise in field data. Systematic noise produces false patterns (signatures) that confuse the net during recognition. We elaborate on this subject in the Recommendations for Future Work section.

Example 2. This example is a buildup test from a gas well completed in the eastern Devonian shales. Tables 1 and 2 in Ref. 12 contain the test data, and the diagnostic plots are presented in Figs. 5 and 6.[12]

Fig. 12 shows the input curve and the activation levels in the output layer. The highest activation level (0.954) indicates that the recorded response can be produced by either a heterogeneous (dual-porosity) model with stimulation in an infinite-acting reservoir (Model 1) or a homogeneous model with stimulation and a linear discontinuity (Model 2). Both models produce similar responses. More evidence now is needed to find the correct alternative. As explained in Ref. 12, Model 1 is more probable from geologic evidence.

The parameters obtained from history matching the test data with an analytical solution for a dual-porosity reservoir accurately

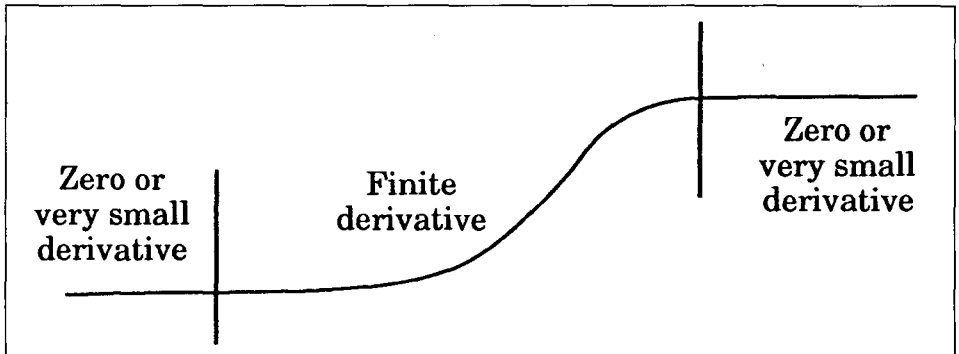

Fig. 6—Schematic of a sigmoidal function showing regions of derivative values.

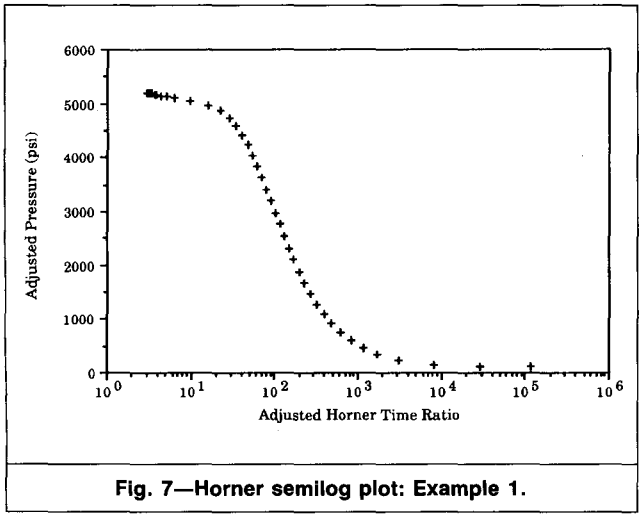

Fig. 7—Horner semilog plot: Example 1.

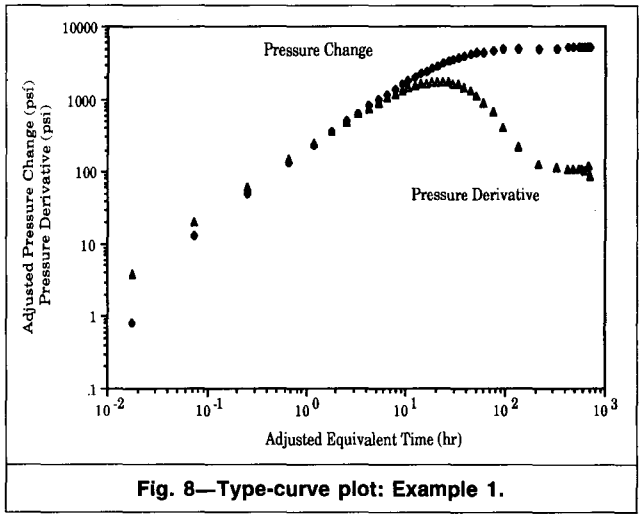

Fig. 8—Type-curve plot: Example 1.

TABLE 1—PRESSURE BUILDUP DATA, EXAMPLE 1

Time (hours)	Pressure (psi)	Derivative (psi)	Time (hours)	Pressure (psi)	Derivative (psi)
0.02	107.65	3.83	23.73	3,197.30	1,737.69
0.07	119.58	20.02	26.74	3,412.70	1,708.73
0.25	156.94	61.88	30.25	3,625.80	1,653.84
0.68	242.27	145.78	34.28	3,835.30	1,566.92
1.20	345.11	243.38	39.00	4,037.70	1,441.65
1.82	465.06	356.20	44.99	4,231.90	1,289.53
2.53	601.47	482.02	52.30	4,415.90	1,095.87
3.36	752.51	625.70	62.15	4,586.20	889.41
4.30	917.56	750.56	76.36	4,736.20	662.70
5.32	1,094.20	877.73	99.06	4,861.70	413.15
6.53	1,281.80	1,026.09	141.33	4,960.30	225.23
7.83	1,477.30	1,167.53	240.75	5,038.60	129.54
9.23	1,681.10	1,291.80	388.95	5,093.20	112.18
10.72	1,889.30	1,418.27	516.02	5,124.30	109.85
12.40	2,103.80	1,516.32	625.94	5,145.80	108.18
14.27	2,319.60	1,594.00	721.87	5,160.80	107.29
16.25	2,538.10	1,654.57	806.27	5,172.60	106.39
18.44	2,758.40	1,706.28	881.07	5,182.20	103.38
20.97	2,976.90	1,740.07	947.81	5,189.70	73.47

TABLE 2—RESERVOIR, FLUID, AND WELL PROPERTIES, EXAMPLE 1

Porosity, fraction	0.150
Net pay thickness, ft	25
Gas viscosity, cp	0.0203
Gas FVF, RB/Mcf	0.855
Gas-law deviation factor	0.924
Total compressibility, psi $^{-1}$	0.000123
Water saturation	0.50
Wellbore radius, ft	0.25
Rate, Mcf/D	190.0
Production time, hours	1,200.0

TABLE 3—INTERPRETATION MODEL PARAMETERS, EXAMPLE 1

Reservoir type	Homogeneous
Permeability, md	0.115
Skin factor	23.96
Dimensionless wellbore storage coefficient	985.96

describe the actual pressure history of the well **(Fig. 13).** Node 11 in the output layer shows an activation level of 0.408, which is considered too low to be significant. The model associated with this node is for a stimulated well in a homogeneous reservoir with closed or constant-pressure outer boundary. Some features from this model are present in our example input curve. We also distorted the same input curve by introducing random noise. As in Example 1, the model was identified again despite this distortion.

Recommendations for Future Work

In this study, we showed that the neural net approach is effective in identifying the well-test interpretation model. In this section, we provide recommendations based on our experience with neural nets.

The performance described in this paper is from the examples we selected for our training set. Other training sets can provide better or worse performance, depending on how representative the training examples are of the pattern recognition space the system will identify. Therefore, we strongly recommend careful selection of training examples.

We noted that the approach in this paper has high tolerance to random noise but that it performs poorly with data affected by systematic noise. Because we do not know how systematic noise is distributed in test data, we recommend that neural nets be trained without examples affected by this type of error. In fact, we recommend use of high-quality data (analytically generated data are preferred) for the training examples so that the net will extract the most significant features of the curve used. Training the net with data affected by systematic noise can result in the net's extracting the wrong features.

As more models are included in the net decision space and more training examples are added to the training set, a general approach like the one presented here reaches a stage where the net cannot learn new models or where training time can become very long (days of CPU time). For this reason, modular design can be very attractive. Smaller nets (the size of the net reflects the number of links) can be trained to recognize one model. The smaller nets can be integrated to act as a larger net. In such a design, training and modifications are applied only to those nets that do not perform well. **Fig. 14** is a schematic of this modular approach.

In this study, the well-test interpretation model was identified from the derivative plot only. We recommend use of the approach summarized here to identify the well-test interpretation model, or at least part of the interpretation model, from other diagnostic plots, such as the semilog graph. The neural net can be trained to recognize such significant features as those caused by phase segregation, skin, and stimulation. We also can train a net to recognize problems in the recorded data, such as those from leaks.

Artificial neural nets are computationally intensive, which implies that they require fast computers during training. In this study, we used a personal computer with a math coprocessor and a 20-MHz accelerator. The simulator was written in C, which allows dynamic memory allocation.

Conclusions

This paper presented a new approach, based on artificial neural nets, to identify a preliminary well-test interpretation model automatically from a derivative plot. This approach can be part of a well-test expert system or a computer-enhanced well-test interpretation.

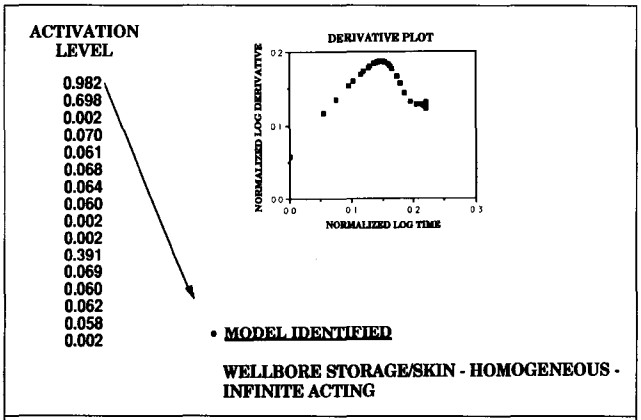

Fig. 9—Normalized derivative curve and activation levels in the output layer: Example 1.

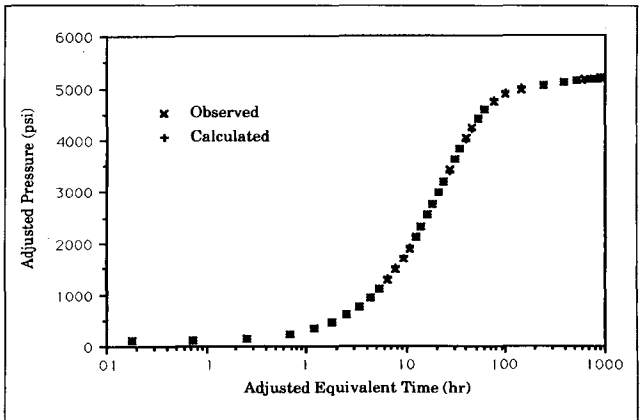

Fig. 10—Observed and calculated pressure data: Example 1.

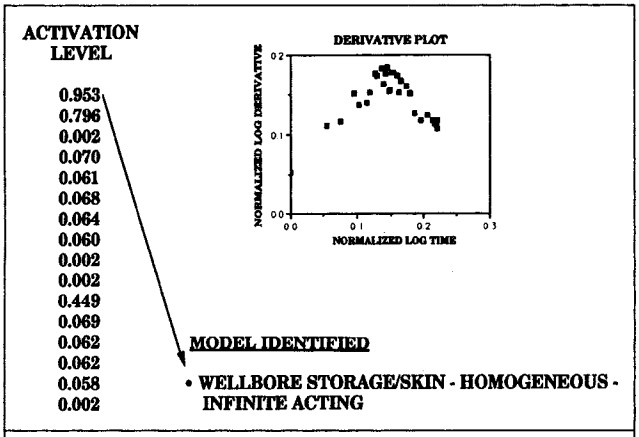

Fig. 11—Distorted normalized derivative curve and activation levels in the output layer: Example 1.

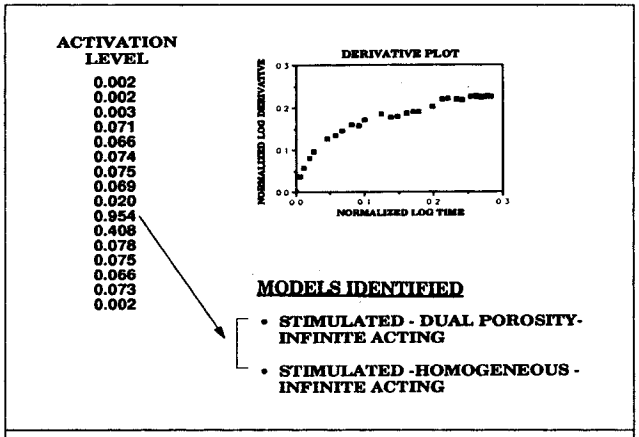

Fig. 12—Normalized derivative curve and activation levels in the output layer: Example 2.

Nomenclature

E = error
$f_k(I_k)$ = sigmoidal function derivative
I = input
n = number of iteration
O = calculated output
t = expected ouptut
w = weight
x_i = coordinate of the ith data point before normalization
y_i = coordinate of the ith data point before normalization
α = momentum
δ = derivative of E with respect to I (Eq. A-8)
η = learning rate constant
θ = threshold

Subscripts

i,j = layers
ij = between Layers i and j
ji = between Layers j and i
jk = between Layers j and k
kj = between Layers k and j
P = Pattern P

Superscript

$'$ = after normalization

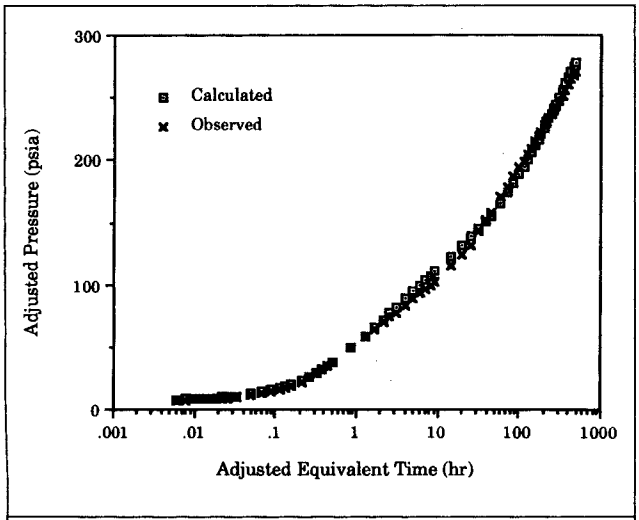

Fig. 13—Observed and calculated pressure data: Example 2.

Acknowledgments

We thank King Fahd U. of Petroleum & Minerals for scholarship support. We also thank the Crisman Inst. for Petroleum Reservoir Management at Texas A&M U. for supporting this research.

References

1. Clark, D.G. and Von Golf-Racht, T.D.: "Pressure Derivative Approach to Transient Test Analysis: A High-Permeability North Sea Reservoir Example," *JPT* (Nov. 1985) 2023.
2. Gringarten, A.C.: "Computer-Aided Well Test Analysis," paper SPE 14099 presented at the 1986 Intl. Meeting on Petroleum Engineering, Beijing, March 17–20.
3. Menke, W.: *Geophysical Data Analysis: Discrete Inverse Theory*, Academic Press Inc., New York City (1989).
4. Allain, O.F. and Horne, R.N.: "Use of Artificial Intelligence in Well-Test Interpretation," *JPT* (March 1990) 342.
5. Fu, K.S.: *Syntactic Pattern Recognition and Applications*, Prentice-Hall Inc., Englewood Cliffs (1982).
6. Stewart, G. and Du, K.F.: "Feature Selection and Extraction for Well-Test Interpretation Model Selection by an Artificial-Intelligence Approach," paper SPE 19820 presented at the 1989 SPE Annual Technical Conference and Exhibition, San Antonio, Oct. 8–11.
7. Pao, Yoh-Han: *Adaptive Pattern Recognition and Neural Networks*, Addison-Wesley Publishing Co., Reading, PA (1989).

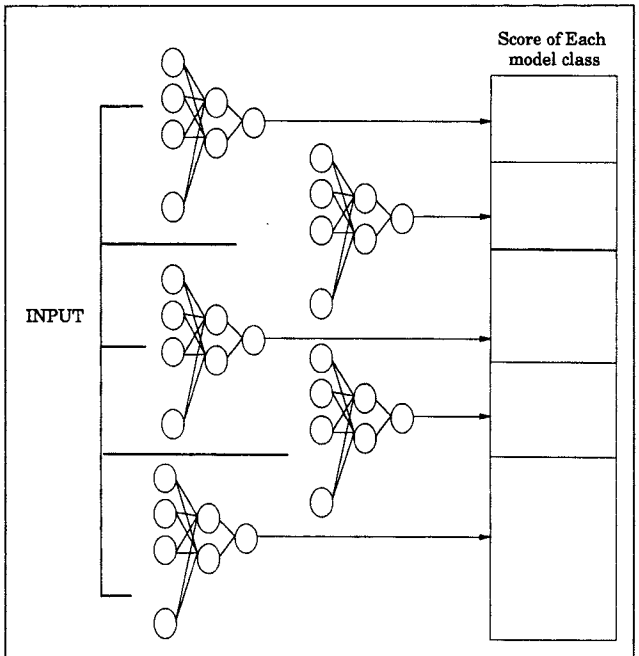

Fig. 14—Schematic of a modular recognition system with neural nets.

8. Wasserman, Philip: *Neural Computing: Theory and Practice*, Van Nostrand Reinhold Co., New York City (1989).
9. McClelland, J. and Rumelhart, D.: *Exploration in Parallel Distributed Processing: A Handbook of Models, Programs, and Exercise*, The MIT Press, Cambridge, MA (1989).
10. Rumelhart, D., McClelland, J., and the PDP Research Group: *Parallel Distributed Processing: Exploration in the Microstructure of Cognition-Foundation*, The MIT Press, Cambridge, MA (1986) Chap. 1.
11. Rumelhart, D., McClelland, J., and the PDP Research Group: *Parallel Distributed Processing: Exploration in the Microstructure of Cognition—Psychological and Biological Models*, The MIT Press, Cambridge, MA (1986) Chap. 2.
12. Al-Kaabi, A.U., McVay, D.A., and Lee, W.J.: "Using An Expert System To Identify the Well-Test Interpretation Model," *JPT* (May 1990) 654.

Appendix A—Algorithm Derivation

In this appendix, we summarize the mathematical derivation of the backpropagation learning algorithm.[7] Then we explain the step-by-step learning procedure. We use Fig. 1 to clarify the derivation procedure.

Backpropagation Learning Rule. The following derivation is for links connected to the outer layer (e.g., links between Layers i and k). Later, a similar derivation procedure will be used to derive an expression for changing weights in links not connected to the output layer (e.g., links between Layers i and j).

Define the net input to a node in Layer j from Pattern P as

$$I_{Pk}=\sum_j w_{jk}O_{pj}. \quad \text{(A-1)}$$

The output, O_{Pj}, from a node in the middle (hidden) Layer j because of Pattern P is defined as

$$O_{Pj}=1/[1+\exp(-I_{Pj})]. \quad \text{(A-2)}$$

Similarly, the output from a node in the output Layer k caused by Pattern P is defined as

$$O_{Pk}=1/[1+\exp(-I_{Pk})]. \quad \text{(A-3)}$$

Define error as

$$E=\frac{1}{2}\sum_P\sum_k (t_{Pk}-O_{Pk})^2. \quad \text{(A-4)}$$

The division by two is for mathematical convenience (as explained later, this 2 will be cancelled by a 2 that results from taking derivatives). Eq. A-4 is the objective function, which we will minimize during learning iterations.

Convergence (learning) is achieved by changing the weights by an incremental value, Δw_{ij}. This value is defined as proportional to E by

$$\Delta w_{kj}=-\eta(\partial E/\partial w_{kj}). \quad \text{(A-5)}$$

The derivative on the right side of Eq. A-5 can be written

$$\frac{\partial E}{\partial w_{kj}}=\frac{\partial E}{\partial I_{Pk}}\frac{\partial I_{Pk}}{\partial w_{kj}}. \quad \text{(A-6)}$$

By taking the derivative of Eq. A-1, we obtain

$$\frac{\partial I_{pk}}{\partial w_{kj}}=\frac{\partial \sum_j w_{kj}O_{Pj}}{\partial w_{kj}}=O_{Pj}. \quad \text{(A-7)}$$

Now, define

$$\delta_{Pk}=-(\partial E/\partial I_{Pk}). \quad \text{(A-8)}$$

By using Eqs. A-6 through A-8 in Eq. A-5, we obtain

$$\Delta w_{kj}=\eta\delta_{Pk}O_{Pj}. \quad \text{(A-9)}$$

Eq. A-7 gives the required weight change within a link between a node in Layer j and a node in the output Layer k. However, we need to find a computable form for δ_{Pk}. If we use the chain rule, we can write

$$\delta_{Pk}=-\frac{\partial E}{\partial I_{Pk}}=-\frac{\partial E}{\partial O_{Pk}}\frac{\partial O_{Pk}}{\partial I_{Pk}}. \quad \text{(A-10)}$$

From the definition of E (Eq. A-4), we obtain

$$\partial E/\partial O_{Pk}=-(t_{Pk}-O_{Pk}), \quad \text{(A-11)}$$

and, from the definition of O_{Pk} (Eq. A-3), we obtain

$$\partial O_{Pk}/\partial I_{Pk}=f_{Pk}(I_{Pk}), \quad \text{(A-12)}$$

where the right side of Eq. A-12 is the derivative of the squashing function. Substituting Eqs. 11 and 12 into Eq. A-10, we obtain

$$\delta_{Pk}=(t_{Pk}-O_{Pk})f_{Pk}(I_{Pk}). \quad \text{(A-13)}$$

Substituting Eq. A-13 into Eq. A-9, we obtain

$$\Delta w_{jk}=\eta(t_{Pk}-O_{Pk})f_{Pk}(I_{Pk})O_{Pj}. \quad \text{(A-14)}$$

Eq. A-14 gives the weight change in a link between Layer j and an output layer. η usually is called the learning rate and takes any value between 0 and 1. The higher the learning rate, the higher the weight changes. We recommend that the learning rate be kept at low values (e.g., 0.1 or 0.2) during early stages of learning and that it be increased as the net begins to converge.

A modified derivation procedure similar to the one outlined previously can be used to find an expression for the weight change in a link not connected to the output layer (e.g., links between Layers i and j). Δw_{ij} is defined as

$$\Delta w_{ij}=-\eta(\partial E/\partial w_{ij}). \quad \text{(A-15)}$$

The derivation that follows is similar to that for the case when the link is connected to the output layer.

$$\Delta w_{ij}=-\eta(\partial E/\partial I_{Pj})(\partial I_{Pj}/\partial w_{ij}) \quad \text{(A-16)}$$

$$=-\eta(\partial E/\partial I_{Pj})O_{Pi} \quad \text{(A-17)}$$

$$=\eta[-(\partial E/\partial O_{Pj})(\partial O_{Pj}/\partial I_{Pj})]O_{Pi} \quad \text{(A-18)}$$

$$=\eta[-(\partial E/\partial O_{Pj})]f_{Pj}I_{Pj}O_{Pi} \quad \text{(A-19)}$$

$$=\eta\delta_{Pj}O_{Pi}, \quad \text{(A-20)}$$

where $\delta_{Pj}=-(\partial E/\partial O_{Pj})f_{Pj}(I_{Pj})$. (A-21)

The partial derivative $\partial E/\partial O_{Pj}$ cannot be evaluated directly because E is based on output in the output layer only. Consider the following indirect approach:

$$-\frac{\partial E}{\partial O_{Pj}}=-\sum_k\frac{\partial E}{\partial I_{Pk}}\frac{\partial I_{Pk}}{\partial O_{Pj}}=\sum_k\left(-\frac{\partial E}{\partial I_{Pk}}\right)\frac{\partial}{\partial O_{Pj}}\sum_j w_{kj}O_{Pj}. \quad \text{(A-22)}$$

Recall that

$$-(\partial E/\partial I_{Pk})=\delta_{Pk}. \quad \text{(A-23)}$$

Substituting Eq. A-23 into Eq. A-22 and evaluating the partial derivative on the right side of Eq. A-22, we obtain

$$-(\partial E/\partial O_{Pj})=\sum_k\delta_{Pk}w_{kj}. \quad \text{(A-24)}$$

Substituting Eq. A-24 into Eq. A-21, we obtain

$$\delta_{Pj}=f_{Pj}(I_{Pj})\sum_k\delta_{Pk}w_{kj}. \quad \text{(A-25)}$$

Finally, substituting Eq. A-25 into Eq. A-20, we obtain

$$\Delta w_{ij}=\eta O_{Pj}f_{Pj}(I_{Pj})\sum_k\delta_{Pk}w_{kj}. \quad \text{(A-26)}$$

Eq. A-26 implies that the weight change in an internal link is based on the weight change in a higher layer (in this case, Layer k), which

Authors

Lee

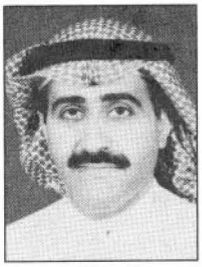

Al-Kaabi

W. John Lee holds the L.F. Peterson chair in Petroleum Engineering at Texas A&M U. He also is executive vice president of S.A. Holditch and Assocs. Previously, he was a technical adviser at Exxon Co. U.S.A. and a senior research specialist at Exxon Production Research Co. Lee holds BChE, MS, and PhD degrees in chemical engineering from Georgia Tech. He is a member of the Career Guidance and Archie Scholarship committees and the Emerging/Peripheral Technical Committee. Lee is a Distinguished Service Award winner and a member of the National Academy of Engineering. Abdul-Aziz U. Al-Kaabi is assistant professor and head of the Petroleum Engineering Section at King Fahd U. of Petroleum and Minerals (KFUPM) Research Inst. He holds BS and MS degrees in petroleum engineering from KFUPM in Dhahran, Saudi Arabia, and a PhD degree in petroleum engineering from Texas A&M U.

also shows that the error is propagated from the output layer back to all the links in the net. In the next section, we describe the step-by-step training procedure using a backpropagation algorithm as the learning rule.

Appendix B—Training Procedure

The following procedure is used to train a neural net with backpropagation as the learning algorithm.

1. Define a maximum node error (large negative number).
2. Randomize the weights in all the net links.
3. Select a pattern from the training set (a pattern includes input and output pairs).
4. Evaluate the outputs at the output layer by propagating the input from the input layer to the output layer in a feed-forward manner.
5. Calculate the error at the output layer. If the node error is larger than the maximum error, set the maximum error equal to the node error. Repeat for all nodes in a feed-forward manner.
6. Use the backpropagation procedure described in Appendix A to calculate the amount of weight change required in each link because of the current pattern. Do not apply any changes to the links yet.
7. Repeat Steps 3 through 6 until the net has been presented with all the patterns in the training set. During this process, accumulate the weight changes in each link caused by the different patterns. When the net is given all the examples in the training set, use the cumulative weight change for each link to change the weight of that link.
8. Evaluate errors at the output layer. If the maximum error is less than the desired error, stop; otherwise, repeat Steps 3 through 7.

Appendix C—Practical Considerations

The shape of the squashing function can be changed to increase the convergence rate for certain problems:[7]

$$O_{Pk}=\frac{1}{1+\exp[(-I_{Pk}+\theta_k)/\theta_0]}. \quad \ldots\ldots\ldots\ldots\ldots\ldots\ldots\ldots (C\text{-}1)$$

θ_k is a bias parameter. If θ_k is positive, the squashing function is shifted to the left, whereas if θ_k is negative, the squashing function is shifted to the right along the horizontal axis. The parameter θ_0 is always positive and modifies the shape of the function. Large values of θ_0 result in a gently increasing function; low values of θ_0 result in a steeper function. The parameter θ_0 can be fixed for all the net nodes or can be variable.

Another popular modification to increase the learning rate of the backpropagation algorithm is the use of a momentum term. The change in the link weight with the momentum term added is defined as[7]

$$\Delta w_{ij}(n+1)=\eta\delta_{Pk}O_{Pj}+\alpha\Delta w_{ij}(n), \quad \ldots\ldots\ldots\ldots\ldots\ldots\ldots\ldots (C\text{-}2)$$

where α takes values between 0 and 1.

SI Metric Conversion Factors

bbl	×	1.589 873	E−01	= m^3
cp	×	1.0*	E−03	= Pa·s
cycles/sec	×	1.0*	E+00	= Hz
ft	×	3.048*	E−01	= m
ft^3	×	2.831 685	E−02	= m^3
psi	×	6.894 757	E+00	= kPa

*Conversion factor is exact.

SPEFE

Original SPE manuscript received for review June 25, 1990. Revised manuscript received Jan. 19, 1993. Paper accepted for publication Sept. 1, 1992. Paper (SPE 20332) first presented at the 1990 SPE Petroleum Computer Conference in Denver, June 25–28.

Discussion of Using Artificial Neural Nets To Identify the Well-Test Interpretation Model

Kacheong Yeung, SPE, U. of Alberta, **Chayan Chakrabarty**, SPE, Golder Assocs. (U.K.) Ltd., and **Sherman Wu**, U. of Melbourne

Use of artificial neural nets (ANN's) to identify noisy and apparently unrecognizable patterns is common for many real-world problems, ranging from applications such as speech recognition to stock-market prediction. ANN approaches are often good candidates for recognizing patterns when rigid mathematical models do not exist or are insufficient to meet a full-scale identification requirement. Al-Kaabi and Lee's[1] proposal of using ANN's to identify the well-test interpretation model is appropriate because well-test data is often highly nonlinear and noisy. The purpose of this discussion is to present some of our results in a similar study and to suggest a simple technique that would enhance the use of ANN's in Al-Kaabi and Lee's approach.

The idea behind an ANN is quite simple: it is a program that classifies samples (patterns) by adjusting its parameters repeatedly until all the samples are correctly classified. When a large number of samples are used in the process (training), a test pattern can be identified if it resembles one of the training samples. However, if the test pattern does not resemble any of the training samples, the neural net would not classify the pattern in the corresponding class.

One of the main problems in interpreting well-test data with ANN's is that, for a particular model, we do not know when the pattern begins and when it ends, let alone the various parameters (k, C_D, s, etc.) that control the pattern shape. Because of this, even one model (with the same reservoir parameters) would require many samples of different beginning and endpoints to identify its class. Al-Kaabi and Lee introduced the scaling of the following forms to reduce this effect.

$$x_i' = \frac{x_i}{\sqrt{\sum (x_i)^2}} \quad \text{..... (D-1)}$$

$$\text{and } y_i' = \frac{y_i}{\sqrt{\sum (y_i)^2}}. \quad \text{..... (D-2)}$$

They further attempted to reduce the sensitivity to pattern size by training the same samples with different sizes, which is done by dividing the data points on the x and y axes after normalization by constant factors (e.g., by 2 and 3). However, we found this scaling method to be undesirable in our neural-net program. To illustrate this, consider a hypothetical well-test response model, Model A (**Fig. D-1**). The model has two similar patterns, one smaller in size with longer beginning and ending positions as compared with the other. Using the scaling method Al-Kaabi and Lee proposed, we obtain scaled versions of the two patterns (**Fig. D-2**). We see that after scaling, the shapes have been altered considerably. Thus, if Pattern 1 was used as a training set for Model A, the neural net probably would not identify Pattern 2 as Model A. The long beginning and ending positions of Pattern 2 shrink the shape relative to Pattern 1 because of the scaling used. Another consequence of the scaling that Al-Kaabi and Lee suggested is that the pattern spans are different. To eliminate this effect, we suggest normalization between 0 and 1; i.e.,

$$x_i' = \frac{x_i - x_{\min}}{x_{\max} - x_{\min}} \quad \text{..... (D-3)}$$

$$\text{and } y_i' = \frac{y_i - y_{\min}}{y_{\max} - y_{\min}}. \quad \text{..... (D-4)}$$

This will ensure that all scaled patterns have the same spans in the x and y directions. However, this still does not solve the problem of shrinking (or expanding) a pattern having longer (or shorter) beginning and ending positions.

A widely applicable technique for efficient algorithms is the "divide-and-conquer" strategy, which consists of breaking a larger problem into smaller problems in such a way that, from the combined solutions to the smaller problems, one can easily construct a solution to the entire problem. In Fig. D-1, Model A has four distinct parts (two horizontal lines and two slope lines). If we modify Eq. 3 to be

$$x_i' = \frac{x_i - x_{\min}}{x_{\max} - x_{\min}} \left(\frac{1}{n}\right), \quad \text{..... (5)}$$

where n is the number of subparts, the resulting scaling of patterns in Fig. D-1 is identical (**Fig. D-3**). Here, we let $y_i'=0$ when the denominator becomes 0 in Eq. 4. From Fig. D-3, we see that if Pattern 1 is used as the training set for Model A, the neural net also can identify Pattern 2 as Model A because the scaled versions of the patterns are identical. For the well-test data, the natural divisions of subparts would be the local minima and maxima of the derivative plots.

In our study, we trained the ANN's with typical well-test models, such as infinite-acting homogeneous and double-porosity formations with and without wellbore storage and skin, etc. We found that

(28151)

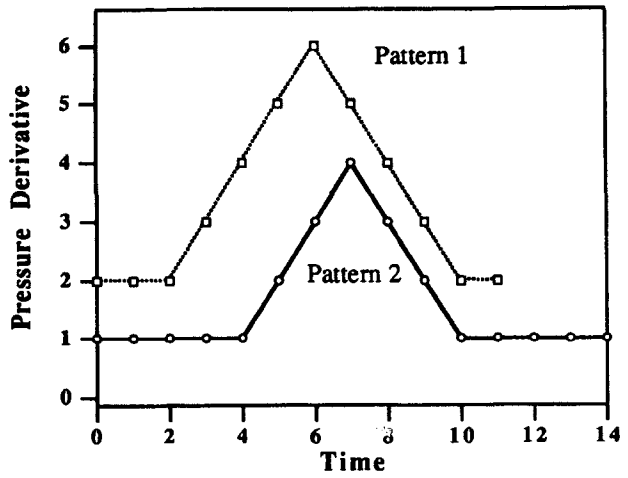

Fig. D-1—Two original patterns for Model A.

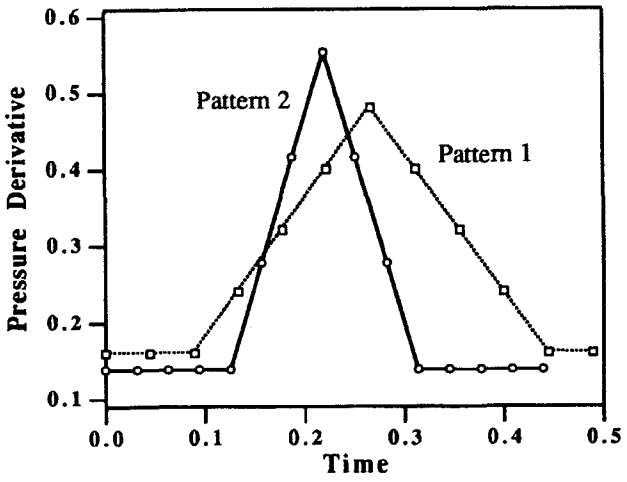

Fig. D-2—Two scaled patterns for Model A (Al-Kaabi and Lee's approach[1]).

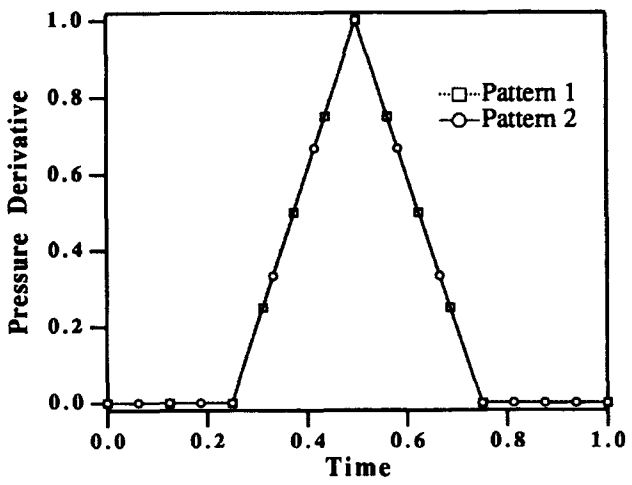

Fig. D-3—Two scaled patterns for Model A (divide-and-conquer approach).

after we had trained the ANN's for a particular well-test model, using Al-Kaabi and Lee's scaling approach, when the same well-test data was truncated by ≈5% of the original data, the ANN's would fail to identify the model. However, with our scaling approach, the truncation has little or no effect on model identification, unless the truncation was so large that a subpart of the pattern was truncated. Thus, using this proposed method of scaling, the training set is reduced significantly. And, as illustrated in our simple hypothetical example, it is more accurate and reliable.

As a final note, other ANN's are more efficient than the backpropagation neural network. For example, we have also programmed this problem with an adaptive logic network (ALN) with a unary encoding scheme; the ALN decreased the training time to minutes instead of the days needed for backpropagation. Other networks, such as the self-organized neural network, are also good candidates.

Acknowledgments

We thank W.W. Armstrong, U. of Alberta, for providing his ALN software, and Yun Wang, who programmed the ALN for the problem.

Reference

1. Al-Kaabi, A.U. and Lee, W.J.: "Using Artificial Neural Nets To Identify the Well-Test Interpretation Model," *SPEFE* (Sept. 1993) 233; *Trans.*, AIME, **295**.

(SPE 28151) **SPEFE**

Authors' Reply to Discussion of Using Artificial Neural Nets To Identify the Well-Test Interpretation Model

Abdulaziz U. Al-Kaabi, SPE, King Fahd U. of Petroleum & Minerals, and **W. John Lee,** SPE, Texas A&M U.

We thank Yeung *et al.* for their discussion[1] about our paper.[2] We agree with Yeung *et al.* that their proposed scaling method (see Eq. 5 in Ref. 1), when applied to patterns with distinct subparts such as the one shown in their Fig. D-1, represents an improvement on the method we proposed. This is particularly true because Yeung *et al.*'s method eliminates the need to train the artificial neural networks (ANN's) on different sizes (scales) of the same pattern of a specific interpretation model. We present the following comments for discussion and suggestions and for further improvement.

1. Yeung *et al.*'s scaling method requires that the number of subparts (segments) of the derivative curve, for which the well-test model will be recognized by a trained ANN, be identified before normalizing and scaling the derivative plot. Deciding on the number of such subparts in derivative plots generated from field well-test data can be difficult and subjective because of noise and interpreter bias. The outcome of pattern scaling will depend on the number of subparts used. The motivation behind using ANN's to identify a preliminary well-test model is to present a method without any interpreter subjectivity or bias.

To minimize such subjectivity in determining the number of subparts that reasonably subdivide a derivative plot, as proposed by Yeung *et al.*, we suggest looking at algorithms, such as the split-and-merge algorithm.[3,4] The objective of the split-and-merge algorithm is to find the minimum number of segments in a plot where, on each of the segments, the data points are approximated by a piecewise linear function with an error norm less than a prespecified quantity. Nonlinear functions can also be used in the previously mentioned algorithm to approximate each segment. It is important to realize that the segmentation that is produced by the split-and-merge algorithm depends on a prespecified error tolerance. Such an approach can give undesirable results when the derivative plot is noisy.

2. Yeung *et al.*'s proposed method assures that all normalized derivative plots of a specific well-test model will be identical only if the corresponding segments of the derivative plots have the same slopes and if the same number of subparts is used to normalize and scale each plot. The normalized and scaled plots using Yeung *et al.*'s method are not identical for similar models if the slopes of the subparts (segments) of their derivative plots are different. This difference in slopes could indicate the need to train the ANN's on more patterns to capture this variation in slopes. Otherwise, the learning may not be general.

The combined effect of using a different number of subparts in scaling patterns of similar models and having corresponding segments of different slopes could be significant. Understanding the extent of such an effect requires further investigation.

References

1. Yeung, K., Chakrabarty, C., and Wu, S.: "Discussion of Using Artificial Neural Nets To Identify the Well-Test Interpretation Model," *SPEFE* (June 1994).
2. Al-Kaabi, A.U. and Lee, W.J.: "Using Artificial Neural Nets To Identify the Well-Test Interpretation Model," *SPEFE* (Sept. 1993) 233; *Trans.*, AIME, **295**.
3. Pavlids, T. and Horowitz, S.L.: "Segmentation of Plane Curves," *IEEE Trans. on Computers* (Aug. 1974) **c-23**, No. 8, 860.
4. Al-Kaabi, A.U.: "Artificial Intelligence Approach to the Identification of the Well Test Interpretation Model," PhD dissertation, Texas A&M U., College Station (May 1990) 79.

(28165) **SPEFE**

Discriminant Analysis and Neural Nets: Valuable Tools To Optimize Completion Practices

Gerrit Nitters, SPE, Shell Intl. Petroleum Mij. and **D.R. Davies,** SPE, and **W.J.M. Epping,**
Koninklijke/Shell E&P Laboratorium

Abstract

This paper describes the application of multi-variate statistical techniques, discriminant analysis and neural networks in identifying drilling and other completion practices that impact on well productivity. Discriminant analysis determines whether a well can be assigned to a group of wells, on the basis of a number of common characteristics and using linear multivariate correlations. Neural nets enable the use of nonlinear correlations for such a classification.

In this study, 47 gas wells from two fields were classified into three groups:

Group 1: no production;

Group 2: production below 5900 std m^3/h (5 MMscf/D);

Group 3: production over 5900 std m^3/h (5 MMscf/D).

The variables used in the discriminant analysis included parameters such as completion type, total height of the perforated interval, mud weight, drawdown during perforation, type of mud and perforation size.

The study has identified and, to some extent, quantified those parameters that either adversely or favourably affect well productivity. The results can be used to adjust operational procedures to maximize well productivity. The parameters identified as increasing productivity reflect, for the most part, sound engineering practices.

Application of neural nets enables further quantification of the effects of petroleum engineering parameters on well productivity and is being developed to make it possible for the most economical preventive and remedial measures to be selected.

However, statistical techniques are applicable only when a sufficiently large data base is available, i.e., they are suitable for reasonably large and fairly mature fields and/or areas.

Introduction

Probably several thousand stimulation treatments are carried out each year with a total expenditure of many millions of US dollars. The prerequisites for successful stimulation are simple:

1. Does the reservoir contain sufficient amounts of hydrocarbons?
2. Are reservoir pressure and permeability high enough to move the hydrocarbons from the reservoir towards the wellbore?

In other words there should be a clear indication that substantial gains are possible, i.e., enough producible hydrocarbons should be present to justify the treatment for a particular well. This holds for both fracturing and matrix treatments.

Hence, the selection of candidates for stimulation treatments requires knowledge about the general performance of oil and gas wells in specific fields or areas. A stimulation campaign should start with the identification of field-wide trends with respect to production-impairing mechanisms, using a statistical evaluation of field data. At the same time, such a statistical approach can, and often will, produce correlations between the productivity in a field and specific drilling and completion parameters. This is very useful, for instance, in identifying those practices that will prevent impairment in future wells.

Even so, the use of statistical techniques is not very popular in petroleum engineering. Only a small number of authors have applied statistics. King *et al.*[1], for instance, derived graphical correlations, based on field data, between permeability, underbalanced perforating pressure and acidization results. Gidley[2] developed design guidelines for mud acid treatments using simple univariate correlations between job result and individual parameters such as permeability and acid volume. More sophisticated techniques, aimed at developing complex correlations between the various parameters, have been rarely used. This is partly because extensive data bases, necessary for such statistical methods, are rarely available.

However, nowadays the widespread application of computers to routine operations calls for the creation of field company-wide data bases. This, coupled with the easy availability of the necessary statistical packages and cheap, powerful computer hardware, enables the routine application of such powerful statistical techniques to petroleum engineering.

Copyright 1995 Society of Petroleum Engineers

Original SPE manuscript received for review April 8, 1991. Revised manuscript received Nov. 9, 1994. Paper peer approved Dec. 19, 1994. Paper (SPE 21699) first presented at the 1991 SPE Production Operations Symposium held in Oklahoma City, April 7–9.

Discriminant Analysis

Discriminant analysis[3] is a powerful multivariate technique for the analysis of data. The analysis determines whether a particular case can be assigned to a group of cases based on a number of common characteristics. In essence, discriminant analysis determines, in the case of N groups, (N-1) linear functions between the parameters, with the general form:

$$F_n(x) = A_n{*}x_1 + B_n{*}x_2 + ...+ M_n{*}x_m + \text{constant};\ \ n=1,...,N-1$$

The value of the functions $F(x)$ for each individual case is called the discriminant score. These values determine whether a case belongs to group 1, 2, etc. In practice, the number of groups is usually restricted to two or three. This technique is often applied in other sciences such as medicine or economics. One example, related to the oil industry, is a publication by Noble,[4] in which he classified acquiring and acquired oil companies, on the basis of a number of economic yardsticks. With this technique he was able to identify consistent differences between these two types of companies. His study showed that acquiring companies are characterised by a number of factors including high asset utilisation and rapid inventory turnover. Acquired companies, however, typically had low finding costs and greater future cash flow potential.

In this paper we will demonstrate the use of discriminant analysis in petroleum engineering by describing its application to a number of gas fields. Previous studies of the area under consideration showed that a variety of factors influenced the performance of the wells. No simple bivariate correlation could be determined between the many variables involved using standard spread-sheet/cross-plot methods. It was therefore decided to carry out a discriminant analysis to identify groups of producing zones based on available reservoir, drilling and production data. To this end the producing zones were classified into three groups, designated by a production indicator:

Group 1: no production;

Group 2: production less than 5900 std m^3/h (5 MMscf/D);

Group 3: production 5900 std m^3/h (5 MMscf/D) or more.

The variables included in the analysis are listed in **Table 1.** Parameters such as porosity and permeability could not be included owing to lack of detailed zone-by-zone data. As a consequence, the effect of reservoir parameters on productivity cannot be extracted from the present study. This is a major limitation since we have, essentially, been forced to assume a fairly uniform permeability, etc., for the wells. Hence, the correlations found are valid strictly for the data sets under study only.

TABLE 1—PARAMETERS INCLUDED IN THE DISCRIMINANT ANALYSIS

Parameter	Name*
Completion type, i.e. perforated or gravel-packed completion	TYPE
Length of the perforated interval	PERFL
Total height of the producing interval	HEIGHT
Well deviation	DEV
Overpressure gradient of the completion fluid	OPGRAD
Under- or overbalance pressure during perforation	DD
Exposure time of the producing interval to completion fluid	EXPOTC
Exposure time of the producing interval to mud	EXPOTM
Overpressure gradient of the mud	MGRAD
Average depth of the producing interval	PERFD
Whether the producing interval was treated with acid	ACID
Type of mud, i.e. Resinex lignosulfonate (RLS) mud (1), inverted oil emulsion mud (2) or chalk mud (3)	MTYPE
Perforation size	PERFS
Perforation phasing	PERFPH
Perforation density	SPF

* Names of variables used in the computations

Input Data

The input data were obtained from a data base that covered two rather similar fields, designated field A, comprising 35 producing zones, and field B, with 12 producing zones. On average, the wells in field B tended to produce at somewhat higher rates than those in field A.

Two discriminant analyses have been performed: one for field A only and one for the combined data from fields A and B together. Missing values with regard to formation exposure times to completion fluid and/or drilling mud were set at the average value for the complete data set. Missing values for the completion fluid overpressure gradient were set at the value indicated for other zones in the same well. Clearly, these omissions affected the analysis, but are typical of the problems to be overcome by an engineer in carrying out such an analysis.

The reliability of multivariate analysis depends on the individual parameters being independent of each other. If dependent variables are included in the analysis, the resulting discriminant scores may become unrealistic and misleading. Univariate scouting analyses for the present study showed a strong correlation between:

(i) the length of the perforated interval and the net formation height;

(ii) well deviation and the exposure time to both mud and completion fluid, although this was less significant.

To avoid any erroneous results arising from the inclusion of such cross-correlated variables, both the length of the perforated interval and the well deviation were excluded from the final analysis.

Furthermore, in the final analysis, only those parameters that have a significant effect on the separation of the groups, and hence on the correctness of the classification, are used. The computer package used has a number of options for doing this automatically.

Results

Field A. The results of the analysis are depicted in **Figs. 1 - 3.** Fig. 1 shows the "territorial map". For each case (i.e., producing zone) two discriminant scores can be calculated using the two discriminant functions determined in the analysis.

$$\text{Score 1} = 0.0325*HEIGHT - 0.000422*DD + 0.0184*EXPOTC + 0.0035*EXPOTM + 9.548*MGRAD - 0.000436*PERFD - 1.74*ACID + 1.247*MTYPE - 0.593$$

$$\text{Score 2} = -0.0273*HEIGHT + 0.00029*DD + 0.0282*EXPOTC + 0.0846*EXPOTM + 0.284*MGRAD + 0.000637*PERFD - 1.212*ACID + 0.914*MTYPE - 6.971$$

A case (producing zone) is classified as a nonproducer (group 1), a moderate producer (group 2) or a good producer (group 3), depending on the coordinates (= score 1, score 2) in the territorial map.

The magnitude of the correlation coefficients for the individual parameters in the discriminant function is misleading as far as the relative importance of each parameter is concerned, since this value is influenced by the units and magnitude of the parameter itself. To correct for this effect, the coefficients are standardised by normalising the values for the parameters to a mean of 0 and a standard deviation of 1. By plotting these standardized coefficients as vectors originating from the total average score, an indication of the relative effect of each individual parameter on the discriminating variable (here the productivity) is obtained. Likewise, the effect of a particu-

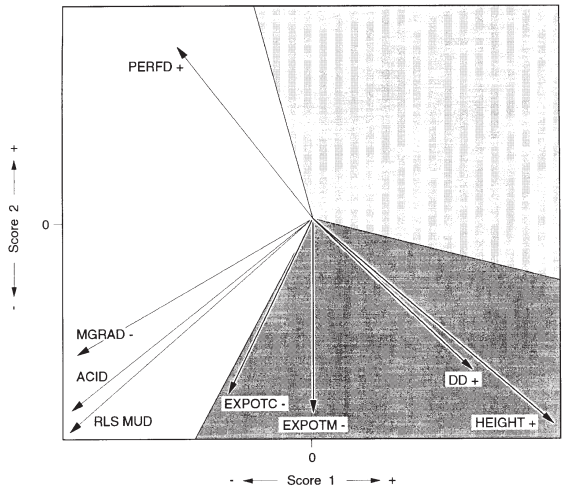

Fig. 1—Territorial classification map of field A data, indicating the effect of individual parameters.

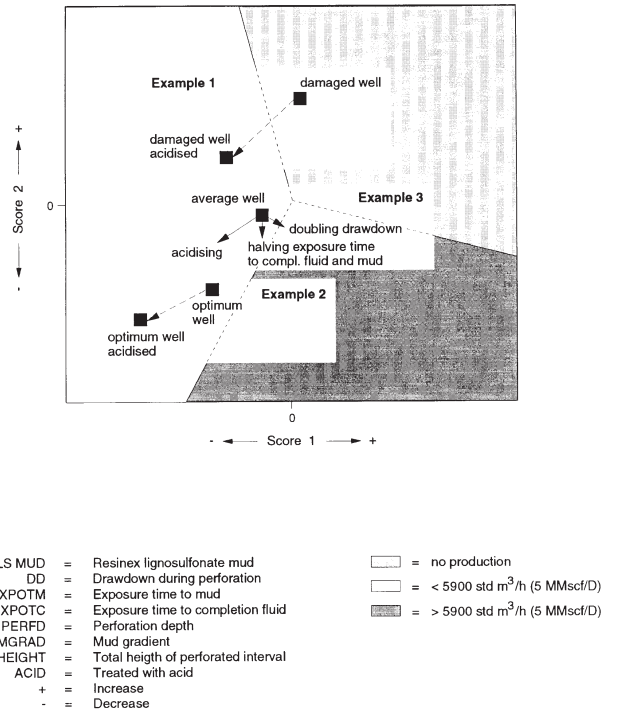

Fig. 2—Effect of individual actions on well productivity (field A)

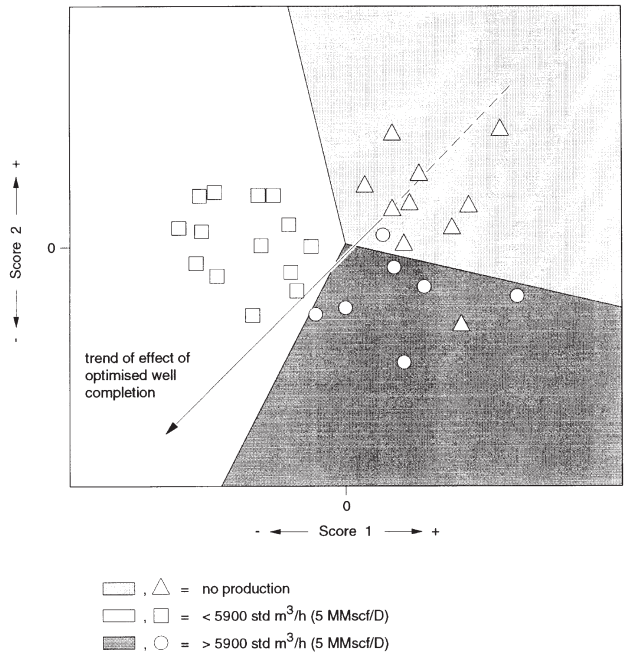

Fig. 3—Classification map of field A data indicating the overall effect of optimized well completion.

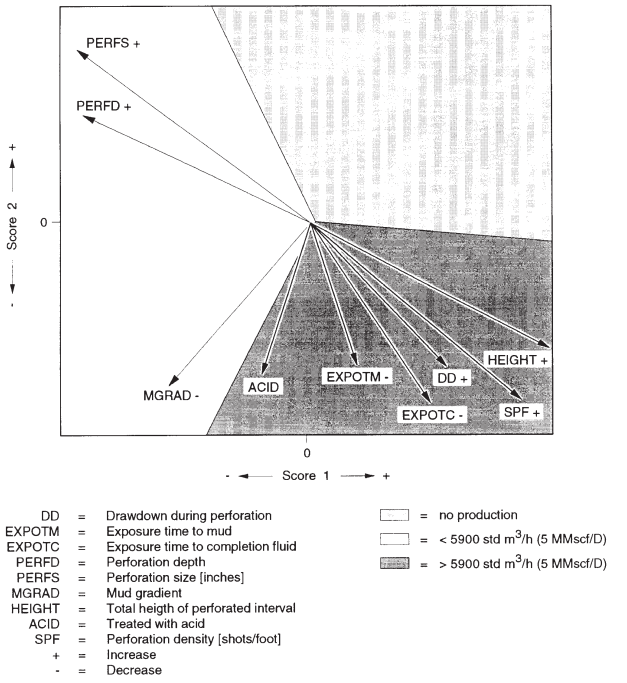

Fig. 4—Classification map of combined fields A and B data indicating the effect of individual parameters.

lar variable on an individual well may be evaluated by drawing the corresponding vector from the coordinates of that well. Although this is not strictly in line with the principle of multivariate statistics, it helps us to visualize and interpret the analysis results. Three examples are shown in Fig. 2:

1. Case 1, a nonproducer is shifted to being a moderate producer by acidizing;
2. Case 2, a (hypothetical) well with optimum productivity is unlikely to improve significantly in productivity by acidizing;
3. Case 3, an average well showing the relative effects of acidizing, doubling the drawdown during perforation and halving the exposure time to mud and completion fluid (by drilling and completing more quickly).

Combining all vectors into one yields the trend (here the overall effect of all drilling and completion parameters on the productivity). This is depicted in Fig. 3.

As is shown in Fig. 3, the application of the discriminant functions for all examined producing zones yields a very good separation of the cases: 91% of all cases are classified correctly, i.e., 3 misclassifications out of 35 cases included in the analysis. Decreasing the number of parameters included in the analysis significantly reduced the success in correctly classifying the wells. Statistically, the number of variables is not excessive in relation to the number of cases.

Fields A and B Combined. The above procedure was also applied to the combined data from fields A and B.* Using the same variables as for field A alone yielded a poorer classification: some 79% of all cases could be classified correctly. However, by including perforation size and shot density in the analysis, a better classification is obtained: 83% correctly classified (8 out of 47 cases are misclassified). This suggests some fundamental differences between the two data sets, for instance, optimum wellbore/reservoir communication is more essential in field B than it is in field A, because the average permeability of field B could be significantly higher than that of field A.

The results are summarised in **Figs. 4 and 5,** these showing the territorial maps with the effects of individual variables (Fig. 4) and the overall trend (Fig. 5). To enable a proper comparison of the two analyses, the data set of field A was also evaluated using the same variables as for the combined case. These results are summarised in **Figs. 6 and 7.** Note that the classification is only marginally less accurate than that obtained previously: 4 misclassifications out of 35 cases instead of 3.

*The data set of field B alone (12 cases) was too small for a meaningful analysis.

Discussion

Field A. From Fig. 1 it may be concluded that, for a particular well or producing zone to be a moderate producer or better (i.e., belong to group 2 or 3), scores 1 and 2 should not both be positive (roughly). Classification in group 2 or 3 is, not surprisingly, favoured by a large formation height. What is somewhat less obvious is that small variations in reservoir depth have a significant effect on the productivity. This is likely to be related to the normally observed decrease in permeability with increasing depth. This effect may be reinforced by these completions being near the porosity/permeability cut-off

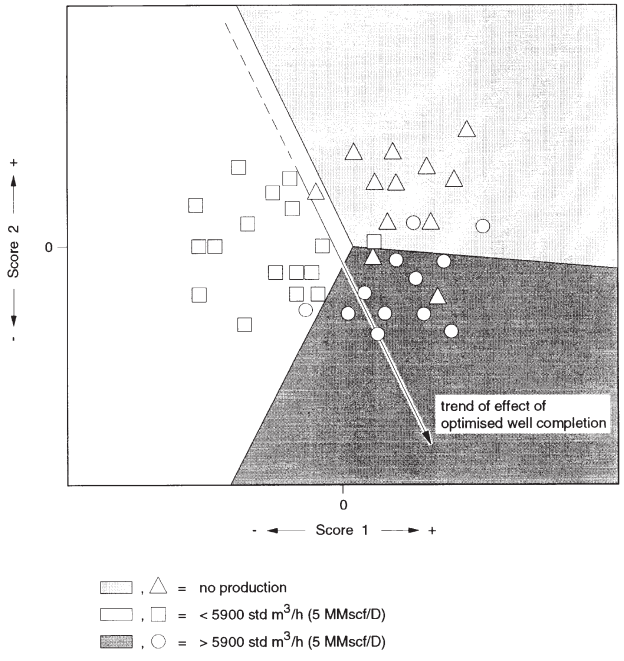

Fig. 5—Classification map of combined fields A and B data indicating the overall effect of optimized well completion.

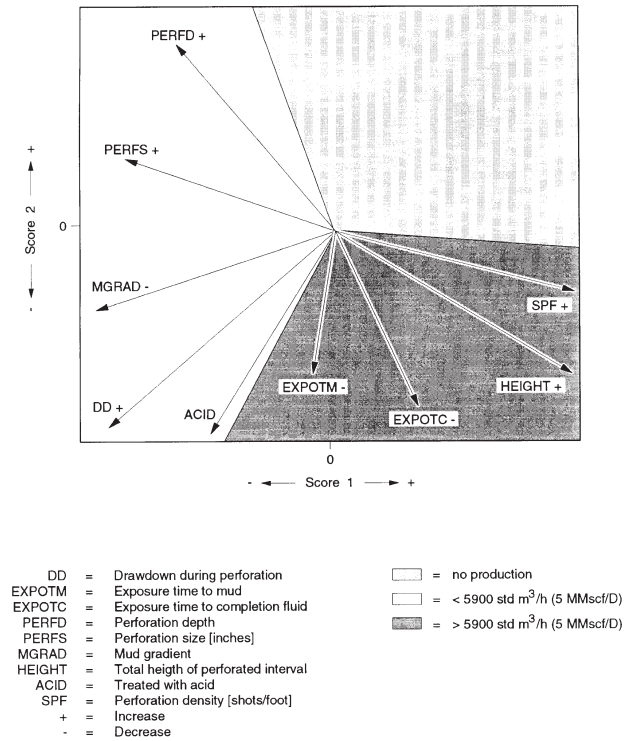

DD = Drawdown during perforation
EXPOTM = Exposure time to mud
EXPOTC = Exposure time to completion fluid
PERFD = Perforation depth
PERFS = Perforation size [inches]
MGRAD = Mud gradient
HEIGHT = Total heigth of perforated interval
ACID = Treated with acid
SPF = Perforation density [shots/foot]
\+ = Increase
\- = Decrease

= no production
= < 5900 std m^3/h (5 MMscf/D)
= > 5900 std m^3/h (5 MMscf/D)

Fig. 6—Classification map of field A data indicating the effect o individual parameters (the same parameters as used for the combined data for fields A and B).

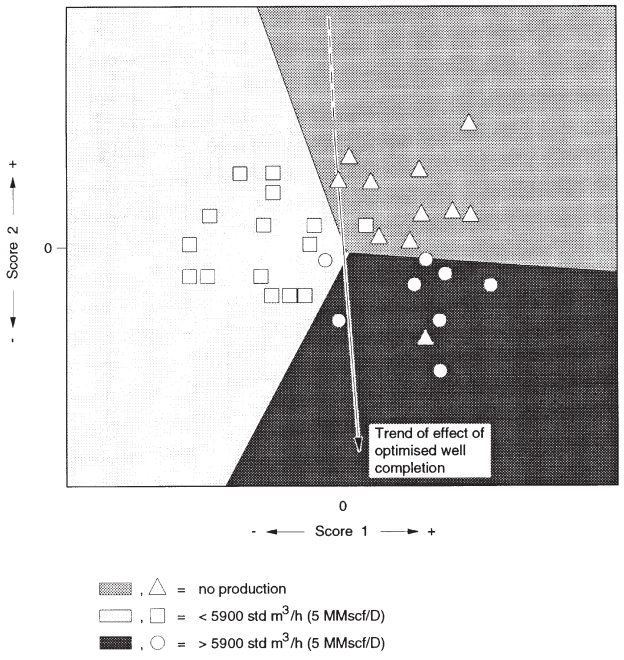

, = no production
, = < 5900 std m^3/h (5 MMscf/D)
, = > 5900 std m^3/h (5 MMscf/D)

Fig. 7—Classification map of field A data based on the same pa rameters as used for the combined field A and B data.

for economic production. However, given a certain height and depth (variables which, after all, are beyond the control of the completion engineer) production is further stimulated by keeping the exposure times to both mud and completion fluids as short as possible, and these fluids should have a minimum overbalance compared with the formation fluid gradient. Group 1, nonproducers, tend to result from long exposure times to drilling and completion fluids with a high overbalance. Thus, a requirement to drill zones with a higher pressure gradient in the same openhole section, for instance, will reduce the potential productivity of completions in formations with a lower pressure gradient. This was current practice in the field under study.

Some other important observations that can be made are (see Fig. 2):

1. The "average" producing interval (case 3) in field A is classified as a fair producer, and in the territorial map is just inside group 2. This agrees with the actual average of 5200 std m^3/h (4.4 MMscf/D).

2. The "optimum" zone (case 2) lies close to the borderline between groups 2 and 3, albeit it is just in group 3.

3. Neither acidizing, nor increasing the perforation drawdown, nor reducing the exposure times to mud and completion fluids will change this situation significantly. Apparently, the "natural" productivity is around 5900 std m^3/h (5 MMscf/D). This implies that any significant improvement of the production above that level may require hydraulic fracturing, rather than acidization.

4. Wells or zones such as case 1, which have been damaged by adverse drilling and completion practices, benefit from acidizing. This non-producer can be converted into a fair producer by such a treatment. Acidization affects both classification functions to roughly the same degree: it tends to shift both scores to smaller or negative values. Hence, acidizing, as currently applied in the area, tends to convert nonproducers into group 2 producers, but has little effect on wells or zones that already belong to group 2 before acidizing.

5. Likewise, the use of Resinex lignosulfonate (RLS) mud reduces the likelihood of a zone becoming a nonproducer, but does not significantly increase the probability of its being classified as a good producer. This particular mud system gives a thin mudcake and is, apparently, more beneficial in protecting the formation from in-depth permeability damage than the other mud systems used in field A.

Fields A and B Combined. Extending the data set by including the data from field B resulted in a (marginally) less accurate classification. As indicated, this is probably because of differences in reservoir properties. These were not available on a zone-by-zone basis and, hence, could not be included in the analysis. Nevertheless, a reasonable classification is obtained (83% correct) by incorporating perforation data.

Now, the "average" zone is classified as a good producer (actual production just over 5900 std m^3/h (5 MMscf/D). A larger percentage of the wells produce at a higher rate, i.e., are group 3 producers. As a result, the optimization of all factors that affect the productivity, such as drawdown during perforation and exposure time to mud and completion fluid, tends to shift the average well or zone further into group 3, rather than into group 2 as is the case for field A alone. In particular, high perforation density, for instance, as is obtained by the use of tubing-conveyed guns, promotes classification into group 3 (see Fig. 4). Apparently, in the combined case the production of a number of wells is restricted by the reservoir/wellbore communication, i.e., the number of open perforations. This explains why an "optimum" well in the combined study will most likely produce more than 5900 std m^3/h (5 MMscf/D) (see Fig. 5).

The application of the same variables to field A alone yields a classification of 88% correct. The effect of increasing shot density, i.e., better wellbore/reservoir communication, is less pronounced. In other words the inclusion of perforation data has a limited (detrimental) effect on the confidence of the classification of field A wells. Still, the overall trend has shifted somewhat towards group 3 (Fig. 7). Hence, increasing the perforation density might have some effect, but, in view of the reduced confidence, more drastic measures—such as hydraulic fracturing—may be required to achieve significantly higher productivities.

Neural Networks

The same data have also been used in an investigation in which a neural network approach[5] was followed. In the past, for instance, neural networks have been applied to identify suitable well test interpretation models based on pattern recognition[6].

Neural networks are a new and promising tool for a large variety of data-analysis procedures. A neural net consists of a number of connected processing units or neurodes, each of which performs a nonlinear transformation on its inputs. Often the neurodes are organised into distinct layers, i.e., input, hidden or associative, and output layers. When the layers are connected in a "feedforward" way

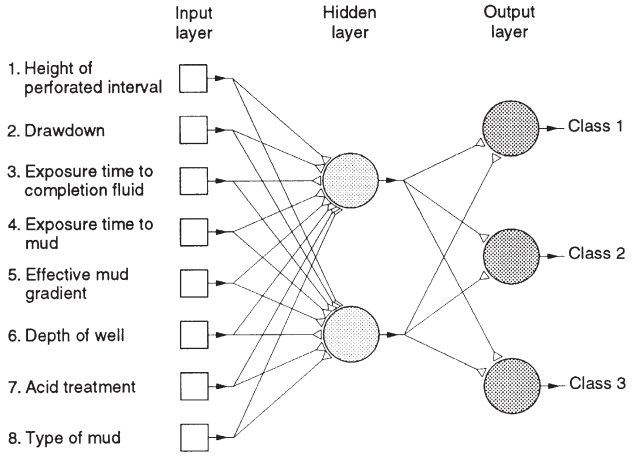

Fig. 8—Neural network for gas-well classification. Number of neurodes: $N_i = 8$, $N_h = 2$, $N_o = 3$. Weights are represented by open triangles.

(so that signals are passed from input to hidden to output layers without feedback or communication within a layer), the net is called a multi-layered perceptron (MLP). The importance of a particular connection is indicated by its weight, which may be positive or negative. Neural nets are powerful because of their self-organising capability. In the training phase a number of examples that are representative of the problem to be learned are provided to the net. By adapting its weights, the net learns the desired input-output relation. A good introduction into neural networks is provided by ref 7.

Actually, a discriminant-analysis system is a special case of a neural net. It can be shown mathematically that an MLP, in which the neurodes have linear transfer functions instead of the usual nonlinear sigmoidal functions, performs a discriminant analysis. In that case the hidden units play the role of the discriminant functions.

The objectives of the present investigation are:
- to evaluate the applicability of neural nets for the classification of gas and oil wells;
- to compare the results of a neural net with the outcomes of discriminant analysis;
- to determine whether neural nets could identify optimal petroleum engineering procedures that improve well production.

The neural-network architecture used is depicted in **Fig. 8.** It consists of three distinct layers: input, hidden and output. The layers are connected by feedforward, weighted connections. The function of the input layer is to distribute values of input parameters into the net. It does not perform any transformation on the inputs, i.e. output is equal to the input:

$$o_i = x_i \, .$$

The hidden and output neurodes compute a weighted sum of their inputs, biased by a threshold:

$$u_i = \sum_j w_{ij} x_j - \theta_i \, ,$$

in which w_{ij} is the connection weight from neurode j to neurode i and θ_i is the threshold of neurode i. The output of hidden and output neurodes is a nonlinear function of the summed input. Generally, a continuous, smooth and bounded sigmoidal function is applied:

$$o_i = \frac{1}{1 + e^{-u_i}} - 0.5.$$

The number of input neurodes N_i is equal to the number of input parameters, which were the same eight drilling, completion and production parameters (Fig. 8) used in the discriminant analysis. To achieve optimal results, these parameters were scaled in such a way that their values were within the range of the sigmoid function (-0.5,0.5). All but the last two input parameters are continuous. The "acid treatment" parameter can only have two values: whether or not the treatment has been applied. The "type of mud" parameter can have three values, depending on the mud type used. The output layer consists of three neurodes whose values indicate the category in which the well should be placed. For example, a Class 1 well would be indicated by a high value of the first output neurode and low values of the other neurodes: (+0.5, -0.5, -0.5). To obtain interesting results, the number of hidden units N_h should be at least two. Such a neural network with two layers of adaptive weights and thresholds is called a two-layered perceptron. The number of adaptive connections, including thresholds, is

$$M = (N_i + 1)N_h + (N_h + 1)N_o.$$

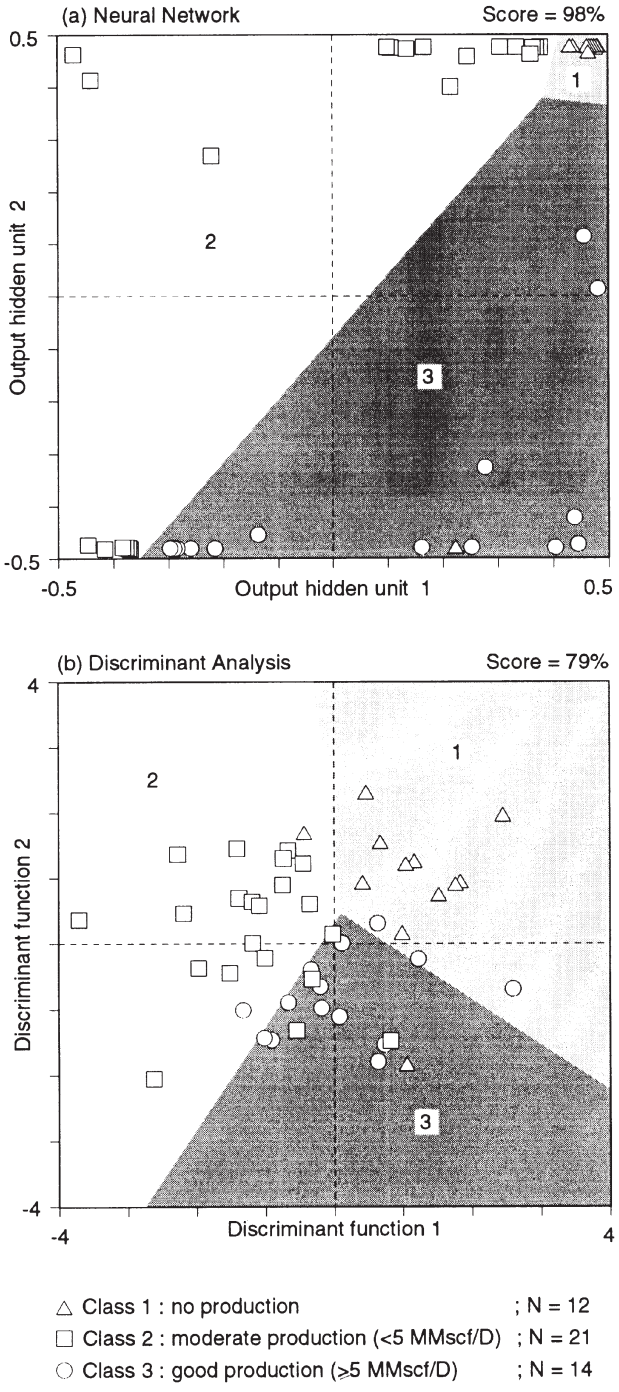

Fig. 9—Comparison of classification performance of neural net and discriminant analyses. Actual production categories are represented by different symbols. Estimated classification regions are indicated by different shades of the background. (a) Internal representation of gas wells on the two hidden units of the neural net. (b) Territorial map of discriminant analysis.

The network in Fig 8 has 27 adaptive connections.

In the training phase, well input parameters are presented to the net. The output classification is then compared to what it should be. Through an iterative, gradient-descent procedure, weights and thresholds are adjusted so that the deviation between net output o and desired output t is minimised. A measure of the deviation is given by the error sum of squares SSE:

$$SSE = \sum_k \sum_i (t_{ki} - O_{ki})^2,$$

in which k is the well index and i the input unit index. The learning rule applied was the error back-propagation rule. Typically, 10^4 iterations are needed for the net to learn the classification task properly. After the training phase the weights and thresholds are fixed. Whereas discriminant analysis forms linear decision regions, it can be shown mathematically that two-layered perceptrons can deal with arbitrarily complex decision regions, provided the number of neurodes is sufficient. The neural network was simulated on a Compaq-386 PC using a commercial software package NeuralWorks Professional II.

Results

Classification of Gas Wells. To compare the neural-net classification with the territorial maps produced by discriminant analysis, the wells were plotted as a function of the two hidden-neurode outputs (**Fig. 9a**). On the hidden layer (but not on the input layer), the classification boundaries are linear, as is the case in territorial maps (**Fig 9b**). The neural net separated the classes better than discriminant analysis. Only one of the 47 wells was classified erroneously by the neural net: it was classified as a Class 3 instead of a Class 1. Hence, the classification score is 98% correct. This score is better than the 79% correct score obtained by discriminant analysis. Another important performance criterion is how well new data—data that were not used as training examples—are classified. To assess this performance criterion, 90% of the wells were used for training and the remaining 10% for testing. The test procedure was repeated 10 times, each time for a different set of test wells. Given such test wells, the classification score of the neural net dropped to 74% correct. For comparison, the score of the discriminant analysis decreased from 79% to 67%. Furthermore, the score on the 10 training sets varied to some extent for both classification procedures. Separate analyses for the two fields did not improve results of neural nets or discriminant analyses; neither did the use of three hidden units instead of two.

Improvement of Well-Performance. The real strength of the neural-net approach lies in its ability to recommend, for instance, the most economic petroleum engineering procedures for improving well production. One can assign quantitative values to the cost effects of the various parameters. This enables a proper cost/benefit analysis to be carried out, in which the costs of altering drilling and completion procedures, etc., can be compared with the potential gain in well productivity. A very convenient way of doing this is to use the net in a "reversed mode".

Once a neural network has been trained, it has captured the feed-forward input-output relation of the underlying problem in its weights. The net may then be regarded as a statistical model of well production. This model can be used to indicate the expected effect of stimulation procedures on well performance. A straightforward way to do this is to change the value of input parameters by hand and observe the influence on the output of the neural net on a well-by-well basis. For optimal results, however, an input parameter should not be investigated on its own; all relevant parameters should be examined in combination. However, performing this job entirely by hand is not feasible.

A more elegant and convenient way to improve production would be to have the neural net calculate an optimal combination of input values on its own. In such a case the net has to operate in reverse: given a desired higher production level, what are the corresponding input values? The original neural net that was used for the classification can in fact perform the reverse task if an extra (new) input layer is added (**Fig 10**). The transfer function of the neurodes in this new layer is the identity function. The original input layer is connected to the new input layer in a one-to-one way between the layers' neurodes. All weights and thresholds are fixed, except the weights between the original and the new input layers. On a well-by-well basis, the current input values and the target enhanced output are provided to the net. By applying the same error back-propagation learning rule as before, the variable weights are updated so that the activation values of the new input layer attain values that result in the desired output.

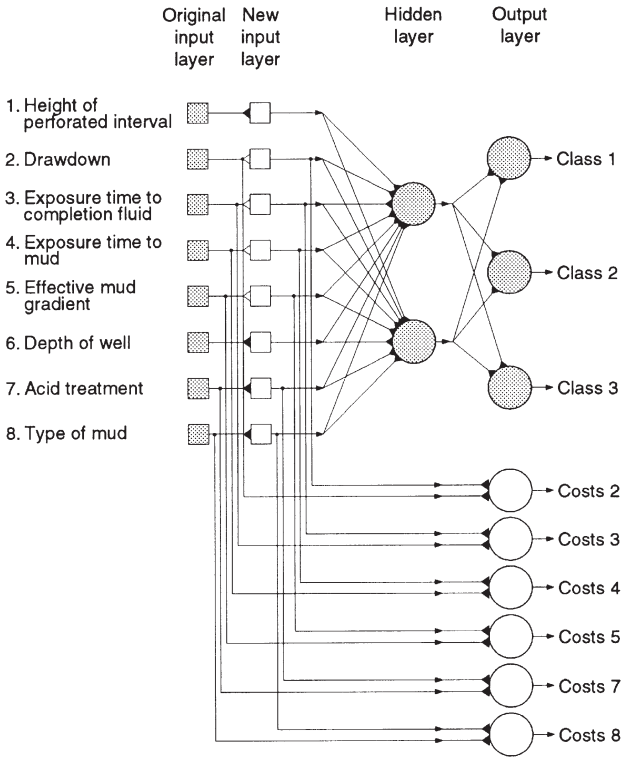

Fig. 10—Neural network for reverse computation of optimal stimulation procedures. The grey subnet isthe original classification net. Fixed weights are represented by closed triangles, adaptable weights by open triangles.

This reverse computation, however, is mathematically ill-defined. It tries to arrive at an 8-D new input vector, based on a desired 3-D output vector. This problem has an infinite number of solutions. Therefore, the solution space has to be reduced by adding constraints:

1. The values of the new inputs should be in the range of those of the training set.
2. The difference between current and new inputs should be as small as possible.
3. Some of the input parameters should be fixed.

The first constraint is added because the reliability of the neural net is guaranteed only for data that are comparable to the training set. It was enforced by including a hard-limiter that clips the linear transfer function of the new input neurodes at -0.5 and $+0.5$. The second constraint minimizes the costs of the proposed stimulation procedure. It was met by extending the output layer with extra neurodes connected to the neurodes of the original and the new input layers. Fixed but oppositely signed weights were given to the connections so that these extra neurodes compute a weighted difference between the original and the new input values. Finally, because the parameters "height of perforated interval" and "depth of the well" cannot be changed readily after the completion process, these two input parameters were not allowed to adapt. Furthermore, the discrete parameters "acid treatment" and "mud type" were fixed as well during adaptation, but were changed by hand outside the adaptation process. Hence, the neural net has to search only in a constrained 4-D input space instead of the original full 8-D space. As an example of the reverse computation, let us consider the conversion of a bad producer (Class 1) into a moderate producer (Class 2). The initial values of the adaptive weights are set at 1, so that the original and the new inputs

TABLE 2—NEURAL NET ADVICE FOR IMPROVEMENT OF WELL PERFORMANCE

Input parameter	Current value	New value
1. height of perforated interval (feet)	55	55
2. drawdown (psia)	−1000	1937
3. exposure time to completion fluid (days)	24	16
4. exposure time to mud (days)	21	21
5. effective mud gradient (psia/feet)	0.338	0.077
6. depth of well (feet)	8998	8998
7. acid treatment	no	no
8. type of mud	1	1

The effective mud gradient is the actual mud gradient minus the reservoir pressure gradient.

are identical at the start of adaptation. Then, the original input and the desired output ($-0.5,+0.5,\ -0.5,0,0,0,0,0,0$) are provided to the net as a "training" example. After about 10^3 iterations, the adaptive weights and hence the new inputs have changed in such a way that the output of the networks has converged to the desired output. Different runs may result in different new-input values with comparable error levels. Runs were also made for all six possible combinations of the two discrete input parameters that were changed by hand. The outcome of the run with the minimum error level is given in **Table 2.**

The net recommends that the avoidance of damage by minimizing drilling time and mud weight and by perforating under drawdown will be the most economic way to optimise the production of a non-producer; i.e., prevention rather than a remedial treatment. Such information can be used in drilling future wells.

Conclusions

1. Well productivity can be related to a number of drilling and completion parameters. Discriminant functions have been determined that correctly classify the performance of 32 out of 35 zones in one field and 39 out of 47 zones from this first field and a second similar field examined together.

2. The studies have identified and, to some extent, quantified those parameters that either adversely or favourably affect productivity. In particular, the productivity is increased by:
- minimizing drilling fluid overbalance;
- minimizing exposure time to drilling and completion fluids;
- maximizing drawdown during perforation;
- using Resinex lignosulfonate mud as a drilling fluid in the area;
- acidizing (damaged) completions.

The parameters identified as increasing productivity reflect, for the most part, sound engineering practices. Operational procedures may have to be adjusted accordingly to maximize productivity. In addition, the effect of not doing so may be assessed.

3. The application of a neural net approach enables further quantification of the most economic way to improve the performance of existing and future wells. This analysis also suggests that, for a number of producing zones in the fields studied, fracturing, rather than acidizing, may be more successful.

4. The usefulness of statistical analysis, such as discriminant analysis and neural networks, can be summarised as follows:

* it pin-points the effects of "standard" engineering practices on a field-wide basis;

* it helps to identify general sources of damage;

* it indicates optimum stimulation techniques.

However, statistical techniques are applicable only when a sufficiently large data base is available, i.e., they are suitable for reasonably large and fairly mature fields and/or areas.

Acknowledgment

The authors wish to express their appreciation for the support of Shell Intl. Research Mij. and their permission to publish this work.

References

1. King, G.E., Anderson, A. and Bingham, M., "A Field Study of Underbalance Pressures Necessary to Obtain Clean Perforations Using Tubing-Conveyed Perforating," paper SPE 14321 presented at the 60th SPE Annual Technical Conference and Exhibition, Las Vegas, Sept. 22–25, 1985.
2. Gidley, J.L., "Acidizing Sandstone Formations: A Detailed Examination of Recent Experience," paper SPE 14164 presented at the 60th SPE Annual Technical Conference and Exhibition, Las Vegas, Sept. 22–25, 1985.
3. Norusis, M.J., SPSSX, Advanced statistics guide, McGraw-Hill Book Co., 1985.
4. Noble, J.E., "A Discriminant Analysis of Acquired and Acquiring Companies in the Oil Industry," paper SPE 14381 presented at the 60th SPE Annual Technical Conference and Exhibition, Las Vegas, Sept. 22–25, 1985.
5. Epping, W.J.M. and Nitters, G., A neural network for analysis and improvement of gas well production. Proceedings of the 1990 Summer Computer Simulation Conference. July 16–18, 1990. Calgary. Eds.: B. Srvcek and J. McRae, pp. 791–796. Society for Computer Simulation, San Diego, CA.
6. Al-Kaabi, A.U., and Lee, W.J., "Using Artificial Neural Networks to Identify the Well Test Interpretation Model," Paper SPE 20332 presented at the 5th SPE Petroleum Computer Conference, Denver, Colorado, June 25–28, 1990.
7. Hertz, J., Krogh, A. and Palmer, R.G. "Introduction to the theory of neural computation," Addison Wesley, 1991.

SI Metric Conversion Factors

ft × 3.048*	E−01 = m
ft^3 × 2.831 685	E−02 = m^3
in. × 2.54*	E+00 = cm
psi × 6.894 757	E+00 = kPa

*Conversion factor is exact.

SPEDC

Gerrit Nitters is a senior production engineer in the well stimulation section at Shell Intl. Petroleum Mij. in The Hague. He joined Shell in 1968 and worked at various locations within Shell. He has 21 year's experience in well stimulation, both in operational as well as theoretical aspects. Since 1985 he concentrated on the development of computerised design methods for matrix treatments and on the promotion of stimulation as an effective means of improving well production. He holds a BSc degree in chemical technology from the Academy Minerva in Groningen. **David R. Davies** is Head of Well Stimulation Research at KSEPL, and has led research groups in production engineering research. He also has worked in operations, responsible for daily operations of 13 drilling rigs. He holds a BSc degree in chemistry and a PhD degree in chemical physics from the U. of Exeter and is active in SPE. He was a 1990-1992 Review Chairman for SPE Production Engineering. **Willem J.M. Epping** is a senior research petrophysicist at Shell Research Rijswijk, The Netherlands. He holds a PhD degree in physics from the University of Nijmegen and has done postdoctoral research on sensory information processing by biological neural networks at the Universities of Nijmegen and Marburg. In 1989 he joint Shell to investigate the application of artificial neural networks in the area of exploration and production.

An Investigation Into the Application of Fuzzy Logic to Well Stimulation Treatment Design

27672

Hongjie Xiong and **S.A. Holditch**, SPE, S.A. Holditch & Assocs. Inc.

Summary

Designing an optimal stimulation treatment for an oil or gas well is a complex procedure requiring in-depth knowledge and experience. This paper describes how fuzzy logic applies to stimulation design and clearly illustrates how to apply fuzzy logic theory. The paper also discusses the advantages and disadvantages of applying fuzzy logic to well stimulation design.

Fuzzy logic evaluators can be applied to study, evaluate, and determine the best methods to improve productivity in oil and gas wells or injectivity in water wells. The approach can be extended to the solution of other problems associated with drilling, completing, and working over wells and with formation damage diagnosis.

Introduction

Well stimulation is a technique that effectively improves hydrocarbon recovery. The success or failure of a stimulation treatment depends heavily on the treatment design. Some of the major decisions that must be made during the treatment design process include (1) the selection of wells that are candidates for stimulation, (2) the selection of the optimal type of stimulation treatment, (3) the diagnosis of the type of damage that is affecting the formation, (4) the evaluation of rock layers that could be barriers to fracture propagation, and (5) the selection of appropriate treatment fluids and additives.

These decisions are crucial to the success or failure of the stimulation treatment, and require comprehensive data sets, knowledge, and experience. Few engineers possess all the skills and/or data required to make these decisions with consistency. Lack of sufficient data is always a problem, and many fuzzy (not clearly defined) linguistic terms are often used to describe reservoir characteristics. Some of the rules that experts use to make decisions during the design are also fuzzy. Designing the optimal stimulation treatments with consistency is important but very difficult to accomplish.

Fig. 1, for example, represents a rule that can be used to select a fluid for a fracture treatment. In this rule, there are three fuzzy linguistic terms: "high," "long," and "highly." The definitions of high temperature, long fracture, and high viscosity are fuzzy; the exact values would depend on a specific engineer and a specific situation. Such fuzzy statements or relationships are common in well stimulation design. We have found that quantifying the problem is much easier using fuzzy logic rules rather than production (if/then) rules.

Fuzzy logic[1,2] provides a method to help us emulate the thought process of the engineer designing a stimulation treatment. Fuzzy logic is an extension of set theoretic multivalued logic in which the truth values are linguistic variables (or terms of the linguistic variable truth). Unlike the classical binary logic (Boolean logic), in which the truth values can be only 0 (false) or 1 (true), fuzzy logic can allow countless truth values that range between 0 and 1.

The three basic components of a fuzzy logic system are fuzzy variables, membership functions, and weighting factors used to connect input and output variables.

Fuzzy Variables. Fuzzy variables are all factors or parameters that have to be considered to make a decision (output). For each fuzzy variable, there is a corresponding fuzzy Set A. For example, if temperature is a fuzzy variable, then its fuzzy set could be {very low, low, medium, high, very high}.

Membership Function. A membership function $\mu_A(x)$ is defined as the degree of truth of the fuzzy variable x in the fuzzy Set A. A membership function can be built based on the input or output, which we call the membership function base. **Fig. 2**, for example, shows the membership functions for temperature based on an input value of temperature.

Weighting Factors. Weights or weighting factors represent the importance of all fuzzy varjables in a fuzzy logic system. The weighting factor of a fuzzy variable indicates its contribution to the output or decisions of the system. The weighting factors are extracted from human expertise (or experience) and can be adjusted for different situations in a fuzzy system.

Fuzzy logic has been applied in the petroleum industry[3-7] to solve numerous problems, including those associated with well stimulation. We have developed fuzzy logic evaluators for selecting the best treatment candidate,[8] evaluating tubular conditions,[9] selecting the optimal treatment type,[10] evaluating potential barriers, diagnosing formation damage mechanisms, and selecting optimal treatment fluids and additives.

The purpose of this paper is to illustrate clearly the methodology that we have used to apply fuzzy logic theory to solve well stimulation treatment design problems. We present the advantages and disadvantages of applying fuzzy logic to well stimulation design and our experience in developing fuzzy logic systems. We conclude this paper by presenting an example of how fuzzy logic can be used to evaluate fracture barriers in layered reservoirs.

Methodology

We have developed a procedure to build a fuzzy logic evaluator for typical well stimulation problems. As shown in **Fig. 3**, the procedure consists of seven steps.

Step 1. One must first determine the objective or purpose of an evaluator. For example, the objective of one fuzzy evaluator, selecting treatment type, is to select an optimal stimulation treatment type based on the given wellbore and reservoir conditions. The treatment type is the output of the fuzzy evaluator.

Step 2. The second step is to structure the output of the evaluator. We try to identify all possible decisions that could be made by a human expert solving this problem. In our selecting-treatment-type-fuzzy evaluator, the possible options include (1) acid fracture treatment, (2) proppant fracture treatment, (3) matrix acid treatment, (4) other matrix treatments, and (5) no treatment.

Step 3. Next, one must identify parameters that affect the output from the fuzzy evaluator. We have to identify the most important fuzzy variables that affect the primary decision. To identify the correct parameters, one must use the domain knowledge for the fuzzy system. For example, the condition of a potential barrier to fracture growth depends on the thickness of all layers, the rock mechanical properties of all layers, and certain fracture fluid properties. One must decide which specific parameters apply and include them in the fuzzy evaluator.

Step 4. The fourth step is to determine the number of membership functions one must include in the fuzzy evaluator. If the membership functions are based on the output, then the number of member-

Copyright 1995 Society of Petroleum Engineers

Original SPE manuscript received for review July 25, 1994. Revised manuscript received Nov. 2, 1994. Paper accepted for publication Nov. 22, 1994. Paper (SPE 27672) first presented at the 1994 SPE Permian Basin Oil and Gas Recovery Conference held in Midland, March 16–18.

If
formation temperature is HIGH
and
expected fracture length is LONG
THEN
use a HIGHLY viscous fracture fluid.

Fig. 1—A typical fuzzy rule.

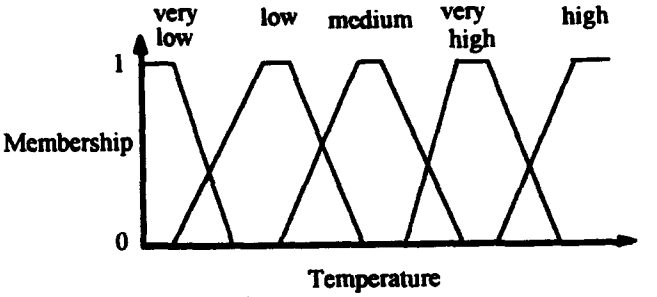

Fig. 2—Membership functions where temperature is input.

ship functions must be the same for all fuzzy variables in the system. On the other hand, if the membership functions are based on the input value, the number of membership functions can be different for different variables. Once the nature of the membership functions is decided for each parameter, then domain knowledge and expertise are used to quantify the membership functions.

Step 5. After the membership functions for each parameter have been constructed, the weighting factors are determined from the domain knowledge and expertise. The weighting factors can be changed for different situations, often called "weighting-factor shifting." For example, skin factor and water saturation are two fuzzy variables in the fuzzy system called well stimulation candidate selection. Usually, the weighting factor for skin factor is larger than that for water saturation. If the water saturation is very high (e.g., >90%), however, the weighting factor for water saturation should be much larger than that for skin factor.

Step 6. After we build membership functions and weighting factors for the fuzzy system, we must determine the evaluation procedure. For a given situation, we usually (1) build our fuzzy matrix $\mathbf{R} = \{F_{ij}\}$ (F_{ij} is the membership value of the ith parameter at the jth membership function of the parameter), which consists of the memberships of all fuzzy variables, and (2) compute the evaluation result matrix:

$$\mathbf{B} = N_o R = [b_1, b_2, b_3, b_4], \quad \ldots\ldots\ldots\ldots\ldots\ldots\ldots\ldots (1)$$

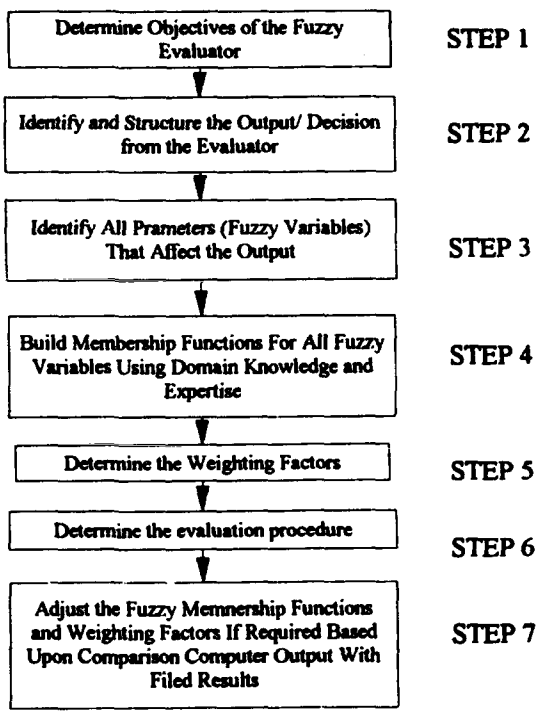

Fig. 3—A typical procedure to build a fuzzy evaluator.

where N is the weighting factor matrix, the operator o represents the operator $M(o, \oplus)$, and the values of b_j are computed as

$$b_j = \min\left\{1, \sum_{i=1} I_i F_{ij}\right\}. \quad \ldots\ldots\ldots\ldots\ldots\ldots\ldots\ldots (2)$$

Step 7. One of the most important steps in building a fuzzy logic system is adjusting membership functions and weighting factors so that the fuzzy logic model will provide the same results as one would receive from a human expert. The membership functions and weighting factors should be reviewed and evaluated by domain experts. They can also be improved by running examples from case histories where the correct results have been documented to be sure the computer logic reproduces the correct results.

Applications

Using the methodology described above, we have built eight fuzzy evaluators that are used in our expert system called Stimulation Expert (STIMEX).[11] All domain knowledge and expertise used to build these fuzzy evaluators and STIMEX were obtained by interviewing industry-wide experts, reviewing technical documents, collecting laboratory data, and reviewing many typical case histories. **Table 1** lists the eight fuzzy logic evaluators. All of them are independent.

Fuzzy Logic Application to Well Stimulation Design

Here we present an example to illustrate how we apply fuzzy logic to evaluate if a layer of rock will be a "good" or "poor" barrier to

TABLE 1—FUZZY LOGIC APPLICATIONS IN STIMEX

	Fuzzy Evaluator	Functions
1	Well stimulation candidate	To identify whether a well is an excellent/good/possible/poor stimulation candidate, or to select optimal stimulation candidates if multiple wells exist.
2	Barrier conditions	To check whether a layer of rock is a good or poor barrier for a fracture treatment.
3	Treatment type	To select an optimal treatment type for a given reservoir and wellbore situation.
4	Injection method	To select an optimal fluid injection method based on tubular conditions and treatment type.
5	Fracturing fluids and additives	To select optimal fracturing fluids and additives
6	Formation damage diagnosis	To diagnose the possible existing formation damage mechanisms
7	Acid fluids	To select acid fluids and additives for acid fracture treatments
8	Matrix treatment fluids	To select fluids and additives for matrix treatments

TABLE 2—RELATIVE CONTRIBUTIONS OF PARAMETERS USED TO DETERMINE BARRIER CLASSIFICATION

Factor	Weighting Factor, I
$\Delta\sigma$	0.40
h_b	0.15
h_p	0.15
E_p	0.1
E_b/E_p	0.075
E_b	0.05
k/μ	0.075
(Total)	1.0

fracture growth. All domain knowledge used to determine the evaluator objectives, to identify fuzzy variables and weighting factors, and to develop membership functions came from domain experts, technical documents, experimental data, and case histories. In addition, a 3D fracture model[12] was used to tune the membership functions and to refine the fuzzy evaluator.

Fuzzy Evaluator Objectives. First, we define the objective of this fuzzy evaluator: to evaluate whether a layer of rock will or will not prevent a fracture to propagate through the layer. The output of the fuzzy system is the barrier condition.

Possible Options of the Output. The possible results from barrier condition evaluation can be strong barrier, weak barrier, questionable barrier, or not a barrier.

Fuzzy Variables in the Evaluator. Several factors must be considered to determine whether a specific layer of rock will act as a barrier to hydraulic fracture growth. We can list the factors in order of importance as (1) in-situ stress difference between the potential barrier and the pay zone, $\Delta\sigma$; (2) barrier thickness, h_b; (3) the ratio of barrier Young's modulus to pay-zone Young's modulus, E_b/E_p; (4) pay-zone thickness, h_p; (5) pay-zone Young's modulus, Ep; (6) barrier Young's modulus, E_b; and (7) the ratio of pay-zone permeability to fluid viscosity in the pay zone, k/μ.

There is essentially an infinite combination of these variables that must be considered in building rules to determine whether a specific layer will act as a barrier to vertical fracture propagation. In most cases, however, we will not have all the data nor the measurements necessary to quantify this problem. However, we can use several fuzzy words or qualitative descriptions to classify potential barriers, such as strong barrier or weak barrier.

Weighting Factors. Using our experience as experts, we developed weighting factors (I) for all fuzzy variables. **Table 2** illustrates our current estimates for these weighting factors.

The importance of each variable listed in Table 2 is dependent on the values of the other variables. For instance, the value of the in-situ stress difference may not significantly affect the barrier classification once it is above a critical value (e.g., 1,000 psi). In this situation, the barrier thickness or other factors, such as fracture fluid viscosity, μ, may become the most important factors in determining whether an interval will act as a barrier.

TABLE 3—BARRIER CLASSIFICATIONS AS DETERMINED FROM COMPOSITE EVALUATION FUNCTION

F_b	Barrier Condition
>= 0.7	Strong
0.7 > F_b >=0.5	Weak
0.5 > F_b >= 0.3	Questionable
< 0.3	No barrier

Membership Functions. For this problem, we determined that the base of all membership functions is the output of the evaluator, which is the barrier condition. Therefore, we have the same number of membership functions for all fuzzy variables, which is one in this specific application. All membership functions are shown in the appendix.

We have developed several membership functions, F, for all parameters on the basis of our experience, observations, and detailed simulation studies. These membership functions are used to quantify the importance of each parameter, on the basis of the actual value of the parameter. For example, as the value of in-situ stress difference increases, the parameter becomes more important in the decision-making process. Thus, once we know the value of the in-situ stress difference, we can obtain the evaluation value, $F_{\Delta\sigma}$, from the evaluation function developed for in-situ stress contrast. The product of the in-situ stress difference weighting factor, $I_{\Delta\sigma}$, and its evaluation value, $F_{\Delta\sigma}$, is then taken to be the overall importance (influence) of in-situ stress on the barrier classification. The sum of the contributions of each factor is used to determine the barrier classification. That is,

$$F_b = \min\left\{1, \sum_{i=1}^{7} I_i F_i\right\} \quad \ldots\ldots\ldots\ldots\ldots\ldots\ldots\ldots\ldots\ldots (3)$$

where the value of F_b represents the comprehensive evaluation of a potential barrier interval. Based on the value of F_b, we can determine if the barrier is strong, weak, questionable, or not a barrier. Eq. 4 presents the detailed expansion of Eq. 3:

$$F_b = \min\left\{1, I_{\Delta\sigma} F_{\Delta\sigma} + I_{h_b} F_{h_b} + I_{h_p} F_{h_p} + I_{\frac{E_b}{E_p}} F_{\frac{E_b}{E_p}} + I_{E_p} F_{E_p} + I_{E_b} F_{E_b} I_{\frac{k}{\mu}} F_{\frac{k}{\mu}}\right\}. \quad \ldots\ldots\ldots\ldots\ldots\ldots\ldots\ldots\ldots\ldots (4)$$

Having determined F_b, we then use **Table 3** to determine the barrier classification.

Example Applications

Some examples have been documented.[13] The following two examples illustrate how this fuzzy logic approach is used to classify potential barriers.

TABLE 4—BARRIER CLASSIFICATION—EXAMPLE 1

Item	Value	Evaluation Value, F	Weighting Factor, I	Contribution, $F*I$	
$\Delta\sigma$	1,000 psi	0.9	0.4	0.36	$F*I$ = 0.7134
h_b	100 ft	0.5159	0.15	0.07739	From Table 3,
h_p	200 ft	0.9785	0.15	0.146776	the barrier is
k/μ	0.1	0.527633	0.075	0.039573	classified as
E_b	2.3×10^6 psi	0.834856	0.05	0.041743	strong.
E_p	4×10^6 psi	0.364982	0.1	0.0364982	
$(E_p - E_b)/E_p$	0.575	0.1528	0.075	0.000181	
	k=0.001 md	=0.01 cp			

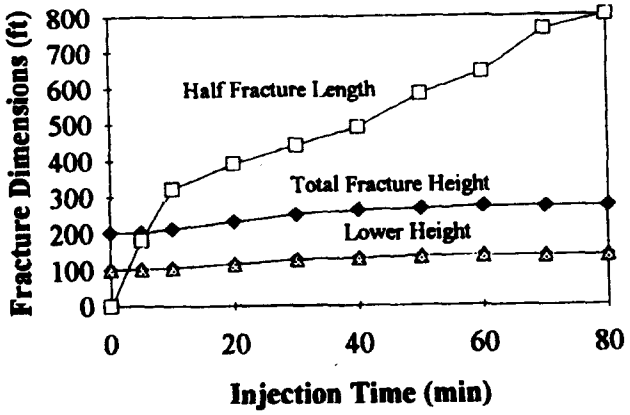

Fig. 4—Fracture dimension propagation for Example 1.

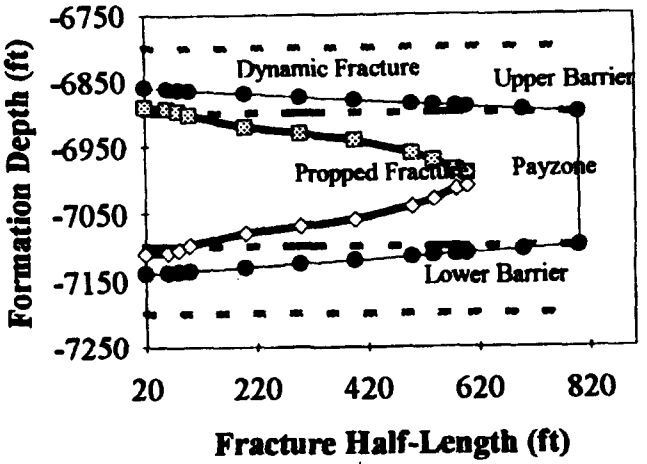

Fig. 5—Fracture after 80 minutes injection.

Example 1. **Table 4** presents the data for Example 1. The in-situ stress difference, $\Delta\sigma$, is 1,000 psi; the barrier thickness, h_b, is 100 ft; the barrier Young's modulus, E_b, is 2.3 million psi; the pay-zone Young's modulus, E_p, is 4 million psi; formation permeability, k, is 0.001 md; the pay-zone thickness, h_p, is 200 ft; and the formation fluid viscosity, μ, is 0.01 cp. The evaluation value, F, for each parameter in Table 4 can be obtained from the corresponding equation in the Appendix. For this case, the nonpay zone is classified as a strong barrier, as shown in Table 4.

Using the data in Table 4 in a 3D fracture propagation model[12] gave the fracture propagation dimensions vs. injection time illustrated in **Fig. 4**. As the injection continues, the fracture length grows very rapidly, and the fracture height remains essentially constant. This problem is a typical case that has a strong barrier to fracture height growth. **Fig. 5** shows the fracture after 80 minutes injection.

Example 2. This example consists of six layers (**Table 5**) where Layer 3 is a pay zone with ratio $k/\mu = 0.05$. The example shows a situation in which the upper and lower barriers are different. Our model predicts that Layer 5 is a questionable barrier (Table 5). Because Layers 4 and 5 are not as strong as Layer 2, the fracture breaks through Layers 4 and 5 (See **Figs. 6** and **7**), which causes Layer 2 to behave like a strong barrier and Layer 5 to behave as if it were not a barrier. When the upper barrier condition is different from the lower barrier, the stronger barrier becomes better and the weaker barrier becomes worse.

Conclusions

1. We successfully applied fuzzy logic to the design of well stimulation treatments. We developed eight fuzzy evaluators: (1) stimulation candidate selector, (2) treatment type selector, (3) barrier condition evaluator, (4) injection method evaluator, (5) fracturing fluids and additives selector, (6) formation damage diagnosis, (7) acid fluids and additives selector (for acid fracture treatments), and (8) fluids and additives selector (for matrix treatments). All these fuzzy logic evaluators were tied together in a well stimulation expert system.

2. The general methodology to build a fuzzy logic system is (1) to determine the objectives of the system, (2) to identify all possible decisions that could be made by a human expert solving the problem, (3) to identify fuzzy variables that affect the output from the

TABLE 5—BARRIER CLASSIFICATION—EXAMPLE 2

Data Item	Layer 1	Layer 2	Layer 3 (pay zone)	Layer 4	Layer 5	Layer 6
In-situ stress, psi	8,900	8,500	8,000	8,200	8,200	8,900
Thickness, ft	500	200	100	200	200	500
Formation fluid viscosity, cp	—	—	0.02	—	—	—
Young's modulus, 10^6 psi	3	3	5	4.6	4.6	3
Permeability, md	0.0001	0.0001	0.001	0.0001	0.0001	0.0001
Barrier evaluation value	0.745	0.55	—	0.237	0.294	0.748
Barrier condition	Strong	Weak	—	No Barrier	No Barrier	Strong

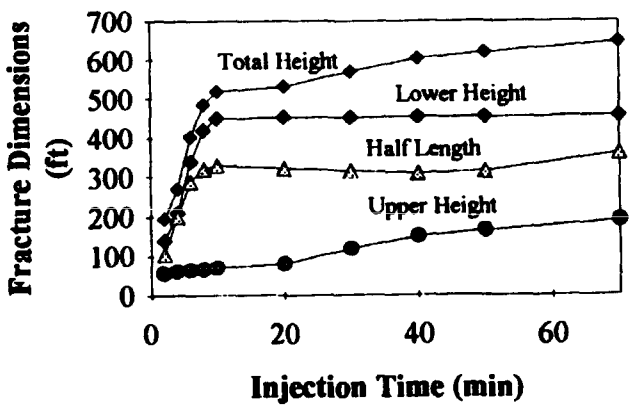

Fig. 6—Fracture dimension propagation for Example 2.

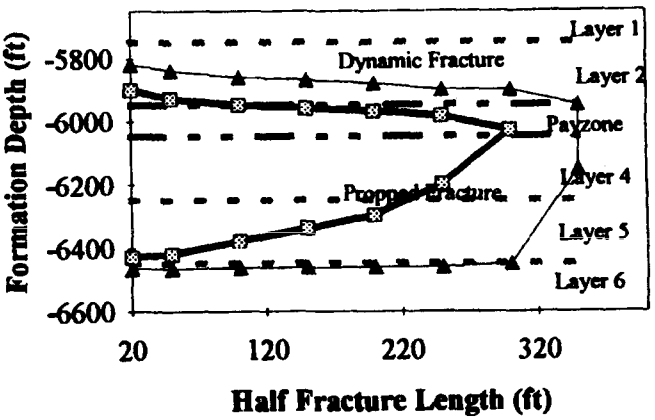

Fig. 7—Fracture after closure for Example 2.

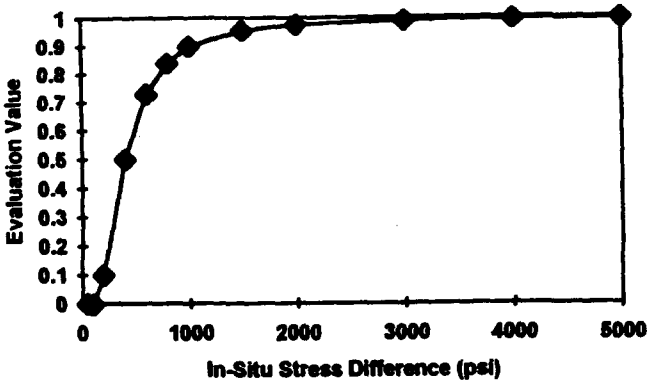

Fig. A-1—In-situ stress difference evaluation function.

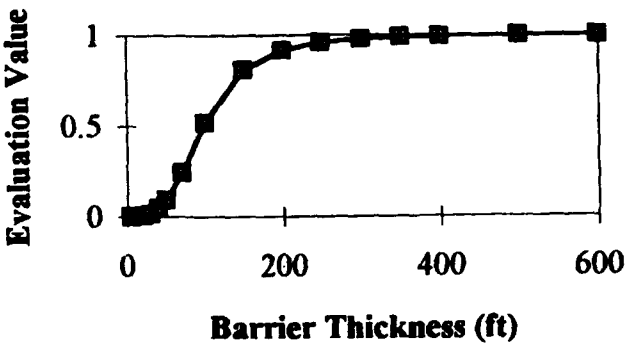

Fig. A-2—Barrier thickness evaluation function.

fuzzy model, (4) to determine the number of membership functions one must include in the fuzzy system and develop all membership functions, (5) to determine the weighting factors and shifting mechanism, and (6) to determine the evaluation procedure and tune the membership functions. The methodology presented in this paper can be used to develop many fuzzy logic systems in other areas, such as drilling, completion, production, and EOR, in which we use a lot of experience to solve the practical problems.

3. Fuzzy logic is an excellent tool to represent domain expertise and knowledge in computer codes, which makes it easier to apply and transfer domain knowledge and expertise. The fuzzy logic reasoning is more approximate to human reasoning and more accurate because it allows fuzzy linguistic terms, a variety of truth values, and no "crisp" cut off.

4. Developing a fuzzy logic system involves substantial knowledge acquisition activities. The available domain experts are crucial in developing a fuzzy logic system. Identifying fuzzy variables and fuzzy sets and determining the base of membership functions and weighting factors are very important. Building and tuning membership functions could be time-consuming.

Nomenclature

A = fuzzy set
b_j = jth element in matrix [B]
[B] = evaluation result matrix
E_b = Young's modulus of barrier, m/Lt^2
E_p = Young's modulus of pay zone, m/Lt^2
F = membership value
F_b = comprehensive evaluation value
F_{ij} = membership value of ith parameter at jth membership function of the parameter
h_b = barrier thickness, L
h_p = pay-zone thickness, L
I = weighting factor
k = permeability, L^2
[R] = membership value matrix
$\Delta\sigma$ = in-situ stress difference between the potential barrier and the pay zone, m/Lt^2
μ = formation fluid viscosity, m/Lt
$\mu_A(x)$ = membership function of Parameter x in its fuzzy set A

References

1. Zimmermann, H.J.: *Fuzzy Set Theory and Its Applications*, Kluwer Academic Publishers, Boston (1991) 131–162.
2. Kosko, B.: *Neural Networks and Fuzzy Systems*, Prentice-Hall, New York City (1992).
3. Lo, T.: "Application of Fuzzy Logic to Seismic Tomography - Method and Preliminary Results," paper presented at the 1991 Conference on Artificial Intelligence in Petroleum Exploration and Production, College Station, TX, May 15–17.
4. Kim, C.S. and Isaksen, G.H.: "Application of Fuzzy Sets and Dempster-Shafer Theory to Organic Geochemistry Interpretation," paper presented at the 1991 Conference on Artificial Intelligence in Petroleum Exploration and Production, College Station, TX, May 15–17.
5. Urwongse, T.: "Predicting Petroleum Potential Using Fuzzy Analogs and Neural Networks," paper presented at the 1992 Conference on Artificial Intelligence in Petroleum Exploration and Production, Houston, July 22–24.
6. Li, L.H., Chen, C.H., and Fang, J.H.: "XPROS 2: A Fuzzy Expert System for Ranking Prospects," paper presented at the 1993 Conference on Artificial Intelligence in Petroleum Exploration and Production, Dallas, May 19–21.
7. Zhou, C.D., Wu, X.L., and Cheng, J.A.: "Determining Reservoir Properties in Reservoir Studies Using a Fuzzy Neural Network," paper SPE 26430 presented at the 1993 SPE Annual Technical Conference and Exhibition, Houston, Oct. 3–6.
8. Xiong, H. and Holditch, S.A.: "Using a Fuzzy Expert System To Choose Target Wells and Target Formations for Stimulation," paper presented at the 1993 Conference on Artificial Intelligence in Petroleum Exploration and Production, Dallas, May 19–21.
9. Xiong, H. and Holditch, S.A.: "An Expert System To Select Injection Method and Evaluation Tubular Conditions for a Stimulation Treatment," paper presented at the 1993 Conference on Artificial Intelligence in Petroleum Exploration and Production, Dallas, May 19–21.

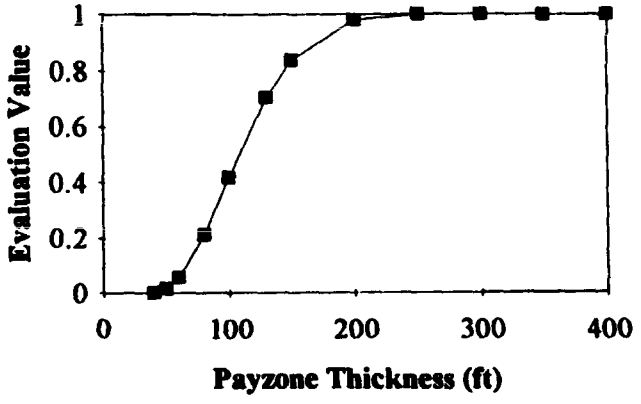

Fig. A-3—Pay-zone thickness evaluation function.

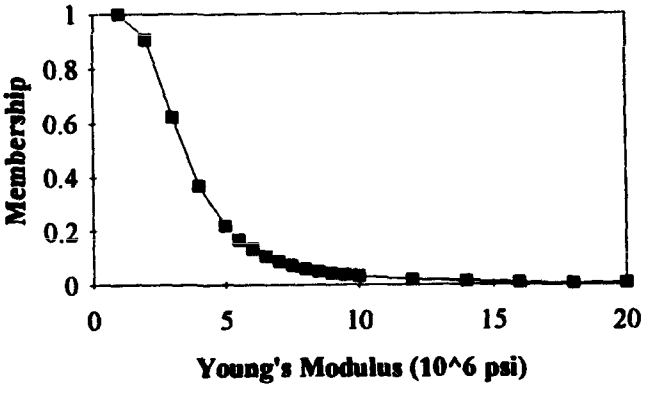

Fig. A-4—Young's modulus evaluation function.

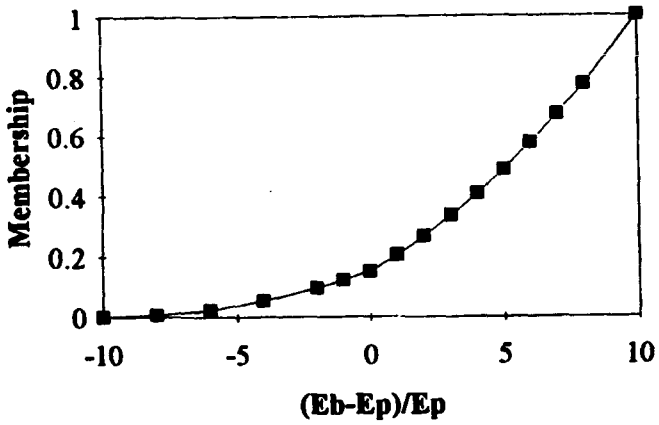

Fig. A-5—Young's modulus ratio evaluation.

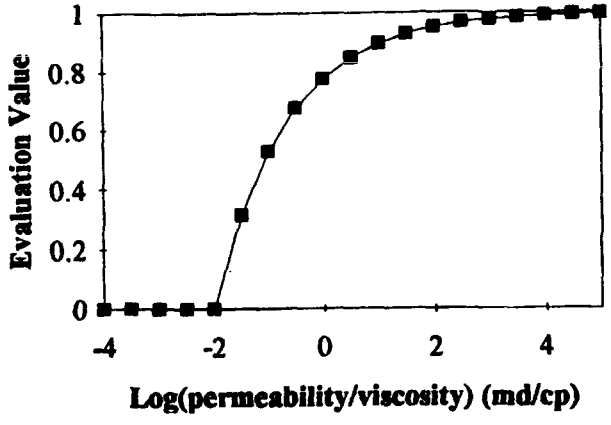

Fig. A-6—Permeability to viscosity evaluation function.

10. Xiong, H., Holditch, S.A., and Lancaster, D.E.: "A Fuzzy Evaluator for Selecting the Optimal Stimulation Treatment Type," paper presented at the 1993 10th Petroleum Technical Conference, Puerto La Cruz, Venezuela, Oct. 20–23.
11. Xiong, H., Sherry, K., and Lancaster, D.: "Intelligent Interfaces for Fracturing Simulators—Part II: System Implementation and Application," paper SPE 28521 presented at the 1994 SPE Annual Technical Conference and Exhibition, New Orleans, Sept. 24–28.
12. *TRIFRAC User Manual*, S.A. Holditch & Assocs., College Station, TX (1992).
13. Xiong, H. and Holditch, S.A.: "An Investigation Into The Application Of Fuzzy Logic To Well Stimulation Treatment Design," paper SPE 27672 presented at the 1994 SPE Permian Basin Oil and Gas Conference, Midland, TX, March 16–18.

Appendix—Membership Functions for Barrier Condition Fuzzy Evaluator

In-Situ Stress Difference Evaluation. The evaluation function we use for in-situ difference is described as

$$F_{\Delta\sigma} = \begin{cases} 0 & \Delta\sigma <= 100 \text{ psi} \\ \dfrac{1}{1 + 90000(\Delta\sigma - 100)^{-2}} & \Delta\sigma > 100 \text{ psi} \end{cases} \quad \ldots (A\text{-}1)$$

Fig. A-1 expresses this function graphically.

Thus, as the in-situ stress difference between the nonpay interval and the pay interval increases, the nonpay interval is more likely to act as a barrier to fracture growth.

Barrier Thickness Evaluation. The evaluation function we use for barrier thickness is described as

$$F_{h_b} = \begin{cases} 0 & h_b <= 5 \text{ ft} \\ \dfrac{1}{1 + \dfrac{2000000}{(h_b - 5)^{32}}} & h_b > 5 \text{ ft} \end{cases} \quad \ldots\ldots\ldots\ldots (A\text{-}2)$$

Fig. A-2 illustrates this function graphically.

As the thickness of the nonpay interval increases (above 5 ft), it is more likely to act as a barrier to fracture growth.

Pay-Zone-Thickness Evaluation. The evaluation function we use for the pay-zone thickness is described as

$$F_{h_p} = \begin{cases} 0 & h_p <= 40 \text{ ft} \\ 1 - e^{-0.00015(h_p - 40)^2} & h_p > 40 \text{ ft} \end{cases} \quad \ldots\ldots\ldots (A\text{-}3)$$

Fig. A-3 presents this evaluation function in graphical form.

Thus, as the thickness of the pay zone increases (above 40 ft), it is more likely that the nonpay interval will act as a barrier to fracture growth.

Young's Modulus of Pay Zone and Potential Barriers. The evaluation function we developed to evaluate the effect of Young's modulus in the pay zone is described as

$$F_E = \begin{cases} 0 & E <= 1 \times 10^6 \text{ psi} \\ \dfrac{1}{1 + 0.1(E - 1)^{2.6}} & E > 1 \times 10^6 \text{ psi} \end{cases} \quad \ldots\ldots (A\text{-}4)$$

Fig. A-4 describes this evaluation function in graphical form.

Thus, the smaller the Young's modulus, the more likely it is that the nonpay interval will act as a barrier to fracture growth. Likewise, the smaller the Young's modulus in the pay zone, the less likely that the fracture will grow into the nonpay intervals.

Young's Modulus Ratio of Barrier to Pay Zone. The evaluation function we developed to evaluate the effect of Young's modulus in the pay zone or potential barriers is described as

$$F_{E_{bpr}} = \begin{cases} 0 & E_{bpr} <= -10 \\ 0.0015\left(E_{bpr} + 10\right)^2 & 0 > E_{bpr} >= -10 \\ 0.0035\left(E_{bpr}^2 + 0.005E_{bpr} + 0.15\right) & 10 > E_{bpr} >= 0 \\ 1 & E_{bpr} >= 10 \end{cases}$$

$$\ldots\ldots\ldots\ldots\ldots\ldots\ldots\ldots\ldots\ldots\ldots\ldots\ldots\ldots\ldots\ldots (A\text{-}5)$$

in which $E_{bpr} = \dfrac{E_p - E_b}{E_p}$.

Fig A-5 describes this evaluation function in graphical form.

The Ratio of Pay-Zone Permeability to Pay-Zone Fluid Viscosity. The ratio of pay-zone permeability (md) to pay-zone fluid viscosity (cp), k/μ, is very important. As the ratio k/μ decreases, the fracture fluid leakoff rate decreases and the treatment size is usually increased (the fracture length and fracture fluid viscosity are increased), which results in the barriers conditions becoming relatively worse.

$$F_{\frac{k}{\mu}} = \begin{cases} 0 & \frac{k}{\mu} <= 0.01 \\ 1 - e^{-0.75\left[\log\left(\frac{k}{\mu}\right) + 2\right]} & \frac{k}{\mu} > 0.0 \end{cases} \quad \ldots\ldots\ldots (A\text{-}6)$$

This function is described graphically in **Fig A-6**.

SI Metric Conversion Factors

cp × 1.0*	E−03 = Pa · s
ft × 3.048*	E−01 = m
psi × 6.894 757	E+00 = kPa

*Conversion factor is exact.

SPECA

Hongjie Xiong is a petroleum engineer with S.A. Holditch & Assocs. Previously he was a lecturer at the Southwest Petroleum Inst. in China. His interests include well stimulation and artificial intelligence applications in petroleum engineering. He holds BS and MS degrees from the Southwest Petroleum Inst., China, and a PhD from Texas A&M U., all in petroleum engineering. **Stephen A. Holditch** is president of S.A. Holditch & Assocs., a professor of petroleum engineering at Texas A&M U., and a consultant. Previously, he worked for Shell Oil Co. as a production engineer, where his interests included well completions, workovers, and fracture stimulation design. He holds BS, MS and PhD degrees in petroleum engineering from Texas A&M U. He was 1991–93 SPE Reprint Series Chairman, a 1989 SPE Distinguished Member, a 1986–89 and 1982–83 SPE Distinguished Lecturer, and a winner of the 1981 SPE Distinguished Award for Petroleum Engineering Faculty.

Xiong

Holditch

SPE 30202

Predicting Production Using a Neural Network (Artificial Intelligence Beats Human Intelligence)

Robert J. Boomer, Texaco Exploration and Production Inc.

SPE Member

Copyright 1995, Society of Petroleum Engineers, Inc.

This paper was prepared for presentation at the Petroleum Computer Conference held in Houston, TX, U.S.A., 11–14 June 1995.

This paper was selected for presentation by an SPE Program Committee following review of information contained in an abstract submitted by the author(s). Contents of the paper, as presented, have not been reviewed by the Society of Petroleum Engineers and are subjected to correction by the author(s). The material, as presented, does not necessarily reflect any position of the Society of Petroleum Engineers, its officers, or members. Papers presented at SPE meetings are subject to publication review by Editorial Committees of the Society of Petroleum Engineers. Permission to copy is restricted to an abstract of not more than 300 words. Illustrations may not be copied. The abstract should contain conspicuous acknowledgment of where and by whom the paper is presented. Write Librarian, SPE, P.O. Box 833836, Richardson, TX 75083-3836, U.S.A. (Facsimile 214-952-9435).

Abstract

Petroleum professionals, that is engineers and geoscientist, routinely make recommendations to drill wells. This process requires the generation of a production profile, oil producing rate versus time, which is a key component in the final economic decision of whether or not to drill the well. The success of the drilling program, and possibly the professional's career, rests, to a high degree, upon the accuracy of this predicted production profile. The more accurate this prediction the more certain the economic value of the recommended drilling location. This paper looks at this predictive process as used in the Vacuum Field of New Mexico. It explores the predictive methods used in the past and reports on their accuracy. A new method, using artificial intelligence, is presented which improves upon the accuracy of this process.

Introduction

Acting upon a recommendation to drill a well, which usually involves hundreds of thousands if not millions of dollars, is a major decision. The final decision of whether or not to drill a well is based, in part, upon the economic evaluation of the anticipated performance of the well. A key component of this economic analysis is the predicted production profile, oil producing rate versus time. This forecasting of the production performance of a new well is one of the most important functions a petroleum professional performs. Both underestimating, predicting a producing rate that is lower than actual, and overestimating, predicting an oil producing rate that is greater than actual, the producing performance of the well is common. Both have a major impact upon the actual economic value achieved by drilling, or not drilling, the recommended well. At the extremes, either overestimating or underestimating oil or gas producing rates results in a potentially disastrous economic decision. Overestimating the production profile will result in the drilling of a well that is not economical while underestimating the production performance causes a well to not be drilled which would have been economical. Usually the result of an inaccurate production forecast is the drilling of a well whose economic performance does not yield the optimum economics for the available drilling investment.

References at the end of the paper.

But this is all part of the risk and uncertainty we face in the oil industry. The industry drilled wells in the past and will continue to drill wells in the future. We accept this uncertainty. However, it raises the question of just how accurate have the forecasts from the past been and can this accuracy be improved. For with improved forecasts come greater economic certainty and greater profitability.

Infill Development Drilling Study Area

A category of significant interest in the Permian Basin of West Texas and Southeast New Mexico is infill development drilling. Infill development drilling is defined as drilling within an existing secondary recovery project to reduce well spacing and consequently the waterflood injection pattern.

San Andres reservoirs in the Permian Basin have produced over 7.7 billion barrels of oil, the majority from secondary recovery projects. This is 46 percent of the total production from the entire basin. This large cumulative combined with low recovery, 30 percent of the oil-in-place, makes this reservoir an excellent candidate for improved development.[1] Since infill development drilling in existing waterflood projects provides many of the drilling prospects for the Permian Basin, it was selected as an area to study the overall accuracy of production performance predictions. Specifically, the Vacuum Field of New Mexico is a good area to study since it is a typical San Andres field and the individual production performance of every well in the field is readily available.

The Vacuum Field, see Figure 1, is located in the southeast corner of New Mexico in Lea County at a distance of approximately 120 miles northwest of the city of Midland, Texas.

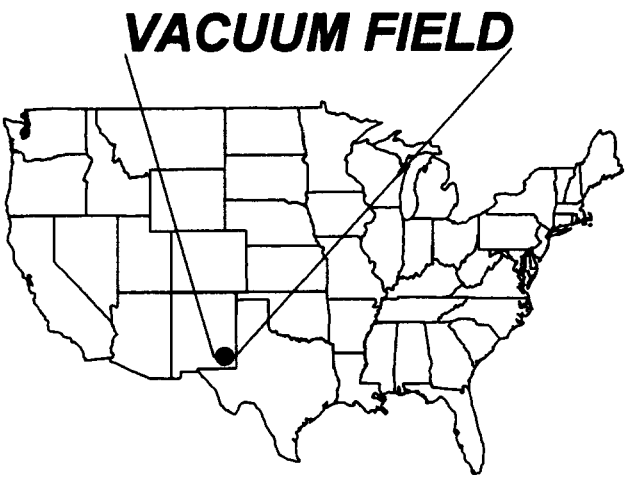

Figure 1 Field Location

The field lies at the north end of the Delaware Basin and Central Basin Platform along a productive east-west-trending shelf area of the Permian Basin. Production is primarily from the Permian Guadalupian age San Andres formation at a depth of 4400 feet. The San Andres is composed of cyclical evaporites and carbonates recording the many transgressings and regressings of sea level occurring around 260 million years ago in a climate very similar to the present day Persian Gulf.[2]

Nine secondary recovery projects constitute the majority of the acreage, wells, and production from the Vacuum Field. Figure 2 shows the outlines of these secondary recovery projects. These projects cover approximately 32 square miles. The field was discovered in 1929 but field development did not start until a pipeline to the field was laid in 1937.

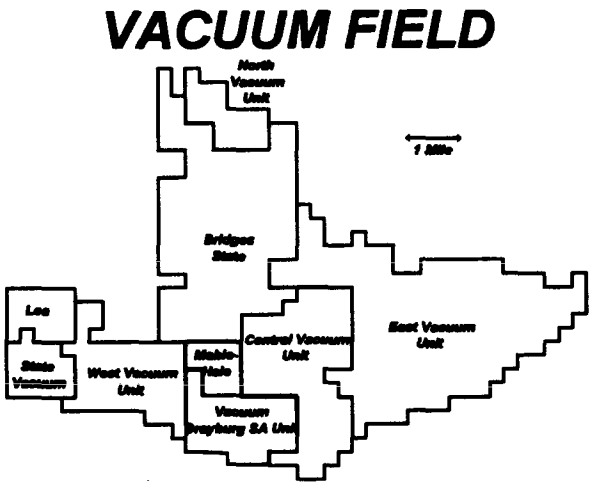

Figure 2 Secondary Recovery Projects

Figure 3 is a plot of monthly oil, water, water injection and well count from 1970 to present. Also shown is oil cut (% Oil), oil volume as a percentage of total produced fluids (oil plus water), and the injection-withdrawal ratio (I/W), water injection rate divided by the total fluid volume. The plot shows that over 300 infill development wells have been drilled in the field since 1970. Field development covers the start of water injection in the 1970's and the down spacing of injection patterns from 80-acre 5-spots patterns to 40-acre 5-spots and to even some 20-acre 5-spots.

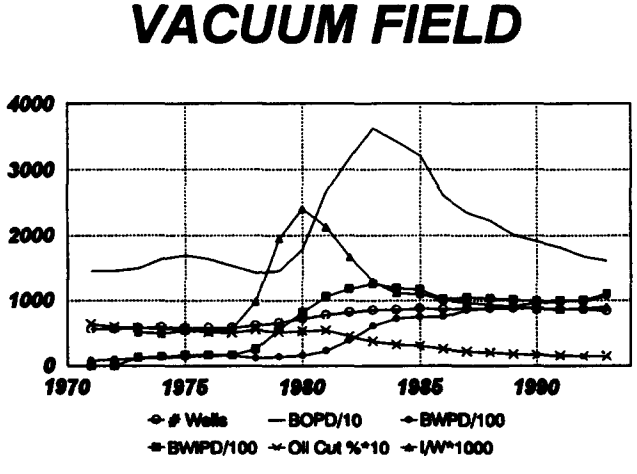

Figure 3 Field Performance

Past Methods of Making Predictions

The Professionals have at their disposal a myriad of tools to predict the production profile of an infill development well. Either a deterministic and/or a statistical method is typically used.

The typical deterministic method for predicting a production profile is a straightforward process. The Professional reviews any geological maps, cross-sections, and existing well logs of the prospect area to determine overall reservoir quality. Next, the Professional reviews the offset well's current and past production performance. Past production performance includes not just the rates and volumes of oil production but also the rates and volumes of water production and water injection. They may also review the production profiles of wells from past drilling programs. It is characteristic of infill drilling for the operator to drill wells in programs with each program including from 2 to 20 wells. In the end the Professionals use this knowledge to generate a production profile for a specific drilling location. Sometimes a numerical reservoir simulator is used to predict a production profile.

Statistical methods consider the actual variability of past drilling programs to generate a single production profile for all proposed drilling locations, knowing that averaging the production performance from every individual well in the drilling program will come close to this statistically generated profile. The actual production performance from each well in the most recent drilling program is first normalized. That is the oil producing rates are normalized with respect to initial completion date not calendar date, production for month number one is the production for the first month after initial completion and not for the month of January. Next these normalized rates are averaged on this monthly basis for every well in that particular drilling program. This resulting production profile is used for the next drilling program. Alternatively, instead of the most recent drilling program the most recent program of "like" wells is used. "Like" in the fashion of 40-acre wells versus 20-acre wells or

geologically similar locations, top of structure versus down dip.

All of these approaches are successful. Successful in that we have used them for decades to recommend wells to be drilled and then to have them drilled. Still, the actual production profile does not match the predicted production profile. Many factors that are not associated with the drilling program itself will influence the long-term forecast, such as changing injection rates or altering injection pattern. If we constrain the time frame over which we compare the actual versus predicted production profile, we might get better accuracy. Monthly production for the first year is a good time frame to use since the profitability of a new well is heavily weighted by the first year's production profile. Accurate prediction of the rate of production for just the first year would improve the certainty of achieving the predicted economical performance of any drilling program. Just how accurate have these approaches been at forecasting oil production over the first twelve months of a well's life?

Prediction Accuracy

A review of the first year's production predictions versus the well's actual performance is enlightening. In the Vacuum Field of New Mexico over 250 producing wells have been drilled since 1970. The Professionals' forecasts were found by searching the well files and correspondence files where Texaco is the operator or where Texaco has a non-operating working interest for the original Authority for Expenditure (AFE) to drill the well. The AFE typically includes the predicted production profile for the proposed location. A sampling of 25 of the 250 wells was used to determine the overall accuracy of the predictions. The production profiles were not biased by a small group of Professionals making forecasts nor were they biased by any particular year's drilling results. Error calculations were based upon the difference between actual and predicted cumulative production, expressed as barrels of oil per day (BOPD), at the one-, three-, six-, and twelve-month time intervals.

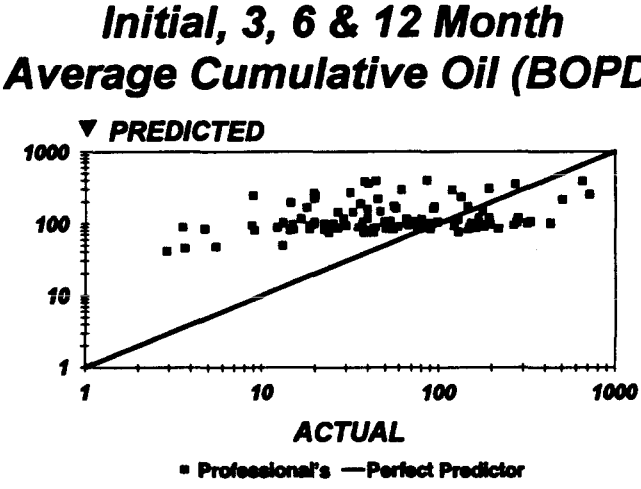

Figure 4 Professional's Performance

Figure 4 shows how accurate the forecasts are by plotting the actual performance versus the predicted performance. This type of plot is called a Confusion Matrix.[3] Included on this figure is a straight line labeled Perfect Predictor. If you had a perfect predictor, then all the points would fall on this line where the actual and predicted values are equal. These Professional predictions have a mean error of 39 BOPD and a mean absolute error of 99 BOPD. The mean absolute error is an excellent measure of the accuracy of the Professional's forecast. For any well their forecast will average within 99 BOPD of the actual rate.

Further statistical analysis reveals that the Professionals predict within ±20BOPD just 8 percent of the time and within ±10BOPD only 5 percent of the time. The Professionals overestimated production 75 percent of the time. It is obvious that the Professionals are not perfect predictors.

One explanation for this poor showing is because of the number of variables considered in making the predictions, variables such as oil rate, cumulative oil, injection rate, and cumulative injection. The Professionals limit the number of offset wells and the

type of data considered from each well in their prediction process. It is very difficult for humans to consider more than a handful of variables at any one time. If a methodology could consider more offset wells and parameters, such as water production, injection withdrawal ratio, etc., then more accurate predictions could be made. What is needed is a tool that provides the professional the means to consider a larger number of variables. Neural Networks are ideally suited to this type of problem.

Neural Network Primer

A Neural Network, as defined by Dr. Robert Hecht-Nielsen (inventor of one of the first commercial neurocomputers), is "a computing system made up of a number of simple, highly interconnected processing elements, which process information by its dynamic state response to external inputs."[4] This definition reflects the basic structure of a Neural Network as that of a computer representation of a biological neuron (nerve cell) that is interconnected with other neurons (a brain).[5] Mathematically, Neural Networks can be viewed as a multi-variable non-linear regression. Neural Networks are not programmed to find a solution, instead they learn by example. Where most computer programs have the principles of chemistry and physics coded into the program itself as equations, Neural Networks do not. Neural Networks do not have any *a priori* knowledge coded into the program at all. Conventional programs apply the coded scientific principles in the program to the problem's inputs to calculate an answer. A Neural Network learns an empirical relationship between the inputs and the desired outputs. The network is presented with different examples of inputs and outputs and relationships are learned after reviewing the examples over and over again, as many as ten million times.[6] It is capable of seeing what Professionals would see if they had the time and inclination to review the inputs and outputs a million times. Professionals who have reviewed inputs and outputs over and over again and have learned a relationship have what is called years of experience. They are considered experts.

A Neural Network initially assumes a random relationship between all the inputs and the desired outputs. By comparing its first attempt at an answer to the desired output, it self-modifies this initial random relationship into a relationship that best fits the outputs. Figure 5 is a graphical representation of a typical Neural Network.

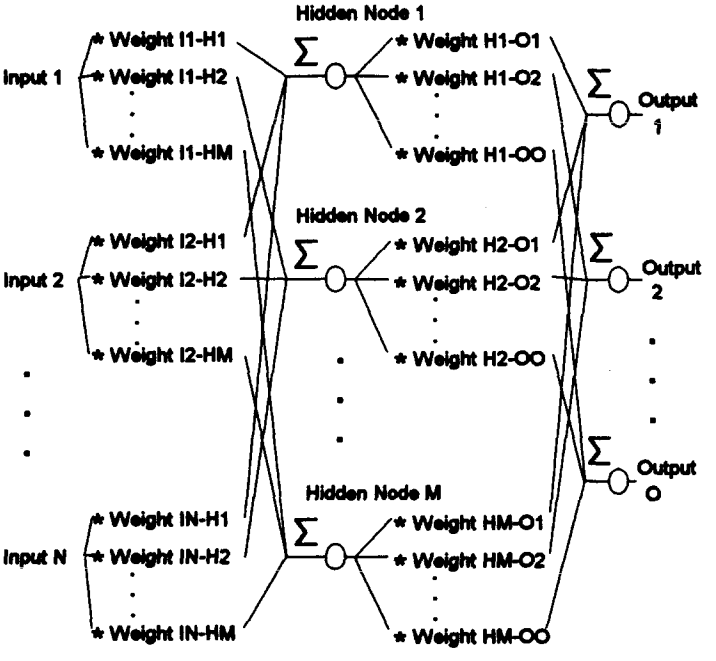

Figure 5 - Typical Neural Network Architecture

The network is made up of a group of interconnected nodes. Biologically, the nodes represent neurons and the interconnections represent the synapse, resulting in a simple brain. The largest network, biggest brain, the author has built has 158 nodes and a total of 5400 interconnections. In comparison, the human brain has over 100 billion neurons and some of these neurons are connected to 10,000 other neurons.

Every input and output is represented by an individual node. The nodes connecting the inputs with the outputs are called hidden nodes. They are called hidden nodes because the end user of the network does not know they exist. Every input node is connected to every hidden node and every hidden node is then connected to every output node. One name for this type of network is a "feed forward"

network. It is called feed forward because the inputs are presented to the network on one side and they flow through the network to the outputs on the other side.

Every connection in a network is associated with a weight factor. These weight factors are independent of each other. The mathematical workings of a network are simple. First the possible range in values for every input and output is determined. Then all inputs and outputs are scaled for their range with 0 for the smallest possible value to 1 for the maximum possible value. At every node, any input to that node is multiplied by its weight factor and then summed with the product of the other inputs and their individual weight factors (see Figure 5). This resulting sum is processed by a transform function within the node.

Two of the more commonly used transform functions are the hyperbolic tangent and logistic. They are "squashing functions;" that is, they pass along a signal with a value between -1 to 1 and 0 to 1, respectively. This transform function provides non-linearity to the network and constrains the node's signal within a fixed range. Regardless of how "excited" an individual node gets, it has a fixed maximum signal that it passes on through the network, just like their biological neuron counterparts. Figure 6 shows a single node and its use of the logistic function.

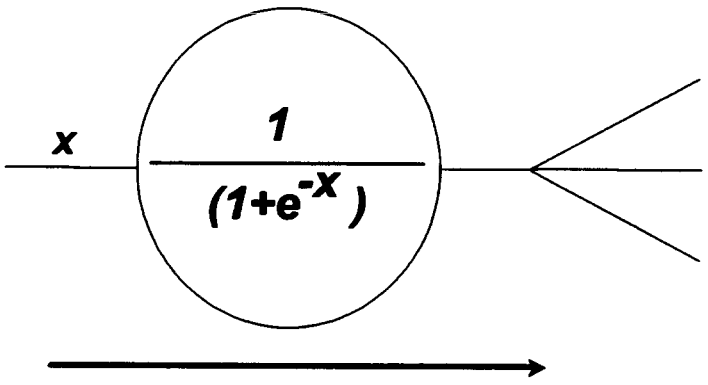

Figure 6 Node's Transform Function

The choice of which transform function and the number of hidden nodes is left to the Network designer, usually several combinations are tried and the one yielding the smallest error is finally chosen. The signals from the hidden nodes proceed in a similar fashion to the output nodes where the final signal is scaled-up to yield the network's answer. The first pass of data through the network produces an answer that is usually way off the mark since all the connection weights are initially random numbers and have not yet learned anything. The networks answer is compared to the correct answer and the network makes self-adjustments to all the connection weights to minimize this error.

This self-adjustment is the reason that another name for this type of network is "back propagation" network. The error is back propagated through the network by adjusting the connection weights in a proportional fashion so the error is minimized. This whole process, feed forward and back propagate, is repeated over and over again for every example the network is supposed to learn. Learning is finished when the average error for all the examples is minimized. This iterative learning may take as many as several million passes of each example through the network before an acceptable average error is reached.

Neural Networks are so good at learning that they can actually memorize all of the training examples. This usually produces a network that does not "understand," it will be poor at applying its newfound knowledge. It is just like the student who had a copy of the answer sheet and just memorized the sequence of answers. He may get a good grade on the test but he does poorly when having to apply this knowledge.

To keep the network honest requires an additional data set of examples for testing the network. Every so often the resulting best network to that point in training time is used on these examples to see how accurate the network is. As long as the network keeps improving on this test set, training will continue. When the network's error starts increasing on this test set, then it is futile to continue training as the network is just memorizing the answers.

The true test of the validity of a network is done by giving the network a "final exam." A third set of examples is used for this testing. The network error on this data set is the true measure of how good the Neural Network performs. The selection of data for the Learning, Testing, and Verifying data sets is not a matter to be taken lightly. To have a Neural Network that you have confidence in requires that the data in each of these three data sets be representative of the problem you are trying to solve. In terms of Artificial Intelligence, the data must cover the Domain of the problem.

It is not unusual to try various combinations of transform functions with a varying number of hidden nodes and selected inputs before deciding upon the final network architecture. This entire process—feed forward, back propagate, stop and test, and then continue training—is easily accomplished with commercially available software.

Production Prediction Neural Network

The first step in building any Neural Network is to develop a data model that captures the data that a professional would use to solve the problem. What inputs would an expert use to generate an output? The review of the past methods of predicting production is the starting point. Data used most often is either offset production data or reservoir characterization data. Since production data is readily available for all wells in the Vacuum Field and reservoir characterization data is not readily available for all the wells in the field, only production data is selected as inputs. The specific production data gathered for every offset well is shown in Table 1.

Current Rate Basis	Cumulative Basis
Oil	Oil
Water	Water
Percent Oil	Percent Oil
Injection	Injection
Inj. - Withdrawal Ratio	Inj. - Withdrawal Ratio

Table 1 Collected Production Data

The professional typically looks only at the nearest offset wells to a prospective drilling location. This usually is the nearest four to eight wells. Since a Neural Network can easily handle more wells than this, a Data Mask is utilized to capture data for wells that are not direct offset wells. The Data Mask is shown in Figure 7. The Data Mask is a 5x5 grid covering 1,000 acres. Each square grid (1,320 feet per side) equals 40 acres. This Data Mask is placed over the drilling location's 40-acre tract and the data listed in Table 1 is collected for every well within the boundaries of the Data Mask. Since the number of inputs in a Neural Network is a fixed number, the number of data values collected by the Data Mask have to be constant for every drilling location. This is impossible as the number of wells within this Data Mask varied between less than 10 to greater than 50. The solution is to divide the Data Mask into three concentric "rings." The "rings," labeled X, 10, and 9, form a bull's-eye target with the drilling location located at the center in the X-Ring. Data collected within each ring is then averaged so the data collected in Table 1 is used with the Neural Network on a per-ring basis instead of a per-well basis. The point in time that this current rate and cumulative data represent is the calendar month preceding the month that oil production for the newly drilled well is first reported to the state of New Mexico, i.e., initial completion.

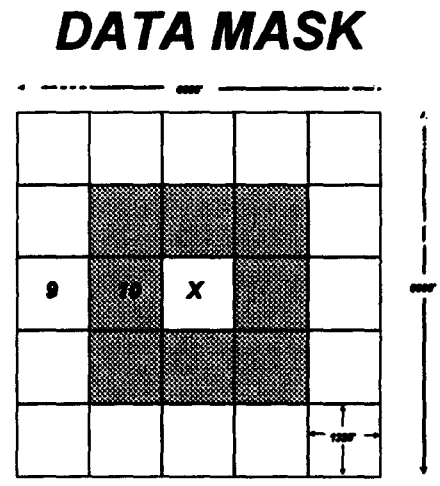

Figure 7 Data Mask

In summary, the data input items, data an expert might use to make a production forecast, for the Neural Network are the current rates and cumulatives for all the wells within a ¾-mile radius of any proposed drilling location expressed as an average for three distinct locations from the drilling location as of the month before the drilling well is initially completed. The outputs for the Neural Network are the one-, three-, six-, and twelve-month cumulative production volumes for the proposed drilling location. All this well data was collected for each of the 250 producing wells completed in the Vacuum Field since 1970. To gather the data for these 250 wells required that data for 7883 offset wells be captured. A schematic of the network is shown as Figure 8.

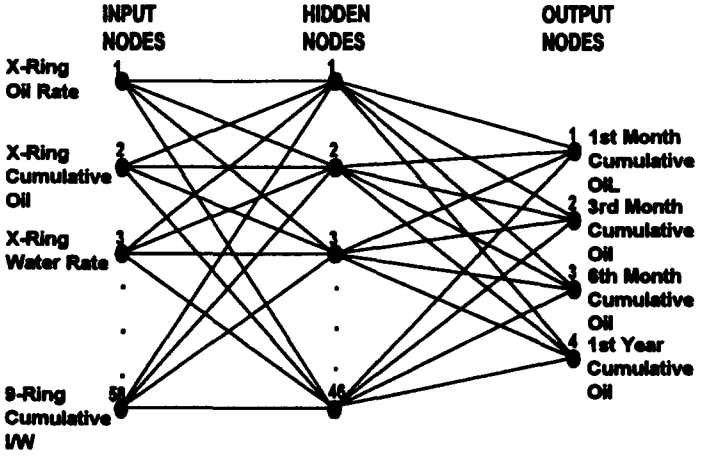

Figure 8 Neural Network

This network learned the relationship between all these variables for about 164 randomly selected wells. An additional 74 randomly selected wells were used to test the network to prevent memorization. The remaining 12 wells were used to verify the accuracy of the Neural Network. Over 30 different network configurations were tested before this network was selected as the best. Training time took approximately four hours on a 33mhz 486 PC.

Neural Network Prediction Accuracy

Figure 9 shows the same Confusion Matrix seen earlier but with the Neural Network's predictions. This is the verify data set, data the network had never seen while training. It shows that the Neural Network slightly underestimates production 38 percent of the time. It has a mean error of -19 BOPD and a mean absolute error of 27 BOPD. This network is over 3.5 times (a mean absolute error of 27 BOPD for the Neural Network versus and a mean absolute error of 99 BOPD for the Professionals) more accurate than the Professionals.

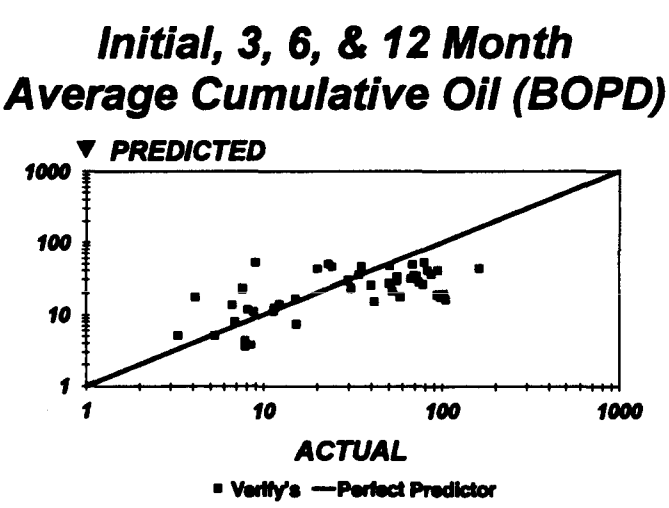

Figure 9 Neural Network's Performance

Conclusions

Statistical analyses of the networks' results are shown in Table 2 along with the analysis of the Professionals' results. As shown in Table 2, the Neural Network is within ±20BOPD 51 percent of the time and within ±10BOPD 39 percent of the time. In a direct comparison, the Neural Network out performed the Professionals 93 percent of the time.

	Accuracy (% of the Time)	
	PROFESSIONAL	NEURAL NETWORK
±20 BOPD	8	51
±10 BOPD	5	39
Optimum	7	93

Table 2 Performance Comparison

While this is quite an improvement, it still is not a perfect predictor. If the Neural Network was presented with additional data that correlates with production, then it would perform even better. An obvious source of this relevant data is geological/geophysical information. Just as the Professionals used this information in making their predictions, a Neural Network would also gain knowledge if it had geological/geophysical data as an input. Figure 10 shows the more familiar rate versus time production plot for an average well. It also shows the predicted profile for both the Professionals and the Neural Network.

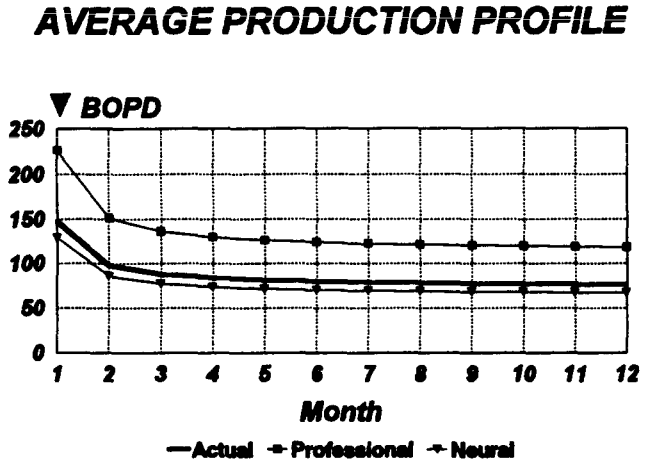

Figure 10 Typical Performance

Another advantage, besides accuracy, the Neural Network has over the Professionals is that it can quickly screen vast areas for those locations with the highest production potential, generating production profiles for all possible drilling locations. Figure 11 shows the results of such a screening that covers several select properties, about eight square miles, within the Vacuum Field. It would take a Professional weeks or even months to generate these production profiles while it takes only a couple of hours to build the data set and execute the Neural Network.

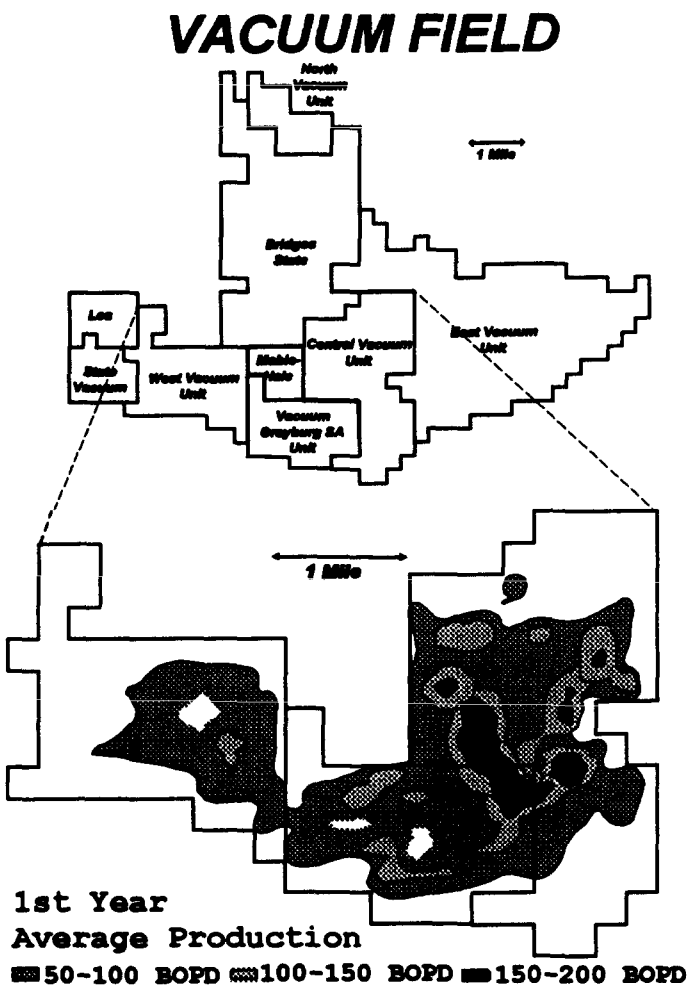

Figure 11 Neural Network Screening

Summary

A Neural Network that predicts production is a powerful tool that can reduce uncertainty in our predictions.

Acknowledgments

The author thanks Texaco Exploration and Production Inc. for permission to publish this paper and to my colleagues for their support during its preparation and review.

References

[1]*Geologic and Engineering Approaches in Evaluation of San Andres/Grayburg Hydrocarbon Reservoirs-Permian Basin*, D. G. Bebout and P. M. Harris (ed.), Bureau of Economic Geology, Austin, Texas (1990) iii

[2]Purves, William J.: "Reservoir Description of the Mobil Oil Bridges State Leases (Upper San Andres Reservoir), Vacuum Field, Lea County, New Mexico," *Geologic and Engineering Approaches in Evaluation of San Andres/Grayburg Hydrocarbon Reservoirs-Permian Basin*, D. G. Bebout and P. M. Harris (ed.), Bureau of Economic Geology, Austin, Texas (1990) 87-112

[3]Klimasauskas, Casimir C.: "Applying Neural Networks: Part III,: *PC AI* May/June 1991 **5 3**, 20-24

[4]Caudill, Maureen: "Neural Networks Primer Part I," *AI Expert* December 1987 **2 12**, 46-52

[5]Klimasauskas, Casimir C.: "Applying Neural Networks: Part I," *PC AI* January/February 1991 **5 1**, 30-33

[6]Wasserman, Phillip D.:*Neural Computing Theory and Practice*, Van Nostrand Reinhold, New York (1989) 1-26

SPE 30600

Application of Neural Networks to Modeling Fluid Contacts in Prudhoe Bay

Manmath N. Panda, SPE, e-mail: mpanda@arco.com;* David E. Zaucha, e-mail: dprdez@arco.com;* Godofredo Perez, SPE, e-mail: gpx@arco.com;* and Anil K. Chopra, SPE, e-mail: anil@arco.com.*
*ARCO Exploration and Production technology, 2300 W. Plano pkwy., Plano, TX 75075.

Copyright 1996, Society of Petroleum Engineers, Inc.

SPE paper 30600 was first presented at the SPE 70th Annual Technical Conference and Exhibition held in Dallas, Texas, USA, 22-25 October, 1995.

Permission to copy is restricted to an abstract of not more than 300 words. Illustrations may not be copied. The abstract should contain conspicuous acknowledgment of where and by whom the paper was presented or published. Write Librarian, SPE, P.O. Box 833836, Richardson, TX 75083-3836, USA, fax 01-214-952-9435.

Abstract

Modeling the dynamic behavior of fluid movement in an oil reservoir is complicated because of non-linear interactions between reservoir heterogeneity and fluid flow. Simple regression, geostatistical, and numerical simulation techniques have been used in the past to model fluid movement with various degrees of success. Most of these methods, however, suffer from common drawbacks that they are time consuming and difficult to automate. This paper presents a new method based on artificial neural networks (ANNs) to model dynamic gas-oil contacts in the Prudhoe Bay reservoir. This method is fast, efficient, and highly automated and requires minimum user intervention.

The proposed method uses oil, gas, and water production, perforation history, permeability, sand and shale distribution, and surveillance data at surrounding wells as ANN input to predict the fluid distribution at a target well. A two-step method is developed to design an ANN. The first step trains the network using previously measured data as input and output, and thus establishing the internal rules of the network. The second step uses the trained network to estimate the fluid distribution at target wells. Results show that the ANN method can predict fluid distribution at target wells more accurately and consistently than conventional methods.

Introduction

The Prudhoe Bay field on the north coast of Alaska is the largest oil field in the North America, with total estimated original oil in place (OOIP) of about 22 billion barrels. The field is overlain by a large gas cap and a major portion of the field is being produced by gravity drainage. Waterflood operations are confined to the down-structure and peripheral areas of the field.[1] Prudhoe Bay can be roughly divided into two regions based on the development strategy and current recovery mechanisms: gravity drainage and water and miscible gas flooding (**Fig. 1**). This paper deals only with the gravity drainage area.

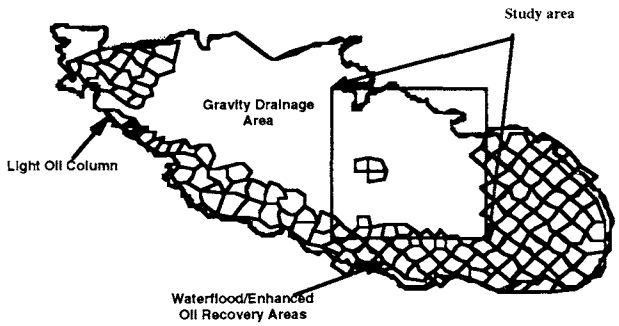

Figure 1. Prudhoe Bay field -- shows regions of water and miscible flooding and gravity drainage.

Characterizing fluid movements in a reservoir is a critical engineering task because it forms one of the key elements for field development, reservoir management, and predicting reservoir performance for different mechanisms. The benefits of such a characterization include reduction of gas and water handling costs, selection of completion and re-completion intervals, and development of better reservoir simulation models.

In Prudhoe Bay, interactions between different drive mechanisms, such as gravity drainage, gas cap expansion, waterflooding, miscible displacement, and reservoir architecture and heterogeneities (shales, faults, and fractures) result in complex gas and water movement through time. Shales of varying sizes, which may not be continuous between wells, have a significant effect on the gas movement. Gas tends to move underneath shales resulting in isolated gas tongues or fingers (also called gas underruns) that break through at different times at wells. Such gas underruns often tend to bypass oil regions, called oil lenses, predominantly above impermeable shales (**Fig. 2**). Cased hole monitor logs for a given well show multiple and different gas-oil contacts. It is difficult to interpret and visualize the inter-well distribution of gas and oil in the reservoir under these conditions.

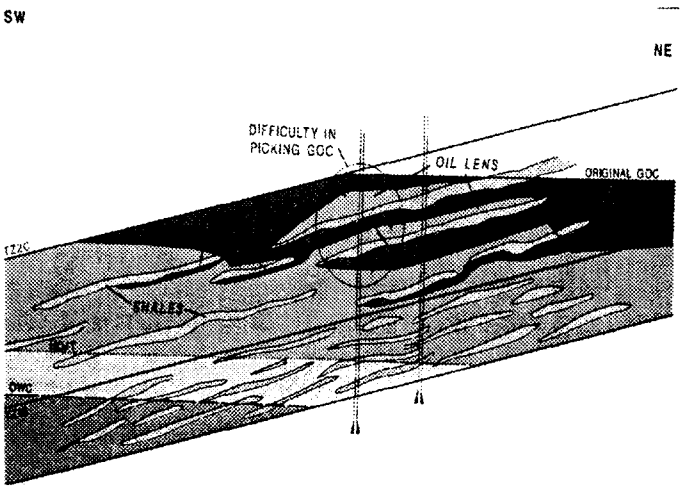

Figure 2. Schematic showing distribution of oil, gas, and shales in Prudhoe Bay. Fluid prediction becomes difficult because of interdependence of these parameters.

The conventional approach to map the interwell movement of fluids is based on simple deterministic approaches. The accuracy of the mapping results depends mainly on the intuition and experience of practitioners because this method relies on visual interpretations of multi-well cross-sections of the surveillance, reservoir description, production, and completion data. This deterministic approach has several drawbacks. Even though conceptually simple, it is extremely time consuming and, in addition, results can be inconsistent. Another approach is to first characterize the reservoir heterogeneity and then use reservoir simulation. This approach is very effective in understanding the effect of different reservoir mechanisms on fluid saturations, but cannot incorporate surveillance data *a priori*. Recently, geostatistical methods have also been used for predicting fluid contacts in Prudhoe Bay.[2] This approach to modeling fluid movement treats data, such as oil, gas, shales, etc., in each layer as independent stochastic variables. The space-time characteristics of these variables are represented by their semi-variograms. Prediction of these variables at any location is done using conditional stochastic simulation. This geostatistical method provides more accurate prediction of fluid distribution than other methods; however, it is difficult to automate and it cannot account for more than two to three variables simultaneously.

This paper presents a new method that uses ANNs to predict time varying characteristics of fluid contacts in the Prudhoe Bay reservoir. By using all available data, such as geological, petrophysical, production, completion, and logging, this method produces a generalized model of the reservoir system. It is fast, efficient, and easily automated and, hence, is suitable for routine applications in the field. Applications of the neural network mapping include estimation of fluid distribution at a given well location, a measure of uncertainty of estimation, and visualization of the interaction between gas movement and shales.

In this paper, first a brief discussion of ANNs is presented followed by strategies to design a network for Prudhoe Bay fluid mapping. Results are then presented to validate the new method and conclusions drawn based on these results.

Artificial Neural Networks

Artificial neural networks (ANNs) are recent developments in computer vision and image processing.[3] ANNs are being routinely used in complex time series prediction.[4] A typical ANN involves processing of patterns that evolve over time—the appropriate response at a particular time depends not only on the current characteristics of the observable event but also on the past events. ANNs, which are simple prototypes of natural neural networks, provide broad-based generalization to complex processes. Examples of their application are numerous in such areas as financial market prediction,[4] medical diagnostics,[5] seismic inversion,[6] computer image analysis,[7] and speech synthesis.[8] Only a limited number of applications[9,10,11] have been reported in petroleum engineering.

ANNs have the ability, under certain conditions, to approximate complex systems by non-linear interpolation of experimental data.[4] They are conceptualized based on the premise that problem solving skill is achieved through interaction of a large number of simple processing units or nodes. This premise is based on observations and current understanding of brain anatomy. For example, the modest brains of

lower animals, like mosquitoes, snakes, etc., can perform tasks that are far beyond the range of the largest and fastest electronic computers. This suggests that the key to efficient solution of complex problems lies in parallel distributed processing; that is, a large system with simple 'hardware' components driven by sophisticated software. Such an artificial prototype of natural neural networks can also have a potentially important advantage of a high degree of tolerance to error or noise in input data to model the system under consideration; similar to the functionality of a human brain. For example, the ease with which a human brain can read several types of hand writing, which is the error ridden input, shows the error tolerance characteristics of a natural neural network.

Three major components of an ANN are: input, hidden, and output nodes. Intermediate results are stored into temporary arrays called hidden nodes. The input nodes are connected to the hidden nodes, which, in turn, are connected to output nodes. These connections, which indicate how nodes are functionally related to each other, are represented by weights, critical internal parameters of the network. When pictorially represented, an ANN appears like a network as shown in **Fig. 3**, where nodes are shown as circles and connections or weights as straight lines.

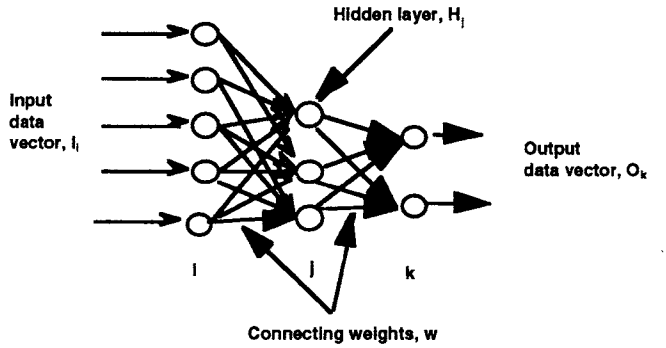

Figure 3. Schematic showing the progression of computation from input to output nodes in a feed forward network.

Figure 3 presents a typical three-layered feed forward network. Information is processed, during both training and prediction phases, from the input to output layer; hence, the name feed forward. Each hidden node is connected with all the input and output nodes. We denote the weights between input and hidden nodes and between hidden and output nodes by w_{ij} and w_{jk}, respectively. Data stored in the input, hidden, and output nodes are denoted by I_i, H_j, and O_k, respectively.

When the processing begins, data stored in each input node is multiplied by the connecting weights. The products of all node values and connecting weights are summed and stored at each hidden node. The resulting sum is passed through non-linear transfer functions called 'squashing functions'. They provide non-linearity characteristics to the network and constrain the node's signal to a fixed range. A widely used squashing function is the hyperbolic tangent function expressed as

$$H_j = \left[1 + \exp(-\sum_i I_i . w_{ij})\right]^{-1} \quad \text{.....(1)}$$

where the summation is evaluated for all input nodes i. Results at output nodes are also computed following a similar treatment.

Now, referring Fig. 3 the hidden nodes are evaluated by convolution (indicated by operator *) as

(Input data) * (Connecting weights) --> (Hidden layer)

$$\text{or, } H_j = \left[1 + \exp(-\sum_i I_i . w_{ij})\right]^{-1} \quad \text{.....(2)}$$

and the output nodes are evaluated as

(Hidden layer) * (Connecting weights)--> (Output)

$$\text{or, } O_k = \left[1 + \exp(-\sum_j H_j . w_{jk})\right]^{-1}$$

$$= \left[1 + \exp(-\sum_j \left\{1 + \exp(-\sum_i I_i . w_{ij})\right\}^{-1} . w_{jk})\right]^{-1} \quad \text{.....(3)}$$

The choice of transfer functions depends on the experience and knowledge of the user about the system under study. Some users also advocate using different transfer functions at different nodes to reflect the complexity of the system.[4,5]

The three phases in any ANN simulation technique are designing, learning (training), and prediction. Designing determines the number of input, hidden, and output nodes. The learning phase consists of iteratively adjusting network parameters so that the ANN output is same as the desired. The iteration is continued until a suitable convergence is achieved. The converged internal parameters of a network, also called weight matrix, are used in the prediction phase.

A critical feature of the learning phase is the algorithm that governs the convergence of the internal

weight matrix. The selection of the learning algorithm depends on the complexity of the system being studied, availability of data, objective of the study, and the prior knowledge about the system. The two main types of learning algorithms available are: unsupervised and supervised. An unsupervised method is predominantly used for pattern recognition where a discriminant is designed based solely on input data. It examines the input data, finds out about some of the properties of the data, and learns to reflect these properties in its output. The exact nature of these properties that the network can learn to recognize depends on the particular network model. A supervised learning, on the other hand, is one where the network output is compared with the actual output and the internal parameters are modified in such a way that the error, defined as the difference between the actual data and network output, decreases. The most widely used example of supervised learning technique is the backpropagation algorithm, which we used. A more detailed discussion on various training algorithms is given by Hertz *et al.*[3]

Before training a network, the input, output, and number of hidden nodes are fixed based on experience, or by trial and error. Random numbers are assigned to the connections or weights. Then, during each iteration of training, the network error is computed. Using a suitable training algorithm the weights are modified. Training continues until the error is less than a user-specified level. Thus, a trained network, which is used to estimate outputs in the prediction phase, is nothing but a set of weights or numbers.[3,4,5]

Methodology

Neural Network Design. The most essential aspect of designing a network is the selection and proper representation of input variables so that the mapping function can be modeled efficiently during training. The input selection is in regard to the number and type of physical properties that influence the output data. These aspects are critical because, if we have too few number of input variables, then the network will have too few internal parameters and will fail to generalize the mapping function. Similarly, if we have too many input parameters, the system will be over determined, and will fail to generalize. Hence, a well planned network design strategy is essential.

One of the strategies often implemented to determine proper input variables is to analyze the physical laws that govern the system. For instance, the fluid distribution at a target location at any time depends on the fluid distribution at the same location at a previous time and the net fluid movement in the drainage volume during that time interval. The fluid distribution at the previous time is usually known from production logs. Generally, fluid distributions at the target location at two previous time intervals are used to extract any local temporal trend of fluid movements. Thus, when trained over a large range of data, the network learns the dynamic behavior of fluid movements - implicitly representing the physics of flow. During the training the network also learns the effects of potentially non-stationary events such as, well shut-ins, cut control, reperforation etc. The net fluid movement from the drainage volume depends on the number and location of injection and production wells, their rate of injection and production, perforation intervals, shale distribution (that controls vertical communication), and the permeability distribution between target and surrounding wells. These data are routinely measured and recorded. We use all these data as input to the network. Such a system's analysis is analogous to energy balance computations.

Scaling. To ensure a fast convergence of the network, input data are usually pre-processed or scaled such that the range of their variation is small.

Scaling facilitates an easy recognition of functional dependence of various parameters by the network. We demonstrate the significance of scaling by way of a simple example in **Table 1**. Variables A and B sample different ranges of values. Where as A varies mostly in the range 900 - 1000, B varies uniformly between its minimum and maximum values. Use of unprocessed A and B may produce an ill conditioned weight matrix yielding an unstable network. A stable network is obtained if variables are represented only within their significant ranges of variations.

Variable	Range	Significant range	Categories			
			1	2	3	4
A	0-1000	900 - 1000	0 - 900	900 - 930	930 - 960	960 - 1000
B	-1 - +1	Uniform	-1 - -0.5	-.5 - 0	0 - 0.5	0.5 -1

Table 1. Example showing the effect of scaling for uniform representation of two variables, A and B.

To represent the significant ranges of all variables uniformly we scale the input data into classes or categories. That means instead of using input variables in terms of their usual physical units they are represented as categories, such as large, medium, small, etc. Such a representation has several advantages. Local variations in input variables are dampened and also, the weight matrix becomes less biased as all input data are uniformly represented. This categorization

scheme helps the network to learn the global functionality of the system more easily.

Different data are scaled differently. Here, we give a brief account of how each data type is scaled. *Continuous Data* - Permeability, gas and oil production: these data are divided into categories or bins, that is, instead of specifying in their usual physical units they are divided into n categories between their observed minimum and maximum values, where n is determined by trial and error. By doing so we suppress all variations that occur over small intervals of time or space. Distance between wells: is specified as classes (or circular regions around the target well) such as, nearest, not so near, far, farthest. The choice of cutoff radii that distinguish between these classes depends on prior information about the field like the range of permeability correlation structure. *Discrete data* - Pay/non-pay, gas/oil distribution: are specified as binary variables.

All available data are presented to the network as a stream or vector of numbers. The final selection of pertinent input data is performed by a process called *pruning*.

Pruning. Not all input data are of the same importance to the network for learning the functionality of the system. For example, fluid withdrawal rates and distribution of shales are of primary importance to predict fluid distributions. Whereas, others, like the perforation interval, angle of dip, and permeability correlation range, may be of secondary importance. The significance of each variable is determined from the magnitude of its connecting weight inside the network. If a variable has a small weight, the weight can be eliminated from the network without a significant loss of accuracy. Such eliminations make the network compact and efficient. This procedure of selective elimination of input data is called *pruning*.

Pruning identifies variables that are important and have significant influence on the output. For example, during the pruning of all Prudhoe Bay data porosity, permeability correlation range, and well deviation angle were found to be of little importance in determining fluid distributions. These variables are removed from the input list. In addition, pruning shows that some of the most important input variables are oil and gas production rates, distance between the target and surrounding wells, distribution of shales, and average permeability in the producing interval. These variables have relatively large weights associated with them.

Input/Output Data Vectors. Input and output data vectors are determined by scaling and pruning all Prudhoe Bay data. **Figure 4** schematically summarizes the space-time coverage of these data. Figure 4(a), which presents the areal coverage of input data, shows locations of the target and four surrounding wells, one from each quadrant around the target well. By choosing the surrounding wells from different quadrants, we provide the local gradient of fluid-contact surfaces to the network.

Figure 4(b) shows the time coverage of input data where T_0 is the current year and T_{-1} and T_{-2} are two previous years and S_1, S_2, S_3, and S_4 are four surrounding wells. This figure shows all available data for the target and surrounding wells for previous two years are used as input to the network. Past fluid distributions in the surrounding wells are used to provide temporal trends in fluid-contact surfaces.

Prediction of fluid distributions in the target well is done at 1 ft resolution in the interval 300 ft above and below a geologic reference marker, which is correlated throughout the study area. This 600 ft interval provides adequate coverage of the producing zones in the gravity drainage area. During the training input and their corresponding output data vectors are created at every foot of this interval. At any depth in the target well the input vector contains all data from the cylindrical volume shown by Fig. 4(b) and (c), namely the following data:

for target well

- depth of interest,
- permeability distribution in the interval 30 ft above and below the target depth - foot-by-foot permeability in the interval 5 ft above and below the target depth, average permeability over intervals 5 - 10 ft, 10 - 20 ft, and 20 - 30 ft above and below the target depth. Missing values are represented by zeros and are excluded from computing averages. These permeabilities are then scaled.
- distance to the nearest perforation zone,
- pay/non-pay information 30 ft above and below the target depth - represented as binary numbers, pay = 1, non-pay = 0,
- previous year's fluid distribution, if available, 30 ft above and below the target depth - represented as binary numbers,
- and scaled monthly oil and gas production rates,

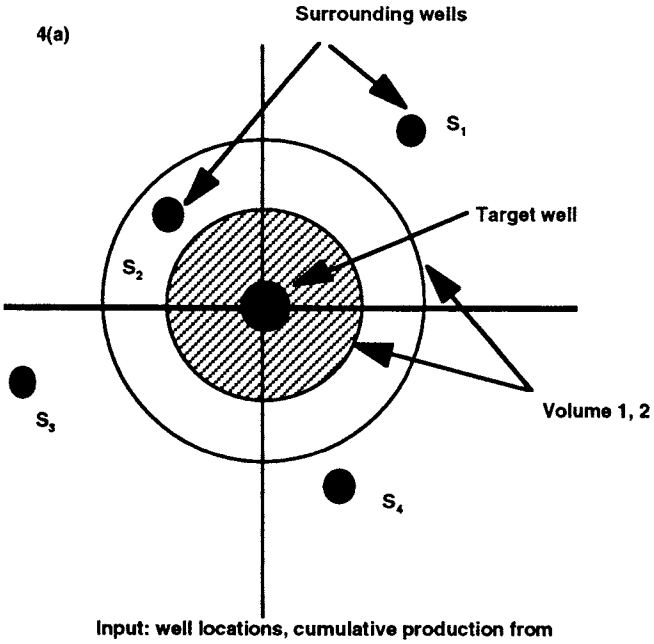

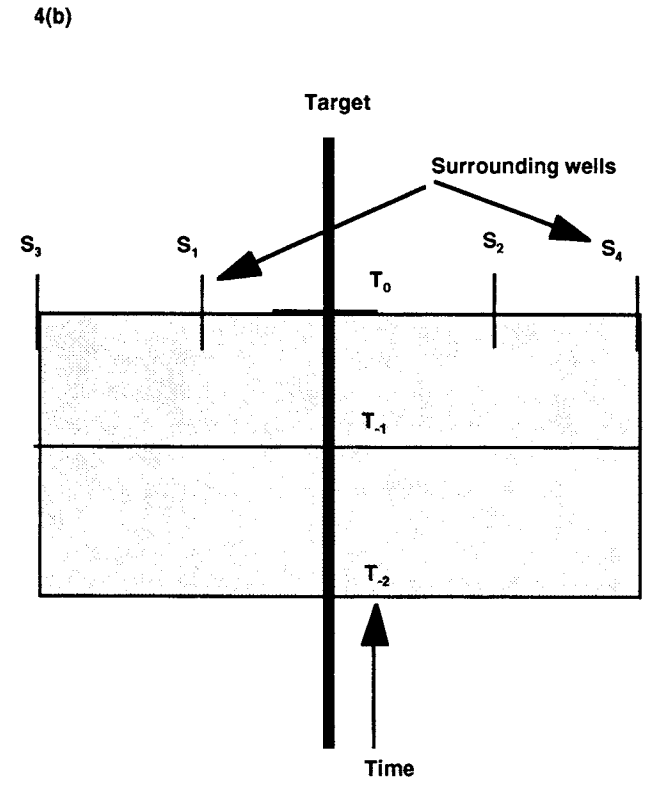

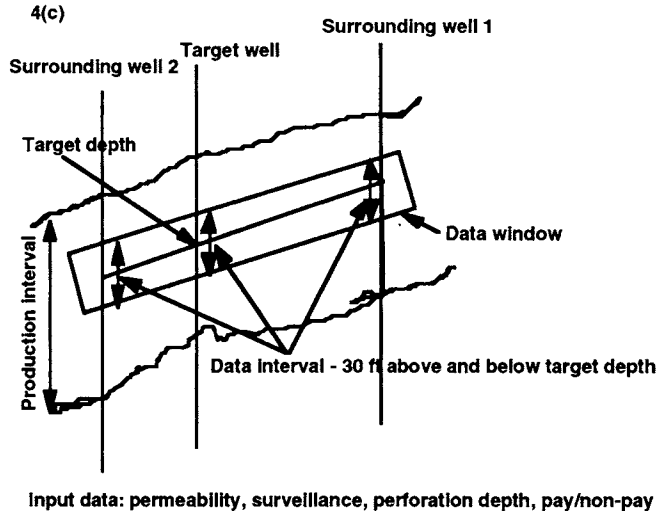

Figure 4. Schematic showing the input data representation for the neural network tool. One surrounding well from each quadrant is chosen.

for each of the surrounding wells

- scaled permeability distribution 30 ft above and below the target depth,
- distance to the nearest perforation zone,
- pay/non-pay information 30 ft above and below the target depth,
- current and previous years' fluid distribution,
- distance from the target well,
- position relative to the target well - the quadrant number,
- monthly oil and gas production rates for the current and previous year, and
- cumulative oil and gas production from incremental volumes around the target well.

The output vector has two elements - one indicates the presence of gas and the other, the presence of oil. If the presence of gas is exactly equal to 1 and the presence of oil is exactly equal to -1 (or vice versa) then the network is predicting the presence of gas (or oil) at the target depth with 100% confidence. If, however, the output is (1,1), (-1,-1), or (0,0) then the network is predicting contradicting results. A 0% confidence (half of the absolute value of the difference between the output elements) is assigned to such results. A low confidence in any interval indicates that the fluid movement is too complex for the network to identify.

Training Strategy. Training, which optimizes the internal weight matrix, is the second phase of the neural network simulation. At the beginning of the training, the weight matrix is initialized randomly by assigning values from a uniform distribution in the

range -0.25 and 0.25 to all the elements. By choosing elements from this narrow range the chances of introducing any fixed structure inadvertently into the weight matrix is minimized. The input and output data are scaled and presented to the network as arrays or vectors. In every iteration during the training the input data is processed using a feed forward operation. Based on the magnitude of the network error, the weights are altered using a standard back propagation algorithm, which is a special case of the well-known Newton-Raphson method. **Figure 5** presents various steps of this approach. Weigend,[4] Al-Kaabi and Lee,[9] Boomer,[10] and Hertz *et al.*[3] present mathematical details of this algorithm.

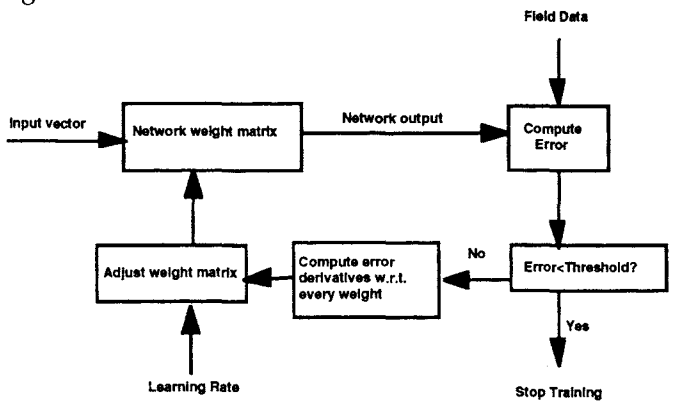

Figure 5. Flow chart of the standard backpropagation training algorithm.

Results and Discussion

A. Setting. We use petrophysical, production, and surveillance data from the Prudhoe Bay reservoir to develop a generalized model of several drillsites in the gravity drainage area. A number of wells are selected as target wells based on the density and quality of data. A feed forward network is trained over eight years' history data.

Model generalization occurs during training, which means the model should not be biased or location dependent, or depend on any other particular parameter, such as production rate, permeability, perforation interval. To accomplish this, we randomize the sample patterns; that is, instead of training the network over systematically ordered locations, like start at drillsite 1, then go to drillsite 2, and so on, the training is performed on randomly ordered well locations. As a result, the network learns global functionality instead of memorizing the local variations.

B. Training. All input and output data are scaled and presented as a vector to the network. During each iteration of the training (and prediction) phase, 600 vectors of input and output data are created. These data, when digitized, give rise to a potentially large network. The complexity increases when the number of years to be processed is large. However, because the computer code is highly automated, the entire process remains transparent to the user.

Steps involved in the prediction process can be summarized as follows:

1. Find at least 4 wells, one from each quadrant, closest to the target well for the current and previous year where surveillance logs are available.
3. Fetch permeability, pay/non-pay, perforation depths, monthly production rates of oil and gas for the current and previous year for the target and surrounding wells.
4. Scale input data—permeability, production, distance of wells from target, etc. — into classes.
5. Digitize input data.
6. Predict fluid distributions in the target well using the trained network.
7. Create PostScript files showing the pay/non-pay and predicted fluid distribution in the interval 250 ft above and below the reference marker in the target well.

C. Validation. The new fluid prediction tool, called Prudhoe Bay neural network simulator (PBNN), is applied to a wide range of regions in the mid-structure of Prudhoe Bay. This section presents some of the results from PBNN runs. Results are validated by comparing with measured data. By running the predictor at a number of well locations not previously used for training, we determine the accuracy and limitations of the tool.

Figure 6(i) presents a typical output from PBNN. The target well is 01-16 in 1988. Four surrounding wells, 01-25, 05-03, 11-03, and 01-12, are chosen based on the quality of field data available for these wells. Locations of the target and surrounding wells are shown in the inset map. As mentioned previously, surrounding wells are selected from different quadrants to obtain the local spatial gradient of the fluid contact surfaces. Measured fluid distributions at target and surrounding wells are compared with neural network estimates at the target well. The geologic reference marker in all the wells is lined up to visualize the effect of dip angle.

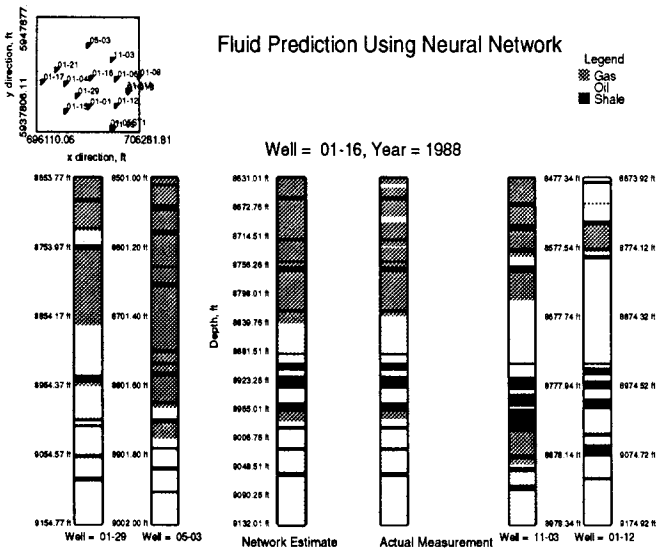

Figure 6(i). Comparison of neural network results with log-measured data for well 01-16.

Figures 6(ii) and 6(iii) present two examples from a number of simulation runs performed at several wells to verify the range of applicability of the tool.

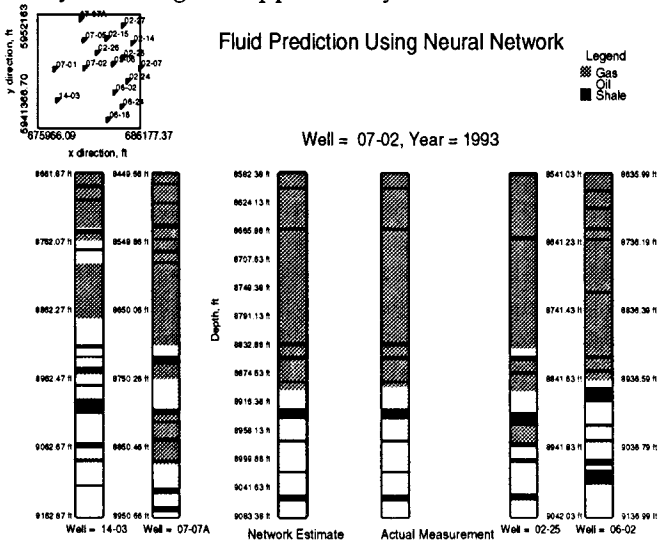

Figure 6(ii). Comparison of neural network results with log-measured data for well 07-02.

Figures 6 show very good matches between neural network estimated fluid distributions and actual data. The error in predicting the thickness of light oil column (LOC) is of the order of the resolution of the surveillance log (≈5 ft). It is also clear that it would be difficult to estimate fluid distributions at target wells accurately by a simple interpolation of fluid picks at the surrounding wells because of complex interactions between the reservoir and fluids.

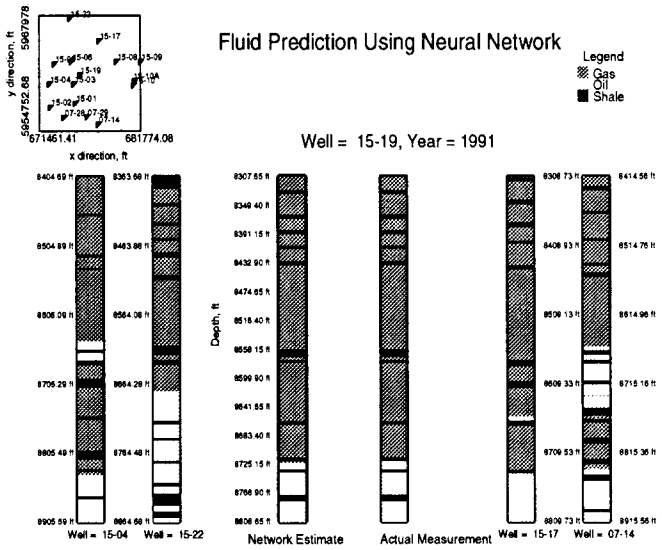

Figure 6(iii). Comparison of neural network results with log-measured data for well 15-19.

Figure 7 compares total light oil column (TLOC) predicted by PBNN for several wells selected in the mid-structure region of Prudhoe Bay with actual data. The TLOC is defined as the sum of oil columns in all pay zones in the interval 300 ft above and below the reference marker. The error in prediction of TLOC is within ±15% for the study area. For a local region comprising drillsites 1, 2, and 5 the estimation error is as low as ±8%. This is expected because the error in the NN approach increases only gradually, rather than abruptly, when applied to a larger area; similar to the characteristics of a natural neural network.

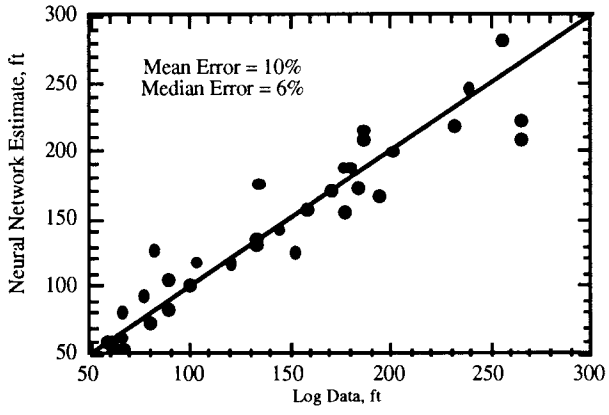

Figure 7. Comparison of neural network estimate of the total oil column in the gravity drainage region of Prudhoe Bay.

A few limitations of the new method are: firstly, it is applicable in data-rich regions and it works best

when surrounding wells are close to the target well. If the density or quality of the data becomes poor, then the accuracy of results also goes down. Secondly, it deals only with the gas and oil presence rather than quantitative fluid saturations.

Conclusions

This paper presents a new fluid prediction method for the gravity drainage area of the Prudhoe Bay field. The method uses artificial neural networks and hence it produces a generalized non-linear interpolation of existing data in three dimensions. It produces a more realistic picture of fluid distributions than existing methods. We derive following conclusions:

1. The new method can integrate reservoir surveillance, production, geological, and petrophysical data to provide a generalized model to predict realistic fluid contacts in a reservoir.
2. This method is validated using the Prudhoe Bay database. It is applicable to most wells in the gravity drainage area.
3. The error in predicting TLOC is within ±15% for the entire study area. For a local region comprising drillsites 1, 2, and 5 the estimation error is as low as ±8%.
4. The error in estimating TLOC decreases when this approach is applied to smaller, geologically similar areas.
5. The results are consistent and reproducible, and not influenced by the bias of practitioners.
6. The method is automatic after the initial training. It is faster and requires less effort than the traditional methods.

Nomenclature

I = input data vector to the network
H = hidden layer
O = output from the network
w = connecting weights
i, j, k = indices for input, hidden, and output nodes

Acknowledgments

We thank Dr. Larry W. Lake of The University of Texas at Austin for his critical insights regarding the use of neural networks. Our thanks are due to the management of ARCO and the Prudhoe Bay Unit Working Interest Owners for permission to publish this paper. We also thank our colleagues for their cooperation, insights, and suggestions, in particular, Matt Maguire, John L. Hand, Dan Kruse, Chuck Severson, and Eric Chang. The techniques and conclusions presented in this paper are those of the authors and may not reflect those of the Working Interest Owners of Prudhoe Bay.

References

1. McGuire, P.L., and Stalkup, F.I.: "Performance Analysis and Optimization of the Prudhoe Bay Miscible-Gas Project," *SPE Reservoir Engineering* (May 1995) 88.
2. Pérez, G., Chopra, A.K., and Severson, C.D.: "Enhanced Geostatistical Mapping of Reservoir Fluids," SPE technical paper no. 29964, presented at the 1995 International Conference on Petroleum Engineering, Beijing, China, Nov. 15-17 (1995).
3. Hertz, J., Krogh, A., and Palmer, R.G.: *Introduction to the Theory of Neural Computation*, Addison-Wesley Publishing Co., New York (1991).
4. Weigend, A.S., and Gershenfeld, N.A.: *Time Series Prediction: Forecasting the Future and Understanding the Past*, Addison-Wesley Publishing Co., New York (1994).
5. Kandel, A., and Langholz, G.: *Hybrid Architecture for Intelligent Systems*, CRC Press, Ann Arbor (1992).
6. McCormack, M., Zaucha, D. E., and Dushek, D.W.: "First-break Refraction Event Picking and Seismic Data Trace Editing using Neural Networks," Geophysics, Vol.. 58, No. 1 (1993) 67.
7. Pati, Y.C., and Krishnaprasad, P.S.: "Analysis and Synthesis of Feed Forward Neural Networks using Discrete Affine Wavelet Transformations," IEEE Transactions on Neural Networks, Vol. **4**, No. 1 (1993) 73.
8. Cadzow, J.A., and Solomon, O.M.: "Algebraic Approach to System Identification," IEEE Transaction on Acoustic, Speech, and Signal Processing, Vol. **ASSP-34**, No. 3 (1986) 462.
9. Al-Kaabi, A., and Lee, W.J.: "Using Artificial Neural Nets to Identify the Well-test Interpretation Model," *SPE Formation Evaluation*, (Sept. 1993) 233.
10. Boomer, R.J.: "Predicting Production Using a Neural Network (Artificial Intelligence Beats Human Intelligence)," SPE 30202, Presented at the 10th Petroleum Computer Conference, Houston, TX., 11 - 14 June (1995).
11. Sinha, S. and M. N. Panda, "Well Test Model Identification using Self Organizing Feature Map", SPE Computer Applications (Aug. 1996).

Manmath N. Panda is a research engineer in the reservoir geostatistics group of ARCO Exp. and Prod. Tech. (AEPT), Plano, TX. He holds B. Tech from the Indian School of Mines, Dhanbad, MS from UAF, Fairbanks, and a Ph. D. from the U. of Texas at Austin, all in petroleum engineering. His current research interests include geostatistics, data scaling, and artificial intelligence. **David Zaucha** is a systems consultant for AEPT. He has a BSEE from U. of Massachusetts and an MSEE from U. of Rochester. His current research interests are trend analysis and forecasting systems using wavelet transforms and neural networks. **Godofredo Pérez** is a senior research engineer in the reservoir geostatistics group of AEPT. He holds B.S., M.S. and Ph. D., all in Petroleum Engineering, from the University of Tulsa. His current research interests include applied geostatistics and evaluation of artificial intelligence techniques to solve reservoir engineering problems. **Anil K. Chopra** is the group leader of Reservoir Geostatistics and Description Research Groups, AEPT. Before joining AEPT he worked at Amoco Production Company Research Center, Tulsa. He holds a B. Tech. from IIT, Kanpur, India and a Ph. D. from the University of Houston, both in Chemical engineering.

Predicting Well-Stimulation Results in a Gas-Storage Field in the Absence of Reservoir Data With Neural Networks

Shahab Mohaghegh, SPE, West Virginia U.; **Dan McVey,** SPE, Natl. Gas and Oil Corp.; and **Khashayai Aminian,** SPE, and **Sam Ameri,** SPE, West Virginia U.

Summary

Selection of candidate wells for stimulation treatment to increase their productivity is a challenging task. A systematic approach that uses a three-layer backpropagation neural network, introduced in this paper, assists engineers in predicting post-stimulation well performance to select candidate wells for stimulation treatment. This approach can also be used to optimize the stimulation design parameters. Unlike conventional simulators that are based on mathematical modeling of the fracturing process, the process introduced in this paper uses no specific mathematical model. As a result, access to explicit reservoir data, such as porosity, permeability-thickness, and stress profile, is not essential. This is a major advantage over conventional hydraulic fracturing simulators, which can translate to considerable savings because it eliminates the need for expensive data collection. The application of this methodology to a gas-storage field is presented in this paper. The developed neural network can predict the postfracture well deliverability with approximately 95% accuracy. These results were achieved in the absence of reservoir data (permeability, porosity, thickness, and stress profiles) that makes conventional fracture simulation impossible. This process is currently being used to select candidate wells for future stimulation treatment in the aforementioned field.

Introduction

Gas-storage fields have numerous wells that are used for both injection during low-demand periods and withdrawal during high-demand periods. As these wells age, their deliverability declines owing to several factors. Stimulation treatments (hydraulic fracturing of the formation) are routinely used in gas industry to improve gas well productivity. Because of the finite financial resources available, engineers must select the candidate wells with the highest potential of improvement after stimulation. This process is best done with two- or three-dimensional hydraulic fracturing simulators that are available in the industry. To use these simulators, however, access to several types of reservoir data is essential. Reservoir data necessary for hydraulic fracture simulation include porosity, permeability, thickness, and stress profiles of the formation. Experience has shown that, given the aforementioned data and assuming availability of a good geologic and structural definition of the reservoir, hydraulic fracturing simulators can predict the outcome of the hydraulic fracturing process with reasonable accuracy.

When dealing with storage fields that are old (this is true for most of the storage fields because they are usually old, depleted gas fields that have been converted to storage fields), the aforementioned information is not available. Acquiring these types of information on an old reservoir is usually very expensive. It involves massive coring of the reservoir, where pieces of the rock from the target formation are brought to the surface and tested in the laboratory under simulated field conditions to measure the reservoir porosity and permeability. It also involves elaborate well-testing procedures and subsequent analysis of well-test data. This paper introduces a new and novel method for predicting the outcome of hydraulic fracture treatments in gas-storage fields, with minimal cost.

Copyright 1996 Society of Petroleum Engineers

Original SPE manuscript received for review 15 August 1995. Revised manuscript received 10 September 1996. Paper (SPE 31159) peer approved 10 September 1996.

Background

This study was conducted on a large natural gas-storage field located in northeastern Ohio. The formation is a tight gas sandstone known as the Clinton sand. The Clinton is a tight gas-bearing sandstone. Natural fracturing is thought to account for production in economic quantities. Sand occurs in lenses and is largely discontinuous from one well to another. Therefore, generalization of field or well reservoir properties from core data is very difficult. Pressure testing is often inconclusive because of insufficient data, reservoir heterogeneities, wellbore storage, interference, and the required duration to achieve steady state.

All the wells in the storage field were initially stimulated by hydraulic fracturing. Since 1970, an average of 25 wells have been refractured each year for a total of around 600 treatments. Most wells in the field have been refractured, some up to three times. The experience with the Clinton sandstone indicates that hydraulic fractures grow vertically out of the zone, regardless of rate and fluid viscosity. Therefore, it appears critical to use high proppant concentrations in a viscous fluid to create a conductive fracture in the pay interval. Treatment design for the storage field currently include a 25- to 30-lbm linear gel with maximum sand concentrations from 3 to 4 lbm/gal.[6]

Currently, the wells are selected to be refractured each year on the basis of maintenance history, past fracture response, years since previous fracture, and overall deliverability potential with mixed results. Postfracture well performance estimates and optimal fracture treatment design are critical in maximizing deliverability enhancements. An accurate estimate of postfracture well deliverability is necessary for engineers to select the candidate wells that would respond with acceptable postfracture deliverability and to avoid investing in the wells with unsatisfactory postfracture deliverability. The use of type-curve matching and computer simulation[1-5] for predicting hydraulically fractured well performance are not practical in this field because obtaining detailed information about rock mechanics and reservoir characteristics by electric logs, well testing, or coring is operationally difficult or cost prohibitive.

Methodology

The challenge was to develop a methodology that would not require expensive well testing, coring, and other operations for data collection but would provide postfracture well deliverability on all wells. Basic well information, such as geographic location, depth, tubular design, completion type, flow tests, past fracture designs, and performance history, is readily available. Most of these data, however, are not considered to be useful engineering data for hydraulic fracturing treatment design. However, many of these variables may contribute to the overall success or failure of a hydraulic fracture treatment in some indirect or complex way.

It should be noted that it is necessary to provide the network with some information on the reservoir being considered. In this study, the historical data on the previous fracture treatments were available and were used for the training. Data available on this field can be divided into three categories: well data, flow data, and hydraulic fracturing data. Well data mainly provide information about the type of the well (injection or withdrawal), its location, and when it was drilled. Flow data are a series of data collected routinely by the field operator with simple two-point flow tests. The company operating this field uses a "yardstick" called Q100, which is the flow rate at $\Delta p^2 = 100{,}000$ psi^2. Hydraulic fracturing data are the parameters used in design and implementation of the hydraulic fracture.

TABLE 1—DATA USED IN THIS STUDY	
Data Type	Parameters
Input	Well number, year well was fractured, date well was fractured (a relative pressure function), number of times well was fractured, type of fracture (water, gelled water, foam), fluid viscosity, total water used, nitrogen used per barrel of water, total sand used, sand concentration, sand type, acid volume and type, chemicals (iron control, bacterial control, etc.), treatment injection rate, occurrence of screen out, contractor, hole size, completion type, well type (injection, production), date of completion, date converted to storage, well group number, sand thickness, minimum 20-year flow test value, maximum 20-year flow test value, average 20-year flow test value, and flow test before refracture.
Output	Maximum flow test after fracture

A three-layer feed forward backpropagation network was used in this study.[7-9] The network consisted of 59 input neurons with linear normalization between zero and one. The single hidden layer had 51 neurons with logistic function as the activation function. The sole output of the network was the peak postfracture gas-storage well deliverability. The neural network developed for this study was trained by use of the information provided in **Table 1.** A complete definition of each of the entries is available in Ref. 6.

Results and Discussion

The available data covers 1968–91. As a first attempt, 13% of the entire data was randomly selected and put aside as the test set and the network was trained on the remaining 87% of the data. Once the network reached convergence, network predictions were compared with actual field results. This comparison provided a coefficient of correlation of 0.97 for training data and 0.98 for the test set. **Fig. 1** shows the result of this part of the study for the entire data.

To simulate a practical situation, the data from 1968 to the end of 1988 were used to train the network. The input/output pairs were presented to the network for training. Once the network reached a stable state, the network prediction on the training data was compared with the output that was provided to the network. It produced a coefficient of correlation of above 0.96. To test the generalization capabilities of the developed network, the input data from the years 1989 through 1991 were given to the network to forecast the postfracture well deliverability. This would be the results upon which candidate wells for fracturing would be selected. **Figs. 2 through 4** show the comparison between network predictions and actual flow test data. The result is quite satisfactory. With a flow test indicator of 500 as the cutoff point, the figures show that a total of nine wells (five wells from 1988, one well from 1990, and three wells from 1991) would not have been chosen for refracturing if this tool had been available at that time. With this tool, the cost involved in fracturing these nine wells would have been saved and nine other wells with acceptable postfracture deliverability would have been fractured, which means even more economic benefits. The time for a well to reach its peak deliverability after a hydraulic fracture (the indicator that is the target of this study) is between 2 to 3 years. At the time this study was being completed, results from 1991 were the most recent peak postfracture deliverabilities that were available. Recently, authors used the developed network to predict the peak postfracture deliverabilities for the wells stimulated in 1992. During 1992, 19 wells were stimulated. By the time this manuscript was being completed, results from 11 wells had become available. **Fig. 5** shows the comparison between network prediction and actual field results for 1992. As can be seen, the network made quite accurate predictions for all but one well, which is the first well in Fig. 5. For this well, neural network predicted a postfracture deliverability of

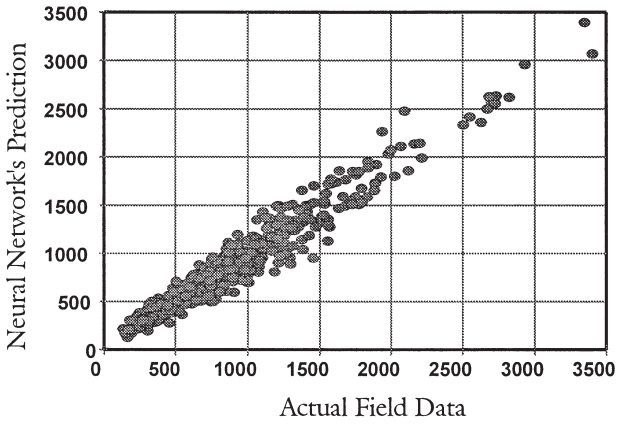

Fig. 1—Neural network prediction for all the available data.

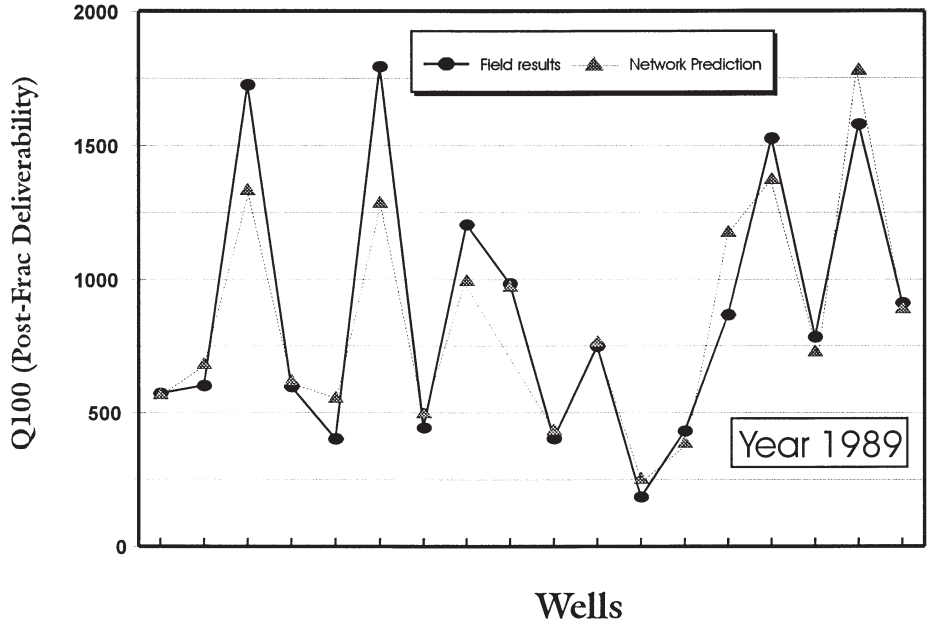

Fig. 2—Comparison between network prediction and field results for 1989. Network was trained with data from 1968 to 1988.

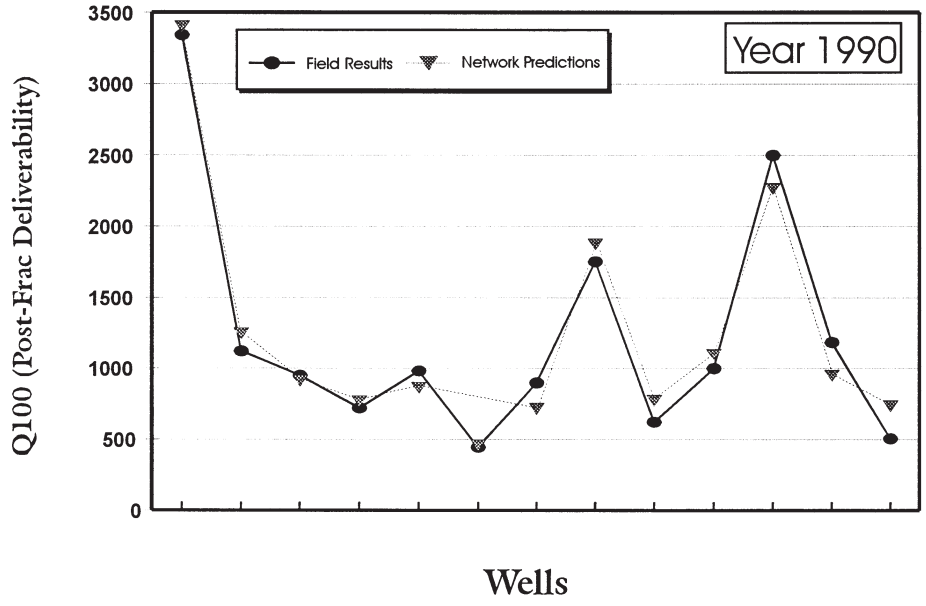

Fig. 3—Comparison between network prediction and field results for 1990. Network was trained with data from 1968 to 1988.

1,400, while the actual deliverability peaked at about 900. Because 500 was used as the cutoff point, the neural network prediction (1,400) would have suggested that hydraulic fracturing be performed on this well. In retrospect, this would have been a good suggestion because the actual deliverability was above 500.

In a separate attempt to demonstrate the power and robustness of this new methodology, the network was trained with data from 1968 to 1974. The coefficient of correlation at this point was almost 0.98. In 1975, a new fracturing fluid was used for the first time (foam). When data from 1975 was introduced to the network, the performance of the network degraded and its prediction accuracy dropped to 0.88. This performance bounced back up by the year 1980, when the network observed and learned the new behavior that was displayed by the new fracturing fluid. This process was repeated two more times, when new fluids were introduced in 1981 and 1989. **Fig. 6** shows the neural network prediction capabilities as new information is added to the network. This further proves the notion that systems developed, based on neural network, do not break down when new situations are encountered; rather, they degrade gracefully.

It is also important to note that the so-called "conventional engineering wisdom" (whatever that may mean) about the available data may not be quite applicable here. In other words, a piece of data that might look very unimportant in terms of information it provides about the reservoir, well, or the fracturing process, may actually contain valuable implicit information useful for the neural network. An example on our experience may clarify this point. During our analysis, it was noted that the well ID number played a role in the overall pattern that has been established between inputs and the postfracture deliverability. It prompted us to look further into the conventions that might had been used in numbering these wells. It was later determined that these wells were numbered according to (1) their date of completion and (2) their relative geographic location in the field. Although this information was not explicit and was unknown to us at the beginning, the network was able to deduce it

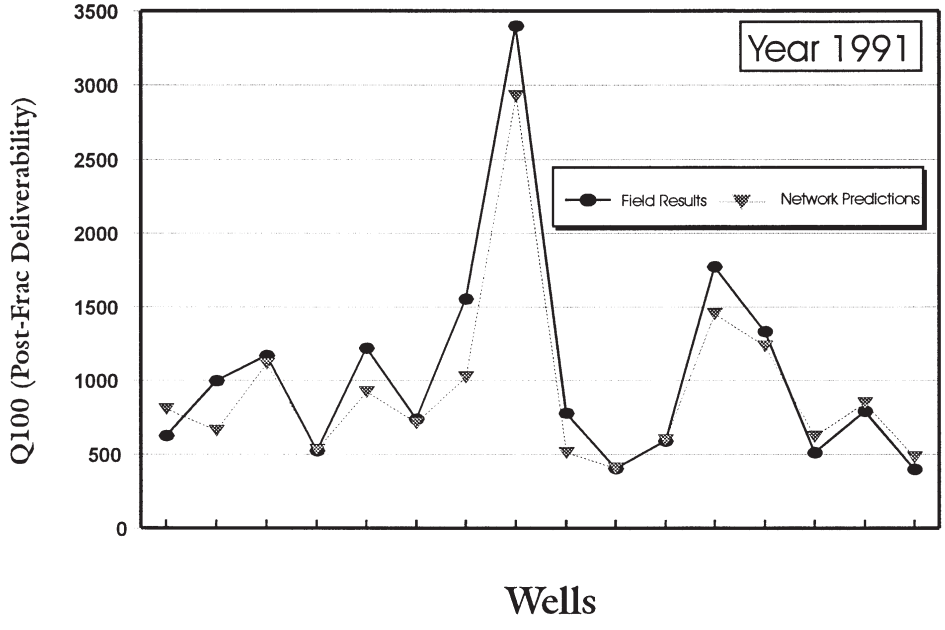

Fig. 4—Comparison between network prediction and field results for 1991. Network was trained with data from 1968 to 1988.

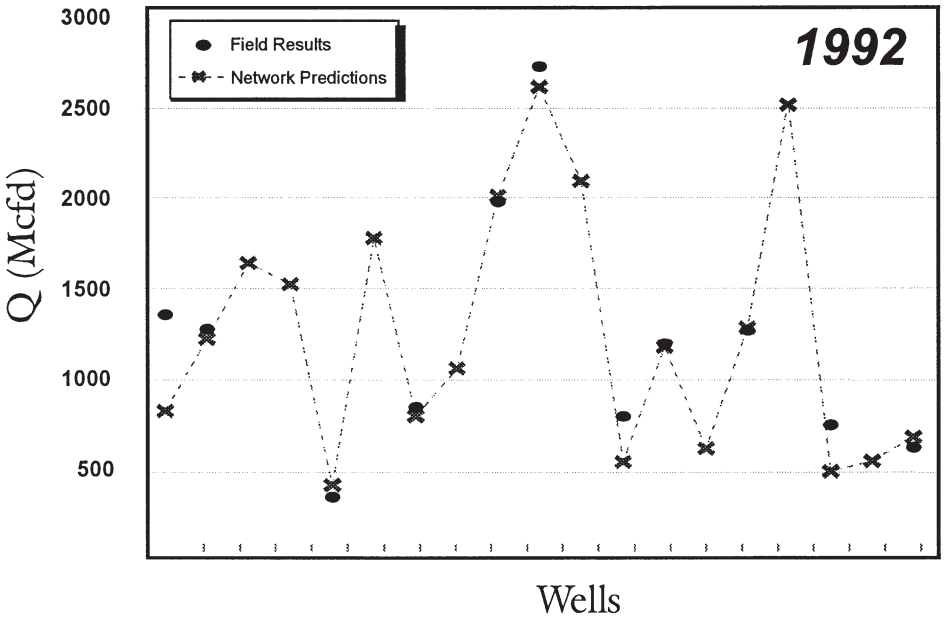

Fig. 5—Comparison between network prediction and field results for 1992.

from the data. It was also interesting to note that, although no information regarding the physics of the problem was provided to the network during the training, once the network was trained, it provided us with information that made perfect engineering sense.[6]

Conclusions

Methodology presented in this paper is capable of forecasting postfracture deliverability on the basis of historical data in Clinton sandstone gas-storage field without detailed reservoir data. This methodology provides considerable cost savings by eliminating the need for costly reservoir data collection in old gas-storage fields. With this methodology, postfracture well deliverability was predicted with approximately 95% accuracy. The neural network developed in this study is currently being used to select candidate wells for hydraulic fracturing in the Clinton sandstone. This procedure can be applied to other fields provided some historical data for training of neural network is available. This methodology not only predicts postfracture well deliverability, but can also assist the practicing engineer in designing the optimal fracture treatment. Development of a hydraulic fracture design tool based on the neural network presented in this paper is near completion.

References

1. Millheim, K.K. and Cichowicz, L.: "Testing and Analyzing Low-Permeability Fractured Gas Wells," *JPT* (February 1968) 193.
2. Gringarten, A.C., Ramey, H.J. Jr., and Raghavan, R.: "Applied Pressure Analysis for Fractured Wells," *JPT* (July 1975) 887.
3. Cinco-Ley, H., Samaniego-V., F., and Dominguez, N.: "Transient Pressure Behavior for a Well With a Finite Conductivity Vertical Fracture," *SPEJ* (August 1978) 253.
4. Agarwal, R.G., Carter, R.D., and Pollock, C.B.: "Evaluation and Performance Prediction of Low Permeability Gas Wells Simulated by Massive Hydraulic Fracturing," *JPT* (March 1979) 362.
5. Hopkins, C.W. and Gatens, J.M.: "Stimulation Optimization in a Low-Permeability, Upper Devonian Sandstone Reservoir: A Case History," paper SPE 21499 presented at the 1991 SPE Gas Technology Symposium, Houston, 23–25 January.
6. McVay, D., Mohaghegh, S., and Aminian, K.: "Identification of Parameters Influencing the Response of Gas Storage Wells to Hydraulic Fracturing With the Aid of a Neural Network," paper SPE 29159 presented at the 1994 SPE Eastern Regional Meeting, Charleston, WV.
7. Josin, Gary: "Integrating Neural Networks with Robots," *AI Expert* (August 1988) 50.
8. Caudill, Maureen: "Neural Networks Primer Part I," *AI Expert* (December 1987) 46.

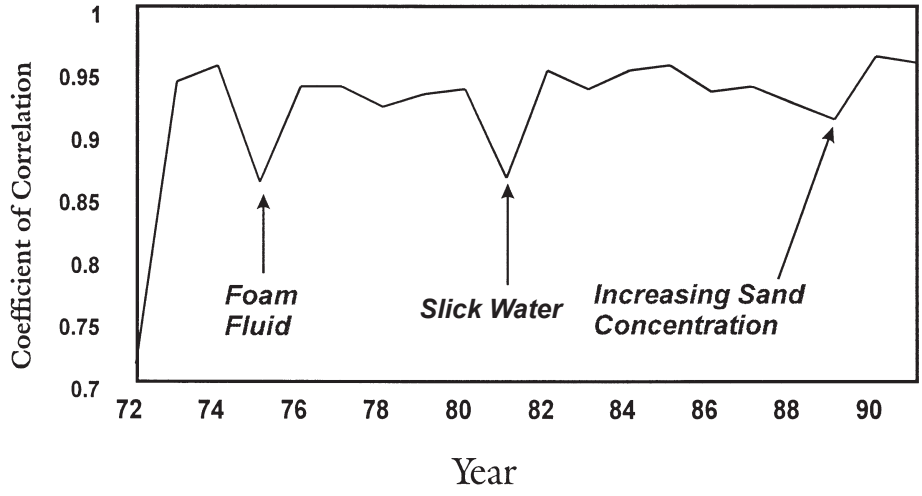

Fig. 6—Robustness of the neural network as new information is added to its database.

9. Caudill, Maureen: "Neural Networks Primer Part III," *AI Expert* (June 1988) 53.

SI Metric Conversion Factors

gal	$\times 3.785\ 412$	$E-03 = m^3$
lbm	$\times 4.535\ 924$	$E-01 = kg$
psi	$\times 6.894\ 757$	$E+00 = kPa$

SPERE

Shahab Mohaghegh is Assistant Professor of petroleum and natural gas engineering at West Virginia U., Morgantown. His research interests include reservoir characterization, formation evaluation, and application of computational intelligence (artificial neural networks, fuzzy set theory, evolutionary programming) to energy and environmental problems. He holds BS and MS degrees in natural gas engineering from Texas A&I and a PhD degree in natural gas engineering from Pennsylvania Sate U. Mohaghegh is a member of the *SPE Formation Evaluation* Editorial Review Committee. **Dan McVey** is Division Superintendent for Natl. Gas & Oil Corp. in Zanesville, Ohio. Previously, he was Storage Operations Engineer for East Ohio Gas Co. in North Canton, Ohio. He holds a BS degree from Marietta College and an MS degree in petroleum engineering from West Virginia U. Photograph is unavailable. **Khashayar Aminian** is Professor of petroleum and natural gas engineering at West Virginia U. Previously, he worked for Michigan Consolidated Gas Co. as a reservoir engineer. Aminian holds MS and PhD degrees from U. of Michigan. He is serving on the SPE U.S. Council and he is an officer for the Northern West Virginia Section. He chaired the 1995 SPE Eastern Regional Meeting and previously served on the *SPE Computer Applications* Committee. **Samuel Ameri** is Chairman and Professor in the Dept. of Petroleum & Natural Gas Engineering at West Virginia U. Previously, he worked at Schlumberger Well Services. Ameri is West Virginia U. SPE Student Chapter Faculty Sponsor. He received the 1989 SPE Regional Service Award. He served on the 1986–89 Continuing Education Committee and was Chairman of the Program Committee for the 1989 SPE Eastern Regional Meeting.

SPE 51080

Candidate Selection for Stimulation of Gas Storage Wells Using Available Data With Neural Networks and Genetic Algorithms

S. Mohaghegh, West Virginia University, V. Platon, Western Atlas, and S. Ameri, West Virginia University

Copyright 1998, Society of Petroleum Engineers Inc.

This paper was prepared for presentation at the 1998 SPE Eastern Regional Meeting held in Pittsburgh, PA, 9–11 November 1998.

This paper was selected for presentation by an SPE Program Committee following review of information contained in an abstract submitted by the author(s). Contents of the paper, as presented, have not been reviewed by the Society of Petroleum Engineers and are subject to correction by the author(s). The material, as presented, does not necessarily reflect any position of the Society of Petroleum Engineers, its officers, or members. Papers presented at SPE meetings are subject to publication review by Editorial Committees of the Society of Petroleum Engineers. Electronic reproduction, distribution, or storage of any part of this paper for commercial purposes without the written consent of the Society of Petroleum Engineers is prohibited. Permission to reproduce in print is restricted to an abstract of not more than 300 words; illustrations may not be copied. The abstract must contain conspicuous acknowledgment of where and by whom the paper was presented. Write Librarian, SPE, P.O. Box 833836, Richardson, TX 75083-3836, U.S.A., fax 01-972-952-9435.

Abstract

The methodology developed in this study uses several artificial neural networks and genetic algorithm routines to help engineers select restimulation candidates based on available data. The neural networks provide realistic models of the hydraulic frac jobs and chemical treatments in this field. The genetic algorithms provide design optimization and economic analysis (capital investment allocation).

Historically wells in this storage field have been stimulated/restimulated by hydraulic fracturing or by being chemically treated using one, two or sometimes three different chemicals. Several neural network models were developed for different stimulation processes. The first series of genetic algorithm routines are used with each of the neural network models to provide optimum treatment design for each of the stimulation processes. A separate genetic algorithm uses several economic parameters and provides the engineer with an optimum stimulation combination of the candidate wells.

A software tool based on this methodology has been developed for a gas storage field in Ohio. Upon the completion of the analysis, the software tool provides a list of the maximum number of candidate wells. This maximum number is based on the provided stimulation budget for a particular year. The list specifies the type of stimulation for each candidate well - whether it should be refraced or chemically stimulated - and recommends a list of possible parameters to be used during the implementation.

Background

This paper presents the continuation of the efforts that were published in two previous SPE publications. In the first paper authors showed the feasibility of using artificial neural networks to accurately model hydraulic fracturing process in a gas storage field[1]. In a second paper as a continuation of that project, genetic algorithm routines were used in an attempt to optimize the design parameters of hydraulic fracturing process[2]. The study being presented in this paper takes into account new realities that the operators are facing in the field. These realities include fundamentally different stimulation jobs such as refracs versus chemical treatments. Each of these restimulation jobs must be treated differently during the model building process. Economic considerations play an important role in restimulation projects. A new economic optimization tool has been added to the process in this study. Therefore, many challenging complexities that were not included in the previous studies have been addressed here.

During a stimulation/restimulation program the engineers face several challenging questions. The hydraulic fractures cost four to five times as much as a chemical treatment, and yet some wells

respond reasonably well to chemical treatments. Given the economic parameters involved, should a well be refraced or chemically treated? What would be the maximum potential post-treatment deliverability if the well were refraced as oppose to chemically treated? Would the decline behavior be different? Would extra cost of the refrac job justify the extra deliverability gains? These are not simple questions to be answered. Considering the fact that every year the engineers must select a handful of wells for restimulation from a total of more than 700 wells emphasizes the complexity of the problem.

In order to address this problem and expect reasonable result it is obvious that many factors must be taken into account. These factors include the history of the well. How it has responded to different hydraulic fractures and refrac processes in the past? Have chemical treatments been performed on the well? If yes, then how did the well responded to those treatments? If the well has been through several fracs, refracs and chemical treatments, do the sequence of these jobs have any significance on the post-treatment deliverability? Has the decline in post-treatment deliverability been sharper in the case of refracs or chemical treatments? These and many other technical questions may be posed.

In addition to the above technical questions many economical considerations also need to be addresses. It is a fact that refracs cost much more than chemical treatments yet many wells have shown that a well designed and implemented chemical treatment may provide the same kind of post-treatment deliverability. Economic parameters other than the cost of the treatment may include the price of the gas, the total budget for the year's stimulation/restimulation program.

The objective of this study is to provide a methodology - and build a software tool based on this methodology - to address the above questions. The ultimate output of the software tool is a list of the restimulation candidates for each year. The list will contain the selected candidates and specifies whether that particular candidate should be refraced or chemically treated. In either case the software tool would provide recommendation on the parameters used in the refrac or the number and amount of chemical used for the chemical treatment.

It is not hard to see that the problem that has been described here is one of process modeling and optimization, and a challenging one. The software tool will take into account all the economic as well as technical concerns that were mentioned here through the use of virtual intelligence techniques. In a nut shell, virtual intelligence - also known as computational intelligence and soft computing - is an attempt to mimic life in solving highly complex and non-linear problems that are either impossible or unfeasible to solve using conventional methods.

In this study authors use a series of artificial neural networks and genetic algorithm routines, integrated with an extensive relational database - specifically developed for this study - to achieve the goals of the project. Since introductory discussions about neural networks and genetic algorithms have been published in the many previous SPE papers by the authors[3-5] and other researchers in this area, further discussion on the nature of these sciences will not be included here.

Methodology

Figure 1 is a schematic diagram of the flow of the information through the software application that was developed for this study. As it is shown in this figure the input data that resides in a relational database is fed into the application. The input data includes general well information, such as well ID number, well location, and some wellbore characteristics, some historical deliverability indicators such as pre-treatment deliverability, maximum and minimum deliverability for the life of the well and average deliverability for the past twenty years, as well as stimulation parameters.

It is worthwhile to mention that an extensive relational database was created for this particular gas storage field. This database is used as input data source for the application as well as a valuable source during the training of the several neural networks that are used as the main engines of the application. The database also provides an

excellent manual rapid screening tool for the engineers. Several useful queries are built into the database in order to simplify visualization of the extensive amount of data that reside in the database.

The software application includes three separate modules. The first module includes the rapid screening neural networks - one network for the refracs and one for the chemical treatments. These networks use general well information and the historical data as input and attempts to predict the post-treatment deliverability. The rapid screening module works as follows: The user specifies a minimum post- deliverability (threshold). The rapid screening module - using the two neural networks - will identify all the wells that have the potential to meet this minimum. These are the wells that are used into the next modules.

To construct the second module, four neural networks - one for refracs three for chemical treatments - are trained to work as fitness functions for the optimization genetic algorithms. The input data into these neural networks include the same data as rapid screening networks plus detail stimulation data. Second module includes four genetic algorithm routines, one for each neural network. Working in the batch mode this module optimizes all possible stimulation treatments for each well and ranks them. The user at this time has the option to inspect the results one well at a time or he/she may continue with the batch mode. Figure 2 provides a schematic diagram of the module two.

In the batch mode, after completion of the second module the third module takes over. This module is a specialized genetic algorithm routine that uses the provided economic parameters to optimize the return on investment. The outcome of this module is a list of candidate wells and the type of the stimulation job that should be performed on each well.

During the second module design optimization is applied to a number of wells that have passed the rapid screening process. At this point the best candidates are identified. But there still remains one question to be answered. Given the cost of frac jobs and chemical treatments - which are inputs to the third module as economic parameters - what is the optimum combination of frac jobs and chemical treatments to be performed? And which wells are to be fractured or treated, in order to maximize the return on the investment?

Module three is an attempt to answer this question. The economic optimization genetic algorithm in this module is designed to provide the optimum list of candidate wells and the corresponding stimulation jobs that should be performed on each well. The function to be optimized in this module is what we call the profit function. As can be seen from Equation 1, the profit function at this time is a simplified function. Increasing the complexity of this function will not in any shape or form change the applicability of this module. The profit function to be optimized is given by the following equation:

$$P = \$g \times [\sum_{1}^{n_F} \Delta Q_F + \sum_{1}^{n_T} \Delta Q_T] - [n_F \times \$F + n_T \times \$T] \quad (1)$$

Where:

P = profit
$g = market gas price
ΔQ_F = total deliverability increase due to applied frac jobs
ΔQ_T = total deliverability increase due to applied chemical treatments
n_F = number of frac jobs performed
n_T =number of chemical treatments performed
$F = average cost of a frac job
$T = average cost of a chemical treatment

In the above equation the only variables are the numbers of frac jobs and chemical treatments to be performed. The goal is to find the optimum combination of these two values such that it would maximize P. There is, however, a constraint that has to be imposed, namely the capital investment available for each stimulation program i.e. annual stimulation budget. Equation 2 provides the constrain:

$$[n_F \times \$F + n_T \times \$T] \leq \$Total \quad (2)$$

Where:

$Total = annual stimulation program budget

While the above equation provides assurance that we are not overspending, Equation 3 is imposed as another constrain so the budget is spent in a fashion that most of it is used:

$$\$Total - [n_F \times \$F + n_T \times \$T] = \min \quad (3)$$

In module three the genetic algorithm maximizes the profit function - as the fitness function - using the two constrain equations. It should be noted that during this optimization process the genetic algorithm uses the list of the wells that have already gone through the stimulation optimization process in module two.

The total number of candidate wells and their optimum stimulation job are identified at this point. The data is stored in a database and can be viewed. A recommended set of parameters for the frac jobs or the chemical treatments - whatever the case may be - accompanies the candidate. Figure 3 shows a schematic diagram of the module three.

Results and Discussion

As was mentioned before historical data in this field included many frac and refrac jobs as well as a variety of different chemical treatments. Upon a closer inspection of the data it was possible to classify the chemical treatments into three categories. The classification was made based on the number of chemicals used in the treatments. They were divided into one, two and three components chemical treatments. Table 1 shows the chemicals used in each category.

Module one of the software application includes the rapid screening neural nets. These nets are constructed and trained to look at the general information of the well and the historical data to estimate a post-stimulation deliverability. The only information provided to the network about the stimulation job at this point is the type of the stimulation jobs i.e. refrac or chemical treatment.

A separate set of neural networks were constructed and trained for module two. These networks are trained using all available data that includes detail stimulation parameters. These are the networks that are used as fitness functions in the genetic algorithm routines.

Figures 4 and 5 show the accuracy of the module one neural networks. Figure 4 shows the result for the frac and refrac network while Figure 5 shows the network accuracy for the chemical treatments. Figures 6 though 9 are the plots of the actual post-treatment deliverabilities versus neural network predictions for the second module. Four different networks were trained for this module. Figure 6 shows the accuracy of the network trained for frac and refrac jobs. Figure 7, 8 and 9 are graphs of network predictions versus actual post- treatment deliverabilities for one, two and three components chemical treatments. These graphs show how well these networks have been trained.

To clearly demonstrate their generalization capabilities correlation coefficients for all the neural networks are provided in Table 2. In this table two separate correlation coefficients are provided for each network. One for the training data set and one for verification data set. The verification data set includes data that have not been used during the model construction and therefore the networks had not seen them before.

Figure 10 shows an example of module two's outcome. In this figure five different candidate wells are shown. For each candidate well three different post-treatment deliverabilities are shown. The first value - going from back to front - is the actual post-treatment deliverability while the second value is the predictor - module two - neural network's prediction. Please note the accuracy of this network's prediction. The exact same neural model that provided the second value has also predicted the third value. The difference between the second and third post-treatment deliverabilities is in the input to the model.

While the input data related to the well's general information and production history is the same in both cases, the stimulation parameters are different. In the case of the second post-treatment deliverability - the value shown by the bar in the

middle - the actual stimulation parameters from the database have been used. But the stimulation parameters to the neural model for the third post-treatment deliverability have been generated by the module two's genetic algorithm. This figure shows the candidate wells potential after an optimum restimulation job.

Figures 11 through 15 show screen shots from the software application that was developed for this study.

Conclusions

A comprehensive software tool has been developed that will assist engineers to select candidate wells for restimulation. The application has been developed using a relational database, six different neural network models and five different genetic algorithm routines. The software application includes three different independent modules that share information. Module one uses two neural models as its main engine and provides a rapid screening tool to identify the wells that need to be studied in more detail.

Module two includes four neural network models as well as four genetic algorithm routines that provide detail stimulation optimization for all the wells that have passed the module one's rapid screening process. Module two results in a ranked list of candidate wells and their corresponding recommended detail restimulation parameters.

Module three uses module two's ranked list accompanied by a set of provided economic parameters to perform an economic optimization. The outcome of the module three is the final list of candidate wells and their corresponding recommended detail restimulation parameters.

This software application has been custom made for a gas storage field in Ohio. The customization of the application is related to the neural network models and the genetic algorithm routines. These models and routines are specific to this storage field since they have been developed using the data from this field. The same methodology may be used to develop similar tools for other fields. This application will make it easier for the engineers to select candidate wells in the situation that other conventional methods can not be used.

References

1. Mohaghegh, S., Mc Vey, D., and Ameri, S.: "Predicting Well Stimulation Results in a Gas Storage Field in the Absence of Reservoir Data, Using Neural Networks", *SPE Reservoir Engineering Journal*, November 1996, pp. 54-57.

2. Mohaghegh, S., Balan, B., McVey, D., and Ameri, S.: "A Hybrid Neuro-Genetic Approach to Hydraulic Fracture Treatment Design and Optimization", *SPE 36602, Proceedings*, SPE 71st Annual Technical Conference, October 6-9, 1996, Denver, Colorado.

3. Mohaghegh, S., Arefi, R., and Ameri, S.: "Determination of Permeability From Well Log Data", *SPE Formation Evaluation Journal*, September 1997, pp. 263-274.

4. Mohaghegh, S., Arefi, R., and Ameri, S.: "Petroleum Reservoir Characterization with the Aid of Artificial neural networks", *Journal of Petroleum Science and Engineering*, December 1996, Vol. 16, pp. 263-274, Elsevier Science Publications, Amsterdam, Holland.

5. Mohaghegh, S., Arefi, R., and Ameri, S.: "Virtual Measurement of Heterogeneous Formation Permeability Using Geophysical Well Log Responses", *The Log Analyst*, Society of Professional Well Log Analysts, March-April 1996, pp. 32-39.

Treatment type	Types of Chemicals Used	
One component	kerosene	
	solvent	
	surfactant	
	water	
Two components	Cold water-based	Paraffin dispersant
		PEN-5
		VISCO 4750
	Hot water-based	B-11
		Drill foam
		Nalco
		Paraffin dispersant
		PEN-5
		Surflo S-24
		Tretolite
		VISCO
		W-121
Three components	Acid-based	Methanol + Water
	Water-based	Methanol + B-11
		Methanol + SEM-7
		Methanol + W-121

Table 1: Chemical Treatment Classification.

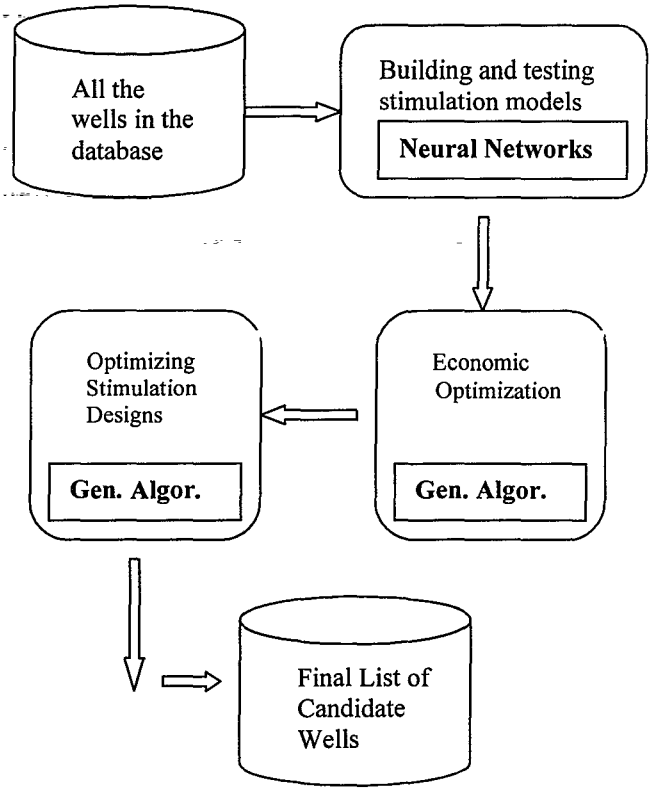

Figure 1. Flow chart of the software application.

Neural Networks	Modules in the Software Application		Training set		Verification set	
			Corr. Coeff.	No. of Records	Corr. Coeff.	No. of Records
Hydraulic Fractures	Rapid screening		94%	477	92%	118
	Optimization		96%	454	91%	112
Chemical Treatments	Rapid screening		96%	1830	92%	783
	Optimization	1 comp	97%	370	91%	157
		2 comp	95%	1492	91%	637
		3 comp	97%	63	94%	25

Table 2: Quality of the neural networks that were trained for this study.

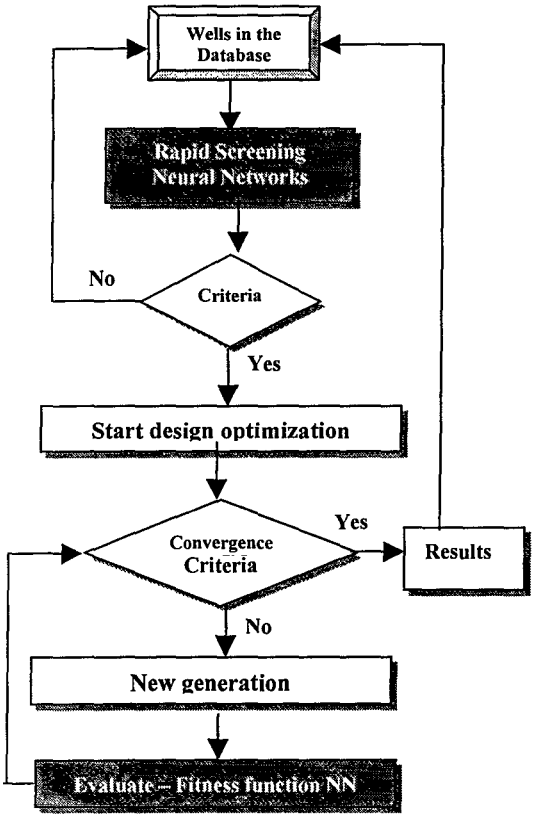

Figure 2. The schematic diagram for the module two process.

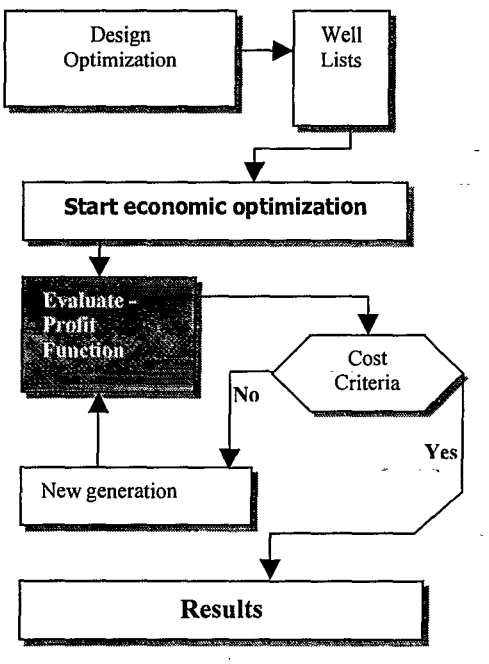

Figure 3: The schematic diagram for the module three process.

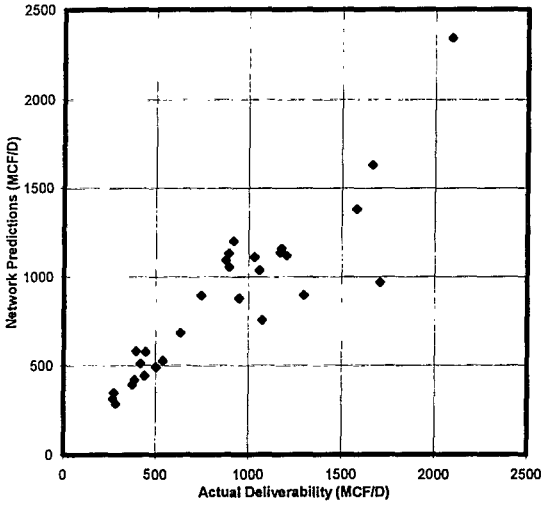

Figure 4: Module one neural net for hydraulic fracs - rapid Screening.

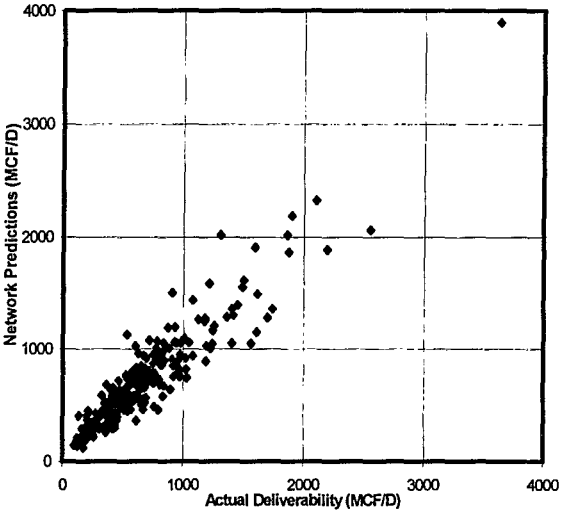

Figure 5: Module one neural net for chemical treatments - rapid Screening.

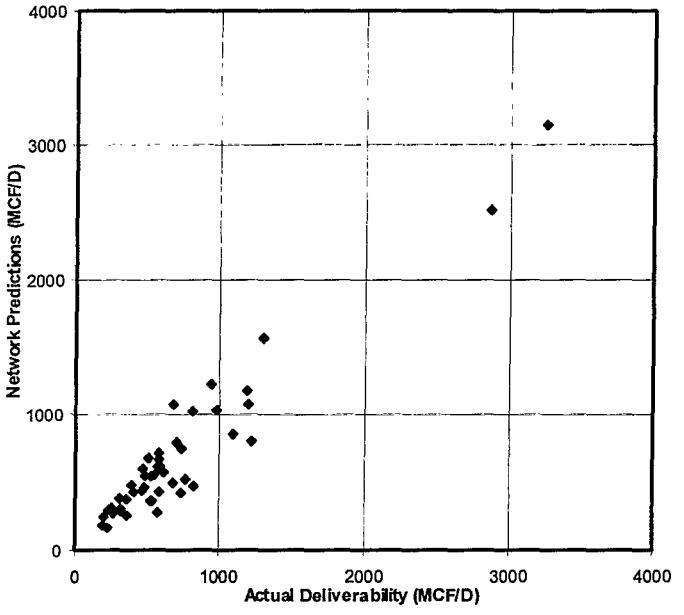

Figure 6: Module two neural net for hydraulic fracs - optimization.

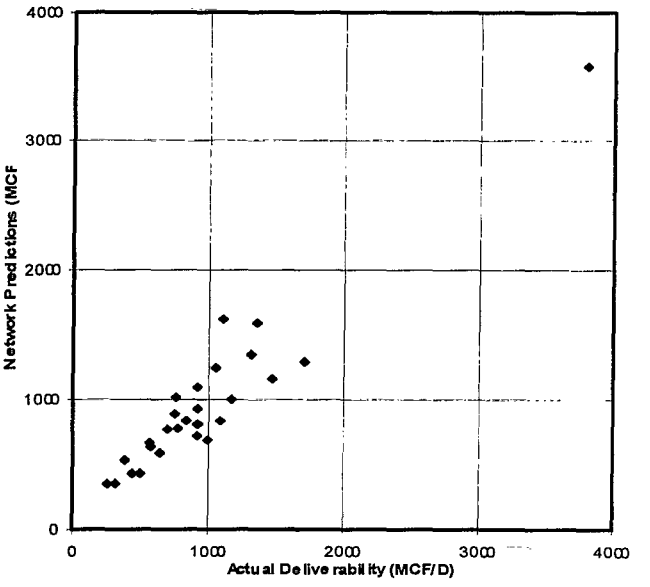

Figure 7: Module two neural net for one component chemical treatments - optimization.

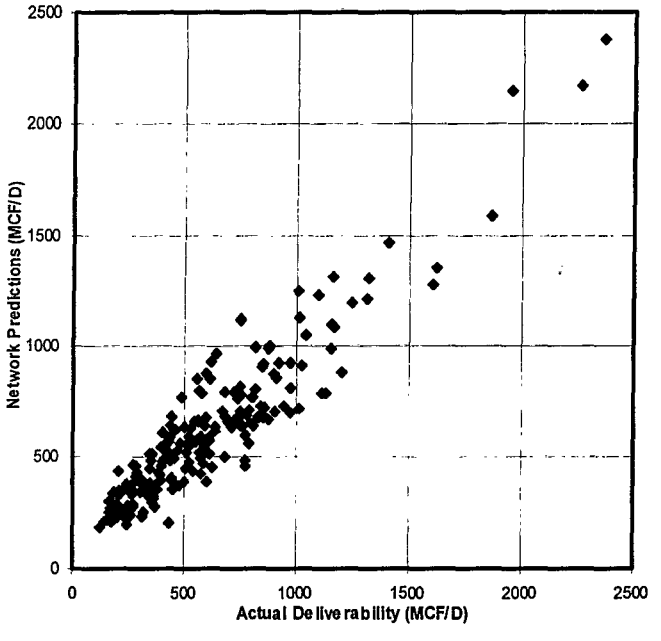

Figure 8: Module two neural net for two component chemical treatments - optimization.

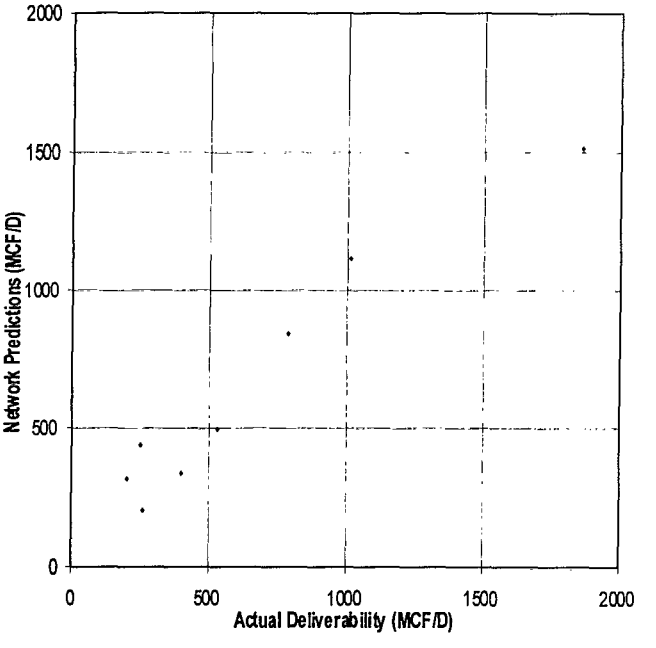

Figure 9: Module two neural net for three component chemical treatments - optimization.

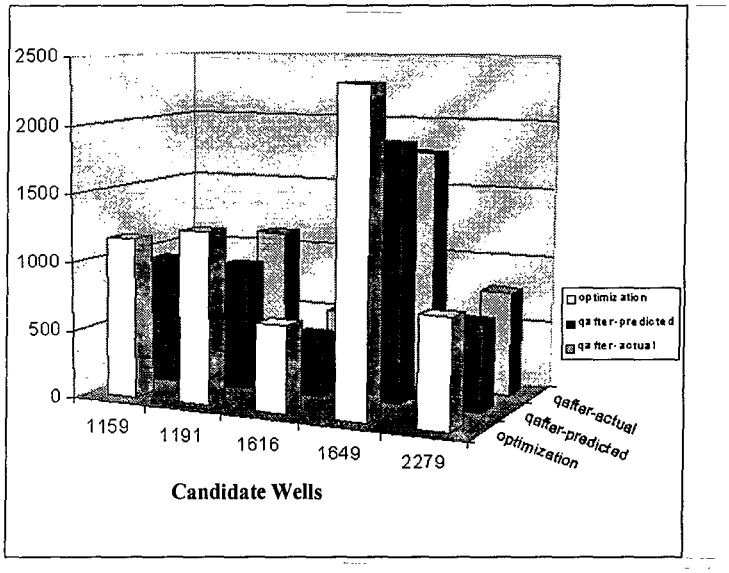

Figure 10: Stimulation optimization of five different candidate wells.

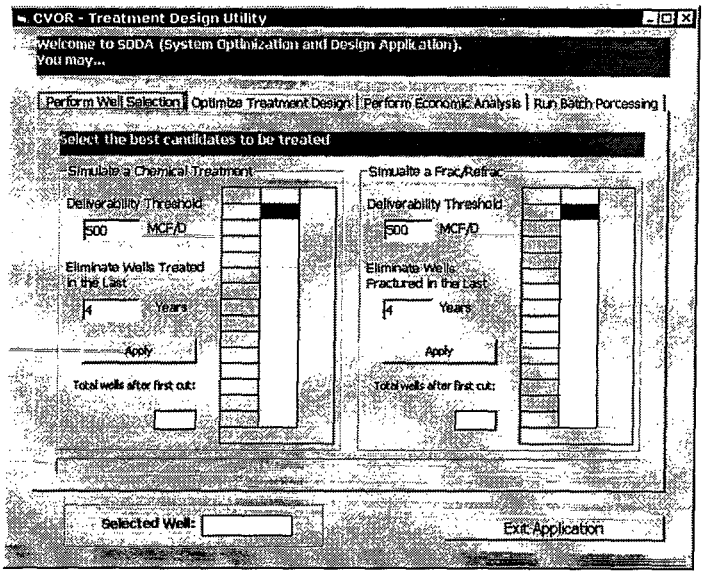

Figure 11: Software application interface for module one.

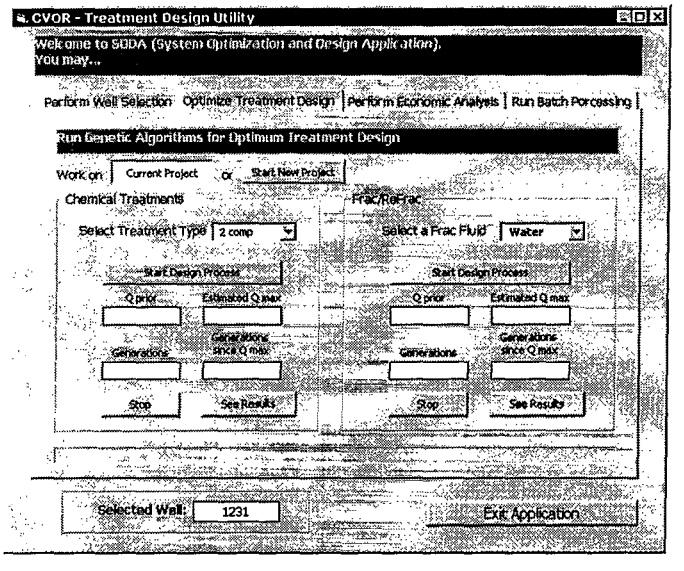

Figure 12: Software application interface for module two.

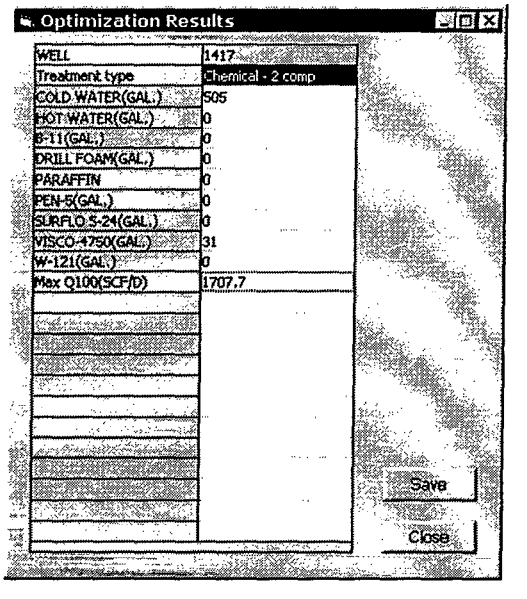

Figure 13: Software application interface.

Neural Network Model for Estimating the PVT Properties of Middle East Crude Oils

Ridha B.C. Gharbi, SPE, and **Adel M. Elsharkawy,** SPE, Kuwait U.

Summary

The importance of pressure/volume/temperature (PVT) properties, such as the bubblepoint pressure, solution gas-oil ratio, and oil formation volume factor, makes their accurate determination necessary for reservoir performance calculations. An enormous amount of PVT data has been collected and correlated over many years for different types of hydrocarbon systems. Almost all of these correlations were developed with linear or nonlinear multiple regression or graphical techniques. Artificial neural networks, once successfully trained, offer an alternative way to obtain reliable results for the determination of crude oil PVT properties.

In this study, we present neural-network-based models for the prediction of PVT properties of crude oils from the Middle East. The data on which the network was trained represent the largest data set ever collected to be used in developing PVT models for Middle East crude oils. The neural-network model is able to predict the bubblepoint pressure and the oil formation volume factor as a function of the solution gas-oil ratio, the gas specific gravity, the oil specific gravity, and the temperature. A detailed comparison between the results predicted by the neural-network models and those predicted by other correlations are presented for these Middle East crude-oil samples.

Introduction

In absence of experimentally measured pressure/volume/temperature (PVT) properties, two methods are widely used. These methods are equation of state (EOS) and PVT correlations. The equation of state is based on knowing the detailed compositions of the reservoir fluids. The determination of such quantities is expensive and time consuming. The equation of state involves numerous numerical computations. On the other hand, PVT correlations are based on easily measured field data: reservoir pressure, reservoir temperature, oil, and gas specific gravity. In the petroleum process industries, reliable experimental data are always to be preferred over data obtained from correlations. However, very often reliable experimental data are not available, and the advantage of a correlation is that it may be used to predict properties for which very little experimental information is available. The importance of accurate PVT data for material-balance calculations is well understood. It is crucial that all calculations in reservoir performance, in production operations and design, and in formation evaluation be as good as the PVT properties used in these calculations. The economics of the process also depends on the accuracy of such properties.

The development of correlations for PVT calculations has been the subject of extensive research, resulting in a large volume of publications.[1–10] Several graphical and mathematical correlations for determining the bubblepoint pressure (P_b) and the oil formation volume factor (B_{ob}) have been proposed during the last five decades. These correlations are essentially based on the assumption that P_b and B_{ob} are strong functions of the solution gas-oil ratio (R_s), the reservoir temperature (T), the gas specific gravity (γ_g), and the oil specific gravity (γ_o), or

$$P_b = f_1(R_s, T, \gamma_g, \gamma_o), \quad (1)$$

$$B_{ob} = f_2(R_s, T, \gamma_g, \gamma_o). \quad (2)$$

In 1947, Standing[1] presented graphical correlations for the determination of bubblepoint pressure (P_b) and the oil formation volume factor (B_{ob}). In developing these correlations, Standing used 105 experimentally measured data points from 22 different crude-oil and gas mixtures from California oil fields. Average relative errors of 4.8% and of 1.17% were reported for P_b and B_{ob}, respectively. Later, in 1958, Lasater[9] developed an empirical equation based on Henry's law for estimating the bubblepoint pressure. He correlated the mole fraction of gas in solution to a bubblepoint pressure factor. A total of 137 crude-oil and gas mixtures from North and South America was used for developing this correlation. An average error of 3.8% was reported. Lasater did not present a correlation for B_{ob}. In 1980, two sets of correlations were reported, one by Vasquez and Beggs[10] and the other by Glasø.[7] Vasquez and Beggs used 600 data points from various locations all over the world to develop correlations for P_b and B_{ob}. Two different types of correlations were presented, one for crudes with °API > 30 and the other for crudes with °API ≤ 30. An average error of 4.7% was reported for their correlation of B_{ob}. Glasø used a total of 45 oil samples from the North Sea to develop his correlations for calculating P_b and B_{ob}. He reported an average error of 1.28% for the bubblepoint pressure and −0.43% for the formation volume factor. Recently, Al-Marhoun[4] used 160 experimentally determined data points from the PVT analysis of 69 Middle Eastern hydrocarbon mixtures to develop his correlations. Average errors of 0.03% and −0.01% were reported for P_b and B_{ob}, respectively. Dokla and Osman[6] used a total of 50 data points from reservoirs in the United Arab Emirates to develop correlations for P_b and B_{ob}. They reported an average error of 0.45% for the bubblepoint pressure and 0.023% for the formation volume factor.

The conventional approach to develop PVT correlations is based on multiple-regression techniques. An alternative approach will be to use an artificial neural network (ANN). PVT models based on a successfully trained ANN can be excellent, reliable tools for the prediction of crude-oil PVT properties. The massive interconnections in the ANN produces a large number of degrees of freedom, or fitting parameters, and thus may allow it to capture the system's nonlinearity better than conventional regression techniques. Recently, artificial neural networks have found use in a number of areas in petroleum engineering.[11–20] The objective of this study is to use ANNs to develop accurate PVT correlations for Middle East crude oil to estimate P_b and B_{ob} as functions of R_s, T, γ_g, and γ_o. With additional experimental data, the neural-network model can be further refined to incorporate these new data. In addition, in this article we evaluate the accuracy of the ANN models developed in this study compared to other PVT correlations.

Copyright © 1999 Society of Petroleum Engineers

This paper (SPE 56850) was revised for publication from paper SPE 37695, first presented at the 1997 SPE Middle East Oil Show, Bahrain, 15–18 March. Original manuscript received for review 19 March 1997. Revised manuscript received 11 February 1999. Paper peer approved 9 March 1999.

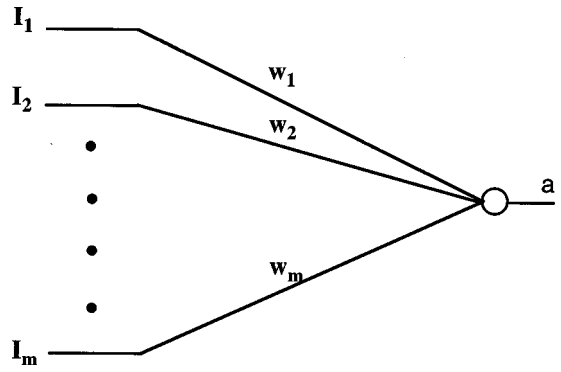

Fig. 1–Typical neuron or a processing unit.

Neural Networks

Artificial neural networks are computing tools composed of many simple interconnected elements called neurons. These neurons are inspired by the biological nervous system. Neural networks have been trained to perform complex problems in various fields of applications, which include visual processing,[21] control systems,[22] and speech synthesis.[23] A typical neuron is shown in **Fig. 1**. A neuron performs two simple tasks: (1) a weighted summation of its input array with components $(I_1, I_2, I_3, \ldots, I_m)$, i.e., $(\Sigma I_i w_i + b)$ and (2) the application of a sigmoidal function (S shaped) to this summation to give an output a, which can serve as input to other neurons. A widely used sigmoidal transfer function, which is used in this study, has the following form:

$$F(x) = \frac{1}{1+e^{-x}}. \tag{3}$$

These elements or neurons are arranged in layers. **Fig. 2** shows a schematic representation of a four-layer neural network. The ANN shown in Fig. 2 has an input layer, an output layer, and two hidden layers. The input layer contains an array of variables into which the input data of the system are read from an external source. Similarly, the predicted data or results, which can be multiple vectors, are written in the output layer. Initially, the input layer receives the input and passes it to the first hidden layer for processing. The processed information from the first hidden layer is then passed to the second hidden layer for processing. Finally, the output layer receives information from the last hidden layer and sends the results to an external source. All the hidden layers have no direct connections to the outside world, and the entire processing step is hidden from us. In general, the output from neuron j in layer k can be obtained by the following equation:

$$a_{jk} = F_k\left(\sum_{i=1}^{N_{k-1}} w_{ijk} a_{i(k-1)} + b_{jk} \right). \tag{4}$$

The coefficients w_{ijk} and b_{jk} in the summation, which are called the connection weights and bias of the network, respectively, are the fitting parameters of the model. The sizes of the input and output layers are fixed by the number of components of vectors **I** and **a**, respectively. The purpose of using an ANN is to obtain a mapping from an input vector **I** to an output vector **a**. It is desired that the difference between the predicted and the observed (actual) values of **a** be as small as possible. The number of neurons in each hidden layer is specified by the user. All neurons operate in parallel and each neuron operates independently of the other neurons. For any given neural network with n layers, the number of the weights in the network is given by the following equation:

$$N_t = \sum_{k=1}^{n-1} N_k N_{k+1}. \tag{5}$$

The operations of an ANN are divided into two phases, a training or ''learning'' phase and a cross-validation phase. The finding of a set of suitable weights that minimizes the error between the predicted and the actual output is called the training of the network. The values of these weights are first set using a random-number generator. During training, the network error is computed using some suitable training algorithm, and the weights in Eq. (4) of all the interconnections between neurons are adjusted based on the magnitude of the error and a parameter called the learning rate until the ANN ''learns'' the correct input-output behavior. The training phase is a time-consuming process and may take days of computer time to obtain adequate input-output performance. ANNs have many training algorithms. The one we used is back-propagation with momentum.[24] The momentum procedure is used to help the search process to not get stuck in a local minimum. The fitting procedure from which the weights w_{ijk} of the model in Eq. (4) are determined is performed using a least-squares minimization routine. In this routine, the sum squared of the relative error between the calculated and the experimental data is to be minimized. In general, backpropagation uses the following steps.

1. Enter a specific input and calculate its corresponding output.
2. If the sum-squared error between this output and the desired output is acceptable, then stop.
3. If step (2) is not satisfied, minimize the error by adjusting the weights between the neurons in the following manner:

- Begin at the output nodes and adjust their weights.
- Propagate backward to the layer adjacent to the output layer by calculating errors and adjusting weights.
- Continue going backward until all errors are calculated and the weights are adjusted.

A general methodology for the back-propagation method with momentum, which is based on the gradient-descent algorithm, was described in detail in a recent paper by Gharbi *et al.*[25]

It should be noted that, even though a good fit of a large number of data is obtained, there is no guarantee that the model can successfully predict data not contained in the learning data set. This is why after the training phase is completed, the cross-validation phase is required to ensure the accuracy and the generalization of the model. This phase is divided into two steps. First, the ANN is subjected to data not seen during the training phase, and hopefully the output prediction by the ANN is acceptable. The most successful ANN architecture is the one which has the smallest prediction error on a data set for which it was not trained. Second, the ANN is subjected to intermediate data points seen

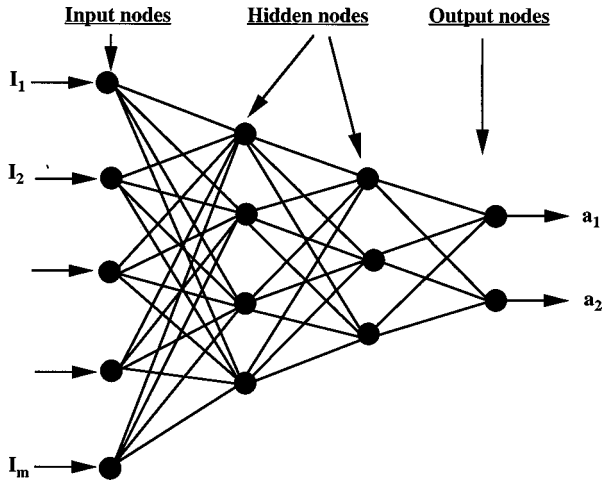

Fig. 2–Multiple layer neural-network model.

during the training phase to ensure that oscillation or ''overfitting'' did not occur.[26] The overfitting problem occurs because of the use of more hidden layers and neurons than actually needed.

Development of the PVT Models

In order to develop accurate PVT models, the artificial neural network must be exposed to enough data points. The data on which the network was trained contain 498 experimentally obtained data sets of different crude-oil and gas mixtures from the Middle East region. This represents the largest data set ever collected to be used in developing PVT models for Middle East crude oils. Some of the data were collected from the literature,[4,6] while the rest were not published previously. The construction of a complete data set representative of typical Middle East crude-oil systems was the most difficult part of this work. Each data point contains the bubblepoint pressure P_b, the oil formation volume factor B_{ob}, the solution gas-oil ratio R_s, the temperature T, the gas specific gravity γ_g, and the oil specific gravity γ_o. The range of the data is shown in **Table 1**. The general relations of P_b and B_{ob} in Eqs. (1) and (2) were considered in this study. The bubblepoint pressure and the oil formation volume factor have been chosen as the output variables, whereas four input variables have been considered: R_s, γ_g, γ_o, and T.

In theory, the output data can have a large domain of variation, as in the case of the bubblepoint pressure. However, if the domain of variation of the output data is large, then the ANN tends to be less stable. Therefore, this difficulty must be eliminated before the ANN enters its learning phase. This is done by preprocessing or scaling the output data in order to have small variation of the range of the output data.[27] This means that, instead of using the output variables in terms of their usual physical units, they are represented in dimensionless forms with values ranging from 0 to 1. The dimensionless output data were obtained using the following formula:

$$O_{new}=\frac{O_{old}-\min(O_{old})}{\max(O_{old})-\min(O_{old})}. \quad (6)$$

TABLE 1–RANGE OF THE PVT DATA

Bubblepoint pressure, psia	121	to	7127
Bubblepoint formation volume factor, rb/STB	1.032	to	2.925
Solution gas-oil ratio, scf/STB	13	to	3366
Gas relative density (air=1)	0.589	to	1.367
Stock-tank oil gravity, °API	19.35	to	50.14
Reservoir temperature, °F	74	to	306

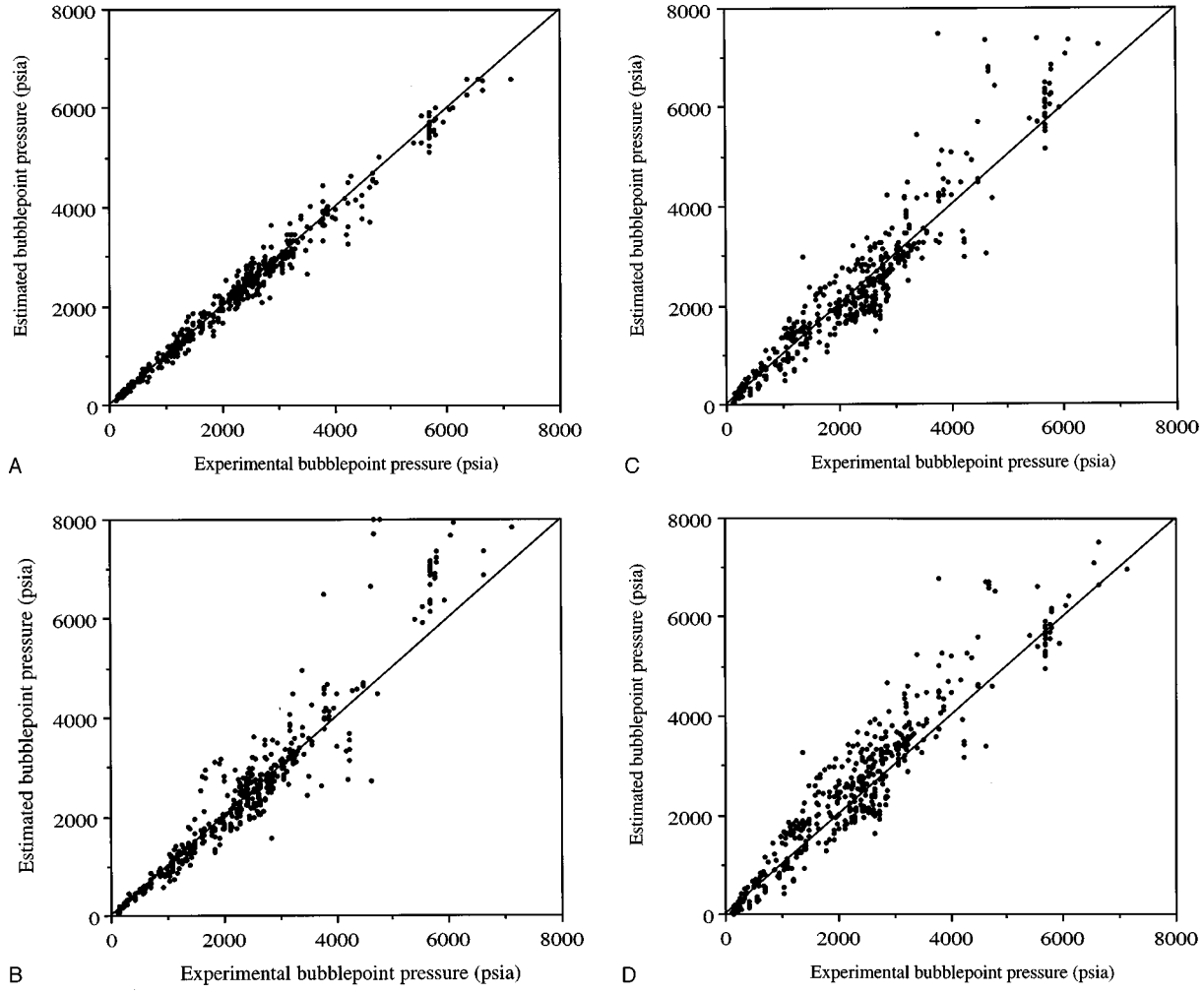

Fig. 3–(A) Comparison of the estimated vs. experimental bubblepoint pressure (ANN model). (B) Comparison of the estimated vs. experimental bubblepoint pressure [Al-Marhoun correlation (Ref. 4)]. (C) Comparison of the estimated vs. experimental bubblepoint pressure [Standing correlation (Ref. 1)]. (D) Comparison of the estimated vs. experimental bubblepoint pressure [Glasø correlation (Ref. 7)].

TABLE 2– STATISTICAL PARAMETERS FOR THE P_b CORRELATIONS (Data used in the training process)

	Neural Network	Al-Marhoun[a]	Standing[b]	Glasø[c]
Average relative error (%)	0.33	2.08	0.13	7.47
Average absolute relative error (%)	7.02	12.29	17.64	22.11
Minimum absolute relative error (%)	0.00	0.00	0.10	0.05
Maximum absolute relative error (%)	27.62	74.96	118.84	139.40
Standard deviation (%)	9.53	18.21	22.88	28.88
Correlation coefficient	0.982	0.812	0.839	0.845

[a]Reference 4.
[b]Reference 1.
[c]Reference 7.

The symbol ''O'' is used to represent the output variable, and it is either P_b or B_{ob}. The symbol O_{old} is the old (original) output, whereas O_{new} is the scaled output.

Various neural-network architectures were investigated to obtain the most accurate models for predicting P_b and B_{ob} as a function of the other four variables. Initially, an attempt was made to develop the two PVT models (P_b and B_{ob}) using a single neural-network design. But its ability to develop accurate models in a reasonable CPU time for the training process was not achieved using a personal computer. Instead, parallel neural-network designs were considered. These designs allow us to have different numbers of neurons for the estimation of P_b and B_{ob},

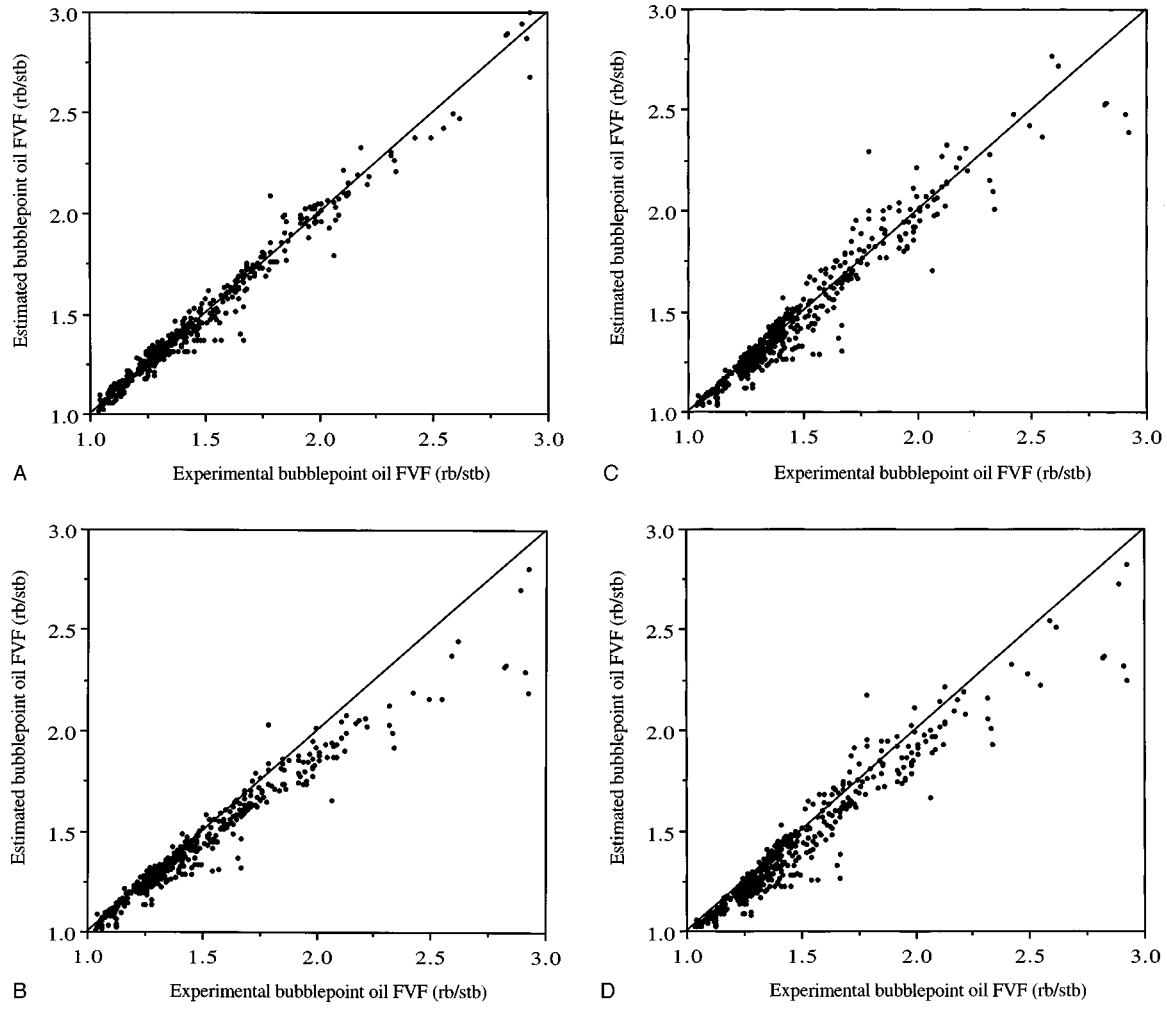

Fig. 4–(A) Comparison of the estimated vs. experimental bubblepoint oil formation volume factor (ANN model). (B) Comparison of the estimated vs. experimental bubblepoint oil formation volume factor [Al-Marhoun correlation (Ref. 4)]. (C) Comparison of the estimated vs. experimental bubblepoint oil formation volume factor [Standing correlation (Ref. 1)]. (D) Comparison of the estimated vs. experimental bubblepoint oil formation volume factor [Glasø correlation (Ref. 7)].

TABLE 3– STATISTICAL PARAMETERS FOR THE B_{ob} CORRELATIONS (Data used in the training process)

	Neural Network	Al-Marhoun[a]	Standing[b]	Glasø[c]
Average relative error (%)	0.09	−2.56	−0.81	−3.58
Average absolute relative error (%)	2.30	3.23	3.29	4.50
Minimum absolute relative error (%)	0.00	0.00	0.00	0.00
Maximum absolute relative error (%)	18.17	25.18	28.76	24.06
Standard deviation (%)	3.19	4.89	4.76	5.95
Correlation coefficient	0.976	0.917	0.938	0.905

[a]Reference 4.
[b]Reference 1.
[c]Reference 7.

and consequently different connecting weights for the two variables.

For each neural-network design, a one-hidden-layer architecture was initially used, and the number of neurons was systematically varied to obtain a good fit to the data. If an acceptable fit was not achieved for a very large number of neurons (greater than 50), then one hidden layer was added, and the procedure was repeated until a given architecture yielded an acceptable fit.

None of the neural networks with one hidden layer yielded acceptable fits, whereas more than one two-hidden-layer networks had an acceptable fit for both P_b and B_{ob}. After the cross-validation phase was carried out, only the architecture with eight neurons in the first hidden layer and four in the second was retained to predict P_b. Also, the architecture with six neurons in both the first and the second hidden layers was retained to predict B_{ob}. All other designs were rejected because they were either characterized by ''overfitting'' or were unable to predict acceptable results from input data not used in the training phase. The corresponding weighting factors and biases for the retained networks of P_b and B_{ob} are shown in the Appendix.

Accuracy of the PVT Models

Data Used in the Training Phase. In this section, the accuracy of the PVT models developed in this study is evaluated against those developed by Al-Marhoun,[4] Standing,[1] and Glasø.[7] The reason these three correlations were chosen is that most of the PVT assessment studies for different hydrocarbon systems have shown that the correlations by Standing and by Glasø perform better than those by Vasquez and Beggs reported in Refs. 28 and 29. In addition, Dokla and Osman's[6] correlation was not used in the comparison because it predicts a decrease in P_b with an increase in temperature, which is physically incorrect.[30]

The scatter diagrams (cross plots) of **Figs. 3(A)–3(D)** compare the experimental P_b versus the computed P_b obtained from the ANN and from the other three correlations. If the calculated results were in perfect agreement with the experiments, then all the

TABLE 4– PVT DATA USED FOR CROSS VALIDATION

No.	R_s (scf/STB)	γ_g	γ_o	T (°F)	P_b (psia)	B_{ob} (rb/STB)
1	104	1.126	0.890	160	408	1.098
2	433	1.188	0.870	100	804	1.215
3	305	0.918	0.840	153	1257	1.223
4	631	1.047	0.858	244	1625	1.489
5	580	0.802	0.834	100	1890	1.259
6	408	0.856	0.836	240	2020	1.393
7	466	0.972	0.830	239	2200	1.36
8	464	0.836	0.847	220	2430	1.291
9	730	0.680	0.799	232	2650	1.674
10	604	0.669	0.842	180	2845	1.331
11	811	0.812	0.842	185	3057	1.445
12	1039	0.910	0.860	193	3320	1.61
13	1172	0.758	0.771	291	3442	2.01
14	1295	0.831	0.855	218	3647	1.772
15	1393	0.900	0.807	306	3870	2.027
16	1052	0.767	0.838	193	4011	1.577
17	891	0.975	0.887	200	4215	1.38
18	1452	1.034	0.790	249	4432	1.901
19	1784	0.827	0.844	231	4640	2.055
20	2216	0.909	0.857	250	5405	2.16
21	1745	0.708	0.817	288	5789	2.1
22	3020	0.708	0.801	297	6358	2.887

TABLE 5– COMPARISON OF P_b ESTIMATED FROM VARIOUS CORRELATIONS
(Data not used in the training process)

No.	P_b Expt.	P_b ANN	P_b Al-Marhoun[a]	P_b Standing[b]	P_b Glasø[c]	E_a(%) ANN	E_a(%) Al-Marhoun[a]	E_a(%) Standing[b]	E_a(%) Glasø[c]
1	408	422	418	468	445	3.31	2.49	14.75	9.14
2	804	773	853	1199	1446	−3.91	6.08	49.13	79.89
3	1257	1188	1088	1047	1180	−5.47	−13.46	−16.74	−6.16
4	1625	1780	1836	2329	2492	9.53	12.97	43.31	53.36
5	1890	1977	1925	1741	2159	4.62	1.84	−7.86	14.25
6	2020	2082	1794	1670	1775	3.09	−11.17	−17.31	−12.15
7	2200	1718	1517	1616	1721	−21.93	−31.06	−26.54	−21.79
8	2430	2281	2062	1940	2135	−6.15	−15.15	−20.15	−12.13
9	2650	2887	3580	2586	2918	8.93	35.09	−2.43	10.10
10	2845	2749	3427	2606	3017	−3.37	20.44	−8.42	6.04
11	3057	3132	2971	2866	3284	2.46	−2.82	−6.26	7.43
12	3320	3828	3111	3610	4021	15.30	−6.31	8.72	21.13
13	3442	3319	4081	3298	3563	−3.58	18.57	−4.18	3.50
14	3647	3782	4457	4798	4989	3.69	22.21	31.57	36.80
15	3870	3861	3964	4319	4198	−0.24	2.42	11.61	8.48
16	4011	3680	3988	3713	4125	−8.26	−0.57	−7.44	2.85
17	4215	3470	2737	3517	3975	−17.66	−35.07	−16.57	−5.70
18	4432	3777	2656	3165	3504	−14.78	−40.08	−28.59	−20.95
19	4640	4248	5568	6077	5941	−8.44	20.01	30.96	28.04
20	5405	5416	5922	7537	6843	0.20	9.57	39.44	26.61
21	5789	5626	7360	6523	5968	−2.82	27.13	12.68	3.09
22	6358	6604	10412	9502	7860	3.87	63.77	49.46	23.63

[a]Reference 4.
[b]Reference 1.
[c]Reference 7.

data will fall on the 45° line. The tighter the cluster about the 45° line, the better the agreement between the experimental and the predicted results. As shown, a tighter cloud of points about the 45° line was obtained by the ANN [Fig. 3(A)] compared to that obtained by the other three correlations [Figs. 3(B)–3(D)]. This indicates that excellent agreement between the experimental and the calculated data was obtained using the ANN. **Table 2** compares the statistical constants obtained from this study and from the other three P_b correlations. The ANN model for the bubble-point pressure of this study achieved the lowest errors (7.02%) and standard deviation (9.53%) with the highest coefficient of correlation, 0.982. Al-Marhoun's correlation showed an average absolute relative error of 12.29% with a standard deviation of 18.21%. The two correlations of Standing and Glasø showed larger values of average absolute relative error and standard deviation with a correlation coefficient larger than that of Al-Marhoun.

The scatter diagrams (cross plots) of **Figs. 4(A)–4(D)** compare the experimental B_{ob} versus the computed B_{ob} obtained from the ANN and from the other three correlations. The excellent agreement between the experimental and the computed data by the ANN is also evident in the estimation of B_{ob} as shown in the scatter diagram of Fig. 4(A). Once again, a tighter cloud is obtained by the ANN compared to that obtained by the other three

TABLE 6– STATISTICAL PARAMETERS FOR THE P_B CORRELATIONS
(Data not used in the training process)

	Neural Network	Al-Marhoun[a]	Standing[b]	Glasø[c]
Average relative error (%)	−1.89	3.95	5.87	11.61
Average absolute relative error (%)	6.89	18.10	20.64	18.78
Minimum absolute relative error (%)	0.20	0.57	2.43	2.85
Maximum absolute relative error (%)	21.93	63.77	49.46	79.89
Standard deviation (%)	8.91	23.73	25.11	26.06
Correlation coefficient	0.962	0.458	0.574	0.787

[a]Reference 4.
[b]Reference 1.
[c]Reference 7.

TABLE 7– COMPARISON OF B_{ob} ESTIMATED FROM VARIOUS CORRELATIONS
(Data not used in the training process)

No.	B_{ob} Expt.	B_{ob} ANN	B_{ob} Al-Marhoun[a]	B_{ob} Standing[b]	B_{ob} Glasø[c]	E_a(%) ANN	E_a(%) Al-Marhoun[a]	E_a(%) Standing[b]	E_a(%) Glasø[c]
1	1.098	1.088	1.105	1.100	1.074	−0.91	0.63	0.15	−2.20
2	1.215	1.213	1.228	1.259	1.239	−0.16	1.05	3.59	1.99
3	1.223	1.24	1.201	1.195	1.166	1.39	−1.78	−2.27	−4.67
4	1.489	1.483	1.439	1.466	1.424	−0.40	−3.33	−1.57	−4.35
5	1.259	1.311	1.272	1.292	1.271	4.13	1.06	2.66	0.94
6	1.393	1.355	1.321	1.303	1.260	−2.73	−5.17	−6.47	−9.54
7	1.36	1.395	1.361	1.353	1.311	2.57	0.11	−0.55	−3.59
8	1.291	1.348	1.323	1.315	1.276	4.42	2.46	1.90	−1.19
9	1.674	1.53	1.452	1.443	1.400	−8.60	−13.27	−13.78	−16.35
10	1.331	1.364	1.328	1.331	1.295	2.48	−0.24	−0.03	−2.67
11	1.445	1.464	1.444	1.480	1.446	1.31	−0.05	2.45	0.07
12	1.61	1.555	1.558	1.648	1.610	−3.42	−3.21	2.37	−0.03
13	2.01	2.032	1.757	1.781	1.717	1.09	−12.58	−11.39	−14.55
14	1.772	1.709	1.678	1.796	1.743	−3.56	−5.30	1.33	−1.66
15	2.027	1.973	1.882	1.989	1.906	−2.66	−7.14	−1.89	−5.96
16	1.577	1.598	1.549	1.611	1.571	1.33	−1.76	2.13	−0.37
17	1.38	1.484	1.490	1.573	1.536	7.54	8.00	13.96	11.29
18	1.901	2.017	1.938	2.066	1.987	6.10	1.93	8.67	4.53
19	2.055	2.064	1.923	2.120	2.029	0.44	−6.40	3.14	−1.26
20	2.16	2.275	2.161	2.482	2.327	5.32	0.04	14.89	7.71
21	2.1	2.113	1.943	2.074	1.978	0.62	−7.50	−1.26	−5.83
22	2.887	2.883	2.604	2.910	2.637	−0.14	−9.80	0.81	−8.65

[a]Reference 4.
[b]Reference 1.
[c]Reference 7.

correlations. The statistical error analyses for the ANN and the three correlations are shown in **Table 3**. This study's correlation for B_{ob} obtained the highest accuracy, with a correlation coefficient of 0.976. Standing's correlation was the second best, with a correlation coefficient of 0.938. Glasø's correlation showed the lowest accuracy, 0.905. This indicates that the ANN was able to predict P_b and B_{ob} more accurately than the correlations of Al-Marhoun, Standing, or Glasø.

Cross Validation. For any correlation to be useful, it should predict results of input data that were not used in its developmental phase even though a good fit was obtained during the training process. This ensures the accuracy and the generalization of the model within the domain of the original data. Twenty-two additional measured PVT data points, which represent crude-oil and gas mixtures from oil fields in the Middle East, were utilized in order to test the prediction capabilities of models presented in this study. **Table 4** lists the 22 PVT data points that were not seen by the neural-network model during its training phase. It should be noted that all of the 22 data points fall in the range of the PVT data used during the training of the neural-network model.

Table 5 compares the 22 experimental bubblepoint pressures with those predicted by the four previously mentioned correlations. The parameter "E_a" represents the percent of relative error between the experimental and the estimated data by a given cor-

TABLE 8– STATISTICAL PARAMETERS FOR THE B_{ob} CORRELATIONS
(Data not used in the training process)

	Neural Network	Al-Marhoun[a]	Standing[b]	Glasø[c]
Average relative error (%)	0.74	−2.83	0.86	−2.56
Average absolute relative error (%)	2.79	4.22	4.42	4.97
Minimum absolute relative error (%)	0.14	0.04	0.03	0.03
Maximum absolute relative error (%)	8.60	13.28	14.89	16.35
Standard deviation (%)	3.65	5.79	6.46	6.74
Correlation coefficient	0.979	0.925	0.923	0.911

[a]Reference 4.
[b]Reference 1.
[c]Reference 7.

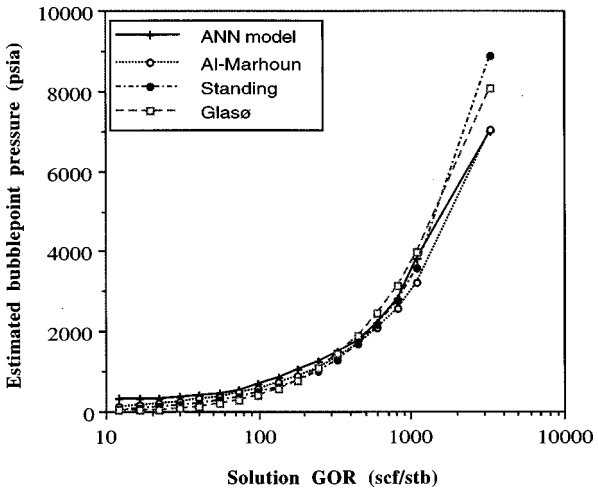

Fig. 5–Effect of the solution gas-oil ratio (GOR) on the bubblepoint pressure (T=195°F, gas spc. grv.=0.889, oil spc. grv. =0.845).

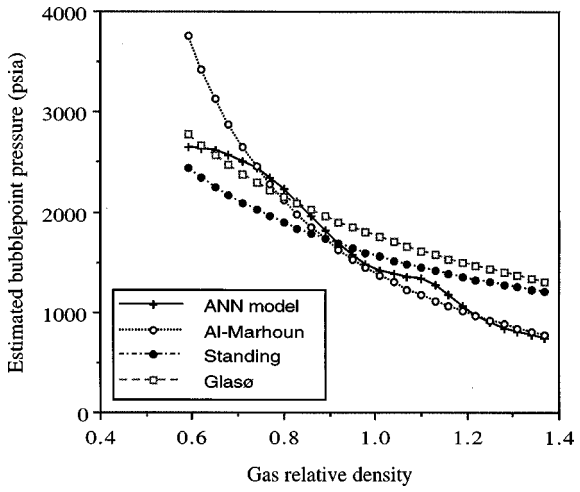

Fig. 7–Effect of the gas specific gravity on the bubblepoint pressure (sol. GOR=465 scf/STB, T=195°F, oil spc. grv. =0.845).

relation. As shown the overall performance of the ANN for the calculation of P_b was better than that of any of the other correlations. The comparison of the statistical parameters obtained by the ANN and by the other three correlations is shown in **Table 6**. The relative error obtained using the ANN ranges from 0.2% to 21.93% with a standard deviation of 8.91%. The other three correlations show a wider range of relative errors with larger values of standard deviations.

Table 7 compares the experimental versus the estimated B_{ob} for the 22 data points, along with the percent of relative error for each of the data points. The comparison of statistical parameters for each correlation is shown in **Table 8**. Once again, the ANN's prediction of B_{ob} was the most accurate, with a relative error that ranges from 0.14% to 8.60% and a standard deviation of 3.65%. Therefore, the prediction capabilities of the neural-network model was validated for a data set not used during the training phase of the model.

Furthermore, in order to show that the model developed in this study is physically correct and no overfitting occurs (i.e., it is stable), the ANN was subjected to intermediate data points. This was done by studying the dependence of both P_b and B_{ob} on a

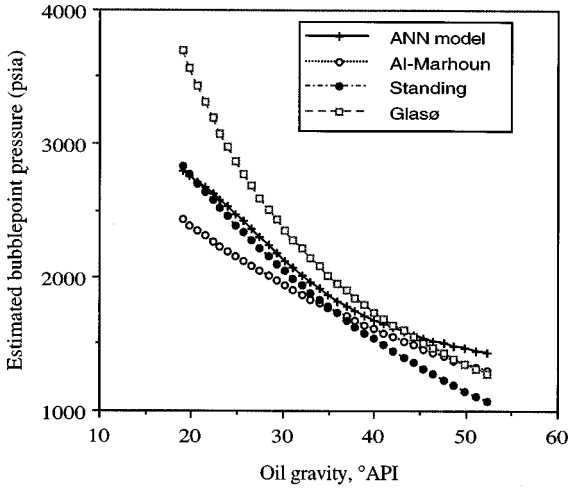

Fig. 8–Effect of the oil specific gravity on the bubblepoint pressure (sol. GOR=465 scf/STB, T=195°F, gas spc. grv.=0.889).

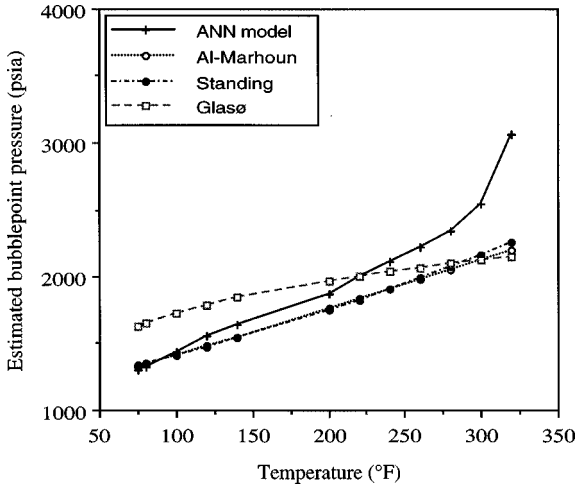

Fig. 6–Effect of the reservoir temperature on the bubblepoint pressure (sol. GOR=465 scf/STB, gas spc. grv.=0.889, oil spc. grv.=0.845).

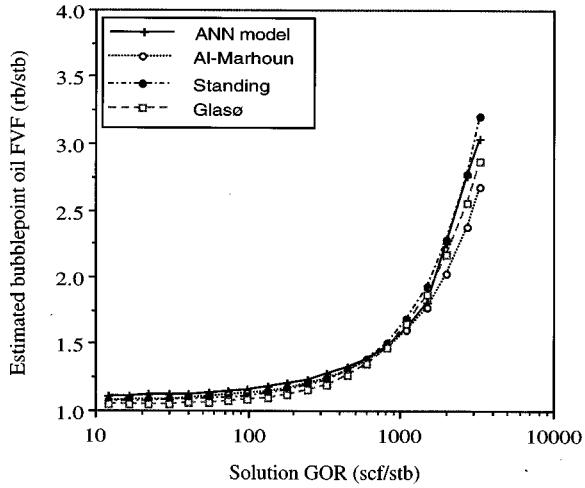

Fig. 9–Effect of the solution GOR on the bubblepoint oil formation volume factor (T=195°F, gas spc. grv.=0.889, oil spc. grv.=0.845).

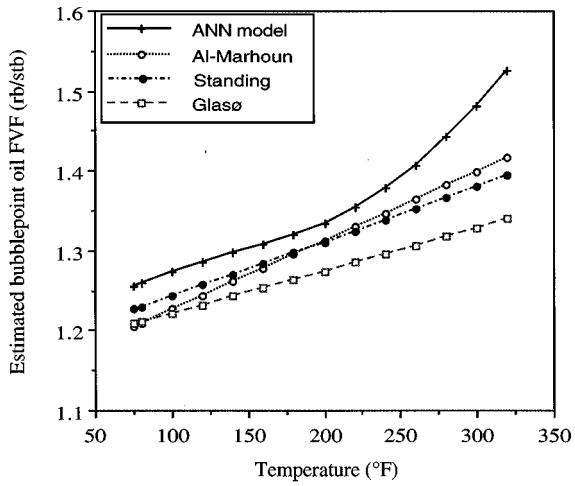

Fig. 10–Effect of the reservoir temperature on the bubblepoint oil formation volume factor (sol. GOR=465 scf/STB, gas spc. grv.=0.889, oil spc. grv.=0.845).

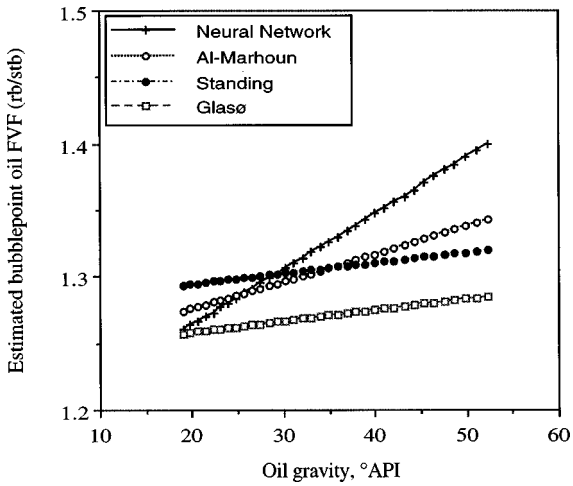

Fig. 12–Effect of the oil specific gravity on the bubblepoint oil formation volume factor (sol. GOR=465 scf/STB, T=195°F, gas spc. grv.=0.889).

single input parameter while maintaining the other three input parameters constant. **Figs. 5, 6, 7, and 8** compare the dependence of P_b on R_s, T, γ_g, and γ_o, respectively, obtained by the ANN and the three correlations. From Figs. 5–8, two conclusions can be drawn. First, P_b is an increasing function with respect to R_s, T, and γ_o and a decreasing function with respect to γ_g, as expected. Hence, the ANN model for P_b is physically correct. Second, oscillation did not occur in these intermediate data points, and therefore overfitting was not a problem in the ANN model of P_b.

The dependence of B_{ob} on R_s, T, γ_g, and γ_o is shown in **Figs. 9, 10, 11, and 12**, respectively, for all the correlations and the ANN model. Once again, the same two conclusions drawn previously in the P_b model can be drawn for the B_{ob} model as well. The ANN and the three correlations show that B_{ob} is an increasing function of R_s, T, γ_g, and a decreasing function of γ_o. In addition, the ANN model did not show oscillation and hence overfitting was not a problem. Therefore, the ANN has successfully captured the system's behavior and is able to correctly predict both P_b and B_{ob} better than other PVT correlations considered in this study.

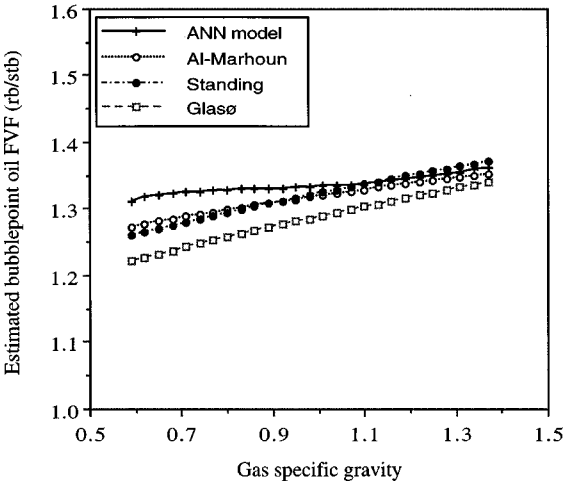

Fig. 11–Effect of the gas specific gravity on the bubblepoint oil formation volume factor (sol. GOR=465 scf/STB, T=195°F, oil spc. grv.=0.845).

Conclusions

This study presents more accurate models for the prediction of PVT properties of Middle East crude oils than existing PVT correlations. Unlike other correlations which were developed using regression techniques, these models were developed using artificial neural networks. Several neural-network designs were investigated to obtain the most accurate PVT models. A back-propagation network with momentum for error minimization was used. A two-layer parallel neural network, which was able to minimize the prediction error on a data set not used in the training phase, was chosen for the prediction of P_b and B_{ob} of Middle East crude oils. The models are able to predict the bubblepoint pressure and the oil formation volume factor as functions of the solution gas-oil ratio (R_s), the temperature, the gas specific gravity (γ_g), and the oil specific gravity (γ_o). The models presented in this study were based on large PVT data analysis (498 data sets), more than those published for Middle East crudes. An additional set of 22 data points were used to check the prediction capabilities of the present models as compared to other correlations. The models are able to predict the bubblepoint pressure and the oil formation volume factor for data falling within the range of data used in this study. The neural-network models can be further refined and weights adjusted to incorporate new additional experimental data.

Nomenclature

$\mathbf{a}$ = output vector
a_{jk} = output of neuron j in layer k
B_{ob} = bubblepoint oil formation volume factor (rb/STB)
b_{jk} = bias for neuron j in layer k
E_a = percent relative error
F_k = transfer function of the neurons in layer k
$\mathbf{I}$ = input pattern
n = total number of layers
N_k = number of neurons in layer k
N_t = total number of weights
P = number of input patterns
P_b = bubblepoint pressure (psia)
R_s = solution gas-oil ratio (scf/STB)
T = reservoir temperature (°F)
w_{ijk} = weight for input i, neuron j, and layer k
γ_g, γ_o = gas and oil specific gravity, respectively (dimensionless)

Appendix—Connection Weights and Biases for the Neural-Network Model

Model for the Bubblepoint Pressure.

Hidden Layer No. 1

	W_{ij}				Bias
j/i	1	2	3	4	b_j
1	8.0228E−04	2.5280E+00	8.4771E+00	8.5291E−03	−1.1104E+01
2	−7.0113E−03	−4.2752E−01	7.6298E+00	−5.6102E−04	−6.4965E+00
3	4.6376E−05	2.9631E−01	7.9591E+00	1.5905E−03	−7.0022E+00
4	−2.2468E−03	−1.3638E+01	−1.3060E+01	4.5893E−02	1.4131E+01
5	6.8922E−03	−2.4546E+00	−3.2147E+00	2.7076E−02	−6.3481E+00
6	−7.2759E−03	−1.0974E+01	−5.3571E−01	7.4948E−02	2.7061E+00
7	−3.6759E−03	−1.4191E+01	1.7926E+01	8.7173E−02	−1.5335E+01
8	−7.7379E−04	3.3960E+00	−4.3077E+00	−4.2351E−04	8.7737E−01

Hidden Layer No. 2

	W_{ij}								Bias
j/i	1	2	3	4	5	6	7	8	b_j
1	1.7747	−4.9792	−2.2483	0.0073	0.6597	−0.2095	−0.2017	−2.1279	−3.9341
2	2.5636	−1.6073	−5.2026	1.7713	2.1588	−0.8285	−7.3801	0.7873	−5.8195
3	−3.2025	1.8759	3.5967	0.5844	2.4276	9.2620	−9.4084	9.5004	8.5087
4	0.8192	−1.5619	−11.5946	−7.3277	−3.7439	4.9106	2.9370	4.9779	7.4471

Output Layer

	W_{ij}				Bias
j/i	1	2	3	4	b_j
1	3.8070E−01	−1.0069E−01	−1.3857E−01	−3.9640E−01	0.5471

Model for the Bubblepoint Oil Formation Volume Factor.

Hidden Layer No. 1

	W_{ij}				Bias
j/i	1	2	3	4	b_j
1	3.4409E−03	−1.6118E+00	−8.2385E+00	1.6280E−03	7.5444E+00
2	−2.0759E−04	2.5652E+00	−2.4135E+00	3.0539E−03	9.5713E−01
3	−2.0828E−03	−6.6452E−02	−8.5894E+00	1.2659E−03	1.0029E+01
4	−8.0186E−04	−8.7802E−01	−1.4093E+00	−5.6451E−03	3.7969E+00
5	−1.4177E−03	−1.1030E+00	5.4724E+00	5.2816E−03	−6.5654E+00
6	−3.0617E−04	1.1743E+00	4.6879E+00	5.0982E−03	−5.2266E+00

Hidden Layer No. 2

	W_{ij}						Bias
j/i	1	2	3	4	5	6	b_j
1	6.2120E−01	2.9407E+00	2.7412E+00	−6.2151E−01	−2.2776E+00	6.4421E−01	−1.1285E+00
2	3.5988E−01	1.2179E+00	−3.6311E−01	−1.7970E+00	2.2254E+00	−1.1461E+00	−1.8388E+00
3	5.4310E−01	1.0527E+00	−6.4833E−01	−1.8828E+00	1.9458E−01	−2.5522E+00	3.0868E+00
4	2.2396E+00	8.2002E−01	2.3519E+00	5.3543E−02	−5.8301E−01	3.4192E+00	6.4497E−01
5	−6.1330E−01	−2.4084E+00	−1.8367E−01	2.0405E+00	−6.3156E−01	−2.3466E+00	−5.9544E−01
6	−1.6987E−01	5.7485E−01	−1.3086E+00	2.3858E+00	1.8950E+00	2.4029E+00	3.7373E+00

Output Layer

	W_{ij}						Bias
j/i	1	2	3	4	5	6	b_j
1	−1.3530E+00	1.5794E+00	2.1993E−01	7.5561E−01	−2.6139E−01	−8.7874E−01	1.3977

References

1. Standing, M.B.: ''A Pressure-Volume-Temperature Correlation for Mixtures of California Oils and Gases,'' *Drill. & Prod. Prac.* (1947) **API**, 275–287.
2. Standing, M.B.: ''Oil-System Correlations,'' *Petroleum Production Handbook*, T.C. Frick (ed.), SPE, Richardson, TX (1962) Chap. 19, 1–42.
3. Standing, M.B.: *Volumetric and Phase Behavior of Oil Field Hydrocarbon Systems*, Millet Print Inc., Dallas, TX (1977) 70–95.
4. Al-Marhoun, M.A.: ''PVT Correlations for Middle East Crude Oils,'' *JPT, Trans.*, AIME **285**, (May 1988) 650–666.
5. Al-Marhoun, M.A.: ''New Correlation for Formation Volume Factors of Oil and Gas Mixtures,'' *J. Cdn. Pet. Tech.* (1992) **31**(3), 22–26.
6. Dokla, M.E. and Osman, M.E.: ''Correlation of PVT Properties for UAE Crudes,'' *SPEFE, Trans.*, AIME (March 1992) **293**, 41–46.
7. Glasø, O.: ''Generalized Pressure-Volume Temperature Correlations,'' *Pet. Technol. Trans.*, AIME (May 1980) **269**, 785–795.
8. Labedi, R.: ''Use of Production Data to Estimate Volume Factor Density and Compressibility of Reservoir Fluids,'' *J. Pet. Sci. Eng.* (1990) **4**, 357–390.
9. Lasater, J.A.: ''Bubble Point Pressure Correlation,'' *Trans.*, AIME (1958) **213**, 379–381.
10. Vasquez, M.E. and Beggs, H.D.: ''Correlations for Fluid Physical Property Prediction,'' *JPT, Trans.*, AIME (June 1980) **269**, 968–970.
11. Briones, M.F., Rojas, G.A., and Corpoven, S.A.: ''Thermodynamic Characterization of Volatile Hydrocarbon Reservoirs by Neuronal Networks,'' paper SPE 27027, Presented at the 1994 SPE Latin American and Caribbean Petroleum Engineering Conference, Buenos Aires, 26–29 April.
12. Habiballah, W.A., Startzman, R.A., and Barrufet, M.A.: ''Use of Neural Networks for the Prediction of Vapor-Liquid Equilibrium *K*-Values,'' *In Situ* (1993) **17**, 227–242.
13. Baldwin, J.L.: ''Using a Simulated Bi-Directional Associative Neural Network Memory with Incomplete Prototype Memories to Identify Facies from Intermittent Logging Data Acquired in a Siliciclastic Depositional Sequence: A Case Study,'' paper SPE 22843 presented at the 1991 SPE Annual Technical Conference and Exhibition, Dallas, TX, 6–9 October.
14. Garcia, G. and Whitman, W.W.: ''Inversion of a Lateral Log Using Neural Networks,'' paper SPE 24454 presented at the 1992 SPE Petroleum Computer Conference, Houston, TX, 21–22 July.
15. Smith, M., Carmichael, N., Reid, I., and Bruce, C.: *Lithofacies Determination from Wire-Line Log Data Using a Distributed Neural Network*, Proc., IEEE Workshop on Neural Networks for Signal Processing, Princeton, NJ, 1991, 482–492.
16. Juniardi, I.R. and Ershaghi, I.: ''Complexities of Using Neural Network in Well Test Analysis of Faulted Reservoirs,'' paper SPE 26106 presented at the 1993 SPE Western Regional Meeting, Anchorage, AK, 26–28 May.
17. Kumoluyi, A.O. and Daltaban, T.S.: ''Higher-Order Neural Networks in Petroleum Engineering,'' paper SPE 27905, Presented at the 1994 SPE Western Regional Meeting, Long Beach, CA, 23–25 March.
18. Waller, M.D. and Rowsell, P.J.: ''Intelligent Well Control,'' *Trans.-Inst. Min. Metall.* (1994) **103**, 47–51.
19. Mohaghegh, S., Arefi, R., and Ameri, S.: ''Design and Development of an Artificial Neural Network for the Estimation of Formation Permeability,'' paper SPE 28237 presented at the 1994 SPE Petroleum Computer Conference, Dallas, TX, 31 July–3 August.
20. Gharbi, R.B. and Elsharkawy, A.M.: ''Neural Network Model for Estimating the PVT Properties of Middle East Crude Oils,'' *In Situ* (1996) **20**(4), 367–394.
21. Pati, Y.C. and Krishnaprasad, P.S.: ''Analysis and Synthesis of Feed Forward Neural Networks Using Discrete Affine Wavelet Transformations,'' *IEEE Trans. Neural Netw.* (1993) **4**(1), 73–80.
22. Bhat, N. and McAvoy, T.J.: ''Use of Neural Nets for Dynamic Modeling and Control of Chemical Process Systems,'' *Comput. Chem. Eng.* (1990) **14**(4/5), 573–582.
23. Cadzow, J.A. and Solomon, O.M.: ''Algebraic Approach to System Indentification,'' *IEEE Trans. Acoust., Speech, Signal Process.* (1986) **34**(3), 462–470.
24. Rumelhart, D.E., Hinton, G.E., and Williams, R.J.: ''Learning Internal Representation by Error Propagation,'' *Parallel Data Processing*, MIT Press, Cambridge, MA (1986) Vol. 1, 318–362.
25. Gharbi, R., Karkoub, M., and Elkamel, A.: ''An Artificial Neural Network for the Prediction of Immiscible Flood Performance,'' *Energy Fuels* (1995) **9**(5), 894–900.
26. Sjöberg, J. and Ljung, L.: ''Overfitting, Regularization, and Searching for Minimum in Neural Networks,'' Proc., Fourth IFAC International Symposium on Adaptive Systems in Control Signal and Processing, Grenoble, France, 1992.
27. Hertz, J., Krogh, A., and Palmer, R.G.: ''*Introduction to the Theory of Neural Computation*,'' Addison–Wesley Publishing Co., New York City (1991).
28. Elsharkawy, A.M., Elgibaly, A.A., and Alikhan, A.A.: ''Assessment of PVT Correlations for Predicting the Properties of Kuwaiti Crude Oils,'' *J. Pet. Sci. Eng.* (1995) **13**, 219–232.
29. Sutton, R.P. and Farshad, F.: ''Evaluation of Empirically Derived PVT Properties for Gulf of Mexico Crude Oils,'' *SPERE* (February 1990) 79–86.
30. Al-Yousef, H.Y. and Al-Marhoun, M.A.: ''Discussion of Correlation of PVT Properties for UAE Crudes,'' *SPEFE* (March 1993) 80–81.

SI Metric Conversion Factors

°API 141.5/(131.5+API)	=	g/cm^3
bbl × 1.589 874	$E-01$ =	m^3
°F (°F−32)/1.8	=	°C
°F (°F+459.67)/1.8	=	K
°F °F+459.67	=	R
psi × 6.894 757	$E+00$ =	kPa
scf/stb × 1.801 175	$E-01$ =	stdm^3/m^3

SPERE

Ridha B.C. Gharbi is an associate professor in the Dept. of Petroleum Engineering at Kuwait U. His e-mail address is Ridha@kuc01.kuniv.edu.kw. His research interests include fluid flow in porous media, numerical simulation, fluid modeling, artificial intelligence, EOR, and horizontal wells. He has authored more than 30 publications in these areas. He holds a BS degree from the U. of Tulsa, and MS and PhD degrees from the U. of Texas at Austin, all in petroleum engineering. **Adel M. Elsharkawy** is an associate professor at Kuwait U. and has teaching and research interests in reservoir fluid modeling, reservoir simulation, and EOR. He holds BS and MS degrees from Suez Canal U., Egypt, and a PhD from Colorado School of Mines, Golden, Colorado.

SPE 57433

Intelligent Systems Can Design Optimum Fracturing Jobs

Shahab Mohaghegh, Andrei Popa, and Sam Ameri, West Virginia University

Copyright 1999, Society of Petroleum Engineers Inc.

This paper was prepared for presentation at the 1999 SPE Eastern Regional Meeting held in Charleston, WV, 21-22 October 1999.

This paper was selected for presentation by an SPE Program Committee following review of information contained in an abstract submitted by the author(s). Contents of the paper, as presented, have not been reviewed by the Society of Petroleum Engineers and are subject to correction by the author(s). The material, as presented, does not necessarily reflect any position of the Society of Petroleum Engineers, its officers, or members. Papers presented at SPE meetings are subject to publication review by Editorial Committees of the Society of Petroleum Engineers. Electronic reproduction, distribution, or storage of any part of this paper for commercial purposes without the written consent of the Society of Petroleum Engineers is prohibited. Permission to reproduce in print is restricted to an abstract of not more than 300 words; illustrations may not be copied. The abstract must contain conspicuous acknowledgment of where and by whom the paper was presented. Write Librarian, SPE, P.O. Box 833836, Richardson, TX 75083-3836, U.S.A., fax 01-972-952-9435.

ABSTRACT

Many computer software programs have been developed to assist petroleum engineers and scientists in designing hydraulic fractures. These programs use analytical, numerical or empirical methods (or a combination of two or all three methods) to model fracture propagation in the reservoir. The user – which is usually experienced petroleum professional – provides the necessary input parameters to the model. These input parameters include reservoir characteristics, fluid and proppant characteristics and treatment schedule. Usually among the major outputs of these models are the fracture geometry and conductivity.

The goal of this study is to provide a tool that allows the engineer to solve the inverse problem in a fast and efficient manner. Using the tool developed in this study the engineer identifies the desired fracture geometry that she/he would like to achieve and enters this value along with the reservoir characteristics into the intelligent software tool. The software tool would then solve the inverse problem and provides the engineer with fluid, proppant and the treatment schedule that would produce the desired fracture in that particular reservoir.

This new tool has been tested and shows to be capable of designing hydraulic fractures replicating those designed by expert engineers. An innovative hybridization of two virtual intelligence paradigms has been used to develop the methodology that is being introduced in this paper. An industry standard three-dimensional fracturing model (FRACPRO) has been used as the data set generator for the study.

INTRODUCTION

Hydraulic fracturing of a formation is a complex process that involves wellbore configuration, reservoir characteristics and fracturing fluid and proppant characteristics. Another factor that plays an important role in the success or failure of a fracture is the method of implementation. A hydraulic fracture is accomplished in several stages that together form the treatment schedule. Design of a job involves selection of fluid and proppant as well as injection rates and volumes and concentration in a specific manner (treatment schedule) that has the highest desirable effect on the target formation.

Designing the treatment schedule that creates the desired fracture propped length is one of the main challenges for an engineer. For given reservoir conditions, the treatment design engineer evaluates the use of several fluid types and volumes, proppant type and concentrations and several injection rates. To evaluate all the possibly usefull combinations, one must perform hundreds of runs for each treatment schedule. Usually on most three dimensional hydraulic fracture simulators a run lasts from one to several minutes. Results of each run should be studied after the completion of each run and input parameters should be altered for the next run to get one step closer to the desired outcome. Overall, designing a job is time consuming, and the process may last from several hours to a whole day. Moreover many hydraulic fracture computer models are not very user-friendly, and require massive amounts of information.

To reduce the complexity of hydraulic fracture design procedure an attempt is made to build an intelligent tool that can help engineers design fracture treatments in a short period of time. This tool is based entirely on the use of virtual intelligence techniques, namely neural networks and genetic algorithms. Neural networks are tools that (once trained properly) provide instantaneous results (output) to a particular set of inputs. Therefore the neural networks were used to replicate the functionality of a three-dimensional hydraulic fracture computer model. A novel two step method that integrates the neural networks with genetic algorithms is proposed. The genetic algorithm searches through all the possible combination of input parameters and finds the most desirable input combinations that provides the best result. Genetic algorithm performs this task based on the Darwinian theory of the survival of the fittest. Several neural networks are trained for the design optimization process. These neural networks are capable of designing ramp treatment schedules as well as stage treatment schedules.

METHODOLOGY

As was mentioned in the previous section, two virtual intelligence paradigms were used in developing the techniques presented in this paper, namely neural network and genetic algorithms. Background information about neural networks and genetic algorithms has been covered in prior publications[1,2] and will not be repeated here. In achieving the objectives of this study these two paradigms were combined and used as a hybrid system. A series of neural networks were trained and used as the hydraulic fracture model. In order to produce the desirable hydraulic fracture design the genetic algorithm was employed. The role of genetic algorithm is to search and find the combinations of variables that satisfies the design specifications.

This innovative approach allows the genetic algorithm to use (without prior dispositions) any conceivable combinations of variables that might not have been thought by an engineer. This would be the true “thinking outside of the box”. On the other hand, specific rules can be introduced in the algorithm that would prohibit production of unrealistic and unacceptable designs. These rules would work as process constraints.

Another tool that was extensively used during the development process was a three-dimensional hydraulic fracture model named FRACPRO[3]. It should be noted that any other hydraulic fracture computer model could have been used. We selected FRACPRO

because of its wide use and favorable reputation in the industry. FRACPRO was used as a tool to train the neural networks. Therefore the designs provided by this methodology is within reasonable accuracy when run on FRACPRO. The difference is that in order to design fracture treatments using our model no specific expertise in hydraulic fracturing design is required. Even experts will find this model to be useful. It can save them many hours of tuning and manipulation of variables to achieve desired fracture geometry by providing a starting point that is very close to the optimum design. Figure 1 shows a general schematic diagram of the model. As it is shown in this figure, the engineer provides reservoir characteristics and the desired fracture geometry as input. The model output consist of fluid and proppant characteristics as well as detail job schedule including the number of stage, and amount of fluid and proppant and the rate at which they need to be pumped.

RESULTS AND DISCUSSIONS

In order to demonstrate the capabilities of the model that is being presented in this study two field examples are presented. In these examples we first introduce a successful job designed by an expert engineer for a particular well. Next the model will be used to generate a fracture design for the same well. The model should be judged by the outcome of its suggested fracture design, and how close it is to the outcome of the expert's design. The issue being addressed here is whether the model is capable of designing fracture treatments that are comparable to those designed by an expert. The only information that is provided to the model are reservoir characteristics and the target fracture length. We will use the same fracture length that the original design has reached as our target length for comparison purposes.

The first desin is a hydraulic fracture that was pumped in Redfork formation. This job is considered to be a successful hydraulic fracture job given the post fracture well response. An engineer with many years of experience in design and implementation of hydraulic fractures designed this job. As demonstrated in Table 1 the engineer has designed a ramp treatment schedule for this fracture. Using FRACPRO to model this design results in a fracture length of about 450 ft as shown in Table 1.

We now use our model by providing the reservoir characteristics and a target fracture length of 450 ft as input to the model. The reservoir characteristics provided to our model are the same information that is provided to FRACPRO. This model provides several potential hydraulic fracture designs that can be used for this well. The model provides detail schedule as well as the fracture length and conductivity that can be expected if any of the jobs are implemented.

The next step is to take the designs provided by the model and test them on FRACPRO, and see how well the model performs against FRACPRO. The fact that our model provides a set of several potential solutions gives the engineer a choice in selecting the design that he feels most comfortable with. Table 2 summarizes the results provided by our model.

The process generates four different near optimum designs that have fracture length close to the desired value of 450 ft. The largest difference between the desired fracture length and those proposed by this methodology is 15 ft or about 3%.

According to the material balance equation the larger the fluid volume pumped the longer the length of the fracture. Consequently, the third treatment design should have provided the longest fracture. However the proppant concentration controls the fracture proppant concentration. So, the higher the fracture proppant concentration, the higher the quantity of proppant needed to be pumped. This translates to higher values of final proppant concentration as well as higher fracture conductivity in the treatment schedule and more fluid to transport the proppant in the fracture.

All four proposed treatment designs create the desired propped length but at the same time the proppant concentration in the fractures are different. This could provide a good starting point for those engineers that are experts in the hydraulic fracturing or have little or no experience using sophisticated three-dimensional computer models such as FRACPRO.

Needless to say that this model is not meant to be in competition or to be used as a substitute for high performance computer models such as FRACPRO. This model can be a useful companion to complement such software and make them accessible and useful to a wider audience such as petroleum professionals that are not necesserily experts in hydraulic fracturing design.

In the second example we tested our model against a fracture designed by another expert in Kaye field, Teapot formation. The original design has eight stages. The detail of this design is shown Table 3. This fracture is considered to be a successful job based on post fracture well performance. Using the original pumped design and modeling it on FRACPRO a fracture length of 403.7 ft and a fracture conductivity of 0.74 lb/ft^2 is achieved.

The reservoir characteristics and the target proppant length of 400 ft are used as input to our model. The model provided four different fracture designs for this well. Three of the designs have nine stages and the fourth includes seven stages. The design details provided by the model is shown in Tables 4 through 7.

All the designs generated by the model are quite comparable to the original design by the expert. The next step in development of this model includes addition of two more modules: First module consists of a set of virtual intelligence routines that would eliminate the need for detail reservoir characteristics as input to the model. The objective of this module is to reduce the need for detail reservoir characterisitcs that might be hard to acquire in many cases and sometimes are substituted by best guesses. Instead of detail reservoir characteristics user can provide a set of wireline logs such as gamma ray, density and resistivity and let the model generate reservoir characteristics based on the log suite. Authors have shown that such objectives are quite achievable[4].

The second module that will be added to this model is an economic module that would help engineers select the most economic design from several potential designs provided by the model. These additions will enhance the productivity of this model extensively.

CONCLUSIONS

A new methodology is introduced that can assists engineers in designing optimum

hydraulic fracture jobs. A software program is developed that implements the introduced methodology. This methodology integrates the power of artificial neural networks and genetic algorithms in order to achieve its objectives. The process includes replication of a sophisticated three-dimensional hydraulic fracturing computer model (FRACPRO) using an ensemble of neural networks. The methodology uses genetic algorithms to search through the entire solution space and finds the best combination of the parameters that provide the hydraulic fracture propped length that is desired.

Two field examples are presented and the capabilities of the model are tested against them. These field examples were designed by hydraulic fracturing experts and have been implemented and shown to be successful.

REFERENCES

1. Mohaghegh, S., Arefi, R., and Ameri S.: "Virtual Measurement of Heterogeneous Formation Permeability Using Geophysical Well Log Responses", *The Log Analyst*, Society of Professional Well Log Analysts, March-April 1996, pp. 32-39.

2. Mohaghegh, S., Balan, B., McVey, D., and Ameri, S.: "A Hybrid Neuro-Genetic Approach to Hydraulic Fracture Treatment Design and Optimization", *SPE 36602, Proceedings*, SPE 71st Annual Technical Conference, October 6-9, 1996, Denver, Colorado.

3. FRACPRO: ”Hydraulic Fracture Treatment Design and Analysis. User’ Manual version 8.1”, Resources Engineering Systems, Inc. (RES).

4. Mohaghegh, S., Popa, A., Koperna, G., Hill, D.: " Reducing the Cost of Field-Scale Log Analysis Using Virtual Intelligence Techniques", *SPE 57454, Proceedings*, SPE Eastern Regional Conference and Exhibition, October 21-22, 1999, Charleston, West Virginia.

Job Designed by an Expert	
Treatment Characteristics	
Total Fluid Volume (gal)	59929
Pad Fluid Volume (gal)	21504
Starting Proppant Conc. (ppg)	1
Final Proppant Conc. (ppg)	7.5
Pump Rate (bpm)	20
FRACPRO's Output for This Design	
Proppant Length (ft)	**451.6**
Fracture Conductivity (lb/ft^2)	**0.5**

Table 1. Job designed by an expert engineer, Redfork formation.

Jobs Designed by our Model				
Treatment Characteristics	**Model Output**			
Total Fluid Volume (gal)	72491	65155	78684	61800
Pad Fluid Volume (gal)	29196	22666	34034	21864
Starting Proppant Conc. (ppg)	1	1	1	1
Final Proppant Conc. (ppg)	7.2	6.5	10.5	6.5
Pump Rate (bpm)	28	22	25	20
Model's Prediction If Above Designs Are Pumped				
Proppant Length (ft)	**450.6**	**450.4**	**450.4**	**448.6**
Fracture Conductivity (lb/ft^2)	**.56**	**.50**	**.78**	**.50**
FRACPRO's Output for the Designs				
Proppant Length (ft)	**451.0**	**465.4**	**459.2**	**457.6**
Fracture Conductivity (lb/ft^2)	**.47**	**.45**	**.69**	**0.46**

Table 2. Potential job designs from our model.

Original Treatment			
Stages	**Fluid Volume (gal)**	**Pump rate (bpm)**	**Propp. Conc. (ppg)**
1	20,762.0	20	0
2	2,585.1	20	1
3	4,570.6	20	2
4	7,223.9	20	3
5	9,152.4	20	4
6	10,950.0	20	5
7	5,087.5	20	6
8	8,886.0	20	0
Total	**69,217.5**		
FRACPRO Results			
Proppant Length (ft)		**403.7**	
Fracture Conductivity (lb/ft^2)		**0.74**	

Table 3. Original job designed by an expert engineer, Teapot formation.

First Treatment Design By Our Model			
Stages	**Fluid Volume (gal)**	**Pump rate (bpm)**	**Propp. Conc. (ppg)**
1	27,054	20	0
2	4,340	20	1.3
3	4,340	20	2.6
4	6,511	20	3.9
5	6,511	20	5.2
6	8,681	20	6.5
7	8,681	20	7.8
8	10,851	20	9.1
9	2,000	20	0
Total	**78,969**		
Model's Prediction If Above Design is Pumped			
Proppant Length (ft)		**400.5**	
Fracture Conductivity (lb/ft^2)		**1.21**	
FRACPRO's Output for this Designs			
Proppant Length (ft)		**400.2**	
Fracture Conductivity (lb/ft^2)		**1.07**	

Table 4. First potential job designed by our model, Teapot formation.

Second Treatment Design By Our Model			
Stages	**Fluid Volume (gal)**	**Pump rate (bpm)**	**Propp. Conc. (ppg)**
1	22,945	24	0
2	4,593	24	1
3	5,741	24	2
4	6,890	24	3
5	8,038	24	4
6	9,186	24	5
7	11,483	24	6
8	6,890	24	7
9	2,000	24	0
Total	**77,766**		
Model's Prediction If Above Design is Pumped			
Proppant Length (ft)		**399.5**	
Fracture Conductivity (lb/ft^2)		**0.91**	
FRACPRO's Output for this Designs			
Proppant Length (ft)		**394.0**	
Fracture Conductivity (lb/ft^2)		**0.81**	

Table 5. Second potential job designed by our model, Teapot formation.

Third Treatment Design By Our Model			
Stages	**Fluid Volume (gal)**	**Pump rate (bpm)**	**Propp. Conc. (ppg)**
1	22,548	22	0
2	4,573	22	1.1
3	5,716	22	2.2
4	6,859	22	3.3
5	9,146	22	4.4
6	10,289	22	5.5
7	11,289	22	6.6
8	4,573	22	7.7
9	2,000	22	0
Total	**76,993**		
Model's Prediction If Above Design is Pumped			
Proppant Length (ft)		**400.2**	
Fracture Conductivity (lb/ft^2)		**1.40**	
FRACPRO's Output for this Designs			
Proppant Length (ft)		**404.2**	
Fracture Conductivity (lb/ft^2)		**1.20**	

Table 6. Third potential job designed by our model, Teapot formation.

Fourth Treatment Design By Our Model			
Stages	**Fluid Volume (gal)**	**Pump rate (bpm)**	**Propp. Conc. (ppg)**
1	26,269	28	0
2	6,565	28	1
3	6,565	28	2.8
4	9,848	28	4.5
5	13,131	28	6.3
6	16,413	28	8
7	2,000	28	0
Total	**80,791**		
Model's Prediction If Above Design is Pumped			
Proppant Length (ft)		**400.8**	
Fracture Conductivity (lb/ft^2)		**1.02**	
FRACPRO's Output for this Designs			
Proppant Length (ft)		**396.7**	
Fracture Conductivity (lb/ft^2)		**0.96**	

Table 7. Fourth potential job designed by our model, Teapot formation.

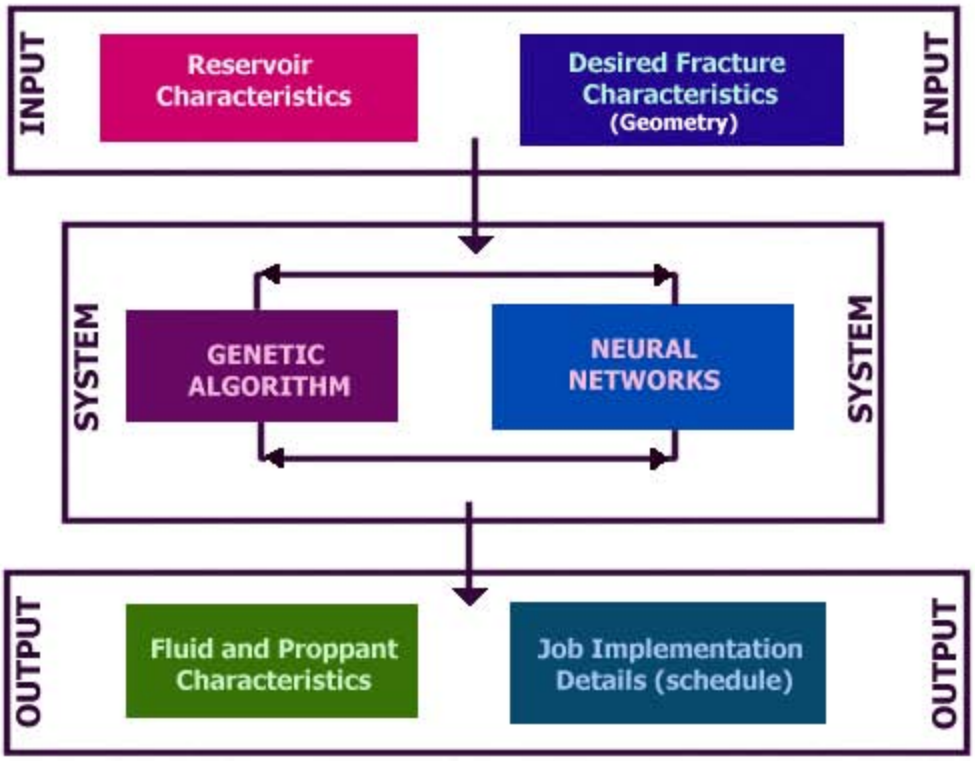

Figure 1. Schematic diagram of model presented in this study.

SPE 68801

Neural-Network Approach To Predict Well Performance Using Available Field Data

Zhong He, SPE, Linyu Yang, John Yen, and Ching Wu, SPE, Texas A&M University

Copyright 2001, Society of Petroleum Engineers Inc.

This paper was prepared for presentation at the SPE Western Regional Meeting held in Bakersfield, California, 26–30 March 2001.

This paper was selected for presentation by an SPE Program Committee following review of information contained in an abstract submitted by the author(s). Contents of the paper, as presented, have not been reviewed by the Society of Petroleum Engineers and are subject to correction by the author(s). The material, as presented, does not necessarily reflect any position of the Society of Petroleum Engineers, its officers, or members. Papers presented at SPE meetings are subject to publication review by Editorial Committees of the Society of Petroleum Engineers. Electronic reproduction, distribution, or storage of any part of this paper for commercial purposes without the written consent of the Society of Petroleum Engineers is prohibited. Permission to reproduce in print is restricted to an abstract of not more than 300 words; illustrations may not be copied. The abstract must contain conspicuous acknowledgment of where and by whom the paper was presented. Write Librarian, SPE, P.O. Box 833836, Richardson, TX 75083-3836, U.S.A., fax 01-972-952-9435.

Abstract

Accurate prediction of future well performance is of great importance for petroleum reservoir management. This paper presents a practical neural network approach to predict existing and infill oil well performance using available filed data, such as well production history and well configuration information. It serves as a practical, cost-effective and robust tool for oilfield production and management. Well production, well spacing and the time-dependent information are used to train the neural network. The time-dependent information of wells are incorporated in a manner of time series for establishment of neural network. After the neural network is established, it is used to predict future performance of existing and infill wells. No reservoir data is currently used in the establishment of neural network, therefore it can predict well production performance in absence of reservoir data. Primary production of two data sets (each has 9 wells) in North Robertson Unit located in west Texas was tested using this approach. The results demonstrate that this approach is powerful in rapid projection of existing wells' future performance, as well as the performance prediction of infill drilling wells.

Introduction

Neural network is a kind of artificial intelligence technology. It mimics characteristics of biological neurons. Like human information processing system, artificial neural system, or neural network, acquire, store, and utilize knowledge by learning. The knowledge is embedded in the networks that can be recalled in response to the presented information.

There are several types of neural networks. The back-propagation neural network is one of them and has been most commonly used for engineering purposes. The structure of back-propagation neural network is sketched in **Fig.1**. The neural network usually consists of at least three layers. They are input layer, hide layer and output layer. Each layer has a number of neurons or nodes. Each input neuron contains actual data introduced to the network externally. The hidden layer between input layer and output layer can be one or more than one according to different applications. Each neuron in output layer give a response for a given data set. The neurons between layers are interconnected by numbers called weights. These weights determine how a particular set of inputs be sent to neurons in hidden layer, and so on from hidden layer to neurons in output layer. These weights are determined by a process called training. Establishment of a neural network is to train the neural network by adjusting the weights between neurons so that the network can give desired output sets for given input data sets by using the trained weights.

In the process of training, the weights are first randomized between the range of 0 to 1. The input data matrix is then multiplied by the weights connecting input layer and hidden layer to produce a new matrix. A transfer function is used to transfer this matrix to another matrix, which is the output of middle layer neurons. The obtained matrix is multiplied by the weights associated with the middle – output layer to generate a new matrix. Similarly, a transfer function is used to transfer the matrix from middle layer to output from the output layer neurons. The obtained output results are compared with the desired outputs to calculated the discrepancy. The weights are updated based on the discrepancy from output layer to input layer (back-propagation) until a specified convergence criterion is satisfied for all input data sets and desired output sets.

In recent years, there are increasing applications in the oil and gas industry [1-7]. Neural network has been used in various petroleum engineering areas, such as geology, geophysics, drilling and completion, formation evaluation, production and stimulation, reservoir engineering and economic etc. Neural network ha s also been proved as a very successful approach on time series prediction problems. Good examples include prices of stock market, etc [8-10].

The purpose of this study is to analyze and predict oil well production performance using neural network technique. Without using the reservoir data, a back propagation neural network is developed to predict the future production performance of wells on account of both spatial variation and time series. In the following, we briefly describe the problem which motivates our research; and analyze our methodology and the architecture of neural network; Testing results of two data sets are presented and finally, some concluding remarks and consideration of future work are given.

The Problem

Consider an oilfield that has multiple wells. These wells were drilled and put into production at different times. Upon a certain period, the production history performance of each well is available. This is such a kind of problem that the production performance is not only controlled by the underground reservoir properties of itself, but also affected by surrounding well performance and various time factors. Therefore, our problem has multiple time series. These time series have different starting points and mutually influence each other. Although it is well known that the reservoir properties, well completion, well interference, and production scheme control and reflect on the oil production performance, it is extremely hard to identify their effect individually.

The objective of this study is to design a neural network based on engineering judgement, to establish the neural network that can map certain kinds of relationships that control previous production performance of wells and to predict future production performance for existing and infill wells. The trained neural network model can serve as a practical, cost-effective and robust oilfield production management tool.

The Architecture of Neural Network

In order to develop an effective neural network, it is very important to observe, recognize, and define problems in a way that will be addressable by neural nets. Critical observation and engineering judgement were used in design and establishment of our neural networks.

The selection of inputs is a key problem in our approach. In other words, how to select as less as possible inputs which can capture the main feature of our prediction problem is most important. From the above section, we know that we are facing two kinds of prediction. The first is the time series prediction of a certain existing well which is based on that well's previous production data. The other one is the spatial prediction of a new infill drilling well which is based on nearby wells' history production data. Our task is to find an effective set of inputs to capture both of the features of these two predictions.

Let's consider the following oil production rate equation for pseudo-steady state flow for a circular reservoir:

$$qo = \frac{KK_{ro}h}{141.2B_o\mu_o(\ln(\frac{re}{rw}) - 0.75 + s)}(\bar{P} - Pwf)$$

Where, q_o – oil production rate
K – formation absolute permeability
K_{ro} – oil relative permeability
h – formation thickness
B_o – oil formation volume factor
μ_o – oil viscosity
r_e – radius of drainage area
r_w – radius of wellbore
$\bar{p}$ – average reservoir pressure
P_{wf} – bottomhole flow pressure
S – skin factor

From the knowledge of reservoir engineering, we know that K and h can be characterized partially by the location of wells. B_o and μ_o are functions of the average reservoir pressure and the average reservoir pressure is a strong function of the cumulative production, reservoir properties, and drainage area. The drainage area of a well is determined by the reservoir characteristics, cumulative production, and the number of wells in the field. K_{ro} is a function of the oil saturation, which is strongly related to the cumulative production. P_{wf} and the skin factor are most likely time-dependent and are usually hard to quantify.

Based on the above observations, four kinds of data are defined to be the inputs of the networks. They are individual well property data, spatial information of well, inter-well interaction data and time series data, respectively. From an alternative perspective, the inputs can be divided as static and dynamic. The static data include well number, the X and Y coordinators of the well. The dynamic data consist of three consecutive production data points of each well, the average cumulative production of surrounding wells and the average distance to the surrounding wells. Although there is no direct reservoir data, the reservoir properties are implicitly included in our inputs. Two back propagation neural networks were developed. Both have a sole output. One uses cumulative production of the fourth point as the output, another uses the incremental production of the fourth point for a specified time interval as the output. Table 1 shows the details of input and output for neural network for cumulative production prediction.

One hidden layer is used in the neural networks. The hidden layer has ten neurons. As shown in table 1, the input layer of the neural networks has 11 neurons plus one bias neuron (=1) while the output layer has one neuron. The sigmoid transfer function was used in the networks.

Results and Discussions

Two data sets of North Robertson Unit in Texas, each has 9 wells, were used to test the effectiveness of our approach. The North Robertson Unit is a low permeable carbonate reservoir and was discovered in early 1950's. The primary production continued until the end of 1986 and the waterflooding began in 1987. The primary production history data were used to train and test the neural networks. Three month production data were summed up as one data point. **Fig.2** shows the areal map of North Robertson Unit and **Fig.3** shows the well configurations and initial producing date of wells for these two data sets. To test our approach, two cases are considered respectively. For case 1, we used the production history data of all nine wells to 1984 to train the networks and testes the networks using the remaining latest 1.5 year data. Case 2 is a case for infill drilling. The latest drilling well was first put aside and another earlier drilled wells were used to train the network. Once the network reached convergence, it was used to predict the performance of the well be put aside and compare actual production results.

Data set 1

Case 1. **Fig. 4 and 5** show the comparisons of NN output of cumulative production vs. actual cumulative production respectively for training data sets and testing data points of all 9 wells. **Fig. 6 and 7** show the comparisons of NN output of 3 month interval production vs. actual data respectively for training data sets and testing data points of all 9 wells. For the cumulative production data, a coefficient of correlation of 0.99 has been obtained for both training data sets and testing data points. The average percentage errors of NN output are 3.12% and 4.57% for training data sets and testing data points respectively. For the 3 month interval production data, a coefficient of correlation of 0.96 has been obtained for training data sets and 0.93 for testing data points. Since the 3 month interval production data themselves have more uncertainties and variations, NN outputs of them have higher prediction errors. For training data sets, the average percentage error of NN calculation is 22.82%. For testing data points, the average percentage error of NN calculation is 16.06%. For projection purposes, this prediction error can be considered to be within reasonable range. **Fig.8** shows the comparison of neural network output of cumulative production versus real cumulative production data for well 802ZL. **Fig. 9** is for 3 month interval production data of same well. The last six points were testing data. Other wells have similar results.

Our results indicate that the neural networks have captured both the magnitude and variation trend of well production performance. They have quite good predictive capacities for short term prediction, for example 1 to 2 years, based on wells' production history data. Because of good predictive accuracy, they can be used to very quickly generate projection of existing wells' future production performance, instead of using decline curve analysis for one well by one well. Another advantage is that prediction of neural networks allows local variation instead of smooth curve projection.

Case 2. The latest drilling well was put aside testing the predicted results while other earlier drilling well's production data before the producing date of latest drilling well were used as training set. This case has the most significance because of its potential application on performance prediction and location optimization of infill drilling wells. **Fig.10** shows the comparison of neural network output of cumulative production versus real cumulative production data for Well 702ZL. All the data points on figure were testing points. The results show that the prediction of infill drilling well is pretty accurate and the trained network has a great potential for selecting an optimum of new infill drilling well location.

Data Set 2. For data set 2, similar works were done. Our approach produced same good results for both case 1 and 2. For case 1, **Fig. 11 and 12** show the neural network results as well as the actual production data for Well 701ZL. For case 3, the performance of an infill drilling well 2215ZL is predicted, as demonstrated as **Fig. 13**. It can been seen that for both projection of existing well production and prediction of infill drilling well performance, the neural network prediction results match quite well with the actual production performance.

Limitation of the approach. Our neural network approach uses current production data point and two previous ones to predict the next future production data point. The results show that it has a good accuracy of short-term prediction, for example, 1 to 2 years, for both existing wells and infill wells. For long-term prediction, this approach doesn't have the guarantee of prediction accuracy.

Conclusions and Future Work

This paper puts forward a neural network approach to predict the oil well production performance. Without any reservoir data, history production data of wells were used to train the neural network. As our inputs include both static and dynamic data, the established neural network is good for both times series prediction and spatial prediction. Two data sets in North Robertson Unit located in west Texas were used to test our approach. By testing two different cases, the results show that the approach is capable of predicting existing well performance, as well as the performance of infill wells. It can serve as a practical, cost-effective and robust tool for oilfield production management.

Additional testing is underway to check the robustness of our neural network approach, and an attempt is being made to extend the approach for waterflood performance projection. We will also incorporate the optimization techniques with our approach to help petroleum engineers find an optimal location for new infill drilling well.

Nomenclature

q_o = oil production rate, STB/d

K = formation absolute permeability, md
K_{ro} = oil relative permeability
H = formation thickness, ft
B_o = oil formation volume factor
μ_o = oil viscosity, cp
r_e = radius of drainage area, ft
r_w = radius of wellbore, ft
S = skin factor
$\bar{p}$ = average reservoir pressure, psi
P_{wf} = bottomhole flow pressure, psi

Acknowledgment
We would like to acknowledge the financial support from the Texas Higher Education Coordinating Board under Grant ATP-036327-066.

References

1. Centilmen, A, Ertekin, and Grader, A.S.: "Applications of Neural Networks in Multiwell Field Development," SPE 56433, presented at the 1999 SPE Annual Technical Conference and Exhibition, Houston, 3-6 Oct. 1999.
2. Doraisamy, H., Ertekin, T., and Grader, A.S.: "Methods of Neuro-Simulation for Field Development," SPE 39962, presented at 1998 SPE Rocky Mountain Regional Meeting, Denver, CO, 5-8 April 1998.
3. Mohaghegh, S., Balan, B., and Ameri, S.: "Candidate Selection for Stimulation of Gas Storage Wells Using Available Data with Neural Networks and Genetic Algorithms," SPE 51080, presented at 1998 SPE Eastern Regional Meeting, Pittsburgh, PA, 9-11 Nov. 1998.
4. Mohaghegh, S., Balan, B., and Ameri, S.: "A Hybrid, Neuro-Genetic Approach to Hydraulic Fracture Treatment Design and Optimization," SPE 36602, presented at 1996 SPE Annual Technical Conference and Exhibition, Denver, CO, 6-9 Oct. 1996.
5. Mohaghegh, S., McVey, D. Aminian, K., and Ameri, S.: "Predicting Well Stimulation Results in a Gas Storage Field in the Absence of Reservoir Data, Using Neural Networks," SPE 31159, SPE unsolicited paper.
6. Mohaghegh, S., and Ameri, S.: "Artificial Neural network as a Valuable Tool for Petroleum Engineers," SPE 29220, SPE unsolicited paper.
7. Mohaghegh, S., Arefi, R., and Ameri, S.: "A Methodological Approach for Reservoir Heterogeneity Characterization Using Artificial Neural Networks," SPE 28394, presented at 1994 SPE Annual Technical Conference and Exhibition, New Orleans, LA, 25-28 Sept. 1994.
8. Chng, E. S., Chen, S. and Mulgrew, B.: "Gradient Radial Basis Function Networks for Nonlinear and Nonstationary Time Series Prediction", IEEE Transactions on Neural Networks, 7(1), pp. 190-194, January 1996.
9. Geva, A. B.: "ScaleNet--Multiscale Neural-Network Architecture for Time Series Prediction", IEEE Transactions on Neural Networks, 9(6), pp. 1471-1482, November 1998.
10. Saad, E. W., Prokhorov, D. V., and Wunsch, D. C.: "Comparative Study of Stock Trend Prediction Using Time Delay, Recurrent and Probabilistic Neural Networks", IEEE Transactions on Neural Networks, 9(6), pp. 1456-1470, November 1998.

Table 1 Input and output data for neural network for cumulative production prediction

Data	Parameters	Unit	Category
Input	Well number		Individual well property
	X coordinate of wells	ft	Spatial information of well
	Y coordinate of wells	ft	Spatial information of well
	Cumulative production at time t-2	STB	Time series
	Cumulative production at time t-1	STB	Time series
	Cumulative production at time t	STB	Time series
	Derivative of cumulative production at time t	STB/day	Time series
	Shut-in switch		Individual well property
	Average distance to surrounding wells	ft	Inter-well interaction
	Average cumulative production of surrounding wells at time t	STB	Inter-well interaction
	Cumulative producing days at time t	day	Time series
Output	Cumulative production at time t+1	STB	

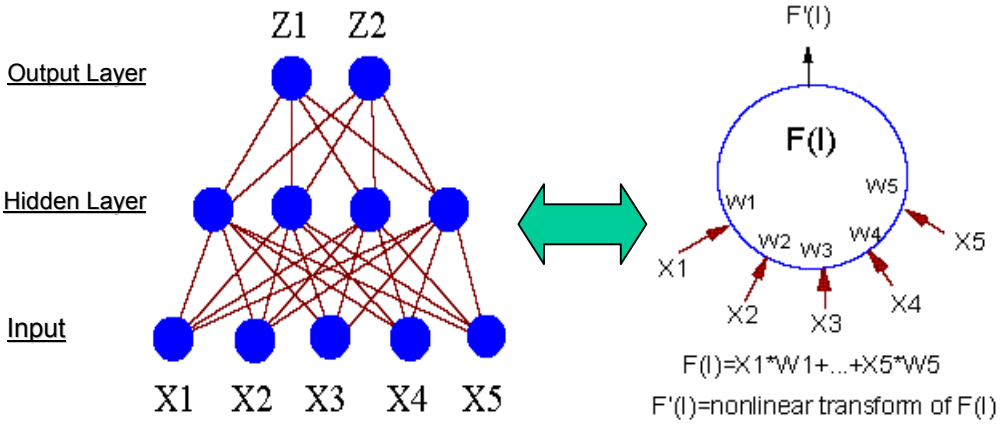

Fig. 1 Principle of neural network

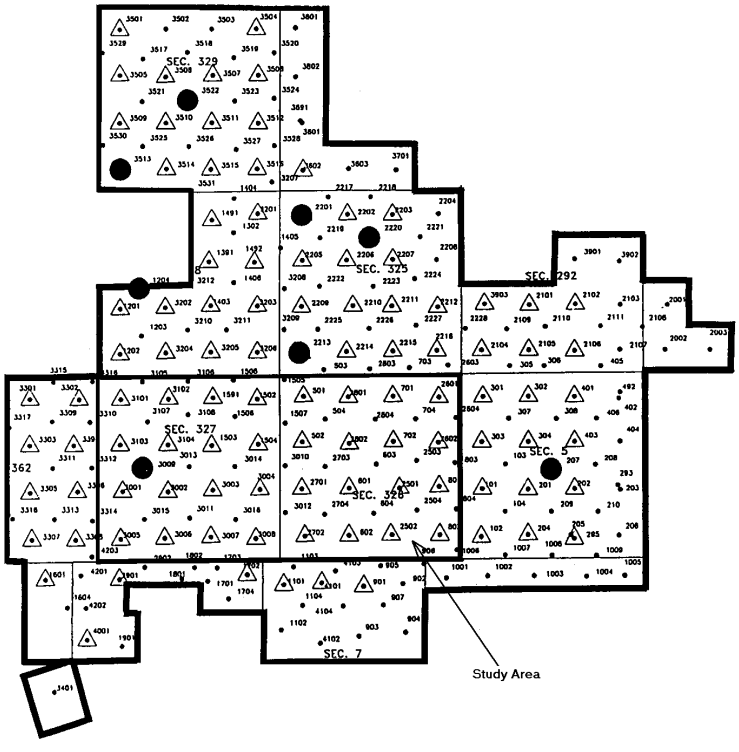

Fig. 2 Areal map of the North Robertson Unit and the study area

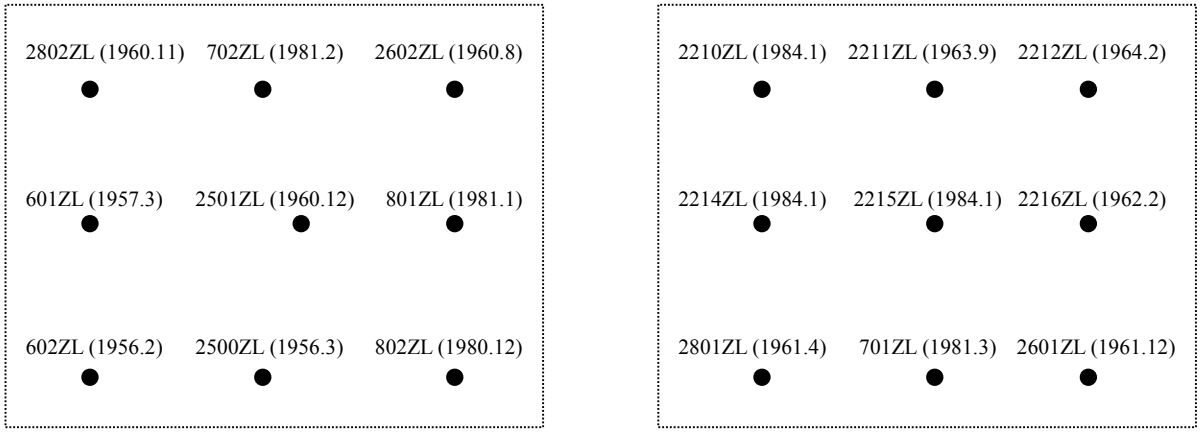

Fig.3 Well configurations of two data sets in North Robertson Unit

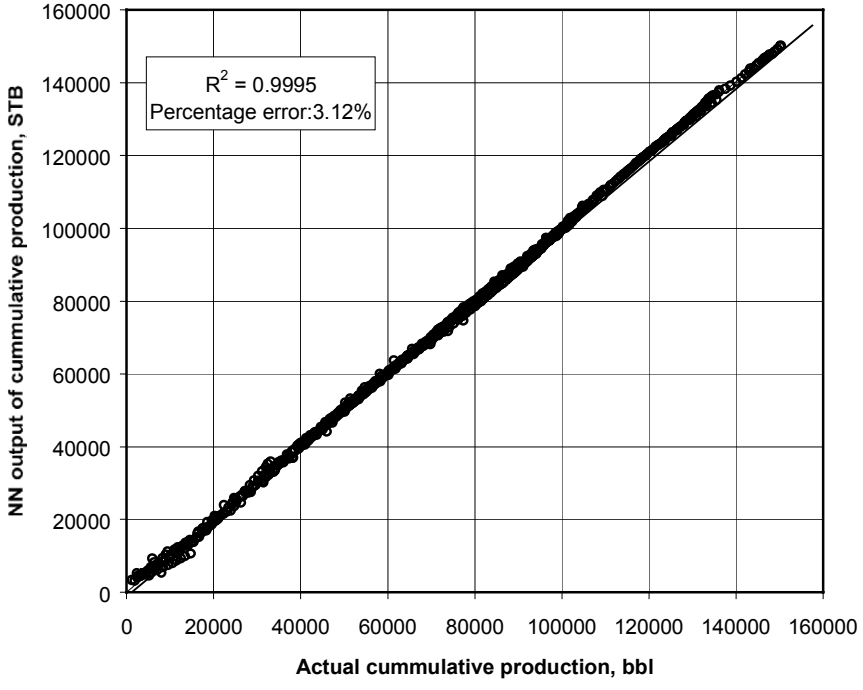

Fig. 4 Comparison of NN output of cummulative production vs. actual cummulative production for training data (Data set 1)

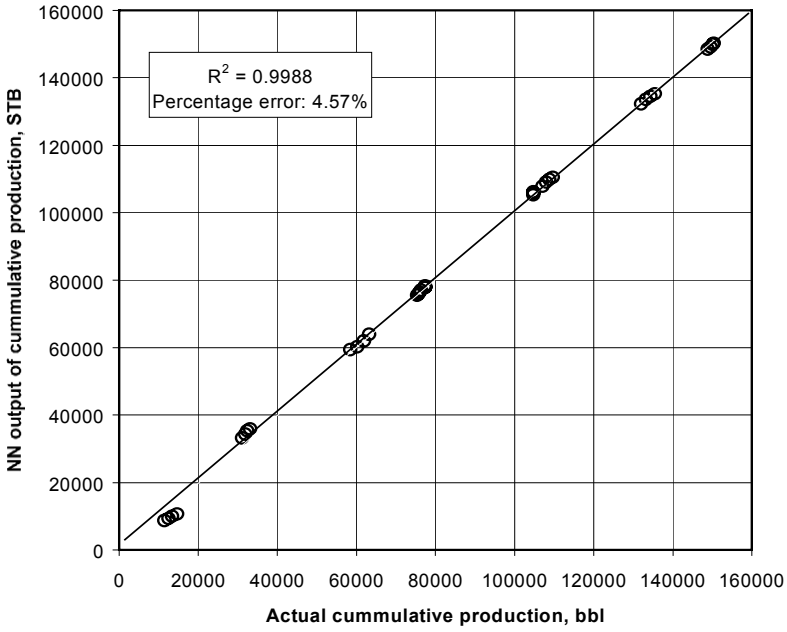

Fig. 5 Comparison of NN output of cummulative production vs. actual cummulative production for testing data (Data set 1)

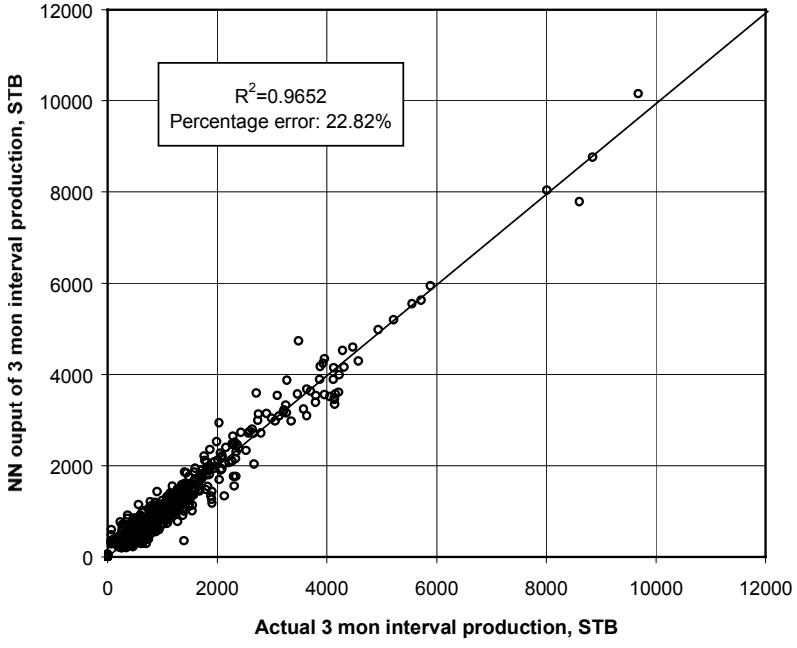

Fig. 6 Comparison of NN output of 3 month interval production vs. actual 3 month interval production for training data (Data set 1)

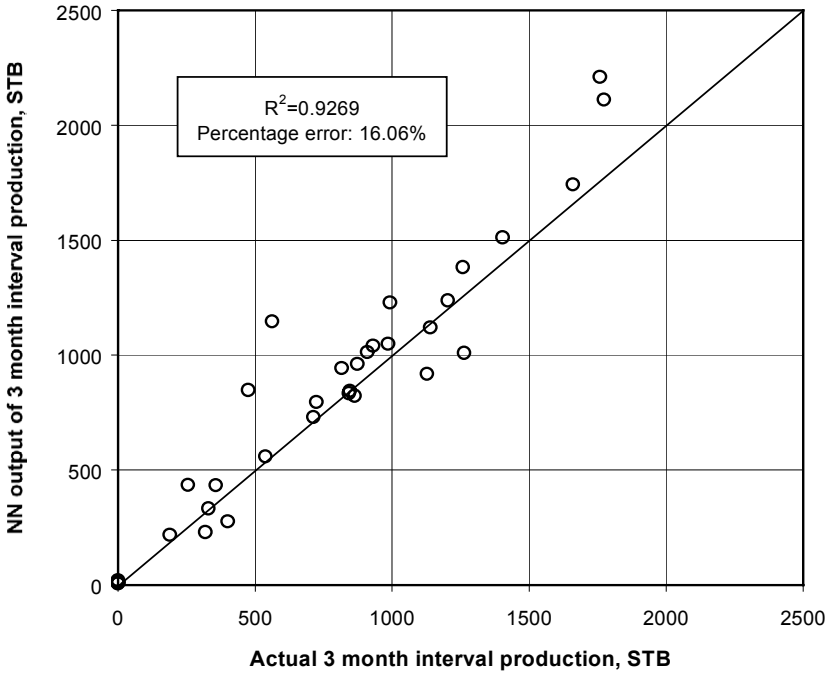

Fig. 7 Comparison of NN output of 3 month interval production vs. actual 3 month interval production for testing data (Data set 1)

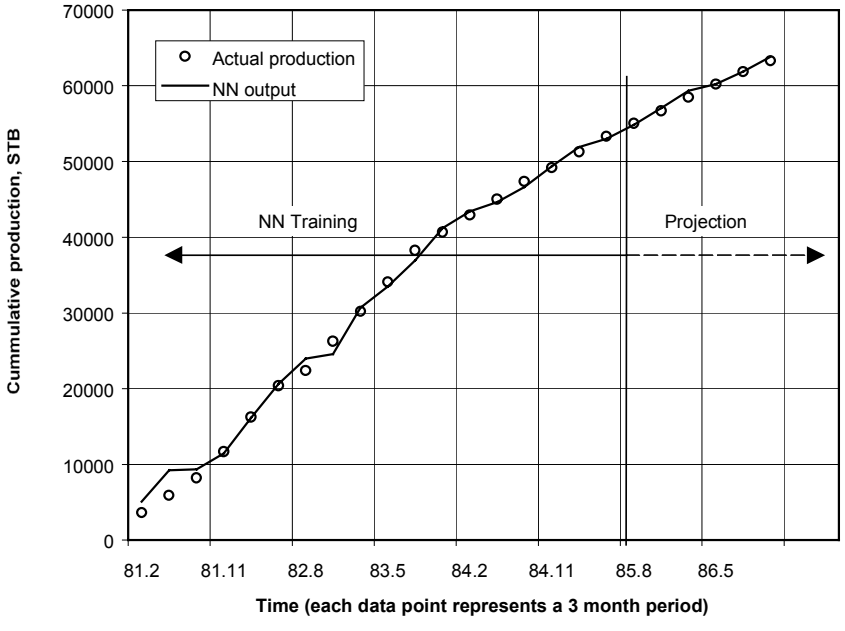

Fig. 8 NN output of cummulative production vs. actual one for well 802ZL

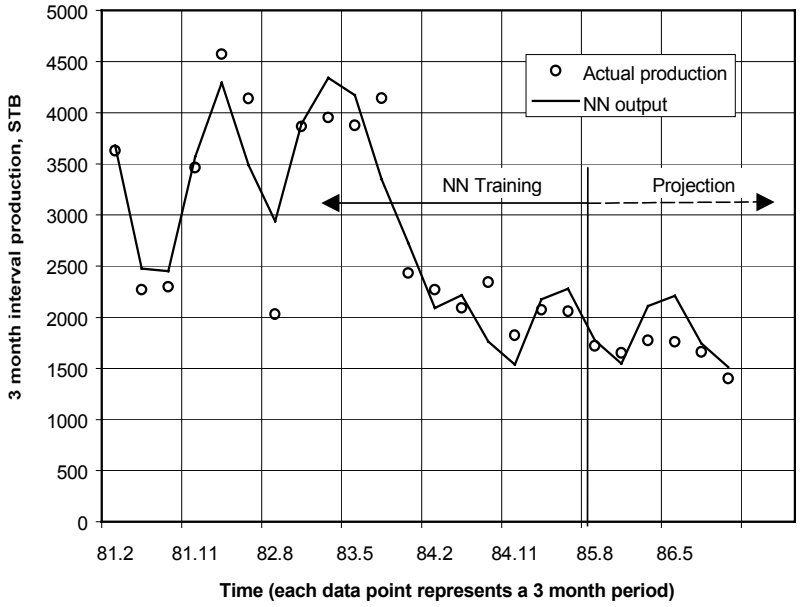

Fig. 9 NN output of 3 month interval production vs. actual one for well 802ZL

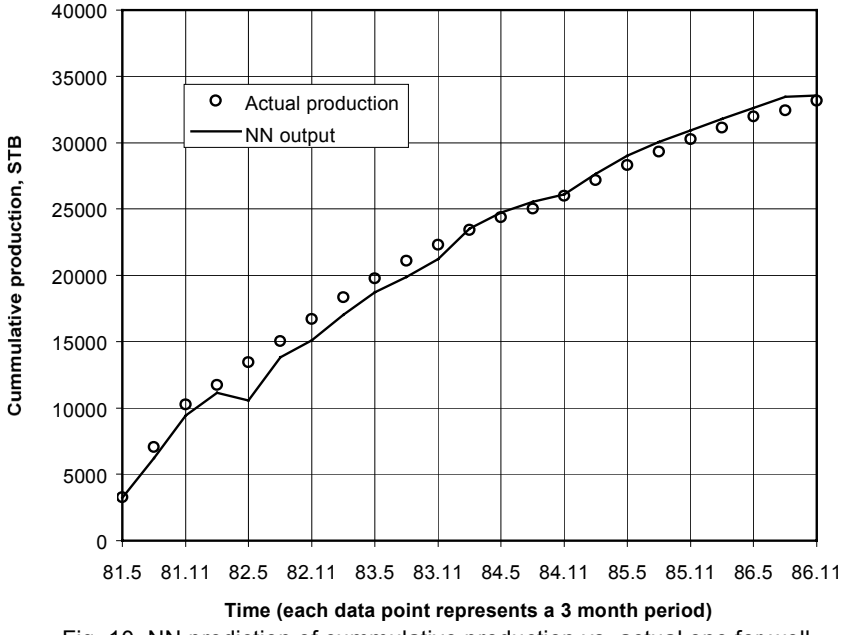

Fig. 10 NN prediction of cummulative production vs. actual one for well 702ZL (Case 2)

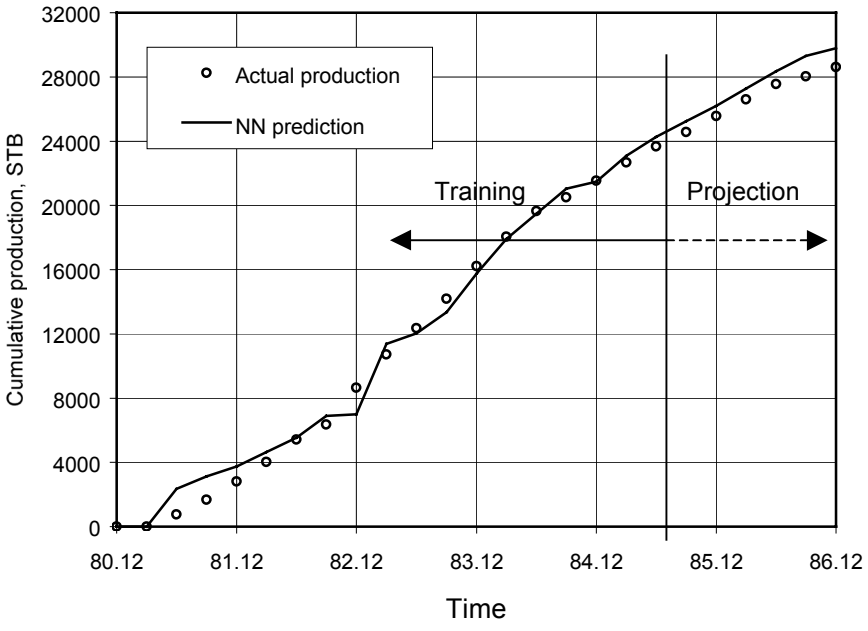

Fig. 11 NN projection of well 701ZL cummulative production
(Data set 2 - Case 1)

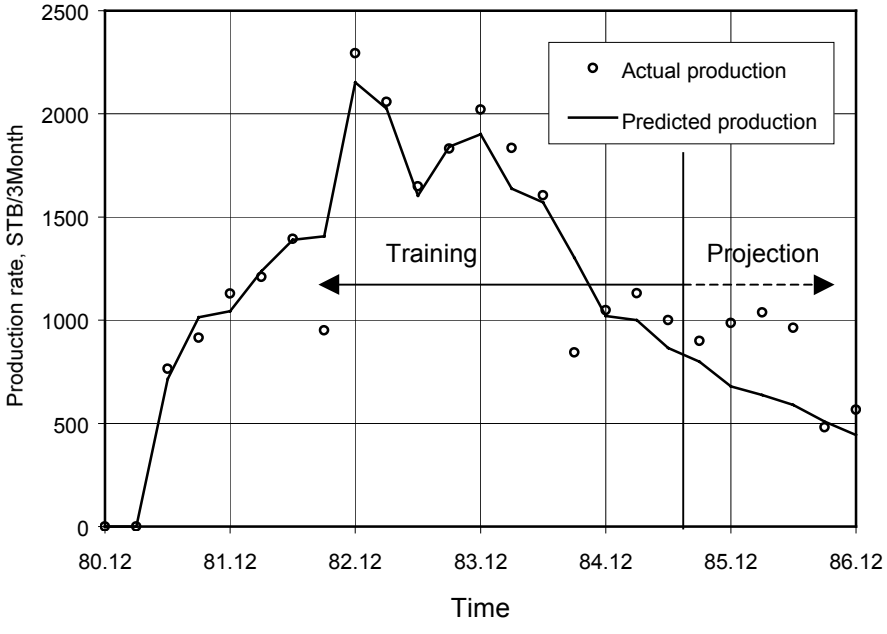

Fig. 12 NN projection of well 701ZL interval production
(Data set 2 - Case 1)

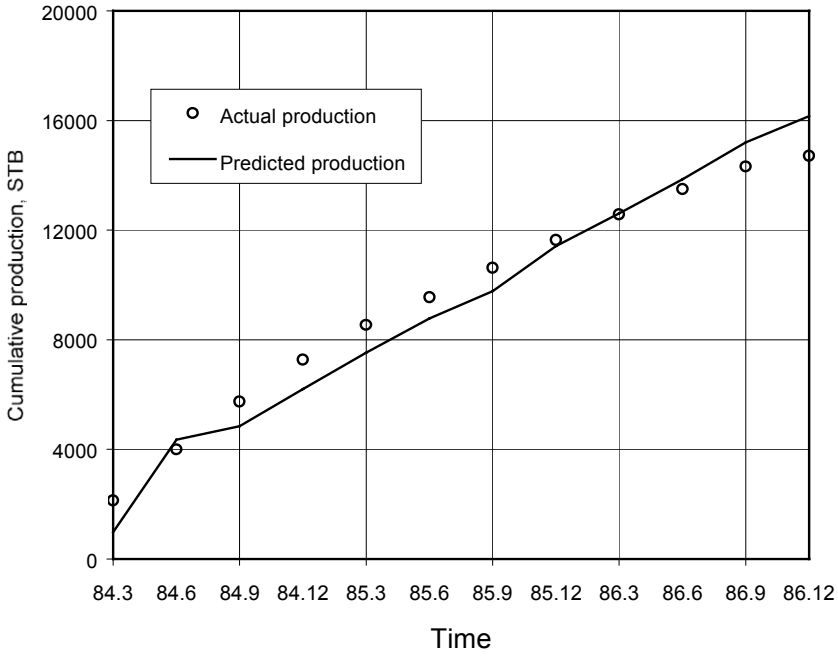

Fig.13 NN prediction of well 2215ZL cummulative production (Data set 2 - Case 2)

Neural Network Approach Predicts U.S. Natural Gas Production

S.M. Al-Fattah, SPE, Saudi Aramco, and **R.A. Startzman,** SPE, Texas A&M U.

Summary

The industrial and residential market for natural gas produced in the United States has become increasingly significant. Within the past 10 years, the wellhead value of produced natural gas has rivaled and sometimes exceeded the value of crude oil. Forecasting natural gas supply is an economically important and challenging endeavor. This paper presents a new approach to predict natural gas production for the United States with an artificial neural network (NN).

We developed an NN model to forecast the U.S. natural gas supply to 2020. Our results indicate that the U.S. will maintain its 1999 production of natural gas until 2001, after which production increases. The network model indicates that natural gas production will increase by an average rate of 0.5%/yr from 2002 to 2012. This increase will more than double from 2013 to 2020.

The NN was developed with a large initial pool of input parameters. The input pool included exploratory, drilling, production, and econometric data. Preprocessing the input data involved normalization and functional transformation. Dimension-reduction techniques and sensitivity analysis of input variables were used to reduce redundant and unimportant input parameters and to simplify the NN. The remaining parameters included data from gas exploratory wells, oil/gas exploratory wells, oil exploratory wells, gas depletion rate, proved reserves, gas wellhead prices, and growth rate of the gross domestic product. The three-layer NN was successfully trained with yearly data from 1950 to 1989 using the quick-propagation learning algorithm. The NN's target output is the production rate of natural gas. The agreement between predicted and actual production rates was excellent. A test set not used to train the network and containing data from 1990 to 1998 was used to verify and validate the network prediction performance. Analysis of the test results showed that the NN approach provides an excellent match with actual gas production data. An econometric approach, called stochastic modeling or time-series analysis, was used to develop forecasting models for NN input parameters. A comparison of forecasts between this study and another is presented.

The NN model has use as a short-term as well as a long-term predictive tool for natural gas supply. The model can also be used to quantitatively examine the effects of the various physical and economic factors on future gas production.

Introduction

In recent years, there has been a growing interest in applying artificial NNs[1–4] to various areas of science, engineering, and finance. Among other applications[4] to petroleum engineering, NNs have been used for pattern recognition in well-test interpretation[5] and for prediction in well logs[4] and phase behavior.[6]

Artificial NNs are an information-processing technology inspired by studies of the brain and nervous system. In other words, they are computational models of biological neural structures. Each NN generally consists of a number of interconnected processing elements (PE) or neurons grouped in layers. **Fig. 1** shows the basic structure of a three-layer network—one input, one hidden, and one output. The neuron consists of multiple inputs and a single output. "Input" denotes the values of independent variables, and "output" is the dependent variables. Each input is modified by a weight, which multiplies with the input value. The input can be raw data or output from other PEs or neurons. With reference to a threshold value and activation function, the neuron will combine these weighted inputs and use them to determine its output. The output can be either the final product or an input to another neuron.

This paper describes the methodology of developing an artificial NN model to predict U.S. natural gas production. It presents the results of the NN modeling approach and compares it to other modeling approaches.

Data Sources

The data used to develop the artificial NN model for U.S. gas production were collected mostly from the Energy Information Admin. (EIA).[7] U.S. marketed-gas production for 1918 to 1997 was obtained from *Twentieth Century Petroleum Statistics,*[8–9] with the EIA's 1998 production data. Gas-discovery data from 1900 to 1998 were from Refs. 7 and 10. Proved gas reserves for 1949 to 1999 came from the *Oil and Gas J.* (*OGJ*) database.[11] EIA provides various statistics on U.S. energy historical data, including gas production, exploration, drilling, and econometrics. These data are available to the public and can be downloaded from the internet with ease. The following data (1949 to 1998) were downloaded from the EIA website.[7]

- Gas discovery rate.
- Population.
- Gas wellhead price.
- Oil wellhead price.
- Gross domestic product (D_G), with purchasing power parity (PPP) based on 1992 U.S. dollars.
- Gas exploratory wells.
  - ➢ Footage and wells drilled.
- Oil exploratory wells.
  - ➢ Footage and wells drilled.
  - ➢ Percentage of successful wells drilled.
- Oil and gas exploratory wells.
  - ➢ Footage and wells drilled.
- Proved gas reserves.

Other input parameters were also derived from the previous data parameters. The derived input parameters include:

- Gross domestic product growth rate. This input parameter was calculated with the following formula.[12]

$$G_{DPi+1} = \left[\left(\frac{D_{Gi+1}}{D_{Gi}} \right)^{\frac{1}{(t_{i+1}-t_i)}} - 1 \right] \times 100, \quad \ldots\ldots\ldots\ldots\ldots\ldots (1)$$

where D_G = gross domestic product, G_{DP} = growth rate of gross domestic product, t = time, and i = observation number.

- Average depth drilled per well. This is calculated by dividing the footage drilled by the number of exploratory wells drilled each year. This is done for the gas exploratory wells, oil exploratory wells, and oil-and-gas exploratory wells, resulting in three additional new input variables.
- Depletion rate. This measures how fast the reserves are being depleted each year at that year's production rate. It is calculated as the annual production divided by the proved reserves and is expressed in a percentage.

Data Preprocessing

Data preparation is a critical procedure in the development of an artificial NN system. The preprocessing procedures used in the construction process of this study's NN model are input/output normalization and transformation.

Copyright © 2003 Society of Petroleum Engineers

This paper (SPE 82411) was revised for publication from paper SPE 67260, first presented at the 2001 SPE Production and Operations Symposium, Oklahoma City, Oklahoma, 25-28 March. Original manuscript received for review 22 April 2002. Revised manuscript received 21 November 2002. Paper peer approved 3 December 2002.

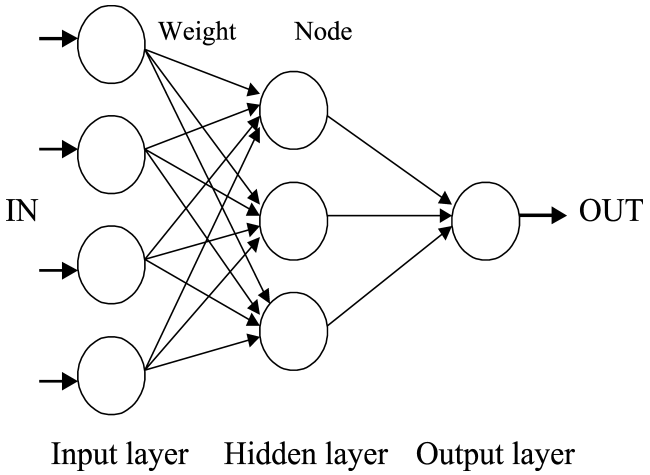

Fig. 1—Basic structure of a three-layer back-propagation (BP) NN.

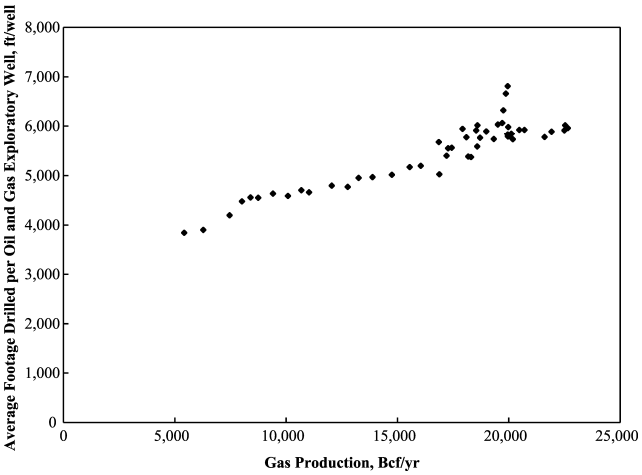

Fig. 2—Scatter plot of gas production and average footage drilled per oil and gas exploratory well.

Normalization. Normalization is the process of standardizing the possible numerical range input data can take. It enhances the fairness of training by preventing an input with large values from swamping out another that is equally important but has smaller values. Normalization is also recommended because the network training parameters can be tuned for a given range of input data; thus, the training process can be carried over to similar tasks.

We used the mean/standard deviation normalization method to normalize all the NN's input and output variables. Mean standard deviation preprocessing is the most commonly used method and generally works well with almost every case. Its advantages are that it processes the input variable without any loss of information and its transform is mathematically reversible. Each input variable, as well as the output, were normalized with the following formula.[13]

$$X_i' = \frac{(X_i - \mu_i)}{\sigma_i}, \quad \ldots\ldots\ldots\

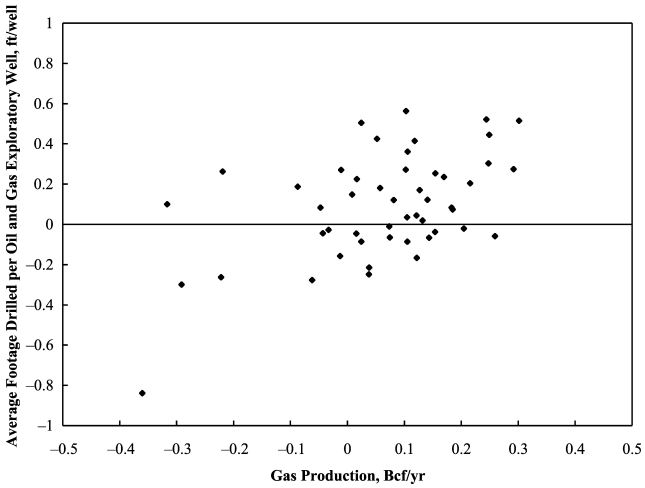

Fig. 3—Scatter plot of gas production and average footage drilled per oil and gas exploratory well after data preprocessing.

of the NN architecture, the learning rule, the number of processing elements in each layer, the number of hidden layers, and the type of transfer function. **Fig. 4** depicts an illustration of the NN model designed in this study.

Architecture. The NN architecture determines the method by which the weights are interconnected in the network and specifies the type of learning rules that may be used. Selecting the network architecture is one of the first tasks in setting up an NN. The multilayer, normal feed forward[1–3] is the most commonly used architecture and is generally recommended for most applications; hence, it was selected to be used for this study.

Learning Algorithm. Selection of a learning rule is also an important step because it affects the determination of input and transfer functions and associated parameters. The network used is based on a back-propagation (BP) design,[1] the most widely recognized and most commonly used supervised-learning algorithm. In this study, the quick-propagation (QP)[14] learning algorithm, which is an enhanced version of the BP one, is used for its performance and speed. The advantage of QP is that it runs faster than BP by minimizing the time required to find a good set of weights with heuristic rules. These rules automatically regulate the step size and detect conditions that accelerate learning. The optimum step size is then determined by evaluating the trend of the weight updates with time.

The fundamental design of a BP NN consists of an input layer, a hidden layer, and an output layer, as shown in Fig. 4. A layer consists of a number of processing elements or neurons and is fully

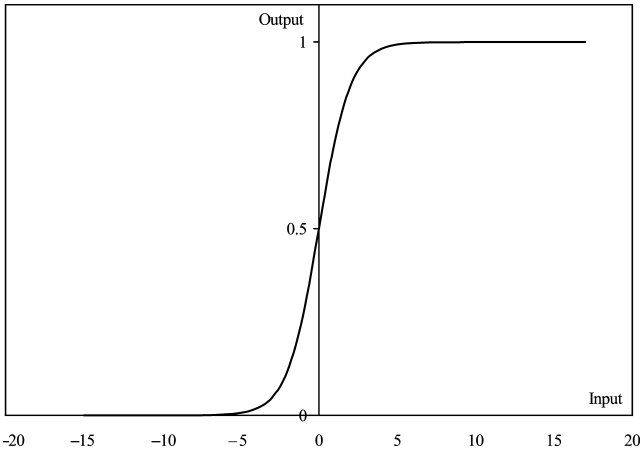

Fig. 5—Sigmoid function.

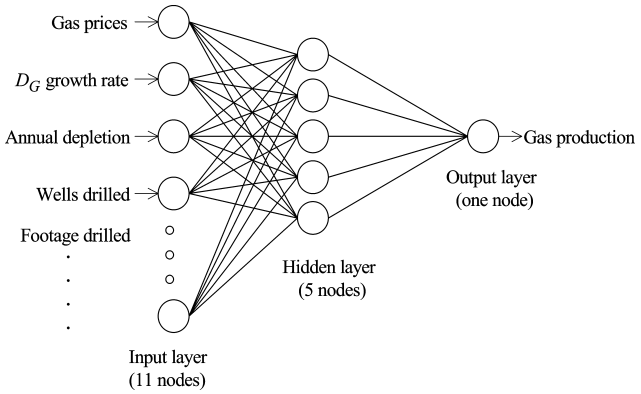

Fig. 4—NN design from this study.

connected, indicating that each neuron of the input layer is connected to each hidden-layer node. Similarly, each hidden-layer node is connected to each output-layer node. The number of nodes needed for the input and output layers depends on the number of inputs and outputs designed for the NN.

Activation Rule. A transfer function acts on the value returned by the input function, which combines the input vector with the weight vector to obtain the net input to the processing element given a particular input vector. Each transfer function introduces a nonlinearity into the NN, enriching its representational capacity. In fact, it is the nonlinearity of the transfer function that gives an NN its advantage vs. conventional or traditional regression techniques. There are also a number of transfer functions. Among those are sigmoid, arctan, sin, linear, Gaussian, and Cauchy. The most commonly used transfer function is the sigmoid function. It squashes and compresses the input function when it takes on large positive or negative values. Large positive values asymptotically approach 1, while large negative values are squashed to 0. The sigmoid is given by[1]

$$f(x) = \frac{1}{1 + \exp(-x)}. \quad \ldots\ldots\ldots\

TABLE 2—INPUT VARIABLES OF THE TRAINED NN

No.	Input	Description
1	I-3	Gas wellhead prices
2	I-6	Average depth drilled per well in gas exploratory wells
3	I-7	Footage drilled in gas exploratory wells
4	I-8	Number of wells drilled in gas exploratory wells
5	I-9	Average depth drilled per well in oil/gas exploratory wells
6	I-10	Footage drilled in oil/gas exploratory wells
7	I-11	Number of wells completed in oil/gas exploratory wells
8	I-12	Average depth drilled per well in oil exploratory wells
9	I-13	Growth rate of gross domestic product
10	I-14	Gas proved reserves
11	I-15	Annual gas depletion rate

TABLE 3—RESULTS OF INPUT SENSITIVITY ANALYSIS FOR TRAINING SET

Input #	Effect	Effect Normalized
I-3	0.145	0.699
I-6	0.187	0.904
I-7	0.202	0.973
I-8	0.168	0.810
I-9	0.212	1.025
I-10	0.155	0.748
I-11	0.193	0.932
I-12	0.158	0.761
I-13	0.264	1.276
I-14	0.285	1.376
I-15	0.310	1.496

• The percentage of training- or testing-set samples that are correct based on a chosen tolerance value.
• A plot of the actual vs. the network output.
• A histogram of all the weights in the network.

The three-layer network with all initial 15 input variables was trained with the training samples. We chose the number of neurons in the hidden layer on the basis of existing rules of thumb[2,3] and experimentation. One rule of thumb states that the number of hidden-layer neurons should be approximately 75% of the input variables. Another rule suggests that the number of hidden-layer neurons be approximately 50% of the total number of input and output variables. One of the advantages of the neural software used in this study is that it allows the user to specify a range for the minimum and maximum number of hidden neurons. Putting all this knowledge together with our experimentation experience allowed us to specify the range of 5 to 12 hidden neurons for the single hidden layer.

We used the input sensitivity analysis to study the significance of each input parameter and how it affects network performance. This procedure helps to reduce the redundant input parameters and determine the optimum number of NN input parameters. In each training run, the results of the input sensitivity analysis are examined and the least-significant input parameter is deleted, then the weights are reset and the network-training process is restarted with the remaining input parameters. This process is repeated until all the input parameters are found to have a significant contribution to network performance. The input is considered significant when its normalized effect value is greater than or equal to 0.7 in the training set and 0.5 in the test set. We varied the number of iterations used to train the network from 500 to 7,000 to find the optimal number. Three thousand iterations were used for most of the training runs. In the process, training is automatically terminated when the maximum iterations are reached or the mean square error of the network falls to less than the set limit, specified as 1.0×10^{-5}. While training the network, the test set is also evaluated. This step enables a pass through the test set for each pass through the training set. However, this step does not intervene with the training statistics other than evaluating the test set while training for fine-tuning and generalizing the network parameters.

After training, the network performance was tested. The test set was used to determine how well the network performed with data it had not seen during training.

To evaluate network performance, the classification option used specified the network output as correct based on a set tolerance. This method evaluates the percentage of training and testing samples that faithfully generalize the patterns and values of the network outputs. We used a tolerance of 0.05 in this study (the default value is 0.5), meaning that all outputs for a sample must be within this tolerance for it to be considered correct. Another measure is the plot of the mean square error vs. the number of iterations. A well-trained network is characterized by decreasing errors for both the training and test sets as the number of iterations increases.

TABLE 4—RESULTS OF INPUT SENSITIVITY ANALYSIS FOR TEST SET

Input #	Effect	Effect Normalized
I-3	0.142	0.856
I-6	0.186	1.124
I-7	0.136	0.821
I-8	0.167	1.011
I-9	0.192	1.163
I-10	0.084	0.506
I-11	0.094	0.567
I-12	0.229	1.385
I-13	0.222	1.340
I-14	0.169	1.020
I-15	0.200	1.207

Results of Training and Testing

We used the input sensitivity-analysis technique[2,14] to gauge the sensitivity of the gas production rate (output) for any particular input. The method makes use of the weight values of a successfully trained network to extract the information relevant to any particular input node. The outcome is the effect and normalized effect values for each input variable at the gas-production output rate. These effect values represent an assessment of the influence of any particular input node on the output node.

The results of the input-identification process and training procedure indicated that the network has excellent performance with 11 input parameters. We found that these parameters, described in **Table 2**, contribute significantly to network performance.

Tables 3 and 4 present the results of the input sensitivity analysis for the training and test sets, respectively. The normalized effect values indicate that all 11 inputs contribute significantly to the improvement of the network performance and to the prediction

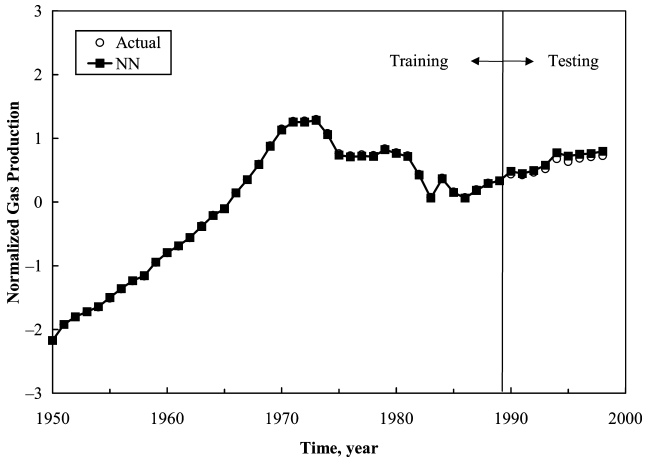

Fig. 6—Performance of the NN model with actual U.S. gas production.

of the U.S. natural-gas production rate for both the training and test sets. The training set input-sensitivity analysis (Table 3) shows that the gas annual depletion rate (I-15) is the most significant input parameter contributing to network performance and, hence, to predicting U.S. natural gas production. Although we found it important to network performance improvement and kept it in the model, the input of gas wellhead prices (I-3) has the least normalized effect value (0.7) of all other inputs in the training set. Table 4 shows that all inputs in the test set exceeded the arbitrary specified threshold value of 0.5, indicating that all inputs contribute significantly to the network model.

The network was trained with 5,000 iterations and the QP learning algorithm. We found that the optimum number of hidden-layer nodes is 5. **Fig. 6** shows the NN model prediction, after the training and validation processes, superimposed on the normalized, actual U.S. gas production. The NN prediction results show excellent agreement with the actual production data in both the training and testing stages. These results indicate that the network was trained and validated very well and is ready to be used for forecasting. In addition, statistical and graphical error analyses were used to examine network performance.

Optimization of Network Parameters. We attempted different network configurations to optimize the number of hidden nodes and number of iterations and thus fine-tune the network performance, running numerous simulations in the optimization process. **Table 5** presents potential cases for illustration purposes only and

TABLE 5—NN PERFORMANCE WITH DIFFERENT HIDDEN NODES AND ITERATIONS*

Case Number	Hidden Nodes	Iteration Number	Training MSE	Training Correct (%)	Testing MSE	Testing Correct (%)
11-9	5	3,000	0.0065	100	0.0321	78
11a	5	5,000	0.0034	100	0.0252	100
11b1	5	6,000	0.0025	100	0.0286	89
11b2	5	7,000	0.0020	100	0.0323	89
11c	6	5,000	0.0012	100	0.0619	44

*All cases were run with the same 11 inputs.

shows that increasing the number of iterations to more than 5,000 improves the training-set performance but worsens the test-set performance. In addition, decreasing the number of iterations to 3,000 yields higher errors for both the training and test sets. The number of hidden-layer nodes also varied by 4 to 22 nodes. Increasing the number of hidden nodes to more than five showed good results for the training set but gave unsatisfactory results for the test set, which is the most important. From these analyses, the optimal network configuration for this specific U.S. gas production model is a three-layer QP network with 11 input nodes, 5 hidden nodes, and 1 output node. The network is optimally trained with 5,000 iterations.

Error Analysis. Statistical accuracy of this network performance is given in Table 5 (Case 11a). The mean squared error (MSE) of the training set is 0.0034 and 0.0252 for the test set. **Fig. 7** shows the MSE vs. the iterations for both the training and test sets. The errors with training-set samples decrease consistently throughout the training process. In addition, errors with the test-set samples decrease fairly consistently along with the training-set samples, indicating that the network is generalizing rather than memorizing. All the training- and test-set samples yield results of 100% correct based on 0.05 tolerance, as shown in **Fig. 8.**

Fig. 9 shows the residual plot of the NN model for both the training and test samples. The plot shows not only that training set errors are minimal but also that they are evenly distributed around zero, as shown in **Fig. 10.** As is usually the case, errors in test samples are slightly higher than in training ones. The crossplots of predicted vs. actual values for natural gas production are presented in **Figs. 11 and 12.** Almost all the plotted points of this study's NN model fall very close to the perfect 45° straight line, indicating its high degree of accuracy.

Forecasting

After successful development of the NN model for U.S. natural gas production, future gas production rates must also be forecast. To

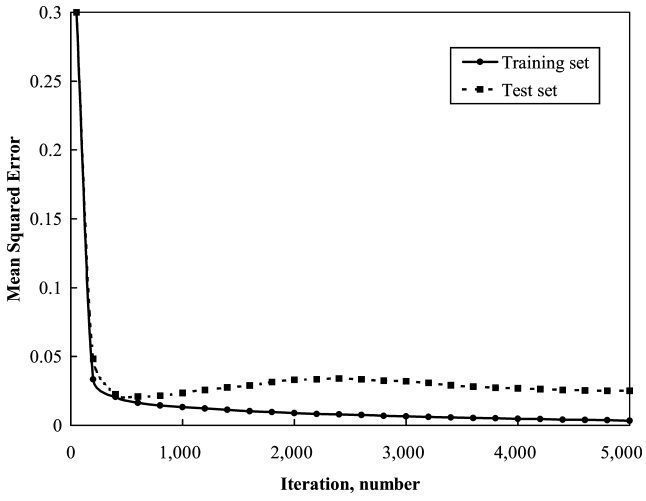

Fig. 7—Convergence behavior of the QP three-layer network (11, 5, 1) that learned from the U.S. natural gas production data.

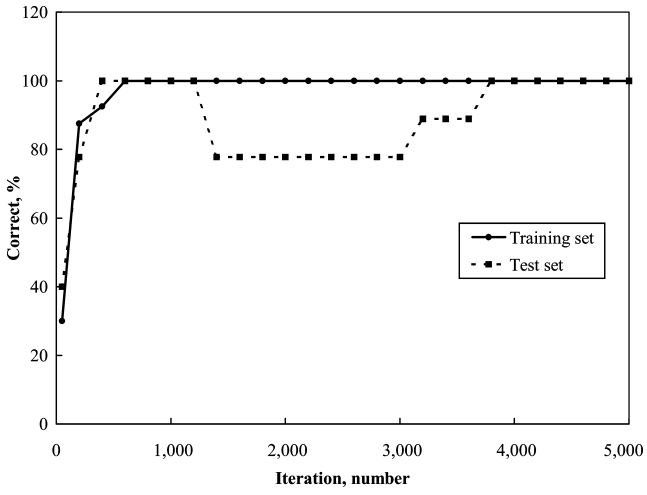

Fig. 8—Behavior of training and testing samples classified as correct.

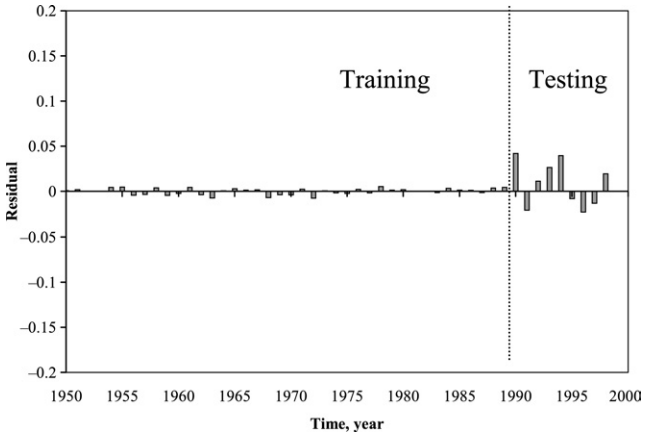

Fig. 9—Residual plot of the NN model.

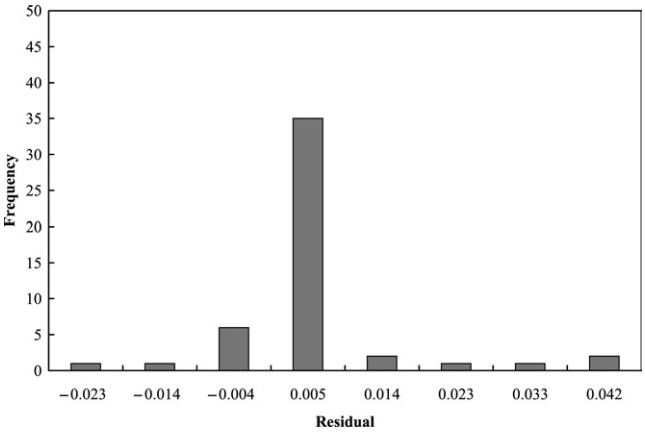

Fig. 10—Frequency of residuals in the NN model.

implement the network model for prediction, forecast models should be developed for all 11 network inputs or obtained from independent studies. We developed forecasting models for all the independent network inputs (except for the input of gas wellhead prices) with the time-series-analysis approach. The forecasts for the gas wellhead prices came from the EIA.[15] We adjusted the EIA forecasts for gas prices, based on 1998 U.S. dollars/Mcf, to 1992 U.S. dollars/Mcf so that the forecasts would be compatible with the historical gas prices used in network development. We developed the forecasting models for the NN input variables with the Box-Jenkins[16] methodology of time-series analysis. Details of forecast development for other network inputs are described in Ref. 17.

Before implementing the network model for forecasting, we took one additional step, taking the test set back and adding it to the original training set. The network could then be trained only one time, keeping the same configuration and parameters of the original trained network intact. The purpose of this step is to have the network take into account the effects of all available data. Because the amount of data is limited, this ensures generalization of the network performance, yielding better forecasting.

Next, we saved data for the forecasted network inputs for 1999 to 2020 as a test-set file, whereas the training-set file contained data from 1950 to 1998. We then ran the network with one pass through all the training and test sets. We retained the obtained data results in their original form by adding the output value at a given time to its previous one. After decoding the first-difference output values, we denormalized the obtained values for the training and test samples with the same normalization parameters as in the data preprocessing.

Fig. 13 shows this study's NN forecasting model for U.S. gas production to 2020. It also shows the excellent match between the NN model results and actual natural gas production data. The NN forecasting model indicates that the U.S. gas production in 1999 is in a decline, at 1.8% of the 1998 production. Production stayed at the 1999 level with a slight decline until 2001, after which gas production started to increase. From 2002 to 2012, gas production will increase steadily, with an average growth rate of approximately 0.5%/yr. The NN model indicates that this growth will more than double from 2013 to 2020, with a 1.3%/yr average growth rate. By 2019, gas production is predicted at 22.6 Tcf/yr, approximately the same as the 1973 production level.

The NN forecasting model developed in this study is dependent not only on the performance of the trained data set but also on the future performance of forecasted input parameters. Therefore, the network model should be updated periodically when new data become available. While it is desirable to update the network model with new data, the architecture and its parameters need not be changed. However, a one-time run to train the network with the updated data is necessary.

Comparison of Forecasts

This section compares the forecasts of U.S. natural gas production from the EIA[15] with the NN approach and with the stochastic modeling approach developed by Al-Fattah.[17] The EIA 2000 forecast of U.S. gas supply is based on U.S. Geological Survey (USGS) estimates of U.S. natural gas resources, including conventional and unconventional gas. The main assumptions of the EIA forecast are as follows:

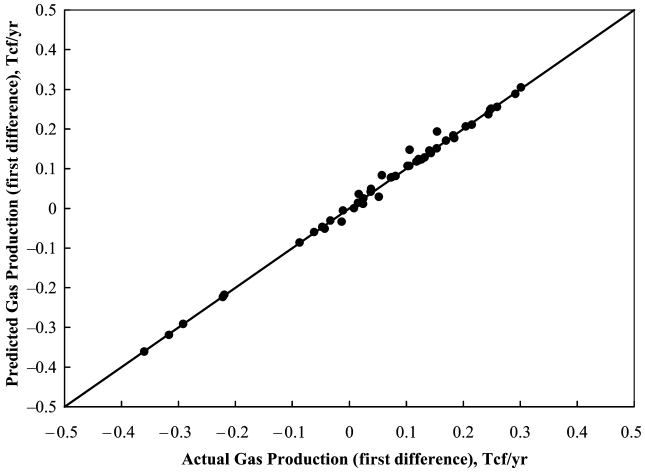

Fig. 11—Crossplot of NN prediction model and actual gas production (first difference).

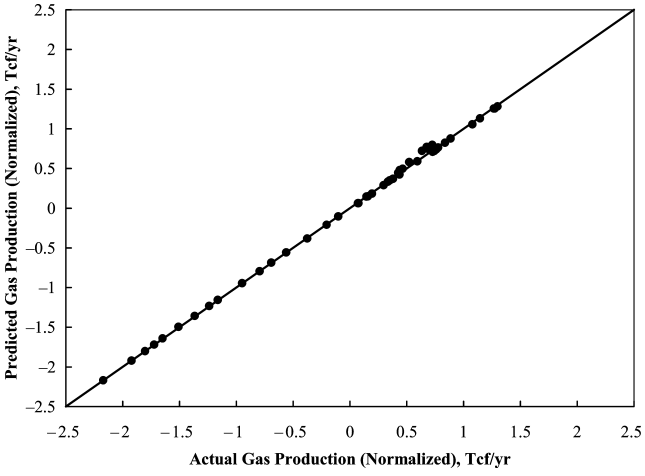

Fig. 12—Crossplot of NN prediction model and actual gas production (normalized).

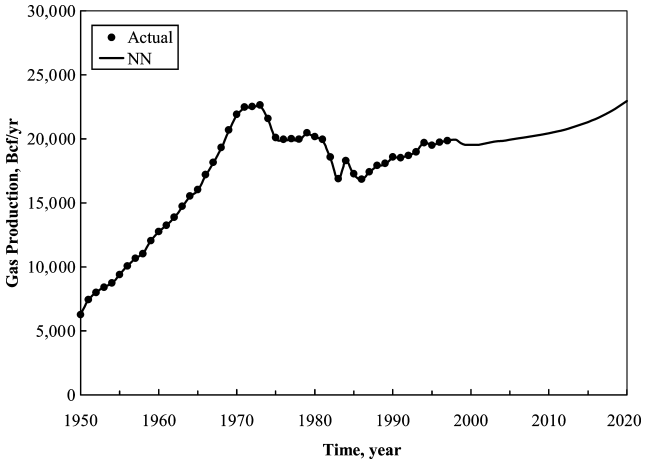

Fig. 13—NN forecasting model of U.S. gas production.

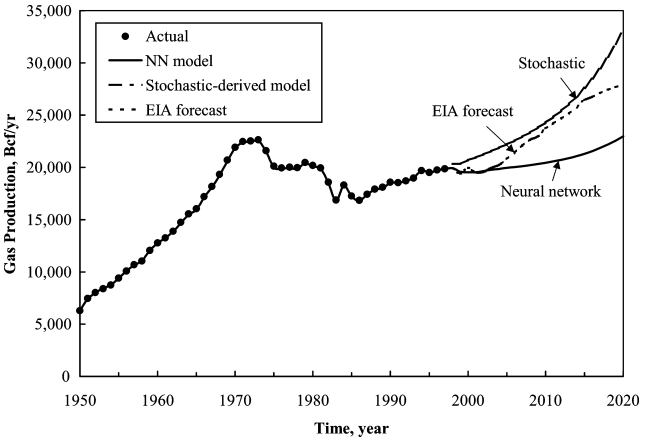

Fig. 14—Comparison of U.S. gas-production forecasts.

• Drilling, operating, and lease equipment costs are expected to decline by 0.3 to 2%.

• Exploratory success rates are expected to increase by 0.5%/yr.

• Finding rates will improve by 1 to 6%/yr.

Fig. 14 shows the EIA forecast compared to those from this study with the NN and time-series analysis (or stochastic modeling).

The stochastic forecast modeling approach we used was based on the Box-Jenkins time series method as described in detail by Al-Fattah.[17] We studied past trends of all input data to determine if their values could be predicted with an "autoregressive integrated moving average" (ARIMA) time-series model. An ARIMA model predicts a value in a time series as a linear combination of its own past values and errors. A separate ARIMA model was developed for each input variable in the NN forecasting model. Analyses of all input time series showed that the ARIMA model was both adequate (errors were small) and stationary (errors showed no time trend).

When we used the ARIMA model to directly forecast gas production with only time-dependent data, we were unable to achieve time-independent errors throughout the production history (from 1918 to 1998). However, because we determined previously that both the depletion and reserves discovery rates were stationary time series, we used these two ARIMA models to forecast gas production by multiplying the depletion rate and the gas reserves. The product of these two time series determines the stochastic gas forecast in Fig. 14.

The EIA forecast of the U.S. gas supply with approximately 20 Tcf/yr for 2000 is higher than the NN forecast of approximately 19.5 Tcf/yr. However, the EIA forecast matches the NN one from 2001 to 2003, after which the EIA forecast increases considerably, with annual average increases of 2.4% from 2004 to 2014 and 1.3% thereafter.

The stochastic-derived model gives a production forecast that is much higher than the EIA and NN forecasts. The forecast of U.S. gas supply from the stochastic-derived model shows an exponential trend with an average growth rate of 2.3%/yr.

The NN forecast is based on the following assumptions of independent input forecasts.

• Gas prices are expected to increase by 1.5%/yr.

• The gas depletion rate is expected to increase by 1.45%/yr.

• Drilling of gas exploratory wells will improve by 3.5%/yr.

• Drilling of oil/gas exploratory wells will increase an average of 2.5%/yr.

• D_G will have an average increase of 2.1%/yr.

The NN forecast takes into account the effects of the physical and economical factors on U.S. gas production, which render forecasts of natural gas supply reliable. The NN model indicates that U.S. gas production will increase from 2002 to 2012 by 0.5%/yr on average. Thereafter, gas production will have a higher increase, averaging 1.3%/yr through 2020.

Conclusions

This paper presents a new approach to forecast the future production of U.S. natural gas with an NN. The three-layer network was trained and tested successfully, and comparison with actual production data showed excellent agreement. Forecasts of the network input parameters were developed with a stochastic-modeling approach to time-series analysis. The network model included various physical and economic input parameters, rendering it a useful short-term as well as long-term forecasting tool for future gas production.

The NN model's forecasting results showed that the 1998 U.S. gas production would decline at a rate of 1.8%/yr in 1999, with 2001 at the 1999 production level. After 2001, gas production starts to increase steadily until 2012, with approximately a 0.5%/yr average growth rate. This growth will more than double for 2013 to 2020, with a 1.3%/yr average growth rate. By 2020, gas production is predicted at 23 Tcf/yr, slightly higher than the 1973 production level.

The NN model is useful as a short-term as well as a long-term predictive tool for future gas production. It can also be used to quantitatively examine the effects of various physical and economical factors on future gas production. With the NN model developed in this study, we recommend further analysis to quantitatively evaluate the effects of the various physical and economic factors on future gas production.

Nomenclature

D_G = gross domestic product, U.S. dollars
G_{DP} = growth rate of gross domestic product
i = observation number
t = time, 1/t, 1/yr
X = input/output vector
X' = normalized input/output vector
μ = mean or arithmetic average
σ = standard deviation

References

1. Haykin, S.: *Neural Networks: A Comprehensive Foundation,* Macmillan College Publishing Co., New York City (1994).
2. Azoff, E.M.: *Neural Network Time Series Forecasting of Financial Markets,* John Wiley & Sons Ltd. Inc., Chichester, England (1994).
3. *Neural Networks in Finance and Investing: Using Artificial Intelligence to Improve Real-World Performance,* revised edition, R.R. Trippi and E. Turban (eds.), Irwin Professional Publishing, Chicago, Illinois (1996).
4. Mohaghegh, S.: "Virtual-Intelligence Applications in Petroleum Engineering: Part I—Artificial Neural Networks," *JPT* (September 2000) 64.
5. Al-Kaabi, A.U. and Lee, W.J.: "Using Artificial Neural Nets To Identify the Well-Test Interpretation Model," *SPEFE* (September 1993) 233.

6. Habiballah, W.A., Startzman, R.A., and Barrufet, M.A.: "Use of Neural Networks for Prediction of Vapor/Liquid Equilibrium *K* Values for Light-Hydrocarbon Mixtures," *SPERE* (May 1996) 121.
7. EIA, Internet Home Page: http://www.eia.doe.gov/.
8. *Twentieth Century Petroleum Statistics,* 52nd ed., DeGolyer and MacNaughton, Dallas (1996).
9. *Twentieth Century Petroleum Statistics,* 54th ed., DeGolyer and MacNaughton, Dallas (1998).
10. Attanasi, E.D. and Root, D.H.: "The Enigma of Oil and Gas Field Growth," *AAPG Bull.* (March 1994) **78,** 321.
11. *Energy Statistics Sourcebook*, 13th edition, *OGJ Energy Database,* PennWell Publishing Co., Tulsa (1998).
12. "World Energy Projection System," DOE/EIA-M050, Office of Integrated Analysis and Forecasting, U.S. Dept. of Energy, EIA, Washington, DC (September 1997).
13. Kutner, M.H. *et al.: Applied Linear Statistical Models,* fourth edition, Irwin, Chicago (1996).
14. *ThinksPro: Neural Networks Software for Windows User's Guide,* Logical Designs Consulting Inc., La Jolla, California (1995).
15. "Annual Energy Outlook 2000," DOE/EIA-0383, Office of Integrated Analysis and Forecasting, U.S. Dept. of Energy, EIA, Washington, DC (1999).
16. Box, G.E., Jenkins, G.M., and Reinsel, G.C.: *Time Series Analysis Forecasting and Control,* third edition, Prentice-Hall Inc., Englewood Cliffs, New Jersey (1994).
17. Al-Fattah, S.M.: "New Approaches for Analyzing and Predicting Global Natural Gas Production," PhD dissertation, Texas A&M U., College Station, Texas (2000).

SI Metric Conversion Factors

ft × 3.048*	E–01 = m
ft^3 × 2.831 685	E–02 = m^3

*Conversion factor is exact.

Saud Al-Fattah is a reservoir management engineer in the Reservoir Management Dept. of Audi Aramco, Dhahran. His specialties include reservoir engineering, operations research, economic evaluation, forecasting, and strategic planning. Al-Fattah holds MS and BS degrees from King Fahd U. of Petroleum and Minerals and a PhD degree from Texas A&M U., all in petroleum engineering. **Richard A. (Dick) Startzman** is currently a professor of petroleum engineering at Texas A&M U. He was employed by Chevron Corporation for 20 years in research, operations, and management in the U.S., Europe, and the Middle East. He joined the faculty of petroleum engineering faculty at Texas A&M in 1982. His research interests include reservoir engineering, economic evaluation, artificial intelligence, and optimization. He was named to the Peterson Professorship in 1993. He has been active in the Society of Petroleum Engineers and was elected a Distinguished Member in 1994.

Integration of Multiphase Flowmetering, Neural Networks, and Fuzzy Logic in Field Performance Monitoring

C. Alimonti, SPE, U. of Rome, La Sapienza, and **G. Falcone,** SPE, Enterprise Oil UK plc*

Summary

The usual approach to the interpretation of producing wells is based on mechanistic models for the simulation of steady-state and transient flow regimes. However, there are significant reservations about convergence problems, computational limits, the need for extensive tuning on field data, the instability of boundary conditions, the limited applicability of existing multiphase flow models, and the uncertainties associated with choke-valve models. The current industry standards are critically reviewed within this framework.

The real-time monitoring of producing wells is recognized as the best way of optimizing field performance. Monitoring a producing well implies the ability to track any changes in fluid composition, flow rates, or pressure and temperature profiles in real time. Multiphase flowmetering (MFM) plays a key role in this scenario. Such information, combined with the critical analysis of historical data from the well itself or from analog wells, allows diagnosis of the system and prediction of future trends. However, field data *per se* do not necessarily generate knowledge. This is particularly true for large databases, which are difficult to manipulate to provide suitable inputs for wellbore simulators.

This paper suggests how MFM, knowledge discovery in databases (KDD), and fuzzy logic (FL) can offer an alternative approach to analyzing producing wells. KDD is the automated extraction of patterns representing knowledge implicitly stored in large information repositories. Distributed, *ad hoc* field measurements (including MFM and downhole measurements) can be processed by means of data cleaning, data integration, data mining, artificial intelligence (AI), and pattern evaluation. FL can then manage the resulting information in terms of flow assurance and production optimization.

The same techniques can also be extended to the reservoir and production network for an integrated approach to production-system analysis.

Introduction

Production wells are the physical connection between the reservoir and the surface facilities. As such, they are part of a production system, which is a network of components through which underground hydrocarbons must flow to reach the surface. It includes and is characterized by the following.

- The reservoir, with its geological and petrophysical properties, and the properties of the fluids stored within it.
- The production wells, particularly their completions and any artificial-lift solutions.
- The flow-control valves, such as the wellhead chokes.
- The flowlines and any flow-assurance solutions associated with them (such as single or multiphase pumping, thermal isolation, and chemical injection).
- The separation and treatment facilities, both subsea and at surface.

Besides this hardware, the properties of multiphase flows within the reservoir and through the production network must also be taken into account for the production system to be fully characterized. It is common knowledge that variations of any of the previous characteristics are reflected in the rest of the system; therefore, none of the system elements can be considered physically disconnected from the others. This means that the production system can be regarded as integrated.

There are several levels of integrated analysis that can be carried out on a production system, depending on what sorts of results are needed. The short-, medium-, and long-term optimization of field management certainly are the main reasons oil companies put so much effort into simulating integrated production systems. Short-term optimization means finding the optimum operational conditions—choke settings, rate and allocation per well of gas lift gas and chemical injection, separator pressure—that maximize the day-to-day production and honor any physical constraints dictated by the system itself (overall capacity of the network, availability of compressors, slug-handling capacity, and flaring restrictions). Medium-term optimization includes planning startups and shutdowns so that the effects of transients can be smoothed and handled throughout the system. Long-term optimization aims at maximizing the recoverable reserves from the system and may include debottlenecking and topsides modifications to handle larger amounts of water or gas from depleting fields.

Optimization can be achieved only by monitoring the field closely and critically reviewing any significant trend in the main parameters of the system. The frequency at which the information must be retrieved from the field is a function of the time dependency of the events being analyzed. Monitoring provides a feel for the lag time between the moment a variation occurs in the system and the moment it is felt by any of the parameters characterizing the system. Thus, *una tantum* measurements can be enough for steady-state conditions, while real-time monitoring is necessary for accurate verification or prediction of fast-changing conditions.

Different levels of analysis may be needed at different stages of field development. The design stage and the early life of a field are the most critical in terms of development planning because very little is known about the potential performance of the field. However, late-life solutions may be critical as well because of the likelihood of more unstable flow conditions associated with depleting systems.

Having introduced the concept of integrated production systems, it follows that the best approach to their interpretation and optimization is the simultaneous integration of information from their individual components. Well monitoring and diagnosis, in particular, are the most direct ways of detecting variations in any key parameter of an integrated production system. However, how can we discern what parameters are most representative of significant changes in system properties? Are variations predictable? Can we measure these in the field? Can the information be inferred from standard software packages when it is not possible to get all the necessary data from the field?

State of the Art

Standard Approach to Integrated Production Systems. To date, several models have been developed to simulate the behavior of multiphase flows within the reservoir and through individual components of a production system. A number of commercial

* Now with TOTAL E&P UK plc, London

Copyright © 2004 Society of Petroleum Engineers

This paper (SPE 87629) was revised for publication from paper SPE 77407, first presented at the 2002 SPE Annual Technical Conference and Exhibition, 29 September–2 October. Original manuscript received for review 20 January 2003. Revised manuscript received 10 November 2003. Paper peer approved 9 December 2003.

TABLE 1—SUMMARY OF OIL PROPERTIES		
Density	Viscosity	Associated GOR
34.5 API	7 mPa • s at 20°C	1,288 to 1,400 scf/stb

simulators are available that can separately model reservoirs, wellbores, gathering systems, and the process plant, and the manufacturers claim they can handle steady-state as well as transient conditions. There are also extensive compositional and black-oil models for simulating the pressure/volume/temperature (PVT) properties of produced fluids and empirical and thermodynamic models for simulating flow through wellhead choke valves. However, compatibility problems often arise when different software packages from different vendors are coupled together.

Because different mathematical codes and convergence procedures are adopted for simulating different elements of a production system, there is always the risk of serious instability when coupling software packages together. In this modular approach to simulating production systems, special attention also must be paid when defining the so-called boundary conditions.[1] These dynamic interactions between different parts of the system guarantee the conservation of mass, energy, and momentum from the reservoir to the process plant. For instance, the multiphase flow correlations must be smooth and consistent throughout the system and the entire range of production conditions, but this is not always possible because of the high complexity and unpredictability of multiphase flows and their strong dependence on the history of the flow. Because of this dynamic interrelation between the various elements of an integrated production system, it is important to account for the overall effects caused by wellhead chokes and other control valves in the process plant.[2,3] Only when critical flow occurs can a wellhead choke decouple the reservoir from the production facilities (although a simulation run with the network model is still needed to establish whether the flow is critical). When the flow is subcritical, the choke must be regarded as a key element of the production system, which creates a pressure drop, affects the upstream/downstream flow, and controls the total production rate.

Another approach to the study of integrated production systems is to combine the equations for the reservoir and the production facilities in a single system and solve them simultaneously.[3] However, despite the need for full-field models that can couple surface facilities to reservoir simulators, no satisfactory solution has been found yet because of the prohibitive computer-processing times associated with conventional techniques. Implicit methods can be computationally intensive if not supported by the use of parallel machines and/or the implementation of acceleration techniques, such as domain decomposition.[3] To treat a system implicitly means to solve the production network first, then use the results as boundary conditions for the reservoir simulator and see if convergence of pressure and flow rate at downhole conditions can be achieved. If not, an iterative process is generated by assuming new well rates as boundary conditions for the production network, but convergence may be very slow for large models and may not be achieved in some cases, especially if choke valves are included. An alternative to implicit methods is represented by explicit methods in which the convergence point at the bottomhole is set at the beginning of the simulation. Although this procedure saves the central processing unit (CPU) time, it may be less accurate, especially when the operating conditions of the system change rapidly.

Both approaches to the study of surface facilities, wells, and reservoirs as integrated systems have the inherent uncertainty of the accuracy of the flow models adopted for simulating the various elements. Each code has its own merits for particular conditions, and it is left to the engineers to judge which combination of tools is the most suitable for simulating a given production system.

With regard to reservoir simulators, it is not unusual to get different answers to the same problem, depending on whether an analytical, deterministic, or streamline-based model is used or whether the reservoir fluids have been characterized by compositional or black-oil techniques.

A similar situation may occur when modeling multiphase flows through wells and pipelines. In this case, mechanistic models, as opposed to empirical ones, can provide more reliable solutions.[4] However, no universal multiphase flow correlations have been developed that can cover any inclination and pipe diameter or be applied to any flow regime. Furthermore, closure laws are generally needed to solve the system of equations, but because they are flow-regime dependent, an error in predicting the flow regime may invalidate the final answer. This is particularly true for transient conditions in which terrain-induced effects and the history of the flow may cause a nonunique solution to the identification of the flow regime, even though the boundary conditions remain unchanged. Because transient simulators are indeed specialized tools, they can generate misleading results unless they are used by a dedicated engineer or group of engineers with experience on the pipeline system under examination.

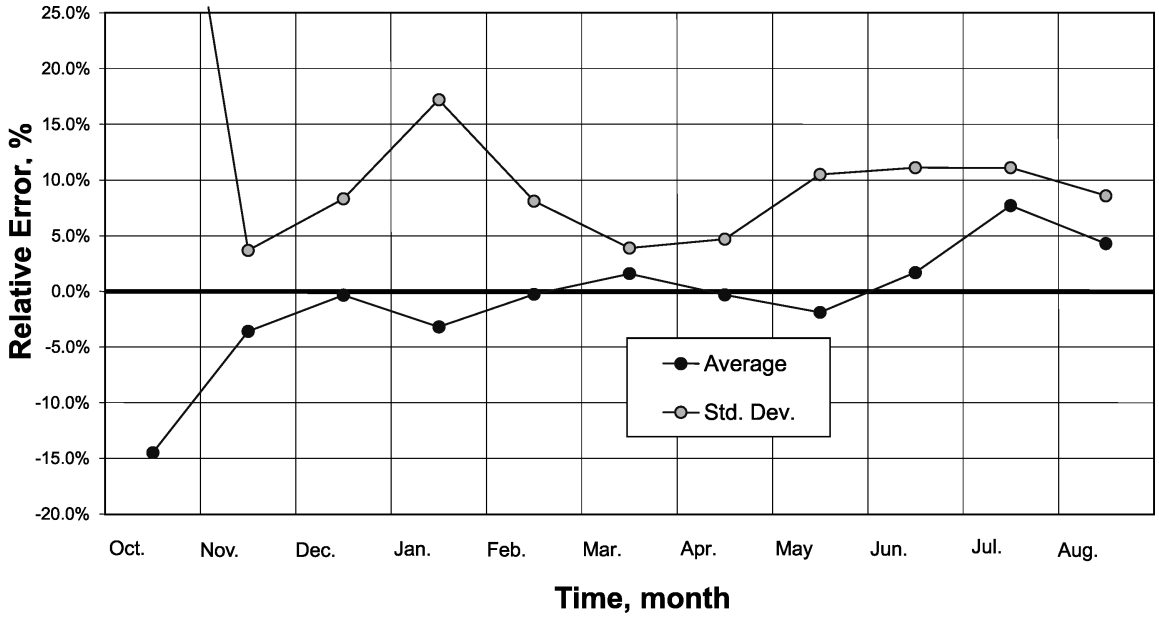

Fig. 1—ANN model vs. field data—relative error in oil flow rate.

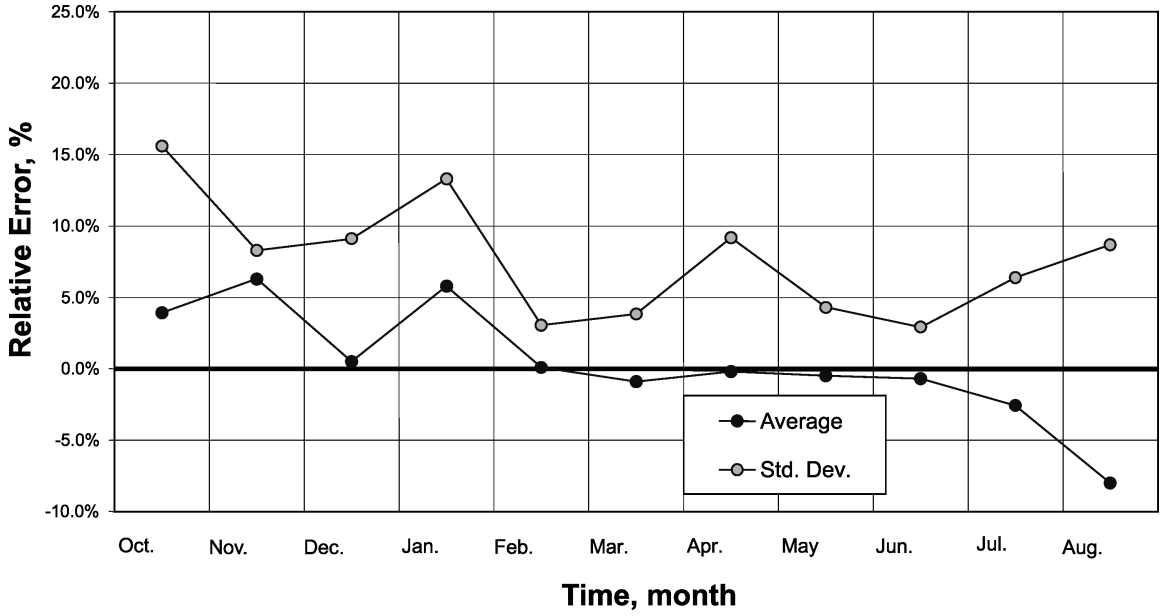

Fig. 2—ANN correction model vs. field data—relative error in oil flow rate.

Tuning Models With Field Data. Another drawback with the two approaches described previously is the need for extensive tuning of the model with field data. This makes the overall process of simulating integrated production systems even longer.

Matching vertical-lift performance curves to measured data and generating families of curves for a large enough water-cut range, gas/oil ratio (GOR), and tubing-head pressure requires long running times and powerful computers. History matching a reservoir model can be very time consuming, especially for fully compositional fluid models and refined simulation grids. Sometimes it is necessary to edit out part of the reservoir, generally part of the aquifer, and assume that its contribution to the pressure support is negligible, at least until depletion becomes significant in the main reservoir. Even when a detailed tuning on historical data is performed, there is no guarantee that the model can run safely in predictive mode.

Multiphase flow correlations also need extensive tuning with field data, yet there may be flow conditions (in the wells, in the pipelines, or through the chokes) that are not satisfied by any of the available correlations.

Data Handling. It is essential that the data gathered from the field contain the information needed for a consistent match of the integrated production system as a whole. The location of reservoir and production monitoring devices throughout the system must be strategic, as must the sampling frequency and any adopted data-filtering technique. Unfortunately, this is not always the case. Many pressure and temperature sensors in the field are not in the desired location to get the necessary information for the multiphase flow models of wells, pipelines, and chokes, usually because of retrofitting (i.e., adding sensors to a field already under development). Also, it is not unusual that downhole pressure gauges are retrieved from the wells long after their memory has become full and are only rarely replaced with new gauges, leaving inference methodologies to estimate pressure values. Thus, retrieved information may be useless unless it is combined with other information from different elements of the system for the same period.

Even when enough instrumentation is put on site, it may become technically challenging to transmit and store large amounts of information to databases from which historical information can be extracted when needed.[5] There may be the risk of storing "noise" or nonessential data along with key information if no filtering techniques are used between the field and the database. However, data can only be filtered when the users know in advance what kind of frequency is to be expected from a given phenomenon, and this frequency may vary during the field's life.

In the last decade, many efforts have been made to offer reliable control tools that provide real-time information for field surveillance. Fiber-optic-based sensors are being used for temperature, pressure, pH, acoustic noise, and strain measurements.[6] So-called intelligent completions have been developed that include not only permanent temperature and pressure downhole sensors but also remote control of downhole chokes for real-time flow control of different producing zones.[7] Continuous measurement of the formation conductivity is now possible by means of water-monitoring radar, which is based on the electromagnetic field generated between a transmitter and two receivers.[7] Permanent geophones are being considered as a potential option for continuously monitoring the fluid migration in the reservoir. Multiphase flowmeters are becoming standard practice for the development of tieback, deepwater, and marginal fields, and they provide invaluable well diagnostics.[8]

Internet-based databases that can retrieve real-time information from the field, make it available to users worldwide, and plot it under different formats, as required, are available to the oil and gas industry. Also, data collected in this way can be downloaded into standard software packages for production allocation and produc-

TABLE 2—SUMMARY OF AVERAGE RELATIVE ERRORS AND STANDARD DEVIATIONS FOR DIFFERENT FLOW-RATE ESTIMATION MODELS

	Oil		Gas	
	Error (%)	Standard Deviation (%)	Error (%)	Standard Deviation (%)
FDM	–3.4	16	2.5	19
ANN	–0.8	13	0.8	7.8
ANN corrector	0.3	7.7	1.8	7.0

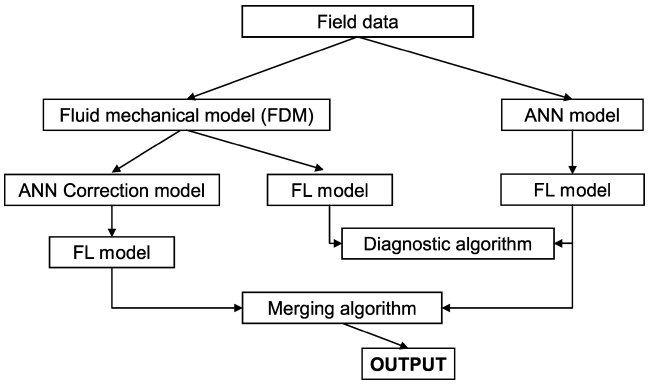

Fig. 3—Flow chart of the data-processing sequence.

tion forecast purposes. A note of caution: such procedures can be quite time consuming, rely on powerful machines, and imply that data are processed and interpreted only after they have been acquired and stored in a databank.

Finally, statistical and probabilistic analysis of reservoir properties (Monte Carlo simulation) and production data (prediction methods such as the linear model fit by least squares and the *k*-nearest-neighbors prediction rule) can now be performed by commercial software packages. Probability theory allows us to model the uncertainty of any process in which the outcomes of any particular realization of it are strictly a matter of chance. This is fine for random processes in which a precise description is available of the statistics of the long-run averages of the process. However, the uncertainty associated with nonlinear, complex systems (and, hence, with integrated production systems) is not random. In such cases, the information available to solve the problem is more qualitative than quantitative and can only be incorporated in engineering models with some tolerance for imprecision.

An Alternative Approach to Well Monitoring and Diagnosis

In the following, we introduce the implementation of AI techniques with the standard methodologies described previously for a more flexible and meaningful approach to interpreting integrated production systems. Although it is not possible to go away without making use of traditional tools, such as reservoir, wellbore, and pipeline simulators, we shall show how key parameters measured at the wellhead and fluid dynamic models can be harmonized by AI to provide real-time information on a flowing system.

In particular, we describe the integrated use of online MFM, *ad hoc* measurements at the wellhead, and AI for a critical approach to well monitoring and diagnosis.

Review of AI Techniques

Knowledge Discovery in Databases: Data Mining and Artificial Neural Networks (ANNs). Data mining, an essential step in the KDD process, is defined as "the automated extraction of patterns representing knowledge implicitly stored in large databases."[9] Thus, data *per se* do not necessarily mean knowledge, and, therefore, some way of uncovering data patterns is usually needed.

KDD has developed continuously since the 1960s, when data collection and database-creation techniques began to make significant progress. The rapid evolution of KDD would not have happened without incredible advances in computing, making it possible to handle huge amounts of data. Hence, now there is the ability to process such data potentially at the same speed at which they are gathered. The KDD process can be summarized as follows:

- Noise and spurious data are removed from the database by means of cleaning/filtering techniques.
- Data that are stored in different databases but belong to the same phenomenon are combined.
- Basic statistics or aggregation techniques are applied to the data for consolidation.
- Patterns are extracted from the data by means of data mining operations, which includes techniques such as machine learning, spatial data analysis, database technology, pattern recognition, and ANNs.
- Once the patterns have been extracted, they must be evaluated to discern new or interesting information from nonessential information.

The previous steps are not necessarily in the order described because they must be tailored to each individual application and its features.

Data mining is not just a deductive database system or a statistical data-analysis tool; it involves an integration of different techniques that rely on the interaction between users and the data mining system. This is particularly true when ANN learning is adopted, because direct user involvement is required to interpret the qualitative meaning behind the learning weights associated with the connections in the network. ANNs, which employ nonlinear functions of linear combinations ("derived features") from the inputs,[10] represent a very general approach to regression and classification problems. Because of their characteristics, ANNs best apply to situations with a high signal-to-noise ratio. ANNs are useful for classification in data mining because of their nonlinear statistical models, from which rules can be extracted and incorporated within FL applications.

FL. The concept of FL was introduced in 1965 by Prof. Lofti Zadeh.[11] FL is a problem-solving control-system methodology that provides a simple way to arrive at a definite conclusion based on vague, ambiguous, imprecise, noisy, or missing input information. It mimics how a person would make decisions, only much faster. In 1973, Prof. Zadeh stated: "As the complexity of a system increases, our ability to make precise and yet significant statements about its behaviour diminishes until a threshold is reached beyond which precision and significance (or relevance) become almost mutually exclusive characteristics."[12]

While it does not bring much improvement in the case of simple linear systems or naturally automated processes, FL best

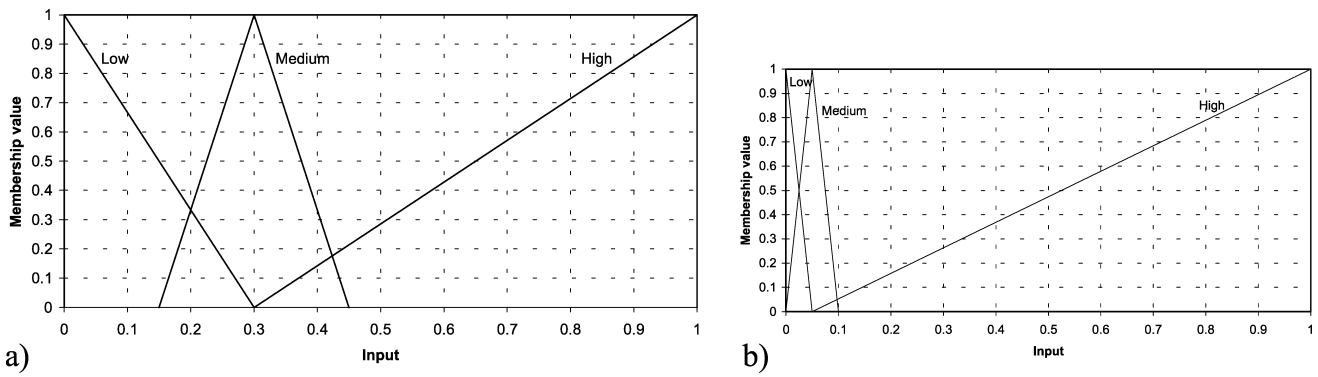

Fig. 4—Membership functions for error Q_o: (a) FDM and (b) ANN model.

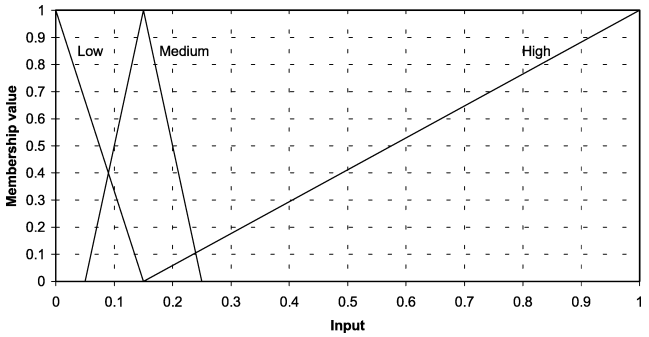

Fig. 5—Membership function for input error GOR.

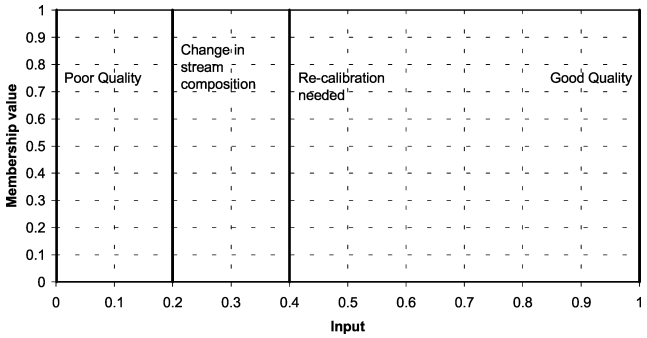

Fig. 6—Membership function for output. Crisp membership function.

applies to areas in which intuition and judgment still play a fundamental role. In Japan, FL is now part of day-by-day life, being successfully implemented to train scheduling, videography, stock tracking on the Nikkei stock exchange, robotics, and domestic appliances.

FL is an infinite-valued logic that allows for degrees of set membership. The three logic operations AND, OR, and NOT return a degree of membership that is a real number between 0 and 1, in contrast to the traditional Boolean values of TRUE, 1, and FALSE, 0.[13]

For a certain number of input parameters, FL identifies the fuzzy variables associated with each parameter of an event. Membership functions, which are assigned to the fuzzy variables to judge the magnitude of their participation in the event, are defined by shape, height, width, shouldering, center points, and overlap. They can be generated in several ways, including use of the so-called genetic algorithms (based upon the concept of Darwin's theory of evolution) and ANNs. Rules that use the input membership values as weighting factors to determine their influence on the final fuzzy output sets are then defined.

The final step in the FL process is so-called defuzzification, converting the fuzzy sets into scalar, single quantities. Defuzzification methods are context-dependent; hence, they may vary from case to case.

Applications of AI to the Oil and Gas Industry. The application of AI techniques to the petroleum industry has been evaluated since the early 1990s. ANNs and FL have already been developed in the following areas.[9, 13–21]

- Geology and geophysics (e.g., reserves estimation, seismic pattern recognition, and sequence stratigraphy).
- Formation evaluation (e.g., porosity and permeability prediction, fracture delineation, and pore pressure determination from log data).
- Drilling [e.g., measurement-while-drilling (MWD) data analysis].
- Production and facilities (e.g., gas-lift optimization, topsides processes optimization, diagnosis and maintenance, and multiphase flowmetering).
- Reservoir engineering (e.g., automatic history matching, pattern recognition of pressure-transient data, and reservoir properties prediction).
- Petroleum economics (e.g., risk analysis and portfolio optimization).

ANNs best reproduce nonlinear phenomena, while fluid dynamic models can be scaled to different flow conditions. Thus, an FL-based integration of both solutions proved to be more accurate than using ANNs and fluid dynamic models separately.

Results

In this section, we present the results obtained from the analysis of the production data gathered during a 10-month extended production test (EPT) on a well of the Val d'Agri field (Italy) carried out between October 1999 and August 2000. The Val d'Agri field is currently being developed in a joint venture between ENI-Agip and Enterprise Oil.** The well considered for this study is located in the northern area of the field and produces oil with the properties shown in **Table 1.**

** Now Shell Italia E&P.

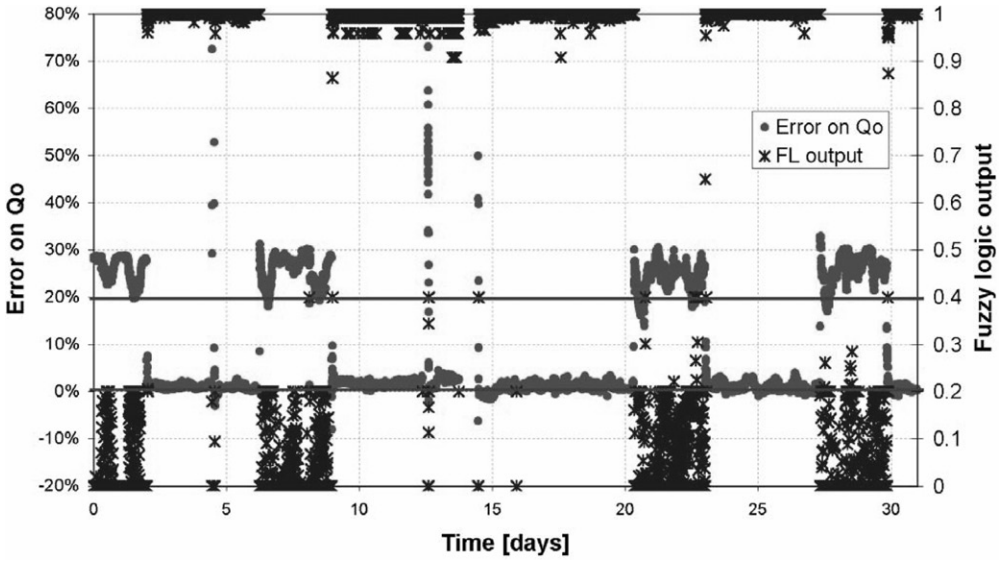

Fig. 7—FL applied to the ANN model—data refer to July 2000.

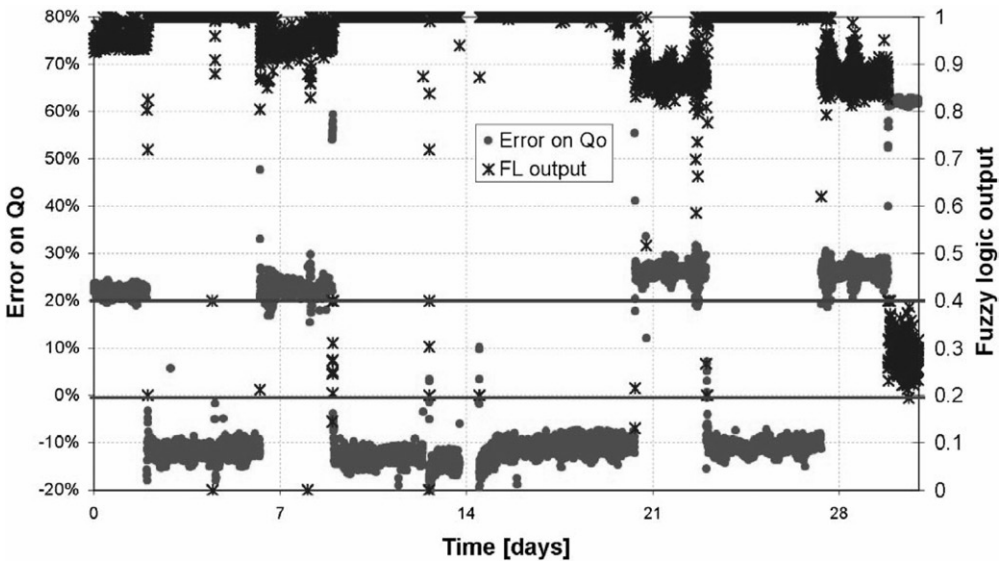

Fig. 8—FL applied to the FDM—data refer to July 2000.

The original aim of the study was to integrate the data measured at the wellhead with the flow rates estimated by a fluid dynamic model (FDM). In particular, an online system based on the existing wellhead choke valve was used together with *ad hoc* measurements of pressure and temperature upstream and downstream of the choke. The results showed that the metering system had achieved the functionality of a multiphase flowmeter. Acceptable oil flow-rate predictions were obtained during the 10-month period, with an average relative error of –3.4% and a standard deviation of 16%. A similar performance was obtained for the gas flow-rate prediction, with an average error of 2.5% and a standard deviation of 19%. A detailed analysis of the results is reported in Alimonti *et al.*[22]

On the basis of those results and previous experience with Venturi meters for the prediction of single and multiphase flow rates,[14] it was decided to try to improve system performance with ANNs. This allowed a critical analysis of data quality as well as process diagnosis. Two approaches were attempted. The first (and more traditional) approach was based on an ANN model that used the same inputs as the FDM to give the flow rates of oil and gas as outputs. The ANN was trained with the data gathered in December 1999 and then used to estimate the flow rates for 9 more months. The results for the oil rates are reported in **Fig. 1,** which shows the mismatch between the measured and predicted oil flow rate. By grouping the errors per month, starting from the data gathered every 5 minutes, an average error of –0.8% and a standard deviation of 13.0% were obtained. It was also possible to observe the effects of opening/closing the well on the model's final response.

The second approach was based on implementing an ANN as a correction algorithm to the FDM. Such an ANN used the flow rates predicted by the FDM as inputs, providing corrected flow rates as outputs. This ANN was trained with the data from February 2000, and the results are presented in **Fig. 2. Table 2** summarizes the relative errors and the standard deviations for the two approaches.

Both ANN approaches lead to a reduced bias and half the standard deviation of the results from the FDM.

For both cases, the higher errors seen for October 1999 and January, July, and August 2000 can be explained as follows. The first 2 months reflected production startups, characterized by high contents of CO_2, and production restarts, characterized by high GORs. The other 2 months reflected the presence of water in the stream, while water production was nil for the data set used to train the ANNs.

Thus, the same kind of information (flow rates, in this case) can originate from different sources (the FDM, the "traditional" ANN model, and the ANN correction model), so that the system becomes redundant. A similar situation occurs when different flowmeters, based on different metering principles, are used at the same time.

On the basis of the previous considerations, a methodology was developed to obtain the most reliable flow-rate values. The idea is to use an FL model to evaluate the performance of different flow-rate-prediction models and adopt a strategic approach from its results. **Fig. 3** shows the flow chart of the data-processing sequence that was followed in this study. Basically, a diagnostic module is obtained by comparing the results of the FL models applied to the FDM and ANN models.

As mentioned previously, FL was adopted to build a model able to perform a quality check on the field data as well as a critical diagnosis of both the production and the online metering systems. To accomplish that, the flow rates measured at the test separator in the field were taken as reference values. The FL model used two inputs (namely, the relative errors in oil and gas flow rate) to give an output parameter ranging between 0 and 1 (0 for low data quality and 1 for high data quality). Besides the output parameter, two more values were selected to represent the need for recalibration of the online metering system (0.4) and a potential change of stream composition (0.2). **Figs. 4 through 6** show the membership functions for this application. **Figs. 7 through 9** show the results of the FL model applied to the ANN and FDM models.

Hence, it remains to define which are the most accurate oil and gas flow-rate values to adopt. The best estimate of flow rates was obtained by a weighted average of the values obtained from the two ANN models, with the weight being the FL output. The results, reported in **Table 3,** are strongly encouraging because they show a strong reduction in the standard deviation (less than 3% for both the oil and gas flow rate).

Conclusions

From the results presented previously, it appears that ANNs and FL can be combined with MFM to provide not only a real-time monitoring of produced flow rates and stream composition but also a valid quality check of this same information.

Field and predicted data can be checked against each other so that it becomes possible, by applying AI techniques, to distinguish between changes in the actual flow conditions of the production system and recalibration issues related to the metering devices.

It also appears that many more combinations of AI techniques and field data can be achieved to perform well diagnosis and monitoring. From a preliminary analysis of the data, the authors believe that the same procedure can be applied, with the well productivity index input in place of the oil rate.

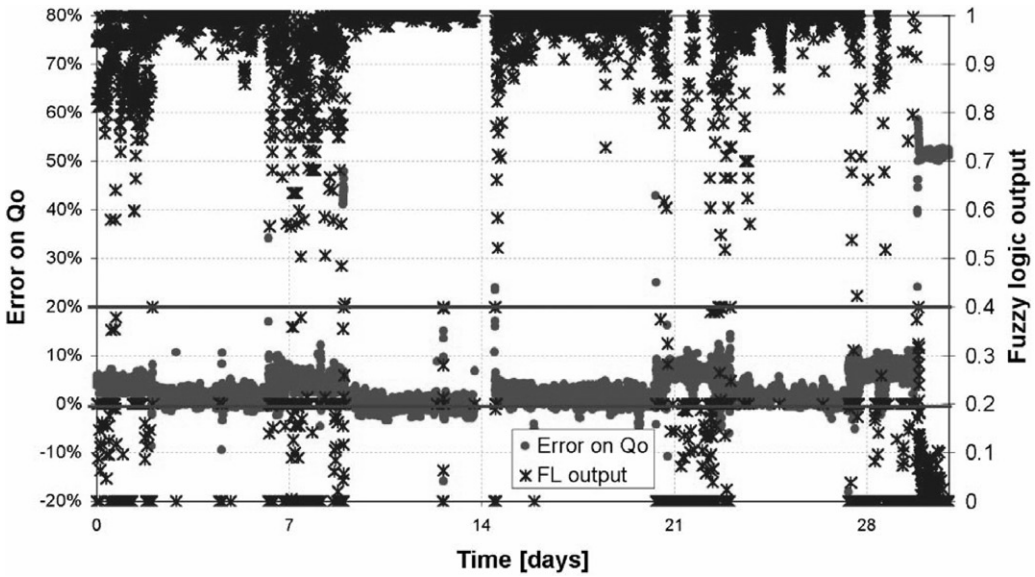

Fig. 9—FL applied to the ANN correction model data refer to July 2000.

To date, no solution has been delivered that integrates all the previously described AI methodologies with regard to integrated production systems as a whole, from reservoir to surface. This may be because expertise in both petroleum engineering and computational techniques is needed to appropriately use AI in the petroleum industry. The dynamic behaviors of oil and gas developments have their own physical characteristics, and the ANNs and FL models must be tailored to such applications. Also, each AI method handles uncertainty differently, and the sequence of steps to be followed when applying AI solutions is not unique. However, these are exactly why an integration of KDD and AI can be expected to be extremely flexible and improve computational speed and imprecision tolerance.

Nomenclature

k = text
Q = oil flow rate

Subscripts

o = oil phase

References

1. Xu, Z.G. and Shea, D.: "Important tips for setting up simulation models for multiphase flow in pipelines," paper presented at the 2001 10th Intl. Conference Multiphase, BHR Group, Cannes, France, 13–15 June.
2. Schiozer, D.J. and Aziz, K.: "Effect of Chokes on Simultaneous Simulation of Reservoir and Surface Facilities," paper SPE 26308 available from SPE, Richardson, Texas (1993).
3. Schiozer, D.J. and Aziz, K.: "Use of Domain Decomposition for Simultaneous Simulation of Reservoir and Surface Facilities," paper SPE 87876 presented at the 1994 SPE Western Regional Meeting, Long Beach, California, 23–25 March.
4. Lopez, D. and Duchet-Suchaux, P.: "Performances of Transient Two-Phase Flow Models," paper SPE 39858 presented at the 1998 SPE International Petroleum Conference and Exhibition of Mexico, Villahermosa, Mexico, 3–5 March.
5. Hunt, A.P. *et al.:* "Real time modelling of multiphase flow systems," paper presented at the 2001 10th Intl. Conference Multiphase, BHR Group, Cannes, France, 13–15 June.
6. Guaita, P.: "Development of a New Fiber-Optic Based Offshore Structural Monitoring System," paper SPE 56435 presented at the 1999 SPE Annual Technical Conference and Exhibition, Houston, 3–6 October.
7. Boe, H.S., Nordtvedt, J.-E., and Schmidt, H.S.: "Integrated Reservoir and Production Management: Solutions and Field Examples," paper SPE 65151 presented at the 2000 SPE European Petroleum Conference, Paris, 24–25 October.
8. Falcone, G. *et al.:* "Multiphase Flow Metering: Current Trends and Future Developments," paper SPE 71474 presented at the 2001 SPE Annual Technical Conference and Exhibition, New Orleans, 30 September–3 October.
9. Han, J. and Kamber, M.: *Data Mining—Concepts and Techniques,* Morgan Kaufmann (2001) ISBN 1-55860-489-8.
10. Hastie, T., Tibshirani, R., and Friedman, J.: *The Elements of Statistical Learning—Data Mining, Inference, and Prediction,* Springer (2001).
11. Zadeh, L.: "Fuzzy Sets," Information and Control 8:338-353 (1965).
12. Ross, T.J.: *Fuzzy Logic with Engineering Applications,* McGraw-Hill Inc. (1995).
13. Ali, J.K.: "Neural Networks: A New Tool for the Petroleum Industry?," paper SPE 27561 presented at the 1994 SPE European Petroleum Computer Conference, Aberdeen, 15–17 March.
14. Alimonti, C. and Bilardo, U.: "Measurement of three-phase flow rates using neural network approach," paper presented at the 2001 4th Intl. Conference on Multiphase Flow, New Orleans, 27 May–1 June.
15. Toral, H. *et al.:* "Esmer Field Tests Multiphase Flow Meter," paper presented at the North Sea Flow Measurement Workshop (1998).
16. Fang, J.H. and Chen, H.C.: "Fuzzy Modelling and the Prediction of Porosity and Permeability from the Compositional and Textural Attributes of Sandstone," *J. of Petroleum Geology* (1997) **20,** No. 2, 185.
17. Rogers, S.J. *et al.:* "Predicting Permeability from Porosity Using Artificial Neural Networks," The American Assoc. of Petroleum Geologists (July 1995)

TABLE 3—SUMMARY OF AVERAGE RELATIVE ERROR AND STANDARD DEVIATION FOR THE MERGING ALGORITHM

	Oil		Gas	
	Error (%)	Standard Deviation (%)	Error (%)	Standard Deviation (%)
Merging algorithm	0.9	2.6	–1.5	2.9

18. Murray, A. *et al.:* "The Applications of Advanced Computing Techniques to Oil and Gas Facility Optimisation," paper SPE 56904 presented at the 1999 SPE Offshore Europe Conference, Aberdeen, 7–9 September.
19. Jansen, B. *et al.:* "Automatic Control of Unstable Gas Lifted Wells," paper SPE 56832 presented at the 1999 SPE Annual Technical Conference and Exhibition, Houston, 3–6 October.
20. Vázquez, M. *et al.:* "Global Optimisation of Oil Production Systems, A Unified Operational View," paper SPE 71561 presented at the 2001 SPE Annual Technical Conference and Exhibition, New Orleans, 30 September–3 October.
21. Annunziato, M. *et al.:* "High Accuracy and Data Fusion in the on-line Measurement of Multiphase Flowrate." paper presented at the 2000 7th Intl. Conference of Multiphase Flow in Industrial Plants, Bologna, Italy, 14–16 September.
22. Alimonti, C., Basso, A., and Pelliccia, A.: "Is it really possible to use a choke valve as multiphase flowmeter? The CVAF from laboratory to the field," paper presented at the 2001 10th Intl. Conference Multiphase, BHR Group, Cannes, France, 13–15 June.

SI Metric Conversion Factors

bbl × 1.589 873	E–01	= m^3
ft^3 × 2.831 685	E–02	= m^3
°API 141.5/(131.5+°API)		= g/cm^3

Claudio Alimonti is an Assistant Professor with the U. of Rome "La Sapienza." e-mail: claudio.alimonti@uniroma1.it. His research interests include multiphase flow modelling and metering. Alimonti holds a first-class degree in mining engineering from the U. of Rome "La Sapienza" and a Ph.D. degree in mechanical engineering from the U. Catholique de Louvain, Belgium. **Gioia Falcone** is currently a Research Reservoir Engineer with Total E&P UK in London. e-mail: gioia.falcone@total.com. She was previously employed as a petroleum engineer with Enterprise Oil UK plc, Aberdeen. Falcone holds a first-class degree in petroleum engineering from the U. of Rome "La Sapienza" and an MSc degree in petroleum engineering from Imperial College, London.

Recent Developments in Application of Artificial Intelligence in Petroleum Engineering

Shahab D. Mohaghegh, West Virginia U. and Intelligent Solutions Inc.

Abstract

With the recent interest and enthusiasm in the industry toward smart wells, intelligent fields, and real-time analysis and interpretation of large amounts of data for process optimization, our industry's need for powerful, robust, and intelligent tools has significantly increased. Operations such as asset evaluation; 3D- and 4D-seismic-data interpretation; complex multilateral-drilling design and implementation; log interpretation; building of geologic models; well-test design, implementation, and interpretation; reservoir modeling; and simulation are being integrated to result in comprehensive reservoir management. In recent years, artificial intelligence (AI), in its many integrated flavors from neural networks to genetic optimization to fuzzy logic, has made solid steps toward becoming more accepted in the mainstream of the oil and gas industry. In a recent set of *JPT* articles,[1–3] fundamentals of these technologies were discussed. This article covers some of the most recent and advanced uses of intelligent systems in our industry and discusses their potential role in our industry's future.

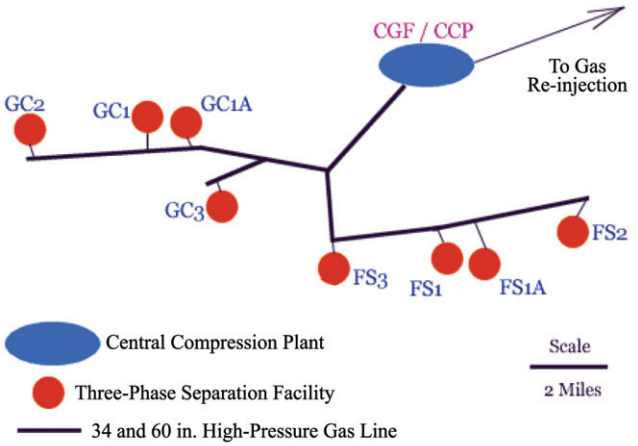

Fig. 1—Simplified overview of the gas-transit pipeline system.

Introduction

On the basis of recent developments, it is becoming clear that our industry has realized the immense potential offered by intelligent systems. Our daily life as petroleum professionals is full of battling highly complex and dynamic problems and making high-stakes decisions. Moreover, with the advent of new sensors that are permanently placed in the wellbore, very large amounts of data that carry important and vital information are now available. To make the most of these exotic hardware tools, one must have access to proper software to process the data in real time. Intelligent systems in their many flavors are the only viable techniques capable of bringing real-time analysis and decision-making power to the new hardware. A search of the available commercial intelligent software tools for the oil and gas industry indicates that although there are some software applications that barely scratch the surface of the capabilities of the intelligent systems (and must be commended for their contributions), the software tool that can effectively implement integrated intelligent systems in our industry has not yet made it to the commercial market.

An integrated, intelligent software tool must have several important attributes, such as the ability to integrate hard (statistical) and soft (intelligent) computing and to integrate several AI techniques (i.e., fuzzy-cluster analysis, neural computing, genetic optimization, and fuzzy inference engine). Software with the above characteristics that targets oil and gas professionals must be able to take serious steps toward changing the "black box" image that has been associated with several AI-related techniques and bring it closer and closer to a "transparent box."

Integrated Intelligent Systems

Today, intelligent systems are used in our industry in many areas. They cover higher-level issues and analyses, from predicting the natural-gas production in the U.S. for the next 15 years[4,5] and decision making at the management level while dealing with incomplete evidence[6] to more-mundane technical issues that concern geoscientists and engineers such as drilling,[7] reservoir characterization,[8-11] production-engineering issues,[12,13] well treatment,[14,15] and surface

Copyright 2005 Society of Petroleum Engineers

This is paper SPE 89033. **Distinguished Author Series** articles are general, descriptive representations that summarize the state of the art in an area of technology by describing recent developments for readers who are not specialists in the topics discussed. Written by individuals recognized as experts in the area, these articles provide key references to more definitive work and present specific details only to illustrate the technology. **Purpose:** to inform the general readership of recent advances in various areas of petroleum engineering.

***Shahab D. Mohaghegh** is a professor of petroleum engineering at West Virginia U. and founder and president of Intelligent Solutions Inc. His research and development efforts in the application of AI in the oil and gas industry date back to 1991. Mohaghegh has published more than 50 papers in this area. He has successfully applied AI techniques to drilling, completion, formation evaluation, reservoir characterization, simulation, and reservoir management. Mohaghegh has served as Technical Review Chairperson for* SPE Reservoir Evaluation and Engineering *from 1997 to 1999, as a discussion leader in SPE Forums, and as a steering committee member in SPE Applied Technology Workshops. He holds BS and MS degrees in natural gas engineering from Texas A&I U. and a PhD degree in petroleum and natural gas engineering from Pennsylvania State U.*

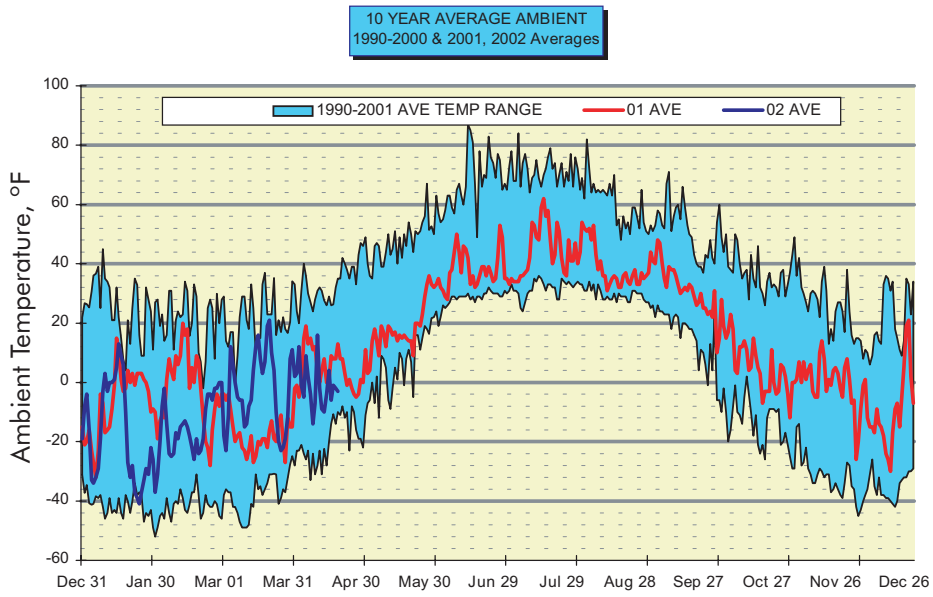

Fig. 2—Historical daily-average ambient-temperature range.

facilities,[16] to name a few. In this article, two of these applications will be reviewed to demonstrate the power of intelligent-systems techniques that address them.

Intelligent systems can be used to address many types of problems that are encountered in our industry. They can be divided into four categories:

1. Fully data driven: examples include developing synthetic well logs, reservoir characterization by correlating logs to seismic and core data, and forecasting U.S. natural-gas production.
2. Fully rule based: examples include well-log interpretation and identification of best enhanced-recovery methods.
3. Optimization: examples include surface-facility optimization for increasing oil rate and history matching.
4. Data/knowledge fusion: examples include candidate-well selection and identifying best practices.

The limit of applicability of intelligent systems in the oil and gas industry is the imagination of the professionals that use them. Like any other analytical technique, intelligent systems have limitations. It is important to understand the limitations of these techniques to increase the probability of their success and their efficiency. As an example, consider the group of techniques in intelligent systems that are developed on the basis of data, such as neural networks. These systems are vulnerable to insufficient data. In other words, the major limitation of such techniques is that they cannot be efficiently developed in cases with scarce data. A major question then will arise, "How much data is enough?" This is a question that, although it seems to be quite simple, does not have a straightforward answer.

Data, Data, Data

The question "How much data is enough?" can be answered only in the context of the problem that is being addressed. What might be enough data in one problem may not be enough for another problem. The amount of data required for modeling the behavior of a system is controlled by that system's complexity. If data are considered snapshots of reality, or "formalized representation[s] of facts" as defined in the U.S. Dept. of Justice's website, then the amount of data that is required to statistically cover a reasonable representation of a system will increase proportionally with the system's complexity. If we take the number of independent variables required for modeling a system as an indication of the system's complexity, then the number of instances of the system's behavior required for developing an intelligent system will be directly proportional to the number of variables. Simply put, as the number of variables in the data sets grows, so should the number of cases or records.

Although not all intelligent systems are fully data driven, this paper mainly concentrates on the paradigms that are used for modeling purposes and are known as data-driven solutions, such as neural networks. It has been the author's experience that developing successful neural models requires integration of fuzzy logic and genetic optimizations. It has been shown that an integrated use of fuzzy-cluster analysis and fuzzy combinatorial analysis[14] plays a vital role in developing successful neural network models. By helping the user identify the most optimum set of independent variables, fuzzy combinatorial analysis addresses the uncertainties associated with input variables during the modeling process. Fuzzy-cluster analysis can be used in a fashion to ensure that training, calibration, and verification data sets are statistically representative of the system behavior. All other issues, such as network architecture, activation-function selection, and tuning of parameters (e.g., learning rate and momentum), although important, pale when compared to these two integration techniques during the model-building process.

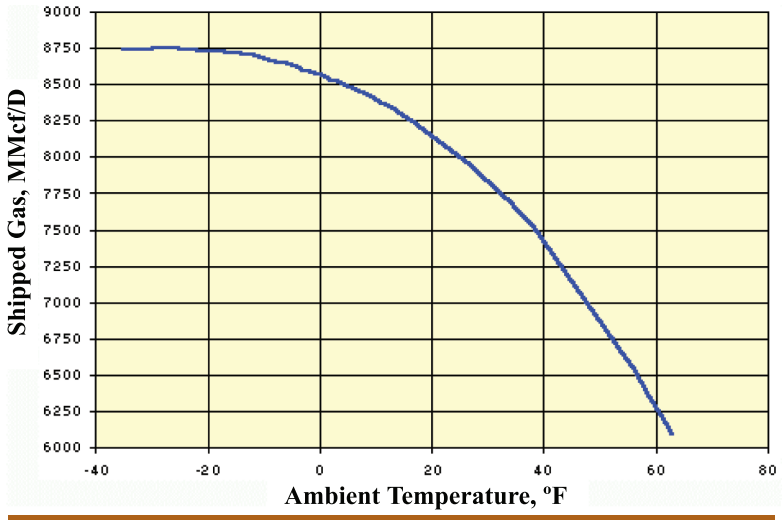

Fig. 3—Shipped gas vs. ambient temperature in 2001.

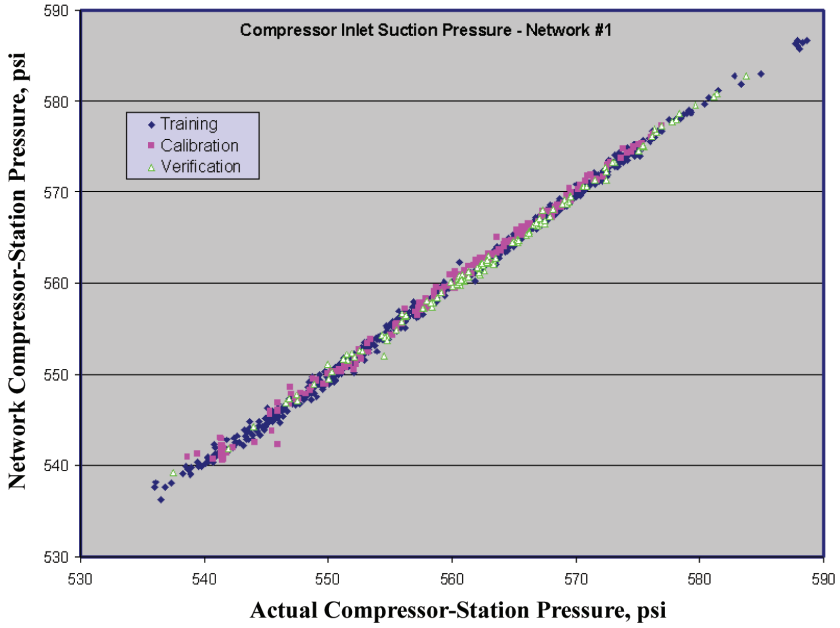

Fig. 4—Crossplot for compressor-inlet suction pressure.

Once intelligent systems are identified as the main tool for solving a certain problem, an important but implicit assumption is made. It is assumed that all the intricacies, nonlinearity, and complexity of the system behavior (that is being modeled for prediction purposes) can be represented through data that can be collected, and that it is either available or can be acquired. Furthermore, it is assumed that the sample data that will be used as the basis for modeling are statistically representative of the system.

When data become the most important component of the modeling process, certain issues must be addressed. Many databases suffer from missing data that are represented by holes in the data matrix. In cases of hard-to-obtain data, being able to patch holes in a database in a way that does not harm the integrity of the entire database can prove very valuable. Currently the only way to deal with such a problem is statistical averaging, a technique that leaves much to be desired. The next issue is outliers. One must be able to identify and deal with outliers in the database. Domain expertise can help in identifying anomalies in the data and passing judgment regarding whether an anomaly is an outlier or an important but unique behavior that must be considered. In the next sections, two recent applications of intelligent systems in oil-and-gas-related problems are covered briefly.

Prudhoe Bay Surface-Facility Modeling

Prudhoe Bay has approximately 800 producing wells flowing to eight remote, three-phase separation facilities (flow stations and gathering centers). High-pressure gas is discharged from these facilities into a cross-country pipeline system flowing to a central compression plant. **Fig. 1** illustrates the gas-transit network between the separation facilities and the inlet to the compression plant.

Ambient temperature has a dominant effect on compressor efficiency and, hence, total gas-handling capacity and subsequent oil production. **Fig. 2** illustrates the range of daily average temperatures during 1990–2000 and the actual daily average for 2001 and 2002. Observed temperature variations during a 24-hour period can be as great as 40°F.

Fig. 3 is a curve fit of total shipped-gas rate to the compression plant vs. ambient temperature for 2001. A significant reduction in gas-handling capacity is observed at ambient temperatures above 0°F. Individual well gas/oil-ratio (GOR) ranges between 800 and 35,000 scf/STB, with the lower-GOR wells in the waterflood area of the field and higher-GOR wells in the gravity-drainage area. Gas-compression capacity is the major bottleneck to production at Prudhoe Bay, and, typically, field oil rate will be maximized by preferentially producing the lowest-GOR wells.

As the ambient temperature increases from 0 to 40°F, the maximum (or "marginal") GOR in the field decreases from approximately 35,000 to 28,000 scf/STB. A temperature swing from 0 to 40°F in 1 day equates to an approximate oil-volume reduction of 40,000 bbl, or 1,000 BOPD/°F rise in temperature.

The ability to optimize the facilities in response to ambient-temperature swings, compressor failures, or planned maintenance is a major business driver for this project. Proactive management of gas production also reduces unnecessary emissions.

As part of a two-stage process to maximize total oil rate under a variety of field conditions, it first is necessary to understand the relationship between the inlet gas rate and pressure at the central compression plant and the gas rates and discharge pressures into the gas-transit pipeline system at each of the separation facilities. Therefore, the first stage of this study was to build an intelligent model that is capable of accurately predicting the state of this dynamic and complex system on a real-time basis.

Fig. 4 shows the accuracy of the predictive model that was built for the pressure at the central compression plant. Similar models were developed for rate and pressure of all the involved separation facilities.

Field oil rate is affected by the manner in which gas is distributed between facilities. A state-of-the-art genetic-algorithm-based optimization tool is built on the basis of neural-network models to optimize the oil rate. The goal of the optimization tool is to determine the gas-discharge rates and pressures at each separation facility that will maximize field oil rate at a given ambient temperature, using curves of oil vs. gas at each facility.

For this project, the development neural model started with a detailed statistical analysis of the data matrix that included patching holes in the data matrix and identifying and addressing the outliers. Next, all variables in the data matrix were analyzed with a combination of analysis of variance, fuzzy clustering, and fuzzy combinatorial analysis to examine the influence of each variable on the model output while making sure that their influences on each other are accounted for. The result was a reduction of the total number of variables that would be considered for predictive modeling. A detailed fuzzy-cluster analysis followed, this time with intention to identify the optimum number of clusters that would best describe the data matrix. Each cluster may be thought to represent a distinct set of behaviors of the system. This information is then used to guide the partitioning of the data matrix into training, calibration, and verification data sets. The fuzzy-cluster analysis provides two major benefits. First, it can guarantee that all three data sets are statistically representative, and, second, it provides the luxury of using as few data as possible for training purposes while leaving a higher percentage of the data for validation and verification of the developed model such that, in this project, less than 30% of the data was used for training.

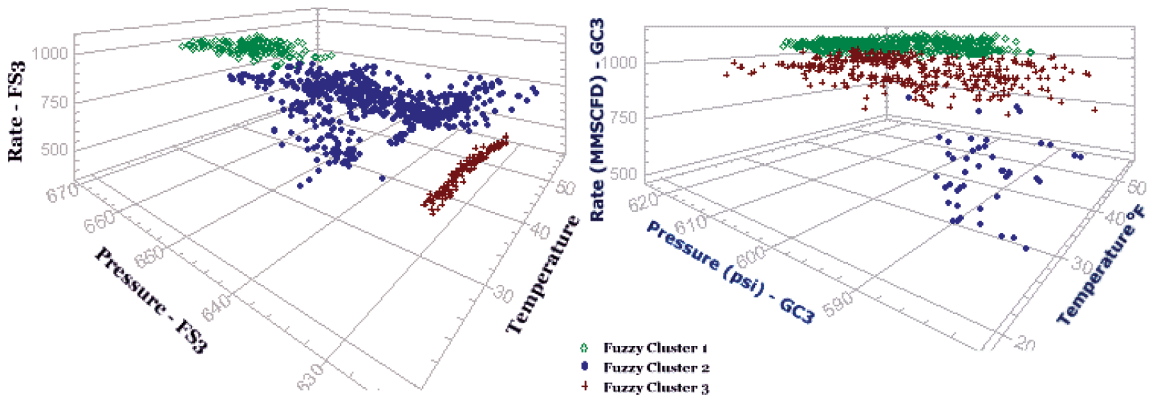

Fig. 5—Partial results of cluster analysis on the data matrix for this project.

Some typical results of fuzzy c-mean clustering analysis are shown in **Fig. 5.** This figure displays pressure/volume/temperature behavior of separation facilities FS3 and GC3. This is an essential step in developing a successful neural-network model.

It should be stressed that the neural models that are the subject of this article cannot be represented by a set of equations. Upon completion of the training process, they can be represented by a series of matrices. This is the main reason they have been referred to as black boxes by engineers who are accustomed to seeing models represented by mathematical equations. But the question is "Do they 'have to be' black boxes?" Are there ways that we can open these black boxes and peek into them to examine their validity? This author believes that, by rigorous analysis of the developed models, engineers and scientists can develop confidence in the capabilities of these models. This confidence can be gained with a thorough analysis of the neural model on the well-known physics of the problem that is being addressed, an example of which is demonstrated in **Fig. 6.**

Looking at Fig. 1, it can be seen that separation facility FS1 is connected to separation facility FS1A. As mentioned before, the dynamic-system model for this complex surface facility included a collection of several smaller but codependent models. The model developed for the separation facility can predict the rate at FS1 as a function of all the parameters that directly influence its behavior. Fig. 6 shows the behavior of the rate at FS1 and FS1A as a function of temperature.

Similar models were developed and analyses were performed for each of the components of the facility shown in Fig. 1. When applied together, they provide an accurate picture of the system's dynamics. Gas-capacity constraints start to affect oil production at approximately 0°F, with increasing effect as the temperature increases. The estimated benefit of this tool for optimizing oil rate during temperature swings and equipment maintenance is 1,000 to 2,000 BOPD for 75% of the year.

The above results show the complexity of the system being modeled as well as the power of the hybrid intelligent systems that make modeling of such complex and nonlinear systems possible. Use of conventional simulation techniques proved inadequate for a system as large and complex as the one mentioned here. The number of facilities, pipe sizes, and fittings and the rigors associated with modeling each component and coupling them all together at the end make it a difficult task. Hybrid intelligent systems on the other hand, when handled properly and with the right set of software tools, can implicitly account for all the intricacies of such a complex system as long as the collected data set is representative of the system and process behavior.

Reservoir Characterization of the Cotton Valley Formation, East Texas

The Cotton Valley formation in east Texas is known for its heterogeneity and the fact that well logs and reservoir characteristics cannot be correlated from well to well.[17] In a recent study,[10] hybrid intelligent systems were used to characterize the Cotton Valley formation by developing synthetic magnetic-resonance-imaging (MRI) logs from conventional logs. This technique is capable of providing a bet-

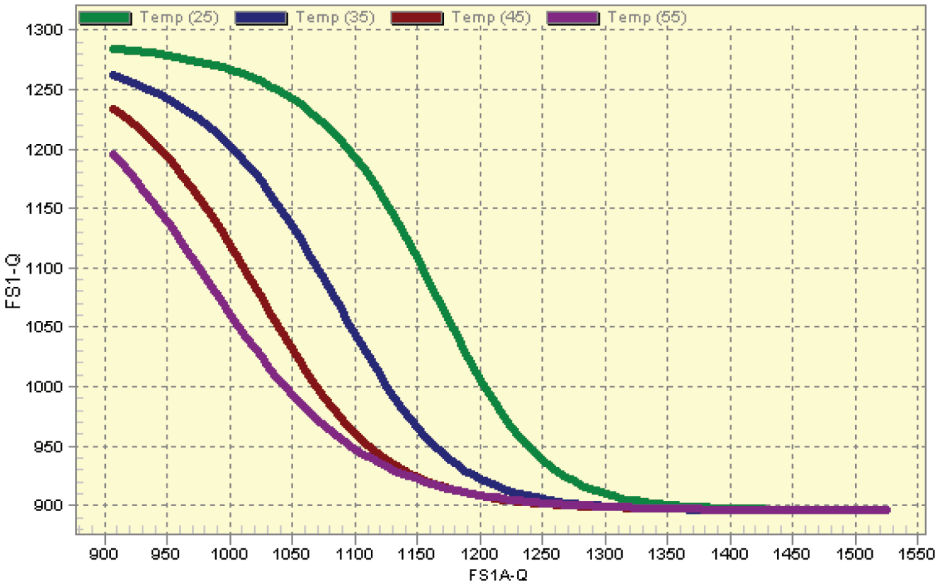

Fig. 6—FS1 and FS1A rate behavior as a function of temperature.

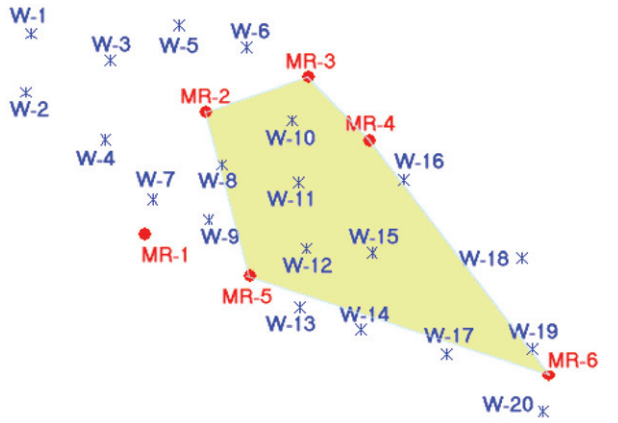

Fig. 7—Relative location of wells used in the study.

ter image of r eservoir-property (effective porosity, fluid saturation, and permeability) distribution and more-realistic reserves estimation at a much lower cost.

The study area included 26 wells. MRI logs wer e available from only six wells, while the other 20 wells had conventional logs but no MRI logs. **Fig. 7** demonstrates the relative location of the wells. In this figure, wells with MRI logs are shown with red circles and are named MR-1, MR-2, etc. W ells that have no MRI logs ar e shown with blue asterisks and are named W-1, W-2, etc. The idea is to use the six wells that have MRI logs and develop a series of intelligent models for Cotton V alley's effective porosity, fluid saturation, and permeability. The inputs to the model would be well location and conventional logs (such as gamma ray, SP, induction, and density).

Upon completion of the development pr ocess, techniques such as kriging can be used to develop a spatial distribution of these r eservoir characteristics thr oughout the domain wher e the intelligent model is applicable. One of the major contributions of this study is that MRI cannot be per formed on wells with casing in place, while many of the conventional logs used in this methodology ar e available from most of the wells in a field.

The intelligent model for this study was developed with five of the wells, MR-2 through MR-6. The MRI logs from Well MR-1 were used as blind well data to validate the applicability of the intelligent model to other wells in the field. Fur thermore, because Well MR-1 is on the edge of the section of the field being studied and is somewhat outside of the interpolation ar ea relative to W ells MR-2 through MR-6, it would push the envelope on accurate modeling. This is because the verification was completed outside of the domain in which modeling was per formed. Therefore, one may claim that in a situation such as the one being demonstrated here, the intelligent, predictive model is capable of extrapolation as well as interpolation. The term extrapolation is used here as a geometric extrapolation rather than an extrapolation of the log characteristics.

Fig. 8 shows the actual and vir tual MRI logs (MPHI—ef fective porosity, and MBVI—irr educible water saturation) for W ell MR-1. If, instead of using data fr om five wells for training and calibration, data from only one or two wells wer e used, chances ar e that the results would not have been as good as those shown in Fig. 8.

Although the quantity of training data is an important issue, the quality of data is equally important. The producing formation consists of rocks of varying quality and characteristics. Quality of data refers to representation of the highest number of rock variations and characteristics. The idea is simple; the network will perform poorly when trying to recognize rocks with characteristics that it has not been trained with. There may be special cases in which only a single well would be sufficient to represent all the available rock variations in the zone of interest. In such a case, the data from this one well would be enough to train a reasonably good network, while in other cases, data from several wells in different parts of the field would be necessary to achieve similar results. Therefore, it is not only the quantity of data but also the quality of data that is impor tant in developing intelligent models.

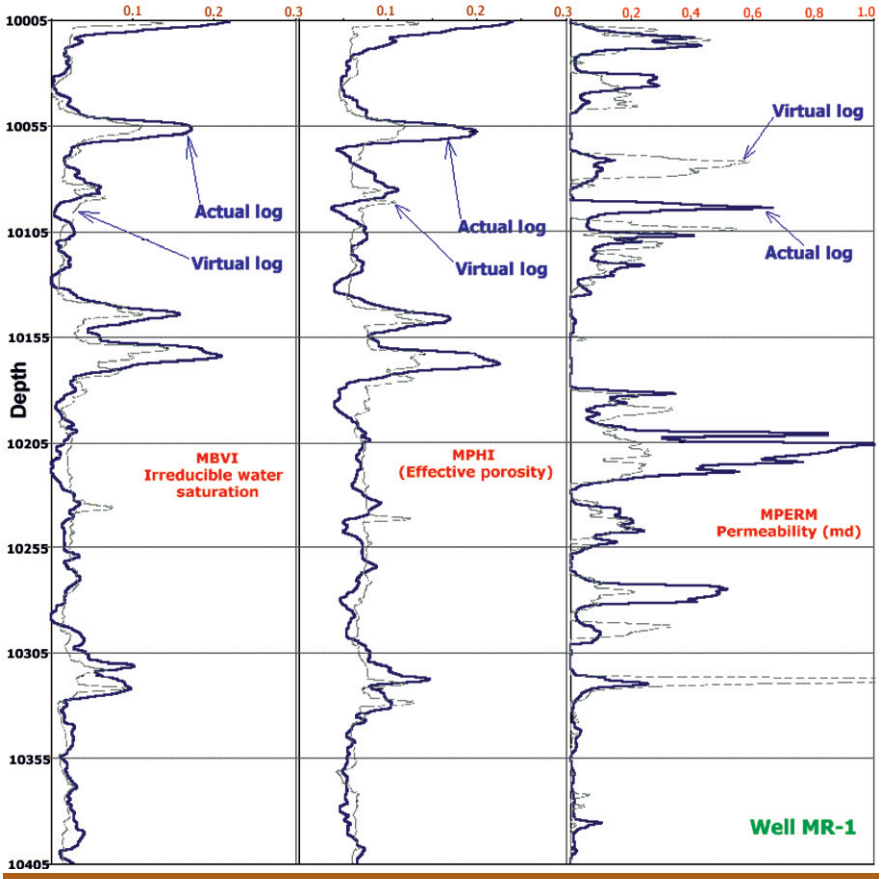

Fig. 8—Actual and modeled MRI logs for Well MR-1.

The logs shown in Fig. 8 wer e used to estimate reserves for this formation. Using the virtual MRI logs, the estimated reserves were calculated to be 138,630 Mscf/acre; while using the actual MRI logs, the calculated r eserves estimates were 139,324 Mscf/acre for the 400 ft of pay in this well. The difference between the two r eserves estimates is appr oximately 0.5%. The small dif ference in the calculated reserves estimates based on virtual and actual MRI logs, r espectively, demonstrates that operators can use this methodology effectively to reach reserves estimates with much greater accuracy at a fraction of the cost. This will allow operators to make better r eserves-management and operational decisions.

Conclusions

The major task for the petr oleum professional is to identify the type of problems that are going to benefit the most from artificial intelligence. An integrated intelligent system, like any other technology, is not going to be the panacea of our industr y, but it will play an important role in moving it into the fr ontiers of information technology. Our industry still awaits the commercialization of software applications that can bring the power of integrated intelligent systems into the mainstream of the oil and gas pr ofession. Implementation of integrated intelligent systems in our daily problem-solving efforts is only a matter time. Companies that recognize the importance of investing in this technology now will be the vanguard that will reap its benefits sooner than others. The future of this technology in our industry has never been brighter. JPT

Acknowledgments

I would like to extend my gratitude to my students and colleagues, Razi Gaskari, Andrei Popa, Carrie Goddard, and Mofazal Bhuiyan, who helped me during several studies that formed the basis of this paper. I also would like to thank Linda Hutchins and Carl Sisk of BP Exploration and Gary Cameron and Rich Deakins of Anadarko Petroleum Corp. for their contributions.

References

1. Mohaghegh, S.D.: "V irtual Intelligence Applications in Petr oleum Engineering: Part 1–Artificial Neural Networks," paper SPE 58046, *JPT* (September 2000) 64.
2. Mohaghegh, S.D.: "V irtual Intelligence Applications in Petr oleum Engineering: Part 2–Evolutionary Computing," paper SPE 61925, *JPT* (October 2000) 40.
3. Mohaghegh, S.D.: "V irtual Intelligence Applications in Petr oleum Engineering: Part 3–Fuzzy Logic," paper 62415, *JPT* (November 2000) 82.
4. Al-Fattah S.M. and Star tzman R.A.: "Predicting Natural-Gas Production Using Artificial Neural Network," paper SPE 68593 presented at the 2001 SPE Hydr ocarbon Economics and Evaluation Symposium, Dallas, 2–3 April.
5. Garcia, A. and Mohaghegh, S.D.: "For ecasting U.S. Natural Gas Production Into Year 2020: A Comparative Study," paper SPE 91413 presented at the 2004 SPE Eastern Regional Confer ence and Exhibition, Charleston, West Virginia, 15–17 September.
6. Fletcher, A. and Davis, J.P .: "Decision Making W ith Incomplete Evidence," paper SPE 77914 pr esented at the 2002 SPE Asia Pacific Oil and Gas Conference, Melbourne, Australia, 8–10 October.
7. Balch, R.S., *et al.*: "Regional Data Analysis To Better Predict Drilling Success: Brushy Canyon Formation, Delaware Basin, New Mexico," paper SPE 75145 pr esented at the 2002 SPE/DOE Impr oved Oil Recovery Symposium, Tulsa, 13–17 April.
8. Mohaghegh, S., Richar dson, M., and Ameri, S.: "V irtual Magnetic Resonance Imaging Logs: Generation of Synthetic MRI Logs From Conventional Well Logs," paper SPE 51075 presented at the 1998 SPE Eastern Regional Confer ence and Exhibition, Pittsbur gh, Pennsylvania, 9–11 November.
9. Bhushan, V. and Hopkinson, S.C.: "A Novel Appr oach To Identify Reservoir Analogues," paper SPE 78338 pr esented at the 2002 SPE European Petroleum Conference, Aberdeen, 29–31 October.
10. Mohaghegh, S.D. *et al.*: "Reservoir Characterization Thr ough Synthetic Logs," paper SPE 65675 presented at the 2000 SPE Eastern Regional Conference and Exhibition, Mor gantown, West Virginia, 17–19 October.
11. Finol, J., Romero, C., and Romer o, P.: "An Intelligent Identification Method of Fuzzy Models and Its Applications to Inversion of NMR Logging Data," paper SPE 77605 pr esented at the 2002 SPE Annual Technical Conference and Exhibition, San Antonio, Texas, 29 September–2 October.
12. Weiss, W.W., Balch, R.S., and Stubbs, B.A.: "How Ar tificial Intelligence Methods Can For ecast Oil Pr oduction," paper SPE 75143 presented at the 2002 SPE/DOE Improved Oil Recovery Symposium, Tulsa, 13–17 April.
13. Alimonti, C. and Falcone, G.: "Knowledge Discover y in Databases and Multiphase-Flow Metering: The Integration of Statistics, Data Mining, Neural Networks, Fuzzy Logic, and *Ad Hoc* Flow Measurements Toward Well Monitoring and Diagnosis," paper SPE 77407 presented at the 2002 SPE Annual T echnical Conference and Exhibition, San Antonio, 29 September–2 October.
14. Mohaghegh, S.D. *et al.*: "Performance Drivers in Restimulation of Gas-Storage Wells," paper SPE 74715, *SPEREE* (December 2001) 536.
15. Mohaghegh, S.D. *et al.*: "Intelligent Systems Application in Candidate Selection and T reatment of Gas Storage W ells," *J. of Petroleum Science and Engineering,* 2001, **31,** No. 2–4, 125.
16. Mohaghegh, S.D., Hutchins, L., and Sisk, C.: "Prudhoe Bay Oil-Production Optimization: Using V irtual-Intelligence Techniques—Stage One: Neural Model Building," paper SPE 77659 pr esented at the 2002 SPE Annual T echnical Conference and Exhibition, San Antonio, Texas, 29 September–2 October.
17. Mohaghegh, S.D. *et al.*: "Reducing the Cost of Field-Scale Log Analysis Using V irtual Intelligence Techniques," paper SPE 57454 presented at the 1999 SPE Eastern Regional Confer ence and Exhibition, Charleston, West Virginia, 21–22 October.

SPE 90266

Zonal Allocation and Increased Production Opportunities Using Data Mining in Kern River

Carrie Popa, SPE, ChevronTexaco; Andrei Popa, SPE, ChevronTexaco; Andrew Cover, SPE, ChevronTexaco

Copyright 2004, Society of Petroleum Engineers Inc.

This paper was prepared for presentation at the SPE Annual Technical Conference and Exibition held in Houston, Texas, U.S.A., 26–29 September 2004.

This paper was selected for presentation by an SPE Program Committee following review of information contained in a proposal submitted by the author(s). Contents of the paper, as presented, have not been reviewed by the Society of Petroleum Engineers and are subject to correction by the author(s). The material, as presented, does not necessarily reflect any position of the Society of Petroleum Engineers, its officers, or members. Papers presented at SPE meetings are subject to publication review by Editorial Committees of the Society of Petroleum Engineers. Electronic reproduction, distribution, or storage of any part of this paper for commercial purposes without the written consent of the Society of Petroleum Engineers is prohibited. Permission to reproduce in print is restricted to a proposal of not more than 300 words; illustrations may not be copied. The proposal must contain conspicuous acknowledgment of where and by whom the paper was presented. Write Librarian, SPE, P.O. Box 833836, Richardson, TX 75083-3836, U.S.A., fax 01-972-952-9435.

Abstract

This paper presents a fast and effective methodology to estimate zonal allocation for commingled producers in a multilayer reservoir using minimal, readily available data (well completion, historical production, sand depths, and location data). A set of data mining tools including regression, neural networks, and fuzzy logic was used to identify candidates for remedial work and the corresponding production increase expected. This approach was applied and executed in a portion of the Kern River field in California with very promising preliminary results.

Introduction

With over 8,000 active producers, 1,200 active injectors and 100 years of production history, Kern River Field presents an interesting challenge for data management and the identification of widespread production opportunities from that data. Despite this vast well count, data is remarkably complete and reliable. However, this high well count also places great demands on production engineering staff, leaving little time for in-depth analysis of this data.

The Kern River field, located in Kern County, California, is a heavy oil reservoir consisting of nine productive sands. Producers are commingled with very little individual zone production test data available. The field is currently produced by steam injection, and the primary production mechanism is gravity drainage, requiring pumps to be set at or below the bottommost oil sand to effectively produce all sands. It is often difficult or inconclusive to determine expected oil/water production by sand for remedial and completion decisions from available reservoir data alone. Often the most reliable method is a time intensive review of completion and production history for a given part of the field to infer oil/water production from each of the zones.

Problem Statement

It has long been observed that some wells in the Kern River field have high production, while nearby neighbor wells are very low producers. One hypothesis is that wells with the pump placed at the bottom of the deeper zones are consistently better producers. Although these deeper zones were targeted 15-30 years ago, the overall strategy since then has been to focus on shallower zones with higher saturation – thus overlooking the bottom sands.

With the sizeable number of wells assigned to each engineer (over 1,200), it becomes very hard to closely monitor each well, much less take the time to investigate this phenomenon. This study was initiated with the intent to use readily available production and wellbore mechanical data without complex, time-consuming reservoir studies to determine the potential of these lower zones.

Background

This paper represents collaboration between production engineering and data management personnel to identify potential opportunities for increased production using minimal amounts of data and avoiding lengthy, complex engineering and modeling analysis.

Benefiting from effective data management, data mining tools such as neural networks and fuzzy logic were rapidly utilized to determine:

- Average zonal allocation (oil and water) from lower sands
- Expected production increase from remedial work designed to effectively drain lower zones
- Prioritized list of wells to further investigate and design remedial work

Data Management. With such a high level of activity taking place in the Kern River field, highly organized electronic data is a must for the success of the field operation. Nearly three years ago, a dedicated team was established for the data management of the business unit. This team introduced a comprehensive data architecture consisting of functionally separate databases with corresponding data bridges to achieve the goals of data accuracy, completeness, and availability.

A considerable effort was then carried out to reconcile and migrate all existing electronic data from historical databases, spreadsheets, and other systems. Due to this effort, data is now available across multiple systems to all user communities (operations, engineering, and earth science). This has resulted

in more interest and occasions to query and learn from existing data.

Neural Networks. Artificial neural networks (ANNs) are one of the most popular artificial intelligence tools available. ANNs are extremely powerful for pattern recognition and non-linear, multidimensional interpolation. Neural networks use distributive parallel processing to capture existing relationships between input parameters and the output of the system. In order to achieve accurate prediction, neural networks must be trained and exposed to adequate and representative data. This study makes use of neural networks to predict the incremental oil production after well workover.

The petroleum industry has found many uses for ANNs such as reservoir characterization, hydraulic fracturing, and other optimization. Neural networks have been thoroughly covered in numerous publications and will not be be repeated here[1,2,3,4,5,6,7,8].

Fuzzy Logic. Fuzzy logic is capable of incorporating natural language to process information. This ability provides maximum efficiency in using imprecise information. In traditional set theory, either an object belongs to a set or not. In fuzzy logic, fuzzy sets are used to determine the degree to which an object belongs – an object may belong to multiple sets in varying degrees.

Many applications for fuzzy logic have been established in the petroleum industry, thus the detailed theory will not be included in this paper[4,9].

Input Data

The intent of this study was to achieve maximum knowledge about the potential of the lower sands quickly, with readily available data. It was correctly speculated by the production engineer that this goal could be accomplished using well completion, zone markers, and production data. All data items under each category are listed in Table 1, and were requested for 550 wells.

In many places, a request of this magnitude could take weeks, if not months, to gather the information from a variety of digital and physical sources. For this request, two structured databases were queried with little effort, and the results were returned to the engineer within the same day.

Well Completion Details. Well completions vary around the field and are a function of location, year drilled, and original intent of the well. Typically, most wells are in 2½ acre five-spot or nine-spot patterns. This configuration is designed for successful steamflood operations.

Most of the producing wells drilled since the 1970s have 7-inch 23# casing cemented to total depth and perforated with four ½-inch jet holes per foot (JHPF) in all of the oil sands. Injectors were completed with 5½-inch 17# casing cemented to total depth. Over time, numerous injectors were converted to producers and perforated similarly with four ½-inch JHPF. The third most common type of completion is a liner. These wells usually have 8⅝-inch 32# casing cemented to 300–400 feet with a 6⅝-inch slotted liner completion below the casing. In addition to these types of completions, many innerliners have been run in wells for sand control since initial completion. As a result, there is a significant number of wells with either 7-inch casing or 6⅝-inch liner with a 5½-inch innerliner.

Sand Markers. Each well drilled in the field has a gamma ray or spontaneous potential log as a minimum. Using this information, field geoscientists have selected picks/markers for the top of each sand interval. These markers are field wide and available in database format. For this study, the marker depths were matched against perforation and pump depths to determine which zones were open in every well of the study area.

The Kern River reservoir has eight major producing sands: C, C1, G, K, K1, R, R1, and R2. The lower zones under investigation in this study are the R sands (R, R1, and R2). The R sand is about 95 feet thick with very little intercalation of shales. Typically, at least 75 feet of perforations are shot in this sand. The R1 sand is approximately 100 feet thick. The thickness of R2 varies across the field and has significant water influx in areas due to an underlying aquifer.

Well Production Indicators. Three sets of production parameters were originally gathered for this study: last well test oil and water, 30-day average oil and water, and 6-month average oil and water. After a thorough analysis, it was concluded that the 6-month averages were in good agreement with the 30-day averages. Since little knowledge would be gained from using both 6-month and 30-day averages, it was decided to use only the more recent 30-day averages.

Next, the 30-day averages were compared against the last well test values. Inaccuracies and fluctuations of the gauging system seemed to cause discrepancies between the two data sets. Consequently, there was concern that the last well test contained significant noise, which may not be representative of overall well performance and could introduce errors into the neural network model. It was decided to eliminate last well test oil and water from the dataset as well.

Data Quality Control. As with any database, the accuracy of the data is never exactly perfect. Errors exist largely due to data entry. Several steps were taken to preserve the integrity of the existing data, identify circumstances that may impact the project, and eliminate any outliers.

The original data set contained 550 wells; however, a recently implemented steamflood in a segment of the study area affected 207 wells. These wells would complicate the review process; therefore, they were eliminated from the data set.

The next step of the quality control process was the correction of inconsistencies found in the database (i.e. pump depth deeper than effective depth). Finally, outliers were identified and removed. For this study, an outlier was considered to be a well with significantly higher production compared to the accepted average production range. This resulted in the identification of only six wells; it is believed that these wells intercept a sand channel or other significant system of microfractures and are therefore not representative of the overall data set. Therefore, these records were removed and not considered in the analysis. The final data set consisted

of 337 records, each corresponding to a well in the project area.

Techniques used for data quality control and data validation have been presented in detail in previous papers by Mohaghegh and Popa[1,2]. These techniques make use of regression plots, frequency distribution plots, and fuzzy curve analysis.

Opportunity Identification Using Data Mining

This study was initiated based on the observation that some wells are high producers while adjacent neighbor wells are very low producers. Figure 1 shows the frequency distribution of number of wells with thirty-day average oil production. Figure 2 shows the ranked regression distribution of thirty-day average production. These plots indicate that more than 50% of the wells in the area of study produce less than 10 barrels of oil per day.

This posed the question: since the wells are so close, what controls well productivity? The first indicator to shed some light was the pump depth. Figure 3 shows a scatter plot of thirty-day average oil production versus pump depth. It can be clearly seen that wells with deeper pumps show the highest production. However, since the reservoir in this area dips 6 degrees from east to west, absolute depth values do not provide the whole picture – plotting pump depth in relation to zones was essential.

Since it appears that 1000 feet (approximately the top of the R sand) represents a defining depth in Figure 3, pump depth was plotted versus top and bottom of the R sand (Figure 4). The graph shows that more than one-third of the wells have the pump depth above the top of the R sand. Figure 3 and Figure 4 show high correlation since together they reflect that low rate producers have the pump depth above the R sand.

Plotting wellbore mechanical data and production data resulted in learning powerful information related to fluid inflow and reservoir behavior. At this point, pump depth was identified as the main driver for high producing wells.

Methodology

The process described in this paper consists of two parts: production increase identification and wellwork candidate selection. The production increase identification involves grouping the wells into clusters based on pump depth and production. Statistics from these groupings helped to determine the amount of oil produced from the R sands.

The wellwork candidate selection uses a neural network model to predict the expected daily oil production for all wells not effectively draining the R sands. The expected oil production is then fed into the fuzzy expert system together with a risk factor based on the completion type. The expert system ranks the candidates based on this information and provides a prioritized list of wells for the engineer to review, write remedial programs, and perform economics.

Data Clustering. In order to extract more information about performance and reservoir potential, it was decided to define four groups of wells based on production and pump depth in relation to the R sand.

For clustering analysis, the depth scale for each well was zeroed at the middle of the R sand as the reference depth. Thirty-day average oil production was ploted versus the difference between pump depth and depth to the middle of the R sand for each well in Figure 5. A negative depth corresponds to a pump above the middle of the R sand, while a positive depth denotes a pump below mid-R.

Four clusters were differentiated:

C1: Wells with < 10 BOPD and pump above mid-R sand
C2: Wells with ≥ 10 BOPD and pump above mid-R sand
C3: Wells with < 10 BOPD and pump below mid-R sand
C4: Wells with ≥ 10 BOPD and pump below mid-R sand

Figure 6 shows the areal distribution of the above clusters for the studied area. The map shows a uniform distribution of high producers around the area. However, there is a high density of low producing wells on the west side of the studied area. Many of these wells are not effective in the deeper sands that exhibit high fluid inflow.

Data Mining Results. Table 2 presents some brief statistics of the study. The average production of the 159 wells that have the pump set above the middle of the R sand is 4.3 BOPD, while the average production for the 178 wells with the pump below the middle of the R sand is 13 BOPD. Of these 178 wells with the pump below mid-R, there is a significant number (77 wells) that make less that 10 BOPD. A closer inspection of these wells shows that not quite half are completed with innerliners, which consistently underperform casing completions. It was then discovered that other wells have the pump placed below mid-R despite the fact that there are few open perforations in the R sands. This indicates that these wells may not be effectively draining the R sands and may have additional potential.

These figures indicate that half of the total daily production in this area, 1600 barrels of oil per day, is being produced from the R, R1, and R2 sands. Taking open perforations into account, a well that is effectively draining the R sands makes on average nearly 15 BOPD more than a well producing above the R sands.

Using merely the statistics from the clusters presented in Table 2, if the 159 wells with the pump set above mid-R had workovers to effectively drain the R sands, an additional 1,300 BOPD would result. Using more aggressive figures that include many of the 77 wells with the pump set below mid-R but not effectively draining the R sands, an upside potential incremental of 3,000 barrels of oil per day exists.

Clearly, the above stated numbers are ideal cases, which assume that all wells are good candidates for workover, there is no interference, and all wells with remedial jobs will be successful. Considering this information, a conservative 1,000 BOPD potential increase in production is anticipated in the project area.

Neural Network Model. Once the potential increase in production was identified, the next step is an efficient workover candidate selection technique, the first part of which is a neural network model. In the absence of reservoir simulation or other time-consuming analytical methodologies that rely on reservoir data, a neural network predictor model was developed. This module is a powerful tool used to predict the expected production if the well would efficiently drain the R sands. The neural net capability is based the information

found from the cluster analysis in Table 2 and on the observed strong relationship between wellbore mechanical and production data.

After a thorough analysis of the entire dataset presented in Table 1, it was determined that eight parameters were most influential in predicting oil production. These parameters were used in the final rendering of the neural network model: bottomhole latitude, bottomhole longitude, casing size, minimum liner/innerliner size, effective depth, pump depth, depth to the top of the R sands, and perforated footage in the R sands. The neural network output is the 30-day average oil production.

The data set consisting of the 101 wells in cluster 4 was divided in three sets: training, calibration, and verification. As the names suggest, the training and calibration sets were used in the training procedure while the verification set was used to check the accuracy of the prediction. Different percentages for training, calibration, and verification sets were tried during the training process. The most confident results were obtained using 73 percent of data for the training set, 16 percent for the calibration set, and 11 percent for the verification set.

Several types of neural networks were also tested. The best results used a back propagation network and three hidden layers with different activation functions. The input layer consisted of the above-mentioned inputs while the output layer consisted of only one parameter, average daily oil production.

The final neural network presented an R^2 of 0.801 and a correlation coefficient of 0.872 for the training set. Figure 7 shows the daily oil production predicted by the neural network compared with actual 30-day average oil production values for the training set. The calibration set presented an R^2 of 0.73 and a correlation coefficient of 0.88, representatively shown in Figure 8. The confidence of the neural network was given by the verification set, which represents data that the neural network has never seen before. Figure 9 presents the response of the neural network when presented with the verification set. It should be noted that the predicted oil production rate is in good accordance with the actual 30-day average oil production with few exceptions. The R^2 value was 0.78 while the correlation coefficient was 0.911.

From the three above-mentioned figures, it can be seen that the neural network is capable of capturing the production behavior in different zones of the area of study. While the majority of the error values fell within two barrels (plus or minus), a few higher differences were observed. Because the 10-25 BOPD range had the highest frequency of records, it is to be expected that the neural network would closely model this behavior. Since there were few wells producing more than 30 BOPD, the neural network had insufficient data from which to learn. In these cases, the neural net became conservative in its predictions and underestimated the expected values. For this study, this is a favorable response, since it is unlikely that many wells will exceed 30 BOPD and overestimation of the forecast is not desired.

Fuzzy Expert System. The fuzzy expert system is the second piece of the wellwork candidate selection. Three parameters are used in conjunction with a set of rules to provide help to the engineers by ranking the high potential workover candidates. This will give the engineering staff a prioritized list of wells to review, write remedial programs, and finalize economics.

The first input parameter is total expected daily oil production, which is the output from the neural network. Secondly, the fuzzy system uses incremental oil as a measure of the increase over current production. The third and final parameter represents the risk associated with each well based on the current completion type and is a combination of total depth, effective depth, smallest casing/liner/innerliner diameter, and damage. This risk factor is meant to incorporate the chances of remedial success, as a result of the impact of the current completion. For example, workovers in 5½" casing have proven to have a higher chance of failure and cannot be sidetracked; therefore, risks and costs are higher and may necessitate a replacement well to drain the deeper sands. Another example of current wellbore status affecting remedial work is casing or liner damage – if damage is severe, certain tools may not be able to enter the wellbore thus requiring a sidetrack (riskier and higher cost). A final example is the difference between effective depth and total depth – the higher the footage to be cleaned out, the lower the chances of a successful workover. This also increases the chances of an expensive and risky fishing job.

The fuzzy system includes 27 rules that are qualified using a set of three truth functions. Figure 10 shows the rule set while Figure 11 displays the fuzzy sets for the risk indicator. By applying the parameter-based rules, the output of the fuzzy expert system defines each well as high, medium, or low priority. The strength of each output is given by the degree of confidence.

The fuzzy expert system, using the engineering knowledge incorporated in the rules, establishes a standard selection process which is unbiased by human interaction. This is extremely beneficial and crucial when the candidate selection includes a large number of wells.

Remedial Recommendations. After the fuzzy expert system generates the prioritized list of wells for review, it is up to the engineers to make the recommendation to work on the well.

There are several different reasons why the pump depth is above the middle of the R sand: total depth is shallower than mid-R (particularly for liner completions); wells were sanded back when upper sands were steamflooded; casing damage prevents the pump to pass through, wells are plugged back to shut off high water production from R2 sand; and others. In addition, there are also wells that have been drilled deep enough, but were never perforated in R sands.

Based on these existing conditions, several types of workover can be defined:

1. Clean-out and lower pump
2. Clean-out, perforate and lower pump
3. Remove innerliner or packer left in the hole, perforate and lower pump
4. Deepen well through TD
5. Sidetrack

The five categories presented above are ordered from cheapest to most expensive. Once the well is identified for workover, the well file is researched for damage or other specific conditions. A flow chart was developed to select the best workover type depending on the current completion.

Using this flowchart and engineering knowledge, the workover type is determined, the remedial program is written, and job costs are estimated for the well. The costs for the workover types described above vary from $5,000 to $40,000. Final economics are run for each well to confirm profitability.

Results

This opportunity identification and candidate selection methodology has been applied to the area of study. The engineer is currently reviewing the wells and making recommendations on remedial work. An initial package consisting of 25 wells has been approved and is currently being executed. To date, 19 remedial jobs have been completed with considerable success. The following are the details of four workovers that are representative of the overall preliminary results.

In the first example, Well #1, a remedial job was completed to clean out, perforate and lower the pump. The neural network estimated a production increase of 8 BOPD. As seen in Figure 12, the actual incremental was 7 BOPD.

Well #2 has been producing 2 BOPD for the past two years. A workover was performed to remove the packer, perforate, and lower the pump. The neural network predicted a daily oil production of 15 BOPD. Currently the well is producing only 11.5 barrels; however, this conclusion may be premature since Figure 13 shows that production is still rising.

Well #3 presents an example that was identified for workover prior to this study. The results of the remedial program are presented in Figure 14. The well was producing around 5 BOPD; a workover was done to clean out and lower the pump. Production jumped to 28 BOPD. Since then, production is still climbing and is currently at 34 barrels. Subsequently, the neural network model was applied and predicted a daily production value of 26 barrels of oil per day. Although the neural net slightly underestimated production, the values are within a range that would not have changed the initial decision to work on the well.

The fourth and final example can be seen in Figure 15. Well #4 has been production 1 BOPD for the past two years. The neural network predicted an incremental production of 15 BOPD, and a remedial job was written to clean out and lower the pump. The current production after the job is 12 BOPD, and production is still climbing after more than one month.

Conclusions

Data mining proved to be a useful technique for examining large data sets and quick screening of the high number of wells for potential opportunitity. Using only completion, production, zone tops, and location data, we were able to accomplish the following:

1. Establish zonal allocation without reservoir indicators or isolated zonal production tests.
2. Identify the opportunity for increased production by recognizing patterns within the large dataset.
3. Build a neural network model to estimate production gain from remedial work without significant reservoir data.
4. Establish a standard, unbiased prioritization list for workover candidates using fuzzy logic rules.
5. Complete and execute an initial package of remedial jobs. Lucrative preliminary results have triggered the expansion of this study to larger areas of the field.

An added benefit of this study is that the zonal allocation, opportunity identification, incremental production predictor, and fuzzy logic prioritization were completed in less than one week – a tribute to the value of effective data management and the use of data mining tools.

Acknowledgments

The authors would like to thank ChevronTexaco for allowing the publication of this work. Special thanks to Mr. Gerry Hall, Mr. Greg Emerson, and Mr. Terry Thompson for encouraging us in the efforts of finding potential production increase.

References

1. Popa, A., Mohaghegh, S., Gaskari, R., Ameri, S.: "Identification of Contaminated Data in Hydraulic Fracturing Databases: Application to the Codell Formation in the DJ-Basin", SPE 77597, Proceedings, 2003 SPE Western Regional/ AAPG Pacific Section Joint Meeting, 19-24 May, Long Beach, California.
2. Mohaghegh, S., Popa, A., Gaskari, R., Ameri, S., and Wolhart, S.: "Identification of Successful Practices in Hydraulic Fracturing Using Intelligent Data Mining Tool; Application to the Codell Formation in the DJ-Basin", SPE 77597, Proceedings, 2002 SPE Annual Technical Conference and Exhibition, 29 September-2 October, San Antonio, Texas.
3. Mohaghegh, S., Popa, A., Mohamad, K., and Ameri, S.: "Performance Drivers in Restimulation of Gas Storage Wells", SPE 57453, Proceedings, 2003 SPE Eastern Regional Conference and Exhibition, 21-22 October, Charleston, West Virginia.
4. Mohaghegh, S., Reeves, S., and Hill, D.: "Development of an Intelligent System Approach for Restimulation Candidate Selection", SPE 59767, Proceedings, 1999 SPE Gas Technology Symposium, 3-5 April, Calgary, Canada.
5. Hosn, N., Popa, A., Popa, C.G.: "A New and Realistic Approach to Pumping Unit Optimization through the Use of Intelligent Systems", SPE 72360, Proceedings, 2001 SPE Eastern Regional Conference and Exhibition, 17-19 October, Canton, Ohio.
6. He, Z., Yang, L., Yen, J., and Wu C.: "Neural-Network To Predict Well Performance Using Available Field Data", SPE 68801, Proceedings, 2001 SPE Western Regional Meeting, 26-30 March, Bakersfield, California.
7. Coste, J.F., Valois, J.P., Mouret, Cl., Guittard, M., and Daniel, O.: "Data Mining Techniques For Optimizing Fast Track Re-engineering of Mature Fields", SPE 78333, Proceedings, 2002 13th European Petroleum Conference, 29-31 October, Aberdeen, U.K.
8. Ali, J.K.: "Neural Networks: A New Tool for the Petroleum Industry?", SPE 27561, 1994 European Petroleum Computer Conference, Aberdeen, U.K., 15-17 March.
9. Ross, T.J.: "Fuzzy Logic with Engineering Applications", McGraw Hill Inc., 1995.

Tables

Table 1: Input Data Gathered for Study

Category	Parameter	Description
Well Identifier	WellName	Commonly used well name
	API	API number
	BottomLatitude	Latitude of the well at the bottomhole
	BottomLongitude	Longitude of the well at the bottomhole
Zone Data	TopR	Measured depth to the top of the R sand, ft
	TopR1	Measured depth to the top of the R1 sand, ft
	TopR2	Measured depth to the top of the R2 sand, ft
	hR	Thickness of the R sand, ft
	hR1	Thickness of the R2 sand, ft
	hR2	Thickness of the R2 sand, ft
Well Completion Data	hpR	Total footage perforated in the R sand, ft
	hpR1	Total footage perforated in the R1 sand, ft
	hpR2	Total footage perforated in the R2 sand, ft
	TD	Total depth of the well measured during original drilling, ft
	ED	Current effective depth of the well, ft
	PumpDepth	Current pump depth intake, ft
	CasingSize	Diameter of the production casing, in
	LinerSize	Diameter of the slotted liner (if present), in
	InnerlinerSize	Diameter of the innerliner (if present), in
	Damage	Minimum depth of recorded casing damage, ft
Production Indicators	LastOil	Measured oil from last well test, BOPD
	LastWater	Measured water from last well test, BWPD
	30DayOil	Average oil production over last 30 days, BOPD
	30DayWater	Average water production over last 30 days, BWPD
	6MonthOil	Average oil production over last 6 months, BOPD
	6MonthWater	Average water production over last 6 months, BWPD

Table 2: Oil and Water Production Values by Cluster

Cluster	Description	Number of Wells	Innerliner Wells	Average Oil Per Well, BOPD	Average Water Per Well, BWPD	Total Oil, BOPD	Total Water, BWPD
C1	<10 BOPD, pump above mid-R	140	53	3.1	49.0	441.0	6,814.0
C2	≥10 BOPD, pump above mid-R	19	4	12.9	205.0	246.0	3,891.9
C3	<10 BOPD, pump below mid-R	77	30	4.6	147.0	360.1	11,347.0
C4	≥10 BOPD, pump below mid-R	101	14	19.3	287.0	1,950.0	29,009.0
C1 & C3	Total < 10 BOPD	217	83	3.7	83.7	801.1	18,161.0
C2 & C4	Total ≥ 10 BOPD	120	18	18.3	274.2	2,196.0	32,900.9
C1 & C2	Total pump above mid-R	159	57	4.3	67.3	687.0	10,705.9
C3 & C4	Total pump below mid-R	178	44	13.0	226.7	2,310.1	40,356.0
All	**Total**	**337**	**101**	**8.9**	**151.5**	**2,997.1**	**51,061.9**

Figures

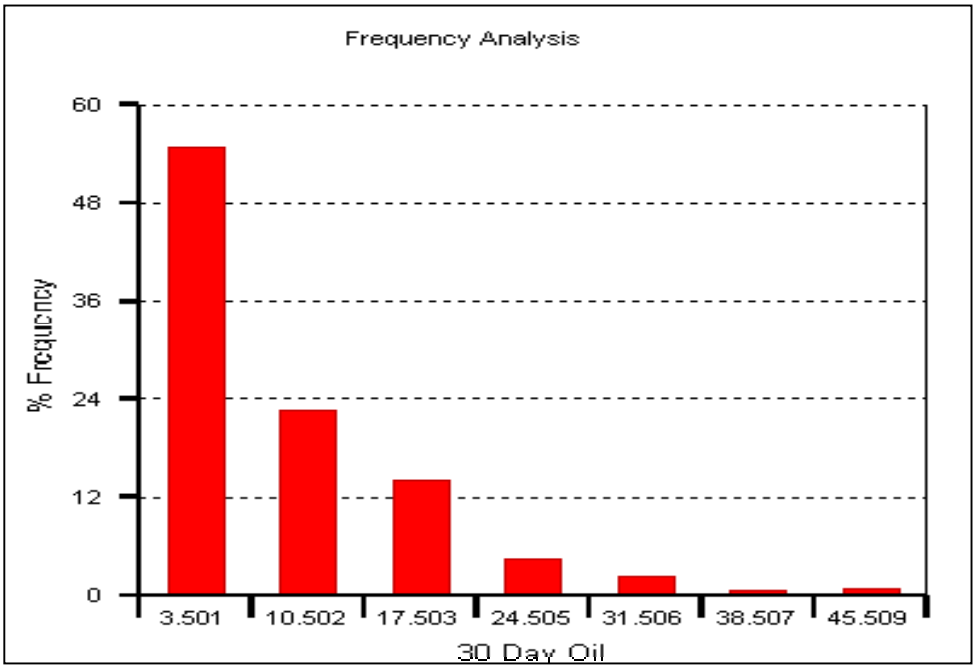

Figure 1: Frequency Distribution of 30-Day Average Production

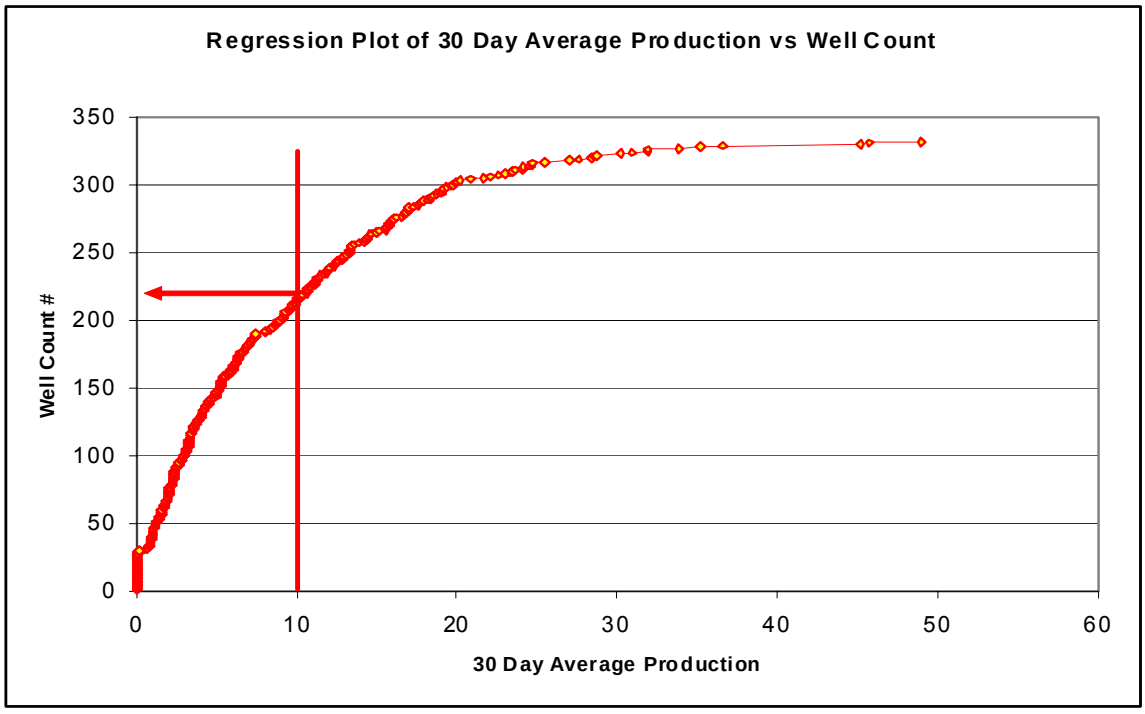

Figure 2: 30-Day Average Production vs. Well Count

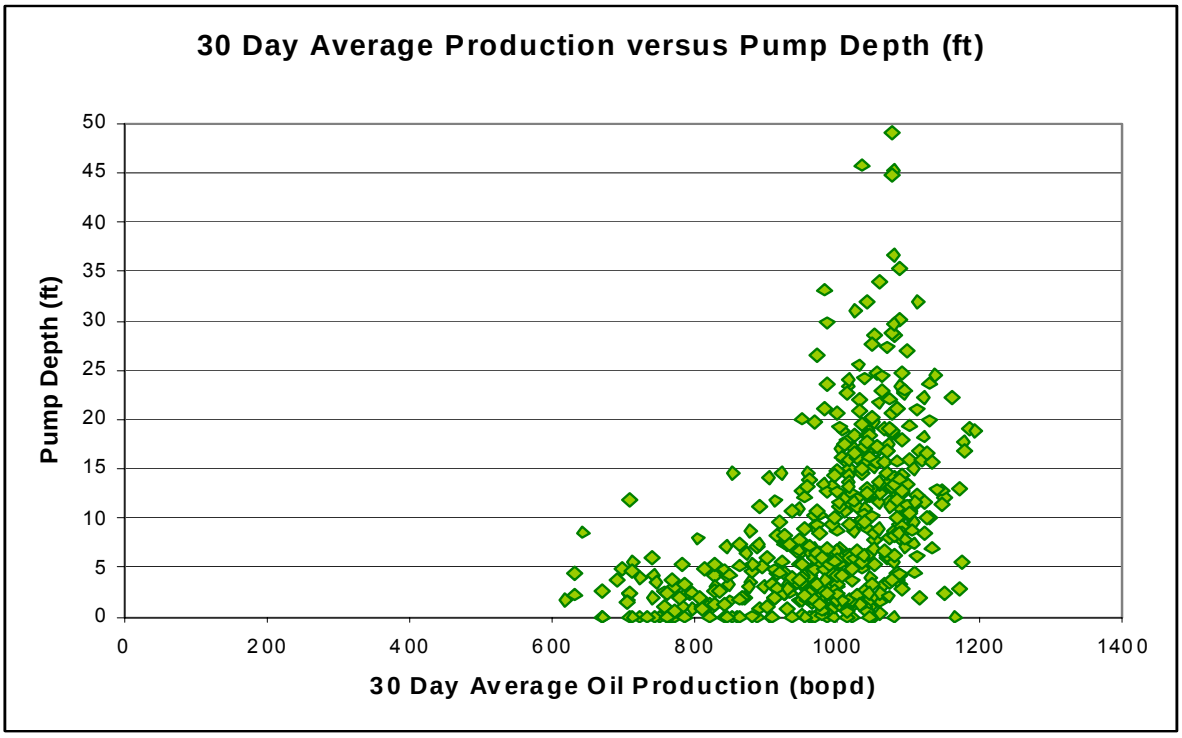

Figure 3: 30-Day Average Oil Production vs. Current Pump Depth

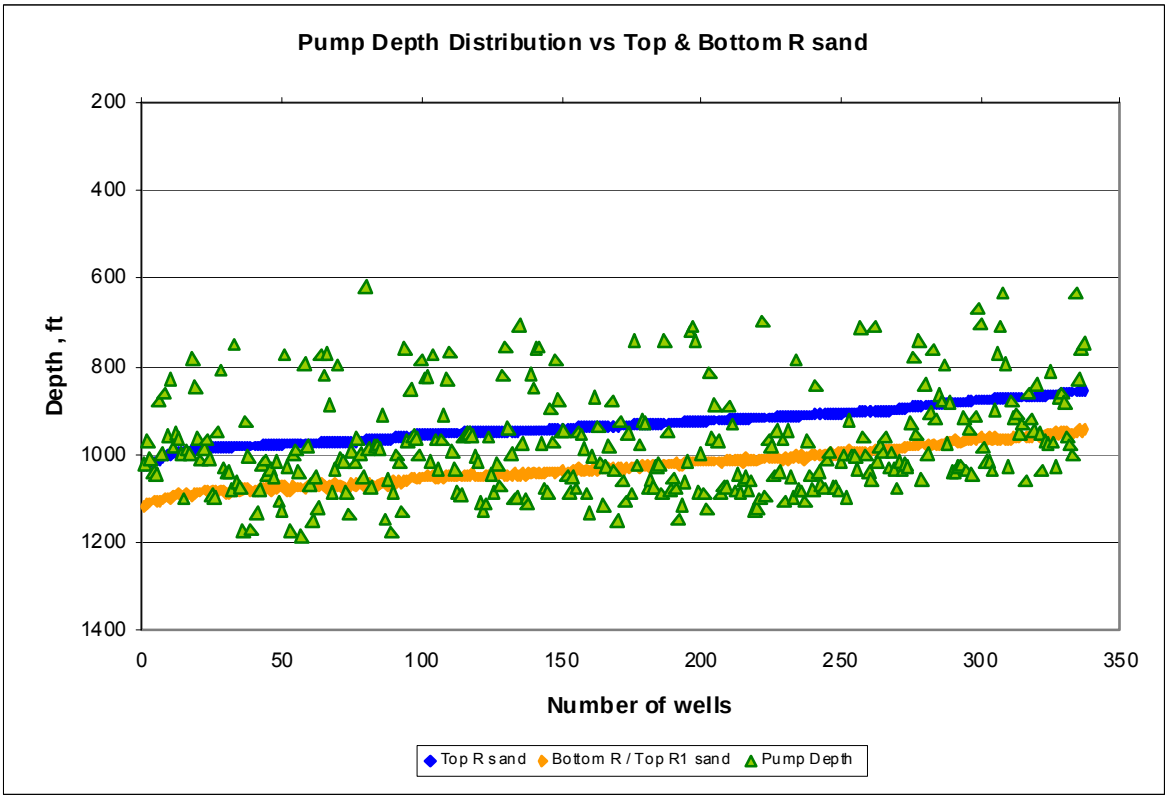

Figure 4: Pump Depth Distribution in Relation to Top and Bottom of R Sand

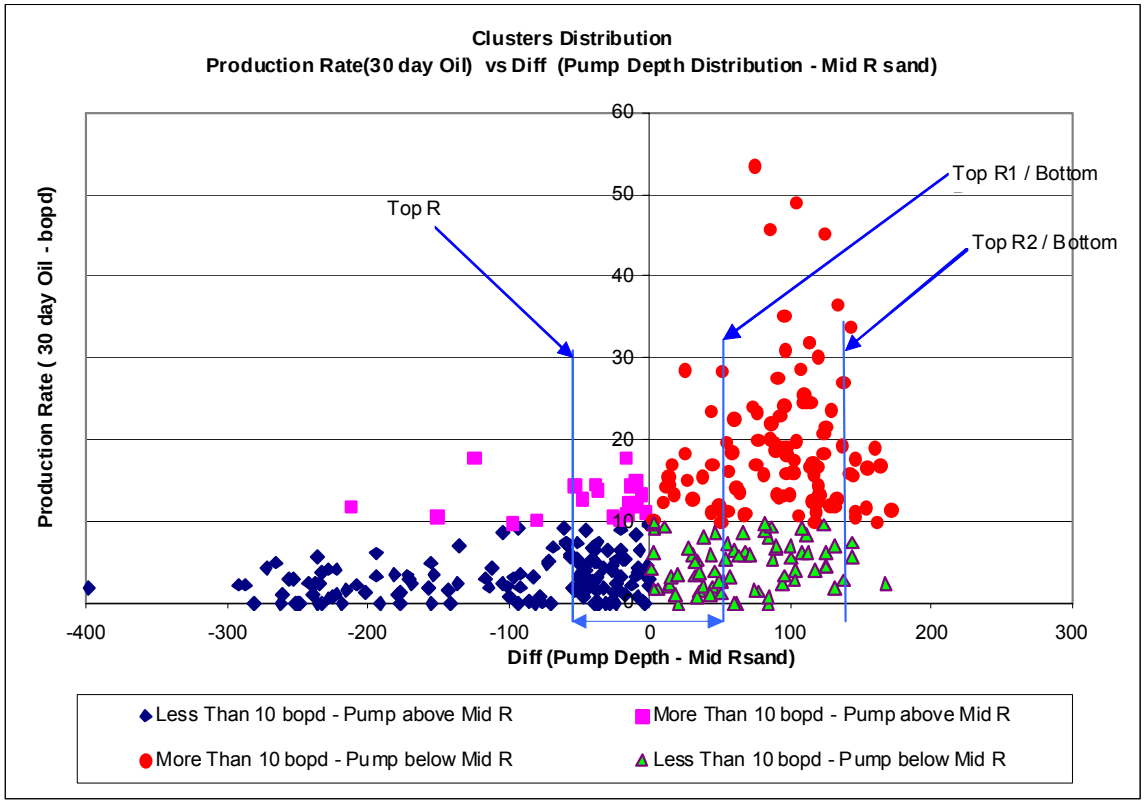

Figure 5: Cluster Determination Based on Production and Pump Depth in Relation to Mid-R Sand

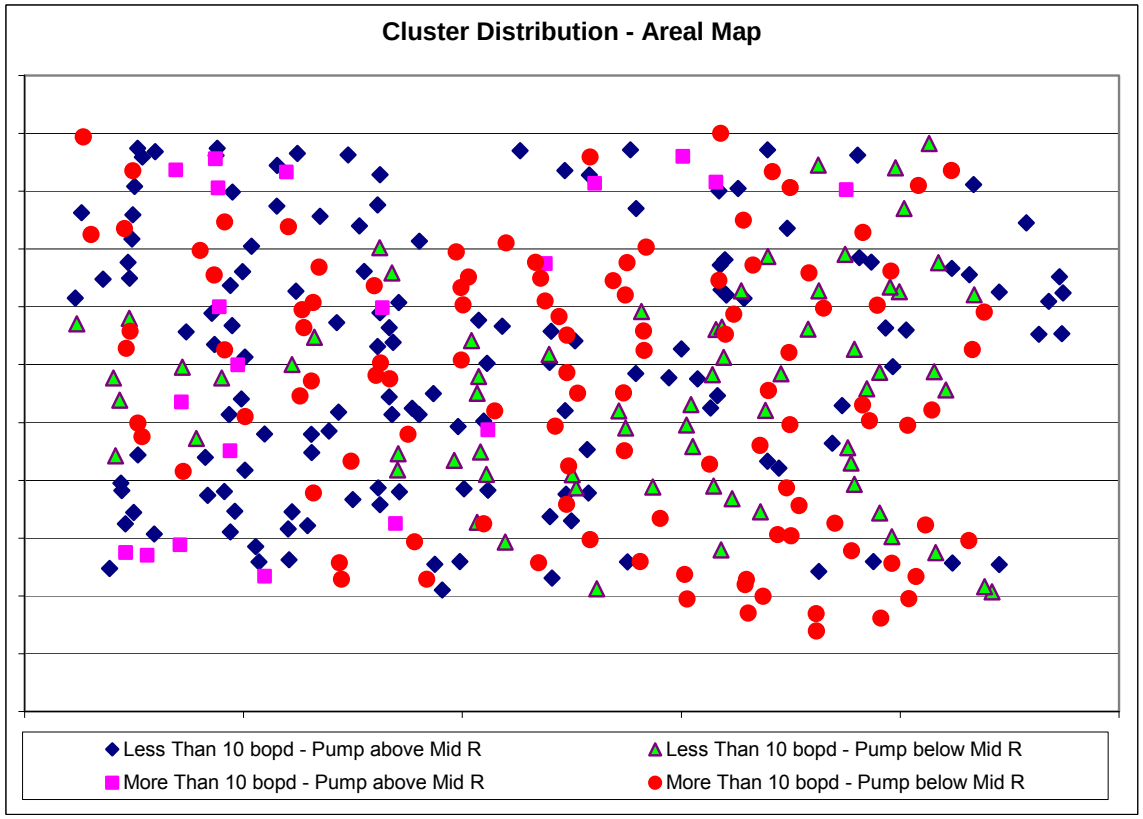

Figure 6: Areal Distribution of Clusters

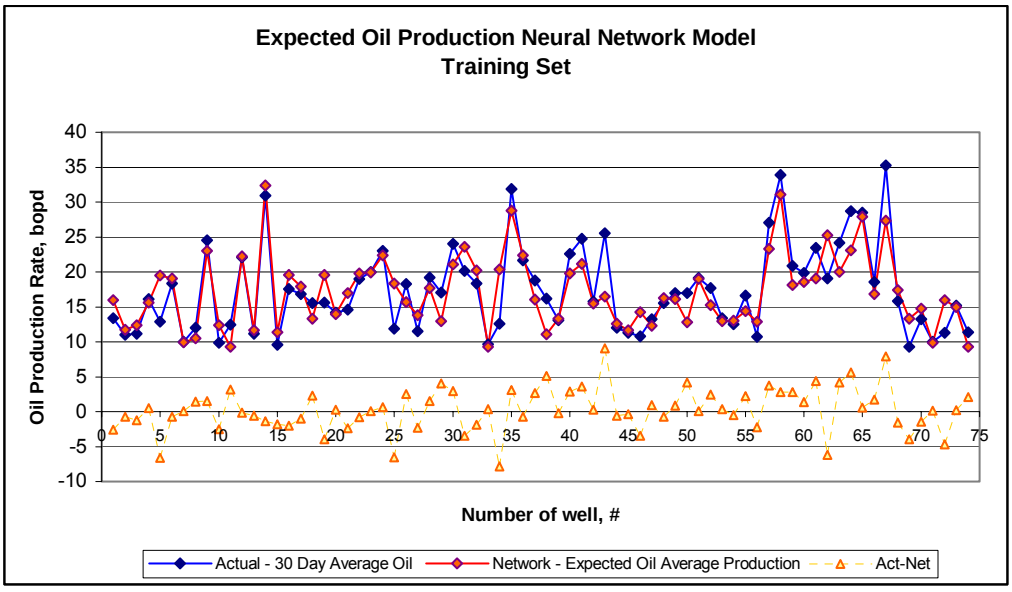

Figure 7: Neural Network Predicted Oil Production vs. Actual for Training Set

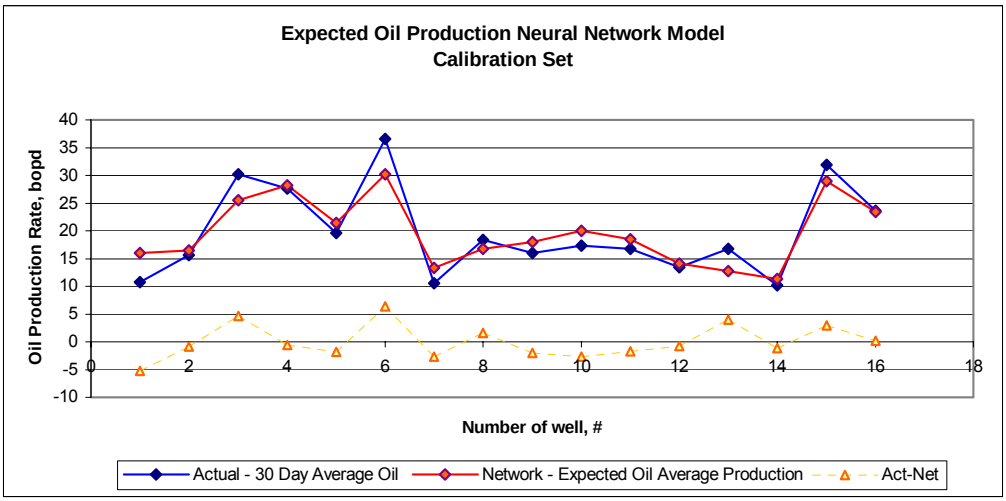

Figure 8: Neural Network Predicted Oil Production vs. Actual for Calibration Set

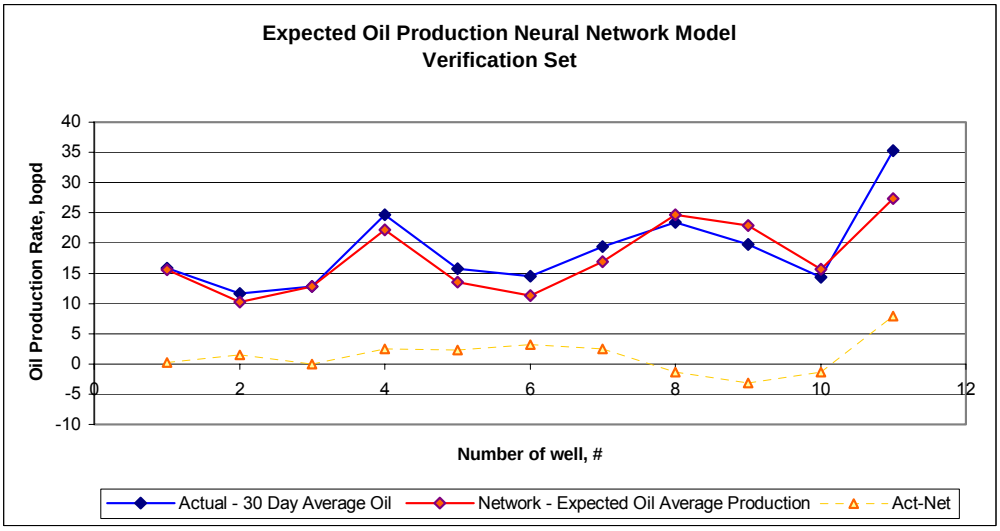

Figure 9: Neural Network Predicted Oil Production vs. Actual for Verification Set

		Risk Indicator				Risk Indicator				Risk Indicator		
		Low	Medium	High		Low	Medium	High		Low	Medium	High
Delta(Actual Oil - NN Predicted Oil)	Low	Medium	Medium	Low	Low	Medium	Medium	Low	Low	Medium	Medium	Low
		T	FT	VT		T	FT	VT		VT	FT	VT
	Medium	Medium	Medium	Low	Medium	High	High	Medium	Medium	High	Medium	Medium
		T	FT	T		VT	T	FT		T	T	FT
	High	High	High	Low	High	High	High	Medium	High	High	High	Medium
		VT	VT	VT		VT	VT	T		VT	VT	T
		Predicted NN Production - LOW				Predicted NN Production - MEDIUM				Predicted NN Production - HIGH		

Figure 10: Rules for Fuzzy Expert System

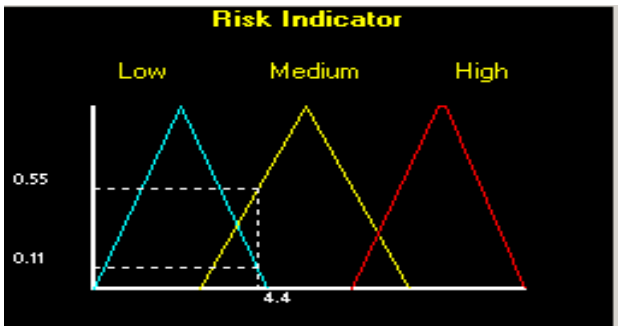

Figure 11: Fuzzy Set for Risk Indicator

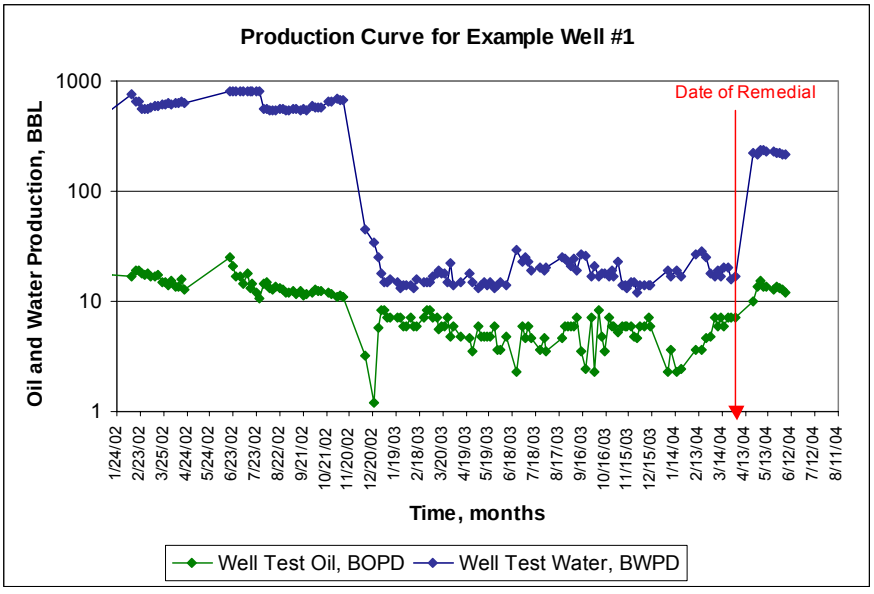

Figure 12: Workover Results for Well #1

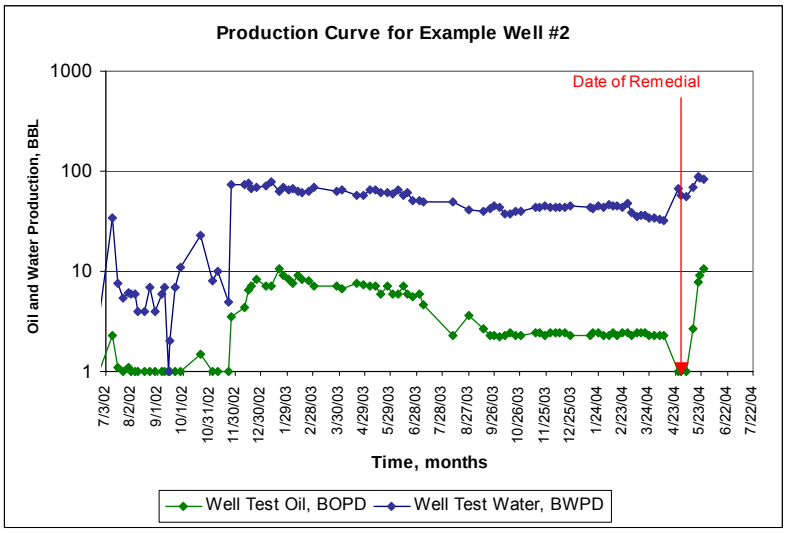

Figure 13: Workover Results for Well #2

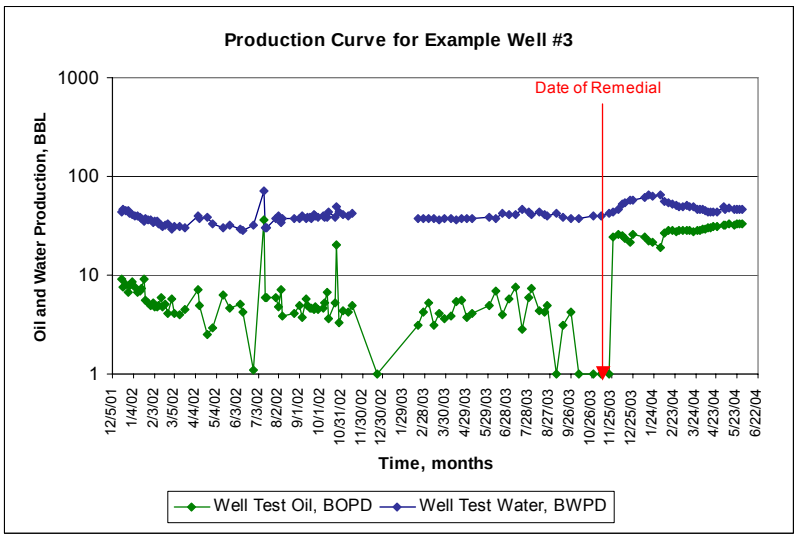

Figure 14: Workover Results for Well #3

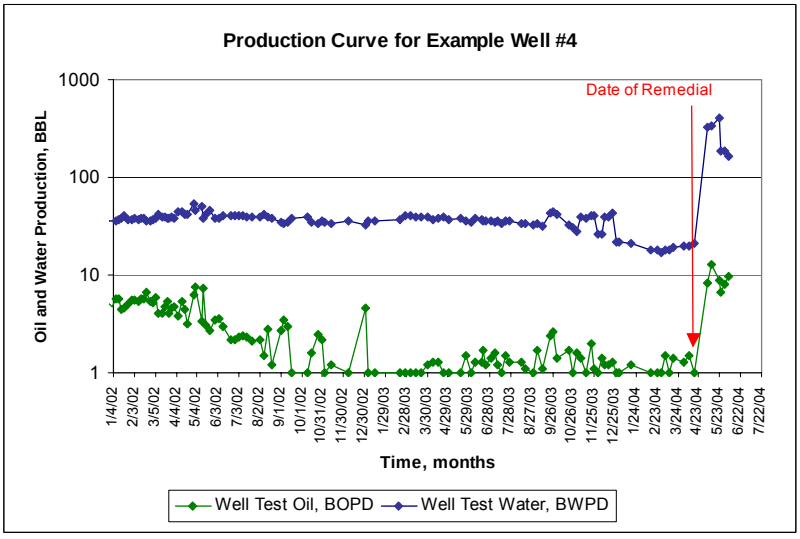

Figure 15: Workover Results for Well #4

SPE 90720

Self-Organizing Maps for Lithofacies Identification and Permeability Prediction

Michael Stundner, Christian Oberwinkler, Schlumberger Information Solutions

Copyright 2004, Society of Petroleum Engineers Inc.

This paper was prepared for presentation at the SPE Annual Technical Conference and Exhibition held in Houston, Texas, U.S.A., 26–29 September 2004.

This paper was selected for presentation by an SPE Program Committee following review of information contained in a proposal submitted by the author(s). Contents of the paper, as presented, have not been reviewed by the Society of Petroleum Engineers and are subject to correction by the author(s). The material, as presented, does not necessarily reflect any position of the Society of Petroleum Engineers, its officers, or members. Papers presented at SPE meetings are subject to publication review by Editorial Committees of the Society of Petroleum Engineers. Electronic reproduction, distribution, or storage of any part of this paper for commercial purposes without the written consent of the Society of Petroleum Engineers is prohibited. Permission to reproduce in print is restricted to a proposal of not more than 300 words; illustrations may not be copied. The proposal must contain conspicuous acknowledgment of where and by whom the paper was presented. Write Librarian, SPE, P.O. Box 833836, Richardson, TX 75083-3836, U.S.A., fax 01-972-952-9435.

Abstract

Methods of Artificial Intelligence like Back-Propagation Neural Networks (BPNN) have become popular software tools to predict permeability and porosity from well logs during the last several years.

Similar to Multiple-Linear Regression models, Back-Propagation Neural Networks are trained with a set of target values from core measurements.

The Self-Organizing Map (SOM) Neural Network method applies an unsupervised training algorithm. Until now this approach has mainly been applied for clustering purposes only, not for predicting reservoir properties.

In a new application, SOM technology has been merged with statistical prediction methods to derive the following types of information from well logs and core measurements in one step:

1) Synthetic lithofacies system (clustering)

2) Porosity and permeability (prediction)

SOM technology also provides a data visualization tool which allows evaluating relationships between input variables (well logs) and output variables (reservoir properties).

SOM models can also be combined with BPNN in order to subdivide the entire set of well log patterns into different lithofacies and run individual BPNN models for each facies.

Application of this method showed increase in prediction accuracy and significant timesavings.

This paper should be viewed and printed in color.

Introduction to Neural Networks

Basically SOM models are a special kind of Neural Networks with an unsupervised training algorithm (Fig.1.).

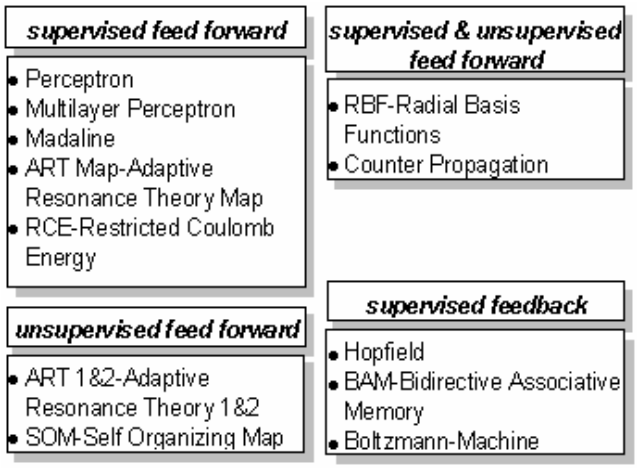

Fig.1: Neural Network methods

Neural Networks (NN) are computational models broadly inspired by the organization of the human brain. Unlike conventional deterministic problem-solving algorithms, Neural Networks can be trained to perform a particular task based on data ("data-driven").

This is done by presenting the system with a representative set of examples describing the problem, namely pairs of input and output samples; the Neural Network will then extrapolate the mapping between input and output data.

After training, the Neural Network can be used to recognize data that is similar to any of the examples shown during the training phase.

The Neural Network can even recognize incomplete or noisy data - an important feature that is often used for prediction, diagnosis or control purposes.

Furthermore, Neural Networks have the ability to self-organize, therefore enabling segmentation or coarse coding of data.

If we take a closer look at a Neural Network model, we find that its interface to the outside world consists of an input - and an output layer of neurons (Fig. 2).

The neurons are the processing units within the Neural Network and are usually arranged in layers. The information is propagated through the Neural Network layer by layer always in the same direction.

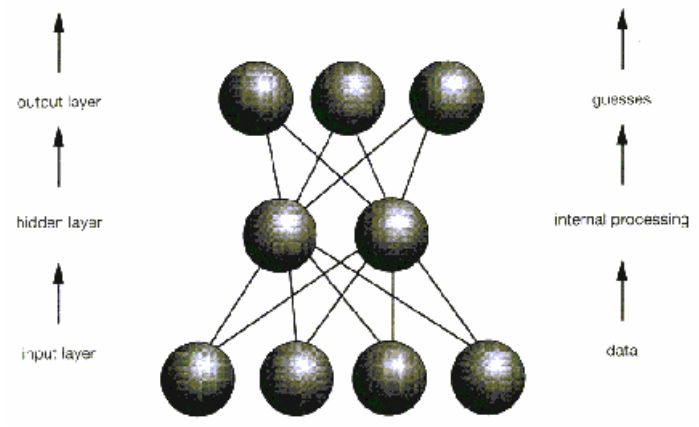

Fig.2: Basic Neural Network architecture

Besides the input and output layer there can be other intermediate layers of neurons, which are usually called hidden layers.

A neuron collects information from all preceding neurons relative to the flow of the information and propagates its output to the neurons in the following layer.

The output of each preceding neuron (o_i) is modulated by a correspondent weight (w_i) before affecting the activity of the neuron (Fig. 3). This process is realized by the formula a = w*o, where a represents the activity of the neuron. This activity is then modified by an activation function f() and becomes the final output (o = f(a)) of the neuron. This signal is then propagated to the neurons of the next layer.

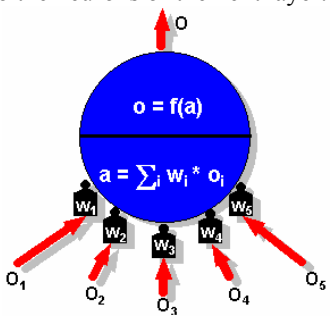

Fig.3: Neuron in a Neural Network

Connections are the paths between neurons where all the information flows within a Neural Network. Very often the neurons of two succeeding layers are fully interconnected, but there are certain exceptions for special applications.

One of the most important aspects of Neural Networks is the storage of information. Each connection is equipped with an individual weight that modifies the signal flow on the respective connection.

The weight works as a factor by which the output of the preceding neuron is multiplied before it becomes an actual input.

This means that information is stored distributed within a Neural Network and even minor destruction of some of the weights will have little effect on the recall of learned information.

The phase when sample patterns of a certain problem are presented to a Neural Network it is called the training phase. During the training the weights of the Neural Network are adjusted. Depending on the type of the Neural Network and on the problem it is going to solve, either a supervised or an unsupervised method can be used for adapting the weights. In both cases however, the training starts with propagating the input through the Neural Network and all its neurons change their activity accordingly.

There are basically 3 different types of Neural Network applications in Well Log Analysis:

- Prediction of permeability and/or porosity
- Generation of synthetic logs
- Determination of lithofacies

The Self-Organizing Map (SOM) method

Many papers have been published to determine lithofacies and predict porosity and permeability from well logs[1-37]. Most authors used Backpropagation Neural Networks (BPNN) which were trained on core data. If core data are not available, an unsupervised method is necessary to generate an artificial lithofacies system. This approach is also applicable if core data are present.

One type of unsupervised competitive learning, is the Kohonen feature map, or Self-Organizing Map (SOM) which is often used for „clustering“ purposes.

In unsupervised learning there are no expected outputs presented to a Neural Network, as in a supervised training algorithm such as Backpropagation. Instead, a network, by its self-organizing properties, is able to infer relationships and learn more as more inputs are presented to it. One advantage to this scheme is that one can expect the system to change with changing conditions and inputs. The system constantly learns.

The algorithm called “Self-Organizing Map” introduced in 1981 by T. Kohonen[38] has been widely studied and applied over the past two decades. SOM was originally devised by Kohonen to model a biological phenomena called retinotopy, a process of self-organization of the neural links between the visual cortex and the retina cells. The SOM is recognized as a gross simplification of this retinotopic process, which occurs in the brain.

The SOM is a particular type of Neural Network that combines multivariate data visualization and clustering capabilities. One particularity of the SOM is that the output layer of neurons is a two-dimensional array (map) that is directly used for data visualization purposes.

A second feature of the SOM is that the learning process is unsupervised or self-organized. This means that class information about the data is not used during the learning process, whether such information is available or not.

The SOM Neural Network takes a set of high-dimensional sample vectors (labeled or not) as input and presents an array of vectors, usually in one, two or three dimensions for visualization purposes as output.

The basic two-layered structure of a SOM Neural Network is shown in Fig.4.

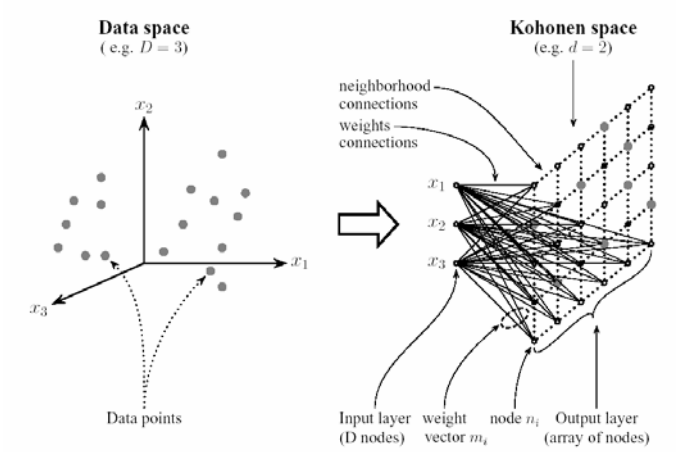

Fig.4: SOM reduces dimensions in data

From the algorithmic point of view, SOM can be seen as an unsupervised version of a supervised learning algorithm called Learning Vector Quantization (LVQ)[40] that was developed as a statistical classification tool.

The idea of LVQ is that in a classification system (a classifier) based on the nearest-neighbor rule a drastic gain of computation speed can be obtained reducing the number of vectors that represent each class.

This reduction of the number of data vectors is clustering. A set of reference vectors is adapted through an iterative process to the data according to a competitive learning rule.

Competitive learning means that only the closest vector (called winning or Best Matching Unit – BMU) is adapted (i.e. moved towards the presented data) at each iteration.

A SOM Neural Network consists of two layers of processing units - an input layer fully connected to a competitive output layer (Fig. 5).

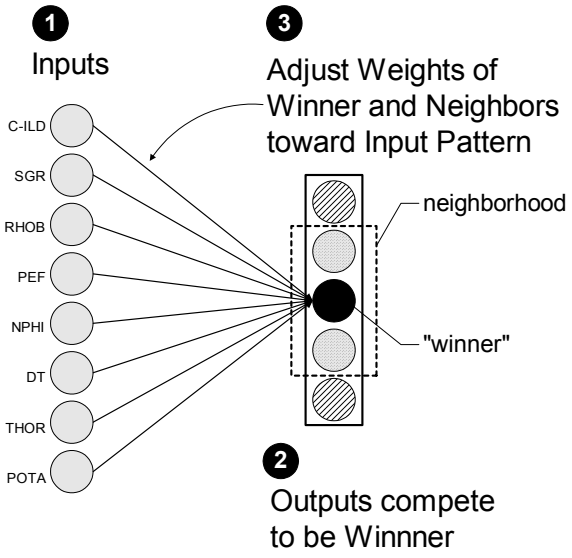

Fig.5: SOM's competitive learning process

There are no hidden neurons. When an input pattern is presented to the feature map, the neurons in the output layer compete with each other for the right to be declared the winner.

The winning output neuron is typically the neuron whose incoming connection weights are the closest to the input pattern (in terms of Euclidean distance).

Thus, the input is presented and each output neuron computes its closeness or match score to the input pattern. The output that is deemed closest to the input pattern is declared the winner and earns the right to have its connection weights adjusted.

The connection weights are moved in the direction of the input pattern by a factor determined by a learning rate parameter. This is the basic nature of competitive Neural Networks.

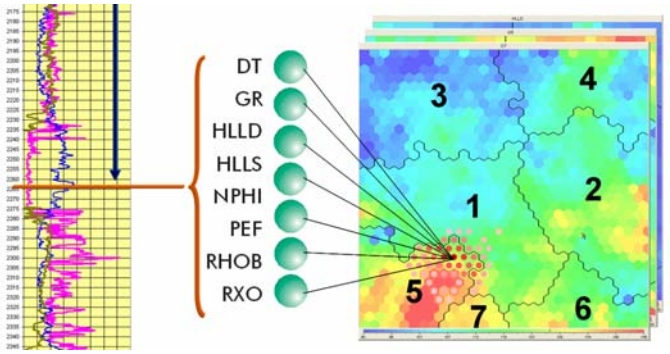

Fig.6: 2D representation of output neurons

The Kohonen feature map creates a topological mapping by adjusting not only the winner's weights, but also adjusting the weights of the adjacent output neurons in close proximity or in the neighborhood of the winner (Fig.6 and 7).

So not only does the winner get adjusted, but the whole neighborhood of output neurons gets moved closer to the input pattern.

Starting from randomized weight values, the output neurons slowly align themselves such that when an input pattern is presented, a neighborhood of neurons responds to the input pattern.

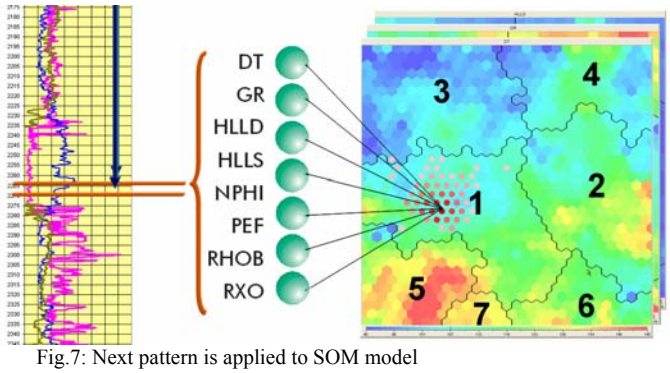

Fig.7: Next pattern is applied to SOM model

As training progresses, the size of the neighborhood radiating out from the winning neuron is decreased.

Initially large numbers of output neurons will be updated, and later on smaller and smaller numbers are updated until at the end of training only the winning neuron is adjusted.

Similarly, the learning rate will decrease as training progresses, and the learn rate may also decay with the distance from the winning output neuron.

Evaluating SOM models

Frequency of input data should be well distributed across the maps (Fig.8, black lines are separators between clusters).

Gaps in the map would introduce less well defined areas, where the capability of prediction is questionable. Therefore the number of output neurons should not be too high.

This leads to good training results, but poor generalization of the trained model.

Fewer output neurons (nodes in the map) lead to higher training errors as several patterns are merged into one node, but the ability to provide reliable prediction results increase (generalization).

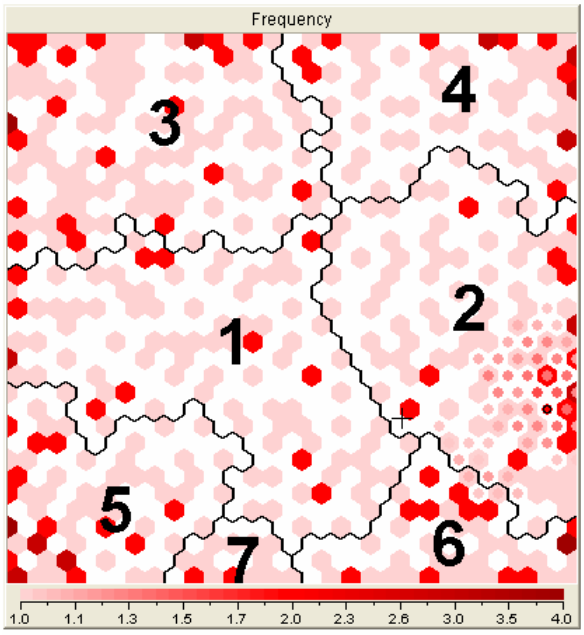

Fig.8: Frequency of input data

Results of trained SOM models may then be evaluated in more detail using the individual parameter maps. Nodes or clusters may be selected and corresponding ranges of input data can be evaluated (Fig.9).

Linear relationships between pairs of input parameters may be evaluated by using crossplots, where cluster membership information of patterns is displayed by color or type of marker (Fig.10).

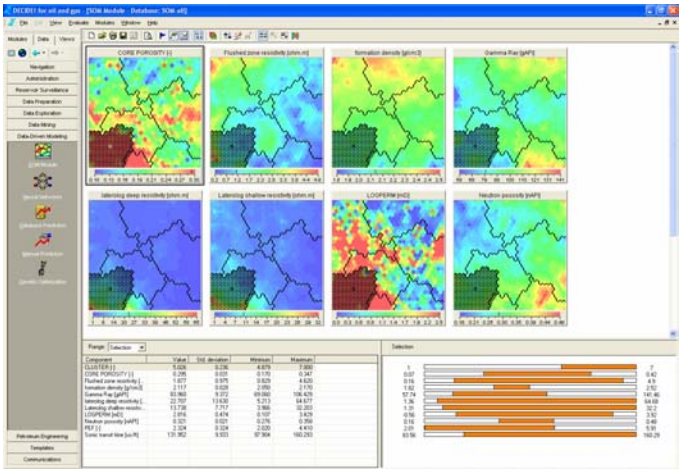

Fig.9: Parameter distribution in SOM models

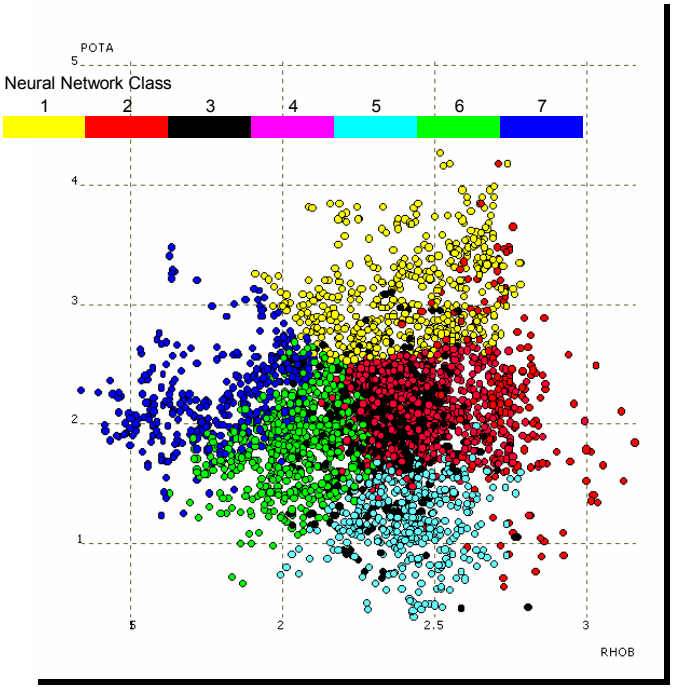

Fig.10: SOM results in crossplot

SOM application to determine lithofacies system

For all patterns the SOM cluster membership can be determined by recalling (kind of prediction) the trained model.

The SOM based lithofacies system can be then compared to available layer systems (Fig.11).

The lithofacies numbers which have been provided by the SOM network are the “winners” within the output array.

Additionally the SOM network assigns values to the neighbors of the winning class.

We received a weighted distribution of values for each pattern which is somehow related to the contribution of the other classes to each pattern.

E.g., the lithofacies “Shale” always contains also other components as “Sandstone” which are taken into account by the SOM network (Fig.12).

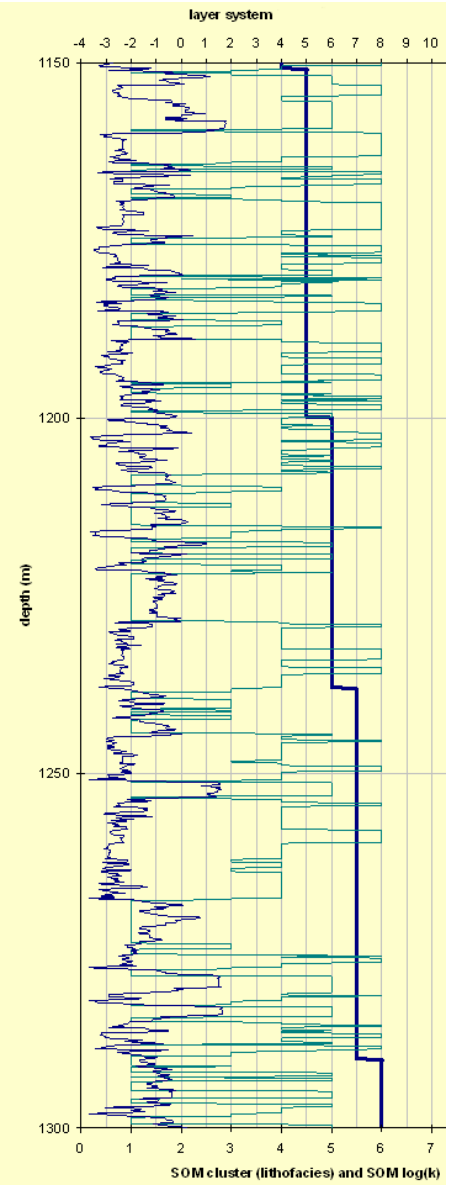

Fig.11: Lithofacies log

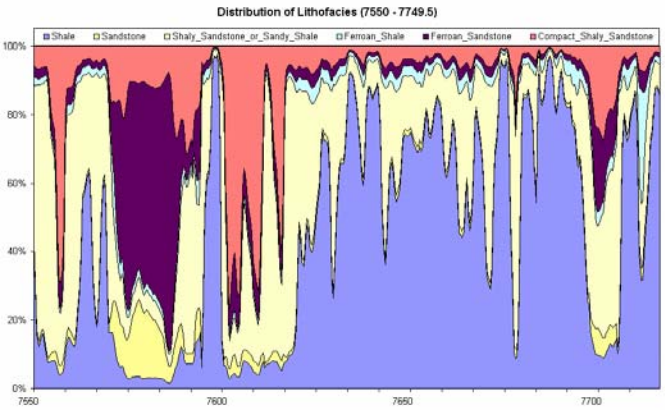

Fig.12: Distribution of lithofacies

The artificial lithofacies system generated by the SOM network is completely data-driven and is therefore a helpful additional source for information in determining the boundaries of geological facies in the investigated wells.

Tune number of clusters

Different to classification algorithms, SOM clustering is not fixed to a predefined number of clusters when applying hierarchical SOM-Ward cluster algorithm[39] (Fig.13).

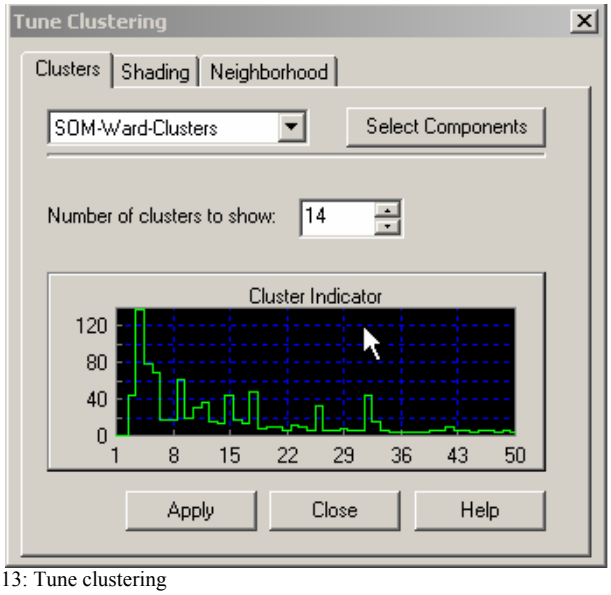

Fig.13: Tune clustering

This clustering method combines the local order information of the map with the classical hierarchical cluster algorithm of Ward.

As in the Ward method, it starts with a clustering where each node by itself forms a cluster. In each step of the algorithm two clusters are merged: those with minimal distance according to a special distance measure, the SOM-Ward distance.

This measure takes into account whether two clusters are adjacent in the map. This means that the process of merging clusters is restricted to topological neighbored clusters.

One might select a certain number of clusters to make comparison with an existing lithofacies (layer) system easy. The applied program shows significance of number of clusters.

The cluster indicator graph (Fig.13) indicates a quality measurement for each cluster count, which can be interpreted as follows: If the indicator is high for a particular cluster count, the clustering may be viewed as "natural" for the map.

If the indicator is low for a cluster count, that clustering is "artificial". Usually, the peaks of the cluster indicator graph indicate interesting clusterings.

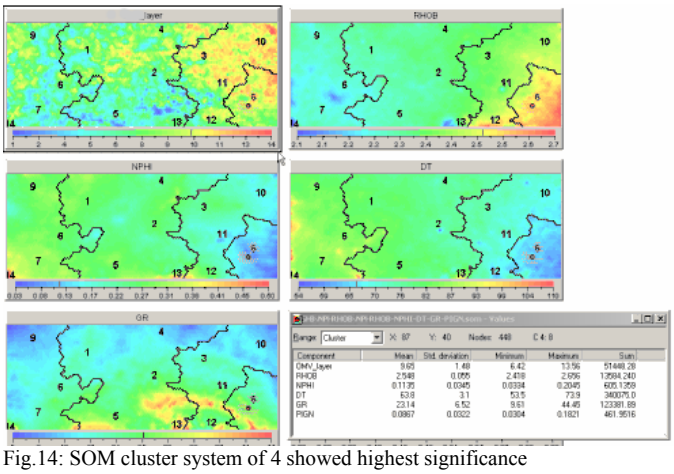

Fig.14: SOM cluster system of 4 showed highest significance

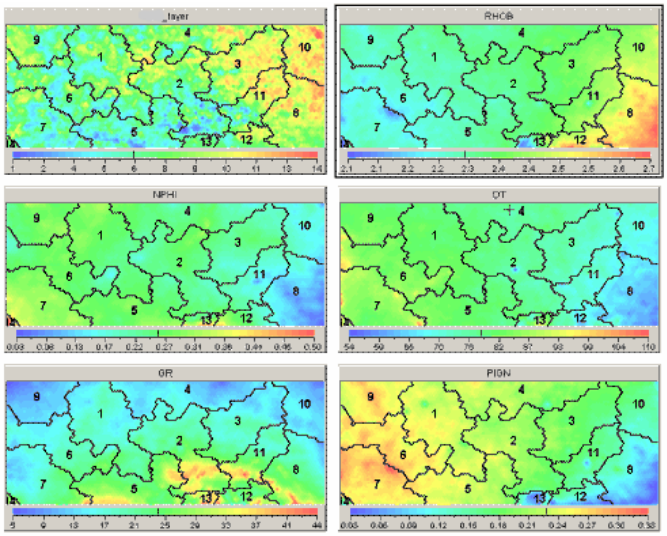

Fig.15: User selected cluster system of 14

Fig.14 and Fig.15 was taken from a field study where the SOM software indicated a cluster system of 4 individual clusters to be the most significant (Fig.14). For comparison reasons this cluster system was further subdivided into 14 clusters (Fig.15).

Prediction of permeability and porosity

Maps for output parameters can be generated with the same distribution of patterns across the map (Fig.16). Nevertheless their weight (priority) during training of the SOM should be zero (Tab.1).

Component	Minimum	Maximum	Mean	Std. deviation	Scaling	Priority	Transformation
Well	1	5	3.091	1.27	Variance	0	None
RHOB	1.925	2.947	2.454	0.129	Variance	1	None
NPHI	0.0511	0.3066	0.144	0.0468	Variance	1	None
DT	59.7	108.6	77.2	7.4	Variance	1	None
GR	40.5	147.5	76.1	21.1	Variance	1	None
PEF	2.6	20.26	6.08	2.92	Variance	1	None
THOR	2.95	24.17	8.24	3.14	Variance	1	None
POTA	0.019	5.161	2.289	1.346	Variance	1	None
LLD	2.85	34.93	6.87	4.19	Variance	1	Logarithmic: offset 2.53
PIGN	0.0001	0.2629	0.1497	0.0536	Variance	1	None
Phi_c	0.08	30.76	14.69	6.64	Variance	0	None
log(K_c)	-2.266	3.655	-0.006	1.541	Variance	0	None
grain_dens	2.63	3.21	2.71	0.082	Variance	0	None

Tab.1: Preprocessing information for SOM model

Output parameters as porosity and permeability do not influence the building of the maps.

The maps can be evaluated as follows (Fig.16):

1. Areas in the map with smooth changes in values provide reliable prediction of uncored intervals/wells.
2. Areas with large differences between neighboring nodes will cause problems in prediction as similar input patterns (neighbors in the resulting map) lead to very different predictions in permeability or porosity. If such a scattered map is experienced for an input parameter, this particular input parameter might have no relationship with the rest of the input vector.

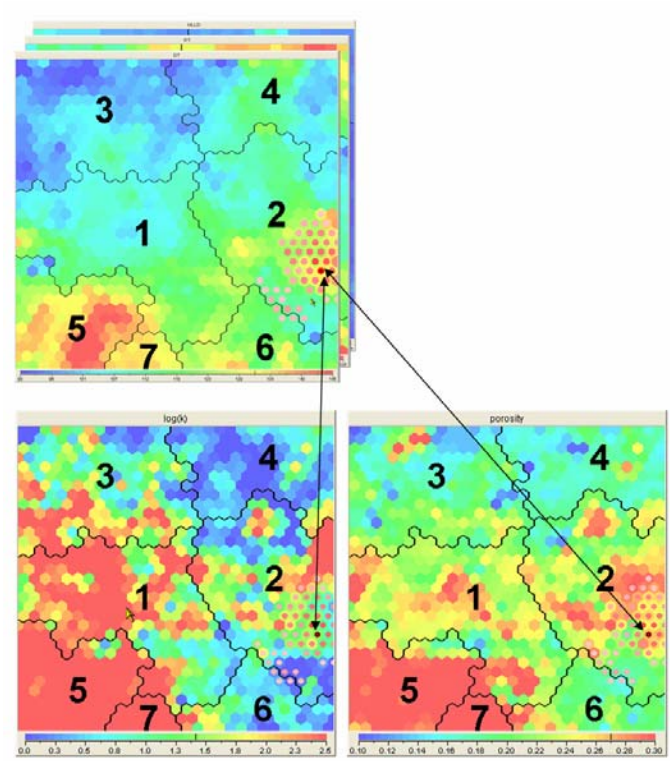

Fig.16: Prediction with SOM models

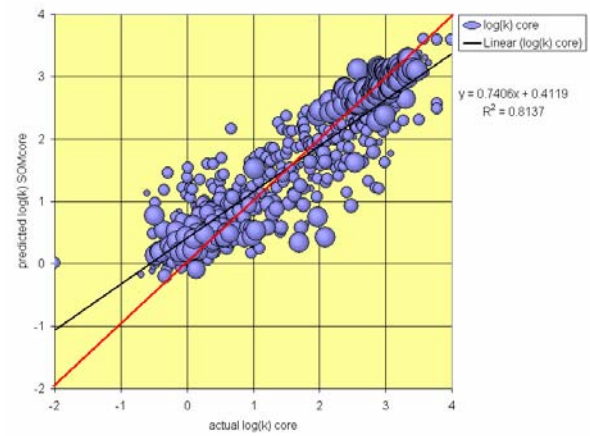

Fig.17: Actual vs. SOM predicted data

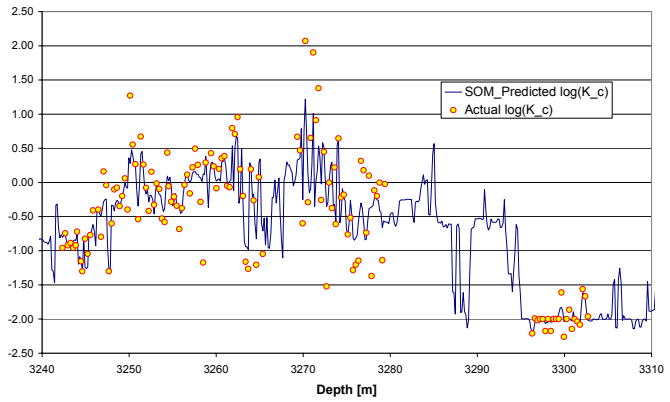

Fig.18: Actual vs. SOM predicted data

Similar to other data-driven methods, one should carefully test the generalization of the SOM models with data which were not seen during the training process (Fig.17 and 18).

Conclusions

SOM models are a valuable alternative to Backpropagation Neural Networks for determining lithofacies systems and predicting porosity and permeability from core data.

BPNN and SOM models can be combined either using SOM cluster membership as additional input parameter for BPNN models or to generate special BPNN models for each SOM cluster.

SOM models can handle missing values, still providing reasonable predictions in intervals where one log might be missing or has been eliminated from input due to erroneous data. Nevertheless majority of input channels for the SOM must be present. In case important well log curves like bulk density is missing, SOM results might be questionable.

References

1. Lee, S.H., Datta-Gupta, A. (1999) Electrofacies Characterization and Permeability Predictions in Carbonate Reservoirs: Role of Multivariate Analysis and Nonparametric Regression. SPE Annual Technical Conference and Exhibition held in Houston, Texas, 3-6 October 1999, SPE 56658, pp. 409 – 421.
2. Baldwin, J.L., Otte, D.N., Wheatley, C.L. (1989) Computer Emulation of Human Mental Processes: Application of Neural Network Simulators to Problems in Well Log Interpretation. SPE Annual Technical Conference and Exhibition held in San Antonio, Texas, 8-11 October 1989, SPE 19619, pp. 481 – 493.
3. Zhou, C.D., Wu, X.L., Cheng, J.A. (1993) Determining Reservoir Properties in Reservoir Studies Using a Fuzzy Neural Network. SPE Annual Technical Conference and Exhibition held in Houston, Texas, 3-6 October 1993, SPE 26430, pp. 141 – 150.
4. Westphal, H., Bornholdt, S. (1996) Lithofacies prediction from wireline logs with genetic algorithms and neural networks. E. Schweizerbart'sche Verlagsbuchhandlung, pp. 465 – 474.
5. Rogers, S.J., Fang, J.H., Karr, C.L., Stanley, D.A. (1992) Determination of Lithology from Well Logs Using a Neural Network. The American Association of Petroleum Geologists Bulletin, V 76, No. 5, pp. 731 – 739.
6. White, A.C., Molnar, D., Aminian, K., Mohaghegh, S., Ameri, S., Esposito, P. (1995) The Application of ANN for Zone Identification in a Complex Reservoir. SPE Eastern Regional Conference and Exhibition held in Morgantown, West Virginia, 19-23 September 1995, SPE 30977.
7. Balan, B., Mohaghegh, S., Ameri, S., (1995) State-Of-The-Art in Permeability Determination From Well Log Data: Part 1 – A Comparative Study, Model Development. SPE Eastern Regional Conference & Exhibition held in Morgantown, West Virginia, U.S.A., 17.-21. September 1995, SPE 30978.
8. Mohaghegh, S., Balan, B., Ameri, S., (1995) State-Of-The-Art in Permeability Determination From Well Log Data: Part 2 – Verifiable, Accurate Permeability Predictions, the Touch-Stone of All Models. SPE Eastern Regional Conference & Exhibition held in Morgantown, West Virginia, U.S.A., 17-21 September 1995, SPE 30979
9. S. Mohaghegh, M. Richardson, S. Ameri, (1998) Virtual Magnetic Imaging Logs: Generation of Synthetic MRI Logs from Conventional Well Logs. SPE Eastern Regional Meeting held in Pittsburgh, PA, 9-11 November 1998, SPE 51075
10. Baldwin, J.L., Malki, H. (1995) Comparision of Neural Network Training and Processing of two Service Company's Data in a Single Wellbore, Artificial Intelligence in the Petroleum Industry, Symbolic and Computational Applications, Chapter 9, pp.282-303
11. Wong, P.M., Shibli, S.A.R., (1998) Use of Interpolation Neural Networks for Permeability Estimation from Well Logs. The Log Analyst, November-December 1998, pp. 18-26
12. Mohaghegh, S., Arefi, R., Ameri, S., (1994) A Methodological Approach For Reservoir Heterogeneity Characterization Using Artificial Neural Networks, 1994, SPE Annual Technical Conference & Exhibition held in New Orleans, LA, U.S.A., 25-28 September, 1994, SPE 28394
13. Mohaghegh, S., Arefi, R., Bilgesu, I., Ameri, S., Rose, D., (1995) Design and Development of an Artificial Neural Network for Estimation of Formation Permeability. SPE Petroleum Computer Conference held in Dallas, 31 July – 3 August 1994, SPE 28237, pp. 151-154
14. Wong, P.M., Henderson, D.J., Brooks, L.J., (1997) Reservoir Permeability Determination from Well Log Data using Artificial Neural Networks: An Example from the Ravva Field, Offshore India, SPE Asia Pacific Oil and Gas Conference held in Kuala Lumpur, Malaysia, 14-16 April 1997, SPE 38034, pp. 149-155
15. Soto, B.R., Ardila, J.F., Ferneynes, H., Bejarano, A., (1997). Use of Neural Networks to Predict the Permeability and Porosity of Zone "C" of the Cantagallo File in Colombia. SPE Petroleum Computer Conference held in Dallas, Texas, 8-11 June 1997, SPE 38134
16. Mohaghegh, S., Arefi, R., Ameri, S., Aminiand, K., Nutter, R. (1996) Petroleum Reservoir Characterization

with the Aid of Artificial Neural Networks. Journal of Petroleum Science & Engineering 16 (1996), pp.263-274
17. Concalves, D.A., Harvey, P.K., Lovell, M.A. (1997) Prediction of Petrophysical Logs using a Multilayer Backpropagation Neural Network. Developments in Petrophysics, Geological Society Special Publication No. 122, pp. 169-180
18. Huang, Z., Williamson, M.A. (1997) Determination of Porosity and Permeability in Reservoir Intervals by Artificial Neural Network Modelling, Offshore Eastern Canada, Petroleum Geoscience, Vol.3 1997, pp. 245-258
19. Mohaghegh, S., Ameri, S., (1996) Virtual Measurement of Heterogeneous Formation Permeability Using Geophysical Well Log Responses. The Log Analyst, March-April 1996, pp. 32-39
20. Mohaghegh, S., Arefi, R., Ameri, S., Rose, D. (1994) Design and Development of an Artificial Neural Network for Estimation of Formation Permeability. SPE Petroleum Computer Conference held in Dallas, U.S.A., July 31 – August 3, 1994., SPE 28237
21. Wong, P.M., Henderson, D.J., Brooks, L.J. (1998) Permeability Determination Using Neural Networks in the Ravva Field, Offshore India. SPE Asia Pacific Oil and Gas Conference, Kuala Lumpur, Malaysia, 14-16 April 1997, SPE 38034
22. Quintero, L., Boyd, A., Gyllensten, A., El-Wazeer, F. (1999) Comparison of Permeability from NMR and Production Analysis in Carbonate. SPE Annual Technical Conference held in Houston, Texas, October 1999, SPE 56798
23. Soto B.R., Holditch, S.A. (1999) Development of Reservoir Characterization Models Using Core Well Logs and 3D Seismic Data and Intelligent Software. SPE Eastern Regional Conference and Exhibition held in Charleston, WV, 21-22 October 1999, SPE 57457
24. Mohaghegh, S., Arefi, S., Ameri, S., Hefner, M.H. (1994) A Methodological Approach For Reservoir Heterogeneity Characterization Using Artificial Neural Networks. SPE Annual Technical Conference & Exhibition held in New Orleans, LA, U.S.A., 25-28 September 1994, SPE 28394
25. Arbogast, J.S., Franklin, M.H. (1999) Artificial Neural Networks And High Speed Resistivity Modeling Software Speeds Reservoir Characterization. Petroleum Engineer International, May 1999, pp. 57-61
26. Garcia, G., Whiteman, W.W. (1992) Inversion of a Lateral Log Using Neural Networks. SPE Petroleum Conference held in Houston, Texas, July 19-22, 1992, SPE 24454, pp. 295-304
27. Xue G., Datta-Gupta, A., Valko, P., Blasingame, T. (1996) Otimal Transformations for Multiple Regression: Application to Permeability Estimation from Well Logs. Improved Oil Recovery Symposium held in Tulsa, Oklahoma, 21 April 1996, SPE/DOE 35412, pp. 115-130
28. Spinler, E.A. (1997) Determination of In-Situ Wettability from Laboratory and Well Log Measurements for a Carbonate Field. SPE Annual Technical Conference and Exhibition held in San Antonio, Texas, 5-8 October 1997, SPE 38733, pp. 167-174
29. Oyeneyin, M.B., Gordon, R., Faga, A.T. (1999) Formation-Grain-Size Prediction Whilst Drilling: A Key Factor in Intelligent Sand Control Completions. SPE Annual Technical Conference and Exhibition held in Houston, Texas, 3-6 October 1999, SPE 56626
30. Chawathé, A., Ounes, A., Weiss, W.W. (1997) Interwell Property Mapping Using Crosswell Seismic Attributes. SPE Annual Technical Conference and Exhibition held in San Antonio, TX, U.S.A., 5-8 October, 1997, SPE 38747, pp. 467-474
31. Mohaghegh, S., Richardson, M., Ameri, S. (1998) Virtual Magnetic Imaging Logs: Generation of Synthetic MRI Logs from Conventional Well Logs. SPE Eastern Regional Meeting held in Pittsburgh, PA, 9-11 November 1998, SPE 51075
32. Spek, A., Thomas, A. (1998) Neural Net Identification of Flow Regime using Band Spectra of Flow Generated Sound. SPE European Petroleum Converence held in The Hague, The Netherlands, 20-22 October 1998, SPE 50640, pp. 93-101
33. Anxionnaz, H.A., Delhomme J.P., De Haan, S. (1999) Reconstructing Petrophysical Borehole Images: Their Potential for Evaluating Permeability Distribution in Heterogeneous Formations. SPE Annual Tehnical Conference and Exhibition held in Houston, Texas, 3-6 October 1999, SPE 56786, pp. 665-675
34. Zhou, Ch., Wu, X., (1993) Neural Network-Based Formation Parameters Estimation From Well Logs in Quantitative Log Analysis: A Comparative Study. SPE Asia Pacific Pil & Gas Conference & Exhibition held in Singapore, 8-10 February 1993, SPE 25359, pp. 357-572
35. Weiss, W.W., Wo, S., Balch, R.S., Roe, J., Fragelius, K., (1999) Integrating Core Porosity and Sw Measurements with Log Values. SPE Rocky Mountain Regional Meeting held in Gilette, Wyoming, 15-18 May 1999, SPE 55642, pp. 477-485
36. Moss, B.P. (1997) The Partitioning of Petrophysical Data: A Review. Development in Petrophysics, Geological Society Special Publication No. 122, pp. 181-252
37. Stundner, M., Lechner, J. (2000) Delineation of Lithofacies based on Well Logs - Application of Stochastic and Neural Network Models for Analyzing and Interpretation, 1st Well Log Analysis/ Formation Evaluation Symposium, Tripoli, Libya, 29th-31st October, 2000
38. Kohonen, T., *Self-Organizating Maps*, second edition, Springer-Verlag, New York (1997).
39. Eudaptics Software GmbH, SOMine Viscovery User Manual, OEM Version 4.0 for DECIDE! FOR OIL&GAS, Wien (2002).
40. Kohonen, T.: Statistical pattern recognition revisited. Elsevier Science Publishers, North Holland, 1990.

SPE 93906

Optimizing Cyclic Steam Oil Production with Genetic Algorithms

A. Patel, ChevronTexaco Energy Technology Co.; D. Davis, Nutech Solutions Inc.; C. Guthrie, and D. Tuk, ChevronTexaco Energy Technology Co.; and Tai Nguyen and J. Williams, ChevronTexaco North America Upstream

Copyright 2005, Society of Petroleum Engineers Inc.

This paper was prepared for presentation at the 2005 SPE Western Regional Meeting held in Irvine, CA, U.S.A., 30 March – 1 April 2005.

This paper was selected for presentation by an SPE Program Committee following review of information contained in a proposal submitted by the author(s). Contents of the paper, as presented, have not been reviewed by the Society of Petroleum Engineers and are subject to correction by the author(s). The material, as presented, does not necessarily reflect any position of the Society of Petroleum Engineers, its officers, or members. Papers presented at SPE meetings are subject to publication review by Editorial Committees of the Society of Petroleum Engineers. Electronic reproduction, distribution, or storage of any part of this paper for commercial purposes without the written consent of the Society of Petroleum Engineers is prohibited. Permission to reproduce in print is restricted to a proposal of not more than 300 words; illustrations may not be copied. The proposal must contain conspicuous acknowledgment of where and by whom the paper was presented. Write Librarian, SPE, P.O. Box 833836, Richardson, TX 75083-3836, U.S.A., fax 01-972-952-9435.

Abstract

This case study describes a project applying a new technology—genetic algorithms—to the problem of scheduling oil production by cyclic steaming at an oil field in the San Joaquin Valley. The paper has seven parts.

In the first part, we discuss the nature of the problem, the importance of solving it well, and the nature of the work process as it occurred before the project began. In the second part, we discuss genetic algorithms and the way that the project adapted them to solve the problem of scheduling cyclical steam injections. In the third section, we describe a pilot project that demonstrated the potential of the approach. In the fourth, we describe the full project that created an optimization tool that has been working daily with oil field personnel to schedule production for the entire field for more than a year. In the fifth, we discuss two types of results of the project—an increase in production and changes to the work process on the part of the oil field personnel owing to their enthusiastic adoption of the optimizer. In the sixth, we discuss some project management factors that led to the success of the project. Finally, we discuss ways in which the success of this project may be relevant to a variety of other types of scheduling and resource allocation problems in the field of oil production.

The paper will center on three themes: the successful solution of a hard production problem with a new technology; the impact of that technology on the oil field personnel; and the potential of that technology to support other types of projects with similar levels of return.

1. Introduction

➢ The Cyclic Steam Process

The Antelope reservoir, located in the Cymric Field, in the San Joaquin Valley, is a siliceous shale reservoir containing heavy oil (12° to 13° API gravity). The reservoir consists primarily of diatomite, characterized by its high porosity (60%), high oil saturation (50-60%) and very low permeability (2 md). Approximately 430 wells are producing from this reservoir with an average daily production of 23,000 BOEG. The oil from the field is recovered using a Chevron-patented cyclic steam process. A fixed amount of saturated steam is injected during a three-to-four day period into the reservoir. The steam's high pressure fractures the rock and the heat from steam reduces oil viscosity. The well is shut in during the next couple of days known as the soak period. Condensed steam is absorbed by the diatomite and oil is displaced into the fractures and well bore. After the soak period the well is returned to production. The flashing of hot water into steam at the prevailing pressure provides the energy to lift the fluids to the surface. The well flows for approximately 20 to 25 days. After the well dies, the same cycle – cycle length of 26-30 days - is repeated.

Scheduling Problem for Cyclic Steam Process

Since there is no oil production during the steaming and soaking period, there is an incentive to minimize the frequency of steaming and increase the length of the cycle. On the other hand, since the well production is the highest immediately after returning to production and declines quickly thereafter, a case can be made for increasing the steaming frequency and reducing the length of the cycle. This suggests there is an optimum cycle length for every well that results in maximum productivity during the cycle. Extend this dilemma for more than 400 wells in the field, combine that with the constraints of steam availability and balancing of the steam distribution system, factor in additional facility constraints, and the result is a formidable scheduling optimization problem.

➢ Other challenges

The production stream is a mixture of heavy oil, associated gas, water and steam. It is quite difficult to accurately measure the rates of each of these components. Furthermore, the production rates for individual wells were measured only

infrequently. As a result, the data have a high degree of uncertainty. Yet another challenge was the lack of available well performance models needed to predict the production during the cycle. The final challenge was to make the new solution / process acceptable to the operational personnel who had been solving this problem quite efficiently for many years.

- Work process prior to this project

There used to be two independent groups of people involved in making a decision regarding which wells to select for steaming. The first group is the well managers who used to recommend a list of wells based on the observed well head pressures, the current performance of the well and its past history. These wells used to be called the PFS (Prep for Steam) wells. Note that once a well makes it to the PFS list, it has the same priority as all the others on the PFS list, thus losing the distinction between the top candidate and the last candidate on the list. The second group is the steam operators would then go through this PFS list and select the wells that can be steamed while honoring the constraints of the steam distribution system. In order to get the optimal response from the field, these two steps (selection of candidates and balancing of steam distribution system) needed to happen simultaneously, but the work process resulted in sequential implementation.

- Business case / opportunity

It was recognized by the engineers and operations that the factors mentioned above (work process, heuristics and uncertain measurements) led to a sub-optimal solution and that there was an opportunity to improve the performance of the field. The project team used historical data and went through an academic exercise to estimate the benefit for this project. They estimated that depending upon the quality of data and frequency of measurements it was possible to achieve a percentage increase in production in the upper single digit range. The consistency and reliability of the new decision making process were thought to be added pluses.

2. Statement of Theory and definition

- Genetic algorithms – background

Genetic algorithms (GA) are global optimization techniques developed by John Holland (Holland 1975). They are one of several techniques in the family of evolutionary algorithms—algorithms that search for solutions to optimization problems by "evolving" better and better solutions. In a genetic algorithm, one begins with a "population" of solutions and then chooses "parents" to reproduce. During reproduction, each parent is copied, and then parents may combine in an analogue of natural cross-breeding, or the copies may be modified, in an analogue of genetic mutation. The new solutions are evaluated and added to the population, and (typically, low-quality) solutions are deleted from the population to make room for them. As this process of parent selection, copying, cross-breeding, and mutation is repeated, the members of the population tend to get better and better. When the algorithm is halted, the best member of the current population is taken as the algorithm's solution to the problem posed.

One critical feature of a genetic algorithm is its procedure for selecting population members to reproduce. Selection is a random process, but a solution member's quality biases its probability of being chosen. Because genetic algorithms promote the reproduction of high-quality solutions, they explore neighboring solutions in high-quality parts of the solution search space. Because the process is randomized, a genetic algorithm also explores parts of the search space that may be far from the best individuals currently in the population, and so some of the solutions found by the algorithm are found in an exploration of the search space.

- **Use of GA in the industry**

In the last twenty years, genetic algorithms have been used to solve a wide range of optimization problems. Problems for which they are well-suited tend to have one or more of these characteristics: the problem cannot be well formulated as a linear programming problem; the problem can be formulated as a linear programming problem, but it takes too long to optimize in this form; or the problem is complex, and brute force and heuristic search techniques are inappropriate or find significantly sub-optimal results.

There are many examples of optimization problems in the petroleum industry for which genetic algorithms are well-suited. At ChevronTexaco, in addition to the cyclical steam scheduling problem, the following problems have been addressed with genetic algorithms: well placement, rig scheduling, portfolio optimization and facilities design. At NuTech Solutions, the following problems have been addressed with genetic algorithms: planning of rig workover projects to that overall workover time is reduced; planning production across multiple plants to reduce costs; planning distribution from multiple plants to large number of customers to reduce costs; and controlling pipeline operations to reduce costs while satisfying pipeline constraints.

All of these problems have the common features that they can not be formulated as linear programming problems, they involve a large number of complex constraints, both hard and soft, and significant increases in profits can be obtained if the problems are solved better than they were being solved before the creation of a computerized optimization procedure.

- **Suitability of a GA for this problem**

Genetic algorithms are applicable to the problem of scheduling cyclical steam injection of heavy oil wells because there does not seem to be a linear formulation of the steam injection problem (production falloff is exponential and constraints are nonlinear). Also, in a pilot project centered on a single gauge setting, ChevronTexaco determined that there seemed to be a significant increase in profit that could be captured if the practices currently in place at the oil field could be supplemented by the output of a global search routine that

could consider hundreds of thousands of possible schedules and "evolve" high-quality schedules that increased production while satisfying the problem's constraints.

- Problem formulation

The scheduling problem is formulated as a GA optimization problem where the objective is to maximize cumulative production over two months' period. The fitness function is calculated as the cumulative production minus the penalties for violating the soft constraints.

- **Hard and soft constraints**

The problem has many constraints. The field level constraints such as the steam availability and maximum # of wells steaming; the GS level constraints such as min amount of steam used and max # of wells on production; the header level constraints such as max # of wells steaming or the individual well constraints such as max / min number of production days. Additionally, there are operational constraints such as communication – where multiple wells must be steamed together and blocked wells due to rig activities.

Although all of the field constraints could have been incorporated in the problem formulation as hard constraints – constraints that absolutely cannot be violated, it was decided to make many of the constraints soft constraints - these constraints can be violated but there is an associated penalty. An example of a hard constraint is the total steam available on a given day for the whole field whereas some of the soft constraints are maximum amount of steam used by a GS and minimum # of wells steaming in a GS or a header.

- **Termination criteria**

The optimization is stopped when one of the following criteria is satisfied:

a) a specified amount of generations have been created
b) a specified amount of time is elapsed, or
c) the fitness function has not improved over a specified number of generations

- **Seed generation**

The genetic algorithm used multiple heuristics to enhance its performance and speed up its search for high-quality solutions. To begin with, when it created the initial population of solutions – "the seed", it used heuristics based on those that the well operators and steam operators used at the oil field. It also used some heuristics developed for the project to find good initial schedules. An example of such a heuristic is "attempt to steam high-production wells at their optimal cycle length—the length of time between steaming at which a well's average daily production is maximized." The constraints of the problem made it impossible to steam all wells at their optimal cycle length, but inserting schedules based on this as a goal into the initial population gave the algorithm some high-quality solutions that could be mutated and cross-bred with other types of solutions in order to find even better solutions.

- **Solution representation (Chromosomes)**

The technique we used for representing solutions was not the approach commonly found in textbooks on genetic algorithms. We used an indirect encoding approach—each solution was a permutation list of wells, with multiple entries allowed for the same well. We then used a decoding procedure that simulated the effects of various schedules to translate the permutation list into an actual schedule. Let us illustrate this process with an example.

The genetic algorithm encoded solutions to the cyclical steam scheduling problem as lists of wells, of the form

<w34, w1832, w196, w34, w9185,>

Such a list contains all the wells that could be steamed, and it typically has duplicate entries. (Note that the example above lists well 34 twice.) This list is not yet a schedule. We used the following procedure to convert a list of this form into a schedule: We began on day one. The schedule builder looks at the first well on the list and simulates steaming it on day 1. If this process violates no hard constraints, then the well is scheduled for steaming on day 1. The schedule builder then looks at the second well on the list—well 1832, in this case. It simulates the effects of steaming that well together with well 34 on day 1. If no hard constraints are violated, this well is added to the schedule for day 1. If hard constraints are violated, the well is not added to the schedule. The process continues, considering each well for steaming on day 1, and adding each well, in order, that can be steamed without violating a hard constraint. Then the process continues with day 2, considering each well in order that was not already steamed in day 1. And so forth. The critical point to note is that the schedule-building process will not build a schedule that violates a hard constraint. It is also worth noting that this schedule-building process uses some clever heuristics and a simulator in order to transform a list of wells into a feasible steaming schedule. Once a schedule is built, it can be evaluated, and its "score" is returned to the genetic algorithm as the evaluation of the original solution—the list of wells.

- **Special operators**

The optimization process uses heuristics to initialize the population, as well as randomly-generated solutions to fill out the initial population. It includes intelligent heuristics in the procedures used to modify new solutions. It uses "cross-breeding" procedures appropriate to combining different permutations in order to combine two parents to produce a child. It includes a good deal of domain knowledge in the schedule builder in order to produce feasible schedules. It includes a post-processor that checks to find simple changes that could be made to the best solution found in order to improve its quality.

- **GUIs, Platforms etc**

The interface to the optimizer gives the well operators and the steam operators at the field a good deal of power and

flexibility in their interactions with the system. The operators can edit the well data that is input to the optimizer. They can select which optimization heuristics and procedures will be used in a run. They can parameterize the objective function that specifies the goals of the run. They can activate, deactivate, and parameterize the hard and soft constraints on the run. They can also edit the solutions found by the optimizer—an essential capability, particularly in cases in which there is a constraint known to the operators that is not reflected in the databases available to the optimizer.

3. Description of application of equipment and process

➢ Pilot test

A pilot test was conducted to demonstrate the feasibility as well as to determine the potential benefit of the approach. A gauge setting comprising of 21 wells was selected and the test was conducted for 60 days. During this period we operated the wells in this gauge setting only on the recommendations of scheduler without any adverse effects. The work process was changed to facilitate the scheduler needs. The operators successfully adopted the new process that relied much more on the production data that were updated daily and used the Visualizer (The next section describes in detail the functionality of Visualizer. At this juncture it is sufficient to mention that this tool /module uses the past data and predicts the well performance) to determine the well performance parameters. Daily logs were kept of the recommendations that were followed. At the end of the test period, a comparison was done against the baselines.

➢ Pilot test results

o **Production during the test increased**

Cumulative production from this GS during the 60 day period increased 11 %. The number of active wells was same as the base period. Thus, implying the well productivity was increased.

o **Steam injection also increased**

The scheduler recommended shorter cycles for many of the wells compared to the field practice. The cumulative steam during the same period increased 17 %.

o **Difficult to separately quantify the benefits due to scheduler and added steam injection**

It is already known that the rate and volume of the steam injection affects the oil production. During the pilot test period, we did not control either of these, since the scheduler was asked only to increase the production. Since the total steam available for the field is constrained, it would not be possible for scheduler to increase the steam usage the way it did in the pilot test. As a result, the increase in the production due to higher steam use was backed out. The final conclusion was that the use of Scheduler would increase the production between 3 to 5%.

o **Operators' response**

During the pilot test, well managers were asked to make a significant process change. They were asked to ignore the well head pressures and rely on the Visualizer which in turn was relying on the gauged information. The steam operators were instructed to strictly adhere to the steaming sequence suggested by the Scheduler. Not only did they quickly and successfully adopted the new work process but also found / suggested more changes that would further improve the process in the future.

o **Other issues**

The pilot test helped identify issues that needed to be addressed before implementing the process field wide such as the need to address the steam system balance and the need for handling uncertainty in the measurements.

4. Description of the Optimization Tool

➢ System Design and Components

Figure 1 describes the overall system which is comprised of four major components: Database, Visualizer, Simulator and Optimizer.

The operator starts the main program interface and retrieves the current model values. The retrieved data can come from the local storage representing previously reviewed results or the field repositories. In either case the information is checked for completeness and consistency. The completeness and consistency checks ensure that there is enough data to run a simulation. Correctness is not ensured although some data integrity checks will be possible. Known errors are brought to the attention of the user who changes the information possibly with suggestions from the program. Results of this process are stored in a local repository.

Individual components are described below.

o **Database**

A local database stores modeling information. This database serves several purposes. First, it is a collection point for field data. It provides quick access to field information, greatly reducing the sometimes extended query times from the main field database. Second, it stores model parameters derived from field data or captured by the interface. Third, this database houses field data that was changed by the operator for data quality or modeling reasons. Finally, it serves as a persistent storage of information that needs to be communicated between models, e.g. between the interface and the Simulation Engine.

- Local Database Functions
- Collects data from the field database
- Supplies raw production data to the Visualizer
- Captures decline characteristics from the Visualizer
- Supplies field data and decline characteristics to the user interface

- Maintains and captures new and adjusted model data not derived from field data. This information will be entered and edited through the interface and supplied as necessary to the Simulation Engine.
- Supplies model data to the Simulation Engine.
- Captures output from the case manager.

Figure 1.

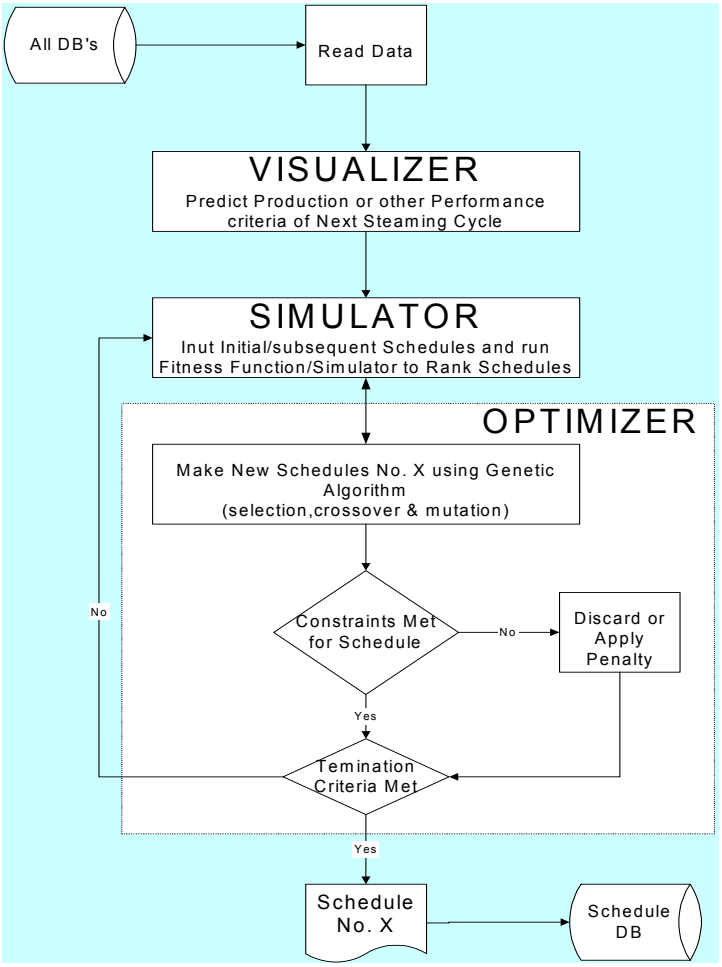

o **Visualizer**

The Visualizer provides a visual interface to the raw well production and pressure data. It can be used to explore well production for the last few steam cycles, as a place for users to correct production measurements, and as the creator of production prediction parameters. The primary function of the visualizer is to determine decline curve parameters for production wells.

- Visualizer Functions
  - Determines decline curve parameters
  - Data reconciliation
  - Allows user intervention to modify parameters

o **Simulator**

The simulator consists of a Simulation Manager and a Simulation Engine. The Simulation Manager acts as the communication vehicle between the user interface, the optimizer, and the Simulation Engine. This is necessary because the system design is for three separate executables to exist along with a common simulation engine: One executable for the HEURO (optimizer) which needs to maintain its own startup entry point, one for the Visualizer, and one for our user interface. When the user instructs the interface to start an optimization run, the interface will start the simulation executable via the Simulation Manager. The Simulation Manager that exists in the optimizer process space will be given control in the HEURO framework main function prior to starting the framework.

- Simulator Functions
  - Accept calls from the user interface to write the simulation data to disk.
  - Launch the simulation executable and obtain evaluation.
  - The Simulation Manager performs initialization, establishes communication with the interface, and proceeds into the HEURO framework.
  - Manage the control of the program.

o **Optimizer**

The Optimizer, HEURO is an engine supplied by NuTech Solutions. It consists of library functions that allow one to carry out all of the GA operations, namely populating, reproduction, crossover, mutation and selection. It also has functions that can be added to carry out any special operations as desired by the user. Finally, it has wrapper functions for easy integration with the rest of the system.

- Optimizer functions
  - Communicate with Simulation Manager.
  - Perform all necessary GA operations.
  - The Optimizer will supply a solution by calling the Simulation Manager with the solution in the chromosome format.

5. Results

As a risk mitigation measure, the plan for developing the Scheduler with all of its functionality was broken down into three Releases. Each subsequent release would be approved to move forward after the prior release was considered to be the success. The Release 1 of the Scheduler for the whole field was deployed in the first week of Jan 2003. It was developed jointly by ChevronTexaco and NuTech Solutions, who were primarily responsible for the optimization module. The system's performance was evaluated as a part of the look back study that is required of all major projects in SJVBU. The evaluation data presented below refers to the first 60 days of operation.

- Increase in Production
  - *Production during the evaluation period has increased*
    - The production from the field during the period Jan 8, 2003 to March 8 2003 increased 6.4% compared to the baseline. Some of this increase, however, is not due to the Scheduler. Since the field situation was dynamic and new wells were drilled, the production from these wells was a part of the increased production.
    - In order to estimate the economic benefit of the scheduler, we needed to deduct the production gain attributable to the factors other than Scheduler. We also wanted to ensure that we erred on the side of underestimating the gain from the Scheduler rather than otherwise. Of the total increase of 6.4%, our best quantitative estimate showed that there was approximately 1.4% gain that cannot be attributable to absolutely any other factor. Although we believe that the use of Scheduler resulted in higher gain than 1.4%, for our economic analysis we assigned only 1.4%production increase to the Scheduler.
      - A preliminary look back of the project indicates that it has DPI of 4.19 and Pay-out of 2.5 months.

- Experience in the field

Scheduler development and deployment have consistently enjoyed the support from the operations personnel. After the installation at the site, the tool has been checked for functionality as well as accuracy by the operators and well managers. They have indicated that the Scheduler correctly provides the answers based on whatever is being asked from it.

- The Scheduler is in daily use since 8/03.
- Operators love it for its consistency and fast response.
- They have added other constraints and continue to ask for more functionality.

- Enthusiastic adoption

They have adopted the new work process which has the following features

- No PFS wells
- Spend time looking at the production curves, adjust visualizer parameters
- Focus on the right amount of steam to be used
- Duplicate this process elsewhere in the business unit

- Intangible benefits

Although the project was justified on the basis of accelerated production from the field, we have noticed additional benefits that cannot be quantified:

- The operators are claiming that the process is now consistent
- Operators are able to focus more on the field problems as the schedule is generated ahead of the time. A typical response is - "…there is no urgency to get back to the computer because the steam operators are waiting…"
- The schedule implementation is done system wide so steam system is always balanced
- The operators are able to analyze the results of the scheduler and are able to justify the results – making the tool more credible

6. Conclusions

Based on our experience on this project, we can reach the following conclusions:

- GAs can be effectively used for production optimization

Production optimization problems can be successfully solved using Genetic Algorithms. Although this specific application was related to scheduling, genetic algorithms can be applied to any kind of resource allocation problems as well as other constrained combinatorial optimization problems.

- Technology implementation is as much about right stakeholders as it is about right technology

The success of Antelope 1Y has been due to the involvement of the stakeholders throughout the development and deployment. The technology, no matter how great, will always need the assistance from right people. From the beginning to the end, the role of each of the stakeholder is critical. Having the right stakeholders in the loop ensures that throughout the project issues are being worked on and a belief in the ultimate success of the project is maintained. Many of the issues and decisions are non-technical in nature and they can only be resolved with the help of right stakeholders.

- Measurement accuracy / frequency very important for optimization

One of the issues that has been identified early on and which is still on our radar is the issue related to the quality of measurements. Since scheduler is a data driven tool, it is very important to have good quality data (measurements) as an input. The business unit operations have also recognized this issue and are in the process of implementing the necessary steps to improve the quality of both steam and oil measurements. We expect that the scheduler benefit will be even more after the data quality is improved.

- Other factors that led to the success of the project
  - Excellent collaboration amongst all partners, and
  - Frequent communication / weekly calls

  The team was comprised of subgroups working from multiple locations – Boston, Richmond & Bakersfield. Constant communications helped resolve the issues quickly.

7. Relevancy and extensibility

The success of this project has led us to look for other areas where Genetic Algorithms and other Artificial Intelligence techniques may be relevant to a variety of other types of scheduling and resource allocation problems in the field of oil production. Indeed, we have already started several other projects in the area of well workovers and rig scheduling (well work scheduling).

Other areas where such applications may be successfully deployed are chemical injection optimization, choke optimization scheduler, and surface steam distribution optimization.

8. Acknowledgements

The authors would like to thank SJVBU –for allowing the publication of this paper, Jim Lederhos and Jim Ouimette for championing this project as well as providing valuable guidance throughout the implementation of this project, and Bob Fragione for providing assistance related to the field operations.

Figure 2.

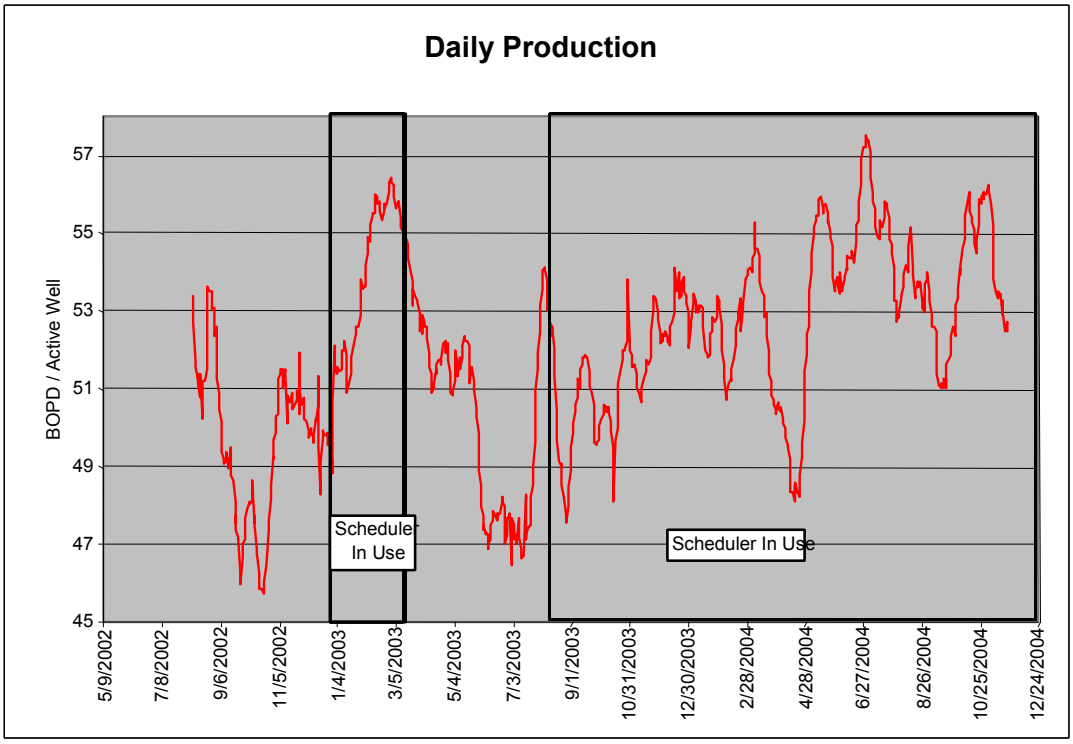

Figure 2 indicates the field performance since the scheduler has been deployed field wide.

SPE 95942

Analysis of Best Hydraulic Fracturing Practices in the Golden Trend Fields of Oklahoma

S.D. Mohaghegh and R. Gaskari, West Virginia U.; A. Popa, Chevron; I. Salehi, Gas Technology Inst.; and S. Ameri, West Virginia U.

Copyright 2005, Society of Petroleum Engineers

This paper was prepared for presentation at the 2005 SPE Annual Technical Conference and Exhibition held in Dallas, Texas, U.S.A., 9 – 12 October 2005.

This paper was selected for presentation by an SPE Program Committee following review of information contained in a proposal submitted by the author(s). Contents of the paper, as presented, have not been reviewed by the Society of Petroleum Engineers and are subject to correction by the author(s). The material, as presented, does not necessarily reflect any position of the Society of Petroleum Engineers, its officers, or members. Papers presented at SPE meetings are subject to publication review by Editorial Committees of the Society of Petroleum Engineers. Electronic reproduction, distribution, or storage of any part of this paper for commercial purposes without the written consent of the Society of Petroleum Engineers is prohibited. Permission to reproduce in print is restricted to a proposal of not more than 300 words; illustrations may not be copied. The proposal must contain conspicuous acknowledgment of where and by whom the paper was presented. Write Librarian, SPE, P.O. Box 833836, Richardson, TX 75083-3836, U.S.A., fax 01-972-952-9435.

Abstract

In the past decades several hundred stimulation procedures have been performed in the Golden Trend fields of Oklahoma. The outcome of these stimulation jobs have not been the same for all wells. The effectiveness of the stimulation is a function of several factors including reservoir quality, completion and stimulation techniques. Completion and stimulation techniques can be further itemized as completion type such as open hole versus cased hole, type and amount of fluids and proppant and the rate at which they are pumped into the formation.

This project was supported by DOE and GTI in connection with the DOE's Preferred Upstream Management Practices (PUMP) project. The project was implemented in three fields in the Golden Trend in Oklahoma. Detailed production and completion data analyses revealed that the most influential controllable parameter effecting the production rate and ultimate recovery was fracture stimulation, and as such, the bulk of efforts were focused on determination of optimized hydraulic fracturing procedure. Detail stimulation data from more than 230 wells in the Golden Trend fields of Oklahoma operated by three independent operators were collected and analyzed using a new best practices analysis methodology.

The study was performed for gas and oil bearing formations. Among the findings of this comprehensive study were the best stimulation practices in carbonate formations that are primarily gas producing, and clastic formations, from which both oil and gas are produced. During his study authors were able to identify the best type of fluid, the most optimal injection rate and proppant concentration for both types of formations.

In this paper application of a new methodology that was used to perform the best practices analysis on the Golden Trend fields of Oklahoma is presented.

Introduction

Identification of best practices in the oil and gas operations is gaining unprecedented momentum. Companies that have gathered large amounts of data now realize that they own a valuable commodity (above and beyond the hydrocarbon) that can play an important role in increasing efficiency in their day to day operations.

The question is how this vast amount of data can be used in order to help the company's bottom-line. This paper attempts to address this question by introducing a newly developed methodology that enables oil and gas companies to deduce information and knowledge from the existing data. The deduced information and knowledge can then be used in developing business rules and decision making.

The new methodology is named "Intelligent Best Practices Analysis" [1]. It incorporates a hybrid form of intelligent systems that includes artificial neural networks [2], genetic algorithms [3] and fuzzy logic [4] to achieve its objective that is the systematic analysis of large amounts of data in order to decipher and deduce relevant knowledge that can be used in business and engineering decision making.

In a previous paper [5] the theory and methodology of "Intelligent Best Practices Analysis" was presented in detail and therefore it will not be discussed in this article. This paper is dedicated to application of this methodology to a database of stimulation practices in the Golden Trend fields of Oklahoma to demonstrate its use and benefits.

In the Golden Trend fields of Oklahoma, like many other oil fields, the outcome of stimulation jobs have not been the same for all wells. The effectiveness of the stimulation is a function of several factors including reservoir quality, completion and stimulation practices. Detail stimulation data from more than 230 wells in the Golden Trend operated by three independent operators were collected and analyzed using this methodology.

Many companies in the oil and gas industry have been collecting large amounts of data over the past several years.

Hundreds of thousands of dollars have been invested in collecting and compiling various types of data. These databases cover all aspects of oil and gas business, from purely technical data that includes certain measurements from the reservoir or the surface facilities to non-technical data such as those related to economics or human resources issues. Now that all this data is available, following questions may be asked: "What can we do with this data?" "How can the company get a return on its data collection and preservation investment?" "Are there stories hidden in the megabytes, or sometime gigabytes of data?" "The collected data is a reflection of the history of the operations that have taken place and sometime are still taking place. What can we learn from our past practices?"

As the volume of data increases, human cognition is no longer capable of deciphering important information from it by conventional techniques. Data mining and machine learning techniques must be used in order to deduce information and knowledge from the raw data that resides in the databases. The Intelligent Best Practices Analysis – IBPA – incorporates the state of the art in data mining and machine learning to assist petroleum professionals in making the most of their existing data. Figure 1 is a schematic diagram of IBPA process in form of a flow chart.

Application to the Golden Trend Fields

In the previous paper [1] the principles of Intelligent Best Practices Analysis was covered in detail. In the next several sections of this paper these principles are applied to hydraulic fracturing practices of the Golden Trend fields of Oklahoma. This study was performed as part of a DOE sponsored project on determining Preferred Upstream Management Practices (PUMP).

Descriptive Best Practices Analysis

The descriptive best practices analysis incorporates fuzzy logic in order to detect any patterns in the records that are in the database. The descriptive best practices analysis can be performed on all the variables available in the database. Table 1 shows the list of parameters that will be analyzed during this study. The list in Table 1 shows 18 parameters that are present in this database. The parameters that will be used during the predictive best practices analysis (next section) are shown in the rows with shades of green. There are 8 parameters that will be studied in detail during the predictive best practices analysis.

The descriptive best practices analysis starts by identifying a parameter that would be used to partition the wells in terms of their productivity. In other words, what constitutes a well to be a poor, an average or a good well. For this study it was decided that the "30 Year EUR" would be the indicating parameter. The "30 Year EUR" has been calculated for all wells using decline curve analysis.

This simply means that, for this analysis, a well that produces up to 30,000 barrels of oil during 30 years is identified as a poor well. A well that produces up to 60,000 barrels of oil during the 30 years is identified as an average well, and wells that produce more than 90,000 barrels in 30 years are considered as good wells. Please note that these ranges are arbitrary and can be changed based on the economic practices of each operator.

Of course we know that in reality there is little difference between a well that produces 1000 bbls/yr and one that produces 1010 bbls/yr. Therefore we will not impose an artificially crisp boundary between such wells. Instead, we define a series of "fuzzy sets" that would resolve such unrealistic situations. This is done by identifying ranges of productivity within which wells are both poor and average and ranges of productivity within which wells are both average and good. This means that in our classification each well is poor to a degree and average to degree, or average to a degree and good to a degree. Let's define these ranges and provide some examples to clarify these definitions before starting the analysis. Based on the fuzzy sets shown in Figure 2, the range between poor and average wells is from 30,000 to 60,000 barrels in 30 years or about 1000 to 2000 bbls/year. The range between an average well and a good well would be from 90,000 to 120,000 barrels in 30 years or about 3000 to 4000 bbls/yr.

In order to clarify the classifications mentioned above please note the following example. In Figure 3 there are five graphs each pertaining to a particular well. In the first row the graph on the left belongs to *well A* which is a well operated by *Company One*. The "30 Year EUR" for this well is 23,402. This productivity makes this well to be a poor well. As shown in this figure *well A* has a member ship of 1.0 in the set of poor wells. In the first row the graph on the right shows the "30 Year EUR" of 35,958 for *Well B* also operated by *Company One*. This level of productivity makes this well to have a membership of 0.8 in set of poor wells and a membership of 0.2 in set of average wells.

In the second row on the left *Well C*, that is operated by *Company Two*, has a "30 Year EUR" of 65,996 that makes it an average well. On the right, *Well D*, has a '30 Year EUR" of 112,163 barrels. This well has a membership of 0.26 in the set of average wells and a membership of 0.74 in the set of good wells. On the bottom, *Well E* has a "30 Year EUR" of 333,940 that makes it clearly a good well.

Now that we are familiar with the classification lets see the existing practices in this field. First of all lets look at the distribution of wells in the database as far as the "30 Year EUR" is concerned. Figure 4 shows this distribution in terms of percentages. As shown in this figure, based on our classification about 85% of the wells are poor, about 35 % of them are classified as average and 9% are classified as good wells. Since we are not using conventional or crisp mathematics the percentage need not to add to 100%. In this methodology if a well has membership in more than one fuzzy set it will contribute to both classes. This simply means that in this database 85+35+9=129-100=29, 29% of the wells belong to more than one set.

In the next several figures we show the distribution of different parameters in our database as a function of the well

quality. For example we will analyze the data to identify the number of poor wells that were hydraulically fractured using a particular fluid and compare it to the number of good and average wells that have been hydraulically fractured using the same fracturing fluid and look for trends. Hopefully these trends will show us if certain parameters and attributes are more predominant in certain quality wells more than others.

For the purposes of this article we will not show the parameters that seem not to have any effect on the well quality. The main fracturing fluids used in the stimulation jobs in the Golden Trend are "Acid", "Water" that includes slick water, salt water, treated water, and fresh water, "Oil" that is predominantly diesel and the last category is "Other". If the majority of the fluid used during the stimulation job was not identified as water, oil, or acid, then it was classified as "Other" which included entries in the database such as mostly "Unknown", some "Gel", and a few "Waxsol".

Figure 5 shows the results of the analysis on these main fracturing fluids. Based on this figure "Water" seems not to be contributing to good fracturing results since the set of poor wells have the highest average value (almost 0.6) of formations that have been fractured using water as the main fluid. This value is about 0.42 for average wells and good wells have an average value of slightly higher than 0.1.

Please note that the average value is a fraction since many wells have been completed in several formations. The numbers that you see in these figures are simply averages over many wells. Oil as main fracturing fluid shows exactly the opposite trend as water. Better wells have been predominantly fractured using diesel oil as the main fracturing fluid. From this figure it is concluded that for those formations that are producing oil, future hydraulic fracturing procedures in this field should be performed using diesel oil as the fracturing fluid, and use of water as the main fracturing fluid should be avoided.

Figure 6 shows the analysis on four stimulation parameters on "per foot of total perforated pay thickness" bases. These parameters are total shots, total fluid amount, total proppant amount, and average injection rate "per foot of total perforated pay thickness". Looking at Figure 6 it seems that there is not an identifiable trend in the average value of "Shot/ft" for different well qualities. Furthermore, it is shown that good wells have been fractured using a lower than average amount of fluid "per foot of total perforated pay thickness". While the average for all the wells is about 1.6 Mgal/ft (which does not change for poor and average wells) the average amount of fluid pumped in good wells is about 1.0 Mgal/ft.

Amount of proppant used during the hydraulic fracturing treatment according to Figure 6, shows a general pattern of higher proppant amounts per foot of pay thickness for average and good wells as compared to poor wells. Given the trend identified for fluid amount, this means that the pattern favors higher proppant concentration for better wells. Average rate of injection "per foot of total perforated pay thickness" indicates that it is preferable for the fluid and proppant to be pumped at lower rates. It seems that the good wells have been pumped at about 0.12 BPM/ft. This may point to the fact that there may not be a significant in-situ stress contrast between the pay zones and the barrier formations.

Predictive Best Practices Analysis

Now that the Descriptive Best Practices Analysis has been completed, let's look at the predictive analysis. The next several sections will cover this analysis for oil production from the Golden Trend fields.

The main idea behind the predictive analysis is to fill the gaps in the solution space in order to make a comprehensive analysis possible. The predictive model that is developed, calibrated and verified based on the existing data provides a continuous hyper -dimensional surface that is full of hills and valleys. This surface covers the entire solution space that the records in the database are discrete points on this surface. Goal of predictive analysis is two folds. First, to develop a predictive model that can accurately approximate this solution space. This goal is achieved using artificial neural networks [2]. The 30 year EUR is used as the network's output and several independent variables (as will be discussed in the next section) are used as the network input. It is important to use the proper variables as the input to the neural network. The input variables have to sufficiently represent the process being modeled and include parameters that identify the uniqueness of each record (well) in the database. Second goal of the multiple-parameter analysis is to exhaustively search through, and query the solution space in order to identify patterns that can be used as guides in the decision making process. This step of the analysis is performed using genetic algorithms [3]. The neural network model developed in the first step is used as the objective function of the genetic algorithms.

Neural Network Modeling

Upon performing some preprocessing on the data and identifying the best set of input parameters to be used during the neural model building a neural model was trained. Table 2 shows the list of the input parameters used in the neural network model.

As shown in this table there are two parameters that have been extracted from the Decline Curve Analysis of the production data. These are Qi (initial flow rate) and Di (initial decline rate). There are two parameters that identify the location of each well, latitude and longitude. These parameters can also be a proxy for the geology of the reservoir at the location where the well is drilled. The two parameters, RRQI and Sub RRQI, relative reservoir quality indices, developed using a process called Intelligent Production Data Analysis [6] and are further indication of the reservoir quality in addition to latitude and longitude.

Number of perforations per foot of the pay zone (Shot / ft) is the parameter that identifies the completion of the well. The next seven parameters out of the total of fourteen are stimulation related. The first one, Date of the First Stimulation, identifies a time stamp for the well. The next four parameters identify the type of fluid that was used as the main

fluid in the stimulation job. The next two parameters identify the amount of fluid and proppant and the rate of injection per foot of the pay zone.

The output of the neural network model is the "30 Year EUR". The data set was divided into three smaller sets. The training data set included 147 records (wells). The calibration data set included 17 records (wells) and the verification data set included 18 records (wells). The training set was used to train the neural network model. The calibration data set was not used for training but served as a criterion in order to identify when the training process has been completed. Finally the verification data set (blind data) served as judging the goodness of the model. Figures 7 and 8 show the results of the model performance on calibration and verification data sets.

The R^2 for the training data set was 0.904 and the correlation coefficient was 0.951. The calibration data set has a R^2 of 0.642 and a correlation coefficient of 0.801. The R^2 and correlation coefficient of the verification data set are 0.905 and 0.951, respectively.

Full Field Analysis

The full field, predictive best practices analysis looks at all the wells in the database and identifies the major trends in the process. The adjective "Predictive" implies the fact that some of the patterns that are identified may not have been already practiced. The analysis would predict what could have potentially happen if certain practices had been employed.

The results of full field predictive hydraulic fracturing best practices analysis in the Golden Trend is summarized in the "Recommendation Matrix" presented in Table 3. This matrix combines the results of single parameter and combinatorial analysis and provides best practices recommendations. Details on how such recommendation matrix is constructed have been presented in [5].

Recommendations are made when both the single parameter analysis and the combinatorial analysis seem to be pointing at the same direction. A good example of such case is use of diesel oil as the main fracturing fluid. During both analyses the dominant trend is toward using diesel oil in order to increase the well productivity.

Other parameters that seem to show clear signs of specific trends are number of perforations per foot of pay thickness, injection rate, and proppant concentration. Number of perforations per foot of the pay thickness is recommended to be on the side of smaller numbers (mainly around one shot per foot). Low injection rates are preferable specifically when the increased proppant concentrations are recommended. Figure 9 and 10 shows the results of combinatorial analysis for full field analysis.

Groups of Wells Analysis

The predictive best practices analysis based on groups of wells are covered in this section. Upon completion of the full field analysis the wells in the database are classified and the process is repeated for each class (category or cluster) of the wells. The classification can be based on several criteria. If there is a class indicator in the database (natural or native classifier) it can be used as the basis for the classification. In the case where each record in the database represents a well in a field (as the case in this application) the classification of the wells can be based on any predetermined classifier such as well quality, operating company, well locations, geology, reservoirs involved, or any other classification that makes sense. In cases that such native (natural) classifier is not present in the database, k-mean clustering or fuzzy c-mean clustering can be used in order to cluster the records in the database. For this study wells were once grouped base on their quality, and once based on the operator. Three operators had participated in this study. In this article only the results that was achieved based on the operators is presented.

Grouping Based on Operators

In this section the predictive best practices analysis is performed on wells grouped based on their operators. This means that the wells in the database are divided into three groups based on the operators i.e. *Company One, Two, or Three*. Initially one might consider this grouping as arbitrary. But we think that valuable information might be deduced using this grouping. This grouping has the potential to shed light on positive or negative practices (regarding hydraulic fracturing) that might exist in a company which can be attributed to the culture (the way things are down around here) within each company. These cultural attributes may contributes to the success of certain practices, in which case must be nurtured, or they may prove not to be very productive, in which case the management may want to revisit them. Some of such attributes may exist in an implicit fashion rather than being enforced explicitly. In such cases studies such as this one may prove helpful in starting productive discussions in the company.

It is a well known fact that certain things are done in certain ways in some companies that might be different from others. Usually the way things are done in a company has its roots in the previous successes that it has brought about and management is reluctant to change things once they have proven to be successful. But sometimes what used to be true may no longer be true, due to changes in the operational landscape. Other factors may have entered the equation, which necessitate another look at the way things were done in the past. On the flip side, by regularly examining the effectiveness of the common practices in a company the management can reinforce the successful productivity of those practices.

Figure 11 shows the location of the wells being in our database that are operated by different companies in the Golden Trend. The Recommendation Matrix for each of the operators is shown in the Tables 4, 5, and 6. For wells operated by *Company One* it is concluded that diesel oil is the most effective fracturing fluid. This conclusion is reached since diesel oil is the only fracturing fluid that results in consistent increase in "30 year EUR" (with the highest range) in both single parameter and combinatorial analysis. Furthermore, it is recommended to use high proppant

concentrations injected at low rates into wells that are completed with about one shot per foot of pay for wells operated by *Company One*.

Table 5 show the combination of the single parameter analysis with the combinatorial analysis for wells operated by *Company Two*. The conclusions reached in this table are analogous to those from *Company One* although some differences appear in the single parameter analysis. These differences are not in directions that would change the recommendations but to make them more or less assertive in different cases. Engineers need to keep an eye on these trends in order to make necessary adjustments when designing new treatments for wells operated by *Company Two*.

In Table 6, where the conclusions for the *Company Three* are presented, the main fracturing fluid seems to still be the diesel oil. But in the case of wells operated by *Company Three* Acid as the main fracturing fluid may provide results that are not so different from oil and in some cases it might even outperform diesel oil. Therefore, for situations that use of diesel oil may not be realistic (for whatever reason) Acid may be the reasonable alternative fluid.

Similar to wells operated by *Company One* and *Company Two*, wells operated by *Company Three* seem to benefit from high proppant concentrations injected at low rates into wells that are completed with about one shot per foot of pay thickness.

The major difference between full field analysis and those made for wells grouped by operators was the clarification of lower number of perforations per foot of pay thickness along with high proppant concentrations.

Individual Well Analysis

Upon completion of full field and groups of wells analysis, the last part of the predictive best practices analysis is the analysis of individual wells. Usually by the time we get to the individual well analysis we have a clear idea of the best practices in a particular field. This is true in the case of the Golden Trend.

The essence of individual well analysis is to look into details of a hydraulic fracture treatment with all the specifications of a particular well. Therefore, an individual well analysis includes running the simulation model for the well that is being considered for a stimulation treatment.

Single Parameter Analysis – Individual Wells

During the single parameter analysis, all the inputs for the well will be kelp at the original value and one by one the controllable parameters will be changed as explained in previous sections. Figure 12 shows the results of the sensitivity analysis for four wells in the database. The reason the following several figures are presented is to show that different behaviors might be observed from different wells.

For example in Figure 12 the top left graph shows the sensitivity of *Well A-1* operated by *Company One* to water as the main fracturing fluid. The blue dot in the graph shows the status of the well in the database. This well did not use water as the fracturing fluid and has two formations present where only one of them has been hydraulically fractured. The fracturing fluid that was used for this well was diesel oil. The graph in Figure 12 shows that if instead of oil, water was used during the fracture treatment for this well, its long term production would have decreased, a practice that would not be recommended for this well.

On the other hand, the graph in the lower right of the Figure 12 shows the hydraulic fracturing behavior for *Well A-4* operated by *Company Three*. This well shows that if instead of one, two of the formations present in this well were treated with water; it would have a positive long term effect on this well's productivity. There are four formations present in this well were three formations were hydraulically fractured using acid as the main fracturing fluid.

Combinatorial Analysis – Individual Wells

The combinatorial analysis for the individual wells can be performed by identifying two or more parameters at a time. First let's examine the situation where two parameters at a time are examined. Figure 13 shows the three-dimensional graphs that are used to show the sensitivity analysis for two parameters simultaneously. The X and Y axes of the three dimensional graphs are "Shot/ft" and "Injection Rate (BPM/ft)". The Z axis of the graph is the "30 Years EUR".

These wells show different types of responses as the number of perforations and average rate of injection per foot of pay thickness changes. As expected all show high production values at low injection rates and number of perforations. The production response is different for each of these wells as number of perforations and the average injection rates start to increase. Well number three shows a monotonic decline in production as these values increase while well number 2 increase to values that are quite high at higher numbers of perforations and injection rates. All three wells show the same kind of behavior at small numbers of perforations that favors lower injection rates.

If more than two parameters are going to be analyzed, then using two and three dimensional graphs will be ineffective. In such cases a Monte Carlo simulation process is used to perform the analysis. To perform a Monte Carlo simulation following procedure must be followed:

- Identify the number of parameters that are going to be studied simultaneously.
- Identify a probability distribution function for each of the parameters.
- Identify the number of simulation runs that should take place.
- Make the simulation runs and plot the results as a probability distribution function.

The result of such a process as mentioned in step 4 would be a probability distribution function that identifies the most probable "30 Year EUR" that would result from the

probability distribution functions that have been assigned to each of the parameters. Figure 14 shows the results of two different Monte Carlo simulations for *Well C-1* operated by *Company One*.

The probability distribution function of the "30 Year EUR" on the left represents 1000 simulation runs when the three identified parameters were selected for the analysis. These parameters were "Shot/ft" that was assigned a skewed triangular distribution function toward lower values, "Proppant Concentration" that was assigned a skewed triangular distribution function toward higher values, and "average injection rate" that was assigned a skewed triangular distribution function toward lower values. The "30 Year EUR" shows a probability distribution function that is skewed toward 29,000 barrels. The figure shows that the probability of long term production slowly reduces toward the 60,000 to 70,000 barrels mark.

The probability distribution function of the "30 Year EUR" on the right represents 1000 simulation runs when all the parameters were assigned a uniform probability distribution function. In this case the probability distribution function of the "30 Year EUR" is closer to a Gaussian distribution than the graph on the left. The mean value of long term production seems to be closer to about 34,000 barrels.

This exercise clearly shows that each well has to be analyzed individually in order to see how the general best practices would apply to it.

Application to Gas Production

The Golden Trend includes several formations. Some of these formations are clastic that are believed to be the main sources of oil production and some others are carbonate that are believed to primarily produce gas. The study detailed in this paper was performed separately for oil production and gas production. The concluding remarks that will follow summarize the conclusions achieved after both analyses had been completed.

Conclusions

Intelligent Best Practices Analysis (IBPA) is a two-step process that includes a descriptive and a predictive analysis. During the descriptive analysis the productivity of the wells in the database is divided into several fuzzy sets and fuzzy-averages of several parameters are then calculated to identify the trends that are present in the database. These trends and patterns usually provide a pretty strong foundation for the best practices that are ultimately identified.

Predictive best practices analysis is a drill-down process where we start with the full field analysis and end with individual well analysis. During the full field analysis we identify the best practices based on all the wells in the database. We then divide wells into groups, based on different criteria, and look at each group more closely and either, verify, refine or dispute the best practices that were identified during full field analysis. The last step of the predictive analysis is working with individual wells and using the results of past two steps as a guide to enhance the production of an individual well. We showed that although the best practices that were identified during the full field and groups of wells analysis would work for most of the wells (since that is how they were identified), there will be wells in the database (or new wells) that would not necessarily follow the identified trends as expected. This makes refining of the design by individual analysis a highly recommended exercise.

All the analysis mentioned above are based on a predictive neural network model that is developed from the data available in the database. Following paragraphs highlights the identification of best practices in the Golden Trend.

Formation Isolation before Stimulation

Wells in the Golden Trend are completed in several formations. The formations that are present in almost all of the wells can be divided into two major categories, clastic and carbonate. Oil production in the Golden Trend is predominantly from the clastic formations while substantial amount of gas is produced from carbonate formations and some from the clastic formations. Based on the findings of this study, formations in the Golden Trend respond positively to different types of hydraulic fractures. Therefore, it is highly recommended that the clastic and carbonate formations be isolated prior to stimulation jobs in order to achieve the best results.

Main Fracturing Fluid

It was identified that the recommended main fracturing fluid for the clastic formations in the Golden Trend is "Diesel Oil". It is concluded that the clastic formations that are producing oil in the Golden Trend seem to have certain amount of clay that is contributing to damage of the reservoir near the well bore by developing hydration spheres, a process that seem to be reversible as long as the water saturation in the reservoir is not at irreducible saturation. This phenomenon has shown to have negative effect on short and long term production. Scientists at the Core Labs, Inc. have concluded that at gas to water permeability ratios (k_g/k_w) of higher than 3 (where Kilnkenberg gas permeability has been measured under reservoir stresses) oil seem to be a better choice for fracturing fluid [7].

On the other hand it was identified that the carbonate formations that produce mainly gas in the Golden Trend, respond positively to acid as the main fracturing fluids. It was further identified that "acid fracs" and not "acid jobs" are the stimulations that should be performed in these formations.

Number of Perforations

It was identified that a relatively low number of perforations (may be less than or equal to one shot per foot of pay thickness) would be the most appropriate practice of completion for wells in the Golden Trend. This seems to be true for both clastic and carbonate formations.

Proppant Concentration

It was identified that higher proppant concentrations work better in the Golden Trend. Figure 15 shows a logarithmic

distribution function of the proppant concentration in the Golden Trend. This figure shows that most of the fracture treatments have used low proppant concentrations (less than 1.0 lbs/gal/ft). The recommendation is to use proppant concentrations of higher than 1.0 lbs/gal/ft.

Average Injection Rate

It is recommended to use average injection rates of less than or equal to 0.2 BMP per foot of pay thickness while stimulating the formations in the Golden Trend. The combination of above three parameters, namely injecting higher proppant concentrations at lower injection rates into smaller numbers of perforations is targeted at avoiding increasing of the bottom-hole pressure during the treatment. While higher proppant concentrations provide a better conduit for the fluid flow and stronger support for keeping the fracture open for longer periods of time, its combination with lower numbers of perforations may contribute to higher bottom-hole pressures that might impede short and long term production. By injecting the treatment at lower injection rates we will try to keep the bottom-hole pressure low. It has been shown that there is a correlation between low bottom-hole treating pressures with higher production indicators [8].

Acknowledgement

This study was performed under a contract from U.S. Department of Energy (DE-FC26-01BC15271). Authors would like to express their gratitude to the USDOE for its support and to Mr. Gary Walker the project manager.

References

1. Intelligent Best Practices Analysis, based on software application available at: http://www.intelligentsolutionsinc.com/ibpa.htm
2. Mohaghegh, S. D., Virtual Intelligence Applications in Petroleum Engineering: Part 1 – Artificial Neural Networks. *Journal of Petroleum Technology*, Distinguished Author Series, September 2000, pp 64-73.
3. Mohaghegh, S. D., Virtual Intelligence Applications in Petroleum Engineering: Part 2 – Evolutionary Computing. *Journal of Petroleum Technology*, Distinguished Author Series, October 2000, pp 40-46.
4. Mohaghegh, S. D., Virtual Intelligence Applications in Petroleum Engineering: Part 3 – Fuzzy Logic. *Journal of Petroleum Technology*, Distinguished Author Series, November 2000, pp 82-87.
5. Mohaghegh, S. D. and Gaskari, R. 'A SoftComputing-Based Method for the Identification of Best Practices, with Application in the Petroleum Industry. CIMSA 2005 – IEEE International Conference on Computational Intelligence for Measurement Systems and Applications Giardini Naxos, Italy, 20-22 July 2005.
6. Intelligent Best Practices Analysis, based on software application available at: http://www.intelligentsolutionsinc.com/ipda.htm
7. Conversations with Dr. Mike Conway of Core Laboratories, inc. June 2003.
8. Johnson, R. L., Dunn, K. P. Hopkins, C. W. and Conway, M. W. "The Pressure Dependence Ratio: A Bottomhole Treating Pressure Diagnostic Tool for Hydraulic Fracturing in Tight, Naturally Fractured Reservoirs," SPE 77916. Presented at SPE Asia Pacific Oil & Gas Conference & Exhibition held in Melbourne, Australia, 8-10 October 2002.

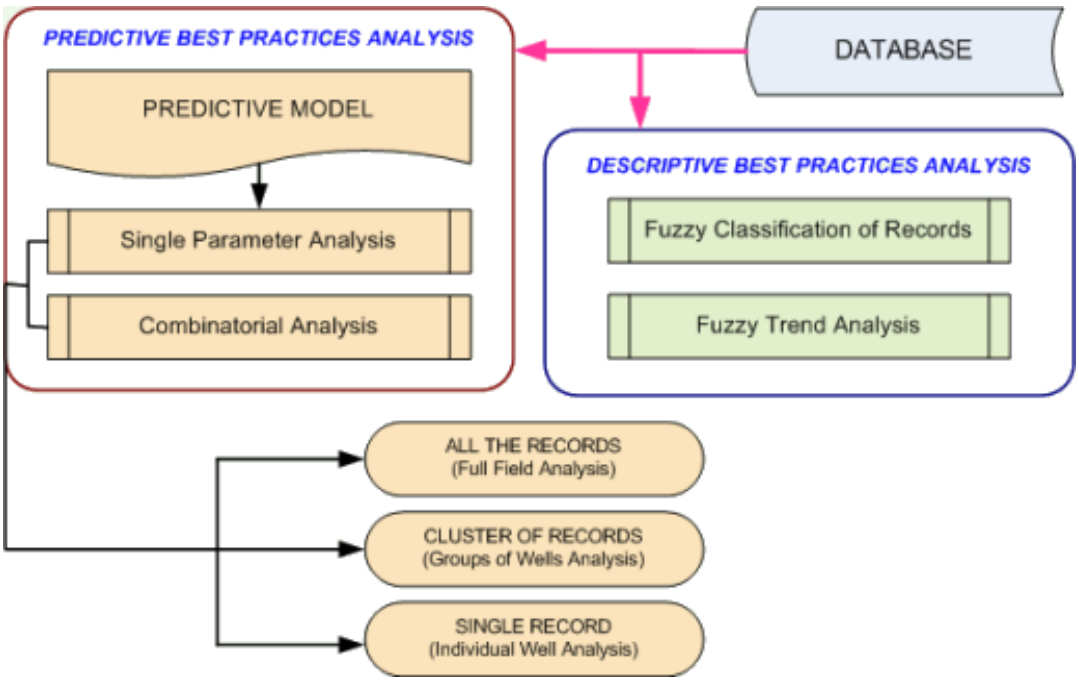

Figure 1. Intelligent Best Practices Flow Chart.

Table 1. Parameters in the database that were used during the "Best Practices" analysis.

No.	Parameter
1	Number of formations present in the well
2	Number of formations stimulated
3	Number of formations with hydraulic fracturing
4	Number of formations with acid jobs
5	Total perforated pay thickness
6	Date of First Stimulation
7	Main Fracturing Fluid - Water
8	Main Fracturing Fluid - Oil
9	Main Fracturing Fluid - Acid
10	Main Fracturing Fluid - Other
11	Total Shots per foot of perforated pay
12	Total Fluid amount (Mgal) per foot of perforated pay
13	Total Proppant amount (Mlbs) per foot of perforated pay
14	Total Proppant Concentration (lbs/gal/ft)
15	Average Injection rate per foot of perforated pay
16	Date of First Production
17	Best 3 months of production
18	Initial Flow Rate – Decline Curve Analysis
19	Initial Decline Rate – Decline Curve Analysis

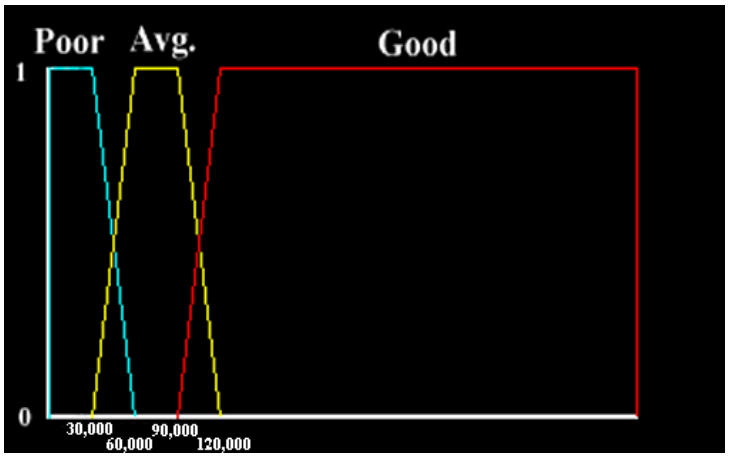

Figure 2. The "30 Year EUR" Productivity Fuzzy sets for wells in the Golden Trend Field.

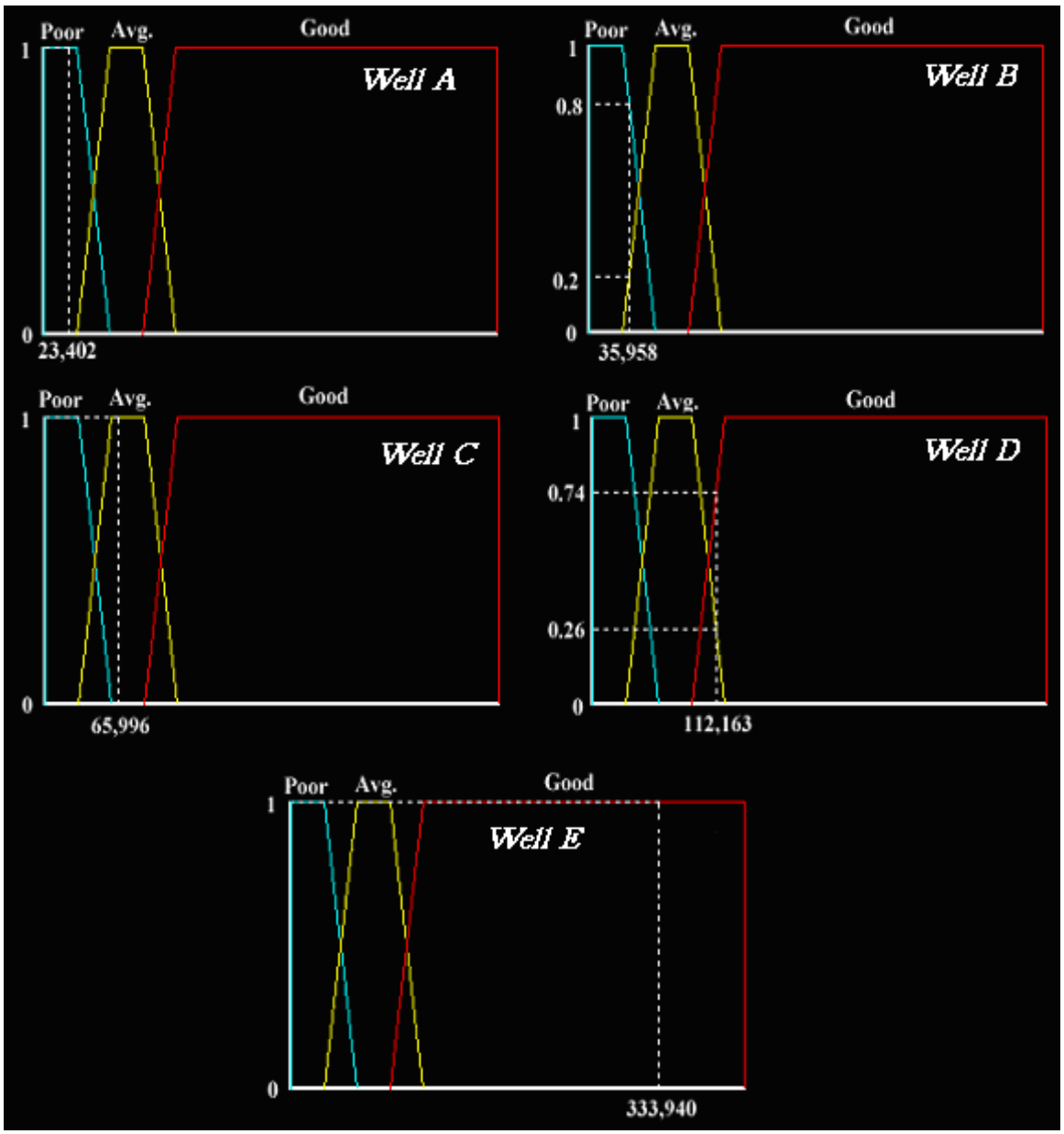

Figure 3. Classification of wells in the database using Fuzzy sets.

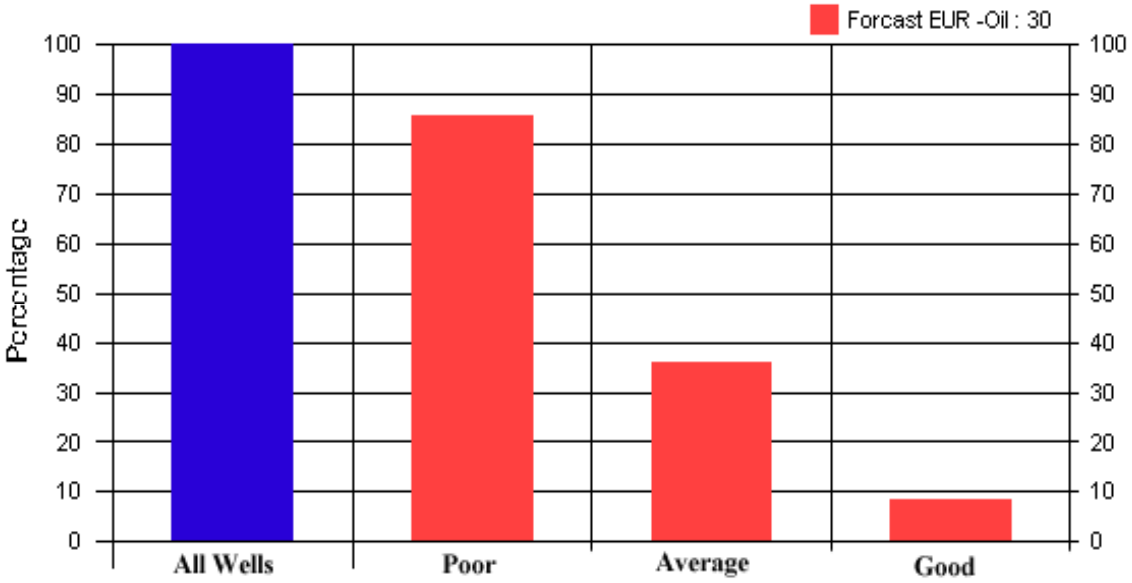

Figure 4. Distribution of the wells based on 30 Year EUR.

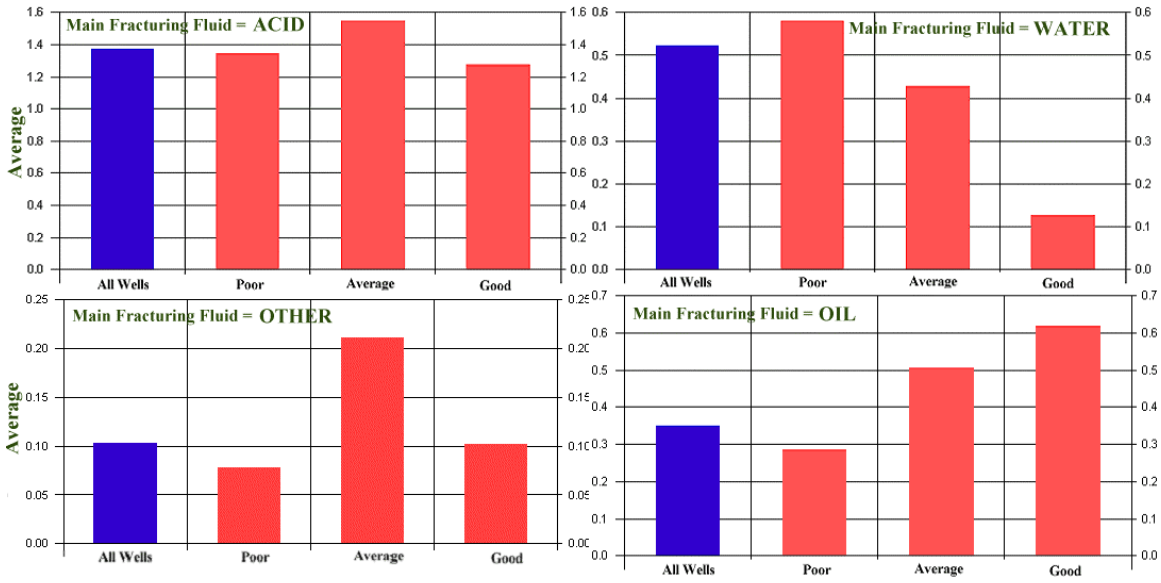

Figure 5. Distribution of the average value of Main Fracturing Fluids in wells of different quality.

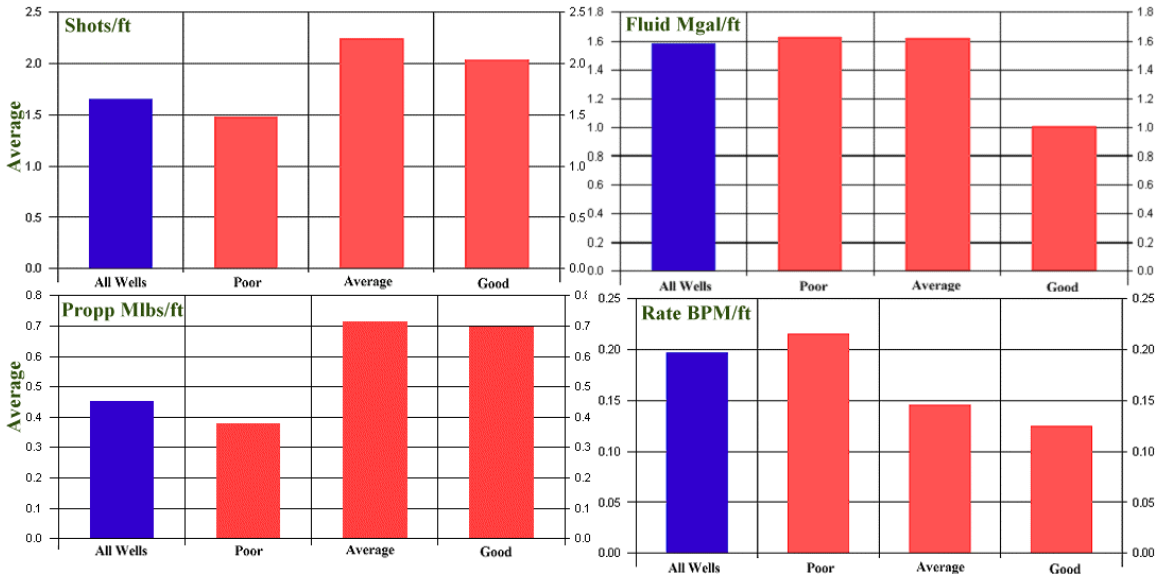

Figure 6. Distribution of the average value of completion parameters in wells of different quality.

Table 2. Parameters used during the neural network modeling process.

Qi
Di
Latitude
Longitude
Sub - RRQI
RRQI
Shots / ft
Date of first stimulation
MF - Water
MF - Oil
MF - Acid
MF - Other
Porppant Concentration (lb/gal/ft)
Ave. Inj. Rate (BMP/ft)

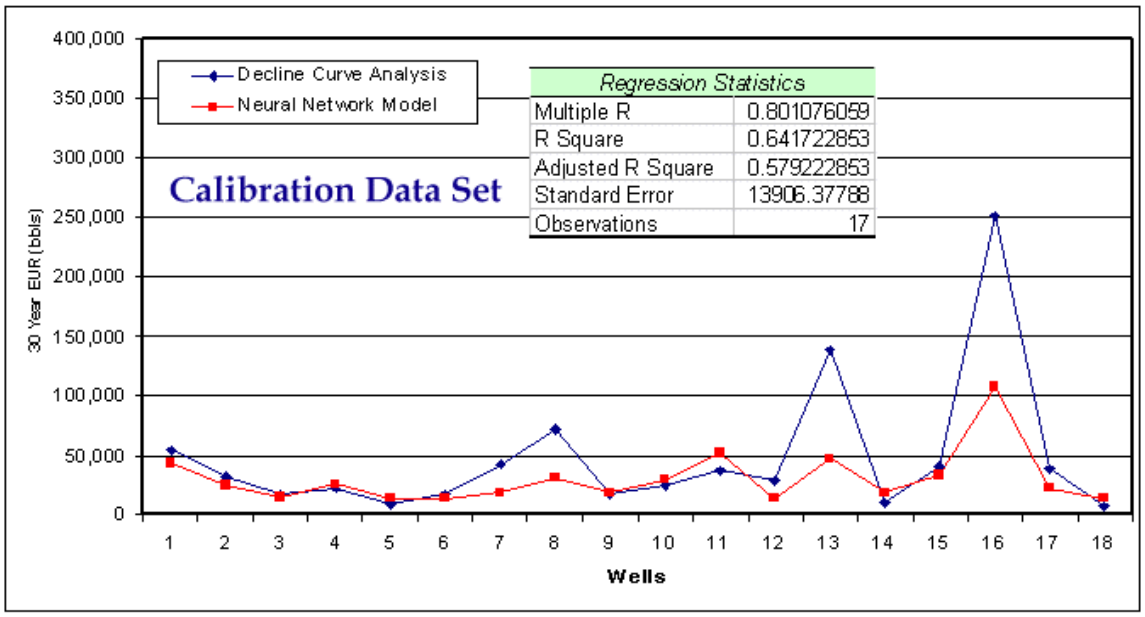

Figure 7. Actual and predicted 30 year EUR of the calibration data set.

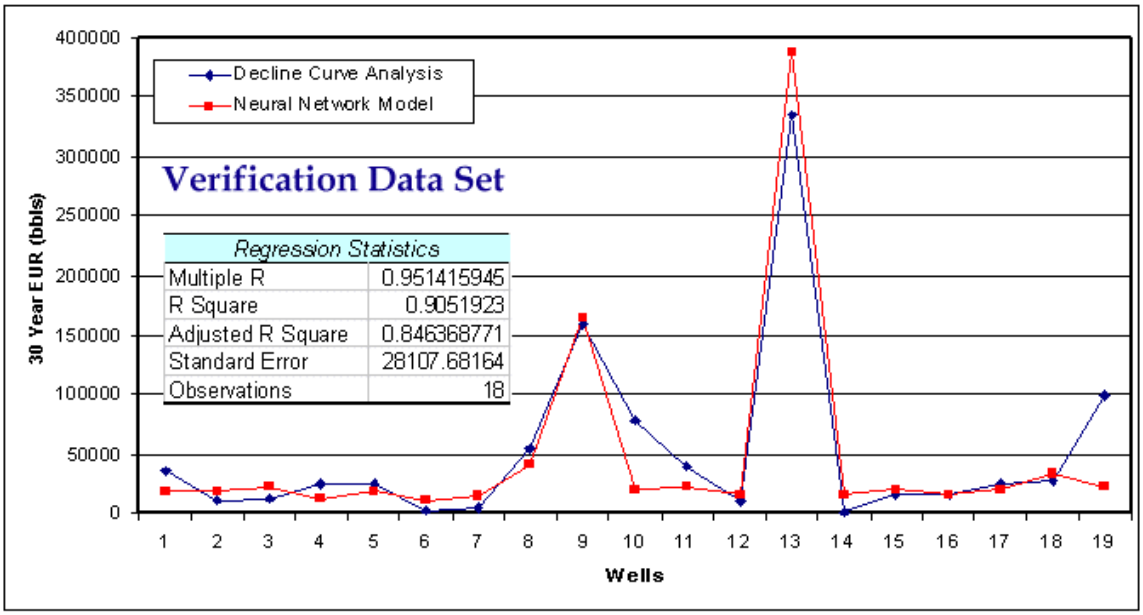

Figure 8. Actual and predicted 30 year EUR of the verification data set.

Table 3. Full field analysis Recommendation Matrix for best hydraulic fracturing practices in the Golden Trend.

	Parameter	Single Parameter Analysis			Combinatorial Analysis		Recommendations
		Percent of Population	Dominant Trend	Change in Value	Distribution	Dominant Trend	
Main Fluid	Water	Majority	Increasing	Moderate	Skewed	Use Little	Use Not Recommended
	Oil	All	Incressing	High	Skewed	Use A Lot	Use Recommended
	Acid	Majority	Decreasing	High	Skewed	Use Little	Use Not Recommended
	Other	Majority	Increasing	Low	Skewed	Use Little	Use Not Recommended
	Shot/ft	All	Decreasing	High	Skewed	Use Little	Use Small Numbers
	Prop Conc. (lbs/gal/ft)	All	Increasing	High	Skewed	Use A Lot	Use Large Amounts
	Rate (BPM/ft)	All	Decreasing	High	Skewed	Use Little	Use Low Rates

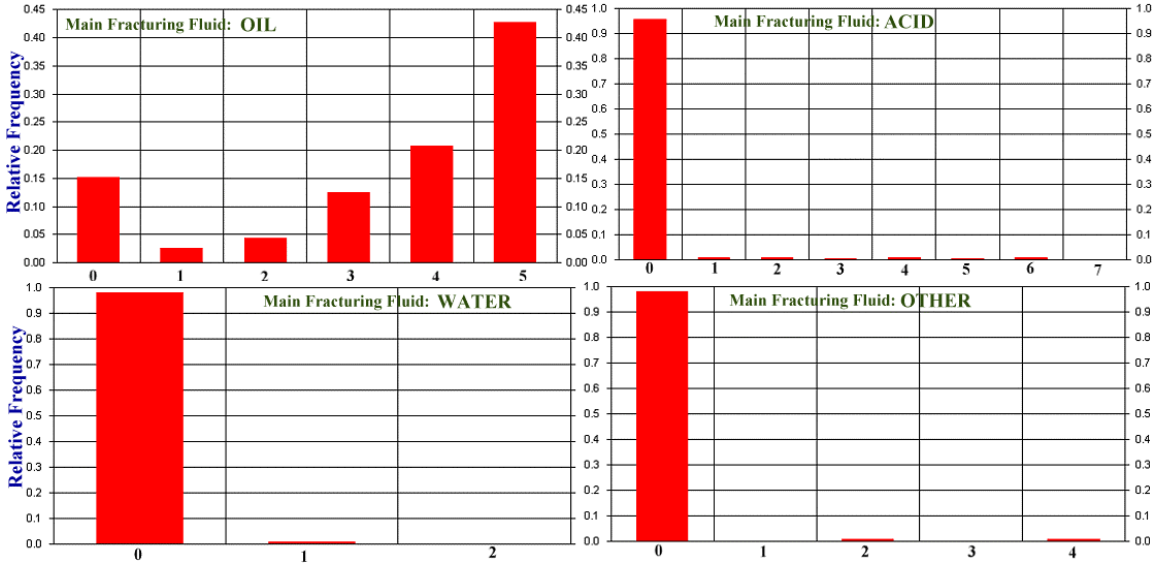

Figure 9. Full Field Combinatorial Analysis, results for main fracturing fluids.

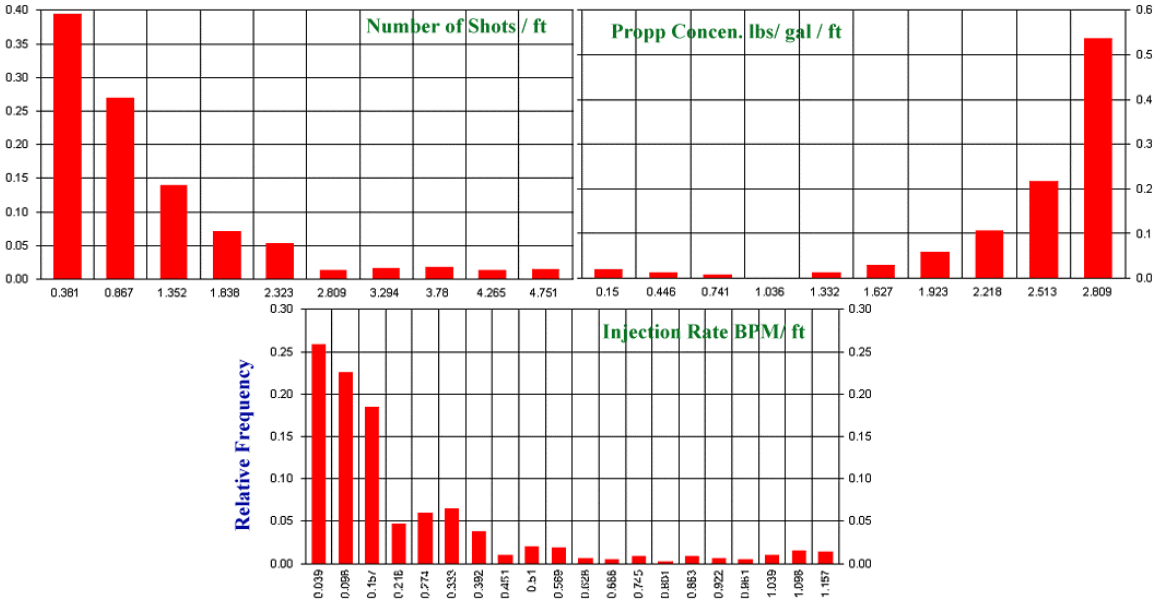

Figure 10. Full Field Combinatorial Analysis, results for other hydraulic fracturing parameters.

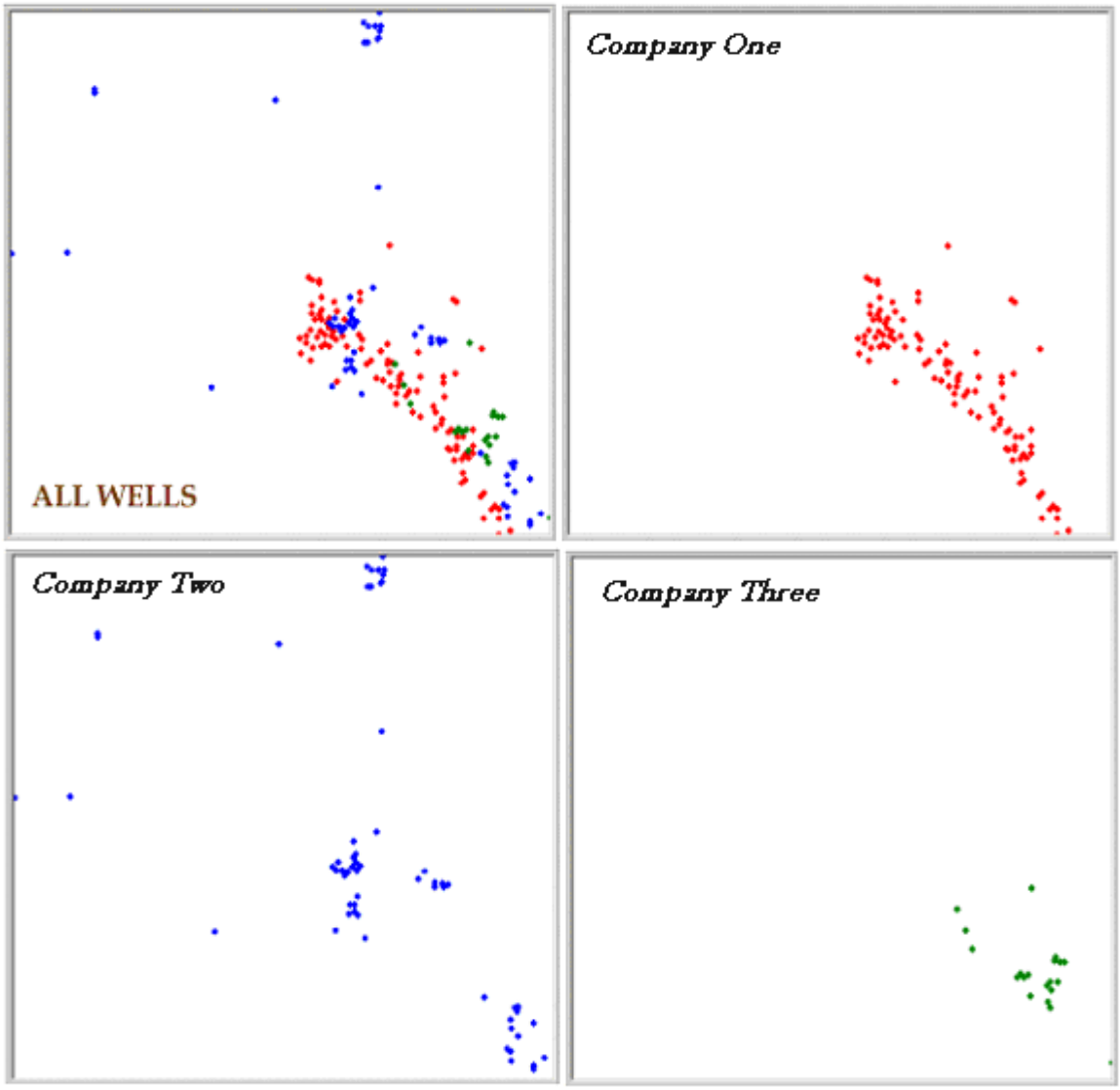

Figure 11. Wells in the database identified by the operating companies.

Table 4. Summary of the groups of wells analysis for Company One.

Company One							
	Parameter	Single Parameter Analysis			Combinatorial Analysis		Recommendations
		Percent of Population	Dominant Trend	Change in Value	Distribution	Dominant Trend	
Main Fluid	Water	Majority	Decreasing	High	Skewed	Use Little	Use Not Recommended
	Oil	All	Incressing	High	Skewed	Use A Lot	Use Recommended
	Acid	All	Decreasing	High	Skewed	Use Little	Use Not Recommended
	Other	Majority	Increasing	Low	Skewed	Use Little	Use Not Recommended
	Shot/**t**	All	Decreasing	High	Skewed	Use Little	Use Small Numbers
	Conc. (lbs/gal/ft)	All	Increasing	High	Skewed	Use A Lot	Use Large Amounts
	Rate (BPM/**t**)	All	Decreasing	High	Skewed	Use Little	Use Low Rates

Table 5. Summary of the groups of wells analysis for Company Two.

Company Two							
	Parameter	Single Parameter Analysis			Combinatorial Analysis		Recommendations
		Percent of Population	Dominant Trend	Change in Value	Distribution	Dominant Trend	
Main Fluid	Water	Majority	Decreasing	Moderate	Skewed	Use Little	Use Not Recommended
	Oil	All	Incressing	High	Skewed	Use A Lot	Use Recommended
	Acid	All	Decreasing	Low	Skewed	Use Little	Use Not Recommended
	Other	Half & Half	Mix	Low / Low	Skewed	Use Little	Use Not Recommended
	Shot/**t**	All	Decreasing	High	Skewed	Use Little	Use Small Numbers
	Conc. (lbs/gal/ft)	All	Incressing	High	Skewed	Use A Lot	Use Large Amounts
	Rate (BPM/**t**)	All	Decreasing	High	Skewed	Use Little	Use Low Rates

Table 6. Summary of the groups of wells analysis for Company Three.

Company Three							
	Parameter	Single Parameter Analysis			Combinatorial Analysis		Recommendations
		Percent of Population	Dominant Trend	Change in Value	Distribution	Dominant Trend	
Main Fluid	Water	Majority	Decreasing	Low	Skewed	Use Little	Use Not Recommended
	Oil	All	Incressing	Moderate	Skewed	Use A Lot	Use Recommended
	Acid	All	Incressing	Moderate	Skewed	Use Little	Inconclusive
	Other	Majority	Increasing	Low	Skewed	Use Little	Use Not Recommended
	Shot/**t**	All	Decreasing	Low	Skewed	Use Little	Use Small Numbers
	Conc. (lbs/gal/ft)	All	Increasing	Moderate	Skewed	Use A Lot	Use Large Amounts
	Rate (BPM/**t**)	All	Decreasing	Low	Skewed	Use Little	Use Low Rates

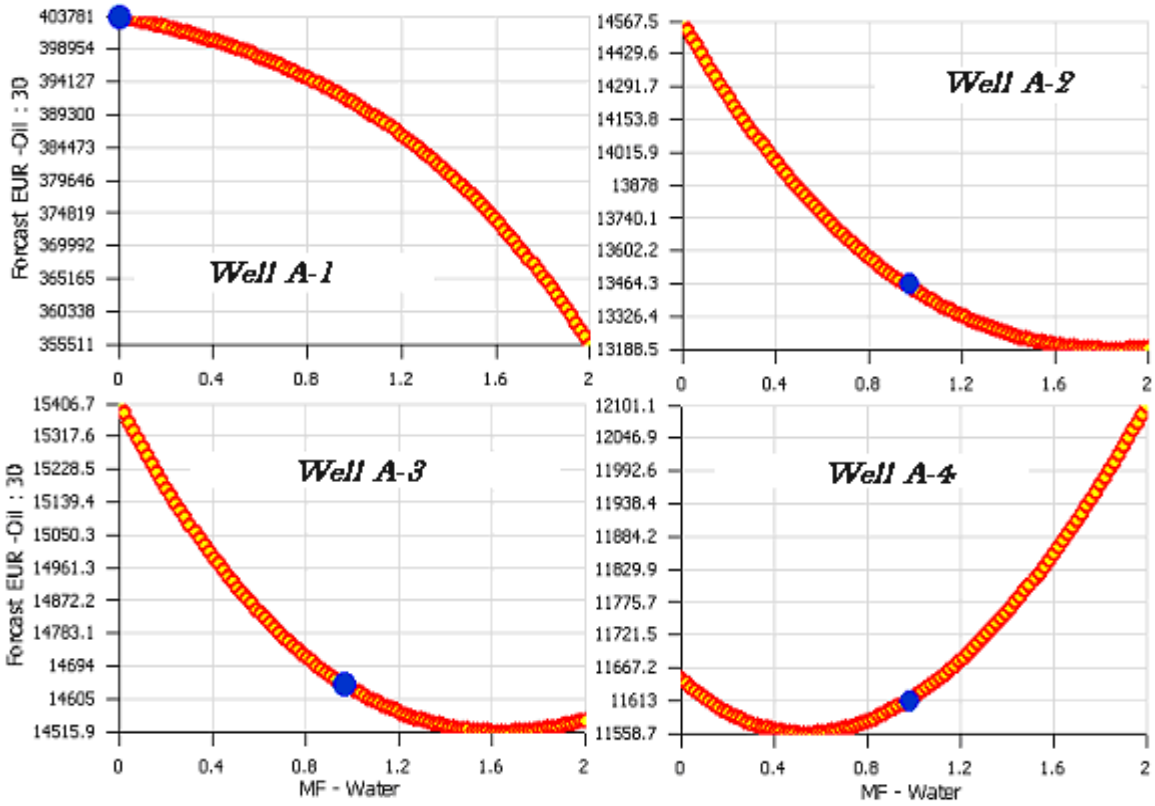

Figure 12. Sensitivity analysis for water as the main fracturing fluid for four wells in the database.

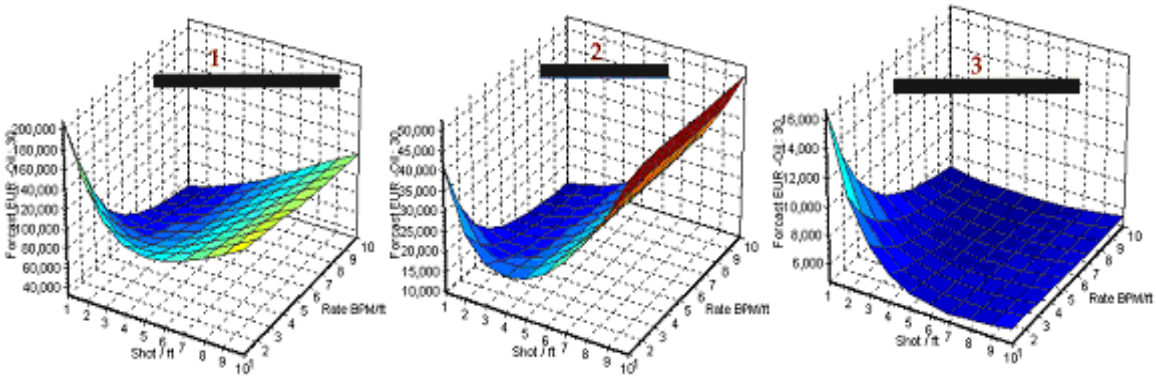

Figure 13. Sensitivity analysis for "Shot/ft" and "Rate" for three wells in the database.

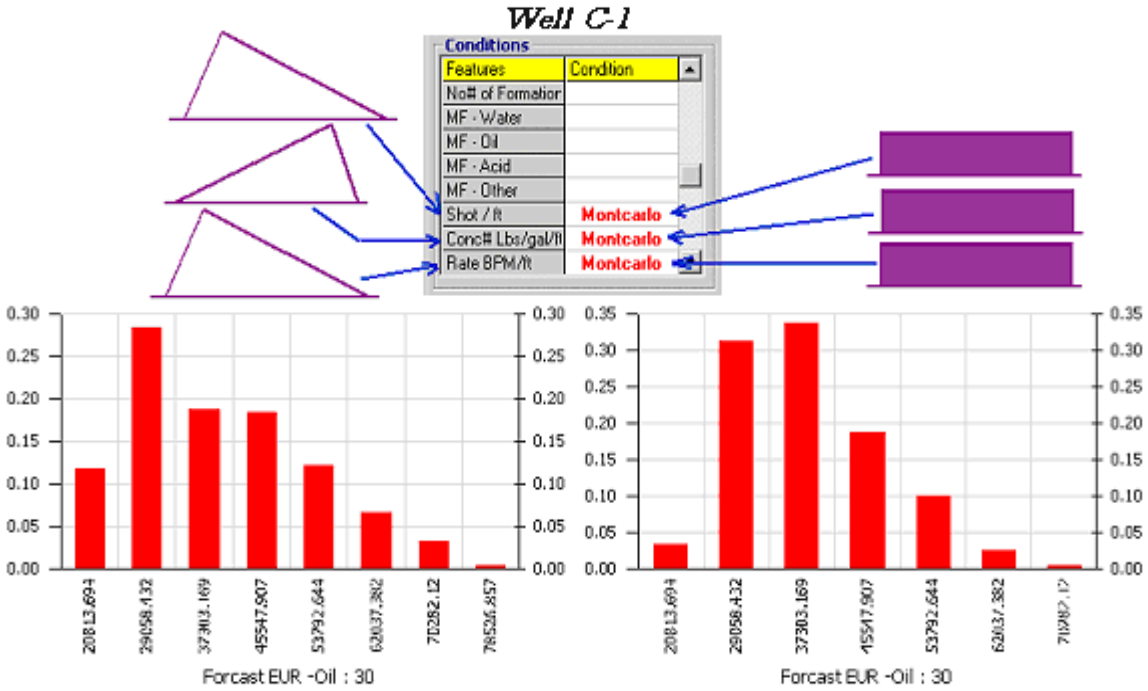

Figure 14. Combinatorial Analysis for *Well C-1* Operated by *Company One*.

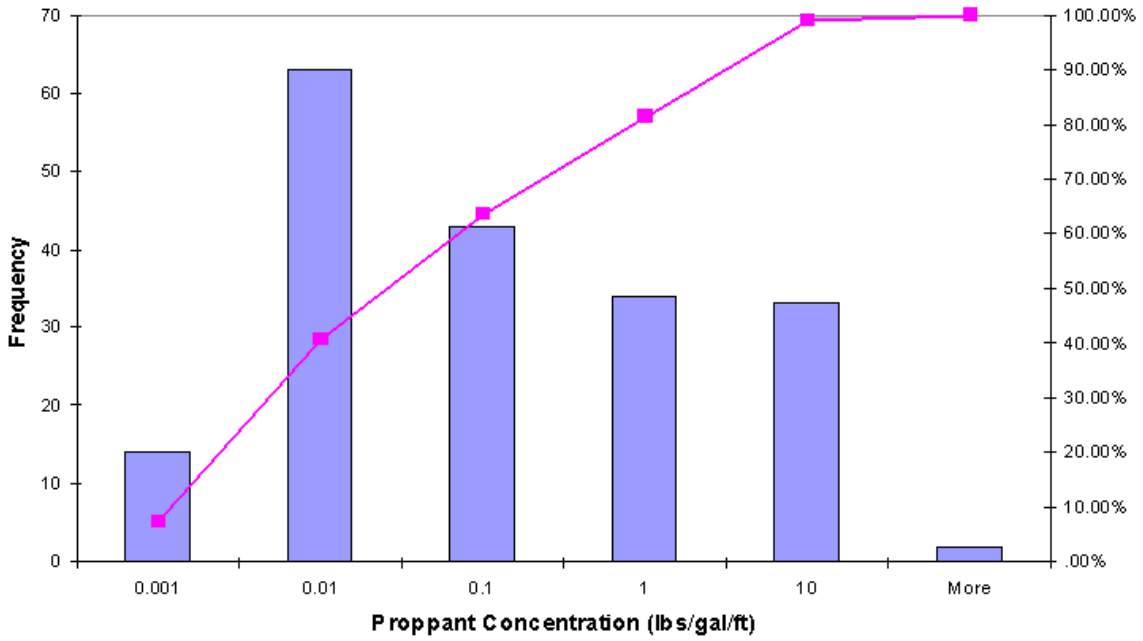

Figure 15. Logarithmic probability distribution function for Proppant Concentration.

SPE 100133

Application of Artificial Intelligence in Gas Storage Management

G. Zangl, M. Giovannoli, and M. Stundner, SPE, Schlumberger

Copyright 2006, Society of Petroleum Engineers

This paper was prepared for presentation at the SPE Europec/EAGE Annual Conference and Exhibition held in Vienna, Austria, 12–15 June 2006.

This paper was selected for presentation by an SPE Program Committee following review of information contained in an abstract submitted by the author(s). Contents of the paper, as presented, have not been reviewed by the Society of Petroleum Engineers and are subject to correction by the author(s). The material, as presented, does not necessarily reflect any position of the Society of Petroleum Engineers, its officers, or members. Papers presented at SPE meetings are subject to publication review by Editorial Committees of the Society of Petroleum Engineers. Electronic reproduction, distribution, or storage of any part of this paper for commercial purposes without the written consent of the Society of Petroleum Engineers is prohibited. Permission to reproduce in print is restricted to an abstract of not more than 300 words; illustrations may not be copied. The abstract must contain conspicuous acknowledgment of where and by whom the paper was presented. Write Librarian, SPE, P.O. Box 833836, Richardson, TX 75083-3836 U.S.A., fax 01-972-952-9435.

Abstract

An approach is investigated, to reduce the amount of CPU time needed to execute a numerical full field model in an optimization loop.

To demonstrate the power of this approach, a real life example is presented. Data from a gas storage reservoir have been used to setup a single tank material balance program. Then, a limited number of simulation runs is carried out. These simulation runs are intended to span over the whole range of input parameter variation (app. 25 runs).

In a next step, a Neural Network (NN) model is setup. By training a Neural Network on the so gained simulation outputs, a model, which is able to interpolate between the individual simulation scenarios is created. In this way, a large variety of different scenarios can be represented with a limited amount of model runs.

The trained Neural Network model is used as a proxy function for an optimization routine. The trained Neural Network has been used as fitness function for the Genetic Algorithm to minimize the output parameter, which is in this example the RMS-error of measured and calculated tank pressure. Due to the very low CPU consumption of the Neural Network, a large number of realisations can be calculated in a short amount of time. By this, the absolute minimum of the desired output parameter (in this case the RMS-error) can be evaluated in a few seconds.

The Genetic Algorithm has succeeded to find a minimum, which is located very close to the absolute minimum of all possible solutions.

Introduction

Numerical models are detailed and powerful predictive tools in reservoir management. While not perfect, they are often the best representation of the subsurface available. Optimization methodologies run these numerical models perhaps thousands of times searching for the most likely or most profitable solution to reservoir management questions. Because of the computational time involved, these methodologies are not used as much as they could be.

An approach is investigated, to reduce the amount of CPU time needed to execute a large number of runs of any CPU intensive numerical model. It can be used to perform a full sensitivity analysis using the uncertainty of the most sensitive input parameter to investigate the uncertainty of important reservoir information, like original hydrocarbon in place, recovery factor or abandonment pressure. This technology can also be used to run thousands of optimization runs in a couple of minutes.

It is proposed to use an artificial neural network (ANN) [1-7] to mimic the behavior of the numerical model. To be able to do that, several runs of the numerical model with a variation of relevant input parameters have to be performed. If all input parameters would have to be modified, the final number of runs would be very large, decreasing the value of this approach to zero.

Experimental Design [8-10]is used to create a set of input parameter variations to reduce the number of sensitivity runs to an affordable minimum. As soon as these runs have been calculated, the variation of the output is correlated to the input variations using an ANN. The neural network learns to behave like the numerical model; it can be described as proxy function of the numerical model. At the same time, the neural network acts as response surface for the Experimental Design. Normally, a polynomial function is used to span a surface over the simulation runs, which have been created using the Experimental Design method. The disadvantage of polynomial functions is their limited capability to represent non-linear dependencies. But exactly the handling of non-linearities is a strong point of neural networks. Therefore, neural networks have been used for the modeling of response surfaces.

Once, the neural network is trained, it needs only a fraction of a second to calculate the result for one set of input parameters. In that way, many thousand runs can be performed in a very short time. If the neural network is used as fitness function for an optimization program (e.g. genetic algorithm) an optimum solution can be found very fast (on a standard PC in less than a minute).

This workflow [11] can be used to either investigate uncertainties of designated input parameters, to optimize operational settings, or shorten the time to history match the numerical model.

In the following, two examples are described. The first one describes how this approach can be used to achieve a history match of a model. The second example uses a NN as single well proxy function, which can be implemented in an

automated surveillance system to monitor the well performance.

After the two examples, the general concept of automated reservoir surveillance is described. In the appendix, the technical terms used in this paper are explained.

Example1: Automated History Match

Data from a gas storage reservoir have been used to setup a single tank material balance program. As a first step, the most sensitive parameters, which affect the material balance model, are determined. In the case of the gas storage reservoir, the reservoir volume, the pressure at start of the simulation and the aquifer transmissivity show the highest impact on the resulting average reservoir pressure.

A limited number of simulation runs is carried out. These simulation runs cannot cover the whole range of possible model realizations, but they are intended to span over the whole range of input parameter variation. For each of the three input parameter, five different values - starting at the minimum and ending at the maximum value of the possible range – create a total number of 5x5x5 = 125 simulation runs. As result (=output parameter) the RMS-error (root mean square error) of the modeled vs. measured average reservoir pressure is calculated. This set is equal to a fully factorial experimental design. If the composite or Box-Behnken experimental design is used, the number of needed simulation runs can be reduced to 25.

In a next step, a neural network (NN) model is setup. The architecture consists of a three layer (input, hidden, output layer) feedforward back-propagation Neural Network having three neurons in the input layer, five neurons in the hidden and one neuron (RMS-error) in the output layer (see figure 1). The Neural Network is trained on 125 patterns, which are represented by the 125 material balance runs. All 125 patterns have been used as training patterns. As a NN model needs also test patterns, 32 randomly chosen patterns have been duplicated and used as test patterns. The training converged very fast, the minimum training and testing error has been achieved after approximately 300 iterations, which takes not more than 5 seconds on a standard PC.

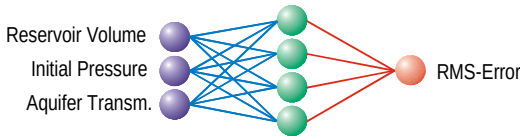

Fig. 1: NN Architecture

By training a neural network on the so gained simulation outputs, a model, which is able to interpolate between the individual simulation scenarios is created. In this way, a large variety of different scenarios can be represented with a limited amount of model runs. The trained Neural Network model is used as a proxy function for an optimization routine. It has been used as fitness function for the genetic algorithm to minimize the output parameter, which is in this example the RMS-error. Due to the very low CPU consumption of the neural network, a large number of realizations can be calculated in a short amount of time. By this, the absolute minimum of the desired output parameter (in this case the RMS-error) can be evaluated in a few seconds.

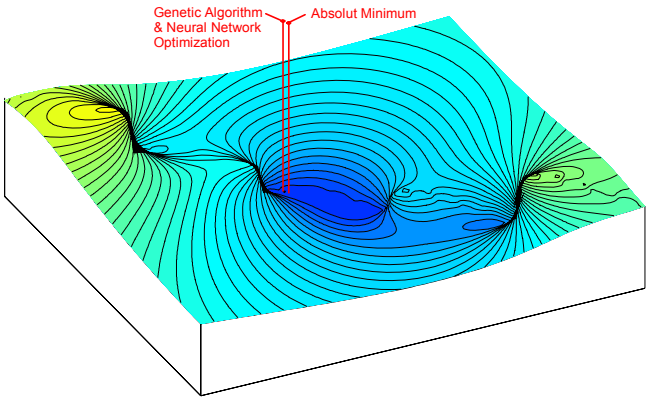

Fig. 2: Optimization Surface & Location of Minima

As can be seen in Fig.2, the Genetic Algorithm has succeeded to find a minimum, which is located very close to the absolute minimum of all possible solutions.

The maximum RMS-error of all runs is 14.16 [bar], the absolute minimum is 5.4. The genetic algorithm has found the appropriate settings for the three input parameters (reservoir volume, initial pressure and aquifer transmissivity) resulting in a RMS-error of 5.49, which is a deviation of 1.67%.

Fig. 3 shows the final history match. The red dots mark the measured pressures; the green line represents the calculated tank pressure from the material balance model. As there is also a dynamic aquifer involved, the blue line depicts the aquifer pressure.

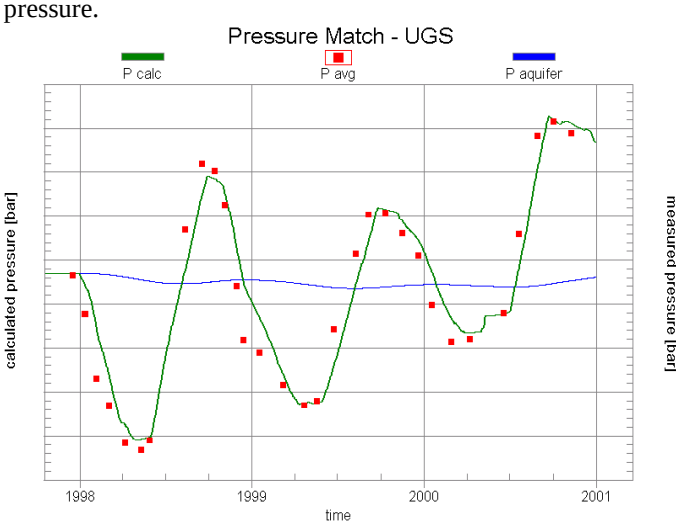

Fig. 3: Final History Match

Example 2: Monitor Horizontal Well Performance

A neural network has been trained to calculate the bottomhole flowing pressure of a horizontal well, which is completed in an underground gas storage reservoir (See Fig. 4). Two different kinds of parameters have been used as input for the ANN. First, production and injection volumes of the well and secondly, model parameters, namely the reservoir pressure and the cumulative water influx into the reservoir. In that way, the input parameters of the neural network capture the behavior of the reservoir and the near wellbore effects. As gas injection and production alternates, it is important to use

both parameters in the input, so that the neural network is able to distinguish between production and injection cycles.

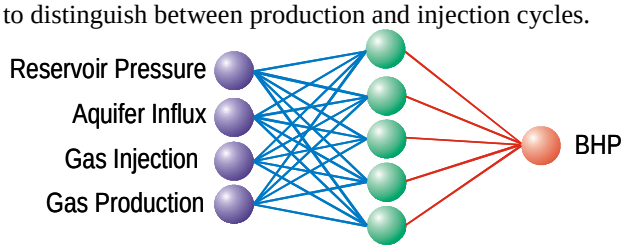

Fig. 4: ANN Architecture for Well Model

The neural network was trained on daily data over one full operation cycle from January 1999 to January 2000 (approximately one year). The test patterns were chosen randomly within this period. The training converged rapidly, which is a good sign for the liability of the network.

After training the neural network, the remaining historical data –daily data for another year – have been used as input values for the neural network together with the results of the reservoir model (reservoir pressure and aquifer influx). The ANN calculated a synthetic bottomhole flowing pressure, which can be compared to the measured one (see Fig. 5).

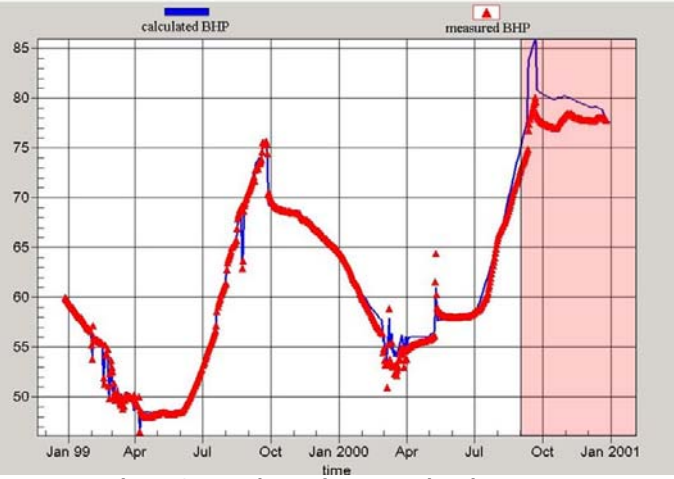

Fig. 5: Comparison of Measured and NN BHP

It is clear to see, that the neural network has predicted the well performance very well up to a time point in late August or early September. The predicted well flowing pressures are higher than the actually measured ones, indicating a change of the well performance, i.e. the well productivity index. This happened shortly before the well changed from injection to production. Several explanations for the reason are possible. In any case, the well needs further investigation by the engineer.

If the reservoir model, that generates the input parameters for the ANN and the ANN itself can be run automatically, a surveillance system can be setup for the whole UGS reservoir. A check of the deviation of the measured value to the calculated value can be implemented, indicating a system change e.g. if the deviation is higher than 10%. Any kind of rules can be setup for all models, making sure to capture the reservoir trend as well as the performance of all wells in operation.

If an automated notification system is included in the surveillance system the engineer receives an alarm and can react timely to reservoir and well changes, saving valuable time.

The next chapter describes some requirements and capabilities of such a surveillance system.

Automated Reservoir Surveillance

Current levels of reservoir surveillance technology like down-hole gauges and fiber optics, sometimes coming along with intelligent well completions create an increasing flow of data. Conventional software cannot help the knowledge worker to cope with high-frequency real-time data. Overloaded with data handling work, the knowledge worker in our industry is not capable to reveal the great potential inherent in this data.

The reservoir's response on the applied production strategy is measured with dramatically increasing resolution in time and space. Conventional reservoir modeling techniques like numerical reservoir simulation were developed to predict reservoir performance with a minimum of individual well production information (i.e. monthly data).

While the well-specific performance data become available at a magnitude of 10.000 to 100.000 (10-seconds data) values per day, CPU time consumption and project turnaround time of numerical simulation models do not allow to run these models in real-time.

A data-hub is needed to condition the high-frequency real-time data into a time increment, which can be handled by any commercial petroleum engineering software. Before dispatching data to the pre-defined models and the engineer's desktop, data are automatically analyzed by an expert system to detect erroneous data.

Erroneous data could be caused by a gauge or reading failure. In this case, an alarm is triggered by the notification system. If data gaps occur, again, an alarm is triggered and the system can automatically suggest a replacement value.

Outliers can be produced by malfunctioning or improper adjusted gauges. The system is able to detect these outliers and remove them. After this extensive data quality check, data are automatically merged to a handy time increment and finally stored on a server in the company's IT-infrastructure. In this way, high quality data are delivered on time at the engineer's desktop.

Automation Task Concept

Automating reservoir surveillance requires the proper definition of tasks, which shall be performed by the surveillance software in an automated way. Reservoir surveillance data arrive on a 24/7 basis in the town office. Therefore software solutions are required which process these data also on a 24/7 basis.

SCADA systems are the first step of automation in oil and gas fields, forwarding the raw data into the town office to visualize the data. Conventional reservoir management tools are designed to work in an offline modus, being not prepared to run with real-time reservoir surveillance data.

The core of such a reservoir surveillance system is an expert system, which allows automation of the reservoir surveillance work process. Faster decisions for short-term production optimization through increased productivity of knowledge workers as well as sustainable work process

optimization and reduced elapsed time for routine reservoir surveillance can be achieved.

An “automation task” concept allows controlling processes inside and outside of the software. These tasks are scheduled in time –these tasks are called master tasks- or are triggered by events detected by other master tasks -these tasks are called slave tasks.

Automation tasks always have the same structure: first scheduled tasks (master tasks), or trigger automation tasks (slave tasks), then run the predictive data mining models and apply rules.

Events in general are either discrepancies from expected trends (actual vs. predicted value – predictive data mining models are applied), or violations of defined constraints.

Triggered actions can be of the following types:

- set alarm (information, warning, alert) in notification system
- execute surveillance software module, e.g. database reporting
- exchange data with 3rd party software and/or run this software
- trigger other slave tasks
- send e-mail or text message

Data Acquisition

Data preparation and quality control is the first crucial step in automating reservoir surveillance. Multi-parameter rules and applied neural networks allow complex cross validation of surveillance data, as outliers may be detected only in the context of other measured data.

The surveillance system should provide information about the quality of the data; sensor errors and transmission errors can be filtered. Statistical reports allow the engineer to evaluate reliability of data and sensors. In a last step, data are aggregated to the defined time increment.

Data Integration

After data preparation, data have to be aggregated at a field sample rate to a rate, which reduces the number of patterns without loosing meaningful reservoir behavior information. Experience has shown that time increments of 15 minutes to 1 day are sufficient for reservoir surveillance data mining models.

Data mining models, like neural networks, are working with patterns, therefore common constant time increments are required for input and output parameters. Raw reservoir surveillance parameters have different

- quality
- frequency
- time delays (transmission)
- ways to be measured (sensors, manually edited).

Therefore, aggregation and interpolation of measured data is required. Better data leads to an increasing utilization of data in the workflow.

Event Detection

Such a process helps to manage assets in the best manner. The engineer is able to react fast on problems occurring. He is able to:

- anticipate the actual reservoir performance and recovery mechanisms which will likely deviate from the planned model
- identify any discrepancies in performance as early as possible
- provide information regarding the cause of these deviations
- use all data available to identify these discrepancies.

Key Performance Indicators are monitored continuously. While SCADA systems are limited to run comparisons with expected trends on a parameter basis, the presented data mining process allows running complex models to health check the reservoir performance.

Appendix A: Experimental Design

Formal experimental design has several advantages over the classic, one-step-at-a-time approach that has been favored by academe. These advantages include improved performance characteristics, reduced costs, and shortened development and testing times.

The formal experimental design examines changes in output variables for a process, given any combination of input variables.

By isolating and better understanding those factors that most affect the outcomes, the researcher can devote fewer resources to investigating the less-important factors. In testing design strategies or troubleshooting established ongoing processes, the experimental design process may be used to gain additional knowledge about the relationships among input and output variables. Formal design also allows the researcher to mathematically model the process and optimize the response.

The goal is to fill a design space with the least number of points (data collection units), yet still fully characterize the system. Researchers accomplish this goal by employing a number of well-defined design types that are standard in the literature. For more adventurous experiments or for modeling a space sufficiently different from the norm, special models are available that are easily implemented in several commercial software programs.

In all of these experiments, the strategy is essentially the same. The first experiment is a screening run. This run isolates those input factors that are most important to the outputs.

The second step is exclusion of those factors deemed to be of minor significance to the desired output, based on the results of the screening experiment. With the remaining factors, researchers can use a response surface design to determine the changes in outputs for any combination of changes in inputs.

The last experiment is a verification run, whereby the outputs are checked against the predictions of the response surface design. Once the suitable input settings have been verified, the process may run at these settings until any inputs are changed.

Screening Designs

The screening run may be designed using one of the following models:

Linear with Center Point

Although the linear-with-center-point design is linear, it does require data collection at the center. This requirement eliminates the drawback of the strictly linear design. These are among the most popular and widely used screening designs.

Factorial Designs

These occur as two types, full and fractional. Full factorial designs are used to estimate all possible effects, including interactions, of the input variables. The number of runs for a design that uses k variables and n levels is nk. This equation means that the number of runs increases dramatically as the numbers of levels and factors increase. The advantages of the full factorial design include orthogonality (ability to exclude confounding, among other properties), lack of aliasing (identical columns in the design), and evaluation of all main effects and interactions. The disadvantages include time, cost, and resource commitment.

Fractional factorial designs retain orthogonality while requiring fewer runs. However, doing fewer runs means acquiring less information. To ensure that subsequent runs capture the most important information, experimenters usually eliminate runs for interactions that are deemed insignificant.

Box-Behnken Designs

An efficient three-level design that uses embedded 2k designs, the Box-Behnken design holds certain factors at their center points. Tables that specify the number of runs to be used are published and readily available. The model drops all corner points in the design space. This elimination of data may be of concern to those who need measurements at the extremities. These designs are close to orthogonal and may be used to estimate main and quadratic effects as well as all linear two-way interactions.

Central Composite Designs

These symmetrical, space-filling designs are flexible and efficient. Also known as Box-Wilson designs, these multidimensional cubes are face-centered and may be easily rotated by choice of appropriate factors. This easy rotation means that the predicted response may be estimated with equal variance regardless of the direction from the center of the design space. The only drawback in these designs is that the number of runs required for the larger designs rapidly becomes very large.

Appendix B: Response Surface (Proxy Function)

The purpose of Response Surface Methodology (RSM) is to approximate a process over a region of interest, often called the operating region. Engineers define a performance measure of the process (the response) and input variables (factors) that are supposed to influence the response. The input variables correspond to the prior uncertainties on the process. RSM provides tools for (1) identifying the variables that actually influence the response (sensitivity), and (2) building a regression model relating the response to the influential variables (modeling). The final model can be used to make predictions of the process over the domain. For the regression model to be computed, the process must be sampled over the operating region through experimentation.

The true response function must be approximated. Usually, a low-order polynomial model is considered valid over a small region of the variable space. Models are generally first-order or second-order, depending on the objective of the study. In this study it is proposed to train an ANN, as it scopes very well with nonlinearities.

RSM provides tests to identify the significant terms of the model and statistics to measure the quality of fit and the predictive power of the model. The power of prediction of the model is estimated on the basis of a computation of the prediction error sum of squares.

In the first case, all that is needed is a model capable of identifying the terms that are significant. In the second case, a model with a good quality of fit and also good prediction power is required.

Appendix C: Artificial Neural Network (ANN)

Artificial Neural Networks (or neural networks for short) are computational models broadly inspired by the organization of the human brain. Unlike conventional problem-solving algorithms, neural networks can be trained to perform a particular task.

This is done by presenting the system with a representative set of examples describing the problem, namely pairs of input and output samples; the neural network will then extrapolate the mapping between input and output data. After training, the neural network can be used to recognize data that is similar to any of the examples shown during the training phase. The neural network can even recognize incomplete or noisy data - an important feature that is often used for prediction, diagnosis or control purposes. Furthermore, neural networks have the ability to self-organize, therefore enabling segmentation or coarse coding of data. The interface of an ANN to the outside world consists of an input layer and an output layer of neurons. Besides the input and output layer there can be other intermediate layers of neurons, which are usually called hidden layers. The neurons are the processing units within the neural network and are usually arranged in layers. The information is propagated through the

Neurons

A neuron collects information from all preceding neurons relative to the flow of the information and propagates its output to the neurons in the following layer. The output of each preceding neuron (oi) is modulated by a correspondent weight (wi) before affecting the activity of the neuron. This process is realized by the formula a = w*o, where a represents the activity of the neuron. This activity is then modified by an activation function f() and becomes the final output (o = f(a)) of the neuron. This signal is then propagated to the neurons of the next layer.

Connections

Connections are the paths between neurons where all the information flows within a Neural Network. Very often the neurons of two succeeding layers are fully interconnected, but additional connections might exist, going to further layers or even missing connections between certain neurons.

Weights

One of the most important aspects of neural networks is the storage of information. Each connection is equipped with an individual weight that modifies the signal flow on the respective connection. The weight works as a factor by which the output of the preceding neuron is multiplied before it becomes an actual input. This means that information is stored distributed within a neural network and even minor destruction of some of the weights will have little effect on the recall of learned information.

Learning

The phase when sample patterns of a certain problem are presented to a neural network it is called the training phase. During the training the weights of the neural network are adjusted. Depending on the type of the neural network and on the problem it is going to solve, either a supervised or an unsupervised method can be used for adapting the weights. In both cases however, the training starts with propagating the input through the neural network and all its neurons change their activity accordingly.

A supervised training is typically chosen when the ANN should map input to output patterns. This requires knowing the output to a given input. After each learning step, the output of the neural network is compared to what should be the resulting output pattern. The observed difference is used to adapt the weights. The adaptation of the weights starts at the output neurons and continues downward toward the input layer. The weight adaptation for one pattern often does not correct the neural network's faulty response completely, but improves it.

However, there are ANNs which can adapt their weights within one training step (this is called one shot learning). Then the next input pattern is chosen and the whole process is repeated until the overall response of the neural network is satisfying. It is important to define the point where the training is terminated, because sometimes it is possible to over-train a neural network. Namely, at some point the neural network starts to memorize exactly the training examples with their inherent noise and later on it will not be able to generalize from the trained examples to new patterns presented during recall.

An unsupervised training is chosen when the ANN has to classify data on its own. Here, the neural network distinguishes certain classes by using the interdependencies it detects within the data. Some of these neural networks are even able to reorganize themselves, e.g. by recruiting new neurons to represent unknown patterns or new classes.

Appendix D: Genetic Algorithm (GA)

Genetic algorithm (GA) is a robust search method based on analogies to biology and genetics. Survival of the fittest among a population of individuals, selection criteria, and reproduction strategies are concepts copied from the natural life and used as operators in this artificial environment.

GA combines survival-of-the-fittest functionality among string structures with a structured, yet randomized, information exchange that emulates somewhat the innovative flair of human search. In every generation, a new set of artificial creatures (strings) is created using bits and pieces of the "fittest" from the previous generation; an occasional new search characteristic is tried for good measure. While randomized, genetic algorithms are no simple random walk, they efficiently exploit historical information to speculate on new search points that will yield improved performance.

Genetic algorithms solve problems by borrowing a technique from nature. They use Darwin's basic principles of survival, mutation, and crossbreeding to create solutions for problems. If more information is needed, extensive descriptions of the technique can be found in the literature.

Conclusions

Artificial neural networks as proxy models can be a powerful tool to save time in the analysis and the calculation of reasonable options. However, the benefit and accuracy of the application of neural networks as proxy model has to be assessed for the specific reservoir / production system. Especially in cases, where too many degrees of freedom, too many constraints, limitations and dependencies are present or where the input space and the output space cannot be correlated at all, neural networks might not be able to be a practical approximation.

ANNs are not a general substitution tool for simulation models. The purpose of the proxy model is to find cases where an ANN can learn the behavior extremely accurately and so eliminating the need for time consuming simulation runs. Especially when regarding real-time applications, the time saving due to the proxy models can be crucial for the system. However, the engineer's reasoning is not replaced.

References

1. Zangl, G. and Hannerer J.:"Data Mining – Applications in the Petroleum Industry", _Round Oak Publishing, Houston, TX (2003), ISBN 0-9677248-1-3.
2. Sharkey, A.J.C., "Combining Artificial Neural Nets," Springer Verlag London Limited, 1999
3. Rao, V.B., Rao, H.V., "Neural Networks & Fuzzy Logic," MIS:Press, New York, 1995
4. Fausett, L., "Fundamentals of Neural Networks," Prentice Hall PTR, New Jersey, 1994
5. Jang, J.-S.R., Sun, C.-T., Mizutani, E., "Neuro-Fuzzy and Soft Computing," Prentice Hall PTR, New Jersey, 1997
6. Tsoukalas, L.H., Uhrig, R.E., "Fuzzy and Neural Approaches in Engineering," John Wiley & Sons Inc., New York, 1997
7. De Jonge,Gert J., Stundner, M., Zangl, G.:" Automated Reservoir Surveillance through Data Mining Software", paper SPE 83974, presented at the Offshore Europe 2003 held in Aberdeen, UK, 2-5 September 2003
8. Lechner, J. P., Zangl, G., "Treating Uncertainties in Reservoir Prediction with Neural Networks", SPE 94357, presented at the 2005 SPE Europec/EAGE Annual Conference, Madrid, Spain.
9. White, C.D., Royer, S. A., "Experimental Design as a Framework for Reservoir Studies", paper SPE 79676, presented at the 2003 SPE Reservoir Simulation Symposium, Houston, TX.
10. Zangl, G., Oberwinkler, C., "Predictive Data Mining Techniques for Production Optimization", paper SPE 90372 presented at the 2004 SPE Annual Technical Conference and Exhibition, Houston, TX
11. De Jonge, Gert J., Stundner, M.:" How Routine Reservoir Surveillance with Neural Networks and Simplified Reservoir Models can Convert Data into Information", paper SPE 78334, presented at the SPE 13th European Petroleum Conference held in Aberdeen, Scotland, U.K., 29-31 October 2002

Using Neural Networks for Candidate Selection and Well Performance Prediction in Water-Shutoff Treatments Using Polymer Gels—A Field-Case Study

A. Saeedi, SPE, Chevron Corp., **K.V. Camarda,** and **J.T. Liang,** SPE, University of Kansas

Summary

Using actual field cases, a neural network model was developed to identify candidate wells and predict well performance for water shutoff treatments using polymer gels. A feed forward back propagation algorithm was used to develop the neural networks. The before and after treatment data for 22 wells treated with polymer gels in the Arbuckle formation in central Kansas were used to train and verify the neural networks.

Polymers and gels have been used extensively in field applications to suppress excess water production and improve oil productivity. Field experience has demonstrated that candidate-well selection is critical to the success of gel-polymer treatments. To date, most candidate-well selections are on the basis of anecdotal screening guidelines, which often results in inconsistent treatment outcomes. With only pretreatment well data as input parameters, the neural networks developed in this work can accurately predict the post-treatment cumulative oil production of the well one month after treatment with an average error of 16%, and the post-treatment cumulative oil production three months after treatment with an average error of 10%. This is a dramatic improvement over the current method of using anecdotal screening guidelines for candidate-well selections.

This method represents a major breakthrough where the candidate selection can now be on the basis of the accurate predictions of treatment outcomes without having to use complicated reservoir models to simulate the well performance after treatment.

Introduction

Excess water production is a major issue in oil field operations worldwide, currently averaging three barrels of water for each barrel of oil produced (Bailey et al. 2000). The situation is even worse in the US where more than seven barrels of water are produced for each barrel of oil (EPA 1999). The annual cost of treating and disposal of this water is estimated to be USD 40 billion (Bailey et al. 2000). Water shutoff and conformance control, therefore, represents a significant financial and environmental challenge/incentive for the petroleum industry. Polymers and gels have been used extensively in field applications to suppress excess water production and improve oil productivity (Seright et al. 2003). Field experience has demonstrated that candidate-well selection is critical to the success of gel-polymer treatments (Seright et al. 2003). To date, most candidate-well selections are on the basis of anecdotal screening guidelines, which often results in inconsistent treatment outcomes (Seright et al. 2003).

Reservoir simulation can potentially be used as a screening tool to predict the post-treatment performance of a candidate well using the pre-treatment historical data (Barati et al. 2006). However, this method is usually expensive and also requires extensive knowledge of the target reservoir (including the rock and fluid properties) the historical production data, and the geological reservoir model. Unfortunately, they are not always available for older reservoirs where the well records are often incomplete or lost (Barati et al. 2006)

Another method that has been investigated is to correlate the historical pre- and post-treatment performance data of the wells treated with polymer gels in the target reservoir. In this method, multivariate analysis is used to correlate the post-treatment performance of the treated wells with the pre-treatment data such as the geographical location of the wells, the depth of the wells, and the production history of the wells, and so on. The correlation could then be used as a predictive tool for candidate selection in the target reservoir. The problem with this method is that the physical processes involved in gel polymer treatment downhole are too complex to be accurately represented by correlations generated between pre- and post-treatment data using multivariate analysis (Alhajeri et al. 2006).

Prediction of the performance of a well after treatment, using the pre-treatment data, is a pattern recognition problem. Neural networks have shown great capabilities in solving pattern recognition problems (Ali 1994; Mohaghegh 1995; Ahmed et al. 1997). The objective of this study is to develop a methodology using neural networks to identify candidate wells on the basis of the predicted outcomes for gel-polymer treatments. The before and after treatment data for 22 wells treated with polymer gels in the Arbuckle formation in central Kansas were used to develop the neural networks (Saeedi 2005).

Arbuckle Formation

The Arbuckle formation is the main oil producer in Kansas, responsible for approximately 36% (~2.2 billion barrels) of the total produced oil in Kansas (Franseen et al. 1999) **(see Fig. 1).** Arbuckle reservoirs are fracture-controlled karstic reservoirs with porosity and permeability influenced by basement structural patterns and subaerial exposures. The subaerial exposure has resulted in weathering and secondary dissolution of the upper beds of the Arbuckle. It is believed that these processes have significantly increased porosity and permeability and created petroleum reservoirs in these strata. (Franseen et al. 1999). Shallow-shelf dolomites predominantly constitute the Arbuckle formation. Porosity of the Arbuckle reservoirs is enhanced by the dolomitization process (Franseen et al. 1999). Most of the Arbuckle's oil and gas zones are perforated in the top 25 ft of the Arbuckle, while some are perforated at a depth of 25 to 50 ft within the formation (Franseen et al. 1999). High initial oil productivity, a rapid decline in oil production rate, and the production of large amounts of water at high water to oil ratios (WOR) are characteristics of Arbuckle wells (Willhite and Pancake 2004). On the basis of these characteristics, Arbuckle reservoirs have been visualized as a column of oil on top of a strong aquifer. To prevent water coning, most of the wells in the Arbuckle were drilled relatively shallow into the formation (less than 10 ft) and completed open hole (Franseen et al. 1999). Because of the absence of field cores and the lack of well log data for the full productive intervals, the reservoir characteristics of the Arbuckle formation are not well understood.

Copyright @ 2007 Society of Petroleum Engineers

This paper (SPE 101028) was accepted for presentation at the 2006 SPE Asia Pacific Oil and Gas Conference and Exhibition held in Adelaide, Australia, 11–13 September 2006, and revised for publication. Original manuscript received 31 August 2006. Revised manuscript received 05 December 2006. Paper peer approved 30 March 2007.

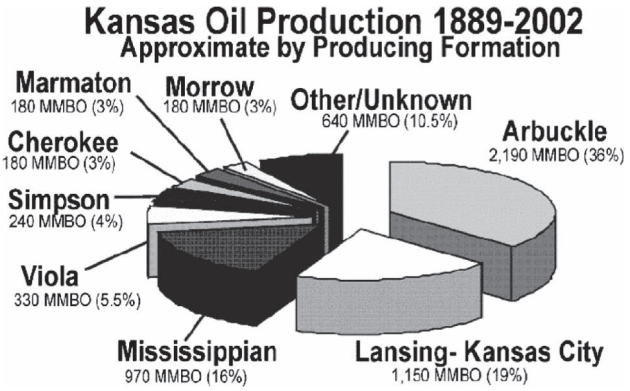

Fig. 1—Kansas oil production, 1889–2002.

Gel-Polymer Treatments in the Arbuckle Formation

Cr(III)-polyacrylamide gels have been used successfully to treat high water-cut wells in the Arbuckle (Willhite and Pancake 2004). The most commonly used crosslinking system in the Arbuckle was Cr(III)-acetate and in some cases Cr(III)-propionate was also used (Alhajeri et al. 2006; www.kgs.) To date, more than 500 water-shutoff treatments were performed using polymer gels (www.kgs). Most successful treatments resulted in an immediate decrease in the water production rate to less than half of the pre-treatment level and an increase in oil production rate to over the pre-treatment level. However, the water and oil production rates usually returned to their pre-treatment levels in less than one year. Some treatments were unsuccessful, that is, the polymer gels had little or no effect on the oil and water rates. Because the lack of understanding of the reservoir characteristics, candidate selections for gel-polymer treatments in the Arbuckle are mostly anecdotal, based mainly on the vendors' past experience in the area (Portwood 2005). In this study, we develop a methodology using neural networks to identify candidate wells on the basis of predicted outcomes for gel-polymer treatments. A feedforward-backpropagation algorithm is used to develop the neural networks. The before and after treatment data for 22 wells treated with polymer gels in the Arbuckle formation in central Kansas are used to train and verify the neural networks (Saeedi 2005).

Feedforward-Backpropagation Neural Networks

An artificial neural network (or a neural network) is an information-processing system that mimics the biological neural network of a human brain. Artificial neural networks are developed on the basis of a mathematical model of biological neural networks (Picton 2000; Pham 1995). In artificial neural networks, information processing is done in many simple individual processors called neurons. Electric signals are passed between neurons through connecting links. Each connection has an associated weight. In typical artificial neural networks, the transmitted signal is multiplied by this weight. After receiving signals from the proceeding neurons, each neuron applies an activation function (a linear or nonlinear function) to its net input to produce its output. The net input of a neuron is the summation of the input signals to that neuron multiply by the weights associated with the links which the signals have passed through (Mohaghegh et al. 2000). **Fig. 2** shows a schematic of an artificial neuron. The output of each neuron upstream is multiplied by the associated connection weight, and then enters the neuron as an input. As shown in Fig. 2, an artificial neuron has many inputs but only one output. Inputs received by the neuron are summed and the summation is applied to the activation function. The result is the output of the neuron (Mohaghegh 2000; Picton 2000; Pham and Liu 1995).

There are different classifications of neural networks on the basis of different characteristics. One of the general classifications is on the basis of training algorithms. On the basis of training algorithms, neural networks can be divided into two major groups, supervised and unsupervised (Ahmed et al. 1997; Mohaghegh 2000; Pham and Liu 1995). Unsupervised neural networks are also known as self-organizing maps. These neural networks are called unsupervised because no feedback is provided during training. In the supervised training algorithm, both inputs and outputs are presented to the network and the network learns on a feedback basis.

There are two steps in preparing neural networks: the training step and the verification step. In the training step, connection weights are adjusted to produce the desired outputs. In the verification step, the accuracy of the trained neural network in predicting the outputs is evaluated using examples that have not been seen by the neural network in the training step. Training is done by adjusting the weights until convergence between the produced outputs and desired outputs is reached. Changing the weights allows the network to modify its behavior in response to the inputs. In the backpropagation algorithm, which is one of the most commonly used supervised training algorithms (Ali 1994; McVey et al. 1994; Centilmen et al. 1999) the network output is compared with the desired output in the training dataset and the difference (error) is propagated backward to the network. During this backpropagation, the weights are adjusted to decrease the error. This process is continued iteratively until the produced outputs are acceptably close to desired outputs (Mohaghegh et al. 2000; Pham and Liu 1995; Swingler 1996; Brierley 1998).

Neural networks on the basis of the supervised training algorithm have the most applications in the oil and gas industries (Ali 1994; Mohaghegh et al. 2000). Among different kinds of neural networks, those which use the feedforward backpropagation learning algorithm are the most popular and heavily applied (Ali 1994; McVey et al 1994; Centilmen et al. 1999). **Fig. 3** shows a schematic of a feedforward neural network. Feedforward neural networks consist of one input layer, one or more hidden layers, and one output layer. The higher the number of hidden layers is, the more complex the correlation between the input and the output variables will be. The number of neurons in the input layer is related to the number of the input variables and the number of neurons in the output layer is related to the number of output

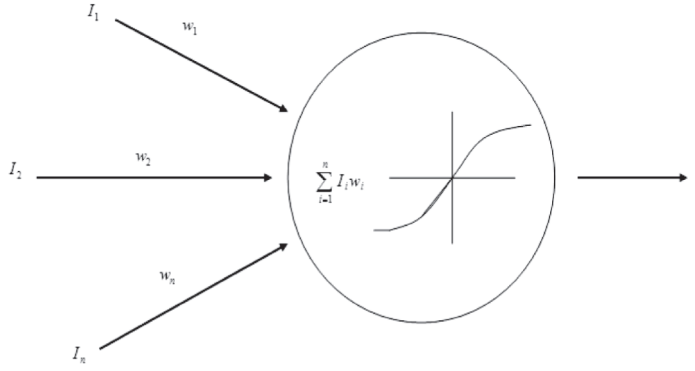

Fig. 2—Schematic of an artificial neuron (Mohagheg et al. 2000).

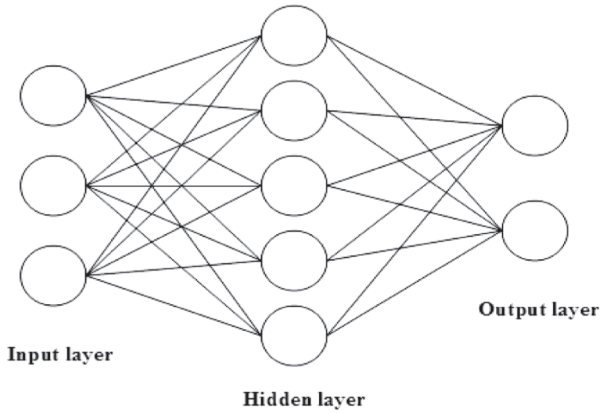

Fig. 3—A three-layer neural network (Mohagheg et al. 2000).

variables. Rules of thumb can be used to determine the number of the neurons in hidden layers, using the number of input and output variables and the number of available training examples.

Example Case

In the following, we use a simple example to demonstrate how a neural network is applied in this study to select candidate wells for gel-polymer treatments. The example case has six production wells **(Table 1).** Five of the wells were previously treated with polymer gels. The objective here is to evaluate if Well 6 is a good candidate well for gel-polymer treatment. The game plan is to develop a neural network using the pre- and post-treatment data of the five previously treated wells to predict the cumulative oil production of Well 6 one month after treatment. **Table 2** lists the input and output parameters that were used in this example. As shown in Table 2, the input parameters include depth to the top of the Arbuckle (ft), the oil production rate before treatment (BOPD), and the water production rate before treatment (BWPD). The output parameter is cumulative oil productions one month after treatment (bbl). In this example, we use three of the five previously treated wells (Wells 1 to 3) as the training set **(Table 3)** and the remaining two (Wells 4 and 5) as the verification set **(Table 4).** The training set is used to train the neural network and adjust the connecting weights. **Fig. 4** shows a schematic of the procedure followed during the training step. In the training step, both the input and output parameters are entered into the network. After entering the input and output parameters, feedforward backpropagation is performed and the weights are adjusted. Next, the accuracy of the trained network is evaluated using the verification set. Please note that example wells in the verification set have not been seen by the network before. **Fig. 5** shows a schematic of the procedure followed during the verification step. In the verification step, the input parameters of the verification set are entered into the trained network and the predicted output is compared with the actual output to evaluate the accuracy of the trained network. In this study, the accuracy of neural network is evaluated using error fraction (EF). EF is the difference between the actual output and the predicted output, divided by the actual output. As shown in **Table 5,** the average EF (AEF) associated with the wells in the verification set is 0.2. In other words, the trained neural network can predict the outcome "cumulative oil production one month after treatment" in the verification set with 80% accuracy. With the neural network successfully trained, it can now be used to predict the cumulative oil production of Well 6 one month after treatment. **Table 6** shows that using the input parameters for Well 6, the predicted cumulative oil production one month after treatment is 1,000 bbl. This information can then be used to determine whether this is a good candidate well for gel-polymer treatment.

Methodology for Developing Neural Networks

During this study, different processes including preprocessing of data, using varied sets of input parameters, choosing different training and verification sets, eliminating outliers, and sensitivity analysis were applied. The following paragraphs give brief explanations on the mentioned processes.

Normalization of Data. In the process of training neural networks, sometimes raw data may not be suitable to be used as input parameters, and thus needs to undergo preprocessing. A situation requiring preprocessing might occur when parameter input values are extremely low, high, or nearly identical. If the range of given input or output parameters is not suitable, normalization of the data should be performed (McVey et al. 1994; Al-Fattah and Startzman 2001). For example, in this project the data on longitudes and latitudes of the wells in the field were too close to each other. This prevented the neural network from being able to find a good correlation between the longitude and the output, or between the latitude and the output. The following formula was used to normalize the data to values between 0 and 1 using

$$X_{\text{Normalized}} = \frac{X - X_{\min}}{X_{\max} - X_{\min}}. \quad \ldots\ldots\ldots\ldots\ldots\ldots\ldots\ldots\ldots\ldots (1)$$

Different Combinations of Parameters. Another situation in which preprocessing is useful occurs when a combination of two or more input parameters will act as a better input parameter than each one of those parameters separately. In this case, preprocessing of data will improve the performance of a neural network (McVey et al. 1994; Al-Fattah and Startzman 2001; Artificial 2004). For example, the ratio of two parameters might be a better input parameter. Mathematical functions can also be used to produce different combinations of parameters. As an example, X^2+Y might produce a better input parameter than X and Y separately.

Randomization of the Dataset. Randomization of the dataset is also a preprocessing procedure. A neural network trained with a randomized sample applies information which is more representative of the population. To randomize the data for this research, the intrinsic FORTRAN random number generator was used. A program was written to produce a series of random continuous integer numbers in a given range. Randomization of the data

TABLE 1—DATASET USED IN THE SIMPLE EXAMPLE

Well No.	Depth to the Top of Arbuckle, ft	Oil Rate Before Treatment, BOPD	Water Rate Before Treatment, BWPD	Cum. Oil Prod. One Month After Treatment, bbl
1	3,670	5.0	475	2,625
2	3,825	9.0	1,125	3,519
3	3,824	3.0	385	2,054
4	3,821	7.0	1,120	1,557
5	3,456	6.4	314	962
6	3,467	7.0	756	?

TABLE 2—INPUT AND OUTPUT PARAMETERS OF THE SIMPLE EXAMPLE	
Input Parameters	Output Parameter
Depth to the top of Arbuckle, ft Oil rate before treatment, BOPD Water rate before treatment, BWPD	cum. oil prod. one month after treatment, bbl

TABLE 3—TRAINING SET OF THE SIMPLE EXAMPLE

Well No.	Depth to the Top of Arbuckle, ft	Oil Rate Before Treatment, BOPD	Water Rate Before Treatment, BWPD	Cum. Oil Prod. One Month After Treatment, bbl
1	3,670	5.0	475	2,625
2	3,825	9.0	1,125	3,519
3	3,824	3.0	385	2,054

TABLE 4—VERIFICATION SET OF THE SIMPLE EXAMPLE

Well No.	Depth to the Top of Arbuckle, ft	Oil Rate Before Treatment, BOPD	Water Rate Before Treatment, BWPD	Cum. Oil Prod. One Month After Treatment, bbl
4	3,821	7.0	1,120	1,557
5	3,456	6.4	314	962

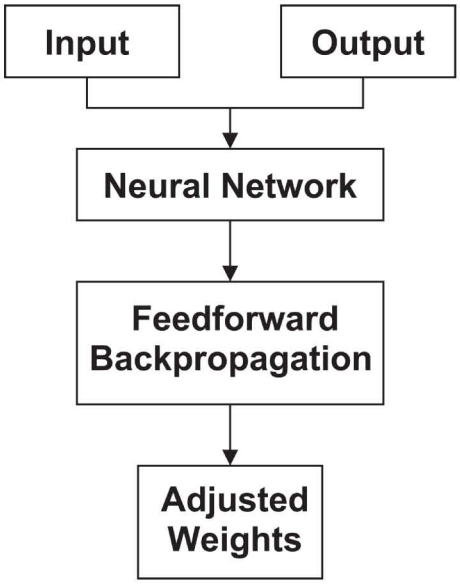

Fig. 4—Procedure for the training step.

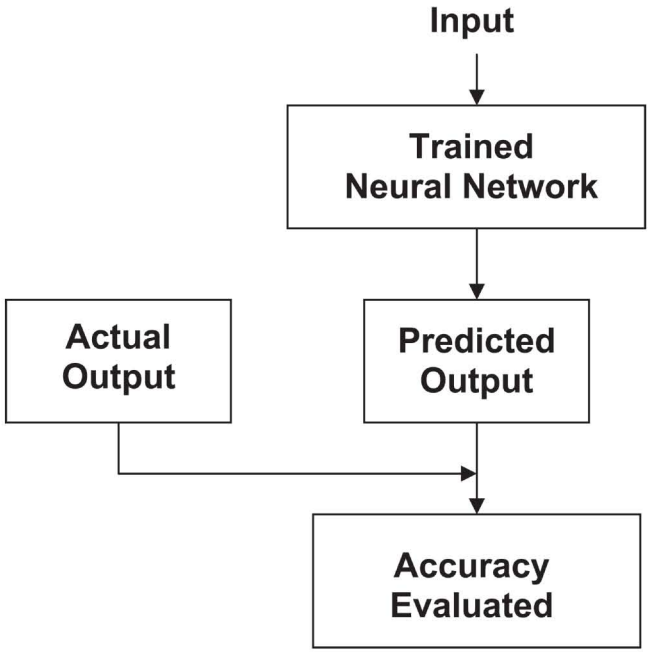

Fig. 5—Procedure for the verification step.

TABLE 5—ACCURACY OF THE TRAINED NEURAL NETWORK

Well No.	Actual Output, bbl	Predicted Output, bbl	Error Fraction	Average Error Fraction
4	1,557	1,219	0.22	0.20
5	962	1,135	0.18	

for this project was performed on the basis of the example (well) numbers.

Different Sets of Input Parameters. Different sets of input parameters result in trained neural networks with different accuracies (Mohaghegh et al. 2000; Ward 2000) For example, assume there are four input parameters to choose from: A, B, C, and D. A neural network trained using A, B, and C as input parameters has a different accuracy than a neural network trained using A, B, and D. The reason is in the way that neural networks function. Neural networks attempt to find an overall pattern between the input parameters and the output parameters. This process is done using the examples presented to the network during the training step (Ali 1994; Artificial 2004). Therefore, a pattern (correlation) must exist between the input parameters and the output parameters for a neural network to be able to correlate the input parameters to the output parameters. Different sets of the input parameters have different correlations with the output parameters. Therefore, neural networks trained with different sets of the input parameters will find totally different overall patterns between the input parameters and the output parameters. These different overall patterns will result in neural networks with different accuracies.

Different Training and Verification Sets. Different training and verification sets result in neural networks with different accuracies. In a dataset, various training and verification sets should be tried in order to obtain the highest accuracy in the verification step (Keltch 2003). Assume that there is a dataset with 100 examples. In the first trial, the first 80 examples could be used as the training set. The remaining 20 examples could be used as the verification set. In the second trial, the first 20 examples could be used as the verification set and the remaining 80 examples could be used as the training set. The only difference between the first and the second trial is in the selection of examples to be used in the training and verification sets. This difference could result in training two neural networks with a huge difference in their accuracy. Other trials which have different numbers of examples in training and verification sets may also be considered.

Elimination of the Outliers. Outliers can exist in any dataset. Outliers decrease the accuracy of networks in predicting the outputs. Therefore, it is necessary to eliminate outliers to train reliable neural networks. In the case of neural networks, outliers can be identified by using the examples in the training step. Examples with the highest errors (difference between the desired output and the predicted output) are most probably the outliers (Oberwinkler and Economides 2003).

Sensitivity Analysis. The goal of this research is to train a neural network which is able to predict the production of a well after gel-polymer treatment. The neural network will be trained using only pretreatment data. There are two important elements to be taken care of to train acceptable neural networks. The first element is having enough training examples to present to the network during the training step. The second element is using a proper set of input and output parameters (Mohaghegh et al 2000; Artificial 2004). The neural network will not be able to perform satisfactorily if it has not been presented with enough training examples. Also, if the right sets of input and output parameters have not been chosen, the trained network will not be a reliable one. A database containing the performance data of Arbuckle gel-polymer treatments is used to provide the neural networks with training and verification examples (Portwood 2005). The accuracy of the predicted outcomes is then used to determine if a sufficient number of examples has been used to train the neural networks.

As far as selecting an effective set of input and output parameters, sensitivity analysis is commonly performed to find the most important parameters (Mohaghegh et al. 2000; McVey et al. 1994; Al-Fattah and Startzman 2001; Shelley 1999; Mohaghegh et al. 1999). In this research, sensitivity analysis is performed using the backward elimination method (Mohaghegh et al. 1999, 2000). The available data is divided into two groups with an equal number of examples. Two different trials are considered. In the first trial, the first group is used in the training step, and the second group is used in the verification step. In the second trial, the second group is used in the training step, and the first group is used in the verification step. Two neural networks are trained using all of the input parameters in the given combination, one for the first trial and one for the second trial. The trial with the best performance [lowest root mean squared error (RMSE)] is identified for analysis using the backward elimination method. In the process of backward elimination, one input parameter is eliminated in each step. A neural network is trained and its performance is evaluated. The most important parameter is the one that, if absent, results in a neural network with the lowest performance.

Sensitivity analysis provides us with a guideline for choosing parameters for the next set of inputs. It identifies the input parameters which have a positive effect on performance of the neural network. It also identifies parameters that do not have an important effect on network performance. These parameters can be replaced by other parameters, in the process of searching for the best set of inputs.

Results and Discussion

Tables 7 and 8 list the available well data in the database (www.kgs) that can potentially be used as input and output parameters, respectively. During this study, ten different sets and combinations of input parameters were considered **(Table 9)** and the performance of the neural networks trained using those different sets and combinations of input parameters was compared (Saeedi 2005). Initially, the neural networks were trained using the gel volume injected as one of the input parameters. Since the objective of this study is to predict treatment outcomes using only the pre-treatment well data, the gel volume injected was later removed from the list of input parameters.

Results from the sensitivity analysis revealed that the number of wells (13 wells) in the database with the information "post-treatment cumulative oil production six-month after treatment" was not sufficient to train the neural networks, and therefore was eliminated from the list of potential output parameters.

TABLE 6—PREDICTED OIL PRODUCTIONS AFTER TREATMENT USING THE TRAINED NEURAL NETWORK

Well No.	Depth to the Top of Arbuckle, ft	Oil Rate Before Treatment, BOPD	Water Rate Before Treatment, BWPD	Cum. Oil Prod. One Month After Treatment, bbl
6	3,467	7	756	1,000

TABLE 7—LIST OF POTENTIAL INPUT PARAMETERS

Latitude and longitude of the well
Total depth of the well, ft
Depth to the top of Arbuckle, ft
Depth completed in Arbuckle, ft
Oil production rate before treatment, BOPD
Water production rate before treatment, BWPD
Water/oil ratio (WOR) before treatment
Gel volume injected, bbl

TABLE 8—LIST OF POTENTIAL OUTPUT PARAMETERS

Output Parameters	Number of Available Examples
Cumulative oil production one month after treatment, bbl	22
Cumulative oil production three months after treatment, bbl	20
Cumulative oil production six months after treatment, bbl	13

At the end, the input sets which resulted in the most accurate neural networks were chosen to train two final neural networks. The input and output parameters selected for the two final neural networks are summarized in **Tables 10 and 11.** As shown in these tables, the output parameter for Network 1 was "post-treatment cumulative oil production one month after treatment" and the output parameter for Network 2 was "post-treatment cumulative oil production three months after treatment." A total of 19 wells was used to develop the neural networks. Of the 19 wells, 15 well were used in the training step and the remaining 4 wells were used in the verification step (Saeedi 2005). **Figs. 6 and 7** show the comparison between the predicted and the actual outcomes for Networks 1 and 2, respectively. **Table 12** shows that with only pretreatment well data as input parameters, Network 1 could accurately predict the post-treatment cumulative oil production one month after treatment with an average error of 16% (AEF = 0.16). **Table 13** shows that Network 2 was even more accurate in predicting the outcome "post-treatment cumulative oil production three months after treatment" with an average error of 10% (AEF = 0.1). The AEFs presented in Tables 12 and 13 are measured in the verification step. This is a dramatic improvement over the current method of using anecdotal screening guidelines for candidate-well selections (Seright et al. 2003).

This method represents a major breakthrough where the candidate selection can now be on the basis of the accurate predictions of treatment outcomes without having to use complicated reservoir models to simulate the well performance after treatment.

Although the neural networks developed in this study are on the basis of field cases in the Arbuckle formation in central Kansas, the same methodology can also be applied in other geological regions where enough historical treatment data are available to train the neural networks.

As an extension of the current application, the neural-network technology could potentially be used to optimize the basic treatment parameters (e.g., gel volume injected, gel pumping rate, polymer-to-crosslinker concentration ratio, treatment overdisplacement volume, and so on), thereby improving the treatment performance. This could be accomplished by correlating the historical treatment outcomes with the basic treatment parameters.

Conclusions

Using actual field cases, a neural-network model was developed to identify candidate wells and predict well performance for water shutoff treatments using polymer gels. A feedforward-backpropagation algorithm was used to develop the neural networks. The before and after treatment data for 22 wells treated with polymer gels in the Arbuckle formation in western Kansas were used to train and verify the neural networks. With only pretreatment well data as input parameters, the neural networks developed in this work can accurately predict the cumulative oil production of the well one month after treatment with an average error of 16%, and the cumulative oil production three months after treatment with an average error of 10%. This is a dramatic improvement over the current method of using anecdotal screening guidelines for candidate-well selections.

This method represents a major breakthrough where the candidate selection can now be on the basis of the accurate predictions

TABLE 9—COMBINATIONS OF INPUT-PARAMETER SETS TESTED

Input Parameters	Set 1	Set 2	Set 3	Set 4	Set 5	Set 6	Set 7	Set 8	Set 9	Set 10
Oil rate before treatment, BOPD	√	√	√	√	√	√	√	√	√	√
Water rate before treatment, BWPD	√	√	√	√	√	√	√	√	√	√
Normalized latitude and longitude	√				√		√		√	
Distance from a reference well, mile		√	√							
Depth to the top of Arbuckle, ft	√	√	√	√	√	√	√	√	√	√
Depth completed in Arbuckle, ft		√			√	√				
Total depth of the well, ft	√		√	√			√	√	√	√
Water/oil ratio (WOR) before treatment		√					√	√		
Gel volume injected, bbl	√	√	√	√	√	√	√	√		

TABLE 10—INPUT AND OUTPUT PARAMETERS FOR NETWORK 1

Input Parameters	Output Parameter
Normalized latitude and longitude of the well	
Total depth of the well, ft	Cumulative oil production one month after treatment, bbl
Depth to the top of Arbuckle, ft	
Oil rate before treatment, BOPD	
Water rate before treatment, BWPD	

TABLE 11—INPUT AND OUTPUT PARAMETERS FOR NETWORK 2

Input Parameters	Output Parameter
Total depth of the well, ft	Cumulative oil production three months after treatment, bbl
Depth to the top of Arbuckle, ft	
Oil rate before treatment, BOPD	
Water rate before treatment, BWPD	

of treatment outcomes without having to use complicated reservoir models to simulate the well performance after treatment.

Nomenclature

X = input parameter
X_{Max} = maximum value of input parameter
X_{Min} = minimum value of input parameter
$X_{Normalized}$ = normalized input parameter

References

Al-Fattah, S.M., and Startzman, R.A. 2001. Predicting Natural Gas Production Using Artificial Neural Network. Paper SPE 68593 presented at the 2001 SPE Hydrocarbon Economics and Evaluation Symposium, Dallas, 2–3 April. DOI: 10.2118/68593-MS.

Ahmed, T., Link, C.A., Porter, K.W., et al. 1997. Application of Neural Network Parameter Prediction in Reservoir Characterization and Simulation—A Case History: The Rabbit Hills Field. Paper SPE 38985 presented at the SPE Latin American and Caribbean Petroleum Engineering Conference and Exhibition, Rio de Janeiro, Brazil, 30 August–3 September. DOI: 10.2118/38985-MS.

Alhajeri, M.M., Green, D.W., Liang, J., and Pancake, R.E. 2006. Gel-Polymer Extends Arbuckle High-Water-Cut Well Life. *Oil & Gas J.* **104** (2): 39–43.

Ali, J.K. 1994. Neural Networks: A New Tool for the Petroleum Industry? Paper SPE 27561 presented at the SPE European Petroleum Computer Conference, Aberdeen, 15–17 March. DOI: 10.2118/27561-MS.

Artificial Intelligence Softwares for Science and Business Ward System Group, Inc., http://www.wardsystems.com. Downloaded 10 October 2007.

Bailey, B., Crabtree, M., and Tyrie, J. 2000. Water Control. *Oilfield Review* **12** (1): 30–51.

Barati, R., Green, D.W., and Liang, J.T. 2006. Simulation of Gelled Polymer Treatments in the Arbuckle Formation, Kansas. Paper SPE 100067 presented at the SPE/DOE Symposium on Improved Oil Recovery, Tulsa, 22–26 April. DOI: 10.2118/100067-MS.

Brierley, P.D. 1998. Some Practical Applications of Neural Networks in the Electricity Industry. Doctor of Engineering thesis, Cranfield University, UK.

Centilmen, A., Ertekin, T., and Grader, A.S. 1999. Application of Neural Networks in Multiwell Field Development. Paper SPE 56433 presented at the SPE Annual Technical Conference and Exhibition, Houston, 3–6 October. DOI: 10.2118/56433-MS.

EPA/310-R-99-006, *Profile of the Oil and Gas Extraction Industry.* 1999. EPA.

Franseen, E.K., Byrnes, A.P., Cansler, J.R., Steinhauff, D.M., Carr, T.R., and Dubois, M.K. 1999. Geologic Controls On Variable Character Of Arbuckle Reservoirs In Kansas: An Emerging Picture. Kansas Geological Survey Open-file Report 2003-59, The University of Kansas, Lawrence, KS.

http://www.kgs.ku.edu/Magellan/Polymer/index.html.

Keltch, B., 2003. Neuro3 software, developed by TRW Inc., http://www.keltch.com/neuro3.html (accessed 10 October 2007).

McVey, D.S., and Mohaghegh, S. 1994. Identification of Parameters Influencing the Response of Gas Storage Wells to Hydraulic Fracturing With the Aid of a Neural Network. *SPE Computer Applications* **12** (4): 54–57. SPE-29159-PA. DOI: 10.2118/29159-PA.

Mohaghegh, S. 1995. Neural Network: What It Can Do for Petroleum Engineers. *JPT* **47** (1): 42. SPE-29219-PA. DOI: 10.2118/29219-PA.

Mohaghegh, S., Mohamad, K., Popa, A., Ameri, S., and Wood, D. 1999. Performance drivers in Restimulation of Gas-Storage Wells. Paper SPE 57453 presented at the 1999 SPE Eastern Regional Meeting, Charleston, West Virginia, 21–22 October. DOI: 10.2118/57453-MS.

Mohaghegh, S., Reeves, S., and Hill, D. 2000. Development of an Intelligent Systems Approach for Restimulation Candidate Selection. Paper SPE 59767 presented at the SPE/CERI Technology Symposium, Calgary, 3–5 April. DOI: 10.2118/59767-MS.

Oberwinkler, C. and Economides, M.J. 2003. The Definitive Identification of Candidate Wells for Refracturing. Paper SPE 84211 presented at the 2003 SPE Annual Technical Conference and Exhibition, Denver, 5–8 October. DOI:10.2118/84211-MS.

Pham, T.D. and Liu, X. 1995. *Neural Networks for Identification, Prediction and Control*. Springler-Verlag London Limited, London.

Picton, P. 2000. *Neural Networks.* PALGRAVE, New York City (2000).

Portwood, J.T. 2005. The Kansas Arbuckle Formation: Performance Evaluation and Lessons Learned from More Than 200 Polymer-Gel Water-Shutoff Treatments. Paper SPE 94096 presented at the SPE Production and Operations Symposium, Oklahoma City, Oklahoma, 16–19 April. DOI: 10.2118/94096-MS.

Saeedi, A. 2005. Candidate Selection and Well Performance Prediction for Gel-Polymer Treatments Using Neural Networks. 2005. M.S. Thesis, The University of Kansas, Lawrence, Kansas.

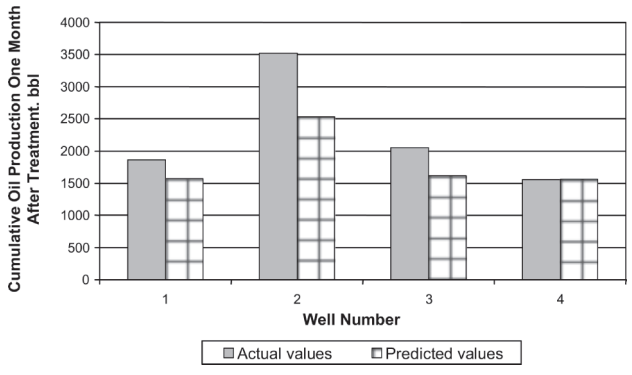

Fig. 6—Comparison between predicted and actual outcomes for Network 1.

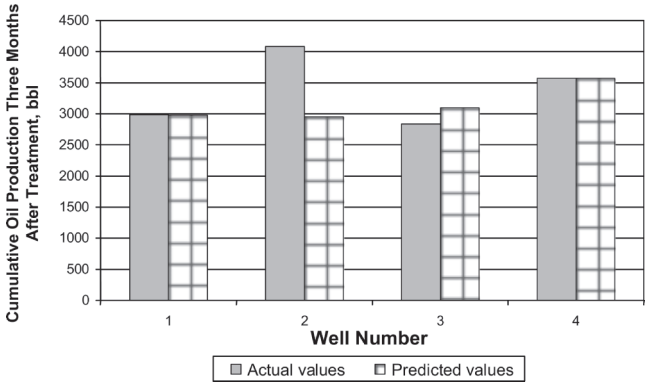

Fig. 7—Comparison between predicted and actual outcomes for Network 2.

TABLE 12—AVERAGE ERROR FRACTION FOR NETWORK 1

Well No.	Actual Value, bbl	Predicted Value, bbl	EF	AEF
1	1,862	1,572	0.155	0.16
2	3,519	2,533	0.280	
3	2,054	1,616	0.213	
4	1,557	1,561	0.003	

TABLE 13—AVERAGE ERROR FRACTION FOR NETWORK 2

Well No.	Actual Value, bbl	Predicted Value, bbl	EF	AEF
1	2,883	3,021	0.048	0.10
2	4,081	2,995	0.266	
3	2,933	3,134	0.069	
4	3,568	3,585	0.005	

Seright, R.S., Lane, R.H., and Sydansk, R.D. 2003. A Strategy for Attacking Excess Water Production. *SPEPF* **(18)** 3: 158–169. SPE-84966-PA. DOI: 10.2118/84966-PA.

Shelley, R.F. 1999. Artificial Neural Networks Identify Restimulation Candidates in the Red Oak Field. Paper SPE 52190 presented at the 1999 SPE Mid-Continent Operations Symposium, Oklahoma City, Oklahoma, 28–31 March. DOI: 10.2118/52190-MS.

Swingler, K 1996. *APPLYING NEURAL NETWORKS, A Practical Guide*, ACADEMIC PRESS INC., San Francisco, California..

Willhite, G.P., and Pancake, R.E. 2004. Controlling Water Production Using Gelled Polymer Systems. Paper SPE 89464 presented at the SPE/DOE Symposium on Improved Oil Recovery, Tulsa, 17–21 April. DOI: 10.2118/89464-MS.

SI Metric Conversion Factors

bbl × 1.5989 873	E–01	$= m^3$
ft × 3.048*	E–01	= m
mile × 1.609 344*	E+00	= km

*Conversion factor is exact.

Alireza Saeedi is a petroleum engineer with the Chevron Corp. in Midland, Texas. email: asdc@chevron.com. Saeedi has an MS degree in petroleum engineering from the University of Kansas and a BS degree in chemical engineering from the Shiraz University of Iran. He is a member of SPE. **Kyle V. Camarda** is an associate professor of the chemical and petroleum engineering department at the University of Kansas. email: carmarda@ku.edu. Camarda holds a PhD degree and an MS degree in chemical engineering both from the University of Illinois at Urbana-Champaign. He also has a BS degree in chemical engineering from the University of California at San Diego. His research interests include the use of high-performance computing to solve optimization problems in product design, process design and bioinformatics, applications of novel optimization techniques for property correlations in chemical and petroleum engineering systems, flux analysis of metabolic networks, and parallel computing applied to chemical engineering optimization problems. **Jenn-Tai Liang** is an associate professor of the chemical and petroleum engineering department at the University of Kansas. email: tliang@ku.edu. Liang holds a PhD degree in petroleum engineering from the University of Texas at Austin, a MS degree in mineral engineering from the University of Alabama, and a BS degree in Chemistry from Tamkang University in Taiwan. Liang has a diverse research and development background with particular expertise in: water shutoff and conformance control, improved oil and gas recovery processes, flow assurance, CO_2 sequestration, and enhanced coal bed methane recovery. He is a member of SPE and a technical editor of SPE *Reservoir Evaluation & Engineering*.

SPE 108604

The Development of an Artificial Neural Network as a Pressure Transient Analysis Tool for Applications in Double-Porosity Reservoirs

M. Alajmi, College of Technological Studies, and T. Ertekin, Penn State University

Copyright 2007, Society of Petroleum Engineers

This paper was prepared for presentation at the 2007 SPE Asia Pacific Oil & Gas Conference and Exhibition held in Jakarta, Indonesia, 30 October–1 November 2007.

This paper was selected for presentation by an SPE Program Committee following review of information contained in an abstract submitted by the author(s). Contents of the paper, as presented, have not been reviewed by the Society of Petroleum Engineers and are subject to correction by the author(s). The material, as presented, does not necessarily reflect any position of the Society of Petroleum Engineers, its officers, or members. Papers presented at SPE meetings are subject to publication review by Editorial Committees of the Society of Petroleum Engineers. Electronic reproduction, distribution, or storage of any part of this paper for commercial purposes without the written consent of the Society of Petroleum Engineers is prohibited. Permission to reproduce in print is restricted to an abstract of not more than 300 words; illustrations may not be copied. The abstract must contain conspicuous acknowledgment of where and by whom the paper was presented. Write Librarian, SPE, P.O. Box 833836, Richardson, Texas 75083-3836 U.S.A., fax 01-972-952-9435.

Abstract

Naturally fractured reservoirs have been studied extensively in the past decades. These reservoirs consist of two distinct porous media: the macropores and the micropores. Several analytical models have been suggested to characterize such reservoirs. In this work, one of the proposed double-porosity pressure transient models is adopted in the description of the naturally fractured reservoirs. The forward solution component of the analytical model is used to generate the pressure transient data, given the characteristic parameters of the double-porosity reservoirs. The double-porosity systems are characterized by a pressure transient signature which is composed of two semi-log straight lines connected by a transitional curve. The pressure transient responses obtained by the analytical forward solution are subjected to a polynomial fit algorithm so that the aforementioned double-porosity signature can be represented by five polynomial coefficients. These coefficients, the known properties of the double-porosity reservoir, and the reservoir fluid and well parameters constitute the principal input given to the artificial neural network (ANN) during the training phase. The ANN, then, inversely predicts the desired unknown properties of the double-porosity system, namely the permeability of the fracture, the porosity of the matrix, the porosity of the fracture, and the permeability of the matrix. This final development of the ANN is achieved by utilizing this inverse protocol in gradually increasing levels of complexity. The complexity of the problem is elevated by increasing the number of unknown characteristics of the double-porosity system. This research demonstrates the efficiency of the ANN utilization in obtaining the desired properties of the double-porosity reservoirs.

Introduction

In reservoir engineering, finding the characteristic properties of the hydrocarbon reservoirs is of paramount importance. These reservoir parameters help the reservoir engineer in the process of reservoir evaluation and development, reservoir-pressure maintenance, reservoir recovery optimization, to name a few. There are number of tools that aid the reservoir engineer in the acquisition of the reservoir properties; one important tool is well testing. Well testing has been utilized to analyze the pressure transient response of different types of reservoirs. An example of such reservoirs is the naturally-fractured reservoirs. Naturally fractured reservoirs play a major role in the world's total production of hydrocarbons that are necessary for the sustenance of today's energy-hungry globe. In fact, according to Knebel et al. (1956), 41% of the proven reserves, which were discovered in 236 major oil-producing fields up to 1956, were in naturally fractured reservoirs[1]. Furthermore, naturally fractured reservoirs include a sizable amount of the world hydrocarbon reserves[2]. These illustrations attest to the importance of the naturally fractured reservoirs in the oil industry.

Barenblatt et al.'s theoretical research paved the way for the development of the future analytical models, which have provided a more rigorous description of the fluid transport and storage in naturally fractured reservoirs. One of these analytical models is the double-porosity model. In fact, it is often considered as the classical model for naturally fractured reservoirs; moreover, it is applied for high fracture intensity reservoirs with intermediate matrix permeability[2]. In a double-porosity model, the naturally fractured reservoir is divided into two subdomains: fracture system and matrix system. . Depending upon the assumptions pertaining to the interaction between the matrix and the fracture, several models have been developed and discussed in the literature. Some of the more prominent models include Warren and Root's model[3], de Swaan's model[4], and Serra et al. model[5]. The mathematical model of interest employed to describe the double-porosity system, in this work, is Serra et al. model[5]. Their research is a continuation of de Swaan's work. In this model, the analytical solution identifies three flow regimes: fracture flow exhibited by the first semi-log straight line, matrix flow demonstrated by the transitional period, and fracture and matrix flow illustrated by the second semi-log straight line.

In this work, the artificial neural network (ANN) is utilized as an unconventional interpretative method of well testing to solve the inverse problem of obtaining the properties of the reservoirs from the pressure transient data collected during drawdown or build-up tests. There are two types of ANNs: unsupervised and supervised[6]; the premises behind the selection of the appropriate kind of ANN used in well testing analysis are explained. The ANN utilized in this work is called the backpropagation neural network (BPNN). Furthermore, the polynomial fit algorithm is utilized in representing the pressure transient data in the form of five characteristic polynomial coefficients. The aforementioned analytical model is used to obtain the pressure transient data for many double-porosity reservoirs, whose characteristics were generated randomly. These coefficients later become part of the input presented to the artificial neural network (ANN).

Polynomial fit procedure

According to the previously described analytical model, the transient behavior of a double-porosity system is characterized by two parallel semi-log straight lines connected by a transitional curve. The first straight line represents the response of the flow in the fracture only. The transitional curve illustrates the response of unsteady-sate flow from matrix to the fracture network. The second straight line represents the response of pseudo-steady state flow from both fracture and matrix. In order to assure the presence of this signature for every generated pattern, during the early phases of the investigation, a "100-point" check criterion was to be met for each pressure transient data generated by the analytical model; although the dual-porosity signature could be observed in some patterns with fewer data, the 100 pressure drop versus time values are chosen for the sake of standardization of the pressure transient data.

In order to effectively maintain the signature integrity of the double-porosity system, a polynomial fit was constructed. This procedure involves the utilization of the following two Matlab®[1] functions: *Polyfit* and *Polyval*. As stated in the Matlab® help manual, *Polyfit* function determines the coefficients of a polynomial of degree N that best matches the given data. To assess the effectiveness of the polynomial fit, *Polyval* function is used to evaluate the polynomial.

Polyfit function is stated mathematically in the following manner:

$$[P, S] = Polyfit(X, Y, N) \qquad [1]$$

In Equation 1, N is the polynomial degree. In this work, N equals 4; P is the polynomial coefficients vector, and it is equal to $N+1$; X vector contains the log(time); Y vector includes the recorded values of Δp. Both X and Y vectors can contain up to 100 entries. S is the structure which contains the Cholesky factor of the Vandermonde matrix, the degrees of freedom, and the norm of the residuals. S is utilized by *Polyval* function to obtain the fitting vector of Y and its error estimates, *delta*.

Polyval function is expressed as follows:

$$[Y_{fit}, delta] = Polyval(P, X, S) \quad [2]$$

Polyval uses *P*, *X*, and *S*, mentioned above, to generate the best fitting of *Y*; Y_{fit} is within *Y* +/- *delta*.

It was observed that with a fitting polynomial of degree four the match between the pressure transient data and the polynomial was very good. Therefore, the 100-point pressure transient data are replaced by the five characteristic polynomial coefficients, which efficiently describe the double-porosity signature of each generated pattern.

Figure 1 illustrates the application of the polynomial fit procedure to the pressure transient data of a certain pattern. Furthermore, **Table 1** shows the coefficients of the polynomial depicted in Figure 1.

An overview of the use of ANN in petroleum engineering applications

The interest in the utilization of neural networks, as unconventional interpretative method used in solving the inverse problems encountered in different areas of the petroleum industry, has grown in recent years. In fact, this interest is illustrated by the plethora of publications in this topic in the past several years. The gamut of ANN applications in petroleum engineering includes analysis of formation lithology, reservoir geological characterization, well testing analysis, to name a few. An example of ANN application in well testing analysis is its utilization in the interpretation of the pressure transient data collected from different types of reservoirs to determine the unknown properties. It should be noted that generally the ANN of choice in the aforementioned applications is the BPNN.

The principal objective of this research is the development of backpropagation neural network whose inputs ideally should consist of the pressure drop with its corresponding time, known properties of double-porosity reservoir, and well and fluid parameters. As previously discussed, the pressure transient data are replaced by the five polynomial coefficients. Furthermore, the target outputs will be the reservoir unknown properties. **Figure 2** shows the general backpropagation neural network structure used in this study.

The development stages of the backpropagation neural network

The development of the backpropagation neural network (BPNN) consists of four principal stages. The degree of complexity of the BPNN is elevated from one stage to the other through the addition of a new output neuron. In the first stage, k_f is the only output of the network. Furthermore, in the second stage, φ_m is removed from the network inputs to be included as the second output of the network. In the third stage, φ_f, once an input, is added to the output neuron list of the network as the third output. In the final stage, k_m becomes the fourth output of the network, after its removal from the list of inputs. It should be noted that in developing these various stages, Neural Network Toolbox[7] was utilized. **Table 2** summarizes the successive changes applied to the input list and the output layer of the artificial neural network designed in this study.

In the final stage of BPNN development, k_m, after being removed from the input list of the network, is introduced as the network's fourth output. In this stage, several testing sets were generated in order to determine the optimum BPNN architecture that would yield the acceptable prediction results. In the first testing of this stage, the network was able to adequately predict five patterns of the last testing set utilized in the third stage. Accordingly, these patterns were added to the training set. After developing several BPNN cases, the remaining five testing patterns were included in the training set; the training set at this point comprises of 154 patterns of pressure transient data. To commence the second testing of the network, a new testing set consisting of ten patterns was generated. When showing this testing set to the network, three patterns proved difficult to be predicted. Since it was observed

[1] Copyright 1984-2002, The MathWorks, Inc.

in the previous stage that the addition of the rather problematical patterns had positive influence upon the prediction performance of the network, the three testing patterns were included in the training set. Based upon the modification of the included testing patterns, three patterns were generated to complete the testing set. To modify these patterns, k_f and φ_f were varied for every pattern. After developing a number of BPNN cases, the network which predicted the testing set accurately was identified. A schematic of this BPNN architecture is depicted in **Figure 3**. It should be noted that the network prediction results indicated that the neural network in fact learned and did not memorize the multi-dimensional input/output relationship. Due to these acceptable prediction results, the entire testing set was incorporated into the training set. Hence, the number of the training patterns has increased now to 167 patterns.

In the third testing of this stage, three patterns were generated to further test the prediction capability of the network. At first, two of the three patterns were poorly predicted by the network. To improve the network prediction performance, several modifications of these patterns were made. For the first pattern, the modifications involved varying the values of k_m, φ_m, h_m, k_f, h_f, φ_f, and r_w. On the other hand, in the second pattern, k_m, k_f, and φ_f were adjusted. After developing several BPNN cases, the third testing set was generally well predicted, and hence it was included in the training set, which now has 170 patterns. The distribution of fracture permeability versus matrix permeability and the distribution of the matrix porosity versus fracture porosity are depicted in **Figure 4** and **Figure 5**, respectively.

Discussion

The BPNN development discussed in this paper underwent several stages in order to accomplish the principal objective of this work. The main objective was realized upon the completion of the fourth stage. Throughout the stages of BPNN development, various cases were investigated. Furthermore, in performing these cases, several procedures were employed.

The principal method which was utilized in all of the stages was the BPNN architecture modification. In changing the architecture of the network, the number of hidden layers, the number of neurons in each hidden layer, the training function, and training function parameters were varied. In most of the sub-stages of the first stage, one hidden layer sufficed in achieving the acceptable results. However, with the inclusion of more network inputs, the utilization of two hidden layers was needed. In fact, two hidden layers were used in all of the following three stages. The utilization of two hidden layers is rather imperative as the complexity of problem increases from one stage to the next. Moreover, the number of neurons in the hidden layers in general increased during the developing of the neural network stages. Nevertheless, the total number of neurons of each layer decreased from left to right, with the largest number of neurons in the first hidden layer and the smallest in the output layer. It is worth noting that the neurons in the first hidden layer are generally more than the inputs of the network. This general rule of thumb was applied in the majority of the BPNN cases. As mentioned before, the functions *traincgf* and *trainscg* were widely used in the training of the network. It was observed that as the training set expanded, the latter training function generally resulted in better network prediction performance. However, in the early phases of the development, the former training function was preferred because *trainscg* at the end of the training progress no longer updated the performance index. Furthermore, it was observed that when using *traincgf* the most influential training parameter was *minsetp*, defined as the minimum step length. In addition to the previous two training functions, other functions were used; the most effective of these functions was *traingdm*.

The breakthrough in the BPNN development was realized with the introduction of the “screen and inject” procedure. In this procedure, the predicted patterns within the acceptable range were screened when presenting the testing set to the neural network; moreover, these patterns were incorporated into the training set to ameliorate the network’s prediction

capability. This procedure was first implemented in the last two sub-stages of the first stage. It was found that the "screen and inject" method was more powerful than the inclusion of more functional links in the inputs of the network. Furthermore, this observation was corroborated by the continuous improvement in the network prediction performance every time this method was invoked. Noting the efficiency of the "screen and inject" procedure, the search for more effective functional links was ceased with the start of sub-stage 11. Instead, the emphasis in the BPNN development was on exercising the former network development procedure through the generation of many testing sets in the last two sub-stages of the first stage and the following stages. In the process of applying the previously mentioned procedure, not only was the quantity of the training set increased but also its quality was improved significantly. Furthermore, with a sizable training set, the incorporation of the testing patterns that were difficult for the network to predict resulted in obtaining acceptable network prediction results.

Results

The results yielded by the BPNN illustrated in Figure 3 are the best results of this stage. To demonstrate the efficiency of the network training for k_f, φ_m, φ_f, and k_m, **Figure 6**, **Figure 7**, **Figure 8**, and **Figure 9** are, respectively, provided. Furthermore, the MSE at the end of network training was reported to be 7E-04. In addition to that, the prediction capability of the neural network of the aforementioned outputs is illustrated by **Figure 10**, **Figure 11**, **Figure 12**, and **Figure 13**, respectively.

Conclusions

In this research, an artificial neural network was developed to be a universal interpretive tool for the pressure transient data originating from double-porosity reservoirs. This objective was achieved through the integration of the knowledge of well testing analysis with the protocols of the ANN.

Within the constraints of this study, the following conclusions are offered:

- The BPNN is a viable tool in the analysis of the pressure transient data collected in a double-porosity reservoir.
- After learning the analytical forward solution, the neural network is able to inversely predict the unknown properties of the double-porosity system.
- During the development of the neural network, the "screen and inject" method was more effective than the incorporation of functional links, which only provided a limited improvement in the prediction performance of the network.
- The continuous application of the "screen and inject" procedure resulted in not only improving the quality of the training set but also exposing the artificial neural network to a larger number of patterns and thus rendering it more robust.
- In modifying the architecture of the network, it was found that invoking the conjugate gradient training functions, namely *trainscg* and *traincgf*, helped in part yield the network acceptable results; moreover, *tansig*, was proved to be the best transfer function because of the algorithm employed in the normalization of the training set.
- The polynomial fit algorithm through the transformation of the pressure transient data into the five polynomial coefficients demonstrated its efficiency by rendering the analysis more flexible because it is usually very difficult to detect the first semi-log straight line when performing the well test.
- The input of the network, consisting mainly of the polynomial coefficients, the system known parameters, and a functional link devised in terms of one of these parameters, provided the much needed convenience in the application of the developed BPNN.
- The developed BPNN provides a good base for future betterment of the network.

References

1. Streltsova, T., *Well Testing in Heterogeneous Formations*, John Wiley & Sons, Inc., New York, 1988.
2. Cinco-Ley, H., "Well-Test Analysis for Naturally Fractured Reservoirs," paper SPE 31162, 1996.
3. Warren, J., and Root, P., "The Behavior of Naturally Fractured Reservoirs," paper SPE 426, 1963.
4. De Swaan, O.A., "Analytic Solutions for Determining Naturally Fractured Reservoir Properties by Well Testing," paper SPE 5346, 1976.
5. Serra, K., Reynolds, A., and Raghavan, R., "New Pressure Transient Analysis Methods for Naturally Fractured Reservoirs," paper SPE 10780, 1983.
6. Hagan, M., Demuth, H., and Beale, M., *Neural Network Design*, PWS Publishing Co., Boston, 1996.
7. Demuth, H. and Beale, M., *Neural Network Toolbox for Use with Matlab®*, The MathWorks, Inc., 1992-1998.

Nomenclature

B	formation volume factor, RB/STB
c_1, c_2, c_3, c_4, c_5	polynomial coefficients
c	total compressibility, psi^{-1}
delta	error estimates obtained when using polynomial fit algorithm
h	thickness (height), ft
h_{ft}	total fracture thickness (height), ft
k	permeability, md
MSE	mean square error
N	polynomial degree
P	polynomial coefficients vector
p	pressure, psi
q	flow rate, STB/D
r_w	wellbore radius, ft
S	Structure used in polynomial fit algorithm
t	time, hours
X	vector containing log(t)
Y	vector containing the recorded values of pressure drop
Y_{fit}	the best fitting vector of Y

Greek

Δp	pressure difference, psi
μ	viscosity, cp
φ	porosity, percent

Subscripts

f	fracture
m	matrix

Table 1: An example of the polynomial coefficients obtained using the polynomial fit algorithm

Polynomial coefficient	Value
c_1	-0.096097
c_2	-0.31526
c_3	5.609
c_4	83.146
c_5	618.22

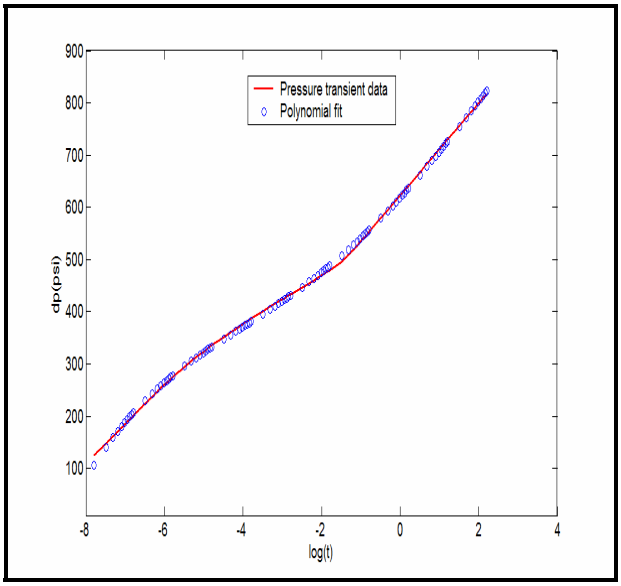

Figure 1: An illustration of the application of the polynomial fit procedure

Table 2: The developmental stages of the artificial neural network

Stage one	
Output:	k_f
Inputs:	c_1, c_2, c_3, c_4, c_5, r_w, B, q, μ, $\mu^{0.25}$, φ_f, c_f, φ_m, c_m, h_m, k_m, h_f
Stage two	
Outputs:	k_f, φ_m
Inputs:	c_1, c_2, c_3, c_4, c_5, r_w, B, q, μ, $\mu^{0.25}$, φ_f, c_f, c_m, h_m, k_m, h_f
Stage three	
Outputs:	k_f, φ_m, φ_f
Inputs:	c_1, c_2, c_3, c_4, c_5, r_w, B, q, μ, $\mu^{0.25}$, c_f, c_m, h_m, k_m, h_f
Stage four	
Outputs:	k_f, φ_m, φ_f, k_m
Inputs:	c_1, c_2, c_3, c_4, c_5, r_w, B, q, μ, $\mu^{0.25}$, c_f, c_m, h_m, h_f

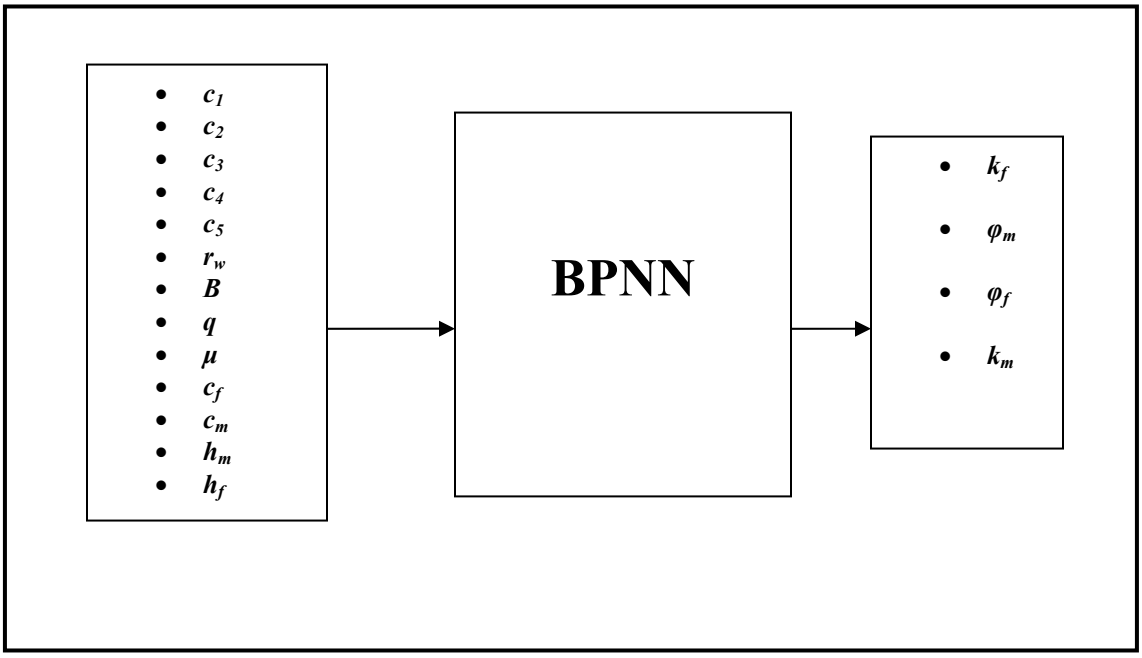

Figure 2: Illustration of a BPNN general structure

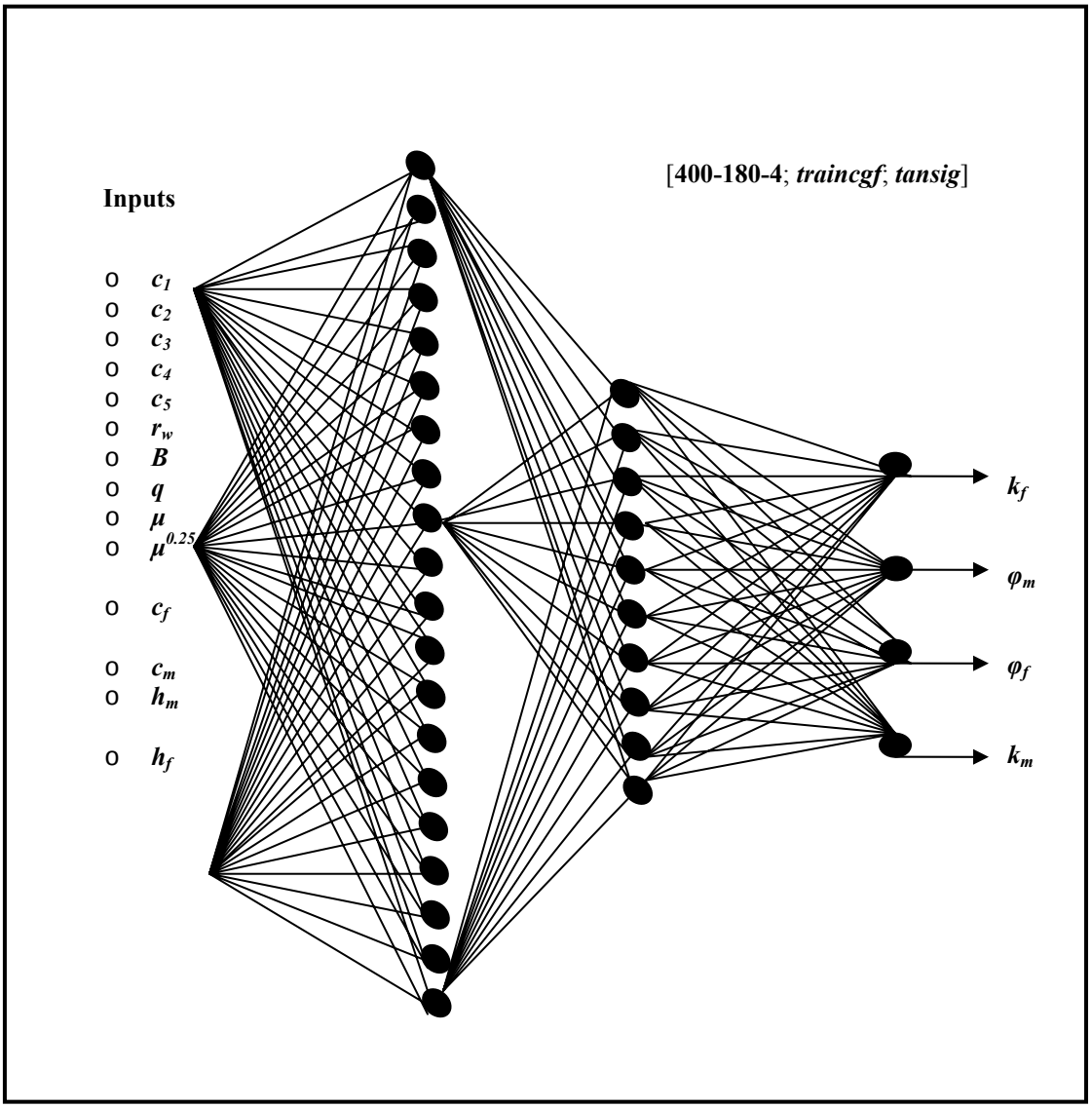

Figure 3: Schematic of stage four BPNN architecture

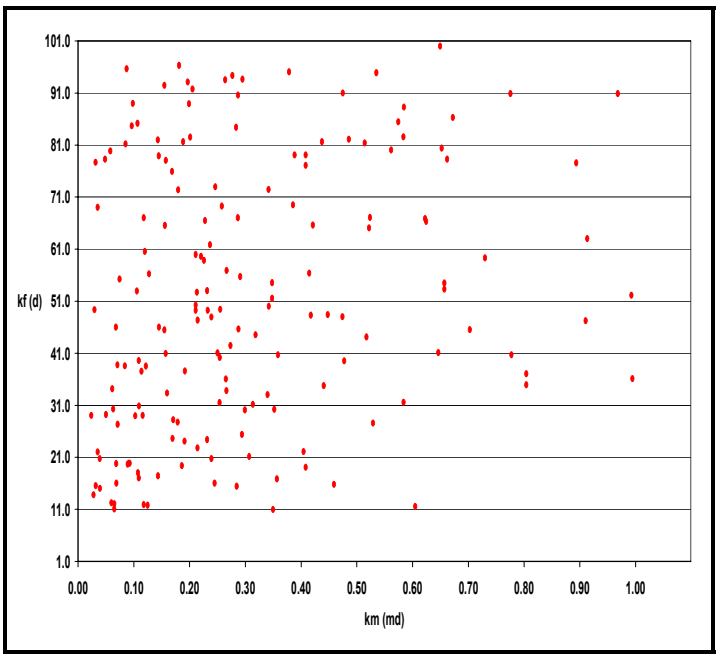

Figure 4: A cross-plot of the fracture permeability versus matrix permeability distribution of the training set

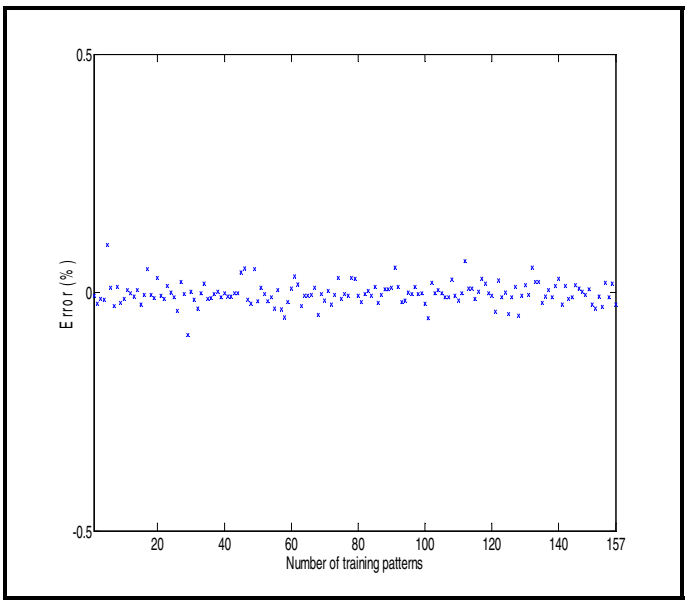

Figure 6: Training error plot of k_f (stage four)

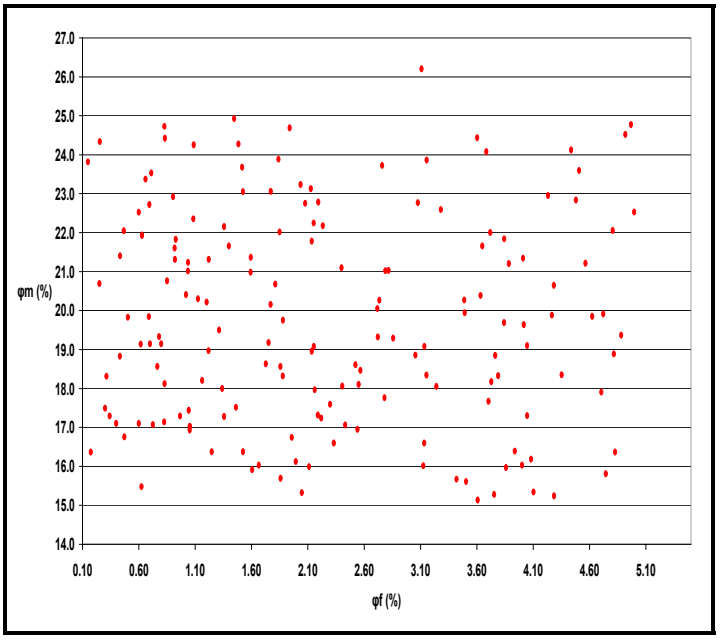

Figure 5: A cross-plot of the matrix porosity versus fracture porosity distribution of the training set

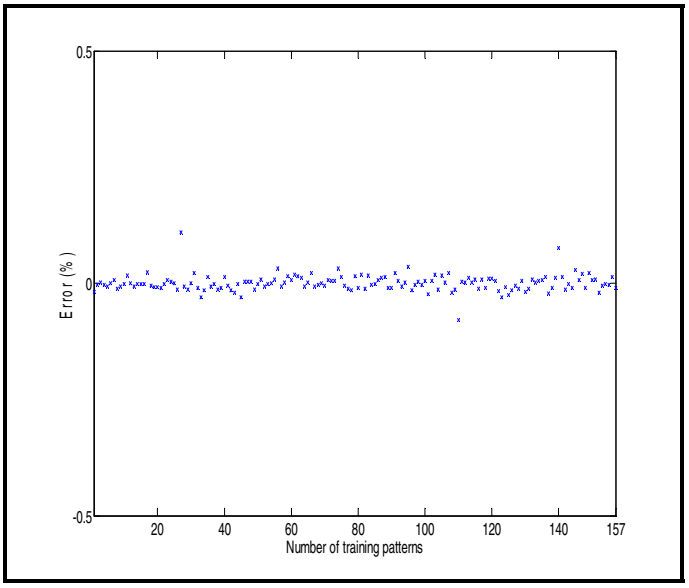

Figure 7: Training error plot of φ_m (stage four)

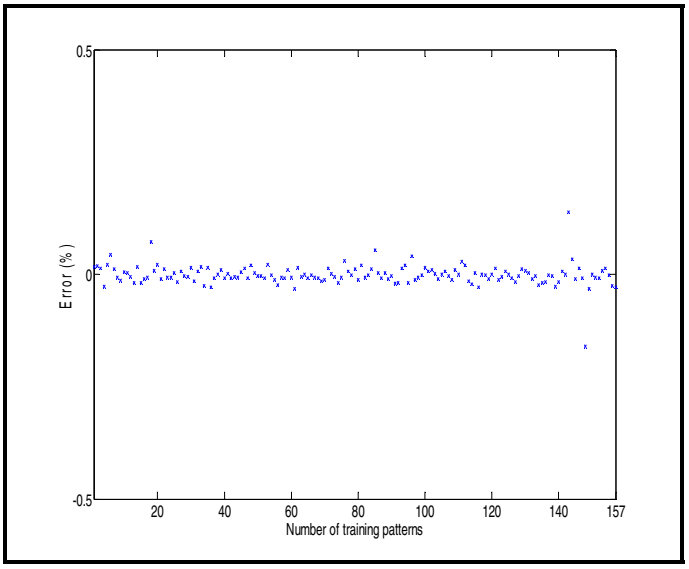

Figure 8: Training error plot of φ_f (stage four)

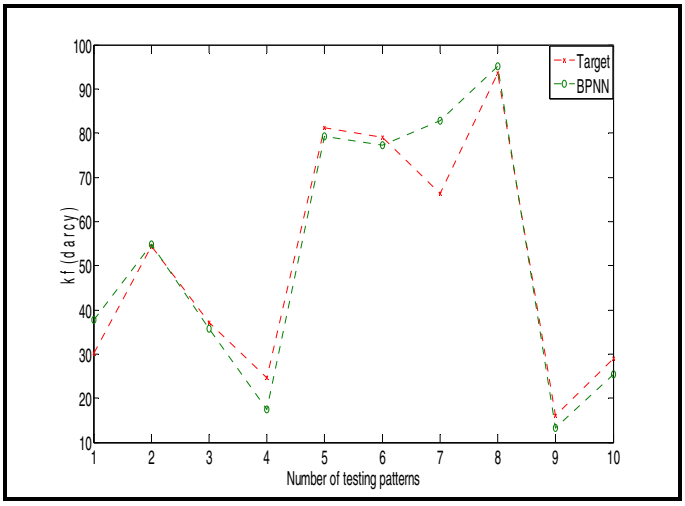

Figure 10: BPNN output and target values of k_f (stage four)

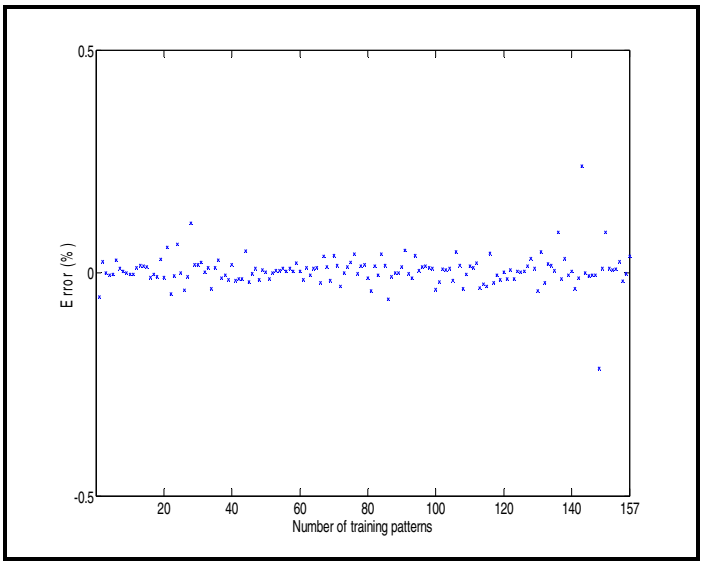

Figure 9: Training error plot of k_m (stage four)

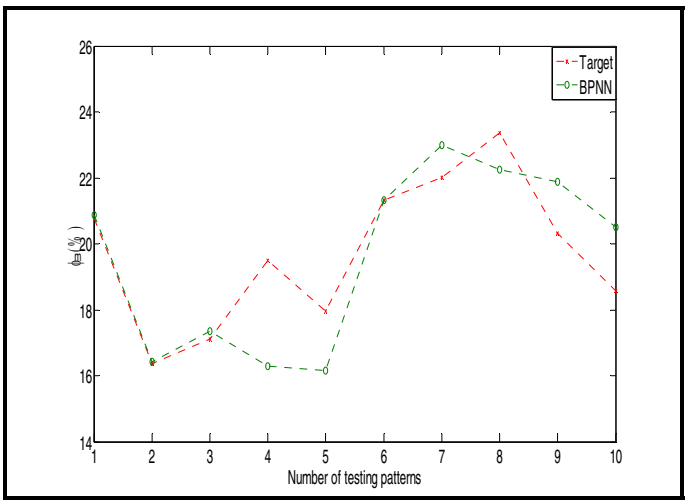

Figure 11: BPNN output and target values of φ_m (stage four)

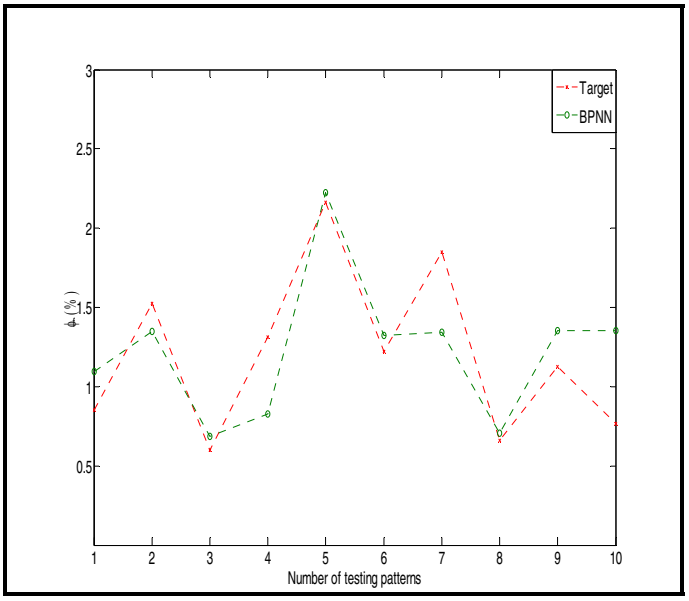

Figure 12: BPNN output and target values of φ_f (stage four)

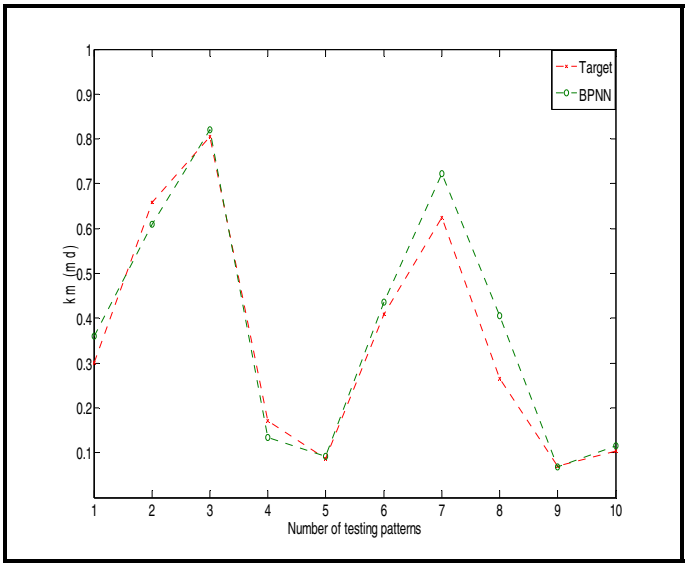

Figure 13: BPNN output and target values of k_m (stage four)

IADC/SPE 108340

Flow Pattern and Frictional-Pressure-Loss Estimation Using Neural Networks for UBD Operations

Evren M. Ozbayoglu, Middle East Technical U., and Murat A. Ozbayoglu, Economy & Technology U.

Copyright 2007
IADC/SPE Managed Pressure Drilling and Underbalanced Operations Conference and Exhibition

This paper was prepared for presentation at the 2007 IADC/SPE Managed Pressure Drilling and Underbalanced Operations Conference and Exhibition held in Galveston, Texas, 28–29 March 2007.

This paper was selected for presentation by an IADC/SPE Program Committee following review of information contained in an abstract submitted by the author(s). Contents of the paper, as presented, have not been reviewed by the International Association of Drilling Contractors or Society of Petroleum Engineers and are subject to correction by the author(s). The material, as presented, does not necessarily reflect any position of the IADC, SPE, their officers, or members. Electronic reproduction, distribution, or storage of any part of this paper for commercial purposes without the written consent of the International Association of Drilling Contractors and Society of Petroleum Engineers is prohibited. Permission to reproduce in print is restricted to an abstract of not more than 300 words; illustrations may not be copied. The abstract must contain conspicuous acknowledgment of where and by whom the paper was presented. Write Librarian, SPE, P.O. Box 833836, Richardson, TX 75083-3836 U.S.A., fax 1.972.952.9435.

Abstract

Underbalanced drilling is a very commonly used technique in many drilling applications. Usually, gasified fluids are preferred for achieving underbalanced conditions. Proper estimation of hydraulic requirements becomes a more important issue for trajectories with highly-inclined angles and longer sections. Flow of two-phase fluids through circular pipes has, relatively, been well understood. However, flow of two-phase fluids through annular sections is still a challenge. Many attempts have been conducted to model two-phase flow through annular geometries, but still there exists an uncertainty at this area. It has been observed that, for annular geometries, hydraulic diameter concept is not applicable for estimating flow patterns or frictional pressure losses using the models developed for circular pipes. This study approaches to estimate the flow pattern and frictional pressure losses of two-phase fluids flowing through horizontal annular geometries using Artificial Neural Networks (ANN) rather than proposing a mechanistic model. Experimental data collected from experiments conducted at Middle East Technical University, Petroleum & Natural Gas Engineering Multiphase Flow Loop, as well as from literature in order to train the ANN. Flow is characterized using superficial Reynolds numbers for both liquid and gas phase for simplicity. The results showed that ANN could estimate flow patterns with a high accuracy (error is less than ± 5%), and frictional pressure losses with an error less than ± 30%. It is also observed that proper selection of ANN is important for accurate estimations.

Introduction

Two-phase flow is the flow phenomenon of two different fluid phases flowing simultaneously through a conduit. Generally, liquid and gas phases are the components of this commonly encountered flow type. As liquid and gas phases are flowing through a conduit, different flow patterns develop as a function of velocities of both phases as shown in Figure-1. Since 1950's, the flow problem of two-phase fluids has been the subject of research in many different engineering practices.

In petroleum industry, the applications of two-phase flow start from drilling and continue till the refining process. In depleted or mature reservoirs, underbalanced drilling techniques are required in order to prevent any possible formation damages while drilling injection/production wells. Thus, in order to determine the design parameters for such wells accurately, the flow behavior of aerated fluids should be well known. Another important usage of two-phase flow takes place during the transportation of the produced oil and gas via the pipelines. Since the oil and gas fields are mainly in remote onshore areas or in offshore, the pipeline systems are of great importance. Reliable engineering calculations should be carried out as the overall distances of these pipeline systems are considered.

With the improving technology, the innovative methods demand for the better understanding of two-phase flow systems. As in case of underbalanced drilling of extended reach wells, the flow problem becomes more complicated when compared with single-phase flow of drilling mud in conventional drilling.

When this wide range of application of two-phase flow in petroleum engineering is considered, the appropriate determination of flow parameters of two-phase fluid systems becomes highly important. The focus of this study is to determine flow patterns and frictional pressure losses of aerated fluid flow through horizontal annuli using artificial neural networks (ANN).

Literature Review

Through the investigation of two-phase flow phenomenon, extensive theoretical and experimental studies have been carried out. The proposed models can be grouped into two categories; namely general models and mechanistic models. The early models developed for two-phase fluid systems were flow pattern independent. These general models ignored the complex flow configurations, named as flow patterns, and treated the two-phase flow as a single-phase fluid flow or as a flow of two separated fluids. The most important models in this category are proposed by Wallis [1], Lockhart and Martinelli [2], and Duns and Ros [3]. These general models are the

starting points through the progress of modeling two-phase fluid flow. The later studies focused on the determination of flow patterns. The flow mechanism of two-phase fluid systems was examined independently for each flow pattern. Then, governing flow equations were proposed for a given flow pattern. These models were called mechanistic models. As the knowledge of flow behavior of two-phase fluid systems has improved, comprehensive and unified models were developed.

Mechanistic Models for Two-Phase Flow Through Horizontal Pipes:

Dukler [4] proposed a model based on dimensionless groups and developed frictional pressure loss correlations using similarity analysis. This model underestimates the liquid holdup. By using correlations proposed by Eaton [5], more accurate liquid holdup can be calculated. In the case of inclined pipe flow, Flanigan [6] proposed a correlation for the determination of the gravitational effects. Beggs and Brill [7] studied two-phase flow through pipes in an entire range of inclination angles, i.e., vertical upward, horizontal and vertical downward. They developed correlations for flow pattern determination by using Froude number and no-slip holdup. The proposed model estimates the actual holdup and the pressure loss for each flow pattern separately. Dukler's method [4] is referred to calculate the two-phase friction factor. Taitel and Dukler [8] analyzed the prediction of transition boundaries between the flow patterns. The model begins with the equilibrium stratified flow assumption. The equilibrium liquid holdup is determined by using the Lockhart and Martinelli parameter. They modified the Kelvin-Helmholtz inviscid theory in order to predict the initiation of slugs. The transition of intermittent to annular flow is assumed to be dependent only on liquid level. Jeffrey's theory for wave initiation is used to determine the transition of stratified smooth to stratified wavy flow pattern. Turbulent and buoyant forces acting on a gas pocket are investigated for the boundary between dispersed bubble flow and intermittent flow. The transition conditions were also expressed as dimensionless parameters. This model, developed for Newtonian flow, was verified with the experiments conducted in small diameter pipes under low-pressure conditions. Dukler and Hubbard [9] investigated the mechanisms and the hydraulic behavior of slug flow. An idealized slug unit concept is introduced. The two main zones that constitute a slug unit are defined as a liquid slug and stratified liquid film/gas pocket. The proposed model estimates the liquid holdup, pressure loss and velocity distributions within the slug unit. Barnea [10] studied the transition mechanisms for each individual boundary and proposed a unified model. The flow chart of the model begins with the dispersed bubble transition. The applicability of the developed mechanisms was presented for the whole range of pipe inclinations. The results were compared with the experimental data. The effects of flow rates, fluid properties, pipe size and inclination angle were incorporated in dimensionless maps. Xiao et al [11] developed a comprehensive mechanistic model for two-phase flow in horizontal and near horizontal pipes. The flow pattern transitions were inherited from Taitel and Dukler's [8], and Barnea et al's [12] models. Two different methods were applied for calculating interfacial friction factor in stratified flow, i.e., Baker et al [13] and Andritsos and Hanratty [14]. Also the effect of pipe roughness was taken into consideration during friction factor calculations. Uniform liquid level in the film zone was assumed for intermittent flow. Empirical correlations were used in order to predict the slug length and liquid holdup of the slug body. Annular flow was treated as stratified flow with different geometrical configuration. Liquid entrainment fraction (Oliemans et al [15]) was also considered while calculating the liquid holdup in the gas core. Gomez et al [16] developed a unified mechanistic model for horizontal to vertical upward flow of two-phase fluid systems. Unified transition flow pattern prediction model and unified individual models for each flow type were presented. Moreover, the proposed model implemented new criteria in order to eliminate the discontinuity problems. The flow mechanisms in the flow pattern boundaries were inherited from the models of Taitel and Dukler [8], and Barnea [10]. Empirical correlations were used for determination of several flow properties such as, liquid/wall friction factor (Ouyang and Aziz [17]), entrainment fraction (Wallis [1]) etc. Petalas and Aziz [18] proposed a mechanistic model applicable to a wide range of pipe geometries and fluid properties. Empirical correlations were developed for interfacial friction in stratified and annular-mist flows, for liquid entrainment fraction and distribution coefficient in intermittent flow. A large amount of experimental and field data were collected in order to develop these empirical correlations. The transition mechanisms between the flow patterns were presented in a similar way to Taitel and Dukler's [8], and Barnea's [10] models. Garcia et al [19] studied a large amount of two-phase flow data and developed composite analytical expressions for friction factor covering both laminar and turbulent flow regimes. Two different approaches were presented. The first method is the universal composite correlation for friction factor estimation regardless of the flow pattern. The second method represents the friction factor correlations for a given flow pattern. This Fanning friction factor definition was based on the mixture velocity and density. Theofanous and Hanratty [20] published a report summary of the study group on flow regimes in multiphase fluid flow. In their work, the importance of experiments, pattern-revealing diagnostics and the computer programs developed for pattern identification was emphasized.

Mechanistic models for two-phase flow through annuli:

Sadatomi [21] developed flow pattern maps for air-water flow through vertical annuli. Hasan and Kabir [22] conducted two-phase flow experiments in inclined annular geometries. Caetano et al [23] investigated the upward vertical flow of two-phase fluid systems through an annulus. A method for flow pattern prediction was proposed by applying the Taitel and Dukler's [8] model to annular concentric and eccentric geometries. Salcudean et al [24,25] investigated the effect of flow obstruction geometry on pressures drops in horizontal two-phase flow. The effect of central and peripheral obstructions on flow pattern transitions was also studied by conducting experiments. Sunthankar [26] modified the model developed by Taitel and Dukler [8] to predict the flow patterns for horizontal and nearly horizontal annular flow. The effect of eccentricity and inner pipe rotation were also investigated. The performance of the proposed model was compared with the

experimental data. Zhou [27] studied the cuttings transport with aerated mud in horizontal annulus under elevated pressures and temperatures. Taitel and Dukler's [8] model was modified for annular two-phase flow. Experiments were also conducted during this study in order to verify the accuracy of developed model. Lage et al [28] conducted an experimental and theoretical study on two-phase flow in horizontal or slightly deviated fully eccentric annuli. Flow pattern prediction and gas fraction and pressure drop calculation procedures were presented.

ANN for two-phase flow through pipes:

There are very limited studies conducted for determination of flow parameters for two-phase flow through horizontal circular pipes using ANN. Ternyik et al[29] explored application of neural networks in predicting the flow pattern and liquid holdup on the basis of experimental data collected by Mukherjee[30]. Osman[31] conducted a study on identification of flow regimes and liquid holdup for horizontal two-phase flow using ANN. He used the experimental data obtained by Minami and Brill[32] and Abdul-Majeed[33]. He applied three-layer backpropagation technique and obtained promising results. Finally, Shippen and Scott[34] conducted a study on liquid holdup prediction using artificial neural networks. They also used backpropagation technique for training the network. Their network estimated the liquid holdup with a reasonable accuracy.

As it can be concluded from the literature review, many studies were conducted for two-phase flow through horizontal pipes. However, there are limited researches focused on two-phase fluid systems in horizontal annular geometries. Due to the complex mechanisms of aerated fluid flow through horizontal annuli, mechanistic models available in the literature are still questionable and in many cases, they are not fulfilling the accuracy demand. Thus, this study aims to determine the flow parameters of aerated fluids flowing through horizontal annuli using various ANN techniques rather than using mechanistic modeling approach.

Theory

Neural networks, in general terms, are input-output mapping models that can be used to attack complex or non-straightforward problems. Neural networks are particularly useful in cases where mathematical or statistical methods, such as linear, nonlinear regression, curve fitting, etc. cannot provide a satisfactory solution, i.e. the solution can be too general, or too specific that the model cannot react well to new data points. A successful model must have a good generalization and should not be affected by the outlier data points, but at the same time be able to successfully respond when new data points are introduced.

Neural networks use a model that imitates the human brain, both structurally and computationally. They are consisted of interconnected neurons that might have several layers input, hidden, output working sequentially and parallel. When an input pattern is introduced to the neural network, the synaptic weights between the neurons are stimulated and these signals propagate through layers and an output pattern is formed. Depending on how close the formed output pattern is to the expected output pattern, the weights between the layers and the neurons are modified in such a way that next time the same input pattern is introduced, the neural network will provide an output pattern that will be closer to the expected response. In that sense, the neural network is a system that will learn from examples or from its own mistakes, just like how a human is expected to behave.

The simple building block for a neural network is the neuron. It consists of several input signals each of which having individual synaptic weights. The weighted input connections are combined inside the neuron and their summation is passed through a nonlinear activation function which generates an output signal from the neuron. Typical activation functions are threshold function (0 when $v < 0$, 1 when $v \geq 0$), piecewise linear function (0 when $v \leq -0.5$, v when $-0.5 < v < 0.5$, 1 when $v > 0.5$), sigmoid function $f(v) = 1 / (1 + e^{-av})$ which has values between 0 and 1 or the hyperbolic tangent function $f(v) = \tanh(v)$ which has the values between -1 and 1. A typical neuron structure is shown in Figure 2.

The bias term is added to the summation at the neuron in order to increase or decrease the input that goes into the activation function. The activation function is a nonlinear input-output mapping function that is generally monotonic and it creates an output that is range bound [0,1] or [-1,1] and can be used as inputs to other neurons at the next layer.

The input-output (x-y) relations for the i^{th} neuron in the k^{th} layer in a neural network system can be described with the following equations:

$$v_i^k = \sum_{j=1}^{n} w_{ij}^k x_j^k + b_i^k$$

$$y_i^k = f^k(v_i^k)$$

When these neurons are combined to form a neural network, the system goes through a training stage where input and output pairs are introduced to the network and the weights in between the neurons are changed so that the network outputs match the desired outputs as close as possible. This training stage is also called as the learning stage. The learning is stopped when the error between the desired and the actual outputs are within an acceptable range. This is accomplished by summing up the error terms at the output and creating a cost function in terms of network inputs and weights and minimizing this cost function with respect to the network inputs. The cost function, generally, is based on Mean Square Error (MSE) of the outputs. Due to the nature of this algorithm, these neural network types are also called supervised neural networks.

One important detail to note is in order to minimize the cost function with respect to the network inputs, the neuron activation function must be differentiable and continuous at every point. As a result, the sigmoid or the hyperbolic tangent functions are better suited to be used in the algorithm, since they satisfy these requirements.

Once the training is terminated, the weights in between the neurons are stored for each layer and the network is ready to be tested. Testing is done by introducing an input-output pattern that was not part of the training pairs. The output is calculated using the stored weights. The difference between the desired and actual output can indicate whether the learning was sufficient and successful, or it can also indicate how similar the new input-output pair is to any of the trained patterns.

The overall structure of a general neural network can be seen in Figure 3. In a typical neural network architecture, there is always 1 input layer and 1 output layer, but depending on the particular network type, there can a different number of hidden layers, some networks even do not have any hidden layers. Several factors can affect the performance of a neural network, such as the number of input features, the number of input-output pairs, the complexity and consistency of the data representation and the network parameters (number of layers, neurons, activation function, learning rate, termination criteria, momentum term, bias values, etc).

ANN structures used in the 2-phase model

Different ANN models have been used in this study for comparing the performances during estimating pressure losses and flow pattern detection. All network models had 2 input neurons representing the liquid superficial velocity (ft/s) and gas superficial velocity (ft/s) respectively and 2 output neurons representing dP/dL (psi/ft) and the type of flow pattern (intermittent, stratified and annular) respectively. In order to determine the type of flow pattern the 3 different patterns were quantified and a numeric output is obtained. The intermediate system configuration (number of hidden layers, neurons, iteration number, etc) is chosen differently in each network model. The network cases used in this study are summarized as follows:

Case – 1: Backpropagation with 5 neurons
Case – 2: Backpropagation with 10 neurons
Case – 3: Backpropagation with 15 neurons
Case – 4: Backpropagation with 20 neurons
Case – 5: Backpropagation with 25 neurons
Case – 6: Backpropagation with 30 neurons
Case – 7: Backpropagation with 2 hidden layers, 20 and 15 neurons, MSE 0.006
Case – 8: Generalized FF with 20 neurons
Case – 9: Modular neural network with 8 modules and 8 hidden neurons
Case – 10: Jordan/Elman with 20 neurons, MSE 0.005
Case – 11: Jordan/Elman with 20 neurons, MSE 0.01
Case – 12: Jordan/Elman with 10 neurons, MSE 0.005
Case – 13: Jordan/Elman with 25 neurons, MSE 0.005
Case – 14: Jordan/Elman with 2 hidden layers, 10 and 10 neurons, MSE 0.005
Case – 15: PCA with 10 principal components and 10 neurons, MSE 0.005
Case – 16: RBF with 30 cluster centers, MSE 0.01
Case – 17: SOM 5x5 feature map connected to 20 neurons, 100 unsupervised iteration, MSE 0.01
Case – 18: SOM 10x10 feature map connected to 20 neurons, 1000 unsupervised iteration, MSE 0.01

Backpropagation Neural Network

Backpropagation is the most commonly used neural network type due to its simplicity in implementation and its successful generalization capabilities for complex data sets. The basic idea behind the backpropagation learning algorithm [36] is the forward propagation of the weighted input signals through a number of layers combined with an error calculation at the output layer and back propagation of the errors at each layer back to the input layer in order to minimize the differences between the desired outputs and the calculated outputs by using the least mean squares (LMS) or Mean square error (MSE) terms [37]. In the 2-phase ANN model, 7 different configurations (Case 1 – 7) for backpropagation network are used. All models had the same input parameters and output parameters, but all had different number of hidden layers and neurons. Cases 1 to 6 had only 1 hidden layer, but had 5,10,15,20,25 and 30 hidden neurons respectively. Case 7 had 2 hidden layers, first one had 20 neurons, and second one had 15 neurons. Tanh function (hyperbolic tangent) is used as the transfer function on the neurons; momentum-learning type is used with a momentum level of 0.7. Batch learning is used for network learning and the training is terminated based on the Mean Square Error (MSE) on the sum of the errors on the training set with an error threshold of 0.01. The maximum number of iterations was set to 100000. The best weight matrices based on the minimum error sum was used in the network in order to find the optimum weights for a given local or global minima within the number of iterations.

Generalized Feed Forward Neural Network

Generalized FF Neural Network is the same as Backpropagation network, except the feedforward connections can jump over layers, whereas in Backpropagation each layer is only connected to the immediate neighboring layer [37]. The Generalized Feed Forward Neural network might solve the same problem faster than a Backpropagation network, but in our experiments (Case 8), we have not observed a better performance from this particular network.

Modular Neural Networks

Modular Neural Network is also very similar to Backpropagation network, except the same inputs are connected to several different backpropagation modules in a parallel fashion, but these modules do not have full connectivity within themselves [37]. There is no specified design methodology for these module structures, so it is unclear how to design these systems to increase the performance. Again in our experiments (Case 9), we have not observed a better performance from this particular network.

Principal Component Analysis (PCA) Neural Networks

Principal Component Analysis is used for reconfiguring the network by finding the most relevant components of the data [37]. Then, these components are used as inputs to a Backpropagation network. This type of network is called as PCA Neural Network. The number of components and other network parameters can be configured in order to accomplish

the best results. As far as how the iterations are performed, it works the same way as a backpropagation network. In the experiments 10 principal components and 10 hidden neurons in 1 hidden layer are chosen (Case 15). The same network parameters are used as in the backpropagation network.

Radial Basis Function (RBF) Neural Network

RBF neural network is another supervised neural network type. In RBF, some centers are chosen within the data clusters and a gaussian or any similar base function is defined at every center. Every data point in the data set is represented as the weighted combinations of the basis functions from all of the centers. The basic idea about RBF networks is to transform a complex data set not linearly separable in its input vector space into a high-dimensional space for better representation by using some nonlinear basis functions [40]. As a result only one weight matrix can represent the whole network as the link between the input and the output layers, therefore there are no hidden layers used. For measuring the difference between the cluster centers and data points Euclidean distance metrics is used. In the output layer, Tanh function is used as the transfer function and momentum-learning type is used with a momentum level of 0.7. Batch learning is used for network learning and the training is terminated based on the Mean Square Error (MSE) on the sum of the errors on the training set with an error threshold of 0.01. The maximum number of iterations was set to 100000. The best weight matrices based on the minimum error sum was used in the network in order to find the optimum weights for a given local or global minima within the number of iterations. In this particular network, various numbers of cluster centers were tested but the best results were obtained when using a 30 clusters model (Case 16).

Self Organizing Maps (SOM) connected to a Backpropagation

SOM Neural Network uses an unsupervised neural network paradigm, the idea is to capture the natural clustering of the data. It is based on competitive learning where with a given input pattern, the output neurons compete with each other in order to best represent the input-output relation [41]. The feature maps are configured as 5x5 neurons in Case 17 and 10x10 neurons in Case 18 connected to each other and the results are used as inputs to a backpropagation network and sent to a hidden layer of 20 neurons. The only key point is the feature maps are obtained by self clustering of the input data and is not affected by the network outputs. Once the feature mapping of the input parameters are finished by SOM, the results are sent to the second module, which is the supervised backpropagation network and that second module is trained using the feature map as inputs and dP/dL (psi/ft) and the type of flow pattern as the 2 output parameters. The same network configuration is used in this module as was used in the backpropagation network.

Computer Work

In order to simplify and generalize the network inputs, superficial Reynolds numbers for both phases are used. Superficial Reynolds number for liquid phase is defined as

$$N_{\mathrm{Re}_L} = \frac{\rho_L v_{SL} \left(D_o - D_i\right)}{\mu_L}$$

and superficial Reynolds number for gas phase is expressed as

$$N_{\mathrm{Re}_G} = \frac{\rho_G v_{SG} \left(D_o - D_i\right)}{\mu_G}$$

In this study, experimental data obtained from Middle East Technical University, Petroleum & Natural Gas Engineering Department, Multiphase Flow Loop[35] as well as data available in the literature[26,27] is used. The information about the experimental data is presented in Table-1.

Results and Discussions

Once the neural network models are trained, they are used for predicting the frictional pressure loss and flow patterns for horizontal annular two-phase flow. The performance of the neural network models used in this study have been observed using tables 2 and 3 as well as Figure-4. Here, Table-2 is the percentage of the number of data points among all data points which gives the corresponding error percent, and Table-3 is the percentage of the number of data points among all data points which shows the corresponding absolute pressure drop difference between the measured and the calculated values. Also, Figure-4 presents the total average error for each neural network model including the frictional pressure loss and flow pattern detection. Analysis of Table-2 and Table-3 showed that case-7 and case-14 showed the best performance among all neural network models for estimating the frictional pressure drop of two-phase flow through a horizontal annulus. The performance of case-7 and case-14 is shown in figures 5 and 6, where x-axis is the measured frictional pressure drop, and y-axis is the calculated pressure drop using the neural network. As seen from figures 4 and 5, most of the data points are estimated with a reasonable accuracy. Among the neural network models, the worst performance is observed for case-2, which the performance is presented in Figure-7. As seen from Figure-7, there exists a scattered distribution of data points which shows a poor agreement between the measured and calculated values.

Figure-8 is the observed flow pattern distribution for all data points used in this study. The neural networks have been trained to match Figure-8. Using Figure-4, the performance of all neural networks could be observed. According to Figure-4, case-13 and case-14 showed the best performance on estimating the flow patterns. The performances for case-13 and case-14 are shown in figures 9 and 10, respectively. However, the worst performance is conducted by case-1, as presented in Figure-11. When figures 9 to 11 are compared, it can be seen that Figure 9 and 10 are very similar to Figure-8, but Figure-11 is totally scrambled, i.e., flow patterns could not be identified properly.

Conclusions

In this study, the flow patterns and frictional pressure losses of two-phase fluids flowing through horizontal annular

geometries are estimated using Artificial Neural Networks (ANN) rather than using conventional techniques. Experimental data used in this study are collected from experiments conducted at Middle East Technical University, Petroleum & Natural Gas Engineering Multiphase Flow Loop, as well as from literature in order to train the ANN. Numerous ANN methods are tested and compared. The followings are concluded.

- ANN can be used to determine the flow patterns and frictional pressure losses for two-phase fluids with a reasonable accuracy.
- Backpropagation with 2 hidden layers, 20 and 15 neurons with a mean square error of 0.006 and Jordan/Elman with 2 hidden layers, 10 and 10 neurons with a mean square error of 0.005 are determined to be the best methods for estimating the frictional pressure losses.
- Jordan/Elman with 25 neurons with a mean square error of 0.005 and Jordan/Elman with 2 hidden layers, 10 and 10 neurons with a mean square error of 0.005 are determined to be the best methods for estimating the flow patterns.

Nomenclature

ρ *density*
μ *viscosity*
b *bias term*
D *diameter*
$f(v)$ *activation function*
N_{Re} *Reynolds number*
v *velocity*
w *weighted*
x *input*
y *output*

Subscritps

G *gas*
i *inner*
L *liquid*
o *outer*
S *superficial*

References

1. Wallis, G.B.: "One-Dimensional Two-Phase Flow," McGraw-Hill Book Co. Inc., New York City (1969).
2. Lockhart, R.W., and Martinelli, R.C.: "Proposed Correlation of Data for Isothermal Two-Phase, Two-Component Flow in Pipes," *Chemical Engineering Progress* 45, No. 1, 39-48 (1949).
3. Duns, H.Jr. and Ros, N.C.J.: "Vertical Flow of Gas and Liquid Mixtures in Wells," *Proc*., Sixth world Petroleum Congress, Frankfurt-am-Main, Germany (1963) 451.
4. Dukler, A.E., Wickes, M. III, and Cleveland, R.G.: "Frictional Pressure Drop in Two-Phase Flow: B. An Approach Through Similarity Analysis" *AIChE J.* (1964) 10, No. 1, 44.
5. Eaton, B.A. and Brown, K.E.: "The Prediction of Flow Patterns, Liquid Holdup and Pressure Losses Occurring During Continuous Two-Phase Flow in Horizontal Pipelines," Technical Report, The U. of Texas (October 1965).
6. Flanigan, O.: "Effect of uphill flow on pressure drop in design of two-phase gathering systems," *Oil and Gas J.* 56-132 (1958).
7. Beggs, H.D., and Brill, J.P.: " A Study of Two-Phase Flow in Inclined Pipes," *JPT* (May 1973) 607; *Trans*., AIME, 255.
8. Taitel, Y., and Dukler, A.E.: " A Model for Predicting Flow Regime Transition in Horizontal and Near Horizontal Gas-Liquid Flow," *AIChE J*. (1976) 22 No. 1, 47.
9. Dukler, A.E., and Hubbard, M.G.: " A Model For Gas-Liquid Slug Flow in Horizontal and Near Horizontal Tubes," *Ind. Eng. Chem. Fundam.* (1975) 14, 337.
10. Barnea, D.: "A Unified Model for Predicting Flow Pattern Transitions for the Whole Range of Pipe Inclinations," *Int. J. Multiphase Flow* (1987) 13, No. 1, 1.
11. Xiao, J.J., Shoham, O., and Brill, J.P.: "A Comprehensive Mechanistic Model for Two-Phase Flow in Pipelines." Paper SPE 20631 presented at the 1990 SPE Annual Technical Conference and Exhibition, New Orleans, 23-26 September.
12. Barnea, D., Shoham, O., and Taitel, Y.: "Flow Patter Transition for Vertical Downward Inclined Two-Phase Flow; Horizontal to Vertical," Chem. Eng. Sc. 37, No. 5, 735-740 (1982).
13. Baker, A., Nielsen, K., and Gabb, A.: "Pressure loss, Liquid Holdup Calculations developed," *Oil & Gas J.,* 55-59 (March 14, 1998).
14. Andritsos, N., and Hanratty, T. J.: "Influence of Interfacial Waves in Stratified Gas-Liquid Flows," *AIChE J*. 33, No. 3, 444-454 (1987).
15. Oliemans, R.V., A., Pots, B.F., and Trope, N.: "Modelling of Annular Dispersed Two-Phase Flow in Vertical Pipes," *Int. J. Multiphase Flow* 12, No. 5, 711-732 (1986).
16. Gomez L.E., Shoham O., Schmidt Z., Chokshi R.N. and Northug T.: "Unified Mechanistic Model for Steady-State Two-Phase Flow: Horizontal to Vertical Upward Flow," SPE Journal 5, No. 3, 339-350 (September 2000).
17. Ouyang, L.B., and Aziz, K.: "Development of New Wall Friction Factor and Interfacial Friction Factor correlations for Gas/Liquid Stratified Flow in Wells and Pipes," paper SPE 35679 presented at the 1996 SPE Western Regional Meeting, Anchorage, 22-24 May.
18. Petalas, N., and Aziz, K.: "A Mechanistic Model for Multiphase Flow in Pipes," *JCPT* 39, No. 6, 43-55 (2000).
19. Garcia, F., Garcia, R., Padrino, J.C., Mata, C., Trallero, J.L. and Joseph, D.D.: " Power Law and Composite Power Law Friction Factor Correlations for Laminar and Turbulent Gas-Liquid Flow in Horizontal Pipelines," *Int. J. Multiphase Flow* 29, 1605-1624 (2003).
20. Theofanous, T.G. and Hanratty, T.J.: " Appendix 1: Report of Study Group on Flow Regimes in Multifluid Flow," *Int. J. Multiphase Flow* 29, 1061-1068 (2003).
21. Sadatomi, M., Sato, Y., and Saruwatari, S.: "Two-Phase Flow in Vertical Noncircular Channels," *Int. J. Multiphase Flow* 8, 641-655 (1982).
22. Hasan, A.R., and Kabir, C.S.: "Two-Phase Flow in Vertical and Inclined Annuli," *Int. J. Multiphase Flow* 18, 279-293 (1992).
23. Caetano, E.F., Shoham, and O., Brill, J.P.: "Upward Vertical Two-Phase Flow Through An Annulus, Part-I: Single Phase Friction Factor, Taylor Bubble Velocity And Flow Pattern Prediction," ASME *J. Energy Resour. Technol.* 114, 1-13 (1992).
24. Salcudean, M., Chun, J.H., and Groeneveld, D.C.: " Effect of Flow Obstructions on Void Distribution in Horizontal Air-Water Flow," *Int. J. Multiphase Flow* 9, 91-96 (1983).

25. Salcudean, M., Chun, J.H., and Groeneveld, D.C.: " Effect of Flow Obstructions on the Flow Pattern Transitions in Horizontal Two-Phase Flow," *Int. J. Multiphase Flow* 9, 87-90 (1983).
26. Sunthankar, A.A.: "Study of the Flow of Aerated Drilling Fluids in Annulus under Ambient Temperature and Pressure Conditions," *M.Sc. Thesis*, The University of Tulsa, 2002.
27. Zhou, L.: "Cuttings Transport with Aerated mud in Horizontal Annulus under Elevated Pressure and Temperature Conditions," *PhD Dissertation*, The University of Tulsa, 2004.
28. Lage, A.C.V.M.; Rommetveit, R.; Time, R.W.: "An Experimental and Theoretical Study of Two-Phase Flow in Horizontal or Slightly Deviated Fully Eccentric Annuli," SPE 62793, IADC/SPE Asia Pacific Drilling Technology, Kuala Lumpur, Malaysia, 11–13 September 2000.
29. Ternyik J., Bilgesu H.I., and Mohaghegh S., "Virtual Measurements in Pipes: Part – 2, Liquid Holdup and Flow Pattern Correlations", SPE 30976 presented at 1995 Eastern Regional Meeting, Morgantown, West Virginia, 17-21 September.
30. Mukherjee H., "An Experimental Study of Inclined Two-Phase Flow", *PhD Dissertation*, University of Tulsa, 1979
31. Osman E.S.A., "Artificial Neural Network Models for Identifying Flow Regimes and Predicting Liquid Holdup in Horizontal Multiphase Flow", *SPE Production and Facilities*, 33, February (2004)
32. Minami K., and Brill J.P., "Liquid Holdup in Wet-Gas pipelines", *SPE Production and Facilities*, 36, February (1987)
33. Abdul-Majeed G.H., "Liquid Holdup in Horizontal Two-Phase Gas-Liquid Flow", *Journal of Petroleum Science and Engineering*, 15, 271 (1996)
34. Shippen M.E., and Scott S.L., "A Neural Network Model for Prediction of Liquid Holdup in Two-Phase Horizontal Flow", *SPE Production and Facilities*, 67, May (2004)
35. Omurlu C., "Mathematical Modeling of Horizontal Two-Phase Flow Through Fully Eccentric Annuli", *M.Sc. Thesis*, Middle East Technical University, 2006
36. Rumelhart D.E, Hinton G.E, and Williams R.J, "Learning representations of back-propagation errors", *Nature*, 323, 533-536, (1986)
37. Haykin S., "Neural Networks: A Comprehensive Foundation, Second Edition", Prentice Hall, Upper Saddle River, NJ 07458, (1999)
38. Elman J.L., "Finding Structure in time", *Cognitive Science*, 14, 179-211, (1990)
39. Jordan M.I., "Attractor dynamics and parallelism in a sequential connectionist machine", Proceedings of 9th Annual Conference of Cognitive Science Society, 531-546, (1986)
40. Powell M.J.D., "Radial basis functions for multivariable interpolation: A Review", IMA Conference on Algorithms for the Approximation of Functions and Data, 143-167, RMCS, Shrivenham, England, (1985)
41. Kohonen T., "The self-organizing map", *Proceedings of the Institute of Electrical and Electronics Engineers*, 78, 1464-1480, (1990)

Appendix

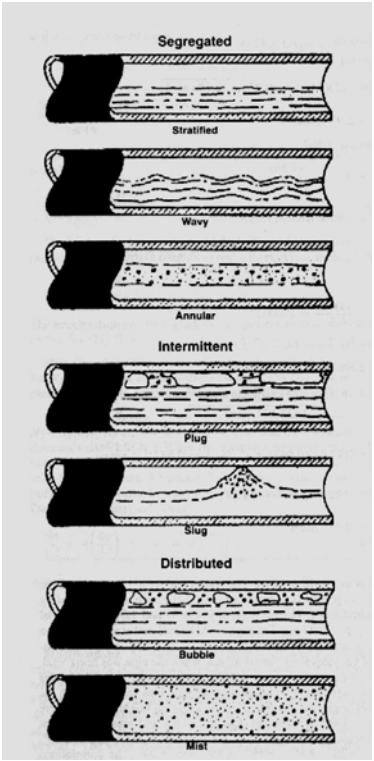

Figure-1 flow patterns of 2-phase flow for horizontal flow, after Taitel and Dukler[8]

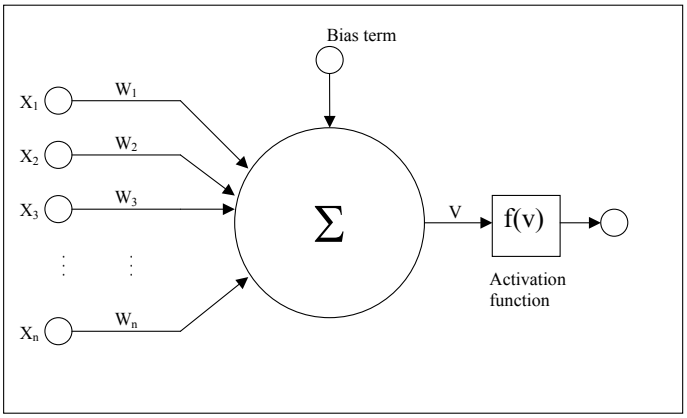

Figure-2 The basic model of a neuron

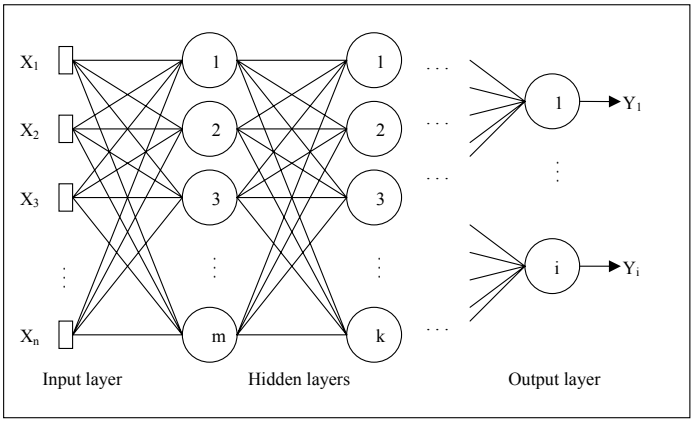

Figure-3 The general architecture of a neural network

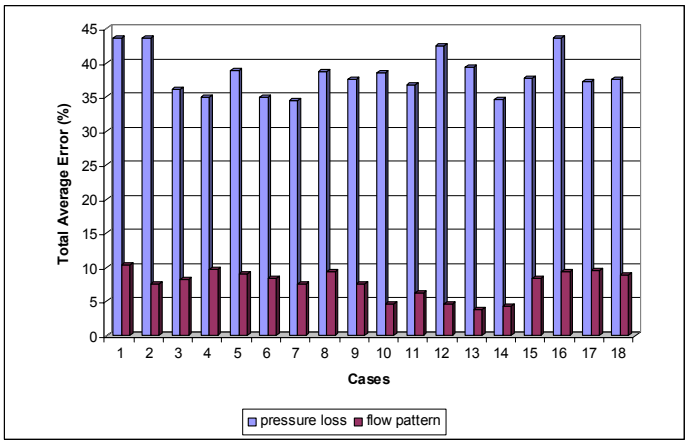

Figure-4 Total average error for all ANN cases

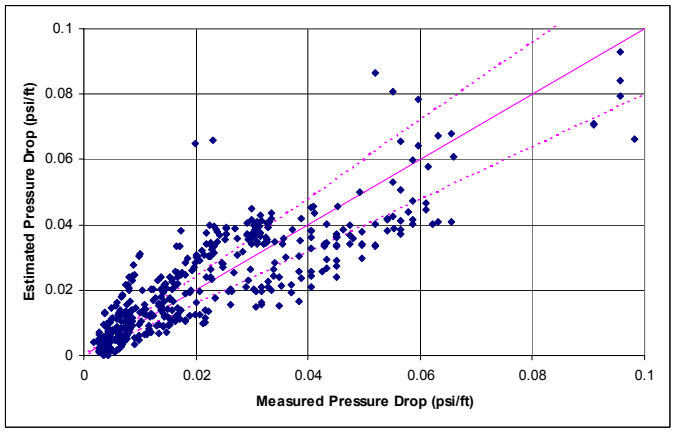

Figure-7 Frictional pressure loss (BP 10 neuron) worst

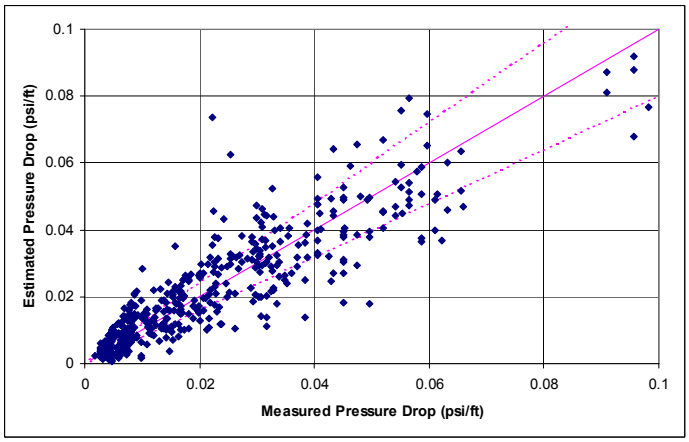

Figure-5 Frictional pressure loss (BP 2h, 20,15n, 0.006) (best 1)

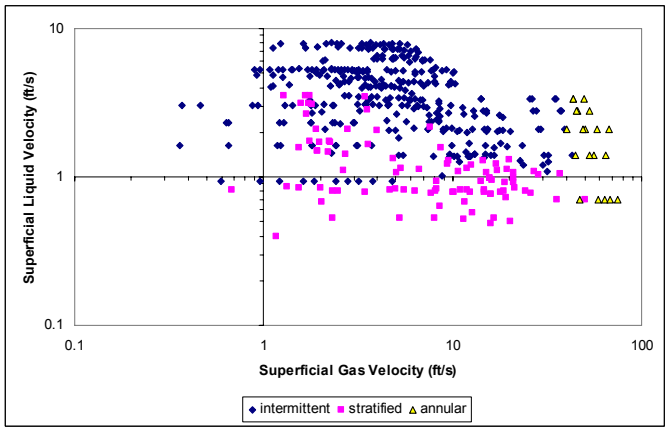

Figure-8 Actual flow pattern map developed using experimental data

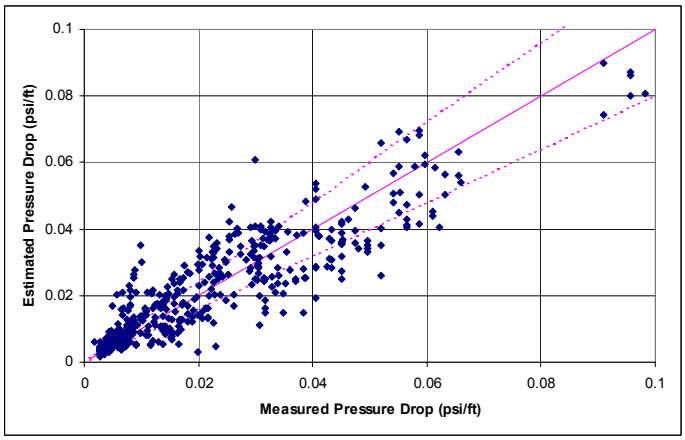

Figure-6 Frictional pressure loss (J_E 2h, 10,10n 0.005) (best 2)

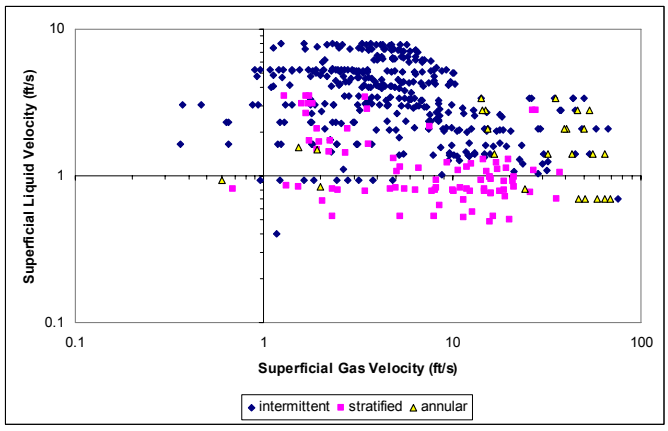

Figure-9 Flow pattern map (J_E 25 n 0.005) (best 1)

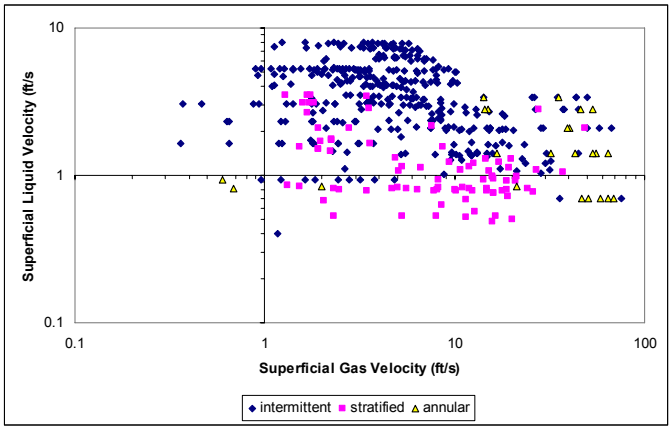

Figure-10 Flow pattern map (J_E 2h, 10,10n 0.005) (best 2)

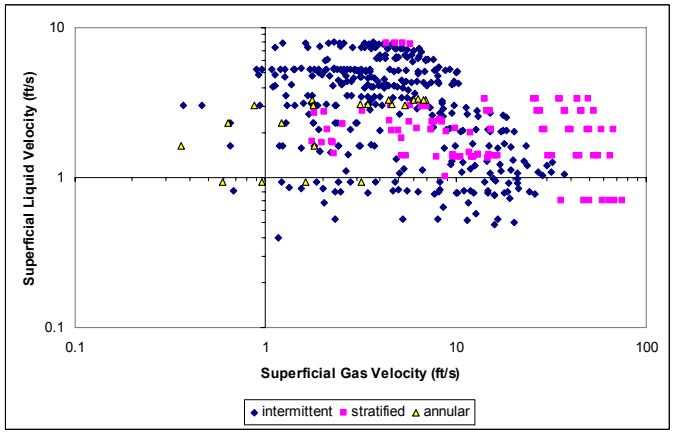

Figure-11 Flow pattern map (BP 5 neuron) (worst)

Table-1 Experimental Data

	fluid used	Well ID (in)	Pipe OD (in)	Superficial in-situ velocity (ft/s)	frictional pressure drop (psi/ft)
liquid	water	1.5 - 4.5	3.0 - 8.0	0.4 - 8.0	0.002 - 0.098
gas	air			0.36 - 75.6	

Table-2 Percentage of data points corresponding to the error percent that the networks can estimate

Error histogram %	Case 1	Case 2	Case 3	Case 4	Case 5	Case 6	Case 7	Case 8	Case 9	Case 10	Case 11	Case 12	Case 13	Case 14	Case 15	Case 16	Case 17	Case 18
<5%	3.76	6.64	7.52	8.19	6.42	7.52	9.51	6.64	5.75	8.85	7.30	6.86	7.30	9.07	6.64	5.31	8.85	8.19
<10%	11.73	12.83	16.59	18.14	13.05	17.48	18.81	13.72	12.83	17.92	17.48	14.82	16.15	18.58	13.27	11.06	18.14	16.37
<15%	20.13	20.13	21.90	28.32	21.46	26.77	28.98	20.35	19.91	27.65	23.89	21.90	24.12	27.21	21.24	20.80	28.32	25.44
<20%	27.43	26.99	31.64	37.83	30.31	37.83	37.61	29.20	30.09	34.51	31.86	28.76	35.18	37.17	29.42	28.32	36.73	34.29
<25%	35.40	35.62	43.36	44.91	40.93	48.01	47.12	40.04	40.93	45.80	42.48	36.06	44.91	48.45	39.38	37.61	46.46	43.58
<30%	44.69	43.58	51.55	54.20	50.22	55.75	55.09	50.88	54.20	53.54	50.22	43.81	52.65	58.63	50.44	48.89	55.09	52.21
<35%	53.10	51.55	60.40	62.39	58.41	63.50	61.73	59.96	63.50	61.06	59.96	53.76	62.17	67.26	60.18	58.41	62.61	61.95
<40%	64.16	62.61	67.70	70.13	67.70	67.48	69.47	67.26	70.58	67.48	66.81	60.18	67.04	73.45	68.14	66.15	67.70	69.25
<45%	72.57	68.36	74.78	75.88	73.67	73.45	74.12	73.67	76.11	74.34	75.88	66.59	72.12	78.10	73.23	71.24	74.12	75.00
<50%	77.65	73.45	80.09	80.31	76.77	78.10	79.20	78.76	79.42	80.75	81.64	71.68	77.21	82.96	79.42	76.77	78.10	78.10
<75%	87.61	87.61	91.59	92.04	88.05	90.93	89.82	91.15	90.49	90.04	92.26	86.73	91.37	92.26	90.93	88.50	90.04	89.38
<100%	91.37	90.71	95.13	95.35	93.36	95.80	95.13	94.25	94.91	94.25	94.47	92.70	94.91	95.13	95.80	92.92	92.92	94.25
>100%	8.63	9.29	4.87	4.65	6.64	4.20	4.87	5.75	5.09	5.75	5.53	7.30	5.09	4.87	4.20	7.08	7.08	5.75

Table-3 Percentage of data points corresponding to the actual absolute pressure drop difference that the networks can estimate

Error histogram (psi/ft)	Case 1	Case 2	Case 3	Case 4	Case 5	Case 6	Case 7	Case 8	Case 9	Case 10	Case 11	Case 12	Case 13	Case 14	Case 15	Case 16	Case 17	Case 18
<0.001	12.39	10.62	13.05	15.04	11.95	14.60	14.60	14.16	13.94	15.27	14.16	11.95	15.27	17.48	13.27	12.83	15.93	14.60
<0.002	21.90	23.67	28.98	31.19	24.34	28.76	30.09	26.33	25.44	28.10	29.42	24.78	26.11	29.87	26.33	27.88	28.98	29.42
<0.003	31.86	32.52	38.50	43.14	36.95	38.94	39.38	37.17	35.40	37.17	35.84	32.74	36.28	39.60	39.38	37.39	42.48	37.83
<0.004	40.27	39.82	48.45	50.44	44.91	50.22	50.44	42.48	43.14	47.35	42.70	41.37	45.35	48.45	46.90	45.13	49.34	44.91
<0.005	46.46	47.35	54.87	57.08	51.11	58.19	57.74	50.00	52.43	54.20	49.78	47.12	51.11	56.19	53.54	49.34	55.97	52.21
<0.006	53.10	54.42	59.51	63.27	55.97	63.94	64.38	56.86	57.74	58.63	55.97	54.87	57.96	61.50	59.07	55.09	61.73	59.29
<0.007	59.29	59.29	64.60	67.04	61.28	67.92	71.24	61.28	63.05	63.50	60.62	58.63	65.49	65.71	62.61	58.85	65.49	64.38
<0.008	63.50	66.37	69.25	71.02	67.04	70.13	76.33	65.27	66.37	67.92	66.81	63.05	70.80	70.58	67.48	63.05	70.58	68.81
<0.009	67.92	70.58	73.89	76.11	72.12	74.34	80.53	69.69	71.02	73.23	72.12	68.58	75.44	75.22	70.80	67.92	74.56	73.45
<0.010	73.01	74.34	77.21	78.32	76.33	77.65	82.96	73.23	75.88	77.43	77.43	73.89	77.88	79.87	75.88	71.90	77.65	76.77
<0.011	76.99	77.65	81.64	81.42	80.31	81.64	86.50	77.65	80.31	80.09	82.08	79.65	81.64	82.52	80.97	75.88	81.64	80.31
<0.012	81.42	82.96	84.29	84.73	83.85	84.29	88.50	80.53	82.74	84.73	84.96	82.30	84.29	86.50	84.07	79.42	84.73	84.07
<0.013	18.58	17.04	15.71	15.27	16.15	15.71	11.50	19.47	17.26	15.27	15.04	17.70	15.71	13.50	15.93	20.58	15.27	15.93

SPE 101474

Uncertainty Analysis of a Giant Oil Field in the Middle East Using Surrogate Reservoir Model

Shahab D. Mohaghegh, West Virginia U. & Intelligent Solutions, Inc.; Hafez Hafez, ADCO; Razi Gaskari, WVU; and Masoud Haajizadeh and Maher Kenawy, ADCO

Copyright 2006, Society of Petroleum Engineers

This paper was prepared for presentation at the 2006 Abu Dhabi International Petroleum Exhibition and Conference held in Abu Dhabi, U.A.E., 5–8 November 2006.

This paper was selected for presentation by an SPE Program Committee following review of information contained in an abstract submitted by the author(s). Contents of the paper, as presented, have not been reviewed by the Society of Petroleum Engineers and are subject to correction by the author(s). The material, as presented, does not necessarily reflect any position of the Society of Petroleum Engineers, its officers, or members. Papers presented at SPE meetings are subject to publication review by Editorial Committees of the Society of Petroleum Engineers. Electronic reproduction, distribution, or storage of any part of this paper for commercial purposes without the written consent of the Society of Petroleum Engineers is prohibited. Permission to reproduce in print is restricted to an abstract of not more than 300 words; illustrations may not be copied. The abstract must contain conspicuous acknowledgment of where and by whom the paper was presented. Write Librarian, SPE, P.O. Box 833836, Richardson, TX 75083-3836, U.S.A., fax 01-972-952-9435.

Abstract

Simulation models are routinely used as a powerful tool for reservoir management. The underlying static models are the result of integrated efforts that usually includes the latest geophysical, geological and petrophysical measurements and interpretations. As such, these models carry an inherent degree of uncertainty. Typical uncertainty analysis techniques require many realizations and runs of the reservoir simulation model. In this day and age, as reservoir models are getting larger and more complicated, making hundreds or sometimes thousands of simulation runs can put considerable strain on the resources of an asset team, and most of the times are simply impractical. Analysis of these uncertainties and their effects on well performance using a new and efficient technique is the subject of this paper. The analysis has been performed on a giant oil field in the Middle East using a surrogate reservoir model.

The surrogate reservoir model that runs and provides results in real-time is developed to mimic the capabilities of a full field simulation model that includes one million grid blocks and takes 10 hours to run using a cluster of twelve 3.2 GHz CPUs. In order to effectively demonstrate the robustness of Surrogate Reservoir Models and their capabilities as tools that can be used for uncertainty analysis, one must demonstrate that SRMs are competent in providing reasonably accurate results for multiple realizations of the reservoir being studied. In order to demonstrate such robustness and their predictive capabilities as well as their limitations, this paper will examine the performance of the surrogate reservoir models on different geologic realizations of the static model.

Introduction

In two previous SPE papers some of the aspects of the Surrogate Reservoir Models were discussed. In the first paper[1] the idea of Surrogate Reservoir Models was introduced and in the second paper[2] its application in quantifying uncertainties associated with a reservoir simulation study was explored.

The conventional approach for uncertainty analysis in our industry is mainly based on geostatistics. One such method that is often used is Response Surfaces[3-5]. Response Surfaces are statistical interpolations (based on fitting some type of pre-determined models – linear or quadratic –) of model responses to different geological, geophysical and petro-physical realizations[6,7]. Another method that has been used more in other industries is called the Reduced Model. Reduced Models are approximations of full three dimensional numerical simulation models that essentially approach an analytical model for tractability[8].

One of the major advantages of Surrogate Reservoir Models, when compared to conventional geostatistical techniques, is the small number of simulation runs that is required for their development. For example, instead of hundreds of simulation runs that would be required to perform a

limited geostatistical study, development of the Surrogate Reservoir Model that is the subject of this paper required only 10 simulation runs. On the other hand, the capabilities of the SRM for analyses are more far reaching than the alternative technique that required hundreds of runs. The reason for being able to do much more with a limited number of simulations runs (about 10 runs as appose to hundreds and sometimes thousands of runs in the case of some geo-statistical analyses) has to do with the efficiency by which SRMs use the resources offered by each simulation run. This efficiency is associated with the way Surrogate Reservoir Models represent the reservoir. The objective of this paper is to demonstrate the approach that is taken by Surrogate Reservoir Models in representation of multiple realizations within a single simulation run. In order to clearly demonstrate this aspect of SRMs, which is a key component in their development, an introduction on the philosophical approach used by the SRM is appropriate.

Surrogate Reservoir Models are prototypes of complete three dimensional numerical reservoir models that are capable of accurately mimicking the behavior of the full field models with all their details and complexity. The word “prototype” is used here in the context of the prototype theory that is defined as “a model of graded categorization, where all members of a category do not have equal status.” This definition becomes clearer once the development process of Surrogate Reservoir Model is considered[1].

Given the above definition of Surrogate Reservoir Model, as a prototype of the full field model, the approach used during the development of the Surrogate Reservoir Models fits more appropriately within the approach summarized in the system theory[9] (depicted in Figure 1) rather than the approach commonly used in our industry that is essentially based on geostatistics.

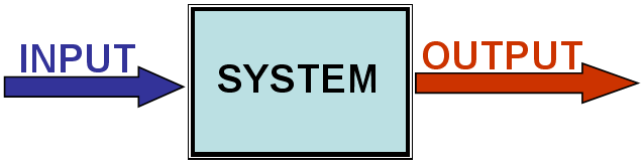

Figure 1. The three components involved in the System Theory, Input, System and Output.

Considering the full field reservoir model within the realm of the System Theory, different reservoir parameters such as permeability, porosity, and capillary pressure, to name a few, from the geologic (static) model are input to the system while the production from the wells is the system output (system being the full field reservoir model as a reasonable substitution for the actual reservoir). When we claim that SRMs are tools that are defined within the real of the System Theory it would mean that the system output reacts to the changes in input. In other words, the Surrogate Reservoir Model is capable of adjust its output as a function of the modeification of the input variables. Moreover, SRMs can perform this task in real-time.

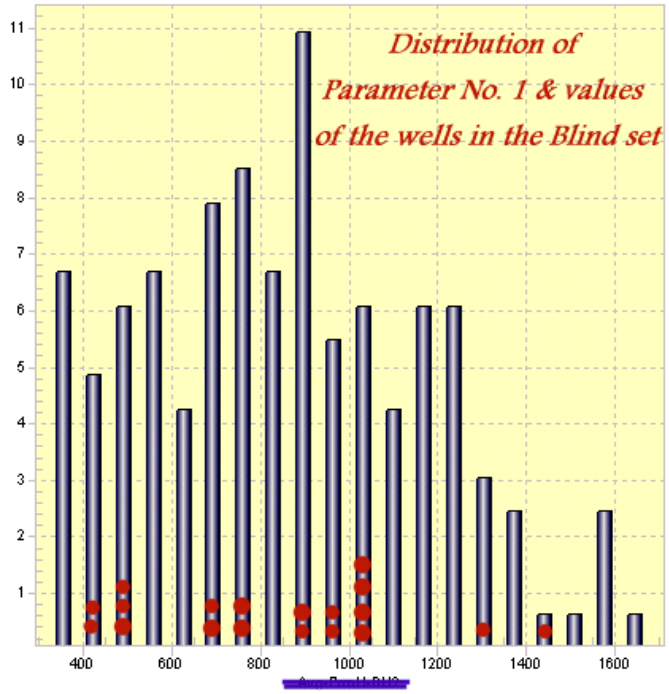

Figure 3. Distribution of reservoir parameter number 1 in the entire reservoir along with the distribution of the 19 blind wells.

During conventional analyses that are categorized as response surface, hundreds of combinations of input parameters are generated (realizations) that upon completion of hundreds of runs, results in hundreds of sets of outputs (production from wells in the field). These outputs are then used to generate surfaces of all the possible responses that can result from the predetermined realizations.

Selection of the realizations is usually made in a way to maximize the coverage of the anticipated

range of input parameters while requiring minimum number of simulation runs. Usually, techniques such as Latin Hyper Cube[10] and Design of Experiments[11] are used to optimize this process. Nevertheless most of the serious studies require hundreds of runs to provide meaningful coverage. Furthermore, once the hundreds or thousands of required simulation runs are made and the response surface is created, the input parameters no longer play any role in the process. In other words, the approach mentioned in the System Theory will not be in effect upon completion of the simulation runs and during the development and use of the response surface.

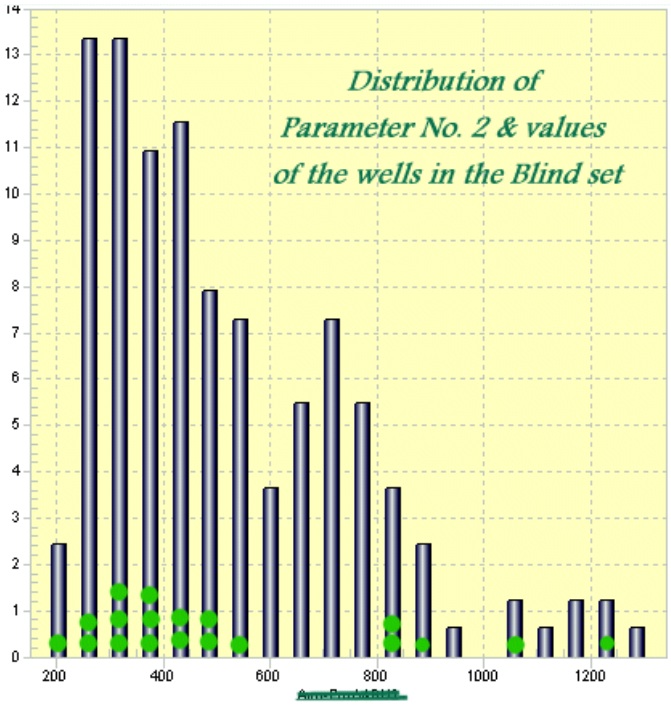

Figure 4. Distribution of reservoir parameter number 2 in the entire reservoir along with the distribution of the 19 blind wells.

Methodology

Figure 2 (at the end of this article) shows the location of the wells in the field along with the approximate drainage area for each well. The approximate drainage areas shown in Figure 2 are identified using the Voronoi Graph theory[12]. During the exercise that is described in this paper the objective is to demonstrate that the Surrogate Reservoir Model can be developed using a certain set of realizations and be validated by another set of independent realizations. In order to do this 19 out of the 165 horizontal wells in the field were randomly selected to serve as the validation wells.

During the remaining parts of this paper, these wells are called the set of blind wells. The validation exercise is performed by predicting the flow behavior in these wells with the Surrogate Reservoir Model that has been developed using the realizations associated with the rest of the wells in the field. The idea is that since the Surrogate Reservoir Model looks at the entire reservoir through the lens of a single well (a representative volume that includes the surrounding area and multiple-layers) then a single simulation run (one realization) actually provides multiple (the total number of wells in the reservoir) realizations. In other words, the realizations that are considered during the development of the Surrogate Reservoir Model include only a segment of the reservoir (the representative volume) rather than the entire reservoir.

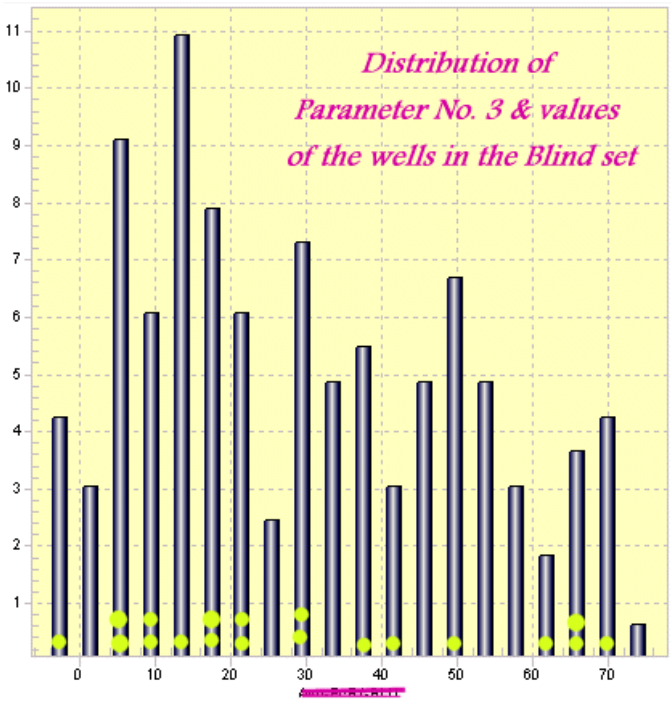

Figure 5. Distribution of reservoir parameter number 3 in the entire reservoir along with the distribution of the 19 blind wells.

Figures 3 through 5 show the distribution of three reservoir parameters in the field along with the values of the set of blind wells identified as small circles in the distribution. It is shown that the values of the parameters for the set of blind wells fall

within the distribution of the entire field. Therefore, one may consider that when cumulative oil production and/or water cut for one of the wells in the blind set is predicted by the Surrogate Reservoir Model the model is essentially predicting the behavior of a new realization with a distribution similar to the ones used during the Surrogate Model development.

As mentioned before, the objective is to develop a Surrogate Reservoir Model that is robust enough to be able to predict the well production behavior as long as the reservoir parameters that contribute to the flow fall within a certain distribution. This certain distribution refers to the distribution of each of the parameters for each of the grid blocks in the full field model.

At this point it would be appropriate to mention that Surrogate Reservoir Models are developed based on several different representative volumes. The size of the representative volume is determined by two factors:

1. The objective of the project.
2. The physics and the dynamics of the reservoir.

The representative volume can be as small as the size of one grid block of the actual full field model or so large that it could include multiple wells. The details on how to actually determine the size of the representative volume and how to implement it in the context of developing a Surrogate Reservoir Model as well as the role it plays in the complexity of the Surrogate Reservoir Model is outside of the scope of this paper and will be discussed in a future paper.

Another capability of the Surrogate Reservoir Models that is discussed in this paper is the development of field-wide type curves. Once the Surrogate Reservoir Model is developed it can be used to generate a large number of type curves for the field (reservoir) being studied. Development of such type curves can provide valuable insight into the general behavior of fluid flow in the field (reservoir) and guide future operational development efforts as well as help and direct future analytical and numerical analysis using the full field model.

The type curves are developed by plotting one of the model outputs (in this study 5 year cumulative oil production or water cut) against another parameter while selecting a third parameter for the type curves. By changing the value of the third parameter from minimum to maximum in several steps a set of type curves can be generated. During this operation one can hold the values of all other involved parameters at overall average or select the minimum or the maximum from the entire data set for all the parameters. Some examples of such type curves are presented in the next section.

Results & Discussions

In order to demonstrate that Surrogate Reservoir Models can predict the flow behavior in a reservoir, a set of 19 wells (these wells were not used during the development process) were used as the set of blind wells to validate the performance of a Surrogate Reservoir Models.

The instantaneous water cut generated by the Surrogate Reservoir Model was plotted against the instantaneous water cut generated by the full filed model for comparison. These plots are shown in Figures 6 though 9 for several of these wells. These figures show that results generated by the Surrogate Reservoir Model are quite accurate and acceptable even for wells in the set of blind wells. In these figures when the water cut goes to zero after increasing for several years indicates that the well has been watered out and has been shut down. It is interesting to note that this phenomenon was predicted correctly in every case.

It was shown in Figures 3 to 5 that values of reservoir parameters for the wells belonging to the set of blind wells falls within the distribution of the same reservoir parameters in this field and thus can be counted as a valid realization.

Figures 10-12 show several type curves that were developed for this particular field. Generating such type curves once the Surrogate Reservoir Model has been developed is an easy task and can be accomplished on ly in a matter of seconds.

Furthermore, one can develop such type curves for a particular well as well as the entire reservoir.

These type curves can provide valuable information to the modeling engineers as well as production engineers. They demonstrate the general tendencies and behaviors of the fluid flow in a particular well or in the antire field. As shown in these figures, three parameters are involved in these type curves. Usually the "y" axis is one of the outputs of the SRM and the user can select one parameter for the "x" axis that would change from the minimum to the maximum of its value in the field database. A third parameter is selected to generate the type curves. The value of the third parameter can be any of the numbers between the minimum and the maximum in several steps. While the model is being run hundreds of times to generate the type curves, other involved parameters can assume average, minimum or maximum values. In the case of developing type curves for a particular well, the other parameters are fixed for the values of the well being analyzed

Conclusions

Surrogate Reservoir Models are accurate prototypes of full field models that can run in real-time. They provide instantaneous results and respond to changes in rock, fluid and rock-fluid characteristics that are used in the model. In this article the robustness of Surrogate Reservoir Models was demonstrated by showing their capabilities to predict fluid flow behavior in several different geological realizations. Furthermore, it was demonstrated that Surrogate Reservoir Models can quickly generate a series of type curves for a reservoir that can help engineers in analysis and operational planning of the reservoir.

Acknowledgment

Authors would like to acknowledge ADCO-PDD for its support of the project and ADNOC for permitting the results to be published. Authors would like to acknowledge Abi Modavi for his valuable contributions to this study.

References

1. "Development of Surrogate Reservoir Models (SRM) For Fast Track Analysis of Complex Reservoirs." Mohaghegh, S. D., Modavi, A., Hafez, H., Haajizadeh, M., Kenawy, M., and Guruswamy, S., *SPE 99667*, 2006 SPE Intelligent Energy Conference and Exhibition. 11-13 April 2006, Amsterdam, the Netherlands.
2. "Quantifying Uncertainties Associated with Reservoir Simulation Studies Using Surrogate Reservoir Models." Mohaghegh, S. D., *SPE 102492*, 2006 SPE Annual Technical Conference and Exhibition. 24-27 September 2006, San Antonio, Texas.
3. "Tahiti: Development Strategy Assessment Using Design of Experiments and Response Surface Methods, " P.E. Carreras, SPE, Chevron Energy Technology Co., and S.E. Turner, SPE, and G.T. Wilkinson, SPE, Chevron North America Exploration and Production Co. SPE 100656, SPE Western Regional/AAPG Pacific Section/GSA Cordilleran Section Joint Meeting, 8-10 May, Anchorage, Alaska, USA.
4. "A Novel Response Surface Methodology Based on "Amplitude Factor" Analysis for Modeling Nonlinear Responses Caused by Both Reservoir and Controllable Factors," B. Li and F. Friedmann, SPE, California Inst. of Technology, SPE 95283, SPE Annual Technical Conference and Exhibition, 9-12 October, Dallas, Texas.
5. "Structured Uncertainty Assessment for Fahud Field through the Application of Experimental Design and Response Surface Methods," M.A. Salhi, and M. Van Rijen, SPE, Petroleum Development Oman; L. Wei and H. Dijk, Shell Intl. E&P; Z. Alias, Petroleum Development Oman; and A. Upadhyaya and H. Lee, Shell Intl. E&P. SPE 93529, SPE Middle East Oil and Gas Show and Conference, Mar 12 - 15, 2005, Kingdom of Bahrain.

6. "Comparison of Response Surface and Kriging models for multidisciplinary design optimization," Simpson, T., Korte, J., Mauery, T., and Mistree, F., Americam Institute of Aeronautics and Astronautics, AIAA-98-4755. 1998.

7. Response Surface Methodology: Process and Product Optimization Using Designed Experiments, Myers, R. H. and Montgomery, D.C., John Wiely & Sons, New York, 1995.

8. "Large-Scale Dynamics of the Convection Zone and Tachocline," Mark S. Miesch. http://solarphysics.livingreviews.org/open?pubNo=lrsp-2005-1&page=articlesu19.html

9. What is Systems Theory? http://pespmc1.vub.ac.be/SYSTHEOR.html

10. A User's Guide to LHS: Sandia's Latin Hypercube Sampling Software, http://www.prod.sandia.gov/cgi-bin/techlib/access-control.pl/1998/980210.pdf

11. Design and Analysis of Experiment, by Douglas C. Montgomery, John Wiley & Sons, ISBN: 047148735X.

12. The Voronoi Web Site. http://www.voronoi.com/cgi-bin/display.voronoi_applications.php?cat=Theory

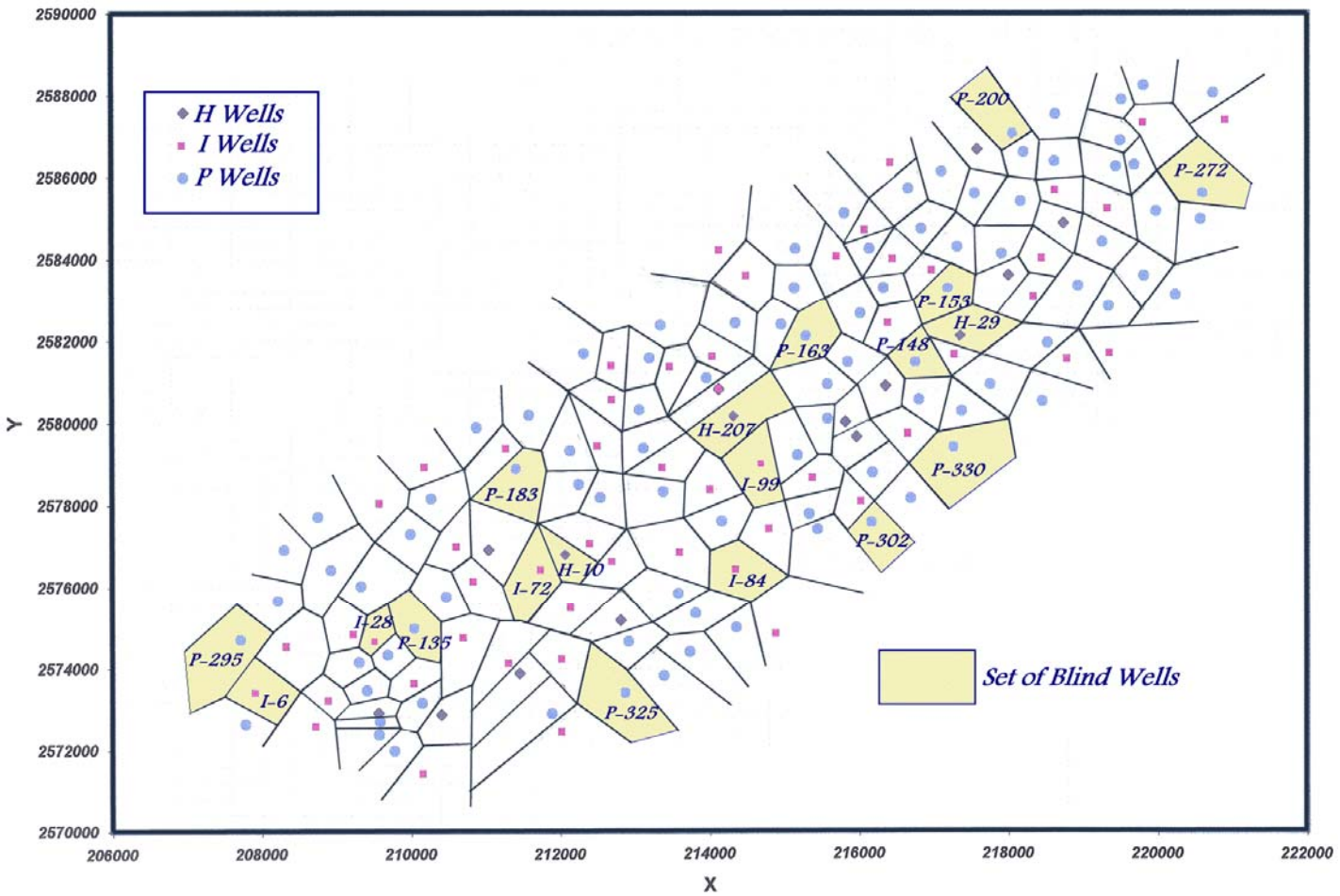

Figure 2. Location of 165 wells in the field. Well identified within colored drainage area are used as blind wells for validation of the analysis.

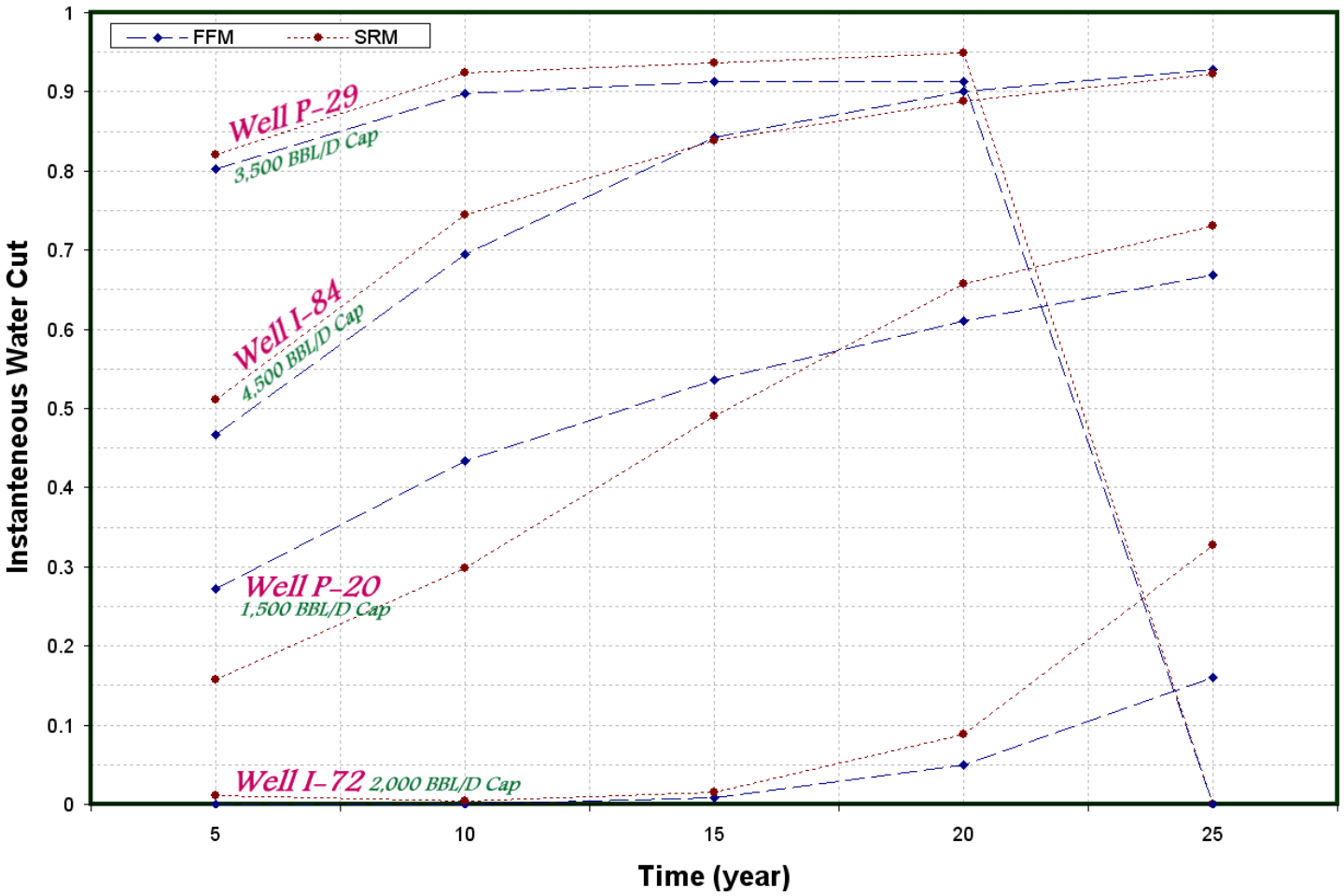

Figure 6. Validation of Surrogate Reservoir Model by comparing the instantaneous water cut as a function of time generated by the full field model (FFM) against those generated by the SRM, for the set of blind wells.

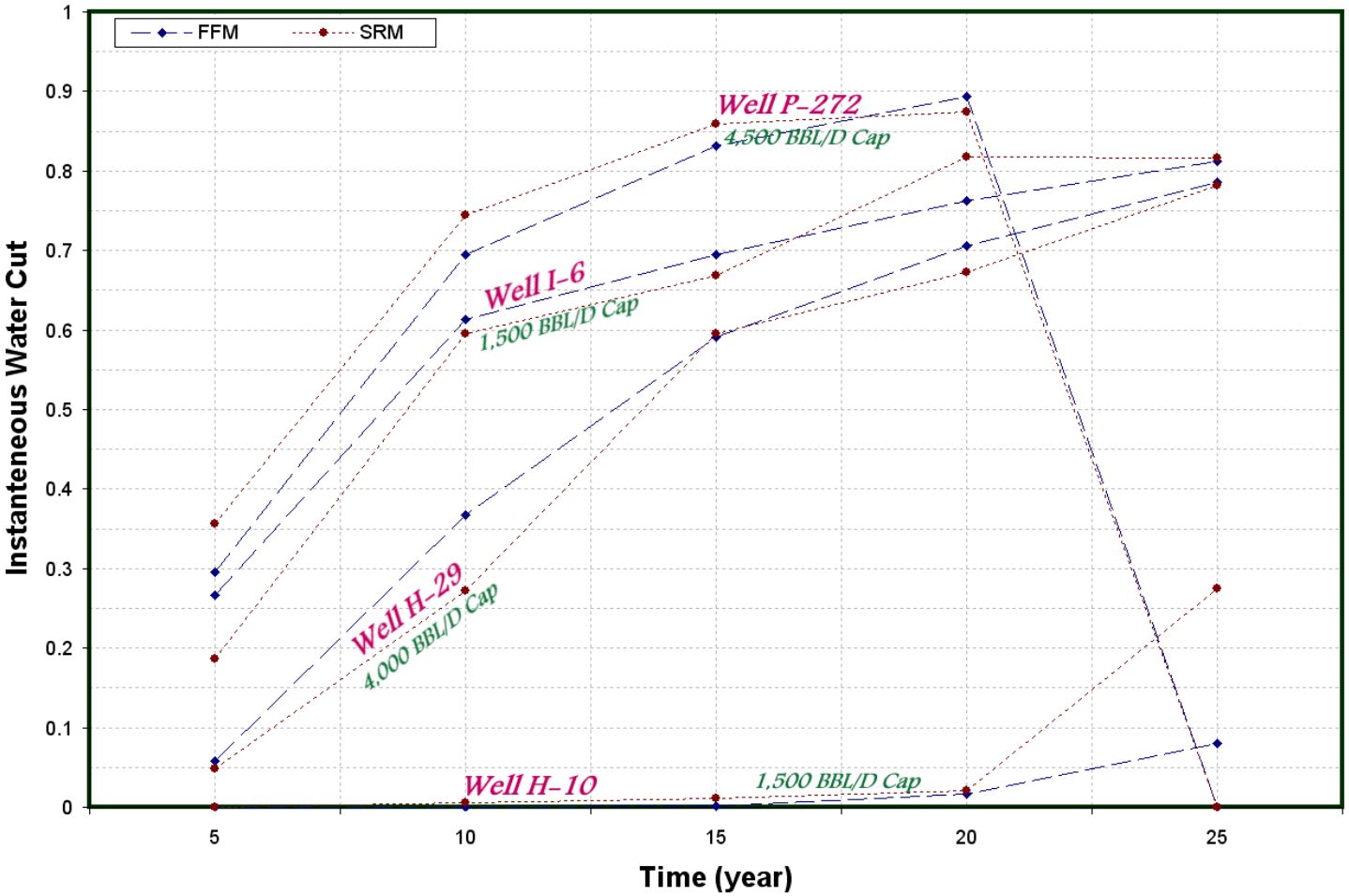

Figure 7. Validation of Surrogate Reservoir Model by comparing the instantaneous water cut as a function of time generated by the full field model (FFM) against those generated by the SRM, for the set of blind wells.

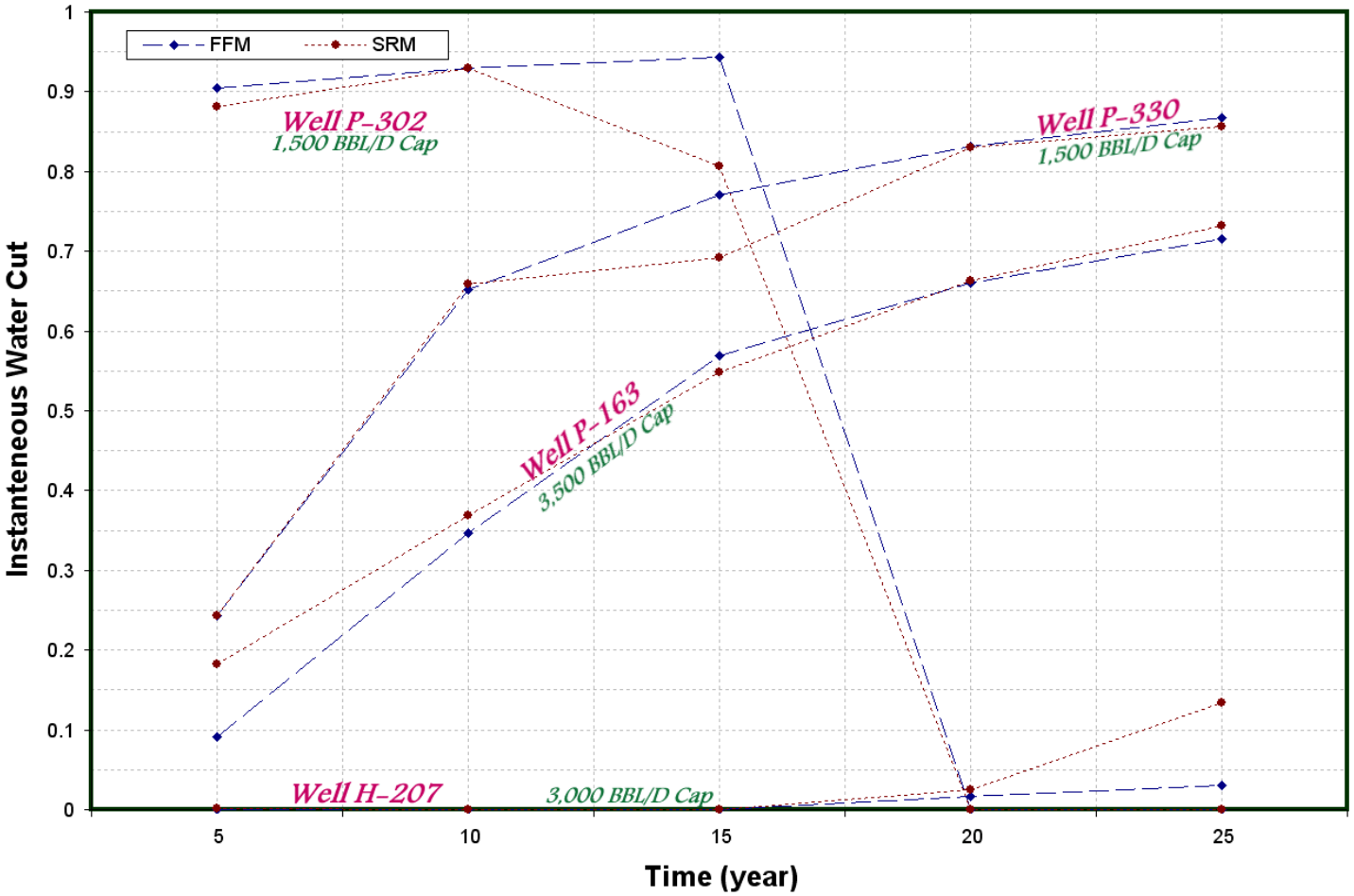

Figure 8. Validation of Surrogate Reservoir Model by comparing the instantaneous water cut as a function of time generated by the full field model (FFM) against those generated by the SRM, for the set of blind wells.

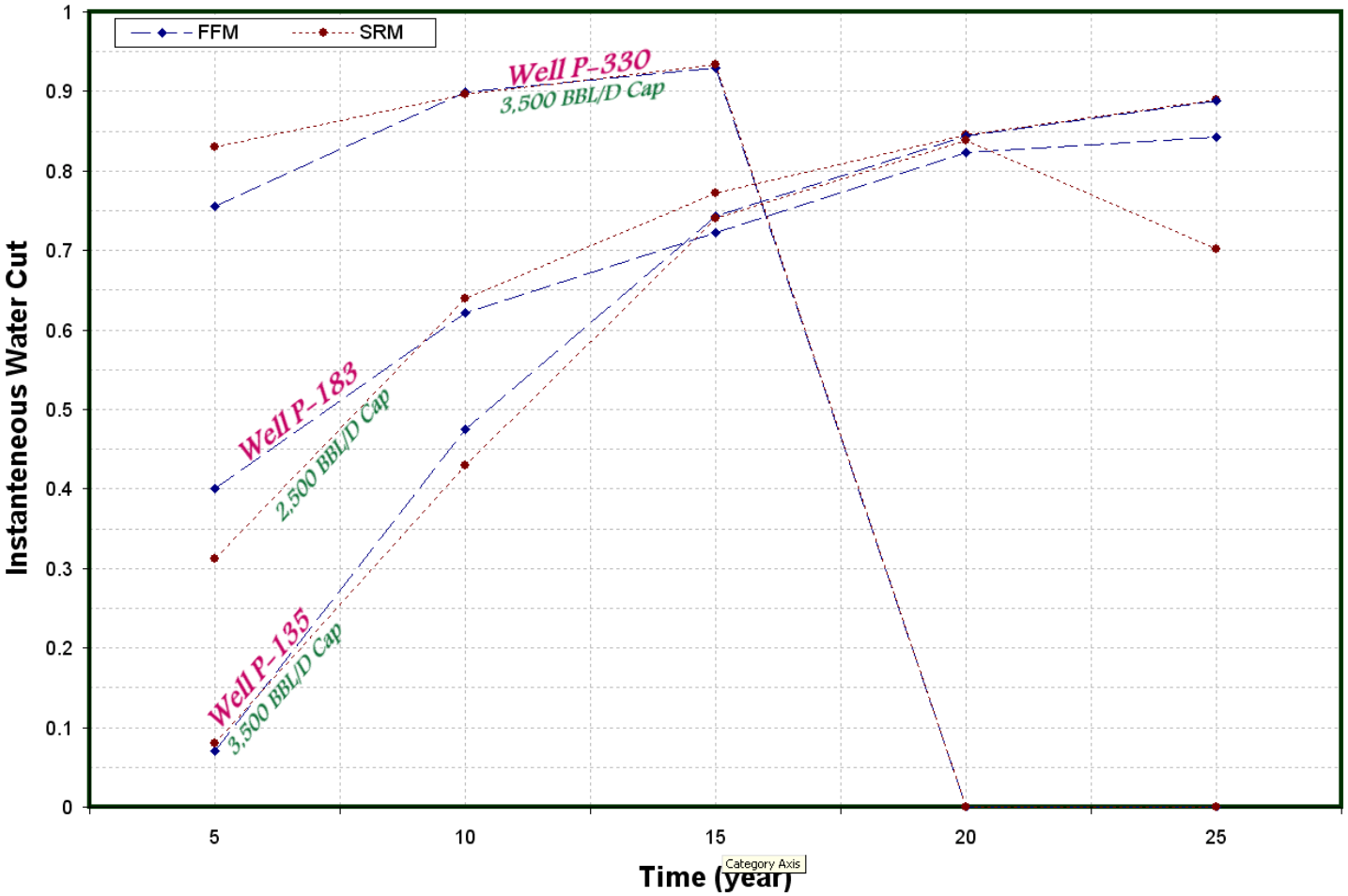

Figure 9. Validation of Surrogate Reservoir Model by comparing the instantaneous water cut as a function of time generated by the full field model (FFM) against those generated by the SRM, for the set of blind wells.

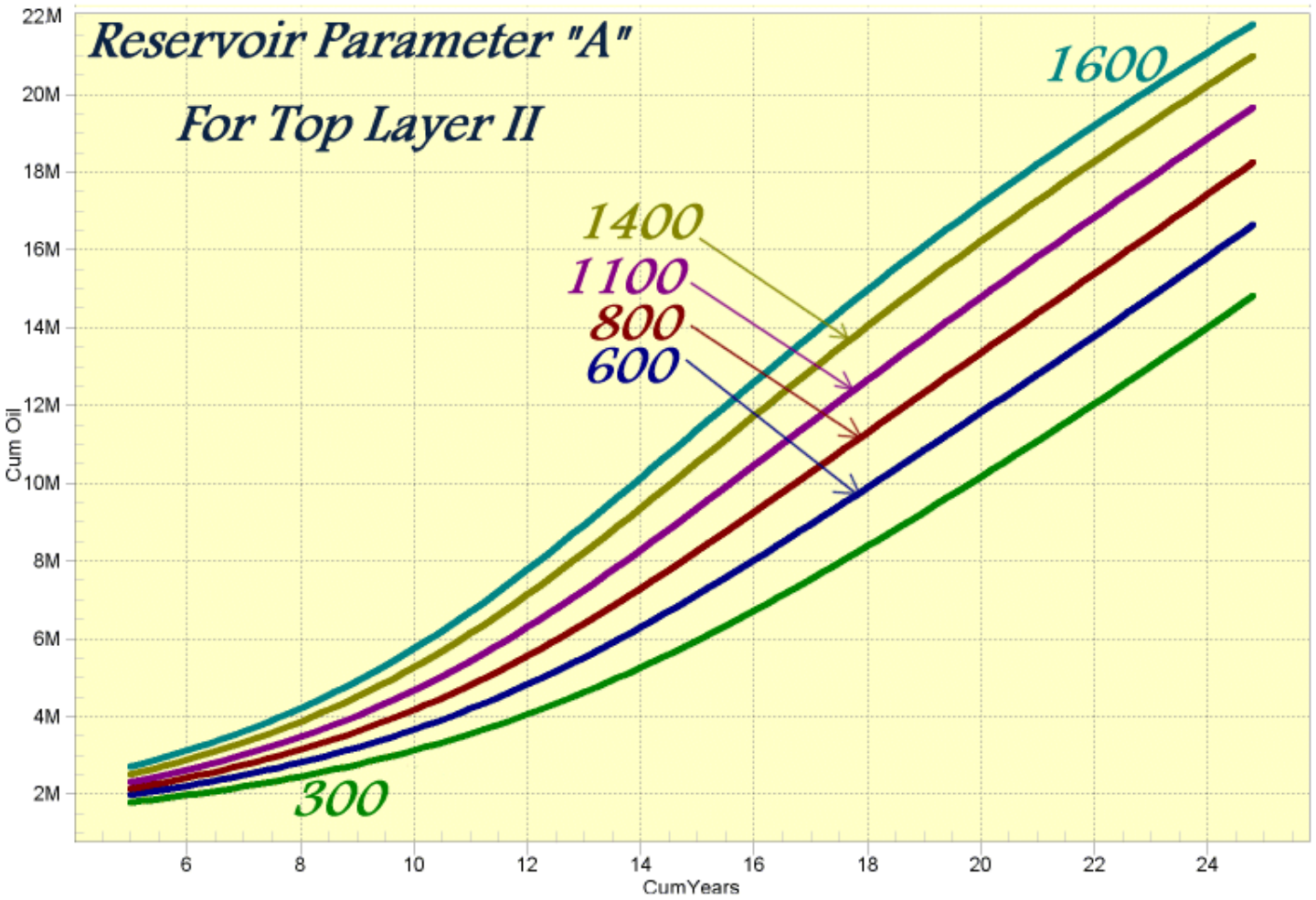

Figure 10. Behavior of 5 year cumulative oil production as a function of time for different values of parameter "A" of Top Layer II. This can be considered as a type curve for this particular reservoir.

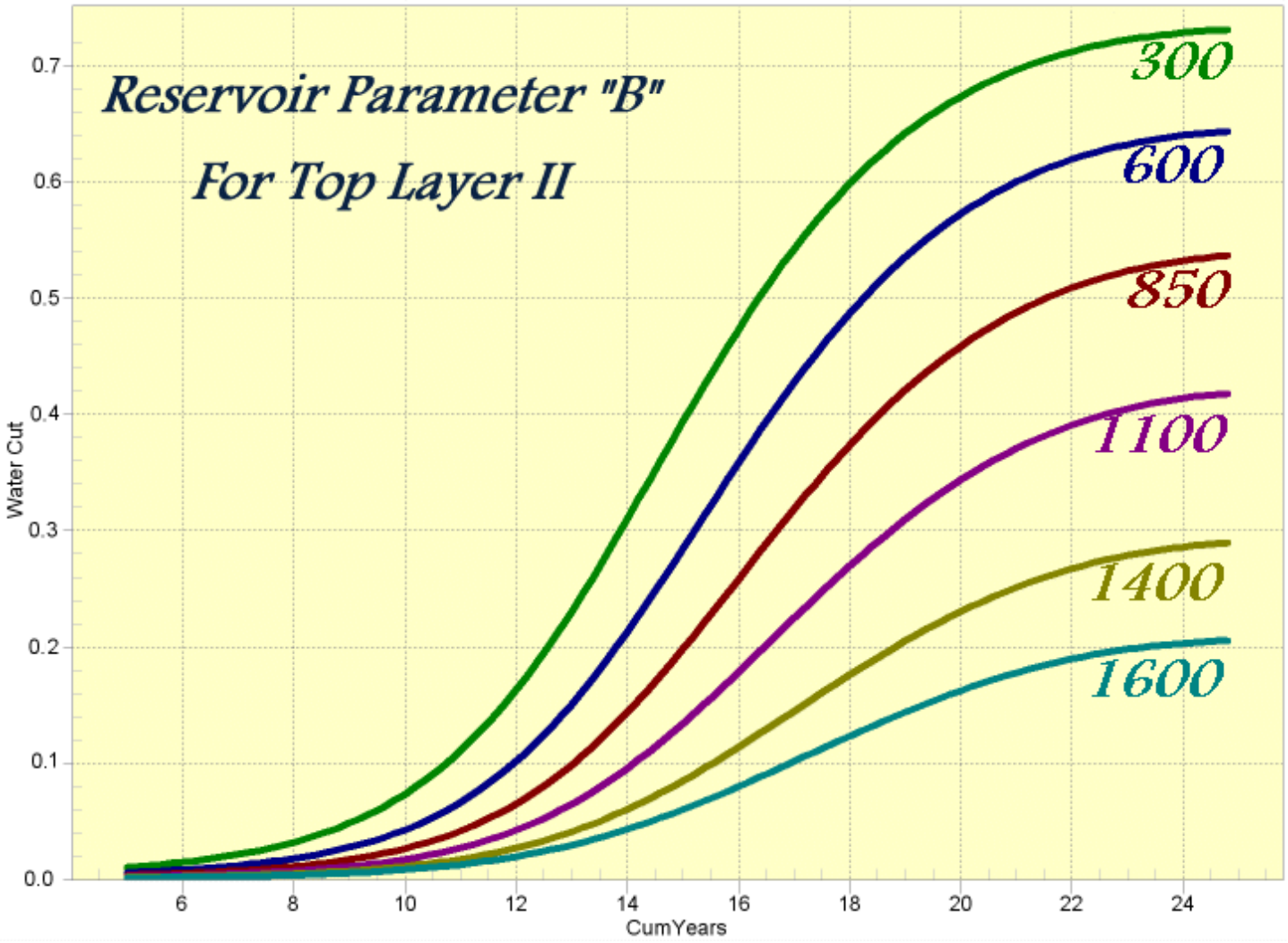

Figure 11. Behavior of instantaneous water cut as a function of time for different values of parameter "B" of Top Layer II. This can be considered as a type curve for this particular reservoir.

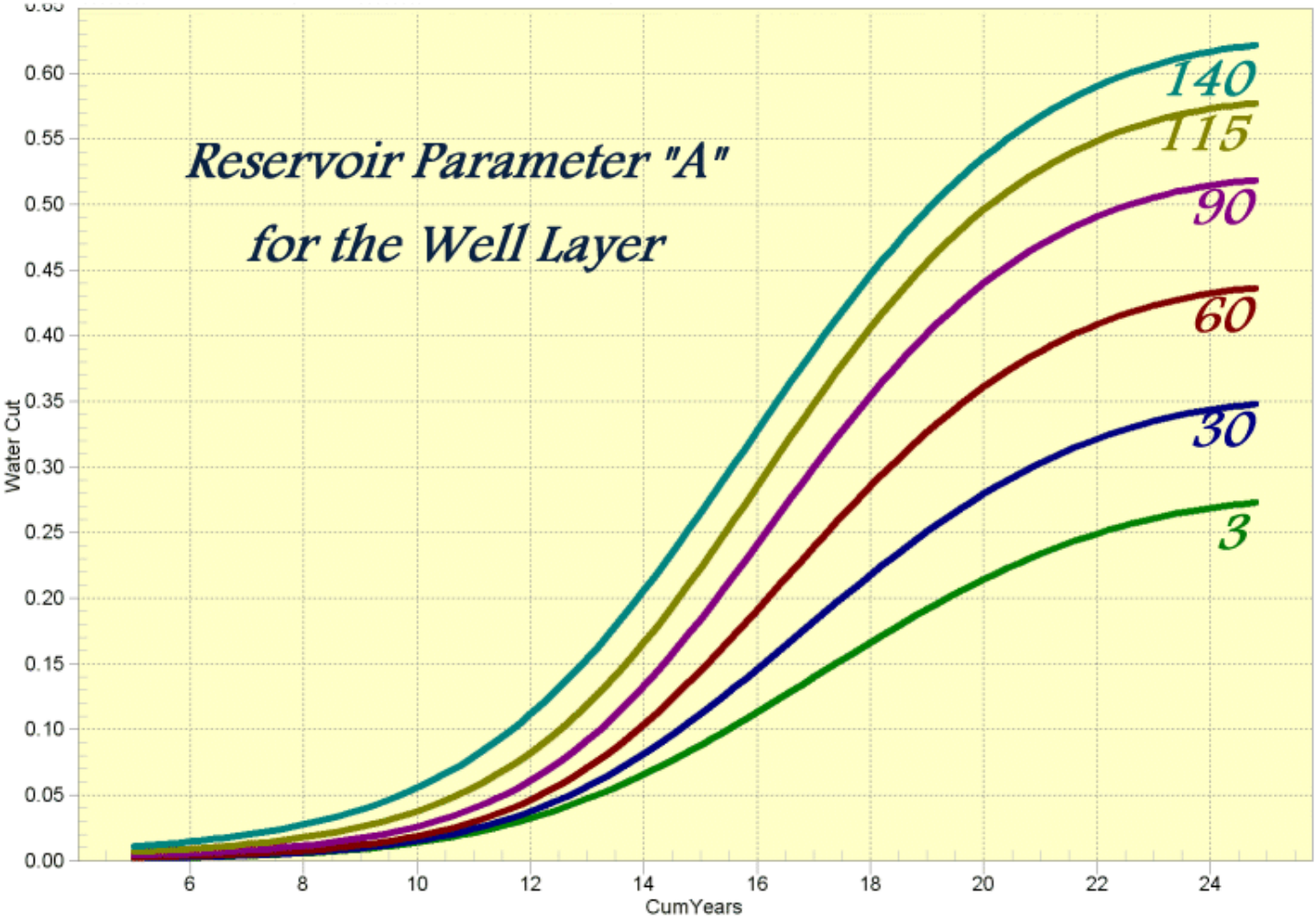

Figure 12. Behavior of instantaneous water cut as a function of time for different values of parameter "A" of Well Layer. This can be considered as a type curve for this particular reservoir.

Artificial-Intelligence Technology Predicts Relative Permeability of Giant Carbonate Reservoirs

Saud M. Al-Fattah, SPE, and **Hamad A. Al-Naim,** SPE, Saudi Aramco

Summary

Determination of relative permeability data is required for almost all calculations of fluid flow in petroleum reservoirs. Water/oil relative permeability data play important roles in characterizing the simultaneous two-phase flow in porous rocks and in predicting the performance of immiscible displacement processes in oil reservoirs. They are used, among other applications, for determining fluid distributions and residual saturations, predicting future reservoir performance, and estimating ultimate recovery. Undoubtedly, these data are considered probably the most valuable information required in reservoir-simulation studies. Estimates of relative permeability are generally obtained from laboratory experiments with reservoir-core samples. In the absence of the laboratory measurement of relative permeability data, developing empirical correlations for obtaining accurate estimates of relative permeability data showed limited success, and it proved difficult, especially for carbonate reservoir rocks.

Artificial-neural-network (ANN) technology has proved successful and useful in solving complex structured and nonlinear problems. This paper presents a new modeling technology to predict accurately water/oil relative permeability using ANNs. The ANN models of relative permeability were developed using experimental data from waterflood-core-tests samples collected from carbonate reservoirs of giant Saudi Arabian oil fields. Three groups of data sets were used for training, verification, and testing the ANN models. Analysis of results of the testing data set shows excellent agreement with the experimental relative permeability data. In addition, error analyses show that the ANN models developed in this study outperform all published correlations.

The benefits of this work include meeting the increased demand for conducting special core analysis (SCA), optimizing the number of laboratory measurements, integrating into reservoir-simulation and reservoir-management studies, and providing significant cost savings on extensive laboratory work and substantial required time.

Introduction

ANNs have seen a great increase of interest during the past few years. They are powerful and useful tools for solving practical problems in the petroleum industry (Mohaghegh 2005; Al-Fattah and Startzman 2003). Advantages of neural network techniques (Bishop 1995; Fausett 1994; Haykin 1994; Patterson 1996) over conventional techniques include the ability to address highly nonlinear relationships, independence from assumptions about the distribution of input or output variables, and the ability to address either continuous or categorical data as either inputs or outputs. In addition, neural networks are intuitively appealing because they are based on crude low-level models of biological systems. Neural networks, as in biological systems, simply learn by examples. The neural-network user provides representative data and trains the neural networks to learn the behavior of the data.

Copyright © 2009 Society of Petroleum Engineers

This paper (SPE 109018) was accepted for presentation at Offshore Europe, Aberdeen, 4–7 September 2007, and revised for publication. Original manuscript received for review 16 September 2007. Revised manuscript received for review 14 April 2008. Paper peer approved 10 June 2008.

Design and Development of ANN Models

In regression problems, the objective is to estimate the value of a continuous variable given the known input variables. Regression problems can be solved using the following network types: multilayer perceptrons (MLPs), radial basis function (RBF), generalized-regression neural network (GRNN), and linear. In this study, we experimented with the first three types: MLP, RBF, and GRNN. The linear model is basically the conventional linear-regression analysis. Since the problem at hand is a regression type and because of its power and advantages, we found that GRNN performs the best for this particular study. This is because GRNN has several advantages.

- It usually trains extremely quickly, making the large number of evaluations required by the input-selection algorithm feasible.
- It is capable of modeling nonlinear functions quite accurately.
- It is relatively sensitive to the inclusion of irrelevant input variables. This is actually an advantage when trying to decide whether input variables are required.

Hence, it is worth giving a brief description of this neural-network type. GRNN uses kernel-based approximation to perform regression (Patterson 1996; Bishop 1995). It is one of the so-called Bayesian networks. GRNN has exactly four layers: the input layer, radial centers' layer, regression nodes' layer, and an output layer, as shown by **Fig. 1.** The input layer has the same number of nodes as there are input variables. The radial-layer nodes represent the centers of clusters of known training data. This layer must be trained by a clustering algorithm such as subsampling, *K*-means, or Kohonen training. The regression layer, which contains linear nodes, must have exactly one node more than the output layer. There are two types of nodes: The first type of node calculates the conditional regression for each output variable, whereas the second type of node calculates the probability density. The output layer performs a specialized function such that each node simply divides the output of the associated first-type node by that of the second-type node in the previous layer.

GRNNs can be used only for regression problems. A GRNN trains almost instantly, but tends to be large and slow. Although it is not necessary to have one radial neuron for each training data point, the number still needs to be large. Like the RBF network, the GRNN does not extrapolate.

There are several important procedures that must be taken into consideration during the design and development of an ANN model. **Fig. 2** is a flowchart illustrating the ANN-development strategies proposed and implemented in this study.

Data Preparation

Data acquisition, preparation, and quality control are considered the most important and most time-consuming task (Fig. 2). The quantity of data required for training a neural network frequently presents difficulties. There are some heuristic rules, which relate the number of data points needed to the size of the network. The simplest of these indicates that there should be 10 times as many data points as connections in the network. In fact, the number needed is also related to the complexity of the underlying function that the network is trying to model, and to the variance of the additive noise. As the number of input variables increases, the number of input data points required increases nonlinearly. Even a fairly small number of input variables (perhaps 50 or less) requires a huge number of input data points. This problem is known as "the curse of dimensionality." If there is a larger, but

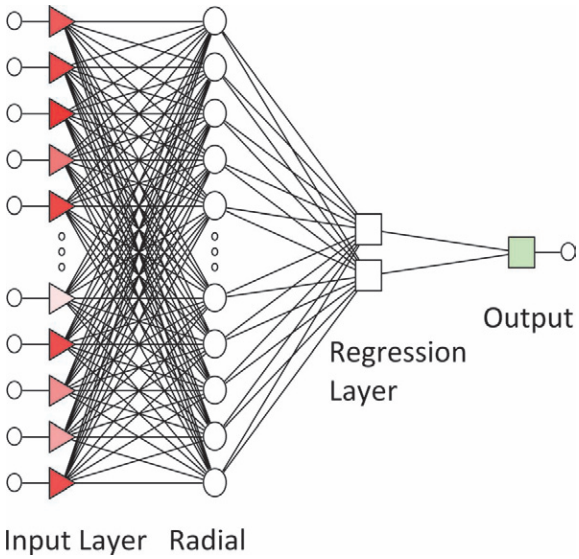

Fig. 1—Design of a GRNN used in this study.

still restricted, data set, then it can be compensated to some extent by forming an ensemble of networks, with each network being trained using a different resampling of the available data and then averaging across the predictions of the networks in the ensemble.

Water/oil relative permeability measurements were collected for all wells having SCAL of carbonate reservoirs in Saudi Arabian oil fields. These reservoirs include Arab-D, Shuaibah, Arab-C, Arab-AB, Fadhili, Upper Fadhili, Hanifa, and Hadriyah. The major fields included in this study are the Ghawar field, which is the largest oil field in the world; and Abqaiq; Shaybah; Qatif; Khurais; and Berri. SCAL reports were studied thoroughly, and each relative permeability curve was carefully screened, examined, and checked for consistency and reliability. Hence, a large database of water/oil relative permeability data for carbonate reservoirs was created. All relative permeability experimental data measurements were conducted using the unsteady-state method.

Developing ANN models for water/oil relative permeability with easily obtainable input variables was one of the objectives of this study. Initial water saturation, residual-oil saturation, porosity, well location, and wettability are considered the main input variables that contribute significantly to the prediction of relative permeability data. We made from these input variables several transformational forms or functional links that are thought to play a role in predicting the relative permeability. **Table 1** presents a list of all input variables and functional links used in this study. The initial water saturation, residual-oil saturation, and porosity of each well can be obtained easily from either well logs or routine core analysis. Wettability is an important input variable for predicting the relative permeability data and is, thus, included in the pool of input variables. We found that not all wells with relative permeability measurements have wettability data. For those wells missing wettability data, we used Craig's rule (Craig 1971) to determine the wettability of each relative permeability curve, which is classified as oil-wet, water-wet, or mixed-wet. It should be noted that Craig's rule helps to distinguish between strongly-water-wet and -oil-wet systems on the basis of relative permeability curves. If no information is available on the wettability of a well, it then can be estimated by use of offset-well data, or sensitivity analysis can be performed. The output of each network in this study is a single variable, either water or oil relative permeability.

Because of the variety of reservoir characteristics, and using data statistics, the database was divided into three categories of reservoirs: the Arab-D reservoir, the Shuaibah reservoir, and all other reservoirs having limited data. This necessitates the development of six ANN models for predicting water and oil relative permeability, resulting in two ANN models for each reservoir category. The database of relative permeability that is used in this

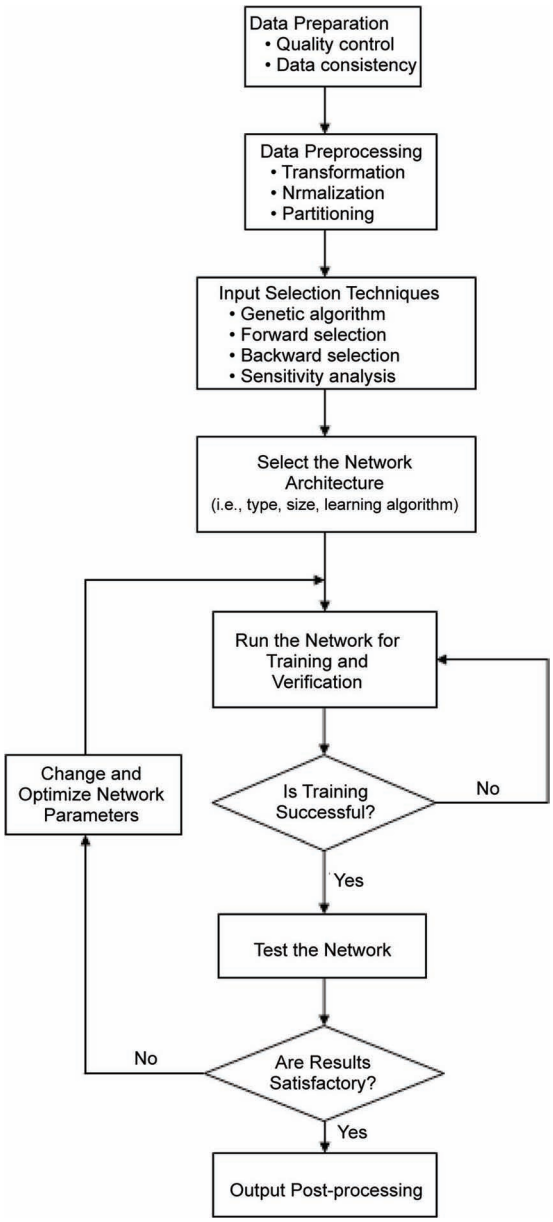

Fig. 2—Flowchart of procedure of ANN design and development proposed in this study.

study comprises of a total of 3,711 records or cases. **Table 2** presents the distribution of these data cases in the three categories of reservoirs (Arab-D, Shuaibah, and the others).

Data Preprocessing

Data preprocessing is an important procedure in the development of ANN models. All input and output variables must be converted into numerical values to be introduced to the network. Nominal values require special handling. Since the wettability is a nominal input variable, it is converted into a set of numerical values. Oil-wet was represented as {1, 0, 0}, mixed-wet as {0, 1, 0}, and water-wet as {0, 0, 1}. In this study, we applied two normalization algorithms—mean/standard deviation, and minimax—to ensure that the network's input and output will be in a sensible range (Al-Fattah and Startzman 2003). The simplest normalization function is the minimax, which finds the minimum and maximum values of a variable in the data and performs a linear transformation using a shift and a scale factor to convert the values into the target range, which is typically [0.0, 1.0]. After network execution, denormalizing of the output follows the reverse procedure: subtraction of the shift factor, followed by

TABLE 1—LIST OF ALL INPUT VARIABLES THAT HAVE BEEN TRIED IN THIS STUDY

Variable	Definition
S_w	Water saturation
S_{wi}	Irreducible water saturation
S_{or}	Residual oil saturation
Por	Porosity
Wet	Wettability (oil-wet, water-wet, mix-wet)
X_{utm}	X-coordinate of the well location
Y_{utm}	Y-coordinate of the well location
S_{on}	$\left(\frac{1-S_w-S_{or}}{1-S_{or}}\right)$
S_{wn}	$\left(\frac{S_w-S_{wi}}{1-S_{wi}}\right)$
S_{o1}	$\left(\frac{1-S_w-S_{or}}{1-S_{wi}-S_{or}}\right)$
S_{w1}	$\left(\frac{S_w-S_{wi}}{1-S_{wi}-S_{or}}\right)$
S_{w2}	$\left(\frac{S_w}{1-S_{or}}\right)$
S_{w3}	$\left(\frac{S_w}{1-S_{wi}}\right)$
S_{w4}	$\left(\frac{1-S_w}{1-S_{wi}}\right)$
S_5	$\left(\frac{S_w-S_{or}}{1-S_{wi}-S_{or}}\right)^2$
S_6	$\phi(1-S_{or})$
S_7	$e^{\phi(1-S_{or})}$
S_8	$e^{S_{w1}}$
S_9	(S_w-S_{wi})
S_{10}	$\left(\frac{S_w-S_{wi}}{\phi}\right)$
S_{11}	$\phi(1-S_{wi})(S_w-S_{wi})$
S_{12}	$\phi(1-S_{or})(1-S_w-S_{or})$
S_{13}	$\left(\frac{S_w-S_{or}}{1-S_{wi}-S_{or}}\right)$
Por1	$\phi(1-S_{or}-S_{wi})$
Por2	$\left(\frac{\phi}{1-\phi}\right)$

division by the scale factor. The mean/SD technique is defined as the data mean subtracted from the input variable value divided by the SD. Both methods have advantages in that they process the input and output variables without any loss of information, and their transform is mathematically reversible.

Input Selection and Dimensionality Reduction

One of the most difficult tasks in the design of the neural network is the decision on which of the available variables to use as inputs to the neural network. The only guaranteed method to select the best input set is to train networks with all possible input sets and all possible architectures, and to select the best. Practically, this is impossible for any significant number of candidate input variables. The problem is complicated further when there are interdependencies or correlations between some of the input variables, which means that any of a number of subsets might be adequate.

To some extent, some neural-network architectures can actually learn to ignore useless variables. Other architectures are affected adversely; and in all cases, a larger number of inputs implies that a larger number of training cases is required to prevent overlearning. As a consequence, the performance of a network can be improved by reducing the number of input variables, even sometimes at the cost of losing some input information. There are sophisticated algorithms that determine the selection of input variables. The following describes the input-selection and dimensionality-reduction techniques that are used in this study.

Genetic Algorithm. A genetic algorithm is an optimization algorithm that can search efficiently for binary strings by processing an initially random population of strings using artificial mutation, crossover, and selection operators, in an analogy with the process of natural selection (Goldberg 1989). It is applied in this study to determine an optimal set of input variables that contribute significantly to the performance of the neural network. The method is used as part of the model-building process, in which variables identified as the most relevant are then used in a traditional model-building stage of the analysis. Genetic algorithm is a particularly effective technique for combinatorial problems of this type, in which a set of interrelated yes/no decisions needs to be made. For this study, it is used to determine whether the input variable under evaluation is significantly important or not. The genetic algorithm is therefore a good alternative where there are large numbers of variables (e.g., more than 50), and it also provides a valuable second opinion for smaller numbers of variables. It is particularly good at spotting interdependencies between variables located close together on the masking strings. The genetic algorithm can sometimes identify subsets of inputs that are not discovered by other techniques. However, the method is time consuming; it typically requires building and testing many thousands of networks, resulting in running the program for a couple of days.

Forward and Backward Stepwise Algorithms. These algorithms (Hill and Lewicki 2006) are usually quicker than the genetic algorithm if there is a reasonably small number of variables. They are also equally effective if there are not too many complex interdependencies between variables. Forward and backward stepwise-input-selection algorithms work by adding or removing variables one at a time. Forward selection begins by locating the single input variable that, on its own, best predicts the output

TABLE 2—DISTRIBUTION OF DATA RECORDS/CASES FOR RELATIVE PERMEABILITY DATA SETS

Reservoir/Data Set	Training	Verification	Testing	Total
Arab-D	1591	457	401	2449
Shuaibah	485	107	84	676
Others	390	93	103	586

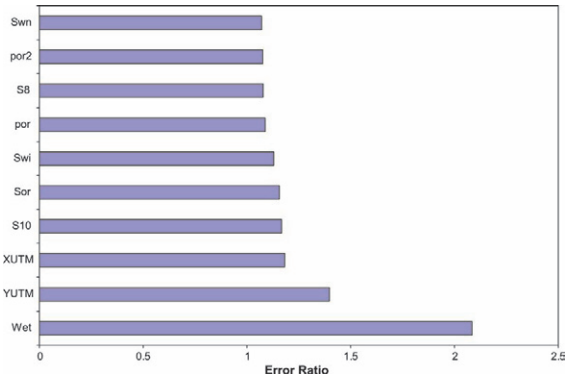

Fig. 3—Error ratio and ranking of the influence of input variables on ANN model for Arab-D-reservoir water relative permeability.

variable. It then checks for a second variable that, when added to the first, improves the model most, repeating this process until either all variables have been selected or no further improvement is made. Backward stepwise feature selection is the reverse process; it starts with a model including all variables, and then removes them one at a time, at each stage finding the variable that, when it is removed, degrades the model least.

Forward- and backward-selection methods each have their advantages and disadvantages. The forward-selection method is generally faster. It may miss key variables if they are interdependent or correlated. The backward-selection method does not suffer from this problem, but because it starts with the whole set of variables, the initial evaluations are most time consuming. Furthermore, the model can actually suffer strictly from the number of variables, making it difficult for the algorithm to behave sensibly if there are a large number of variables, especially if there is only a few weakly predictive ones in the set. In contrast, because it selects only a few variables initially, forward selection can succeed in this situation. Forward selection is also much faster if there are few relevant variables because it will locate them at the beginning of its search, whereas backward selection will not whittle away the irrelevant ones until the very end of its search.

In general, backward selection is to be preferred if there is a small number of variables (e.g., 20 variables or less), and forward selection may be better for larger numbers. All of the above-mentioned input-selection algorithms, including the genetic algorithm and forward and backward selection, evaluate feature-selection masks. These are used to select the input variables for a new training set, and a GRNN is tested on this training set.

Sensitivity Analysis. This is performed on the inputs to a neural network to indicate those input variables that are considered most

TABLE 3—STATISTICAL ANALYSIS OF ANN MODEL FOR K_{ro} ARAB-D RESERVOIR

	Training	Verification	Testing
Data standard deviation	0.198159	0.133331	0.214694
Error mean	–4.47 E-05	0.002488	–0.000804
Error standard deviation	0.019920	0.014860	0.032760
Absolute Error mean	0.004571	0.005582	0.009307
Standard deviation ratio	0.100502	0.111487	0.152606
Correlation Coefficient	0.994949	0.993845	0.988549

TABLE 4—STATISTICAL ANALYSIS OF ANN MODEL FOR K_{rw} ARAB-D RESERVOIR

	Training	Verification	Testing
Data standard deviation	0.236330	0.225397	0.230525
Error mean	–0.001382	–0.000521	–0.003320
Error standard deviation	0.065039	0.065243	0.070861
Absolute Error mean	0.041148	0.042435	0.044872
Standard deviation ratio	0.275205	0.289457	0.307389
Correlation Coefficient	0.965349	0.960761	0.956011

important by that particular neural network. Sensitivity analysis can be used purely for informative purposes or to perform input pruning, which is removing excess neurons from input or hidden layers. In general, input variables are not independent. Sensitivity analysis gauges variables according to the deterioration on modeling performance that occurs if that variable is not available to the model. However, the interdependence between variables means that no scheme of single ratings per variable can ever reflect the subtlety of the true situation. In addition, there may be interdependent variables that are useful only if included as a set. If the entire set is included in a model, they can be accorded significant sensitivity, but this does not reveal the interdependency. Worse, if only part of the interdependent set is included, their sensitivity will be zero because they carry no discernable information. In summary, precautions should be exercised when drawing conclusions about the importance of variables because sensitivity analysis does not rate the usefulness of variables in modeling in a reliable or absolute manner. Nonetheless, in practice, sensitivity analysis is quite useful. If a number of models are studied, it is often possible to identify variables that are always of high sensitivity, variables that are always of low sensitivity, and ambiguous variables that change ratings and probably carry mutually redundant information.

Another common approach to dimensionality reduction is the principle-component analysis (Bishop 1995), which can be represented in a linear network. It can often extract a very small number of components from quite high-dimensional original data and still retain the important structure.

Applying the above-mentioned input-selection methods in this study, we first used the genetic algorithm to identify redundant input variables from the 25 variables given in Table 1. For the Arab-D-reservoir ANN model, this step identified four redundant input variables that can be removed from the input pool. In the second step, we applied forward and backward stepwise selection on the remaining input variables. Both the forward and the backward algorithms yielded the same results by identifying six additional redundant input variables. We then ran the network with the remaining 15 input

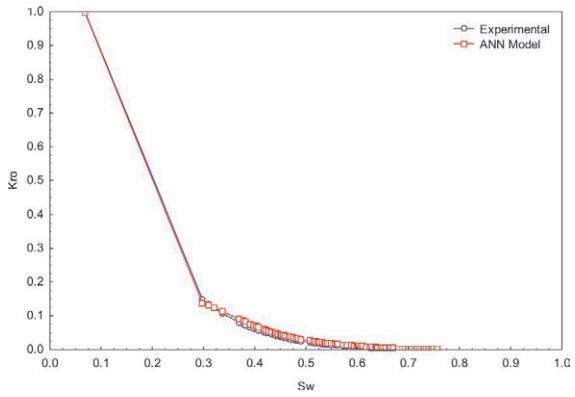

Fig. 4—Results of ANN model compared to experimental data for oil relative permeability.

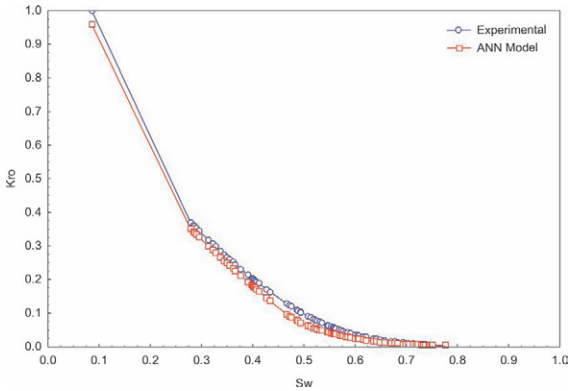

Fig. 5—Results of ANN model compared to experimental data for oil relative permeability.

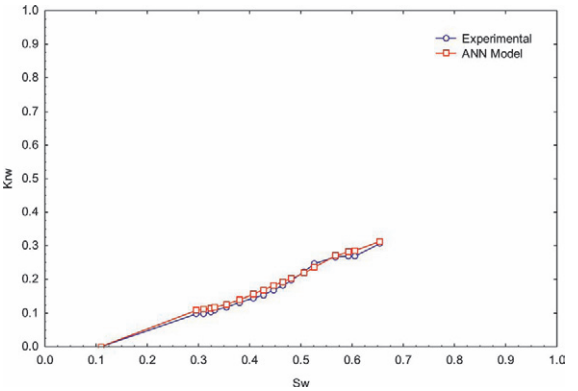

Fig. 6—Results of ANN model compared to experimental data for water relative permeability.

variables while running the sensitivity analysis simultaneously. The network gave a very good performance; however, sensitivity analysis indicated that two input variables can be removed from the network without affecting the performance of the ANN model. **Fig. 3** presents the results of sensitivity analysis for the top 10 most influential input variables for the Arab-D-reservoir ANN model. Fig. 3 shows the error that will be given by the model if that particular input variable is excluded from the network. Fig. 3 shows that the wettability gives the highest error if it is removed from the network, indicating its significance to the performance of the ANN model; thus, it was ranked the first among other variables. In this study, we determined that input variables that have error ratios greater than one are significant and influential to the network performance. Input variables having error ratios less than one are removed from the network. The final ANN model consisted of 13 input variables as an optimum input set.

Training, Verifying, and Testing

By exposing the network repeatedly to input data, the weights and thresholds of the post-synaptic potential function are adjusted using special training algorithms until the network performs very well in predicting the output correctly. In this study, the data are divided into three subsets: training set (50–60% of data), verification or validation set (20–25% of data), and testing set (20–25% of data), as presented in Table 2. Typically, the training-data subset is presented to the network in several or even hundreds of iterations. Each presentation of the training data to the network for adjustment of weights and thresholds is referred to as an epoch. The procedure continues until the overall error function has been minimized sufficiently. The overall error is also computed for the second subset of the data, which is sometimes referred to as the verification or validation data. The verification data act as a watchdog and take no part in the adjustment of weights and thresholds during training, but the networks' performance is checked against this subset as training continually. The training is stopped when the error for the verification data stops decreasing or starts to increase. Use of the verification subset of data is important because with unlimited training, the neural network usually starts "overlearning" the training data. Given no restrictions on training, a neural network may describe the training data almost the perfectly but may generalize very poorly to new data. The use of the verification subset to stop training at a point when generalization potential is best is a critical consideration in training neural networks. A third subset of testing data is used to serve as an additional independent check on the generalization capabilities of the neural network, and as a blind test of the performance and accuracy of the network. Several neural-network architectures and training algorithms have been attempted to achieve the best results. The results were obtained using a hybrid approach of genetic algorithm and neural network.

Results

All the six networks developed in this study were successfully well trained, verified, and checked for generalization. An important measure of the network performance is the plot of the root-mean-square error vs. the number of iterations or epochs. A well-trained network is characterized by decreasing errors for both the training and verification data sets as the number of iterations increases (Al-Fattah and Startzman 2003). Statistical analysis used in this study to examine the performance of a network are the output-data SD, output error mean, output error SD, output absolute error mean, SD ratio, and Pearson-R correlation coefficient (Hill and Lewicki 2006). The most significant parameter is the SD ratio, which measures the performance of the neural network. It is the best indicator of the goodness of a regression model, and it is defined as the ratio of the prediction-error SD to the data SD. One minus this regression ratio is sometimes referred to as the explained variance of the model. The degree of predictive accuracy needed

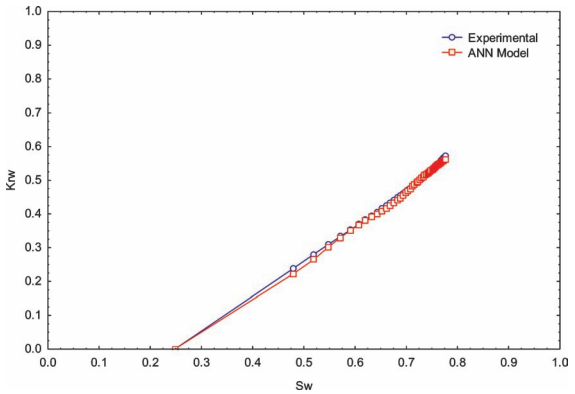

Fig. 7—Results of ANN model compared to experimental data for water relative permeability of Well U-628.

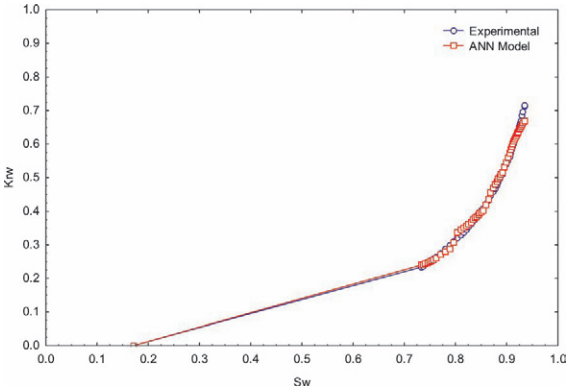

Fig. 8—Results of ANN model compared to experimental data for water relative permeability of Well SB-50.

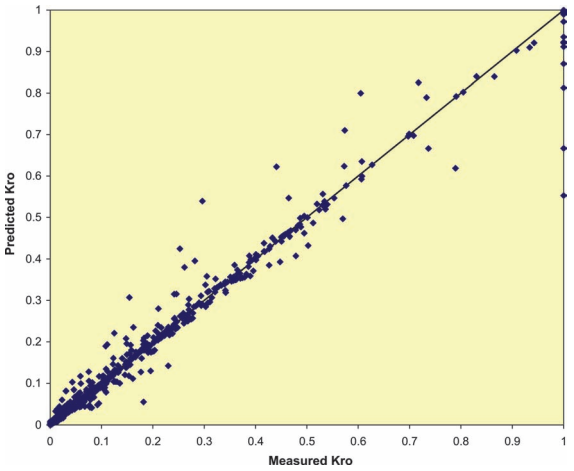

Fig. 9—Crossplot of ANN predicted vs. measured k_{ro} for Arab-D reservoir.

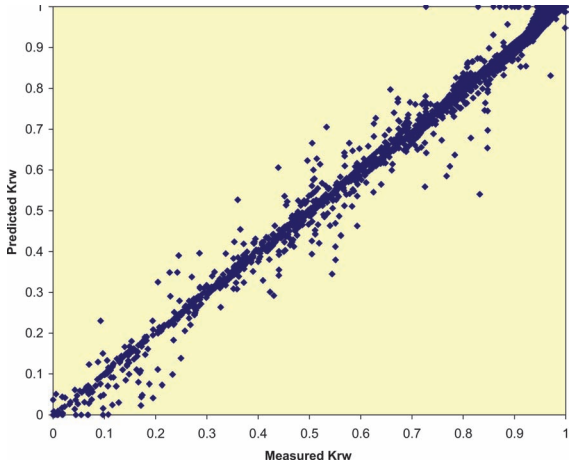

Fig. 10—Crossplot of ANN predicted vs. measured k_{rw} for Arab-D reservoir.

varies from application to application. Generally, an SD ratio of 0.3 or lower indicates a very good regression-performance network. Another important parameter is the standard Pearson-R correlation coefficient between the network's prediction and the observed values. A perfect prediction will have a correlation coefficient of 1.0. In this study, we used the network verification-data subset to judge and compare it with the performance of a network among other competing networks.

Because of its large quantity of data (70% of the database), most of the results presented in this paper belong to the ANN models developed for the Arab-D reservoir. **Tables 3 and 4** present statistical analysis of the ANN models for determining oil and water relative permeability, respectively, for Arab-D reservoir. Table 3 shows that Arab-D-reservoir ANN models for predicting oil relative permeability achieved excellent accuracy by having low values of SD ratios, which are lower than 0.2 for all data subsets including training-, verification-, and testing-data set. Table 3 also shows that a correlation coefficient of 99% was achieved for all data subsets of the Arab-D-reservoir model, indicating the high accuracy of the ANN models for predicting the oil relative permeability data. Table 4 shows that the water relative permeability ANN model yielded a correlation coefficient of 96% for all all three data subsets of the Arab-D-reservoir model, with SD ratios less than 0.3 indicating a high degree of accuracy and excellent performance.

Figs. 4 through 8 show that the results of ANN models are in excellent agreement with the experimental data of oil and water relative permeability. Crossplots of measured vs. predicted data of oil and water relative permeability are presented in **Figs. 9 and 10,** respectively. The majority of the data fall close to the perfect 45° straight line, indicating the high degree of accuracy of the ANN models. **Figs. 11 and 12** are histograms, respectively, of residual errors of oil and water relative permeability ANN models for Arab-D reservoir.

Sensitivity analysis was performed on all input variables to identify significant variables that are influential on the network's performance. Wettability was not found to be an important input parameter for determining oil relative permeability for all ANN models. On the other hand, wettability was found to be the most influential input parameter for determining water relative permeability. Fig. 3 presents the most influential input variables that play an important role on the network's outcome for determining water relative permeability. As can be seen from this figure, wettability is placed first as the most significant input parameter for predicting water relative permeability. To study the effect of wettability on the network predictions, we removed the wettability from the input variables and ran the network. Statistical analysis of the network performance is presented in **Table 5.** The results of accuracy are badly deteriorated after removing the wettability, indicating the significance of the wettability on determining water relative permeability. Without using the wettability as input, the ANN model has a correlation coefficient of 79% for the verification subset and 51% for the testing subset. In addition, SD ratios of more than 0.6 were given by this model, indicating the poor performance of the ANN model for water relative permeability after removing the wettability as input.

Comparison of ANN against Correlations

The newly developed ANN models for predicting water/oil relative permeability of carbonate reservoirs were validated using data that were not used in the training of the ANN models.

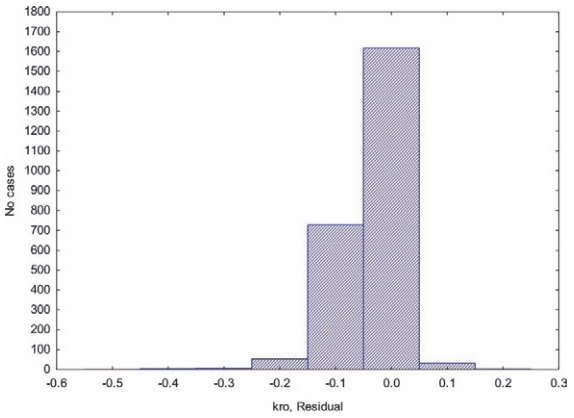

Fig. 11—Histogram of k_{ro} residual error for the Arab-D-reservoir model.

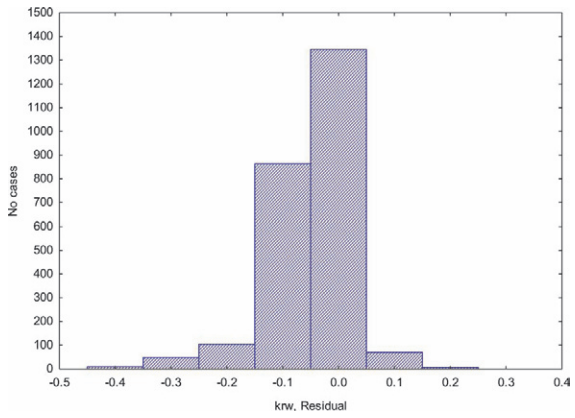

Fig. 12—Histogram of k_{rw} residual error for the Arab-D-reservoir model.

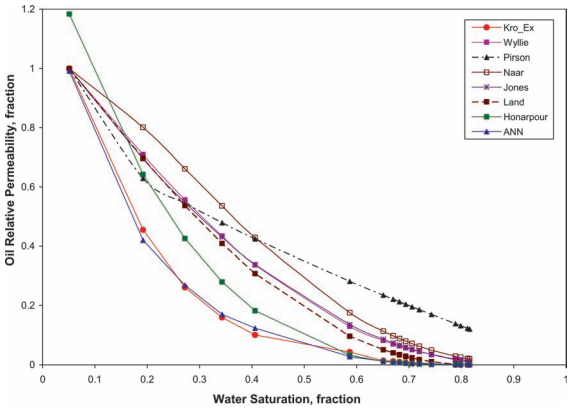

Fig. 13—Comparison of ANN model and correlations for predicting k_{ro} for one well in the Ghawar field.

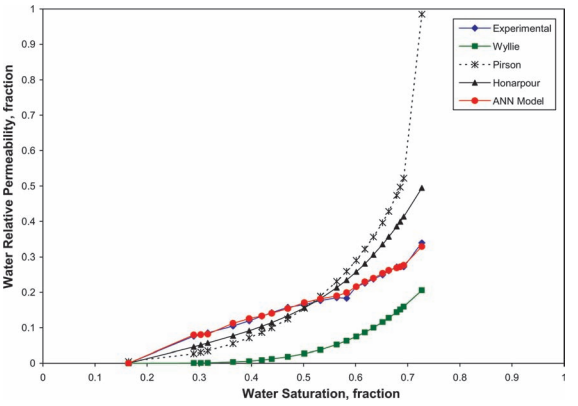

Fig. 14—Comparison of ANN model and correlations for predicting k_{rw} for one well in the Ghawar field.

This step was performed to examine the applicability of the ANN models and to evaluate their accuracy against correlations previously published in the literature. The new ANN models were compared with published correlations of Wyllie (1951), Pirson (1958), Naar et al. (1962), Jones and Roszelle (1978), Land (1968), and Honarpour et al. (1986, 1982). The relative permeability data used for the comparison are for wells in the testing-data subset. No attempt was made in this study to generate new coefficients of the published correlations by use of the same data used for the comparison. The correlations were used with their original coefficients to be compared with the GRNN predictions using the testing-data subset. **Fig. 13** shows the results of comparison of the ANN model against published correlations for predicting oil relative permeability for one of the oil wells in the carbonate reservoir. The results of comparison showed that the ANN models reproduced more accurately the experimental relative permeability data than the published correlations. Although the Honarpour et al. (1986) correlation gives the closest results to the experimental data among other correlations, it does not honor the oil relative permeability data at the initial water saturation by yielding a value greater than one.

Fig. 14 presents a comparison of results of ANN models against the correlations for predicting water relative permeability data for an oil well in the Ghawar field. The results clearly show the excellent agreement of the ANN model with the experimental data and the high degree of accuracy achieved by the ANN model compared to all published correlations considered in this study.

This study differs from others' ANN work (Slipngarmlers et al. 2002) in that this study used a large database of relative permeability for giant carbonate reservoirs, it used fewer input variables such that the developed ANN models use mainly six input variables that can be obtained easily without performing additional complicated experiments, it used a different network type (GRNN), and it achieved a higher degree of accuracy and performance. In addition, for the development of the ANN models, this study implemented several input-selection methods and also used three data subsets (training, verification, and testing), making sure that the network trained very well and avoiding the overlearning problem. Slipngarmlers et al. (2002) used only two data subsets (training and testing).

TABLE 5—STATISTICAL ANALYSIS OF ANN MODEL FOR K_{rw} ARAB-D RESERVOIR WITHOUT THE WETTABILITY

	Training	Verification	Testing
Data standard deviation	0.206744	0.270242	0.265920
Error mean	−0.000831	−0.012651	−0.099167
Error standard deviation	0.058208	0.166682	0.231691
Absolute Error mean	0.036350	0.141533	0.179689
Standard deviation ratio	0.281546	0.616790	0.871281
Correlation Coefficient	0.963740	0.787427	0.508382

Conclusion

In this study, we developed new prediction models for determining water/oil relative permeability using ANN modeling technology for giant and complex carbonate reservoirs. The ANN models were developed by use of a hybrid approach of genetic algorithms and ANNs. The models were successfully trained, verified, and tested using the GRNN algorithm. To the authors' knowledge, this is the first study that uses this type of network, GRNN, in the application of relative permeability determination. Variable-selection and dimensionality-reduction techniques, critical procedures in the design and development of ANN models, were also presented and applied in this study.

Analysis of results of the blind testing-data set of all ANN models shows excellent agreement with the experimental relative permeability data. Results showed that the ANN models outperform all published empirical equations by achieving excellent performance and a high degree of accuracy.

It is hoped that this study will have a great impact on reservoir-simulation and reservoir-management studies. It minimizes the cycle time of the history-matching process, which leads to improved performance predictions. It provides best estimates of relative permeability for existing and newly drilled wells for which experimental data are unavailable.

Nomenclature

S_{on} = normalized oil saturation
S_{or} = residual-oil saturation, fraction
S_w = water saturation, fraction
S_{wi} = irreducible water saturation, fraction
S_{wn} = normalized water saturation
ϕ = porosity, fraction

Acknowledgments

The authors would like to thank Saudi Aramco management for their permission to publish this paper. Special thanks to Ahmed A. Al-Moosa, Faisal Al-Shuraidah, and Fawzi Al-Matar, all of Saudi Aramco, for the great support received during the course of this project. Thanks are extended to the Petrophysics Unit of Saudi Aramco's EXPEC Advanced Research Center for providing the data used in this work.

References

Al-Fattah, S.M., and Startzman, R.A. 2003. Neural Network Approach Predicts US Natural Gas Production. *SPEPF* **18** (2): 84–91. SPE-82411-PA. DOI: 10.2118/82411-PA.

Bishop, C.M. 1995. *Neural Networks for Pattern Recognition*. Oxford, UK: Clarendon Press.

Craig, F.F. 1971. *The Reservoir Engineering Aspects of Waterflooding*. Monograph Series, SPE, Richardson, Texas **3.**

Fausett, L. 1994. *Fundamentals of Neural Networks Architectures, Algorithms, and Applications.* Englewood Cliffs, New Jersey: Prentice-Hall Inc.

Goldberg, D.E. 1989. *Genetic Algorithms in Search, Optimization, and Machine Learning*. Columbus, Ohio: Addison-Wesley.

Haykin, S. 1994. *Neural Networks: A Comprehensive Foundation*. New York City: MacMillan Publishing.

Hill, T. and Lewicki, P. 2006. *Statistics: Methods and Applications*. Tulsa: StatSoft.

Honarpour, M., Koederitz, L., and Harvey, A.H. 1986. *Relative Permeability of Petroleum Reservoirs*. Boca Raton: CRC Press Inc.

Honarpour, M., Koederitz, L., and Harvey, A.H. 1982. Empirical Equations for Estimating Two-Phase Relative Permeability in Consolidated Rock. *JPT* **34** (12): 2905–2908. SPE-9966-PA. DOI: 10.2118/9966-PA.

Jones, S.C. and Roszelle, W.O. 1978. Graphical Techniques for Determining Relative Permeability from Displacement Experiments. *JPT* **30** (5): 807–817; *Trans.,* AIME, **265.** SPE-6045-PA. DOI: 10.2118/6045-PA.

Land, C.S. 1968. Calculation of Imbibition Relative Permeability for Two- and Three-Phase Flow From Rock Properties. *SPEJ* **8** (2): 149–156; *Trans.,* AIME, **243.** SPE-1942-PA. DOI: 10.2118/1942-PA.

Mohaghegh, S.D. 2005. Recent Developments in Application of Artificial Intelligence in Petroleum Engineering. *JPT* **57** (4): 86–91. SPE-89033-MS. DOI: 10.2118/89033-MS.

Naar, J., Wygal, R.J., and Henderson, J.H. 1962. Imbibition Relative Permeability in Unconsolidated Porous Media. *SPEJ* **2** (1): 13–17; *Trans.,* AIME, **225.** SPE-213-PA. DOI: 10.2118/213-PA.

Patterson, D. 1996. *Artificial Neural Networks*. Singapore: Prentice Hall.

Pirson, S.J. 1958. *Oil Reservoir Engineering*. New York City: McGraw-Hill.

Slipngarmlers, N., Guler, B., Ertekin, T., and Grader, A.S. 2002. Development and Testing of Two-Phase Relative Permeability Predictors Using Artificial Neural Networks. *SPEJ* **7** (3): 299-308. SPE-79547-PA. DOI: 10.2118/79547-PA.

Wyllie, M.R.J. 1951. A Note on the Interrelationship Between Wetting and Nonwetting Phase Relative Permeability. *Trans*., AIME **192:** 381–382.

Saud M. Al-Fattah is a researcher currently at Saudi Aramco's corporate planning in Dhahran, Saudi Arabia. E-mail: saud.fattah@aramco.com. He worked in several departments of E&P at Saudi Aramco including reservoir management, production and facilities development, and petroleum engineering applications services. Al-Fattah's areas of specialty include reservoir engineering, artificial intelligence, operations research, economic evaluation, and energy forecasting. He holds a PhD degree from Texas A&M University, College Station, Texas, and MS and BS degrees with honors from King Fahd University of Petroleum and Minerals (KFUPM), Dhahran, Saudi Arabia, all in petroleum engineering. Al-Fattah was awarded the 2006 SPE Saudi Arabia Technical Symposium's Best Paper of the Year award (first place). Al-Fattah is an active member of SPE; he is a technical editor of *SPE Reservoir Evaluation and Engineering*, a mentor in the SPE e-Mentoring program since 2005, vice chairman of the 2006 SPE Saudi Arabia Annual Technical Symposium, and chairman of the 2007 SPE Saudi Arabia Annual Technical Symposium. **Hamad A. Al-Naim** is currently on assignment as a reservoir engineer in the reservoir management department at Saudi Aramco, Dhahran, Saudi Arabia. E-mail: hamad.naim@aramco.com. He worked previously as a petroleum engineering systems analyst in the petroleum engineering applications services department at Saudi Aramco. Al-Naim holds a BS degree from KFUPM, Saudi Arabia, in computer engineering in 2001, and an MS degree in petroleum engineering from the University of Calgary in 2006.

SPE 114229

Case-Based Reasoning Approach for Well Failure Diagnostics and Planning

Andrei Popa, SPE, Carrie Popa, SPE, Mike Malamma, and John Hicks, Chevron North America Exploration and Production

Copyright 2008, Society of Petroleum Engineers

This paper was prepared for presentation at the 2008 SPE Western Regional and Pacific Section AAPG Joint Meeting held in Bakersfield, California, U.S.A., 31 March–2 April 2008.

This paper was selected for presentation by an SPE program committee following review of information contained in an abstract submitted by the author(s). Contents of the paper have not been reviewed by the Society of Petroleum Engineers and are subject to correction by the author(s). The material does not necessarily reflect any position of the Society of Petroleum Engineers, its officers, or members. Electronic reproduction, distribution, or storage of any part of this paper without the written consent of the Society of Petroleum Engineers is prohibited. Permission to reproduce in print is restricted to an abstract of not more than 300 words; illustrations may not be copied. The abstract must contain conspicuous acknowledgment of SPE copyright.

Abstract

Case-based reasoning, also known as computer reasoning by analogy, is a simple and practical technique that solves new problems by comparing them to ones that have already been solved in the past, thus saving time and money. The technique constantly incorporates dynamic data, which empowers the system to learn and adapt from new experiences. A general framework for case-based reasoning is presented, along with a review of the four-step cycle that characterizes the technology: retrieve, reuse, revise and retrain.

This paper presents a specific application of case-based reasoning to determine the optimum cleaning technique (bailing, washback, or foaming) for sanded/seized well failures. The methodology extracts only the most relevant information from the historical database, utilizes a rule-based system to make adaptations, and then suggests the most appropriate solution for a given well intervention. This technique was used for production operations as a front end tool for well workover planning and design and was applied to sample data from a large oil field where the main artificial lift system is rod pump. This simple case demonstrates how case-based reasoning can be applied to improve the planning and execution of well interventions, thus reducing cost, rig time, and well turnaround time, while maximizing reliability and production.

Introduction

In large fields with thousands of wells, an immense amount of data and experience build up in databases over time. Typically engineers have access to this data, but rarely have time to analyze the entire dataset before making a recommendation for a well intervention or job. Furthermore, much of the data is irrelevant to a given case and reviewing it can waste the engineer's highly valuable time. Even human memory is of little help in a field with a high activity level or significant turnover where the same engineer, operator, or crew rarely works on the same set of wells. In any and all of the above cases, the well failure dataset represents a tremendous amount of knowledge that can and should be exploited for better decision-making. Case-based reasoning is an excellent technique to maximize the value of historical data for better decisions regarding well intervention planning and execution.

Case-Based Reasoning. Case-based reasoning (CBR) is a basic problem solving technique that uses and adapts the solutions of analogous past problems to solve new problems. Its roots are steeped in human cognitive research from the early 1980s, and the technique has gained traction in the last decade. CBR can be described as a common human problem-solving behavior that has been adapted for computer use. It is based on recall and reuse of specific "cases" and offers techniques for acquiring, representing and managing previous experiences. The formalized four-step process of retrieve, reuse, revise, and retain is detailed below and depicted in Figure 1.

- Retrieve: The process of finding cases, and their corresponding solutions, in the dataset or knowledge base that are most relevant to the given case.
- Reuse: The process of mapping the most common solution from the knowledge base for the given case. The reuse process also allows for adaptation of the most common solution, as needed, through the use of rules or "if statements" incorporated into the system.
- Revise: The process of testing the new solution. If the new solution is successful, the process moves directly to retain. If the new solution does not work as expected or needs additional fine-tuning, the solution is further adapted to achieve the desired result.

- Retain: The process of storing the new case and its final solution in the knowledge base for future use in the case-based reasoning process.

Authors such Kolodner[1] and Rissland[2] divide case-based reasoning tasks into two segments: interpretive CBR and problem solving CBR. Aamodt and Plaza[3] denote interpretive CBR as exemplar-based reasoning and refer to it as a classification task, where a new case is clustered into the right class. Problem solving CBR then generates a new solution from adaptation of previously stored solutions.

The power of case-based reasoning technology resides in its potential for developing a system that learns as new cases are solved. Learning occurs as a natural by-product of the process[3]. It is important to note that case-based reasoning systems learn from both successes and failures. For example, each time a new solution is generated and a problem is solved, the experience is stored through the retain process to be used later on in solving similar problems. On the other hand, when the proposed solution to the problem fails, the reason for failure is identified and retained in order to avoid the same failure in the future.

Research in the area of case-based reasoning has grown from isolated university centers to a field of widespread interest. The application of case-based reasoning can now be found in the full spectrum of tasks such as classification, interpretation, scheduling, planning, design, diagnostics, explanation, projection of effects, and execution monitoring[4]. Case-based reasoning is already utilized in other industries including software (design, sales support and help desk)[5,6], manufacturing, airline, construction, real-estate, law, medicine, and education.

In the oil industry, the application of case-based reasoning is still at the beginning. One of the first applications of case-based reasoning was documented by Irrgang et al[7] where the technique was applied to derive alternate drilling plans based on previously drilled wells. The system utilized past experiences recorded in drilling data and reports. In 2002, Bhushan et al[8] applied case-based reasoning to globally search for reservoir analogues as an important step in planning a new field development. Perry et al[9] describe the development of a case-based knowledge repository for drilling optimization as a tool for the capture, representation, and dissemination of lessons learned.

Well Intervention and Planning. In fields where rod pump is the main artificial lift system, wells experience many failures during their lifetime. These failures lead to significantly decreased or complete loss of production, requiring well interventions to restore production. Although most interventions are reactive (after well failure), some are proactive, designed to increase production prior to failure. Most stimulation jobs are considered proactive (fracturing, acidizing, cyclic steam, pressure wash, capacity upsize/downsize, effective depth change, etc), while reactive examples include pump failure, tubing failure, rod failure, and sanded/seized. This study is focused on the second category, reactive well work, specifically on sanded/seized failures.

Sanded/seized failures occur when unconsolidated reservoir sands flow into the bottom of a well and cause the pump to become stuck. After a well has been diagnosed as a sanding failure, one of three cleaning methods is typically employed to correct the situation and return the well to production: bail, washback or foam. For each method, the job length varies and different equipment is required, so job costs for each method are also significantly different.

- Bailing uses a wireline device to remove sand from the tubing and/or casing. This procedure is effective when there is a small amount of sand to be removed. The equipment required is a bailer.
- Washback is the process of washing sand back into the formation by means of water circulation through tubing. This method is applied only for highly permeable formations. A water source, along with a wash pump or adequate water pressure, is required on location.
- Foaming is the practice of circulating foam through tubing to remove sand by bringing it to surface. This technique is applied when there is a large amount of sand and/or the well is damaged. A foaming unit and tank are required on location.

The success of a well intervention is determined by accurate failure diagnosis and appropriate planning. An accurate diagnosis of failure leads to appropriate planning and results in faster and shorter intervention time with significant cost reductions. When proper planning is done, the rig moves on location with the correct equipment and the job is completed as scheduled. However, situations arise when the diagnosis is not accurate and/or the selected method does not work. This is particularly true in a field with a high activity level where a substantial amount of time cannot be dedicated to planning each well intervention. Furthermore, bailing, washback, and foaming are progressively more expensive and time-consuming, so it is natural for operations to select one of the less expensive methods. If that method does not work, it leads to the necessity of using multiple cleaning methods during a single well intervention, causing even longer downtime and a significant increase in job cost.

As an example, a well has a sanded/seized failure and the engineer or operator plans a bailing job. The rig moves in and after a few hours, no significant progress is made. At this point, a decision is made to move to washback or foaming. For a washback, tubing must be run back into the well leading to additional time and cost. If foaming is required, then a foaming unit and a tank must be brought on location. While the foaming unit is brought on location the rig is on downtime or, worse still, a foaming unit might be available but a tank is not. This creates even longer downtime and increase in job costs. The worst case scenario is when all three cleaning methods end up being used during execution: the original plan calls for bailing, but the crew decides to switch to washback, but then must foam in the end before the well can be successfully returned to production.

The execution and decision-making process described above is shown in Figure 2. It is clear that accurately planning for the proper sanded/seized cleaning method is the best outcome. The critical opportunity in this example is to utilize a case-based reasoning system to reduce the number of well interventions where multiple cleaning methods are needed. A correct diagnosis of failure and planning for the most suitable job type can lead to significant improvements in job time, costs, well turnaround time, and returned down production. Improvements in sanded/seized programs can also lead to better allocation and usage of equipment, allowing more jobs to be completed, along with lower operating expenses and increased revenues.

Methodology

Case-based reasoning applications rely entirely on a complete and well-organized database or knowledge domain that contains historical cases and their solutions. The data collected in this study contained nearly 5000 well interventions from the past three years (approximately 2500 bailing, 1000 washback, and 1500 foaming). Of these cases, roughly 800 were instances where the cleaning method was changed during the job, highlighting a one-in-six opportunity for improvement. Quality control was a significant effort, repairing inconsistent data and typos, deleting incomplete records, and analyzing outliers for accuracy.

Data Types for Knowledge Domain. In this study, multiple data types were collected for the knowledge domain including well location, completion, artificial lift, and production, as well as job dates and events. The data collected were intended to represent the knowledge, experience, and thought process an engineer would use for planning a sanded/seized well intervention. Table 1 shows the data attributes for each record in the knowledge domain.

- Location data, specifically latitude and longitude (X,Y coordinates), are useful during the retrieval process when searching for certain behaviors in the field. For example, if past history shows that certain parts of the field experience more sanding than others, then the case-based reasoning system can include this.
- Completion data includes effective depth, total depth, casing/liner/innerliner size and wellbore damage. The pipe size offers information on the amount of sand to be removed (the larger the casing, the more sand accumulated). Wellbore damage, both the extent and number, may lead to excluding a well from being a bailing candidate. Furthermore, wells completed with liners or innerliners should never be washed back.
- Artificial lift data included attributes such as pump type and pump depth. Pump type is advantageous since washback or foam jobs can be completed without pulling tubing if the well has an insert pump, while wells with tubing pumps will take longer since the pump cannot be removed without pulling the tubing. Also, the distance between effective depth and pump depth, also known as rat hole, is an important factor in the planning process.
- Production data was utilized to compare the performance of wells cleaned by bailing, washback or foaming.
- Job dates were not ultimately used as a direct input in the described system, but instead were used to calculate the frequency of well interventions for each well. Low well intervention frequency implies that the sanding rate for a well is low and is likely an excellent candidate for bailing. On the other hand, high sanding frequency points to highly unconsolidated formation around the wellbore, making it a likely candidate for foaming.
- Job events data included the sanded/seized cleaning method and statistics for the job, such as amount of sand fill cleaned out, circulation time, and total job duration. Past job information, particularly the amount of sand fill cleaned out, provides valuable knowledge about the behavior of a particular well and allow for better prediction of the appropriate cleaning type for a sanded/seized well intervention.

Retrieve. When the case-based reasoning system is presented with a new case, the retrieval process searches the previously described database or knowledge domain and returns the most similar cases. In this example, the k-Nearest Neighbors technique was used for the similarity function. The algorithm uses the distance between examples and retains the closest cases based on a certain criteria, where k represents the number of cases retrieved. Since the k-Nearest Neighbors algorithm uses the Euclidean distance to calculate the closeness of the cases, all data in the knowledge domain must be numeric or converted to a numerical scale. A metric is defined for each dimension or data type. Additional reasoning is also incorporated into the calculations in the form of a weighting factor. The weighting factor is typically defined by the user, and the sum of the attribute weights should equal 1. Equation 1 represents the similarity function[10] for numeric attributes between two cases used in this example.

$$similarity(p,q) = \sqrt{\sum_{A} w_A \times f(p_A, q_A)}$$

where,

- p is the new case presented to the case-based reasoning system
- q is a case from the knowledge domain for comparison
- A is the number of attributes in each case in the knowledge domain
- p_A is the numerical value of attribute A for case p
- w_A is a non-negative real value parameter that represents the relative weight of attribute A

Equation 1: Euclidean distance equation used in k-Nearest Neighbors technique

The similarity calculations are performed until all cases in the knowledge database have been compared. The cases are then ranked based on their similarity to the given case and the most similar cases are kept for the reuse process.

Reuse. The most common solution from the retrieved cases becomes the starting point for the reuse process. The reuse process then runs though a series of adaptation algorithms to ensure solution validity. The adaptation algorithms are basically rules or "if statements" that the engineer can incorporate into the system to change the proposed solution based on exceptions or other experience. Since the retrieval process returns cases from many different wells, most of the adaptation algorithms focus on well-specific information that could determine the outcome of a well intervention. Although the adaptation algorithms can get as complex and elaborate as the system designer would like, most used in this example were relatively simple (although the combination and order became quite intricate and complicated). A small subset is listed below:

- If the well has a liner or innerliner, it should never be washed back.
- If the well has had prior failures being bailed or washed back, it should be foamed.
- If the well has considerable wellbore damage, it is not a candidate for bailing.
- If the well has a low sanding frequency, it is a bailing candidate.
- If the well has a high sanding frequency, it is a foaming candidate.
- If the well has been successfully returned to production in the past using different cleaning methods, use the cleaning method that resulted in the best production response.
- If the well has had 100 feet or more of sand cleaned out during numerous prior jobs, it is a foaming candidate.

Safety concerns are critical for well intervention planning and were another key source of adaptation algorithms for the case-based reasoning system. The dataset used in the pilot is from a large, thermally operated field with very tight well spacing. In areas of active steam injection, wells can reach a very high temperature, making bailing a safety risk. Additionally, compact well density can restrict certain types of equipment from reaching particular well locations.

During the reuse step, the system will change the proposed sanded/seized cleaning method if any of the adaptation algorithm rules are violated; otherwise, the most common solution from the retrieved cases will persist as the final proposed well intervention type.

Revise and Retain. The final solution proposed by the reuse process is then used by the engineer or operator to write the job program for execution in the field. If the job performs as expected, the revise process is skipped. However, if the proposed cleaning method does not achieve the desired result (i.e. the system proposed bailing, but no progress was made and the crew switched to washback), then the case solution is revised to the final cleaning method before the next step.

At the successful completion of the well intervention, the job is added as a new case into the knowledge domain or database. This retain process is the key feature that allows for continuous learning by using new data which ensures that the system never needs retraining.

Results

To test this methodology, a small subset of historical jobs was withheld from the dataset to compare the case-based reasoning proposed solution with the actual job results. The testing subset was a mixture of two types of well interventions: (1) jobs where one cleaning method was able to successfully return the well to production, and (2) jobs where the initial cleaning method did not work and required another cleaning method(s) before the sand was successfully removed. In the first instance, success was defined as the case-based reasoning system proposing the same well cleaning method actually used during the job. In the second, success was defined as the case-based reasoning system proposing the final cleaning method used during the job. For these jobs in the second category, implementation of the case-based reasoning system would have saved time and money by avoiding the initial well cleaning method(s) that was not able to successfully return the well to production.

Using the above definitions of success, the case-based reasoning system was able to correctly propose the successful well cleaning method for approximately 80 percent of cases. The following four examples are representative of the testing data subset and demonstrate the effectiveness of the case-based reasoning system.

The first example demonstrates how the case-based reasoning system worked for a simple case in the testing data subset. In this example, the well has a perforated completion and is located in the northwest part of the field. It has wellbore damage, but the damage is below the pump and a bailer is still able to pass. The effective depth is less than 50 feet below the 2 ¼ inch tubing pump. The well has one prior successful bailing job in the knowledge domain. 109 similar cases were retrieved, and the most common solution was bailing. This example did not trigger any adaptation algorithms in the reuse step, so the case-based reasoning system proposed bailing as the well cleaning method. The actual job type was also bailing, which was successful.

The second example was from a well located in the southwest part of the field. The well has an innerliner, no damage, and a moderate well failure frequency. The well has a history of successful bailing and foaming jobs, depending on pump depth, in the knowledge domain. The 2 ¼ inch pump is currently set approximately 80 feet above the effective depth. The retrieval step found 71 similar cases, where the most common solution was washback. In this case, the reuse process triggered the innerliner adaptation algorithm and changed the proposed well cleaning method to foaming. The actual job type was also foaming, which was successful.

The third example depicts a well in the eastern part of the field. This well has a perforated completion with a 2 ¼ inch tubing pump set 40 feet above the effective depth. Although the well has a low failure frequency, one successful prior bailing job is listed in the knowledge domain. The retrieval step found 92 similar cases. The most common cleaning method was bailing, and this proposed solution did not change as a result of any adaptation algorithms. In actuality, a washback was recommended and successfully performed on this well. In the reported results, this example was considered a failure since the system proposed a different cleaning method than the one executed in the field. It is unknown whether or not bailing could have been successful for this job since it was never tried. There is still a possibility, then, that bailing could have been the preferred cleaning method, thus saving time and money.

The fourth and final example presented is a well located in the central part of the field. The well has a perforated completion, no damage, and moderate well failure frequency. The 1 ¾ inch tubing pump is set more than 70 feet above the effective depth. The well has a history of one foaming job in the knowledge domain. The most common solution in the 83 similar cases from the retrieval step was foaming. During the actual job, the crew initially attempted bailing. After three hours and only 18 feet of cleanout, the crew switch to foaming and successfully returned the well to production. The total job duration was 21 hours, compared to the typically job duration for foaming only of 14 hours. In this example, the case-based reasoning system accurately proposed the successful well cleaning method and could have saved time and money if implemented.

Since the methodology presented in this paper is still under development, it has not yet been implemented in the field using the revise and retain steps. For field implementation, a new data type will be added to the database where the system will store its proposed solution. Over time, this system-proposed solution will be compared against the actual well intervention solution to enable the ability to statistically prove its effectiveness. Furthermore, the system is very flexible in that it has the ability to add other parameters for storage and use in the knowledge domain. As the system is implemented and utilized, the engineer may determine other data, factors, or exceptions that can enrich the knowledge base and suggest more effective and viable solutions.

Conclusions

Case-based reasoning technology was successfully applied as a methodology to improve sanded/seized well intervention planning. The significance and unique advantage of case-based reasoning over other technologies, including neural networks, is the fact that it integrates dynamic data. This enables the system to continuously learn and become even more beneficial over time as the knowledge domain grows. Every day that new well interventions are executed, the database will be populated with new data for retrieval, which increases the success of the system.

Testing results demonstrate the effectiveness of the case-based reasoning system and indicate that implementation will save time and money by accurately proposing the appropriate well cleaning method. In addition to saved job costs and time, the case-based reasoning system has the potential for better allocation and usage of equipment, allowing more jobs to be completed, leading to lower operating expenses and increased revenues.

The case-based reasoning system presented in this paper is relatively simple and focuses only on reactive sanded/seized well failures. The vision of the authors is to take this technology one step further by transforming or combining reactive well interventions into proactive work. For example, after a well failure is identified, the case-based reasoning system would have the ability to search for additional proactive work such as opening other reservoir zones by adding perforations or deepening the well past the current effective depth. This enhancement would add incremental oil production and avoid the need for another job by taking advantage of completing additional work while the well is down.

Acknowledgments

The authors would like express appreciation to Chevron North America Exploration and Production for permission to publish this paper. Special thanks to Jack Stevenson and Art Lewis for their support and encouragement in completing this work and reviewing the manuscript. Thanks also to Debbie Priddy and Robert Altmiller for their assistance in data collection.

References

1. Kolodner, Janet. “Case-Based Reasoning”, San Mateo, Morgan Kaufmann, 1993.
2. Rissland, E.L. and D.B. Skala. “Combining case-based and rule-based reasoning: A heuristic approach”, Eleventh International Joint Conference on Artificial Intelligence, IJCAI-89, pp. 524-30.
3. Aamodt, Agnar and Enric Plaza. “Case-Based Reasoning: Foundational Issues, Methodological Variations, and System Approaches”, Artificial Intelligence Communications 7, No. 1, 1994, pp. 39-52.
4. Watson, Ian. “Applying Case-Based Reasoning: Techniques for Enterprise Systems”, Morgan Kaufmann, 1997.
5. Delany, Sara, and Padraig Cunningham. “The Application of Case-Based Reasoning to Early Software Project Cost Estimate and Risk Assessment”, Contract TCD-CS-2000-10.
6. Maher, Mary Lou, M. Bala Balachandran, Dong Mei Zhang. “Case-Based Reasoning in Design”, Lawrence Erlbaum Associates, 1995.
7. Irrgang, R., C. Damski, S. Kravis, E. Maidla. “A Case-Based System to Cut Drilling Costs”, SPE Annual Technical Conference and Exhibition, Houston, Texas, 3-6 October 1999.
8. Bhushan, V., S.C. Christopher Hopking. “A Novel Approach to Identify Reservoir Analogues”, SPE 13th European Petroleum Conference, Aberdeen, Scotland, 29-31 October 2002.

9. Perry, P.B., D.A. Curry, J.D. Kerridge. “A Case Based Knowledge Repository for Drilling Optimization”, SPE IADC/SPE Asia Pacific Drilling Technology Conference and Exhibition, Kuala Lumpur, Malaysia, 13-15 September 2004.
10. Pal, Sankar and Simon Shiu. “Foundations of Soft Case-Based Reasoning”, Wiley Series on Intelligent Systems, 2004.

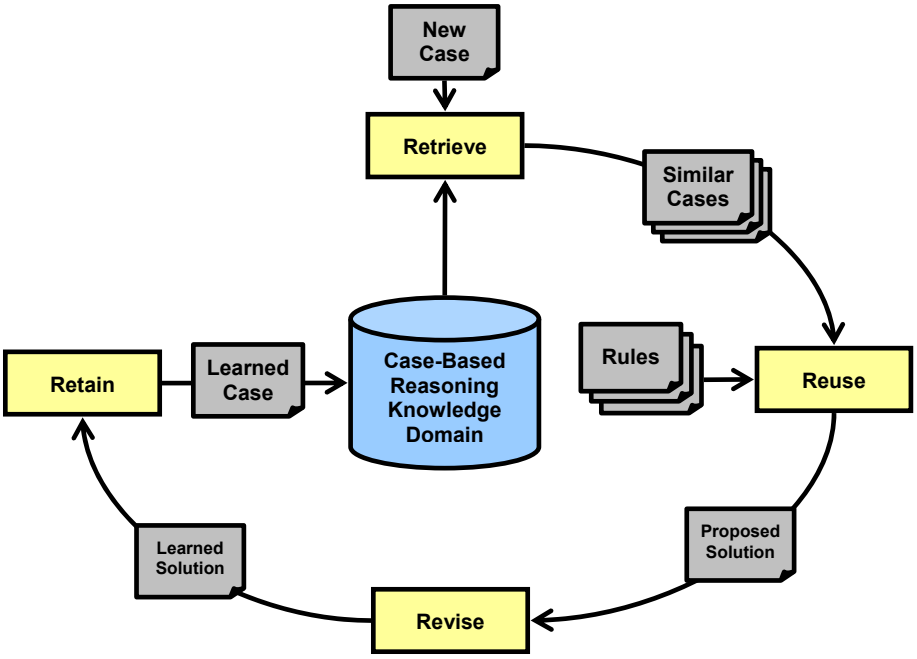

Figure 1: Case-Based Reasoning Process, adaptation from Aamodt and Plaza[3]

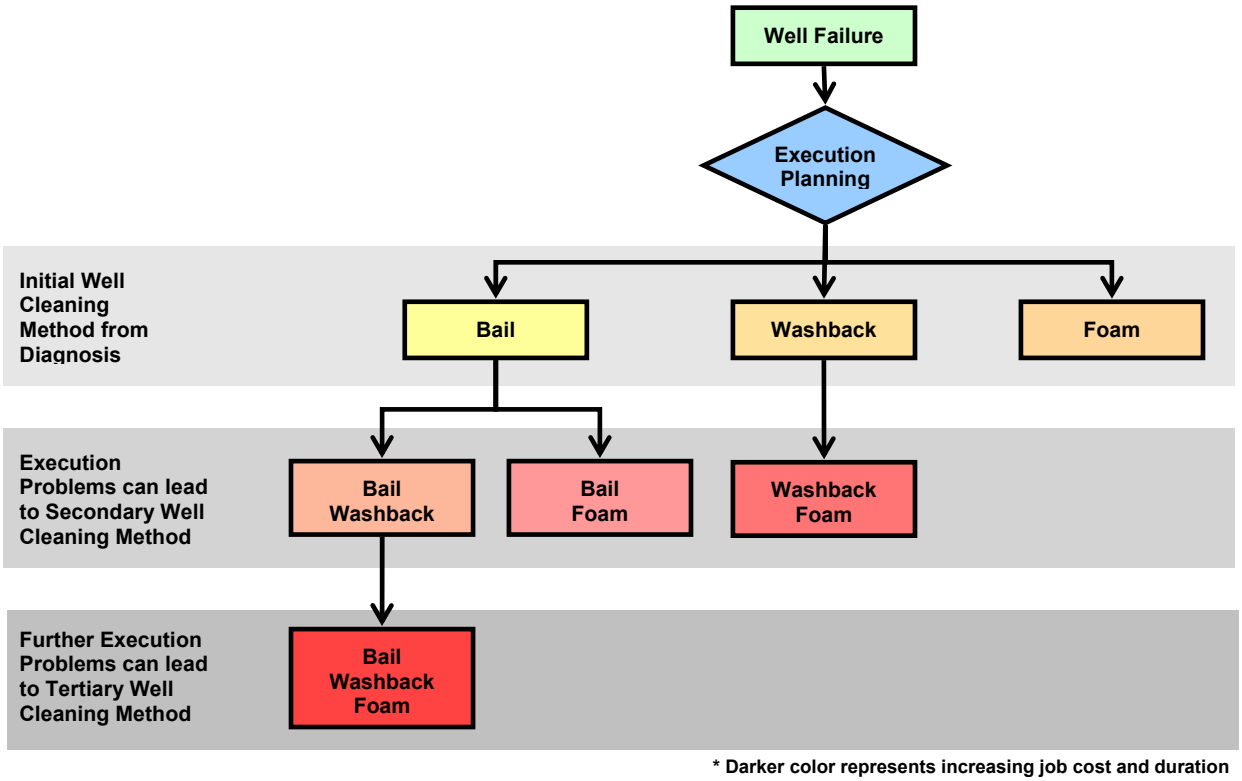

Figure 2: Sanded/Seized Well Cleaning Method Progression

Attribute	Data Type: Value
API_Number	character
Well Name	character
Surface X Coordinate	real: discrete
Surface Y Coordinate	real: discrete
Bottom X Coordinate	real: discrete
Bottom Y Coordinate	real: discrete
Total Depth	real: continuous
Effective Depth	real: continuous
Casing/Liner Diameter	real: continuous
Casing/Liner Description	character
Pump Depth	real: continuous
Pump Type	character
Job ID	integer: unique
Job Type	integer: 1=proactive 2=reactive
Failure Reason	integer: 1=Pump, 2=Tubing, 3=Rod, 4=Sanded/Seized
Event Type	integer: 1=Bailing, 2=Circulating, 3=Foaming
Cleaning Method	integer: 1=Bail, 2=Wash, 3=Foam
Planned Job Date	date: discrete
Job Start Date	date: discrete
Job End Date	date: discrete
Job Duration	real: continuous
Tool Size	real: continuous
Tag Depth	real: continuous
Cleaned Depth	real: continuous
Bail Duration	real: continuous
Feet Bailed	real: continuous
Wellhead Temperature	real: continuous
Pre-Job Avg Oil Prod	real: continuous
Pre-Job Avg Water Prod	real: continuous
Post-Job Avg Oil Prod	real: continuous
Post-Job Avg Water Prod	real: continuous

Table 1: Data Attributes in Case-Based Reasoning Knowledge Domain

SPE 124204

Top-Down Intelligent Reservoir Modeling (TDIRM)

Y. Gomez, Y. Khazaeni, and S.D. Mohaghegh, SPE, West Virginia University, and
R. Gaskari, Intelligent Solutions, Inc.

Copyright 2009, Society of Petroleum Engineers

This paper was prepared for presentation at the 2009 SPE Annual Technical Conference and Exhibition held in New Orleans, Louisiana, USA, 4–7 October 2009.

This paper was selected for presentation by an SPE program committee following review of information contained in an abstract submitted by the author(s). Contents of the paper have not been reviewed by the Society of Petroleum Engineers and are subject to correction by the author(s). The material does not necessarily reflect any position of the Society of Petroleum Engineers, its officers, or members. Electronic reproduction, distribution, or storage of any part of this paper without the written consent of the Society of Petroleum Engineers is prohibited. Permission to reproduce in print is restricted to an abstract of not more than 300 words; illustrations may not be copied. The abstract must contain conspicuous acknowledgment of SPE copyright.

Abstract

This paper examines the validity of a recently introduced reservoir simulation and modeling technique. The technique, that is named Top-Down Intelligent Reservoir Modeling, TDIRM (not to be confused with BP's TDRM history matching technique), integrates traditional reservoir engineering analysis with Artificial Intelligence & Data Mining (AI&DM) technology in order to arrive at a full field model and to predict reservoir performance in order to recommend field development strategies. The distinguishing feature of this technology is its data requirement for its analysis. Although it can incorporate almost any type and amount of data that is available in the modeling process, it only requires field production rate and some well log data (porosity, thickness and initial water saturation) in order to start the analysis and provide a full field model. Presence and incorporation of other types of data can increase the accuracy and validity of the developed model.

In this work three different reservoir models with varying criteria have been generated using a commercial simulator. The models are built to investigate TDIRM's capabilities in predicting different aspects of an oil reservoir. The models include different reservoir saturation conditions (saturated or under-saturated), different number of wells and different distributions of reservoir characteristics. Production rates and well log data from the wells in the simulation model are imported into the TDIRM to develop a new empirical reservoir model and make predictions on new well performance and potential infill locations. The results from the TDIRM analysis are compared to the original simulation models. Investigation and validation of TDIRM's predictive capabilities include identification of gas cap development in the formation, identification of infill locations by mapping the remaining reserves as well as predicting flow performance of the wells that are planned to be drilled in the reservoir.

Introduction

Understanding the reservoir depletion and achieving high recovery factor has always been a challenge for reservoir engineers. In the past several years efficient techniques have been developed to study reservoir behavior and to build models that would allow analysis and predictions, however, the techniques that are based on numerical solution of the fluid flow equation required a large amount of reservoir data and are expensive from a time and man-power stand point. The analytical approaches to building such models usually limit the analysis to single-well models and include approximations and assumptions that limit their use for full field analysis.

In recent years, a new empirical modeling technique has been introduced that is called Top-Down Intelligent Reservoir Modeling (TDIRM) (1) (2) (3) that approaches full field reservoir modeling from a different angle. The TDIRM's advantage is its flexibility in data requirement. It needs only production rate data and well logs (for some wells not all) in order to start its analysis and build full field model. It has also the capability of incorporating other data such as core analysis, well tests, pressure data and seismic, in cases where such data is available. The main disadvantage of TDIRM is that it is recommended to be used in fields with at least 50 wells and about five years of production history. This has to do with the fact that TDIRM uses the production history and well log data in order to generate a large spatio-temporal database of the reservoir static and dynamic behavior. It uses Artificial Intelligence and Data Mining (4) (5) (6) techniques to deduces field-wide patterns from the large spatio-temporal database. The result of these analyses is a full field model with impressive predictive capabilities.

The large spatio-temporal database of the reservoir behavior is developed using combination of statistical analyses of the production data and a series of classics reservoir engineering techniques such as decline curve analysis, type curve matching, and production history matching using single-well numerical simulation as well as estimation of volumetric reserves and recovery factor. These analyses are performed on single-well basis (for all the wells in the database) and are then fused together using Fuzzy Pattern Recognition technology and an ensemble of artificial neural networks in order to generate a full field model.

Validation Methodology

The Top-Down, Intelligent Reservoir Modeling (TDIRM) was first validated (3) for gas reservoirs using a commercial reservoir simulator (4). The objective of this study is to investigate TDIRM's capabilities when applied to oil reservoirs. The methodology used for this study is similar to the previous study where a commercial reservoir simulator (5) is used in order to develop several reservoir models. The reservoir models are produced for several years and the production rate and well log (porosity, thickness, and initial water saturation) data are extracted and used as input to the TDIRM. In each case an empirical full field model is developed using the TDIRM and certain predictions are made according to the objectives of the specific model /study. The predictions from the TDIRM are then compared with the reservoir simulation model. Schematic diagram of this process is shown in Figure 1.

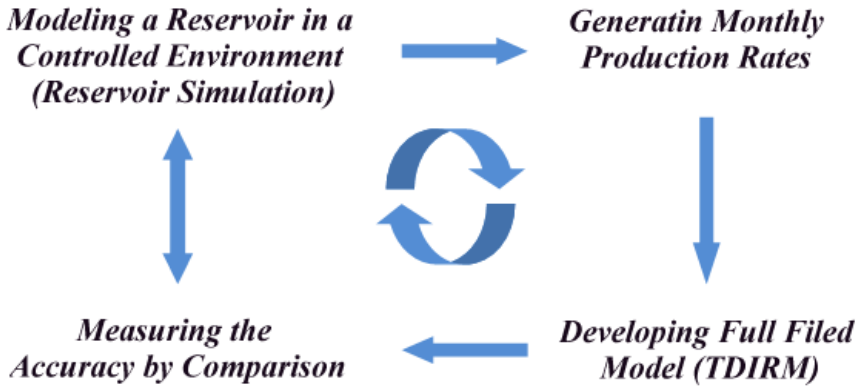

Figure 1. Methodology used in developing an empirical full field model in TDIRM.

Three models were developed and studied for the purposes of this article. The three models developed for this study have several things in common while differing in many characteristics. For example all models are oil producing reservoirs with initial water and oil saturations of 35% and 65%, respectively. All three models include highly heterogeneous distribution of porosity, permeability, formation tops, and thickness. All wells in these models were vertical with 0.25 ft open-hole completion, and they were produced with constant bottom-hole pressures.

There are some activities that are performed during a TDIRM analysis that is common to all models and reservoirs. These activities are performed on production data and on the well log data. Some of the common activities that are performed on the production data include generation of production rate statistics upon importing the production data. These statistics include 3, 6 and 9 months cumulative productions as well as 1, 3, 5 and 10 years cumulative productions. Conventional decline curve analysis is performed on all production rate data. Unconventional (intelligent) decline curve analysis is performed on data such as Gas Oil Ratio where a negative decline is the normal behavior. The "Intelligent" decline curve analysis refers to a TDIRM-specific process of using a time-series adaptive modeling techniques to model the behavior non-declining production characteristics such as GOR and water cut.

The common activities that are performed on the well log (including well locations – Latitude and Longitude) data include generation of a series of Voronoi cells (9). These analyses generated estimations of the parts of the reservoir that are impacted by the production from each well. Hydrocarbon pore volume as well as time and amount of production can play a role in identifying the extent of each Voronio cell. Figure 2 shows the process of generating Voronio cells in TDIRM and associating each Voronoi cell with a collection of Cartesian cells that will be used in order to build an "earth model". It is helpful if an estimation of the structure of the reservoir is available that could serve as the outer boundary of the reservoir as shown in Figure 2Figure 2. In this figure the well location are plotted (a), a Cartesian grid is generated (b), the outer boundary of the reservoir is identified (c), and finally the Voronoi cells are generated (d). The Voronoi cells are then associated with the collection of Cartesian grids for any given well.

Geostatistical techniques such as Kriging or Sequential Gaussian Simulation are used for the generation of the earth model. Using the earth model and the associated Voronoi cells volumetric reserves are estimated and by integrating the volumetric reserves with the results of the decline curve analysis, a recovery factor for each well is estimated. Furthermore, during this process the top five "Closest Offset Wells (COWs)" along with their static and dynamic properties are identified and associated with each of the wells in the field. Static and dynamic properties of the top five "Closest Offset Wells (COWs)" carry important information about the interferences that take place amongst neighboring wells throughout the production process. This information is an important part of developing predictive models at the later stages of TDIRM analysis.

Upon completion of the two common activities that were mentioned in the above paragraphs the results are used in a process called Field-Wide Pattern Recognition. The Field-Wide Pattern Recognition employs Fuzzy Pattern Recognition (FPR) (6) technology in order to extract non-trivial, implicit, previously unknown, and potentially useful information and patterns from the large database that has been generated as the result of activities that were mentioned above. The process of Field-Wide Pattern Recognition using Fuzzy Pattern Recognition (FPR) is demonstrated briefly in Figure 3.

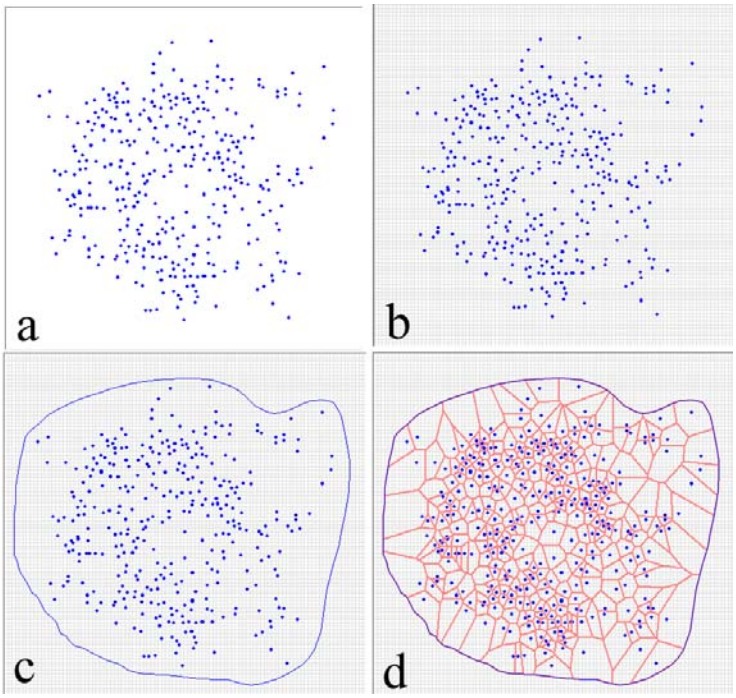

Figure 2. Generating Voronoi cells for the wells during the TDIRM analysis process.

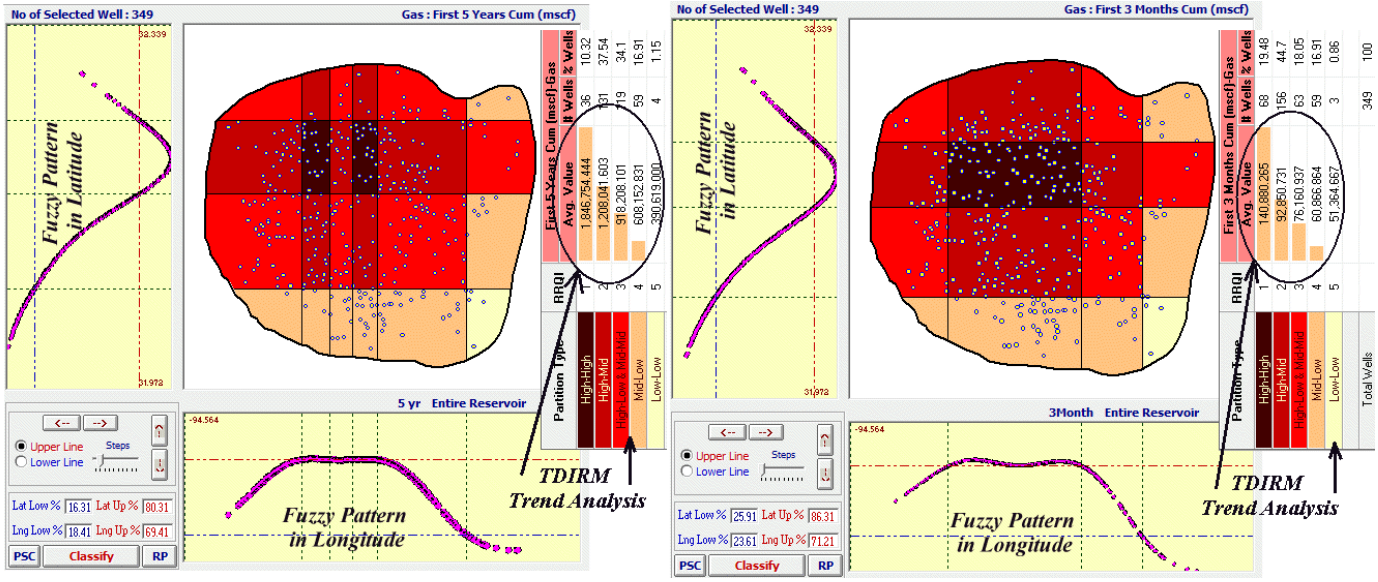

Figure 3. Results of Fuzzy Pattern Recognition showing the sweet spots in a field after the first 3 months (left) and 5 years of production (left).

This process includes generation of fuzzy patterns (from actual data that is usually quite scattered and a trend cannot be observed in a cross plot) of a given attribute (such as 3 months cumulative and 5 years cumulative production) against latitude and longitude as indicated in Figure 3. Then each of these patterns (that are now essentially a two dimensional plot) are divided into three segments using two horizontal lines (the red-top and the blue-bottom lines in the figure). These lines divide the pattern into high (the segment above red line), average (the segment between red and blue lines), and low (the segment below the blue line). At locations where these lines cross the fuzzy pattern (the 2D profile along the latitude and longitude) a vertical line is generated and projected on to the field map (latitude vs. longitude). These projection lines delineate the reservoir into Relative Reservoir Quality Indices indicating the high from the latitude and high from the longitude as "high-high" to be the best portion of the reservoir. Similarly where low from the latitude and low from the longitude are crossed, it would be indicated as "low-low" or the worst portion of the reservoir. Other RRQIs are identified accordingly as indicated in Figure 3. The TDIRM "Trend Analysis" that is shown in Figure 3 as "tornado charts" is provided to serve as qualitative indications for moving the red and the blue lines appropriately in order to create trends that are consistent with the RRQIs 1 through 5.

Results from Fuzzy Pattern Recognition (FPR) process and development of earth model using Voronio cells are used in developing the final cohesive model that emerges from the TDIRM and subsequent analysis and conclusions are made from the FPR and final full field model. In the following sections each of the three models that have been investigated for this study will be explained in some details. For each of the models the purpose and the objective are identified along with the simulation model details followed by the results of the TDIRM analysis. The TDIRM analysis results are then compared with the results generated by the commercial reservoir simulator.

It is important to note that TDIRM analyses (especially Fuzzy Pattern Recognition as shown in Figure 3) are qualitative in nature and should only be used as trend and pattern identifiers. The quantities represented in these analyses may not necessarily be accurate or represent specific physical meaning.

Model #1, Predicting Well Performance

Figure 4 shows the reservoir characteristics that have been used in this model. Permeability, porosity, formation tops and thickness distribution for the modeled reservoir is shown in this figure. The distributions in this figure clearly show the degree of heterogeneity that has been incorprated in this reservoir model . Details of this model is shown in Table 1. The modeled reservoir has a porosity range of 20% to 35%, horizontal permeability range of 30 to 60 md, vertical permeability range of 3 to 6 md and pay thickness range of 100 to 200 ft. It is produced at a bottomhole pressure of 600 psi while the initial pressure of the reservoir is 2500 psi.

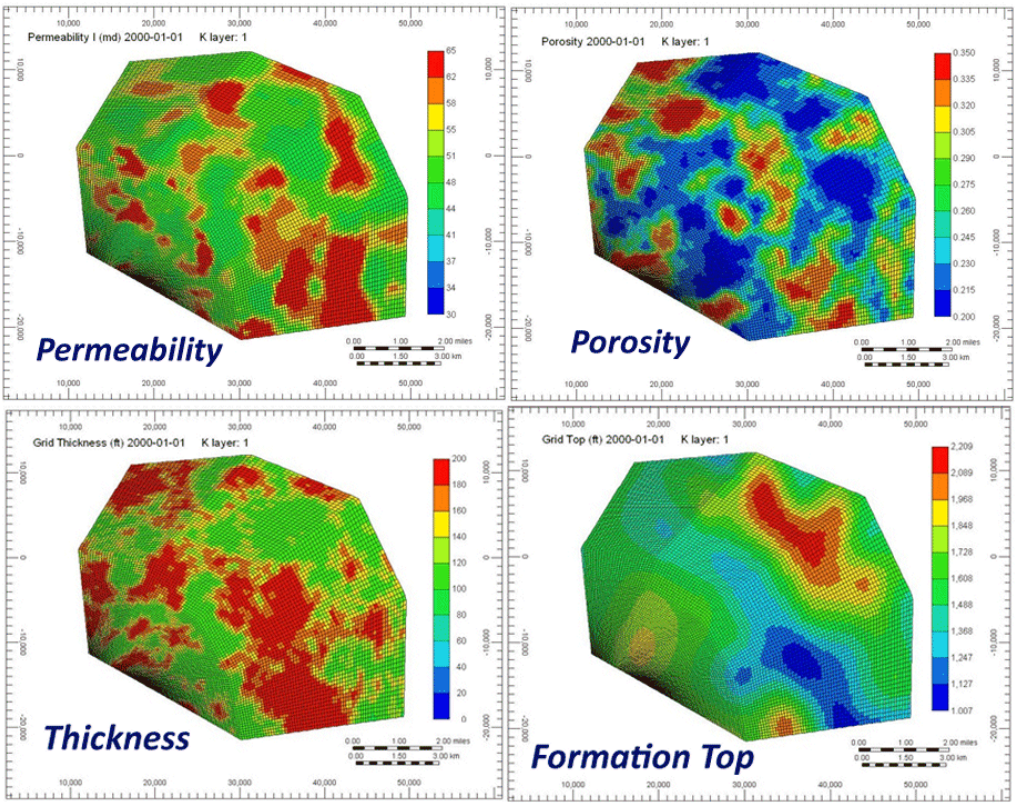

Figure 4. Permeability, Porosity, formation tops and thickness distribution that was used in model #1.

A total of 150 irregularly spaced wells were drilled and produced for 10 years in this filed. In order to investigate the predictive capabilities of Top-Down, Intelligent Reservoir Modeling (TDIRM) 15 of these wells were removed from the analysis to be used as blind verification wells. The objective was to build a TDIRM model using the production rate and well log data (porosity, formation thickness and initial water saturation) from the the remaining 135 wells and then use the model to predict the production from the 15 wells used as blind verification wells. Locations of the 15 wells that were randomly selected as blind verification wells are shown in Figure 5.

Upon completion of the TDIRM analysis that was briefly summarized in the previous section, the TDIRM predicted production of the 15 blind-verification wells. These predictions were compared with the production of these wells generated by the commercial reservoir simulation model.

Table 1. Reservoir Characteristics used in model #1.

Property	Value
Porosity (%)	20 - 35
Permeability I and J (md)	30 - 60
Permeability K (md)	3 - 6
Thickness (ft)	100 - 200
Initial Reservoir Pressure (psi)	2500
Bubble Point Pressure (psi)	600
BHP (psi)	700
Oil Saturation (%)	65
Water Saturation (%)	35
Depth (ft)	Top: 2210 Bottom: 1190
Total field size (acres)	23,340

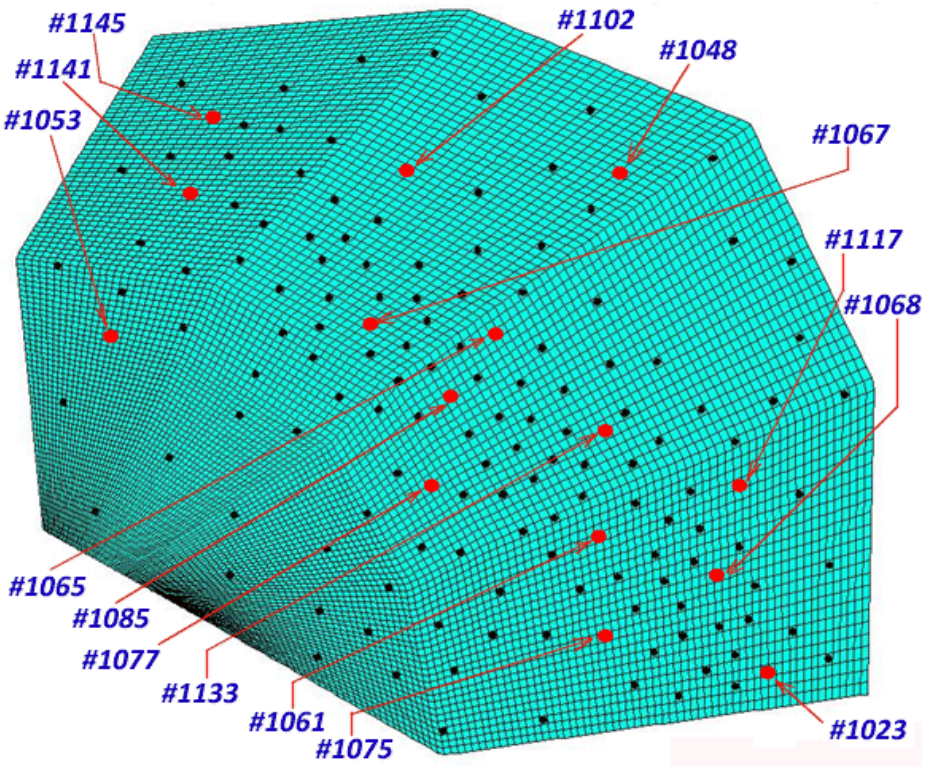

Figure 5. Wells used as blind test in this study for verification of TDIRM are identified in red.

Figure 6 provides the comparative results for four out of the 15 blind-verification wells. The results shown in this figure are typical of the 15 wells. In this figure cumulative production is plotted against time. The blue continuous profile is the cumulative production from each well generated by the commercial simulator and the red dots are the predictions made for these wells by TDIRM using the data (production data and well logs) from the other 135 wells. The TDIRM predictions were made at 3, 6, 9, 12, and 60 months of production. Almost in all cases the predictions made by TDIRM are accurate.

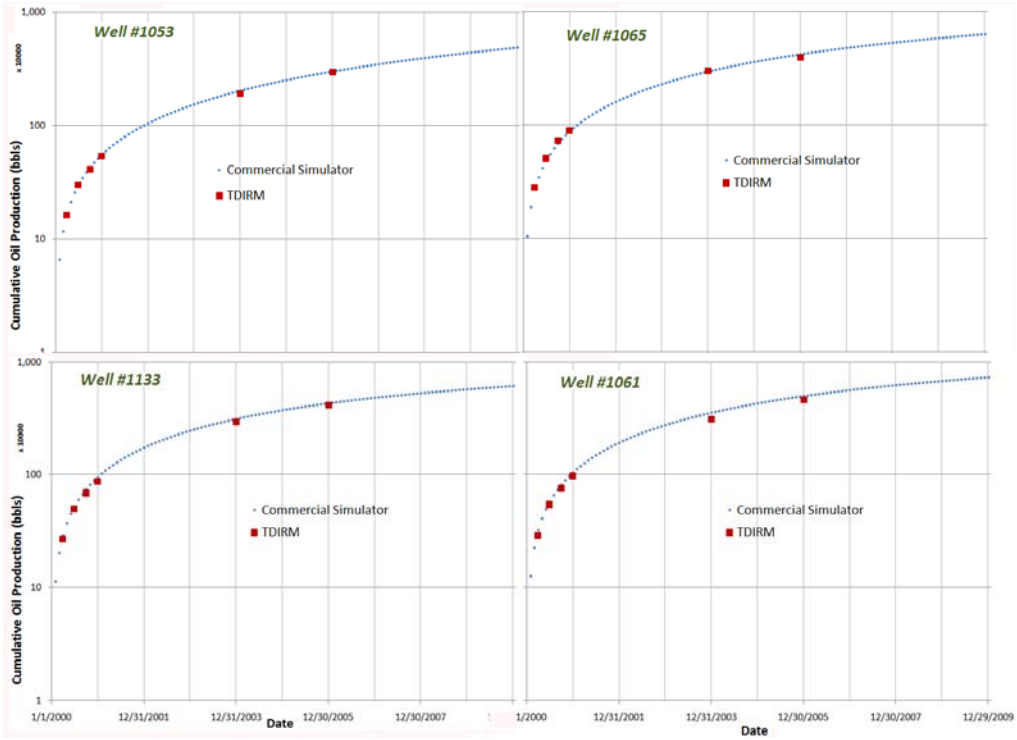

Figure 6. TDIRM's predictions versus the actual (modeled) production profile for four of the 15 wells used as blind test to verify the TDIRM's predictive capabilities.

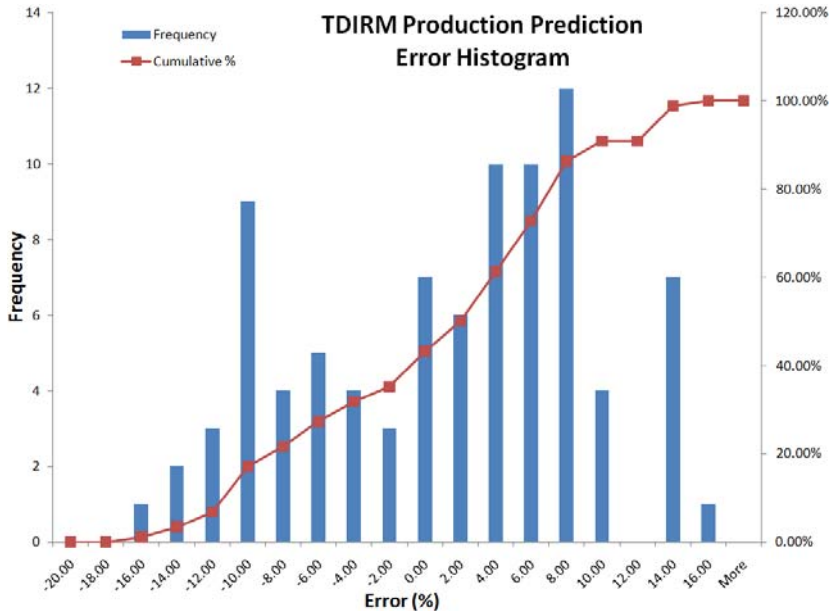

Figure 7. Error statistics for TDIRM production prediction.

To better analyze the accuracy of TDIRM predictions, all the predictions from TDIRM was tabulated and analyzed. Figure 7 provides statistics of TDIRM's predictions throughout this analysis. This figure shows that the range of TDIRM production prediction error is between -17% and +14%. Furthermore, the statistical analysis of the error show that about 75% of the predictions made by TDIRM is within ±10% of the actual values and 36% of the predictions is within ±5% of the productions from the reservoir simulator.

Model #2, Estimating Remaining Reserves

The model used to investigate the capabilities of TDIRM technology in estimating the remaining reserves is similar to the previous model as far as the range of the reservoir characteristics and the number of wells are concerned. There are two major differences between models #1 and #2. First, although the ranges of the reservoir characteristics are the same as shown in Table 2, the reservoir properties distribution are quite different between the two models. The reservoir properties distribution for model #2 is shown in Figure 8 and can be compared to that of model 1 that is shown in Figure 4. Furthermore, the initial reservoir pressure in the model #2 is 4,500 psi that is larger than the initial pressure of model #1. These changes were made in order to investigate the robustness of the TDIRM in making predictions and to evaluate its performance under different reservoir conditions.

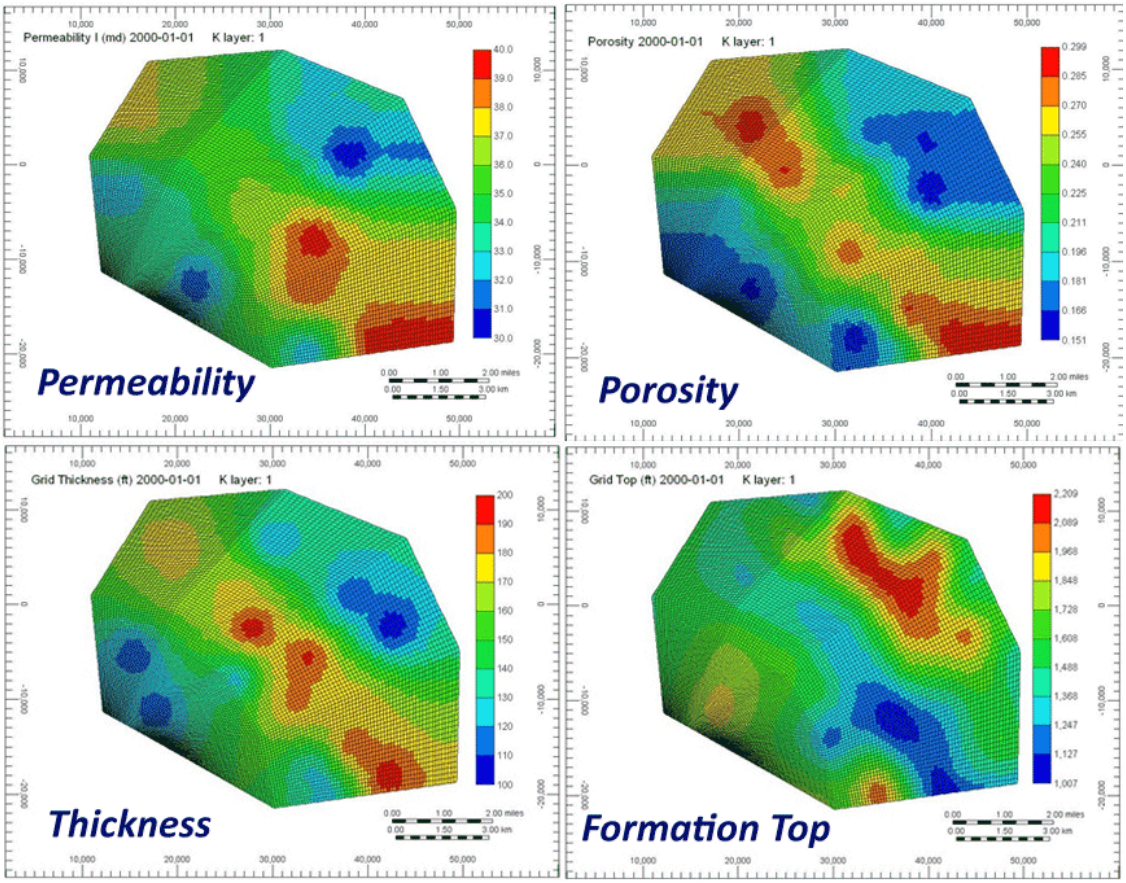

Figure 8. Permeability, Porosity, formation tops and thickness distribution that was used in model #2.

Table 2. Reservoir Characteristics used in model #2.

Property	Value
Porosity (%)	15 - 30
Permeability I and J (md)	30 – 40
Permeability K (md)	3 - 4
Thickness (ft)	100 - 200
Initial Reservoir Pressure (psi)	4500
Bubble Point Pressure (psi)	600
BHP (psi)	700
Oil Saturation (%)	65
Water Saturation (%)	35
Depth (ft)	Top: 2210 Bottom: 1190
Total field size (acres)	23,340

Similar to the previous model a total of 150 irregularly spaced wells were drilled in this reservoir but this time only produced for 8 years. To test the capabilities of TDIRM in estimating the remaining reserves as an important inducator for identification of infill locations, remaining reserves distribution was mapped (generated) by the TDIRM at two different times (after one and eight years of production).

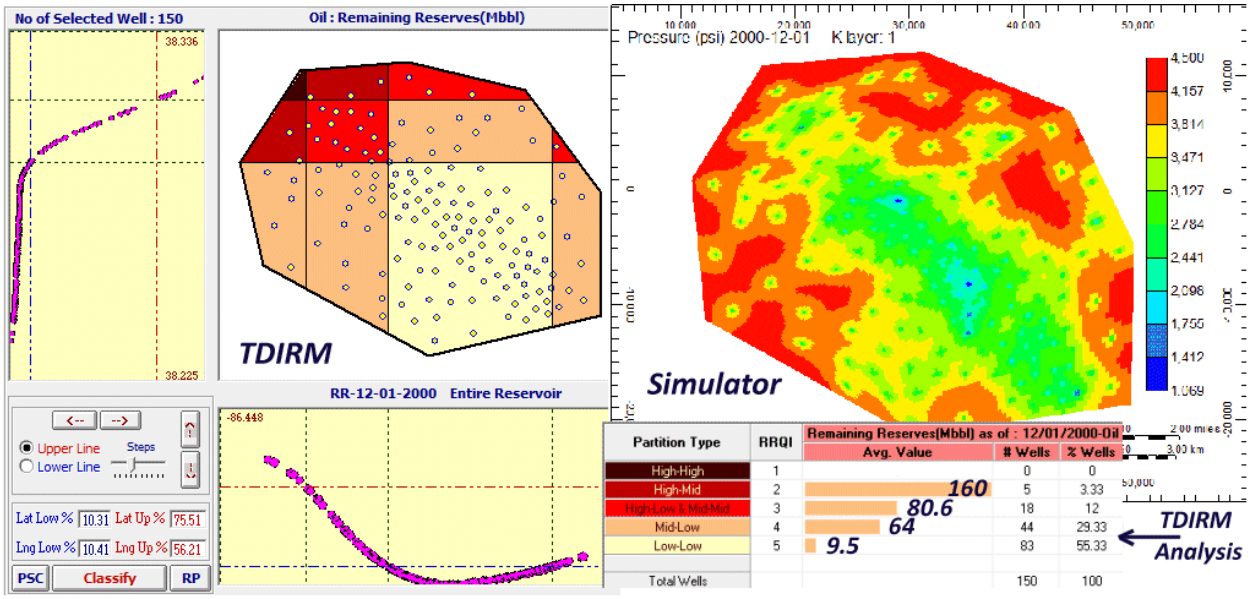

Figure 9. Map of remaining reserves from TDIRM (left) compared to reservoir pressure distribution generated by the commercial simulator, both after one year of production by the 150 wells.

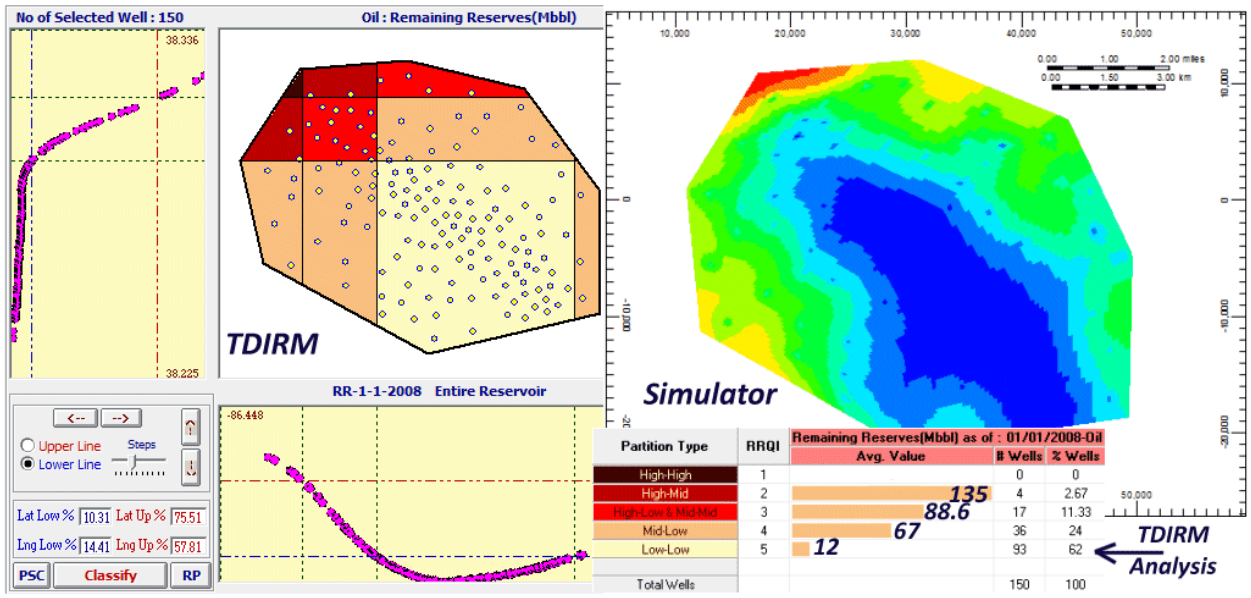

Figure 10. Map of remaining reserves from TDIRM (left) compared to reservoir pressure distribution generated by the commercial simulator, both after eight years of production by the 150 wells.

To investigate the validity of the remaining reserves distributions generated by the TDIRM, similar maps needed to be generated in the reservoir simulator for comparison purposes. It was concluded that to generate similar maps some calculations needed to be performed at the grid block level in the reservoir simulation model. Since such functions were not readily available in the simulator (or we were not say enough in using all available functions in the reservoir simulator) and it had to be formulated, to avoid any potential miscalculation or misinterpretation, it was decided to use a readily available function such as pressure distribution as a valid indicator of a similar property such as remaining reserve. Given the fact that the recovery factor is embeded in the formulation that is used to calculate and map the remaining reserves in TDIRM, reservoir pressure at a given time seemed to be an appropriate measure for comparison between the remaining reserves generated by the TDIRM and the appropriate infill locations in the reservoir simulator model.

Figure 9 and Figure 10 show the comparison between remaining reserves mapped by TDIRM and the reservoir pressure distriution generated by the reservoir simulator after one and eight years of production. In these figures the analyses generated by TDIRM are shown on the left. The pressure distribution in the reservoir generated by the commercial reservoir simulator are shown on the right in each figure. The "TDIRM Analysis" that are shown at the bottom of each figure indicates the average value of remaining reserves in each of the RRQI (Relative Reservoir Quality Index) segments. As mentioned before these number are to be viewed as qualitative indicators rather than quantitavily accurate.

In both figures, the TDIRM analysis indicates no RRQI(1). In Figure 9 the RRQI(2) has a value of 160 Mbbls followed by RRQIs(3) thruogh 5 with average values ranging from 80 to 9 Mbbls after one year of production. After eight years of production, as shown in Figure 10, these values changes slightly but the trend (in both cases) are consistent (lower RRQIs having larger value). In both cases figures show that TDIRM analyses have captured the overall trend of the remaining reserves in the field and can serve as guide for identifying infill locations (especially when aggregated with other TDIRM predictions and analyses). Once again it is important to note that TDIRM analysis was performed only with production rate data and well logs (porosity, thickness, and saturation) and no pressure data was furnished to the TDIRM for this analysis.

Model #3, Estimating the Location of Gas Cap Development

In the previous two models the reservoir was producing above the bubble point. In this model that is quite different from the previous two models, the reservoir is produced below the bubble point in order to allow the formation of gas cap in the reservoir. The objective here is to see if TDIRM analysis can help identify the locations in the reservoir where gas cap is formed. TDIRM's attempt in accomplishing this task is based on two sets of analyses. First, an "intelligent" decline curve analysis is performed (where negative decline in GOR as a function of time is modeled adaptively) and the predictions is made on each well's GOR based on the negative decline analysis. Second, Fuzzy Pattern Recognition is used to identify the patterns in the reservoir where GOR may propagate based on the production pattern of the wells in the reservoir.

Ranges of the reservoir characteristics used in this model are shown in Table 3. The reservoir properties distribution for this model (model #3) is shown in Figure 11 and can be compared to that of models 1 and 2 that were shown in Figure 4Figure 4 and Figure 8Figure 8, respectively. Initial reservoir pressure in this model is 2,500 psi while the bottom hole pressure for the 345 wells producing from this reservoir is kept at 300 psi. Furthermore, the bubble point is set at 1000 psi.

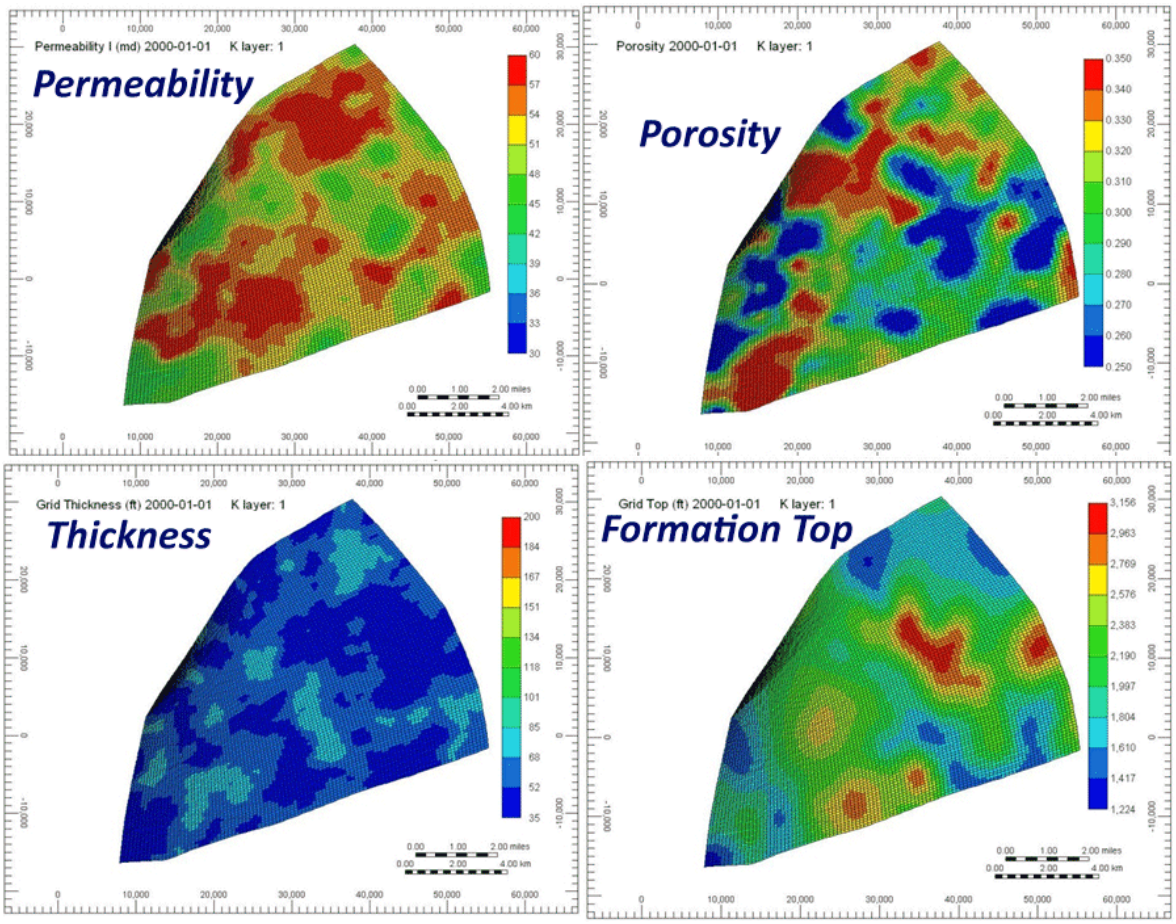

Figure 11. Permeability, Porosity, formation tops and thickness distribution that was used in model #3.

Table 3. Reservoir Characteristics used in model #3.

Property	Value
Porosity (%)	25 - 35
Permeability I and J (md)	30 – 60
Permeability K (md)	3 - 6
Thickness (ft)	35 - 200
Initial Reservoir Pressure (psi)	2500
Bubble Point Pressure (psi)	1000
BHP (psi)	300
Oil Saturation (%)	65
Water Saturation (%)	35
Depth (ft)	Top: 3156 Bottom: 1265
Total field size (acres)	29,750

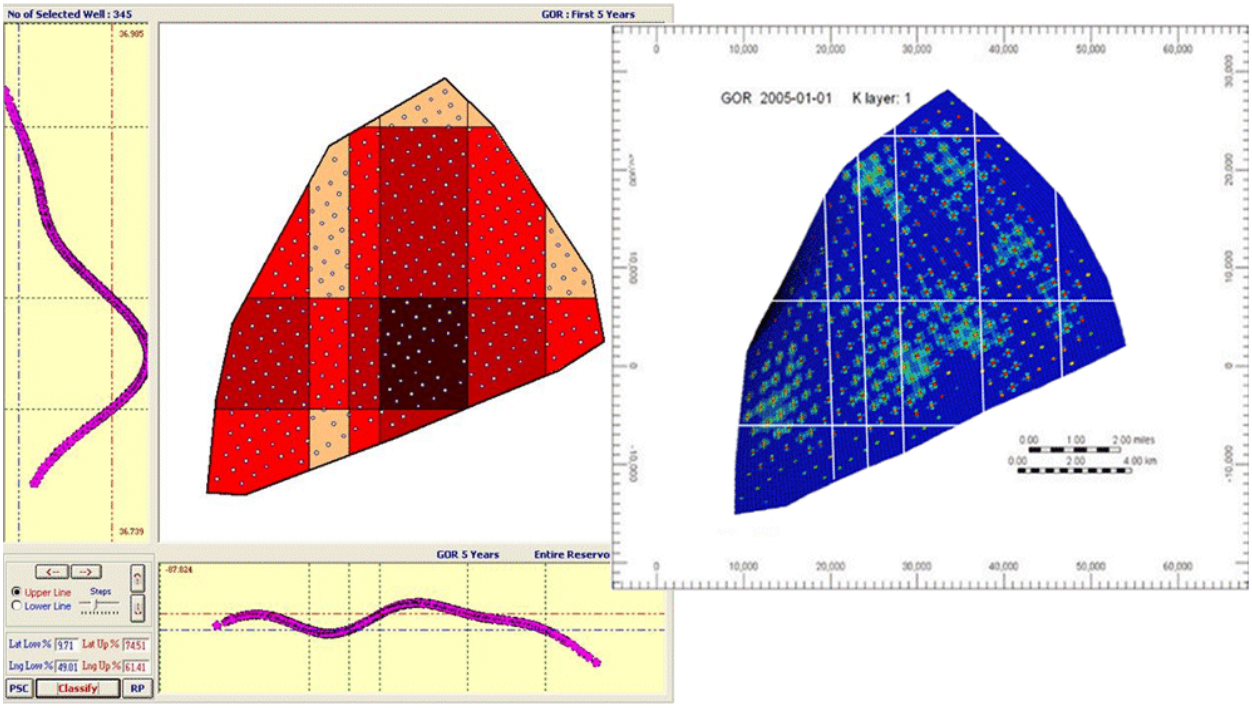

Figure 12. Gas cap analysis by TDIRM and comparison with the reservoir simulator. The gas cap formation is shown after 5 years of production. The delineation lines identified by the TDIRM analysis are projected on gas saturation distribution from the simulator.

To perform this analysis the reservoir was produced for five years. Oil and gas production from all the 345 wells were imported into TDIRM. GOR profiles were calculated and modeled using an "intelligent" decline curve analysis technique that can model, analyze and make predictions based on negative declines. Fuzzy pattern recognition was used in order to map the GOR in the field. Reservoir was delineated in order to identify the pattern of gas saturations in the reservoir. Figure 12Figure 12 shows the result of this analysis. The figure on the left shows the TDIRM analysis and delineation while the figure on the right shows the gas saturation distribution after 5 years of production from the commercial reservoir simulator. In the TDIRM analysis the darker colored areas indicate the location identified with highest probability of gas cap presence in this reservoir. Similarly the lightest colored areas are the locations in the reservoir where no gas cap is being formed. Comparing the TDIRM's analysis and predictions and comparing to the reservoir simulation output of gas saturation after five years of production indicates that TDIRM's prediction are reasonably accurate. This is important to note, since TDIRM has only used production rate data in order to perform its analysis.

Conclusions

In this article it was demonstrated that Top-Down, Intelligent Reservoir Modeling (TDIRM) can provide reasonably accurate results when it is being used to analyze oil producing reservoirs. TDIRM integrates classic reservoir engineering analysis with Artificial Intelligence and Data Mining (AI&DM) techniques such as artificial neural networks, fuzzy set theory, and genetic optimization in order to build reservoir models. In this article it was demonstrated that TDIRM can predict production profiles of new wells based on the production performance and well logs of offset wells, with good accuracy. Furthermore, it was demonstrated that TDIRM can be used as a tool to locate remaining reserves in the reservoir and to identify the presence of gas cap. It is important to note that TDIRM is capable of performing these tasks while only using production rate and well log data. It was also mentioned that some results from the TDIRM (especially those from Fuzzy Pattern Recognition) are qualitative in nature and should be used accordingly.

Acknowledgement

Authors would like to acknowledge and thank Computer Modeling Group for providing West Virginia University with license to use their reservoir simulation software, IMEX.

Bibliography

1. *Top-Down Intelligent Reservoir Modeling (TDIRM); a New Approach in Reservoir Modeling by Integrating Classis Reservoir Engineering with Artificial Intelligence and Data Mining (AI&DM).* **Mohaghegh, S. D.** Denver, Colorado : AAPG, 2009.

2. *An Integrated Technique for Production Data Analysis (PDA) with Application to Mature Fields.* **Gasakri, R., Mohaghegh, S.D. and and Jalali, J.** 4, s.l. : SPE Production and Operations Journal, 2007, Vol. 22. pp. 403-426.

3. *Field-Wide Reservoir Characterization Based on a New Technique of Production Data Analysis.* **Mata, D. and Gaskari, R. and Mohaghegh, S.D.** Lexington, Kentucky : SPE 111205 Eastern Regional Conference, 2007.

4. *Virtual Intelligence Applications in Petroleum Engineering: Part 1 ; Artificial Neural Networks.* **Mohaghegh, S.D.** s.l. : SPE Journal of Petroleum Technology, Distinguished Author Series, September 2000. pp 64-73.

5. *Virtual Intelligence Applications in Petroleum Engineering: Part 2 ; Evolutionary Computing.* **Mohaghegh, S. D.** s.l. : Journal of Petroleum Technology, Distinguished Author Series , October 2000. pp 927-939.

6. *Virtual Intelligence Applications in Petroleum Engineering: Part 3 ; Fuzzy Logic.* **Mohaghegh, S.D.** s.l. : Journal of Petroleum Technology, Distinguished Author Series , November 2000. pp 82-87.

7. **Schlumberger.** ECLIPSE Reservoir Engineering Software. [Online] http://www.slb.com/content/services/software/reseng/index.asp?entry=ad_google_sis_eclipse&gclid=CMH40ZKnsJsCFU1M5QodS1XhDw.

8. **Group, Computer Modeling.** IMEX: IMplicit-EXplicit Black Oil Simulator. [Online] http://www.cmgroup.com/software/imex.htm.

9. **Erwig, M.** *The graph Voronoi diagram with applications.* s.l. : Copyright © 2000 John Wiley & Sons, Inc., 2000.

SPE 132621

New Insight into Integrated Reservoir Management using Top-Down, Intelligent Reservoir Modeling Technique; Application to a Giant and Complex Oil Field in the Middle East

Amirmasoud Kalantari-Dahaghi, Shahab D. Mohaghegh, Yasaman Khazaeni, SPE, West Virginia University

Copyright 2010, Society of Petroleum Engineers

This paper was prepared for presentation at the SPE Western Regional Meeting held in Anaheim, California, USA, 27–29 May 2010.

This paper was selected for presentation by an SPE program committee following review of information contained in an abstract submitted by the author(s). Contents of the paper have not been reviewed by the Society of Petroleum Engineers and are subject to correction by the author(s). The material does not necessarily reflect any position of the Society of Petroleum Engineers, its officers, or members. Electronic reproduction, distribution, or storage of any part of this paper without the written consent of the Society of Petroleum Engineers is prohibited. Permission to reproduce in print is restricted to an abstract of not more than 300 words; illustrations may not be copied. The abstract must contain conspicuous acknowledgment of SPE copyright.

Abstract

This paper demonstrates the validity of a recently developed reservoir modeling technique called "Top-Down, Intelligent Reservoir Modeling" (will be referred to Top-Down Modeling for short). This new modeling technology integrates reservoir engineering analytical techniques with Artificial Intelligence & Data Mining (AI&DM) in order to arrive at an empirical, cohesive and spatiotemporally calibrated full field model. The model is used to predict reservoir performance in order to recommend field development strategies. One of the distinctive features of this technology is its data requirement for analysis. Although Top-Down Modeling can incorporate almost any type and amount of data that is available in the modeling process, it only requires monthly production rate and some well log data (porosity, initial water saturation and thickness) in order to start the analysis and provide a full field model. Presence and incorporation of other types of data such as core analysis, pressure data, reservoir characteristics and seismic data can and will increase the accuracy and validity of the developed model.

In this work, we apply Top-Down Modeling to a large and complex Oil field in the Middle East that produces from a combination of clastic and carbonate formations. Production rates and well log data from 210 wells have been analyzed and imported into the Top-Down Modeling software to develop a new empirical reservoir model and make predictions on new well performance and potential infill locations. Results from Top-Down Modeling analyses are compared with results concluded from a comprehensive reservoir management study (that included use of large amount and various types of data and a commercial numerical reservoir simulator) performed by an IOC. Analytical reservoir engineering techniques used in the Top-Down Modeling presented in this study include production decline analysis, volumetric reserve and recovery factor estimations and are integrated with Voronoi graph theory, geostatistics, two-dimensional Fuzzy Pattern Recognition (FPR), and discrete, data driven predictive modeling.

The resulting full field Top-Down Modeling is used to identify the distribution of the remaining reserves, sweet spots for infill locations and under-performer wells and also identify the locations in the reservoir where gas cap is formed. Furthermore, the fullfield model is used to predict new well's performance.

Introduction

Top-Down Modeling approaches reservoir simulation and modeling from an opposite angle compared to conventional reservoir simulation. Top-Down Modeling attempts to provide insight into fluid flow in the reservoir by starting with actual field measurements such as well production history and well logs. Other data such as core analysis, well test, and seismic can be used in Top-Down Modeling in order to increase model accuracy. Although not intended as a substitute for the conventional reservoir simulation of large, complex fields, this unique approach to reservoir modeling and management can be used as an alternative to traditional reservoir simulation and modeling in cases where performing conventional modeling is cost and man-power prohibitive specially for independent producer of mature fields. In cases where a conventional model of a reservoir already exists, Top-Down Modeling may be considered a compliment to the conventional technique that provides

an independent look at the data coming from the reservoir/wells for optimum development strategy and recovery enhancement. Time and resources required to perform Top-Down Modeling is only a small fraction of that required for a conventional reservoir simulation and modeling.

In this study, Top-Down Modeling is performed on a giant and complex oilfield in the Middle East that is producing for half-century. The reservoir has been producing under natural depletion, with a strong water drive maintaining the reservoir energy. The formation is complexes intermix of clastics and carbonates of variable reservoir qualities. Like many of such reservoirs in the Middle East, this prolific reservoir is highly complex in its flow behavior. Recently an IOC performed a comprehensive field development study on this field. The conclusions reached by the IOC study included recommendations on infill locations. Upon completion of the Top-Down Modeling, the conclusions from the two studies are compared.

Top-Down, Intelligent Reservoir Modeling may be used as an alternative to conventional reservoir simulation and modeling in cases where reservoir data is scarce or when the resources are limited. On the other hand, in cases where a conventional reservoir simulation model already exists for a given asset such as this study, Top-Down Modeling can be used as an independent and complementary modeling technology. Time and resources required to perform Top-Down Modeling is only a small fraction of that required for a conventional reservoir simulation and modeling.

Methodology

The IOC in charge of this study constructed a geological model for this field with the aim to obtain the best possible conceptual model of flow heterogeneities at all scales. The three dimensional geological model was developed based on stochastic modeling techniques and formed the basis for the simulation model used for history matching and production forecasting. This model is the basis for estimation of initial and remaining hydrocarbons volumes in the reservoir. Results obtained from of this comprehensive reservoir simulation and modeling using conventional reservoir simulator have been used to examine the validity of Top-Down Modeling.

Top-Down, Intelligent Reservoir Modeling starts with well-known reservoir engineering techniques such as Decline Curve Analysis, Type Curve Matching, and (single-well) production History Matching as well as Volumetric Reserve Estimation, and calculation of Recovery Factors. All these analyses are performed on individual wells. Using statistical techniques, multiple Production Indicators (First 3, 6, and 9 month cumulative production as well as 1, 3, 5, and 10-year cumulative oil, gas and water production and Gas Oil Ratio and Water Cut) are calculated. To model the behavior of non-declining production characteristics such as GOR and water cut, intelligent decline curve analysis is performed on Gas Oil Ratio where a negative decline is the normal behavior. The “Intelligent” decline curve analysis refers to a process that is specific to Top-Down Modeling. It is performed using an adaptive time-series modeling techniques that trains itself based on the existing data and predicts system behavior in specific length of time in future.

In order to identify segments of the reservoir that are impacted (quantifiably, from a production point of view) by the production from each well, a series of Voronoi cells are generated. Hydrocarbon pore volume as well as time and amount of production determine the extent of each Voronoi cell. Figure1 shows the process of generating Voronoi cells in Top-Down Modeling and association of each Voronoi cell with a collection of Cartesian cells that will be used in order to build a high-level earth model. In the process that is shown in Figure 1 the well locations are plotted (a), a Cartesian grid is generated (b), the outer boundary (structure) of the reservoir is identified (c), and finally the Voronoi cells are generated (d). The Voronoi cells are then associated with the relevant Cartesian grids for any given well. It should be noted that Voronoi grids are dynamic and are modified as a function of time.

Geostatistical techniques such as Kriging or Sequential Gaussian Simulation are used for the generation of a high-level earth model. Using the earth model and the associated Voronoi cells, volumetric reserves are estimated. By integrating the volumetric reserves with the results of the decline curve analysis, well-based and field-wide recovery factors are calculated. Optimization of the field-wide recovery factor is one of the objectives of the Top-Down, Intelligent Reservoir Modeling.

A large volume of data that is representative of the reservoir behavior in both space and time is generated at the conclusion of the above analyses. It is important to note that these spatiotemporal snap shots of reservoir behavior are discrete representatives of fluid flow in the reservoir, while a full-field model must possess a continuous nature in order to be a useful tool for reservoir management. One of the contributions of Top-Down Modeling is the ability of fusing a large number of discrete data and single-well models into a cohesive and continuous full field model. This process is performed using Fuzzy Pattern Recognition (FPR) integrated with a carefully orchestrated ensemble of artificial neural networks. Therefore, the essence of Top-Down Modeling relates to its ability in pattern discovery and predictive, data driven modeling based on a database that include discrete snap shots of spatiotemporal reservoir behavior.

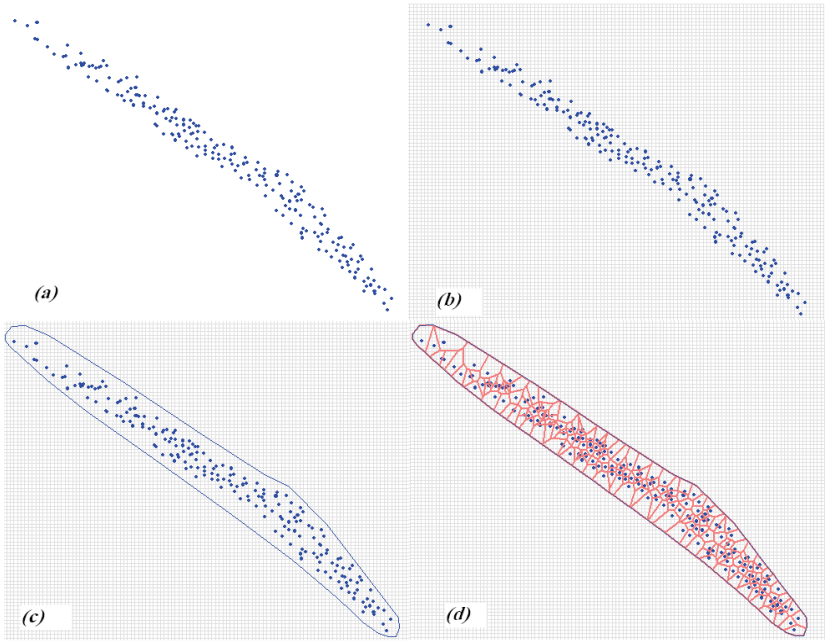

Figure 1.Generating Voronoi cells for the wells during the Top-Down Modeling analysis process

The objective of pattern recognition as part of data mining is to extract non-trivial, implicit, previously unknown, and potentially useful information and patterns from the spatiotemporal database generated in the preliminary steps of Top-Down Modeling. This process includes generation of fuzzy patterns from actual data that is usually quite scattered and a trend cannot be observed in cross plots of attribute (such as 3 months cumulative and 5 years cumulative production) versus latitude and longitude. Figure 2 shows the fuzzy pattern partitioning for the first 3 month and the first 5 years of cumulative production in which the reservoir has been divided into different regions qualitatively.

In the two dimensional maps (Figure 2) reservoir is delineated with Relative Reservori Quality Index (RRQI) being the first 3 month and the first 5 years of cumulative production. The delineation shown in this figure are indicated by colors. Higher quality regions (regions with high values of cumulative production) are shown in darker colors and as the average value of cumu.production reduces in each region, the color becomes increasing ly lighter. The difference between these two figures shows the depletion in the reservoir and identifies the parts of the field that still have potential for more recovery.

Top-Down, Intelligent Reservoir Model is calibrated using the most recent set of wells that have been drilled in the field through a process that is analogous to conventional history matching practices. The calibrated model is then used for field development strategies and reservoir management to improve and enhance hydrocarbon recovery.

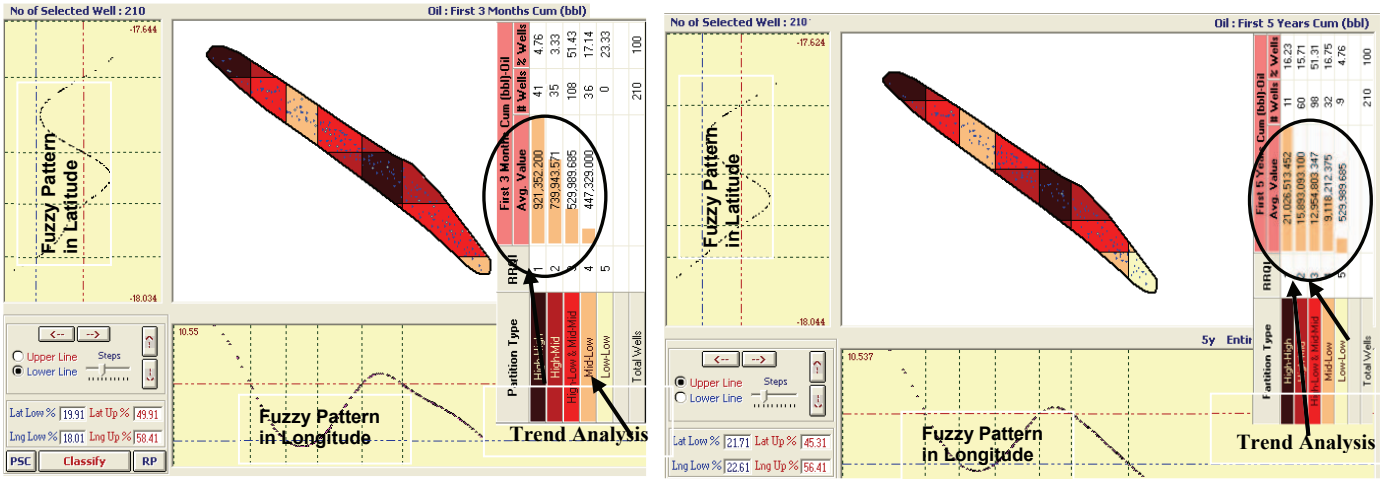

Figure 2. Results of Fuzzy Pattern Recognition (Top-Down Modeling) showing the sweet spots in a field after the first 3 months (left) and 5 years of production (right).

Results from Fuzzy Pattern Recognition (FPR) process along with the high level earth model are used in developing the final cohesive model. In the following sections, the results of Top-Down Modeling application on the aforementioned oilfield are discussed.

Figure 3 shows the geostatistical distribution of porosity, permeability and water saturation for entire reservoir. As it is shown in the following graphs the middle section of reservoir has higher value in terms of storativity and flow conductivity. Also the middle part has lower water saturation.

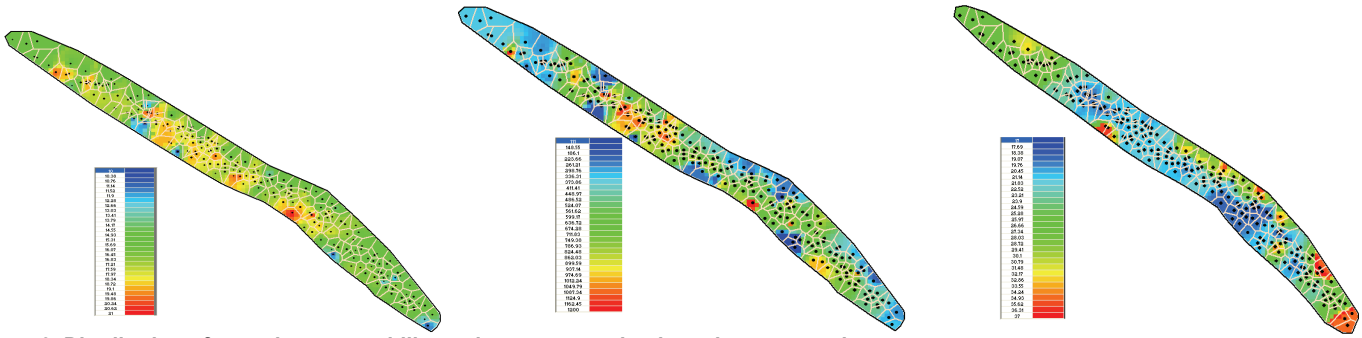

Figure3. Distribution of porosity, permeability and water saturation in various reservoir zones

Estimating the Location of Gas Cap Development

The objective here is to see if Top-Down Modeling can help identify the locations in the reservoir where gas cap is formed.

According to reservoir simulation results (Full field study) the gas cap has primarily expanded in a south-east direction. In addition, there is evidence of a secondary gas cap in the reservoir.

There are two gas caps which are in communication (Primary and Secondary). The GOC is therefore, tilted along the main axis of the anticline. The southern gas cap (Primary) has however expanded deeper than the central gas cap (Secondary). There is an imbalance between two gas caps may be explained by the combined lack of aquifer support from the east, and the relatively high oil production from that section of the reservoir.

Wells in this formation have experienced free gas breakthrough. These wells are identified through an increased well head pressure (WHP), and are subsequently shut in when the WHP increase beyond the maximum working pressure of the wellhead. When the wells are put on production, at a later time, they may produce gas-free for an extended period. There is evidence of a secondary gas cap in the central part of the field.

Figure 4 represent the gas cap formation as a function of time. As shown in this figure, primary gas cap has been generated at around the fifth years of production. Moreover, the secondary one has been formed during the nineteenth years of production.

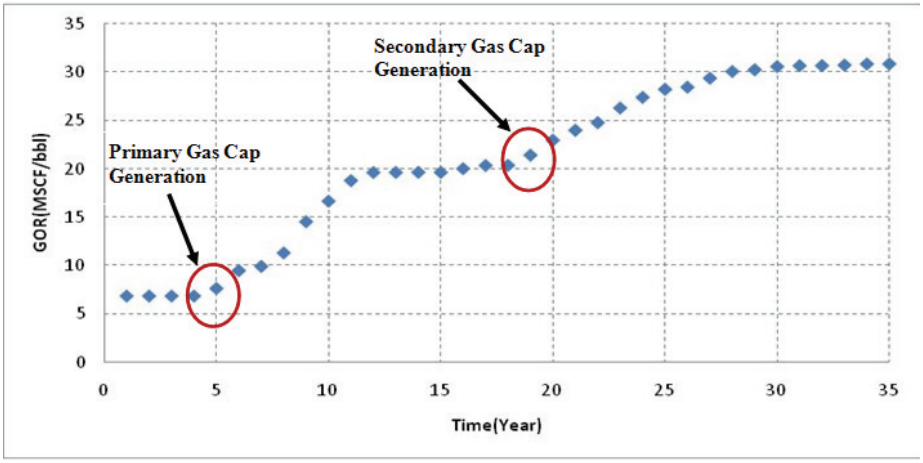

Figure 4.Identification of primary and Secondary Gas cap generation based on total Field GOR.

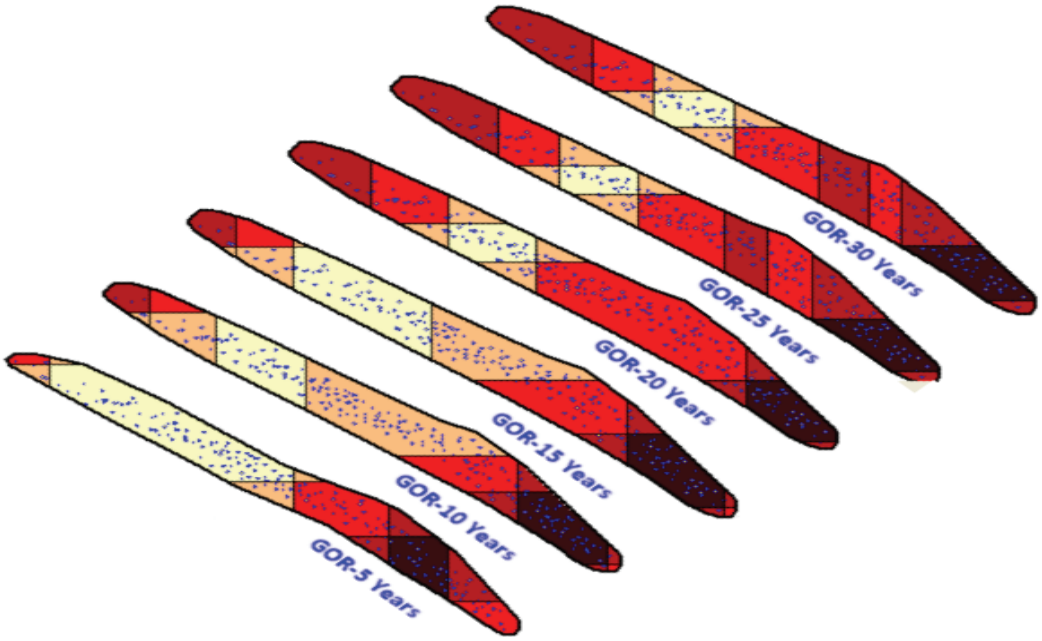

Figure 5.Results of Fuzzy Pattern Recognition (TDIRM) showing the distribution of Gas oil ratio (GOR) in various reservoir zones as a function of time.

Oil and gas production from all 210 wells were used to perform Top-Down Modeling. GOR profiles were calculated and modeled using an "intelligent" decline curve analysis technique, which can model, analyze, and make predictions based on negative declines. Fuzzy pattern recognition was used in order to map the GOR in the field. Reservoir was delineated in order to identify the pattern of gas saturations in the reservoir.

Figure 5 shows the distribution of GOR as a function of time in various reservoir zones. In Top-Down Modeling, the darker colored areas indicate the location identified with highest probability of gas cap presence in this reservoir. Similarly, the lightest colored areas are the locations in the reservoir where no gas cap is being formed. Comparing the Top-Down Modeling's analysis and predictions to the reservoir simulation result indicates that Top-Down Modeling has predicted the primary and secondary gas cap formation with reasonable accuracy.

Figure 6 clearly shows that reservoir is not behaving the same in all zones. The upper part of reservoir has a very low GOR respect to the lower section even though the gas oil ratio is increasing through the reservoir as time goes on. Red dots represent the GOR for entire reservoir.

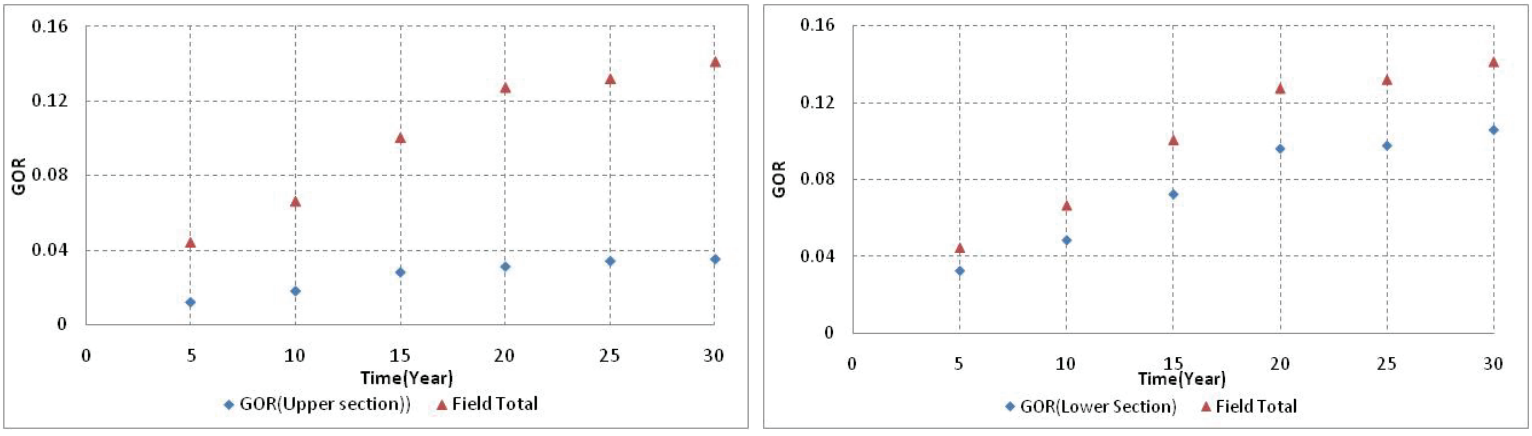

Figure6. Gas oil ratio (GOR) variation in upper (left) and lower (right) section of reservoir

Water Cut Analysis

The current reservoir performance indicates that water production is limited, but is on the increase. Figure 7 shows the water cut distribution as a function of time in various reservoir segments. In Figure 7 the darker colored areas indicate the location identified with highest probability of water production in this reservoir. Similarly, the lightest colored areas are the locations in the reservoir with little or no water production. Please note that the extent of each identified section of the reservoir (sections of the reservoir with similar water production behavior) changes as a function of time.

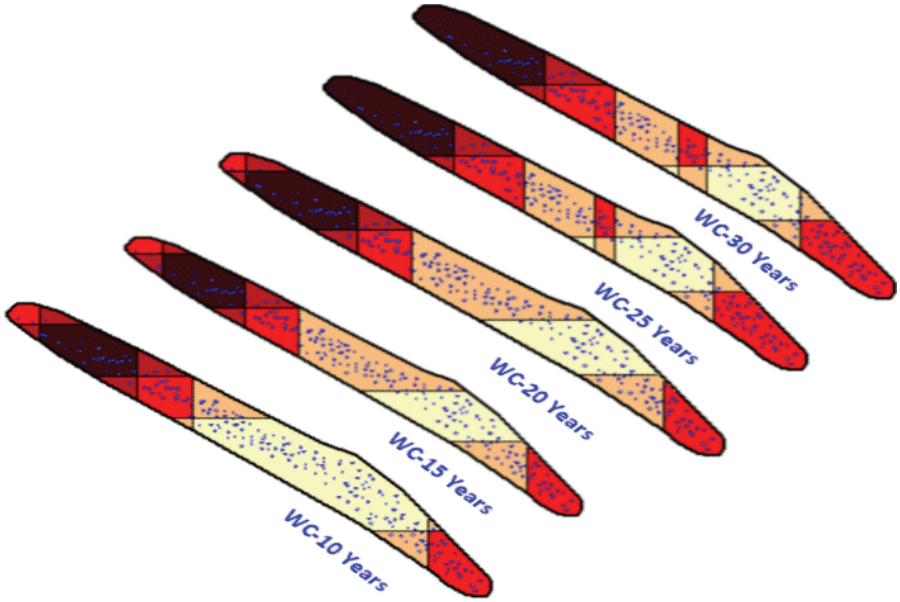

Figure 7.Results of Fuzzy Pattern Recognition (TDIRM) showing the distribution of water cut (WC) in various reservoir zones as a function of time.

As illustrate in Figure 8 the upper section of reservoir has higher water cut respect to the lower section. Red dots represent the field water cut for entire reservoir.

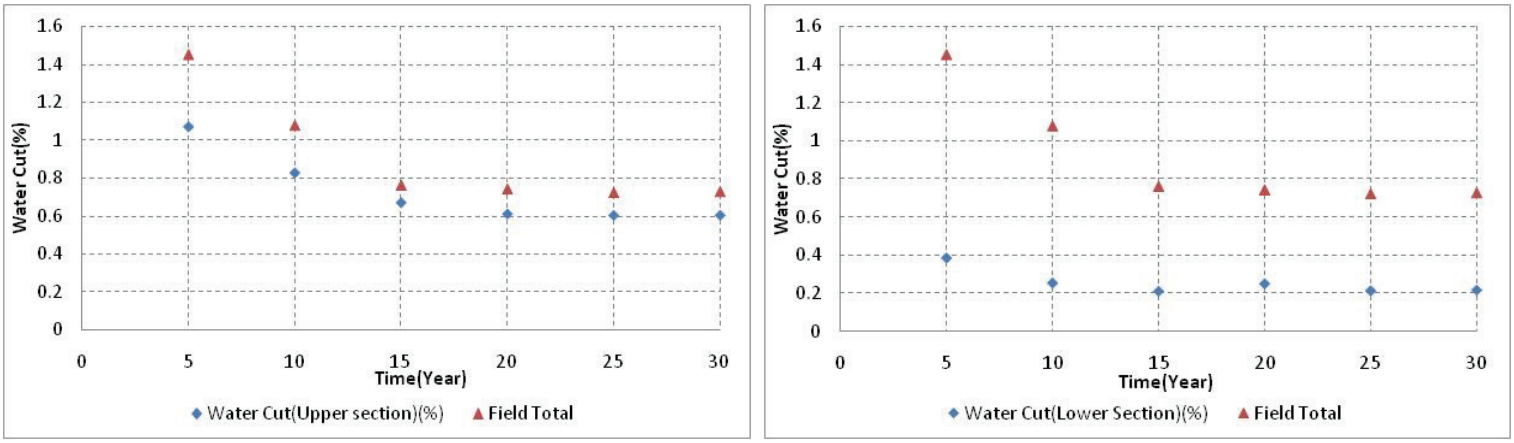

Figure8. Water cut (WC) variation in upper (left) and lower (right) section of reservoir

Estimating Remaining Reserves

Estimation of remaining hydrocarbon in place is an important step in any reservoir analysis since it contributes significantly to decision making during reservoir management. It plays an important role in proposing new infill drilling locations. In this part of study, the result of estimated remaining reserve with Top-Down Modeling has been compared with that of conventional reservoir simulation-based analysis (Figure9).

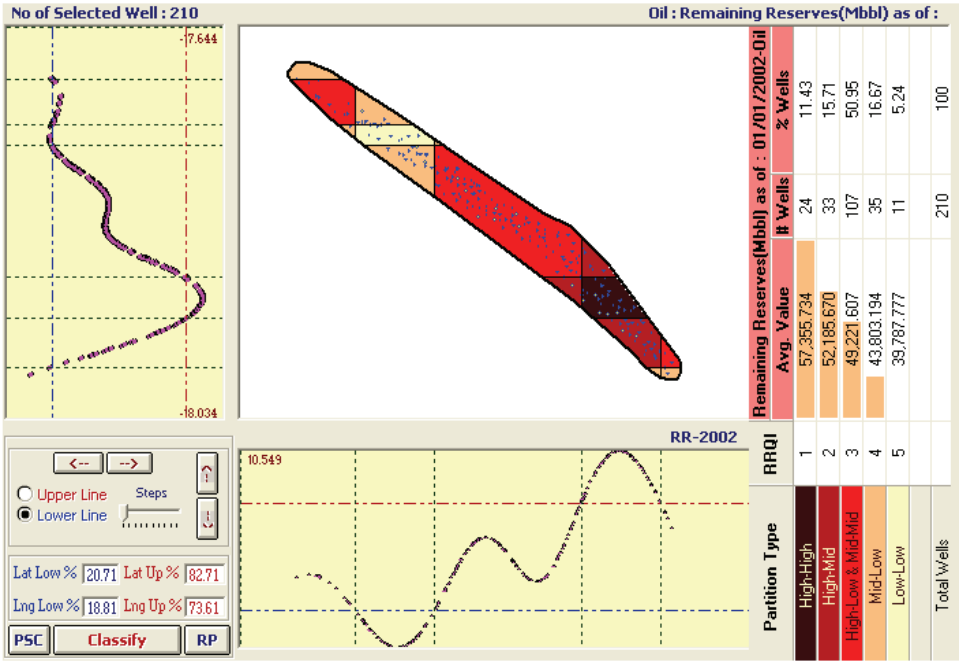

Figure9.Results of Fuzzy Pattern Recognition (TDIRM) (Left) with correspondence conventional reservoir simulation model(right) showing the distribution of remaining oil in various reservoir zones at end historical production period

As represented in Figure 9 the reservoir simulation indicates large areas of remaining reserves in the southeast and central areas of the reservoir. The red spots in this figure (right) indicate highest remaining oil columns, which have good correspondence to the dark areas in fuzzy pattern recognition model of Top-Down Modeling.

Figure 10 shows the results of fuzzy pattern recognition of Top-Down Modeling that identify remaining reserve as function of time (if no new wells are not drilled).

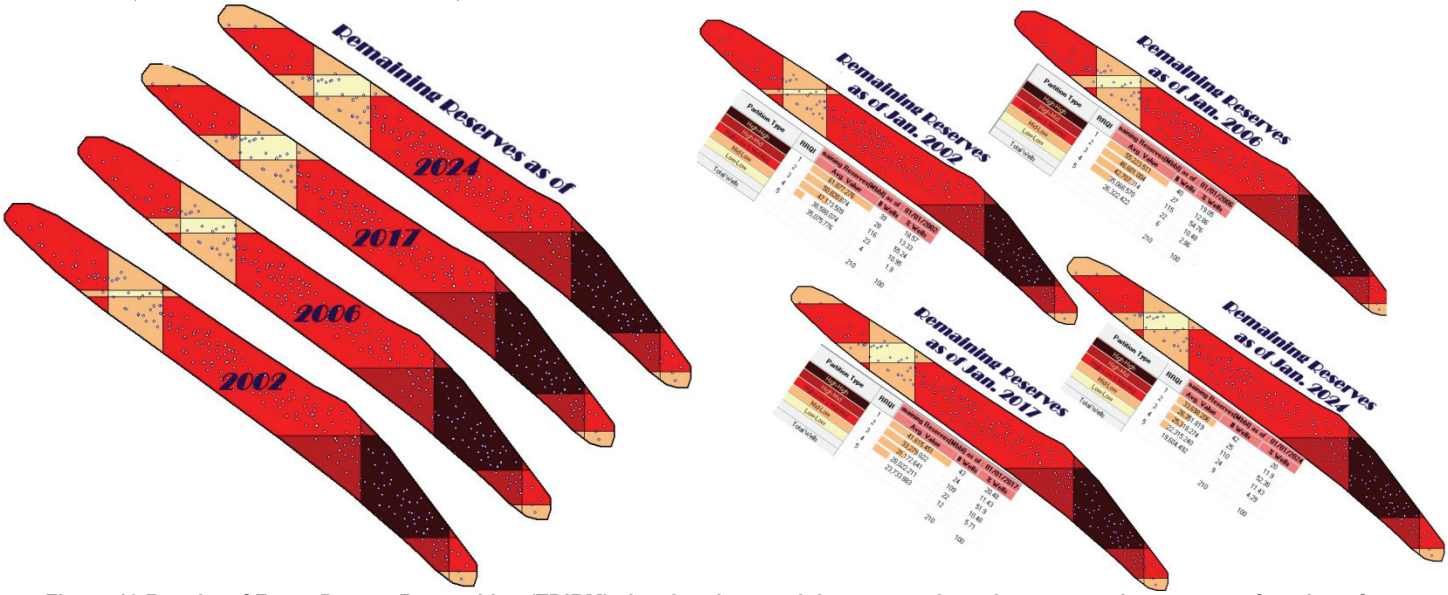

Figure 10.Results of Fuzzy Pattern Recognition (TDIRM) showing the remaining reserve in various reservoir zones as a function of time.

Proposed infill drilling locations

The final goal of building high-resolution geological model, solving flow equations and in one word creating a complex reservoir simulation model and employing the other reservoir management techniques is to predict the sweet spots in the reservoir in terms of remaining hydrocarbon in place, storativity and flow conductivity.

Figure11 demonstrate the proposed infill drilling location, which are based on the result of conventional reservoir simulation model. In this period of drilling, the drainage targets are set to the north-eastern part and middle of reservoir that has higher remaining oil, which can be simply identified using Top-Down Modeling. According to Top-Down Modeling the northeast and middle section of the reservoir have the higher remaining reserves. The upper part of reservoir has a higher permeability but because this area has problem with water production has not been proposed for drilling.

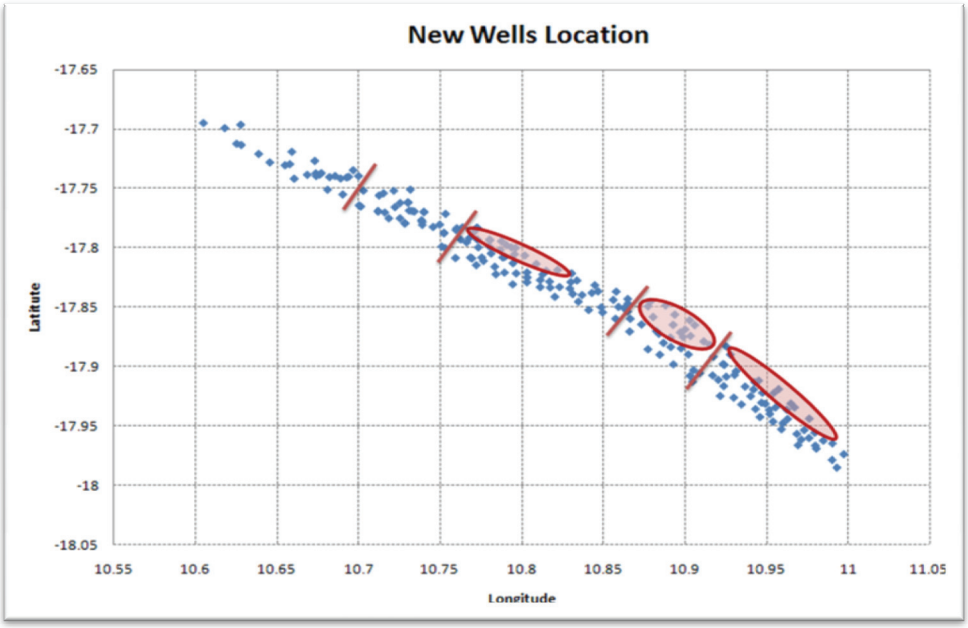

Figure 11.Proposed infill drilling locations

Model Calibration and Validation

One of the steps that are taken upon building the Top-Down, Intelligent Reservoir Model is to calibrate and validate the model. To calibrate the Top-Down models about 10 % of wells for are removed from the analyses. This constitutes removal of 21 wells from the analysis. The models are developed using the remaining 189 wells. The objective is to make sure that the Top-Down model can predict the 5 year cumulative production for these removed wells (blind data set). The results are shown in Table 1 .

For example in table 1 the four Relative Reservoir Quality Indices (RRQI) are shown as well as the model results that indicates the prediction for the blind/validation wells. As indicated in this table the Top-Down model predicted that the average 5 year cumulative production for wells drilled in the RRQI “1” (the darkest area) will be more than 18 MM bbl. Two bind wells (wells removed from the analysis and used as validation wells) in RRQI “1” have an average 5 year cumulative production of more than 23 MM bbl (correct prediction).

Furthermore, the Top-Down model predicted that the average 5 year cumulative production for well in the RRQI “2” will be between 14.8 MM and 18.1 MM bbl. Table 1 shows that there were 8 wells drilled in RRQI “2” and the average 5 year cumulative production for this well was 17.3 MM bbl (correct prediction).

The Top-Down model predicted that the average 5 year cum. for 3 wells drilled in the RRQI “3” will be between 13.3 MM bbl and 14.8 MM bbl and the average 5 Year cum. For wells drilled in this RRQI turned out to be 14.4 MM bbl(correct prediction).

For RRQI “4” ,the average 5 year cumulative production for wells drilled in the RRQI “4” were predicted to be between 9.4 and 13.3 MM bbl while the 8 wells drilled in RRQI “4” had an average 5 year cumulative production of 7.5 MM bbls, so the Top-Down Modeling over-estimates the results for this RRQI .

Table1. Results of Top-Down modeling

5 Year Cumulative Production(bbl)					
	Model Results			Removed Wells	
RRQI	More Than	&	Less than	Average 5 Yr Cum.	No. of Wells
1	18,141,338			23,306,515	2
2	14,795,838	&	18,141,338	17,317,949	8
3	13,339,641	&	14,795,838	14,417,578	3
4	9,496,060	&	13,339,641	7,471,294	8
5			9,496,060	Total	21

Predictive modeling

A predictive model has been developed using neural networks. Networks has been trained by backpropagation technique to be able to predict the future production of this field. After completing the neural network training and verification process the predictive model has been used to forecast the cumulative production of two most recent drilled wells (Figure 12), therefore those wells have been removed from the modeling process in order to verify the accuracy of model in time basis. These wells have not been used in neural network training process. Production predicted of these two wells is compared with the real production history. Results are shown in Figure13. As shown in this graph (Figure 13) a reasonably good prediction of cumulative production is achieved.

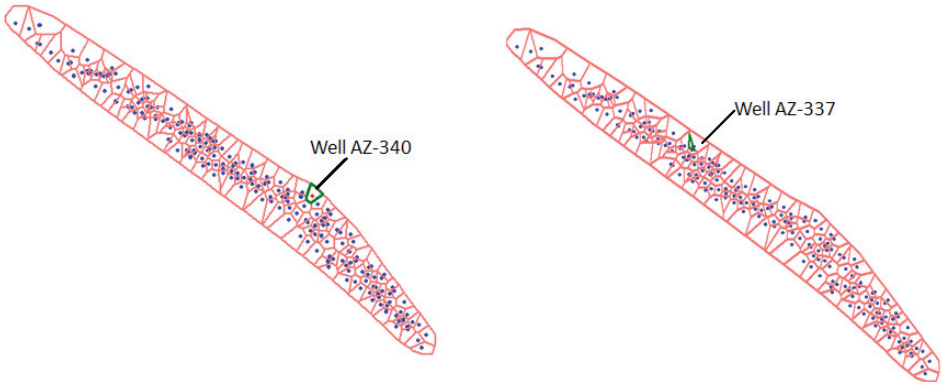

Figure 12.Two Verification Wells' Locations

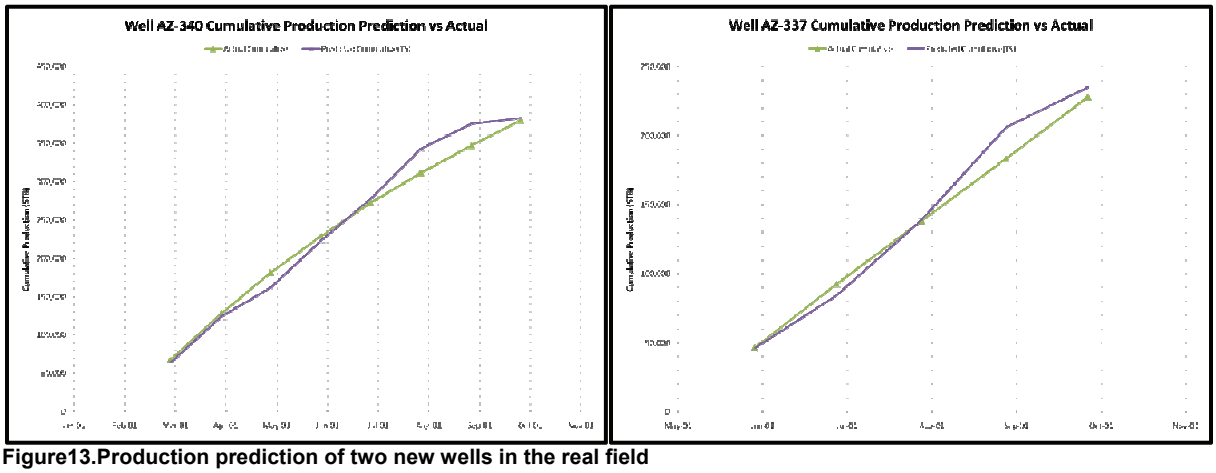

Figure13.Production prediction of two new wells in the real field

Conclusion

In this study, a new reservoir modeling technology has been applied to a giant and complex oilfield. This new modeling technology, Top-Down, Intelligent Reservoir modeling incorporates Artificial Intelligent and Data Mining techniques such as data driven Neural network modeling and fuzzy pattern recognition in conjunction with classic reservoir engineering analyses in order to combine single well analyses into a cohesive full field model.
Top-Down intelligent reservoir modeling allows the reservoir engineer to plan and evaluate future development options for the reservoir and continuously updated the model that has been developed as new wells are drilled and more production data and well logs become available.

Top-Down Modeling demonstrate its capability by estimating reservoir and petrophysical parameters, remaining reserve, gas cap location predication, proposed infill drilling locations and estimation new well performance with acceptable accuracy in comparison with the result of fullfield analysis, which has been done by an IOC utilizing conventional reservoir simulator.

One of the important advantages of Top-Down intelligent reservoir modeling is its ease of development. It is designed so that an engineer or a geologist will be able to comfortably develop a Top-Down model in a relatively short period with minimum amount of data (only monthly production data and some well logs are enough to start modeling). This new technique can be performed on the other types of oil and gas reservoirs. (Conventional and Unconventional resources)

Our Studies have shown that Intelligent Top-Down Reservoir Modeling holds much promise and can open new door for developing reservoir models using field measurement data.

References

1. Virtual Intelligence Applications in Petroleum Engineering: Part 1; Artificial Neural Networks. S.D.Mohaghegh. Journal of Petroleum Technology,Distinguished Author Series, 2000.
2. Virtual Intelligence Applications in Petroleum Engineering: Part 2; Evolutionary Computing. S.D.Mohaghegh. Journal of Petroleum Technology, 2000.
3. Virtual Intelligence Applications in Petroleum Engineering: Part 3; Fuzzy Logic. S.D.Mohaghegh. Journal of Petroleum Technology, 2000.
4. Top-Down Intelligent Reservoir Modeling of New Albany Shale. A .Kalantari-Dahaghi, S.D. Mohaghegh, SPE, West Virginia University, SPE, 2009. 125859.
5. New Method for Production Data Analysis to Identify New Opportunities in Mature. Mohaghegh, S. D., Gaskari, R. and Jalali, J. Morgantown : Society of Petroleum Engineers, 2005. SPE 98010.
6. Identifying Infill Locations and Underperformer Wells in Mature Fields using Monthly. Jalal Jalali, Shahab D. Mohaghegh, Razi Gaskari,. Canton, Ohio : Society of Petroleum Engineers, 2006. SPE 104550.
7. An Integrated Technique for PDA with Application to Mature Fields. R. Gaskari, S.D. Mohaghegh, and J. Jalali,SPE Production & Operations, 2007, Vol. 22.
8. Top-Down Intelligent Reservoir Modeling .Y .Gomez, Y. Khazaeni, S.D. Mohaghegh, SPE, West Virginia University, R. Gaskari, Intelligent Solutions, Inc. SPE, 2009. 124204.

Getting Up To Speed

Our new series of paper collections provide engineers with a basic introduction to technical topics.

Additional series available for download from the SPE bookstore at **www.spe.org/store**.

Society of Petroleum Engineers

ISBN 978-1-61399-064-3